

**DESIGN, SYNTHESIS, CHARACTERIZATION AND BIOLOGICAL  
EVALUATION OF SOME NOVEL HETEROCYCLIC COMPOUNDS  
AS ANTI-TUBERCULAR AGENTS**

**THESIS**

**Submitted to  
THE TAMIL NADU DR.M.G.R MEDICAL UNIVERSITY,  
CHENNAI**

*In partial fulfillment for the award of the degree of*

**DOCTOR OF PHILOSOPHY**

**IN**

**PHARMACY**

**By**

**K.M.NOORULLA**

*Under the Guidance of*

**DR. A. JERAD SURESH, M.Pharm., Ph.D., M.B.A.,**



**COLLEGE OF PHARMACY,  
MADRAS MEDICAL COLLEGE, PARK TOWN,  
CHENNAI-600003.**

**JANUARY - 2016**

# CONTENTS

CHAPTER	TITLE	PAGE NO.
1.	<b>INTRODUCTION</b>	
	1.1. History of Tuberculosis	1
	1.2. Epidemiology: prevalence, airborne transmission	3
	1.3. Pathogenesis and Immune Response : the interactions between MTB and the host cell	4
	1.4. Treatment and vaccines: antituberculosis drugs, BCG vaccine, and drug resistance	6
	1.5. Drug Discovery	10
	1.6 Medicinal Chemistry	11
	1.7 <i>In Silico</i> Screening Approach	11
	1.8. Biological Target	16
	1.9. Significance of Heterocyclic Compounds	20
2.	<b>LITERATURE REVIEW</b>	
	2.1. Based on In Silico	22
	2.2. Based on Chemistry	28
	2.3. Based on Pharmacology	40
	2.4. Conclusion	47
3.	<b>RESEARCH ENVISAGED AND PLAN OF WORK</b>	
	3.1 Objective of the Present Study	48
	3.2 Work Flow	49

4.	<b><i>IN-SILICO</i> APPROACH</b>	
	5.1. Materials	51
	5.2. Experimental	52
	5.3. Results and Discussions	57
5.	<b>CHEMISTRY</b>	
	5.1. Materials	100
	5.2. Experimental	101
	5.3. Physical properties of the synthesized compounds	119
	5.4. Results and Discussions	126
6.	<b><i>IN-VITRO</i> ANTI-MYCOBACTERIAL ASSAY</b>	
	6.1. Materials	159
	6.2. Experimental	159
	6.3. Results and Discussions	160
7.	<b>MULTIPLE <i>DOcKING</i> ANALYSIS AND MOLECULAR DYNAMIC SIMULATION STUDIES</b>	
	7.1. Multiple Docking Analysis	166
	7.1.1. Materials	166
	7.1.2. Experimental	167
	7.1.3. Results and Discussions	167
	7.2. Molecular Dynamic Simulation	177

	7.2.1. Materials	177
	7.2.2. Experimental	177
	7.2.3. Results and Discussions	178
8.	<b><i>IN-VIVO</i> EFFICACY</b>	
	8.1. Acute Toxicity Study	186
	8.2. In-vivo antimycobacterial activity	188
9	<b>SUMMARY AND CONCLUSION</b>	
	9.1. Summary	192
	9.2. Conclusion	195
10.	<b>BIBLIOGRAPHY</b>	197

## LIST OF TABLES

Table No.	Title of Table	Page No.
1	2D and energy minimized 3D structures of the selected molecules	59
2.	Docking results of the selected 30 analogs	70
3.	Residue interaction pattern for the synthesized compounds against target enzyme InhA	74
4.	<i>In-silico</i> ADME properties of the selected 30 ligand molecules	87
5.	<i>In-silico</i> toxicity assessment results of the 30 ligand molecules	89
6.	List of synthesized compounds with their IUPAC name	119
7.	Melting Point, Percentage Yield and TLC Profile of the synthesized compounds	123
8.	Solubility data of the synthesized compounds	125
9.	Ranking of the compounds based on the <i>in-vitro</i> antimycobacterial activity	165
10.	Glide docking scores of selected compounds (N10, N11 to N20 and GAT) against multiple target enzymes	168
11.	Cross observational analysis of top three ranked compounds with docking ranks	169
12.	Residue interaction pattern for all the studied compounds (N10, N11 to N20 and GAT) against thymidylate kinase	172
13.	Lung CFU lung values in animals treated with test samples and standard controls	191

## LIST OF FIGURES

Figure No.	Title of the Figure	Page No.
1.	<i>Mycobacterium tuberculosis</i>	02
2.	Estimated TB incidence rates, 2013	04
3.	Sequence of events in the natural history of tuberculosis	06
4.	First-Line Treatment of Tuberculosis (TB) for Drug-Sensitive TB with their mode of actions	08
5.	Multidrug-Resistant Tuberculosis (MDR TB) and Possible Effective Treatments with their mode of actions	08
6.	Extensively Drug-Resistant Tuberculosis (XDR TB) Diminishing Options for Treatment	09
7.	New Tuberculosis (TB) Drugs under Development with their mode of actions	09
8.	Energy minimized 3D structure of prepared protein (PDB ID-2NSD)	68
9.	Docked poses of all the 30 ligands at the active site of target enzyme InhA	68
10.	Ligand Interaction Diagrams of all the 30 ligand molecules against active site of target enzyme InhA	78
11.	Screen shot of <i>In-silico</i> toxicity assessment results	90
12.	ORTEP diagram of compound N1	158
13.	<i>In vitro</i> Antimycobacterial activity of 30 synthesized compounds	162
14.	The docked poses of the all the studied compounds (N10, N11 to N20 and GAT) at the active site of thymidylate	171

	kinase	
15.	Ligand interaction diagrams of all the studied compounds (N10, N11 to N20 and GAT) against the binding site of target enzyme thymidylate kinase (1G3U)	174
16.	Plot showing Protein-Ligand (N18-1G3U) RMSD evolution	178
17.	Plot showing Protein-Ligand (N11-1G3U) RMSD evolution	179
18.	Plot showing Protein-Ligand (N20-1G3U) RMSD evolution	179
19.	Ligand interaction diagram before and after simulation and BAR representation of the ligand N18 against 1G3U	182
20.	Ligand interaction diagram before and after simulation and BAR representation of the ligand N11 against 1G3U	183
21.	Ligand interaction diagram before and after simulation and BAR representation of the ligand N20 against 1G3U	184
22.	Lung CFU lung values in animals treated with test samples and standard controls	191

# CHAPTER 1

## INTRODUCTION

Tuberculosis, MTB, or TB is a deadly infectious disease caused by various strains of mycobacteria; usually *Mycobacterium tuberculosis*.<sup>1</sup> According to World Health Organization (WHO) TB is a global pandemic, which has become an important world-wide public health menace with one-third of the world's population infected by the TB bacillus.<sup>2</sup> Most infections do not have symptoms, known as latent tuberculosis and about one in ten latent infections eventually progresses to active disease which, if left untreated, kills more than 50% of those so infected. People with weak immune systems (those with HIV/AIDS, those receiving immunosuppressive drugs and chemotherapy) are at a greater risk of contracting TB disease. There is currently a growing concern about the progress and spread of multidrug and extensively drug-resistant tuberculosis (MDR/XDR-TB), which has the potential to paralyze TB care schemes.

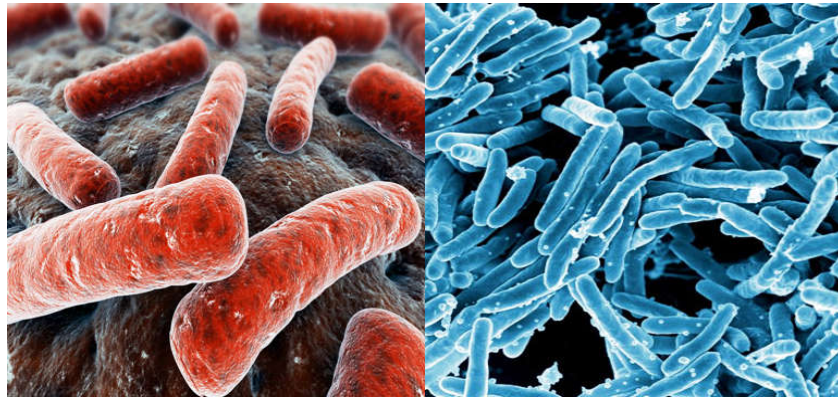
The focal theme of this thesis is the exploration of new strategies in the field of modern drug discovery for the development of new drugs, capable of overcoming MDR/XDR-TB. In order to put things in perspective, a brief introduction to the history, epidemiology and pathogenesis of tuberculosis, modern drug discovery aspects and their applications in the medicinal chemistry are given in the following sections.

### ***1.1. History of Tuberculosis***

Tuberculosis, an airborne disease that typically affects the lungs leading to severe coughing, fever and chest pains, but can also affect other parts of the body.<sup>3,4,5</sup> It may have killed more persons than any other microbial pathogen. It has been assumed that the genus *Mycobacterium* originated more than 150 million years ago.<sup>6,7</sup>



This peculiar disease, whose Latin-originated name describes the rod shape of the bacillus (**Figure 1**), became implicit when the German microbiologist Robert Koch announced that *Mycobacterium tuberculosis* caused TB in the year 1882.<sup>8,9</sup> This finding, along with the later discoveries of tuberculin in the year 1890 and the Bacillus-Calmette Guerin (BCG) vaccine in 1908 and anti-tuberculosis drugs starting in 1943, offered hope for the eradication of a disease deadlier than the plaque.



**Figure 1:** *Mycobacterium tuberculosis*

Mortality rates significantly turned down from the early to mid-20<sup>th</sup> century; in spite of this, funding for research was attenuated and between 1970 to 1990, drug and vaccine developments were decelerated.<sup>3</sup> With the advancement of the AIDS pandemic and the emergence of TB resistant strains, interest in TB research and prevention increased.<sup>3</sup> Strategies to control and prevent the disease were developed. The Directly Observed Treatment Short-Course (DOTS) program was introduced in 1993, with the addition of a DOTS-plus program to address multidrug resistant (MDR) TB in 1998.<sup>3,9</sup>

Though current research in recent years has given valuable insight into TB transmission, diagnosis, and treatment, much needs to be done to efficiently decrease the incidence of and eventually eliminate TB.<sup>3,10</sup> The disease still puts a strain on public health, being only second to HIV/AIDS with high mortality rates.<sup>4</sup>

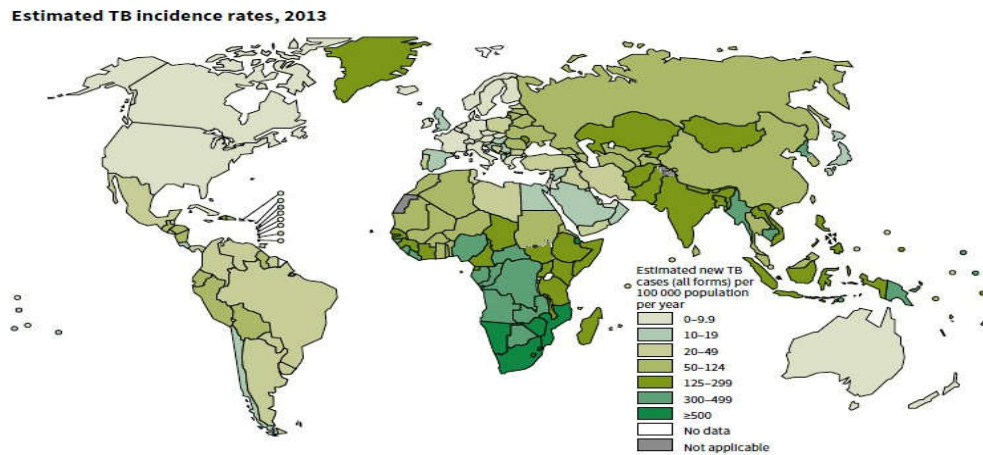
## ***1.2. Epidemiology: prevalence, airborne transmission***

There are a number of risk groups that are more susceptible to acquire infected including: young adults, those in developing countries, health care workers who are in the vicinity of the disease frequently, and those whose immune systems are feeble, as in those who have HIV or smoke.<sup>10,11</sup> Furthermore, foreign-born individuals and those who reside in indigent areas or where malnutrition is ubiquitous are more likely to get infected.<sup>4</sup> The host's own deficiency in interleukin (IL)-12 promoting the T helper (T<sub>H</sub>) 1 response is another factor in the increased susceptibility to infection.<sup>12</sup>

MTB infection is acquired by inhalation of infectious aerosol particles released from close contacts.<sup>11,13</sup> A majority of individuals who inhale MTB build up an effective response in the lungs leading to successful inhibition in the growth of MTB, resulting in the bacteria turning out to be dormant; this condition is often referred to as latent tuberculosis;<sup>14</sup> immuno-competent latent individuals are infected with MTB but do not present symptoms and do not transmit the disease to others.<sup>4,11</sup> It is well-known that one third of the entire world's population is latently infected with MTB.<sup>11</sup> On or after latent infection, the infection can progress to an active state.<sup>15</sup> About 5-10% of latent tuberculosis infection cases are at risk to progressing from infection to active (primary) TB.<sup>11</sup> Those with HIV and other immuno-compromised individuals, such as those with cancer or those currently taking immune suppressing medication have a greater risk of developing active TB.

The World Health Organization (WHO) reported that “one-third of the world's population has been infected with TB”.<sup>4</sup> An estimated 13.7 million chronic cases were active globally,<sup>16</sup> and in 2013, an estimated 9 million new cases occurred.<sup>17</sup> In 2013 (**Figure 2**) there was between 1.3 and 1.5 million associated deaths,<sup>17,18</sup> most of which

occurred in developing countries.<sup>19</sup> While TB can be present in any civilization in any country, a majority of those deaths reported, about 95%, occurred in developing and under-developed countries where resources are inadequate, with a majority of cases appearing in India and China.<sup>4,10</sup>



**Figure 2: Estimated TB incidence rates, 2013**

### ***1.3. Pathogenesis and Immune Response: the interactions between MTB and the host cell***

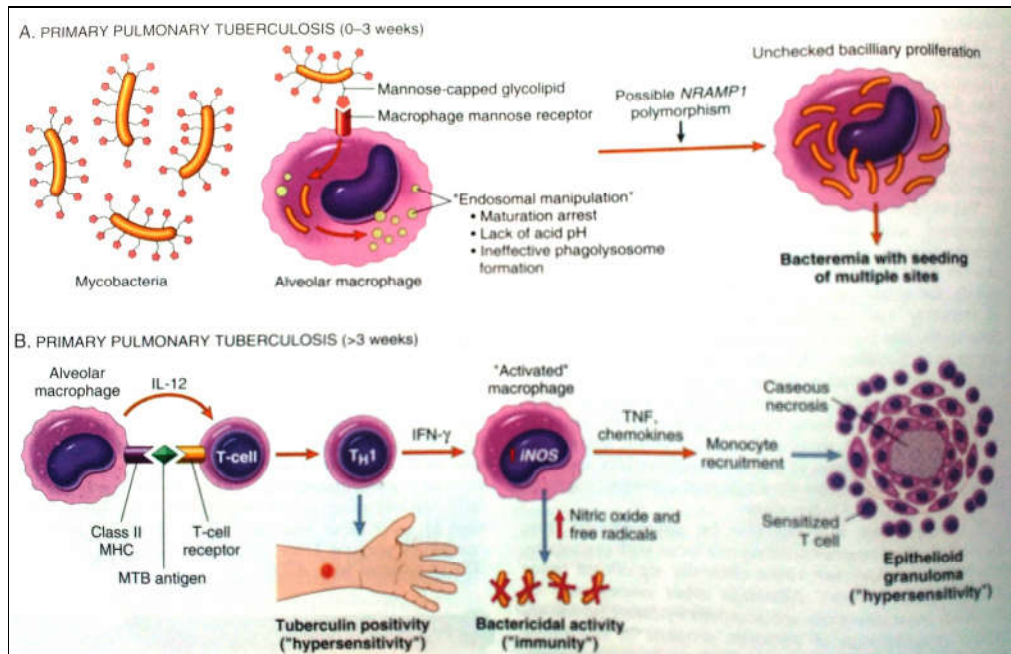
Once the bacterium *M. tuberculosis* (MTB) is inhaled via droplets, spread through person-to-person contact, macrophages can phagocytose and kill the bacilli, during that initial interaction.<sup>20</sup> However, if the bacilli are not killed, they inhibit normal microbial responses by averting the fusion of the lysosomes with the phagocytic vacuole. The prevention of phagolysosome formation allows unhindered mycobacterial proliferation. Thus, the initial phase of primary tuberculosis (first three weeks) in the nonsensitized patient is exemplified by bacillary proliferation inside the pulmonary alveolar and seeding of multiple sites. Regardless of the bacteremia, most persons at this stage are asymptomatic or experience a mild flu-like illness.<sup>21</sup>

The genetic makeup of the patient may have an effect on the course of the disease. In some people with polymorphisms of the NRAMP 1 (Natural Resistance-Associated Macrophage Protein 1) gene, the disease may possibly progress from this point without the improvement of an effective immune response. NRAMP 1 is a transmembrane ion transport protein found in endosomes and lysosomes that is held to contribute to microbial killing.<sup>21</sup>

The event of cell-mediated immunity occurs approximately 3 weeks after exposure. Processed mycobacterial antigens arrive at the draining lymph nodes and are accessible to CD4 T cells by means of dendritic cells and macrophages. Under the influence of macrophage-secreted IL-12 (Interleukin-12), CD4+ T cells of the T<sub>H</sub> 1 (T-helper 1) subset are produced that are capable of secreting IFN- $\gamma$  (Interferon- $\gamma$ ).<sup>21</sup>

IFN- $\gamma$  released by the CD4+ T cells of the T<sub>H</sub> 1 subset is vital in activating macrophages. Activated macrophages, sequentially, release a variety of mediators and upregulate expression of genes with essential downstream effects, including (1) TNF (Tumor necrosis factor) differentiation into the “epitheloid histocytes” that characterize the granulomatous response; (2) expression of the inducible nitric oxide synthase (iNOS) gene, which ends in elevated nitric oxide levels at the site of infection, with exceptional antibacterial activity; and (3) generation of reactive oxygen species, which can have antibacterial activity.<sup>21</sup>

Defects in any of the steps of T<sub>H</sub> 1 response (including IL-12, IFN  $\gamma$ , TNF, or nitric oxide production) result in deprived formation of granulomas, absence of resistance and disease progression. Persons with inherited mutations in any component of the T<sub>H</sub> 1 pathway are notably susceptible to infections with mycobacteria.<sup>21</sup> The Sequence of events in the natural history of tuberculosis was shown in Figure 3.



**Figure 3: Sequence of events in the natural history of tuberculosis**

#### ***1.4. Treatment and vaccines: antituberculosis drugs, BCG vaccine, and drug resistance***

The choice of TB treatment depends on whether the individual is in the latent or active stage and about the probability of risk. Treatment of TB typically necessitates a drug cocktail, or a combination of multiple drugs, with an intensive initial 2-month phase followed by a slower 4 to 6 months continuation phase.<sup>10</sup>

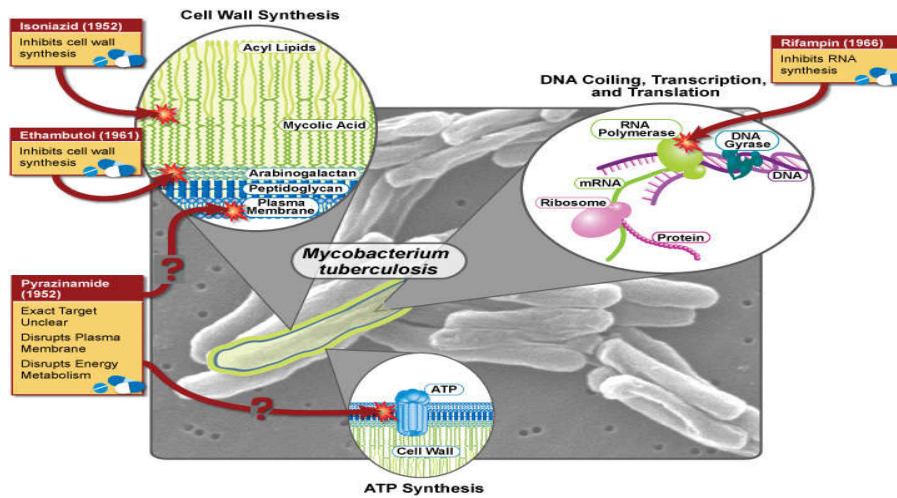
The classical antitubercular agents are divided into two categories: first-line and second-line drugs. The first-line drugs include isoniazid (INH), rifampicin (RIF), pyrazinamide (PZA), ethambutol (EMB), and Streptomycin (SM).<sup>10,13</sup> The second-line drugs including kanamycin, cycloserine,  $\beta$ -aminosalicylic acid, ethionamide, prothionamide, thiacetazone and fluoroquinolones are regarded as a kind of supplement to the first-line drugs. They are usually used in cases of retreatment, resistance, or intolerance to the first-line drugs. Second-line drugs are classified as cell wall, nucleic

acid, energy, or protein synthesis inhibitors; however, no two second-line agents can be used together owing to their nephrotoxicity and ototoxicity.<sup>22</sup>

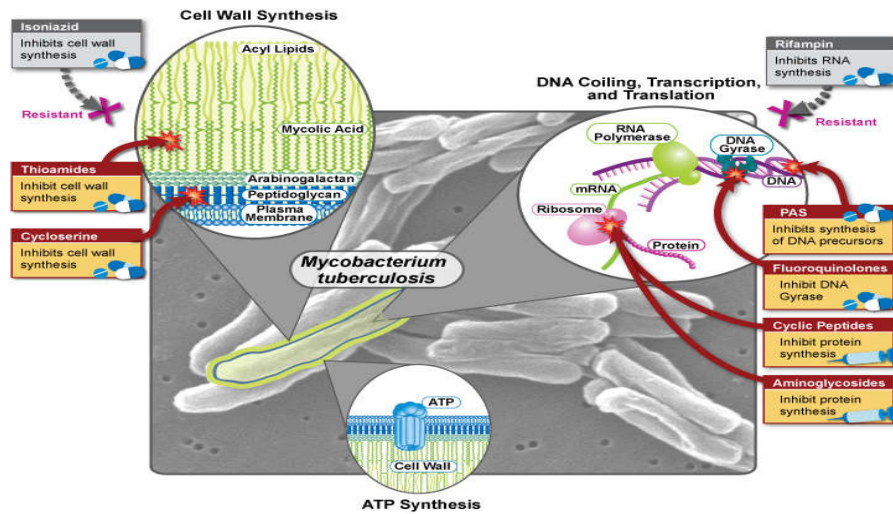
Current front-line therapy consists of two months' treatment with four first-line agents including RIF, INH, and PZA, (with or without EMB), followed by four months' follow-up therapy with INH and RIF.<sup>23</sup> MDR-TB infection requires treatment with second-line drugs such as amikacin, kanamycin, fluoroquinolone,  $\beta$ -aminosalicylate, capreomycin, cycloserine, or ethionamide, and this treatment often lasts for up to two years.<sup>13</sup> In addition to the five main antituberculosis drugs, the *Mycobacterium bovis* BCG vaccine is the current vaccine used to mimic the natural immune response to infection.<sup>24</sup> Although the BCG vaccine has been widely administered for more than eighty years and strongly induces T<sub>H</sub> 1 cells, its efficacy is highly variable, according to a recent review by Andersen.<sup>24</sup>

Drug resistance persists to pose a major health concern. Although drug susceptibility tests are always performed to monitor resistance,<sup>13</sup> previous treatments, not completing treatment, not complying with treatment, and improper or inadequate regimens can confer drug resistance.<sup>11, 13</sup>

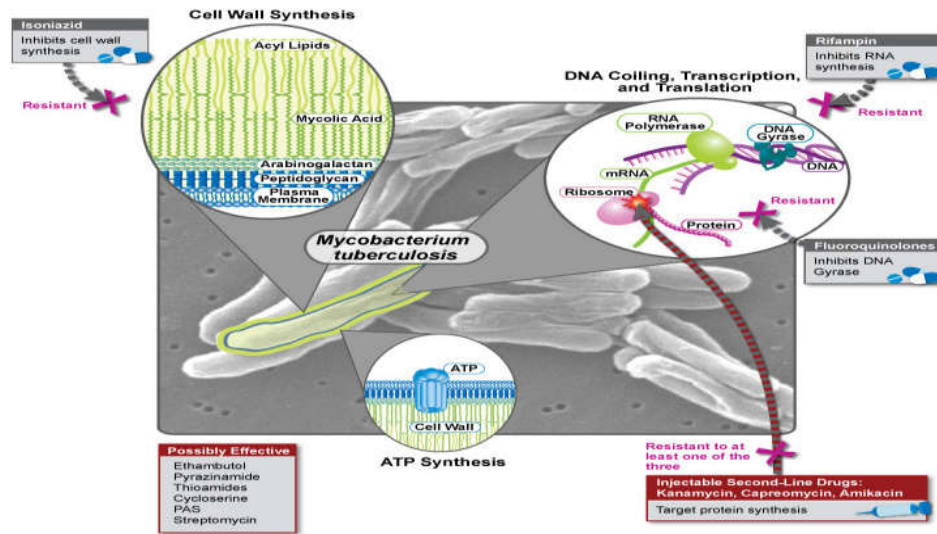
Schematic diagrams of First-Line Treatment of Tuberculosis (TB) for Drug-Sensitive TB (Figure 4), Multidrug-Resistant Tuberculosis (MDR TB) and Possible Effective Treatments (Figure 5), Extensively Drug-Resistant Tuberculosis (XDR TB) Diminishing Options for Treatment (Figure 6) and New Tuberculosis (TB) Drugs Under Development with their mode of actions (Figure 7).<sup>25</sup>



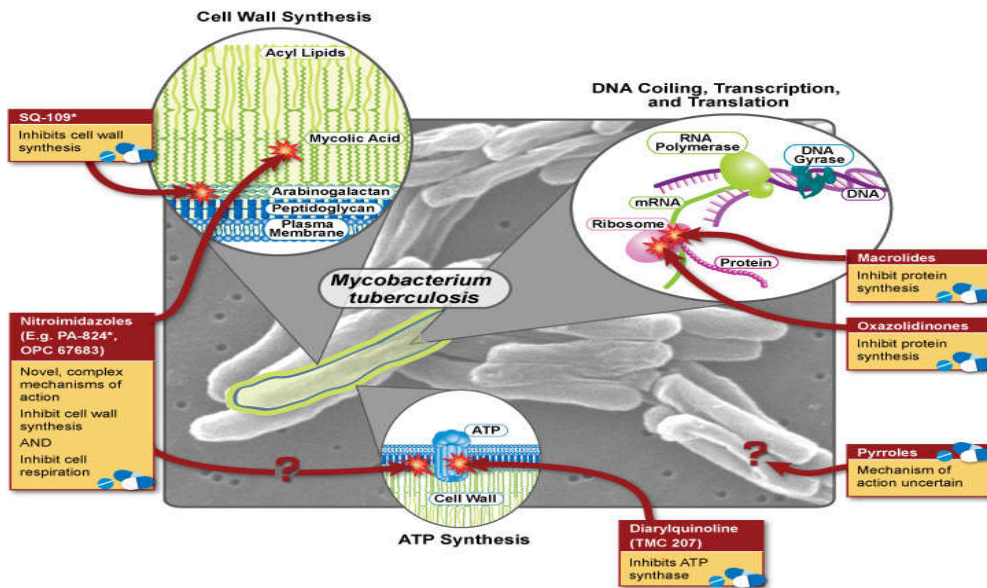
**Figure 4: First-Line Treatment of Tuberculosis (TB) for Drug-Sensitive TB with their mode of actions**



**Figure 5: Multidrug-Resistant Tuberculosis (MDR TB) and Possible Effective Treatments with their mode of actions**



**Figure 6: Extensively Drug-Resistant Tuberculosis (XDR TB) Diminishing Options for Treatment**



**Figure 7: New Tuberculosis (TB) Drugs under Development with their mode of actions**



## 1.5. Drug Discovery

Modern drug discovery and development plays an imperative role in transforming a molecule from laboratory into a drug candidate. Drug discovery process can be generally segregated into two segments.

- Identification and optimization of lead molecules to put up their selectivity towards the target including their toxicity profile.
- Development of a pertinent biological system to test the compounds in *in-vitro* and *in-vivo* models to accelerate the drug discovery process and to enrich the screening efficiency and success rate.<sup>26</sup>

Drug discovery and development is a composite, protracted and an expensive process since the safety, efficacy and other issues are obligatory. By and large, it takes about more than 10 years to end in a new drug developed from its preliminary screening stage to final FDA approval and has a huge failure rate at each phase of the developmental process. To aid this various new techniques are available such as, combinatorial chemistry, green organic synthesis, high-throughput purification, molecular docking and QSAR analysis. In spite of such modernization and evolution in research and development, the number of new chemical entities reaching the market has decreased noticeably, giving an impression that, selection of the appropriate molecules for synthesis turn out to be one of the most challenging tasks.<sup>26</sup>

The assessment of ADMET profiles of drug candidates during preclinical development represents one of the decisive parts of the drug discovery process. Effective profiling operations are now run in parallel to potency screening during lead optimization. *In-vitro* assays are employed during early drug development and high-throughput ADMET screens are also accessible. The advantage of exploiting *in silico* approaches over *in-vitro* assays is that less investment is needed in resources, time and technology.<sup>27</sup>

## ***1.6. Medicinal Chemistry***

Medicinal chemistry is an interdisciplinary science, which deals with a wide domain situated at the interface of organic chemistry with life sciences such as biochemistry, pharmacology, molecular biology, genetics, immunology, pharmacokinetics, and toxicology on one side, and chemistry-based disciplines such as physical chemistry, crystallography, spectroscopy, and computer-based techniques of simulation, data analysis and data visualization on the other side.<sup>28</sup>

“Medicinal chemistry concerns the discovery, the development, the identification and the explanation of the mode of action of biologically active compounds at the molecular level”.<sup>29</sup> Medicinal chemistry is also concerned with the “study, identification, and synthesis of the metabolic products of the drugs and related compounds”.<sup>29</sup> Thus, medicinal chemistry remains a challenging science which provides profound satisfaction to its practitioners. Medicinal chemists have a chance to participate in the fundamentals of prevention, therapy and understanding of diseases and thereby to contribute to a healthier and happier life.<sup>30</sup>

## ***1.7. In Silico Screening Approach***

Over the past decade, the use of computerized models to predict outcomes in biological studies has become apparent. This concept is better known as *in silico* biology. It eventually aids a better understanding and prediction of chronic human disease pathogenesis and ultimately facilitates to design better and more rational approaches for developing and analyzing new drug candidates.

In general, Rational Drug Design (RDD) is “the ingenious process of discovering new molecules based on the knowledge of the biological target”. The drug is most commonly a small organic molecule which stimulates or inhibits the function of

a bio-molecule such as a protein which in turn produces therapeutic benefit to the patient. Thus the fundamental concept of drug design involves “design of small molecules that are complementary in shape and charge to the biomolecular target to which they interact and therefore will bind to it”. Drug design often but not necessarily relies on computer modeling techniques. This type of modeling is often referred as Computer Aided Drug Design (CADD).

CADD computational tools and software's are used to simulate drug receptor interactions. In traditional based approach, drugs were discovered by the means of trial and error methodologies making research and development process more time consuming and expensive. Computational drug discovery helps scientists to get an insight into the drug receptor interactions and also helps to reduce the time and cost.<sup>31</sup>

RDD methods fall into two different categories

- ✓ Ligand- based (Pharmacophore modeling)
- ✓ Structure- based (Molecular docking)

➤ *Ligand- based drug design:*

Ligand based drug design (or indirect drug design) relies on the perception of other molecules that bind to the biological target of interest. These and other molecules may be used to derive a pharmacophore model which describes the minimum necessary structural characteristics for a molecule to possess, so as to bind to the target. conversely, quantitative study (QSAR) in which a correlation between calculated properties of molecules and their related biological activity may be derived. QSAR relationship is used to predict the activity of new analogs.

➤ *Structure-based drug design:*

Structure based drug design (or direct drug design) relies on empathizing the three dimensional structure of the biological target obtained through methods such as X-Ray crystallography or NMR spectroscopy. Using the structure of the biological target, candidate drugs that are expected to bind with high affinity and selectivity to the target may be designed using interactive graphics based on the intuition and ingenuity of the medicinal chemist. Alternatively, diverse automated computational procedures may be used to contemplate the molecular targets for which drugs are contemporarily designed.

### ***1.7.1. Molecular Docking***

Molecular Docking is the technique which envisages the “preferred orientation of one molecule to a second when bound to each other to form a stable complex in three dimensional spaces”. In cell biology, the function of proteins is a result of its interaction (i.e. docking) with other proteins as well as other molecular components; if we could understand how proteins interact (dock) with other molecules, the function of the protein can be inferred. Thus the results of the docking are exceptionally beneficial in finding drugs which are effective against particular disease.<sup>32</sup>

#### ***Docking Principle***

The two main components that are important for docking studies are:

- Secondary structure of our protein of interest.
- Library of ligands from suitable data base.

Docking tools are based on the search, algorithm and the scoring function. A search algorithm finds the best docking pose measured by the scoring function. A scoring function differentiates correct docking poses from incorrect ones.

The quality of any docking results depends on the reasonable starting structures of both the protein and the ligand. The protein and ligand structures require preparation before docking in order to achieve the best docking results.<sup>33-35</sup>

### ***1.7.2. In-Silico Toxicity Risk Assessment***

Toxicity is accountable for ~20-40% of drug failures to reach the market and for the withdrawal of a considerable number of compounds from the market once they have been approved. Commercially *in-silico* tools are available and can be used for predicting potential toxicity issues; they are generally classified into two groups. The first approach uses “expert systems that develop models on the basis of abstracting and codifying knowledge from human and the scientific literature sources”. The second approach relies on “generating the descriptors of chemical structure and statistical analysis of the relationships between those descriptors and the toxicological end-point”. Modern software packages primarily lay emphasis on carcinogenicity and mutagenicity, although some packages do also comprise tools and/or knowledge bases for other end-points, such as “teratogenicity, irritation, sensitization, immunotoxicology and neurotoxicity”.<sup>36</sup>

### ***1.7.3. In-Silico ADME Predictions***

Generally drug discovery and development are expensive and time-consuming processes. In pharmaceutical research several new drug failures occur in the clinical trial phase due to absorption, distribution, metabolism and excretion (ADME) properties. Therefore, *in-vitro* approaches are comprehensively used to explore the

ADME properties of new chemical entities and more recently, computational (*in silico*) modeling has been investigated as a tool to optimize the choice of the most suitable drug candidates for development.

The advantage of using *in silico* tools is that, being high-throughput and low cost, they can be used very early in discovery to virtually screen thousands of compounds in a matter of hours to help prioritize compounds and assays for ADME/toxicity testing. These tools are used to forecast physicochemical and pharmacokinetic (PK) properties, which in turn helps prioritize compounds for screening and facilitates early decision making in drug discovery. ADME prediction is an exceptionally challenging area as many of the properties predicted are a result of multiple physiological processes.<sup>37</sup>

#### ***1.7.4. Molecular Dynamic Simulation Studies***

The structure of a protein cannot be resolved solely from its sequence. Instead, the structure can be obtained experimentally for some proteins either by X-Ray crystallography or by NMR Spectroscopy. These experimental methods cannot give detailed information on the dynamic properties of a protein and consequently provide only very limited insights on the folding process itself.

Molecular dynamics (MD) simulations can be used to study the dynamic properties of a system in full atomic details. Thus MD simulations can be used “to gain a better understanding of the interactions between protein-protein and between ligand-protein in order to predict how proteins or some of their elements associate with one another to achieve their lowest free energy conformation”. The ability to accurately determine differences in free energy is therefore of great practical interest in biophysics and structural biology as it would allow the prediction of phenomena such as

conformational changes or protein-ligand interactions. Free energy differences can be calculated from numerical simulations using a variety of statistical mechanical approaches. The accuracy of such calculations is primarily limited by two factors, the nature of the underlying model or force field and the extent of the sampling during the simulation.<sup>38</sup>

### ***1.8. Biological Target***

There are various biosynthetic enzymes that are essential for the survival of the *Mycobacterium* and are considered as potential drug targets. A comprehensive *in silico* target identification pipeline for *Mycobacterium tuberculosis* was identified and reported. It comprises a total of 451 high-confidence targets.<sup>19</sup>

The identification of 451 high-confidence targets of *Mycobacterium tuberculosis* was studied by passing the whole *Mycobacterium tuberculosis* proteome into various filters/analysis such as “network analysis of the protein-protein interactome (molecular interaction network), flux balance analysis of the reactome (Mathematical method for simulating metabolism in genome-scale reconstructions of metabolic networks), experimentally derived phenotype essentiality data (genes that are indispensable for the survival of an organism), sequence analysis (process of subjecting a DNA, RNA or peptide sequence to any of a wide array of analytical methods to recognize its features, function, structure, or evolution) and a structural assessment of targetability (availability of crystal structure of the proteins in order to increase the targetability)”.<sup>19</sup>

From those 451 high confidence targets of *Mycobacterium tuberculosis*, ten critical targets which pass the major filters of the above study were selected for the computational study.

The target enzymes are as follows,

- ✓ *Mycobacterium tuberculosis* Diaminopimelate Decarboxylase,
- ✓ *Mycobacterium tuberculosis* cyclopropane Synthase,
- ✓ *Mycobacterium tuberculosis* Antibiotic Resistance Protein,
- ✓ *Mycobacterium tuberculosis* TrpD essential for lung colonization,
- ✓ *Mycobacterium tuberculosis* Thymidylate Synthase X,
- ✓ *Mycobacterium tuberculosis* InhA, the enoyl acyl carrier protein reductase,
- ✓ *Mycobacterium tuberculosis* Thymidylate Kinase,
- ✓ *Mycobacterium tuberculosis* Protein Kinase G,
- ✓ *Mycobacterium tuberculosis* Gyrase TypeIIA Topoisomerase and
- ✓ *Mycobacterium tuberculosis* L, D Transpeptidase 2.

#### ***Mycobacterium tuberculosis* Diaminopimelate Decarboxylase:**

The *Mycobacterium tuberculosis lysA* gene has encoded the enzyme *meso*-diaminopimelate decarboxylase (DAPDc), a pyridoxal-5'-phosphate (PLP)-dependent enzyme, which catalyzes the final step in the lysine biosynthetic pathway converting *meso*-diaminopimelic acid (DAP) to L-lysine. Thus *lysA* gene of *M. tuberculosis* H37Rv has been established as essential for bacterial survival in immunocompromised mice, demonstrating that *denovo* biosynthesis of lysine is essential for *in-vivo* viability.<sup>39</sup>

#### ***Mycobacterium tuberculosis* Cyclopropane Synthase:**

Mycolic acids are major components of the cell wall of *Mycobacterium tuberculosis* has acyl chain that are important for pathogenesis and persistence. There are at least three mycolic acid cyclopropane synthases (PcaA, CmaA1, and CmaA2) which are responsible for these site-specific modifications of mycolic acids. They have a seven-stranded  $\alpha/\beta$  fold similar to other methyltransferases with the location and interactions with the cofactor *S*-adenosyl-L-methionine conserved. Mycolic acid



substrate active binding site which reveals electron density represents a bicarbonate ion. In addition, comparison of the enzyme structures reveals a possible mechanism for substrate specificity. These structures provide a foundation for rational-drug design, which can lead to the development of new inhibitors effective against persistent bacteria.<sup>40</sup>

#### ***Mycobacterium tuberculosis* Antibiotic Resistance Protein:**

Putative aminoglycoside *N*-acetyltransferase, is a gene product of an open reading frame Rv1347c. The crystal structure of Rv1347c protein coupled with functional and bioinformatic data, suggests its role in the biosynthesis of mycobactin, which is the siderophores of the *M. tuberculosis*.<sup>41</sup>

#### ***Mycobacterium tuberculosis* TrpD essential for lung colonization:**

The tryptophan biosynthesis pathway is thought to be non-essential for many pathogens but not in the case for *M. tuberculosis*. The *trpD* gene, anthranilate phosphoribosyltransferase, which catalyses the second step in tryptophan biosynthesis could be an essential target.<sup>42</sup>

#### ***Mycobacterium tuberculosis* Thymidylate Synthase X:**

A novel flavin-dependent thymidylate synthase was identified recently as an essential gene in many archaeobacteria and some pathogenic eubacteria. This enzyme, ThyX, is a potential antimycobacterial drug target, since humans and most eukaryotes lack the *thyX* gene and depend upon the conventional thymidylate synthase (TS) for their dTMP requirements.<sup>43</sup>

#### ***Mycobacterium tuberculosis* InhA, the enoyl acyl carrier protein reductase:**

InhA, the enoyl acyl carrier protein reductase (ENR), is one of the key enzymes involved in the type II fatty acid biosynthesis pathway of *M. tuberculosis*. The direct

InhA inhibitors require no mycobacterial enzymatic activation and thus circumvent the resistance mechanism to antitubercular prodrugs such as Isoniazid (INH) and Ethionamide (ETA) that is most commonly observed in drug-resistant clinical isolates.<sup>44</sup>

#### ***Mycobacterium tuberculosis* Thymidylate Kinase:**

Thymidylate mono-phosphate (TMP) kinase is a binary complex with its natural substrate TMP. Its main features involve: (i) a clear magnesium-binding site; (ii) an alpha-helical conformation for the so-called LID region; and (iii) a high density of positive charges in the active site. There is a network of interactions involving highly conserved side-chains of the protein, the magnesium ion, a sulphate ion mimicking the  $\beta$  phosphate group of ATP and the TMP molecule itself.<sup>45</sup>

#### ***Mycobacterium tuberculosis* Protein Kinase G:**

A crucial virulence factor for intracellular mycobacterial survival is protein kinase G (PknG), a eukaryotic-like serine/threonine protein kinase expressed by pathogenic mycobacteria that blocks the intracellular degradation of mycobacteria in lysosomes. Inhibition of PknG with the highly selective low molecular-weight inhibitor AX20017 results in mycobacterial transfer to lysosomes and killing of the mycobacteria.<sup>46</sup>

#### ***Mycobacterium tuberculosis* Gyrase TypeIIA Topoisomerase:**

DNA topoisomerases are essential enzymes that can overwind, underwind, and disentangle double-helical DNA segments to maintain the topological state of chromosomes. Nearly all bacteria utilize a unique type II topoisomerase, gyrase, which actively adds negative supercoils to chromosomes using an ATP-dependent DNA strand passage mechanism; however, the specific activities of these enzymes can vary

markedly from species to species. *Escherichia coli* gyrase is known to favor supercoiling over decatenation, whereas the opposite has been reported for *Mycobacterium tuberculosis* gyrase.<sup>47</sup>

### ***Mycobacterium tuberculosis* L, D Transpeptidase 2:**

Traditional  $\beta$ -lactam antibiotics that inhibit D, D-transpeptidases are not effective against mycobacteria, in part because mycobacteria rely mostly on L, D-transpeptidases for biosynthesis and maintenance of their peptidoglycan layer. This reliance plays a major role in drug resistance and persistence of *Mycobacterium tuberculosis* (*Mtb*) infections.<sup>48</sup>

### ***1.9. Significance of Heterocyclic Compounds***

One half of all therapeutic agents consist of heterocyclic compound, as revealed by Organic Chemical Society. Small heterocyclic ring system in many cases comprises the very core of the active moiety as pharmacophore. The last decade saw the development of heterocyclic compounds emerging as compounds of chemotherapeutic value. The presence of heterocyclic structure in compounds of carbohydrates, amino acids, vitamins, alkaloids or antibiotics is a strong by indicative of the profound effect of such structures on the physiological activity.<sup>49</sup>

“Small ring heterocyclic’s containing nitrogen; sulfur and oxygen have been under investigation for a long time because of their important medicinal properties”. Among this type of molecules, 4-thiazolidinones and some fused ring systems like thieno-pyrimidines, thieno-pyridines, thieno-thiazines and benzo-thiophenes were shown to have various important biological activities such as antibacterial, antifungal, antiviral, diuretic, tuberculostatic, anti-HIV, antihistaminic, anticancer, anticonvulsant, anti-inflammatory and analgesic properties.<sup>50-71</sup>

Considering the above facts and statements, the research attempt has been undertaken to frame the strategy as per the protocol of drug discovery to design and synthesize new chemical entities of diverse heterocyclic scaffolds like 4-thiazolidinones, thieno-pyrimidines, thieno-pyridines, thieno-thiazines, benzo-thiophenes and to screening them for their anti mycobacterial activity.

# CHAPTER 2

## LITERATURE REVIEW

The aim of the literature survey is to establish a complete knowledge, based upon the various *in-silico* approaches attempted in the modern drug discovery. The survey also aimed to understand the chemistry and biology involved in the drug discovery of anti-tubercular agents. Thus, a detailed literature survey was carried out based on *in-silico* approaches, chemistry aspect and on pharmacological aspect.

### ***2.1. Based on In Silico***

1. **Kondreddi R R *et al.*,<sup>72</sup> (2013)** reported the design, synthesis and biological evaluation of indole-2-carboxamides, as a promising class of anti-tuberculosis agents from phenotypic screening against mycobacteria.
2. **Soumendranath B.,<sup>73</sup> (2012)** reported SAR and pharmacophore based designing of some antimalarial and antiretroviral agents using internet based drug design approach. The study predicted that the molecules designed on the basis of SAR and pharmacophore to be more effective and potent in nature than that of all prototype molecules.
3. **Wermuth C G.,<sup>74</sup> (2006)** reviewed the similarity in drugs with the importance and reflections on analogue design. He also clarified the terminology of analogue design by establishing a clear distinction among three kinds of analogues.
4. **Ntie Kang F *et al.*,<sup>75</sup> (2015)** reported an *in silico* evaluation of the ADMET profile of the StreptomeDB database. An assessment of the “drug-likeness” and

pharmacokinetic profile of >2,400 compounds of natural origin, currently available in the recently published StreptomeDB database was also reported.

5. **Ghorpade S R *et al.*,<sup>76</sup> (2013)** studied a pharmacophore-based search led to the identification of thiazolopyridine ureas as a novel scaffold with antitubercular activity acting through inhibition of DNA Gyrase B (GyrB) ATPase.
6. **Martins F *et al.*,<sup>77</sup> (2014)** reported the QSAR oriented design, synthesis and *in vitro* antitubercular activity of several potent isoniazid derivatives (isonicotinoyl hydrazones and isonicotinoyl hydrazides) against H37Rv and two resistant *Mtb* strains.
7. **Kore P P *et al.*,<sup>31</sup> (2012)** reviewed a brief history of CADD, DNA as target, receptor theory, structure optimization, structure-based drug design, virtual high-throughput screening (vHTS) and graph machines.
8. **Nalini C N *et al.*,<sup>78</sup> (2011)** synthesized a series of novel 5-substituted Isatin derivatives and evaluated for antimicrobial activity. These compounds were further subjected to toxicity parameters such as mutagenicity, tumorigenicity, skin irritation, reproductive effect using Osiris software.
9. **Bamane R V *et al.*,<sup>79</sup> (2011)** studied the binding modes of a series of quinoline-3-carbohydrazide as novel PTP1B inhibitors as potential antihyperglycemic agents by using molecular modeling techniques.
10. **Raparti V *et al.*,<sup>80</sup> (2009)** synthesized a series of 4-(morpholin-4-yl)-N'-(arylidene)benzohydrazides. The synthesized compounds were screened for antimycobacterial activity and percentage reduction in relative light units (RLU) was calculated using luciferase reporter phages (LRP) assay.

11. **Renuka J et al.,** <sup>81</sup> (2014) discovered and optimized ethyl 5-(piperazin-1-yl) benzofuran-2-carboxylate series of mycobacterial DNA gyraseB inhibitors, and the compounds were tested for their biological activity against *Mycobacterium smegmatis* DNA gyraseB enzyme.
12. **Haouz A et al.,** <sup>82</sup> (2003) reported the chemical synthesis of derivatives designed as inhibitors of *Mycobacterium tuberculosis* TMP kinase.
13. **Frederick W G et al.,** <sup>83</sup> (2015) outlined general principles that should be applied to ensure the building block collection's impact on drug discovery projects.
14. **Santhi N et al.,** <sup>84</sup> (2011) performed the docking of 26 withanferin and 14 withanolides from *Withania somnifera* into the three dimensional structure of PknG of *M. tuberculosis* using Glide. The inhibitor binding positions and affinity were evaluated using scoring functions-Glidescore.
15. **Alegaon S G et al.,** <sup>85</sup> (2014) reported synthesis of twenty-two 1,3,4-trisubstituted pyrazole its anti-inflammatory activity, in which some of the compounds possess thiazolidinone core. They also reported the molecular docking study of the synthesized compounds in order to support the observed activity.
16. **Romano T K.,** <sup>86</sup> (2007) reported an introduction of ligand-receptor docking and illustrated the basic underlying concepts. Virtual screening for the rapid identification of small molecule ligands of macromolecular targets was also established.

17. **Alegaon S G *et al.*,<sup>87</sup> (2014)** reported synthesis, pharmacophore modeling, and *in vitro* anticancer activity of a series of 2-thioxothiazolidin-4-one derivatives.
18. **Eleftheriou P *et al.*,<sup>88</sup> (2012)** reported fragment-based design, docking, synthesis, biological evaluation and structure activity relationships of 2- benzo/ benzisothiazolimino-5-arylidene-4-thiazolidinones as cyclooxygenase/ lipoxygenase inhibitors.
19. **Joshi S D *et al.*,<sup>89</sup> (2015)** reported the synthesis, evaluation and *in silico* molecular modeling of sixty eight novel pyrrolyl-1, 3, 4-thiadiazole inhibitors of InhA by three-step optimization processes.
20. **Nasr T *et al.*,<sup>90</sup> (2015)** reported the design, synthesis and *in vitro* antimicrobial evaluation of new functionalized 2, 3-dihydrothiazoles and 4-thiazolidinones tagged with sulfisoxazole moiety.
21. **Spadola L *et al.*,<sup>91</sup> (2003)** reported the model of the three-dimensional structure of VZV TK resulting from a homology modelling study. Subsequent docking studies of the natural substrate deoxythymidine (dT) and known antiviral drugs were performed and shed new light on the binding characteristics of the enzyme.
22. **Saha R *et al.*,<sup>92</sup> (2014)** synthesized thirty two novel hybrid-pyrrole derivatives, and the compounds were evaluated against *Mycobacterium tuberculosis* H37Rv strain.
23. **Mohan S B *et al.*,<sup>93</sup> (2012)** designed a series of 1,2,3,4-tetrahydropyrimidine-5-carbonitrile derivatives and the target compounds were synthesized by multicomponent reaction which involves one-pot organic reactions.



24. **Vilar S *et al.***,<sup>94</sup> (2011) explored the applicability of docking-based virtual screening to the discovery of GPCR ligands and defined the methods intended to improve the screening performance.
25. **Zhou Z *et al.***,<sup>95</sup> (2007) studied the problem of docking and scoring flexible compounds which are sterically capable of docking into a rigid conformation of the receptor. They also showed that docking into multiple receptor structures can decrease the docking error in screening a diverse set of active compounds.
26. **Kim M *et al.***,<sup>96</sup> (2012) elucidated the mechanism of allosteric inhibition of the human form of peroxiredoxin (Prx), 2-Cys proliferation associated gene (PAG) by molecular modeling.
27. **Friesner R J *et al.***,<sup>97</sup> (2004) reported the new computational algorithms for docking and scoring for Glide and evaluated the performance of these algorithms in predicting binding modes over a wide range of cocrystallized structures.
28. **Friesner R A *et al.***,<sup>98</sup> (2006) developed a novel scoring function to estimate protein-ligand binding affinities and implemented as the Glide 4.0 XP scoring function and docking protocol.
29. **Halgren T A *et al.***,<sup>99</sup> (2004) describes a new approach for rapid, accurate docking and scoring-enrichment factors in database screening.
30. **Halgren T.**,<sup>100</sup> (2007) describes a new method for fast and accurate binding-site identification and analysis.
31. **Halgren T.A.**,<sup>101</sup> (2009) reported a new approach for identifying and analyzing binding sites and for predicting target druggability.

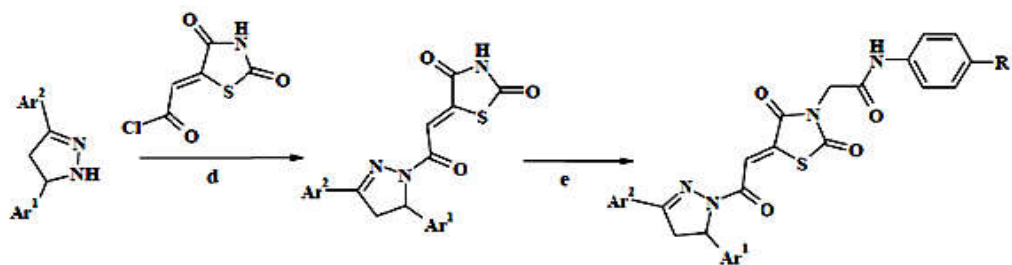
32. **Sastry G M *et al.***,<sup>102</sup> (2013) reported the protein and ligand preparation, its parameters, protocols and influence on virtual screening enrichments.
33. **Douguet D *et al.***,<sup>103</sup> (2005) described LEA3D, a new structure-based drug design program aimed at identifying novel structures that were predicted to fit the active site of a target protein.
34. **Unsal-Tan O *et al.***,<sup>104</sup> (2012) designed and synthesized a series of novel 2-aryl-3-(4-sulfamoyl/methylsulfonylphenylamino)-4-thiazolidinones were designed, synthesized and evaluated for their *in vitro* COX-1/COX-2 inhibitory activities.
35. **Raghu R *et al.***,<sup>105</sup> (2014) reported the virtual screening and discovery of novel Aurora Kinase inhibitors by using molecular modeling with 3UOK and identified 9 promising fragment molecules considering the interaction pattern and synthetic feasibility. Biological activity was also performed against breast and colorectal cancer cell lines.
36. **Shahlaei M *et al.***,<sup>106</sup> (2011) reported the homology modeling, molecular docking and molecular dynamics simulation to explore structural features and binding mechanisms of some inhibitors of chemokine receptor type 5 (CCR5).
37. **Xiao J *et al.***,<sup>107</sup> (2004) reported the homology modeling and molecular dynamics studies of a novel C3-like ADP-ribosyltransferase. The protein 3D structure was built by using homology modeling based on the known crystal structure of exoenzyme C3 from *C. botulinum* (1G24), then the model structure was refined by the energy minimization and molecular dynamics methods.
38. **Park H *et al.***,<sup>108</sup> (2013) studied the homology modeling and virtual screening approaches to identify the potent inhibitors of slingshot phosphatase 1. They

identified eight novel inhibitors of SSH1 through the computer-aided drug design protocol involving homology modeling of SSH1 structure, virtual screening of a large chemical library with docking simulations, and *in vitro* enzyme assays.

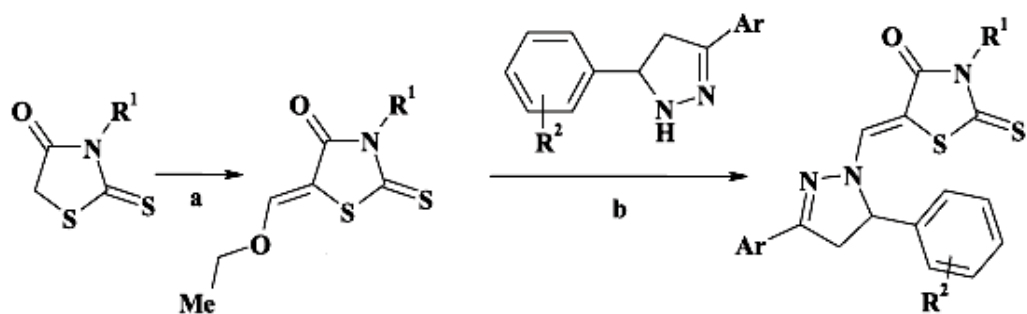
39. **Guo Z *et al.***, <sup>109</sup> (2010) studied probing the  $\alpha$ -helical structural stability of stapled p53 peptides by molecular dynamics simulations and analysis. They determined that how and to what extent the introduction of hydrocarbon cross-links at various locations in the sequence modifies the equilibrium conformational population of the peptides in solution.
40. **Shivakumar D *et al.***, <sup>110</sup> (2010) studied that the predictions of absolute solvation free energies for a diverse set of 239 neutral molecules using molecular dynamics/free energy perturbation (MD/FEP) and the OPLS force field.

## ***2.2. Based on Chemistry***

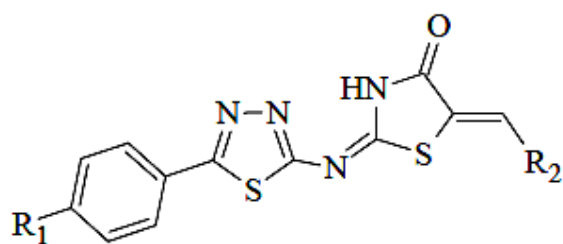
41. **Hamama W S *et al.***, <sup>111</sup> (2008) reported the recent development in the chemistry of 4-thiazolidinones which includes structure, basicity, synthetic aspects, reactions and its applications.
42. **Havrylyuk D *et al.***, <sup>112</sup> (2013) synthesized and evaluated anticancer activity of novel 4-thiazolidinone based conjugates with pyrazoline moiety. The screening of antitrypanosomal and antiviral activities of 5-(3-naphthalen-2-yl-5-aryl-4,5-dihydropyrazol-1-yl)-thiazolidine-2,4-diones was also carried out.



43. Havrylyuk D *et al.*,<sup>113</sup> (2014) synthesized a series of novel 4-thiazolidinone-pyrazoline conjugates and tested for trypanocidal activity.

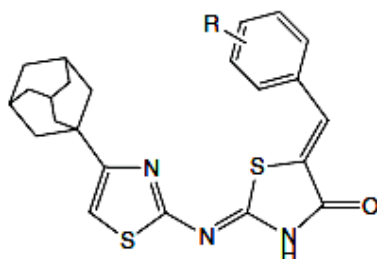


44. Küçükgülzel I *et al.*,<sup>114</sup> (2013) reported the design, synthesis and evaluation of some novel allosteric inhibitors bearing the 4-thiazolidinone scaffold as inhibitors of HCV NS5B polymerase.

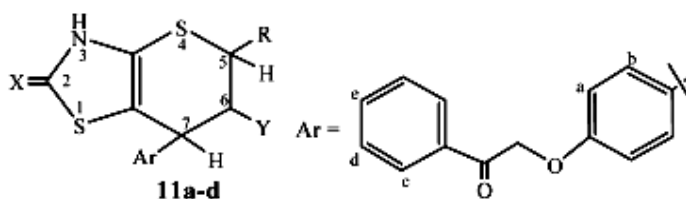


45. Metwally M A *et al.*,<sup>115</sup> (2010) reviewed and reported that 2-amino-4-thiazolidinones are synthetically versatile substrates, as they can be used for the synthesis of a large variety of biologically active compounds, such as thiazolo-dihydropyrazoles, thiazolo-triazines, and thiazolo-tetrahydropyrimidones, and as a raw material for drug synthesis.

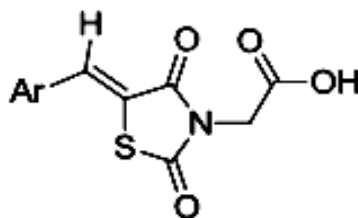
46. **Omar K *et al.***,<sup>52</sup> (2010) reported the synthesis of novel 4-thiazolidinone derivatives incorporating three known bioactive nucleus such as thiazole, thiazolidinone and adamantane.



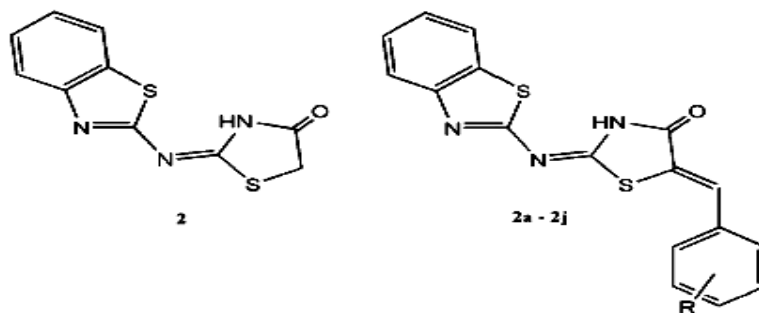
47. **Metwally N H *et al.***,<sup>116</sup> (2008) synthesized the new *Z*-5-arylmethylene-4-thioxo-thiazolidine derivatives by condensation of  $\omega$ -(4-formylphenoxy)acetophenone derivatives with 4-thioxothiazolidine derivatives.



48. **Alegaon S G *et al.***,<sup>117</sup> (2013) described the synthesis of new (*Z*)-2-(5-arylidene-2, 4-dioxothiazolidin-3-yl) acetic acid derivatives. The compounds were also evaluated for their anti-microbial and anti-cancer activities.



49. **Vicini P *et al.***,<sup>118</sup> (2008) synthesised 2-heteroarylimino-5-benzylidene-4-thiazolidinones and assayed *in vitro* for their antimicrobial activity against Gram positive and Gram negative bacteria, yeasts and mould.

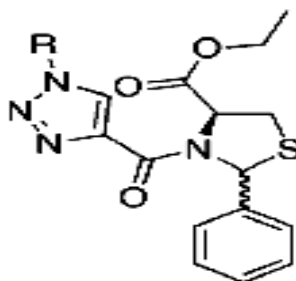


50. **Aneja D K et al.,** <sup>119</sup> (2011) synthesized a new pyrazolyl-2,4-thiazolidinediones by Knoevenagel condensation and the synthesized compounds were tested for *in-vitro* their antibacterial and antifungal activities.

51. **Babaoglu K et al.,** <sup>63</sup> (2003) synthesized substituted thiazolidinones for the inhibition of enzymes-dTDP-rhamnose synthesis which is essential in the biosynthetic pathway of *Mycobacterium tuberculosis*.

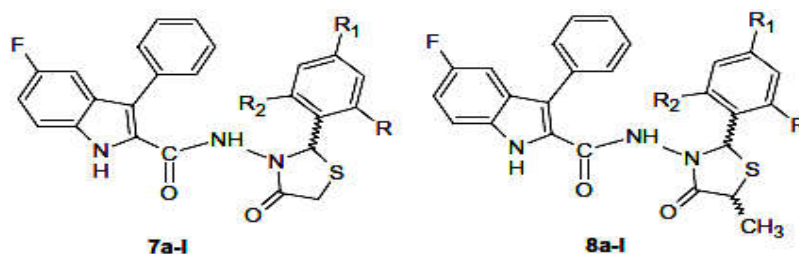


52. **Onen F E et al.,** <sup>120</sup> (2008) synthesized three series of compounds based on thiazolidine core which possess potent inhibitory action on thymidylate synthase X, and evaluated the catalytic activity of the enzyme.

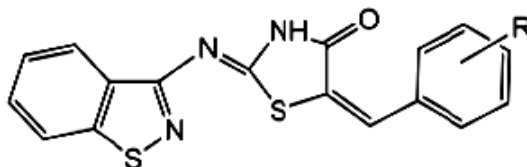


53. **Onen-Bayram F E et al.,** <sup>121</sup> (2012) developed a novel anticancer agent to activate apoptosis-induced cell death in cancer cell lines. They synthesized a novel thiazolidine compound and evaluated for their cytotoxicity to several human cancer cell lines.

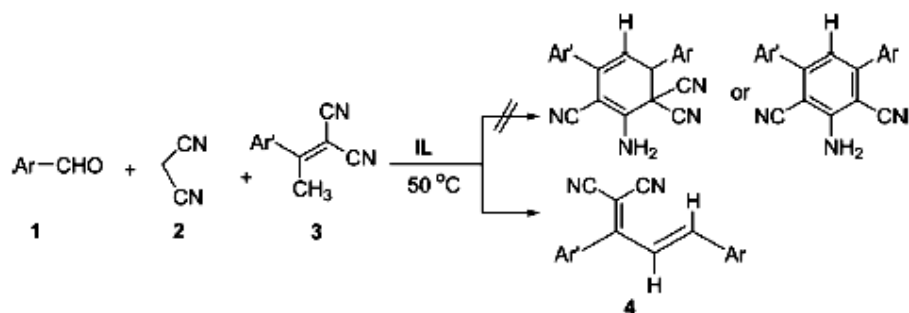
54. **Ustundag G C et al.,** <sup>122</sup> (2015) reported the synthesis of novel hydrazone and 4-thiazolidinone derivatives and evaluated them for *in-vitro* antitubercular activity against *Mycobacterium tuberculosis* H37Rv and anticancer activity against different human-derived cell lines. The results were found to be showing 99% inhibition at MIC values ranging from 6.25-25 $\mu$ g/ml for antitubercular activity. The anticancer activity for one compound was found to be active at sub-micromolar concentrations.



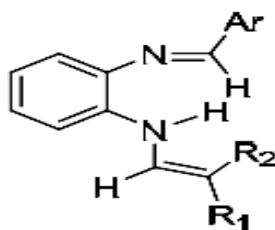
55. **Crasci L et al.,** <sup>123</sup> (2015) synthesized 2-Benzisothiazolylimino-5-benzylidene-4-thiazolidinones and the chondroprotective capability related to antioxidant activity and to inhibition of MMPs was studied by *in-vitro*, by determining nitric oxide production and glycosaminoglycan release.



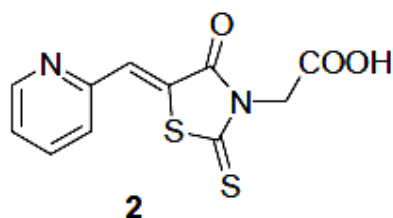
56. **Wang X S et al.,** <sup>124</sup> (2009) discovered a green and highly selective method for the synthesis of 2-((E)-1,3-diaryllallylidene)malononitriles in ionic liquid using 10 mol% malononitrile as catalyst.



57. **Química C et al.**,<sup>125</sup> (2009) reported that, the disubstituted *o*-phenylenediamine by reaction with substituted ethoxymethylene compounds and aromatic aldehydes were highly stable structure even under microwave irradiation.



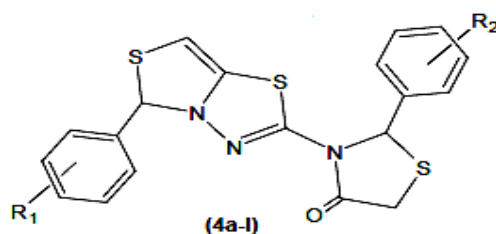
58. **Dolezel J et al.**,<sup>126</sup> (2009) synthesized rhodanine-3-acetic acid derivatives and its lipophilicity was analyzed using RP-HPLC method. The compounds were evaluated for antifungal effect against selected fungal species. Most compounds exhibited no activity, and only one compound strongly inhibited the growth of *Candida tropicalis* 156, *Candida krusei* E 28, *Candida glabrata* 20/I and *Trichosporon asahii* 1188.



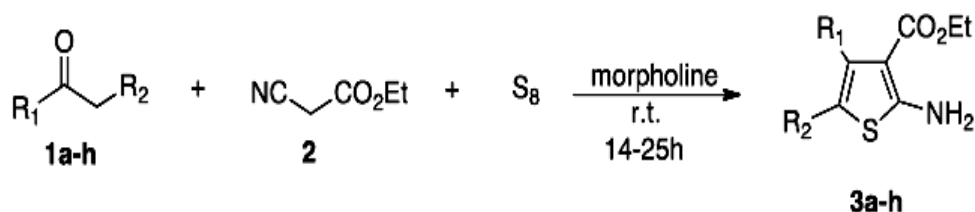
59. **Jain A K et al.**,<sup>127</sup> (2012) reviewed on the recent developments and biological activities of thiazolidinone derivatives.



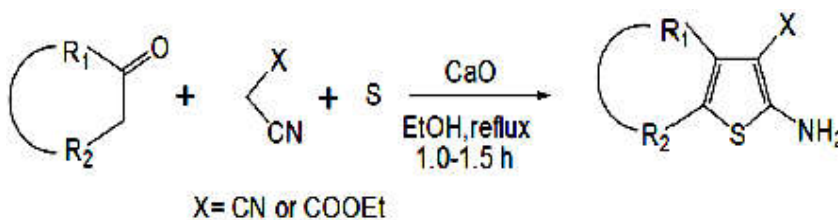
60. **Malipeddi H *et al.*,** <sup>128</sup> (2012) synthesized a series of twelve novel thiazolidinones by cyclocondensation of various Schiff base of amino thiadiazole with thioglycolic acid and the compounds were evaluated for *in vitro* antitubercular activity by Microplate alamar assay method showed that, two compounds showed higher antitubercular activity than standard drugs.



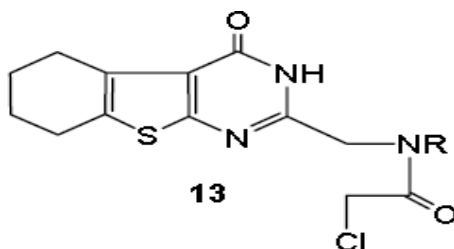
61. **Forero J S B *et al.*,** <sup>129</sup> (2011) reported a new set of green conditions in developing the preparation of tetra substituted 2-aminothiophene derivatives through the Gewald reaction between the respective ketones, ethyl cyanoacetate and elemental sulfur in the presence of morpholine.



62. **DurgaReddy G A N K *et al.*,** <sup>130</sup> (2013) reported a simple and efficient protocol for the synthesis of 2-aminothiophenes via Gewald reaction from ketones with an active nitrile or ethyl ester and elemental sulphur using CaO in ethanol under reflux in 1 to 1.5h.

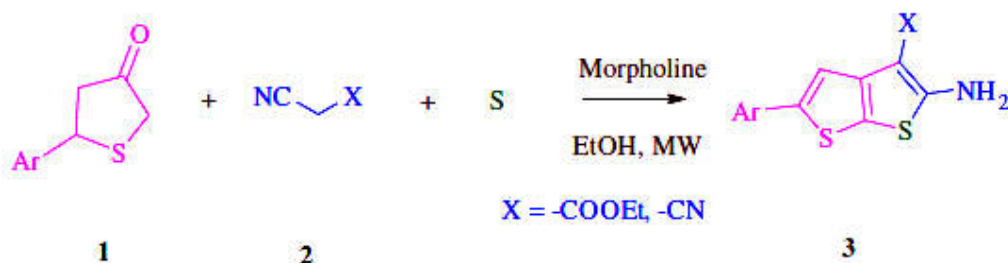


63. **Kanwar S *et al.***,<sup>131</sup> (2005) reported a facile and efficient method for the synthesis of 4-hexyl substituted  $\beta$ -lactams from substituted thienopyrimidinone.

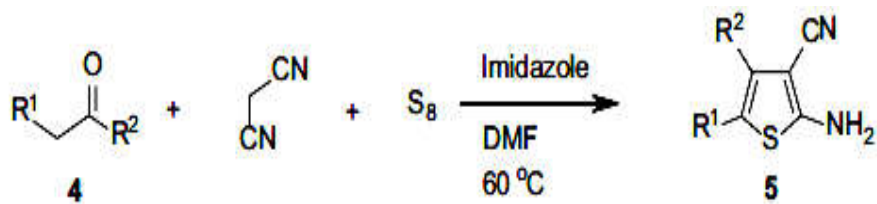


64. **Puterova Z *et al.***,<sup>132</sup> (2010) reviewed and summarized the synthetic strategies for substituted 2-aminothiophenes.

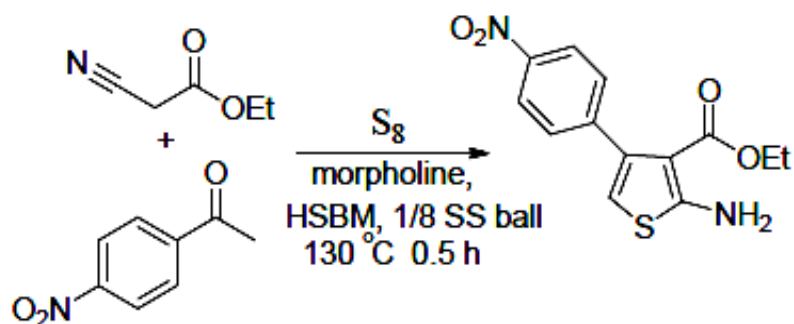
65. **Balamurugan K *et al.***,<sup>66</sup> (2009) synthesized regioselective novel series of 2-amino-5-arylthieno [2, 3-b]thiophenes via domino Gewald reaction-dehydrogenation sequence and evaluated for their *in vitro* activity against *Mycobacterium tuberculosis* H37Rv and MDR-TB. They concluded that, one compound was found to be more potent at MIC value of 1.1  $\mu$ M among the 12 compounds which was screened.



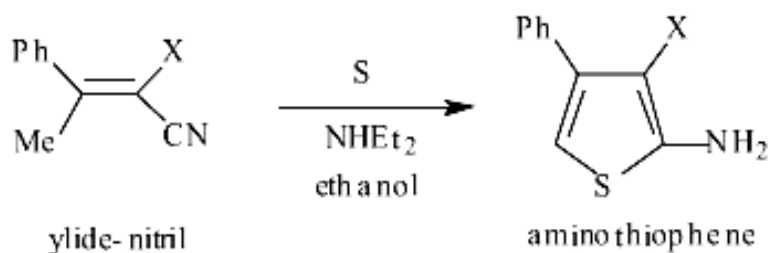
66. **Huang X-G *et al.***,<sup>133</sup> (2011) developed a simple and efficient procedure for the synthesis of multisubstituted 2-aminothiophene derivatives through the reaction of aldehydes, or ketones with dicyanomethane and elemental sulfur in DMF in the presence of catalytic amount of imidazole



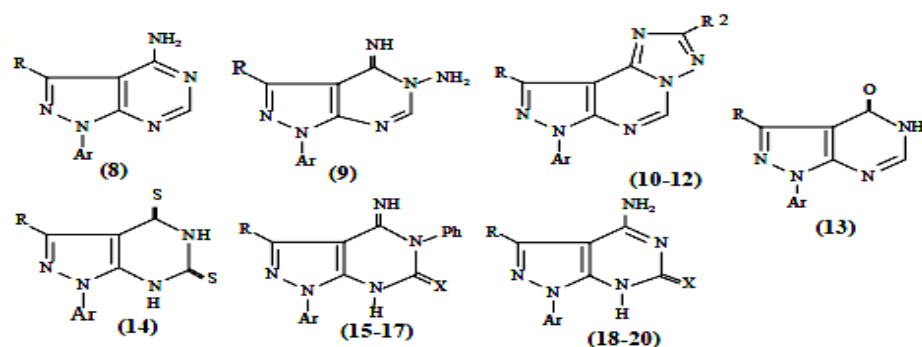
67. Shearose W C *et al.*,<sup>134</sup> (2014) reported the solvent-free synthesis of 2-aminothiophenes via the Gewald reaction, utilizing high speed ball milling conditions, heated in a conventional oven using catalytic base.



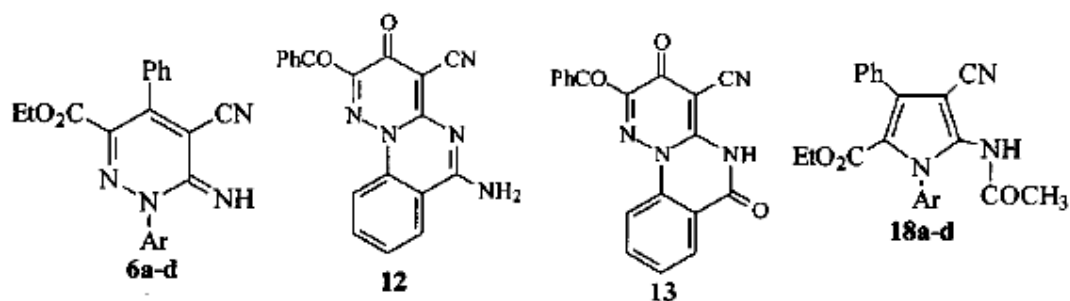
68. Tumer F *et al.*,<sup>135</sup> (2004) reported a facile synthesis of substituted-2-aminothiophenes via a stepwise Gewald reaction.



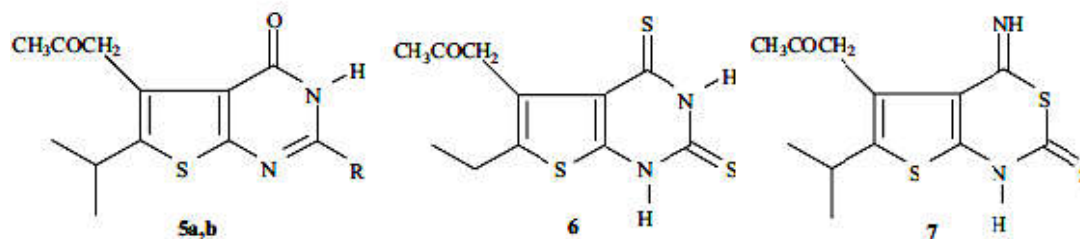
69. Al-Afaleq E I *et al.*,<sup>136</sup> (2001) reported the various methods for the synthesis of novel pyrazolo[3,4-d]pyrimidines with a pyridazine moiety at the 1-position.



70. Abdelrazek F M *et al.*,<sup>137</sup> (2001) reported a novel synthesis of some pyridazine, pyridazino[2,3-a]quinazoline and pyrrole derivatives.

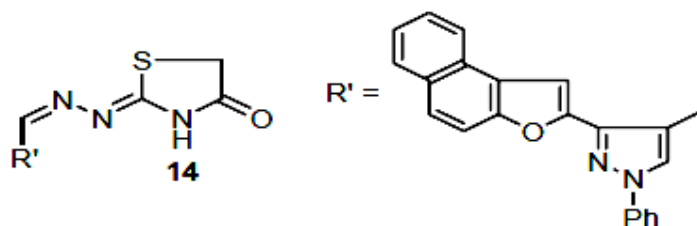


71. El-Gazzar ARBA *et al.*,<sup>67</sup> (2007) reported the synthesis of thieno [2, 3-d] pyrimidine derivatives and the compound evaluated for their anti-inflammatory, analgesic and ulcerogenic activities.

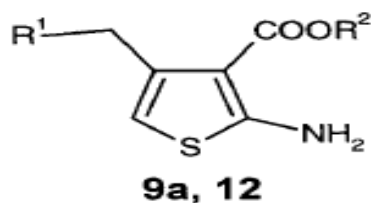


72. Abd El-Wahab A H F *et al.*,<sup>68</sup> (2011) reported the synthesis of some new naphtho[2,1-b]furan derivatives by Vilsmeier formylation reaction. The antimicrobial activities of these compounds were evaluated against Gram-positive, Gram-negative bacteria and fungi. They concluded that, one compound showed highest antibacterial

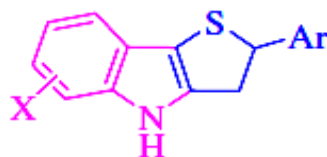
activity, while one compound showed moderate activity and the remaining compounds showed no activities against any of the test microorganisms.



73. **Buchstaller H P *et al.***,<sup>138</sup> (2001) synthesized a novel 2-aminothiophene 3-carboxylates using the two-step variations of the Gewald reaction, particularly of compounds exhibiting a functionalized alkyl group at position 4.

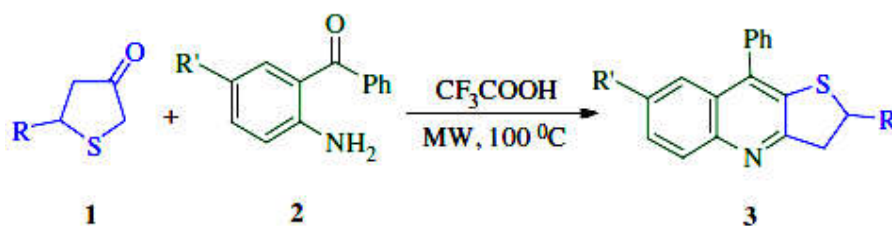


74. **EL-mahdy K M *et al.***,<sup>69</sup> (2013) reported the synthesis, characterization and biological evaluation of some new thieno[2,3-*d*]pyrimidine derivatives by using Vilsmeier-Haack reaction. The synthesized compounds were screened for their antimicrobial activity. The result suggested that, the synthesized compounds were found to be lower to mid active in antimicrobial screening.
75. **Karthikeyan S V *et al.***,<sup>70</sup> (2009) reported a microwave assisted facile, efficient and rapid regioselective Fischer indole synthesis of new 2-aryl-3,4-dihydro-2H-thieno[3,2-*b*]indoles in excellent yields under mild reaction conditions. It also displayed good *in-vitro* antimycobacterial activity against MTB and MDR-TB.

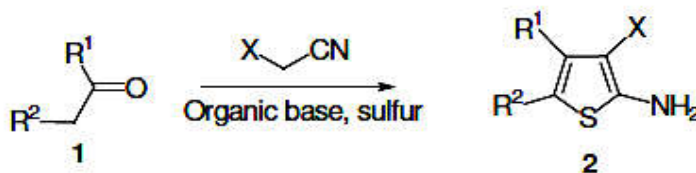


6

76. **Balamurugan K et al.**,<sup>71</sup> (2010) reported a facile, regioselective synthesis of 2,9-diaryl-2,3-dihydrothieno-[3,2b]quinolines by Friedlander annulations under microwave irradiation at 100°C. They were screened *in-vitro* antitubercular activity against *Mycobacterium tuberculosis* H37Rv and MDR-TB. They concluded that, two compounds were exhibited maximum activity among the 17 compounds which was screened.

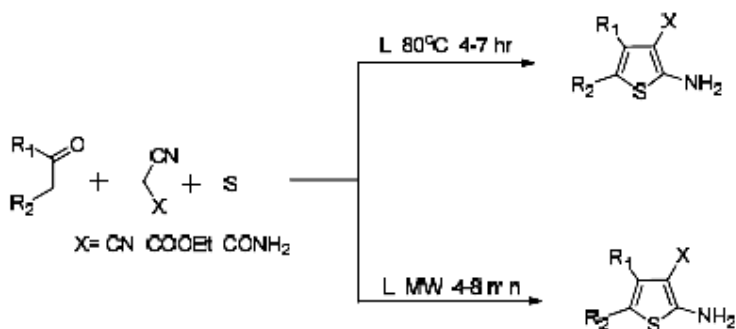


77. **Tormyshev V M et al.**,<sup>139</sup> synthesized 2-aminothiophene-3-carboxylate containing various aryl groups at the position-4 by one pot Gewald reaction of aryl alkyl ketones with ethyl cyanoacetate and elemental sulphur in the presence of morpholinium acetate and excess morpholine.

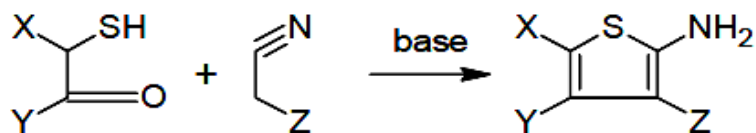


78. **Fleming F F *et al.***,<sup>140</sup> (2010) reported the efficacious roles of the nitrile pharmacophore in Nitrile-containing Pharmaceuticals. They were also reviewed the importance of aryl nitrile-containing pharmaceuticals,  $\alpha$ -aryl acetonitriles, alkenenitrile-containing pharmaceuticals, N-cyanoguanidine containing drugs,  $\alpha$ -amino nitrile drugs and drug leads.

79. **Chavan S S *et al.***,<sup>141</sup> (2012) developed a simple, rapid, and green one-pot process for the synthesis of 2-aminothiophenes via three-component Gewald reaction utilizing cost-effective guanidine based ionic liquid.



80. **Eller G A *et al.***,<sup>142</sup> (2006) reported a synthesis of novel 3-acetyl-2-aminothiophenes from cyanoacetone and 1,4-dithianyl-2,5-diols using a modified Gewald reaction.



### 2.3. Based on Pharmacology

81. **Fogel N.**,<sup>20</sup> (2015) reviewed about the history of tuberculosis, its epidemiology, transmission and diagnostic tools, its pathogenesis, its treatment regimen and its control. He also concluded about the importance of complete understanding of pathological immune responses and interactions in TB in the development of efficacious drugs and vaccines.

82. **Daniel T M.,** <sup>5</sup> (2006) reported a historical review of history of tuberculosis from ancient to mid 19<sup>th</sup> century. He also reviewed about the evaluation of drug and vaccine developments to eradicate TB.
83. **Awasthi D et al.,** <sup>143</sup> (2013) reported an extensive SAR study for the optimization of trisubstituted benzimidazoles as inhibitors of Mtb FtsZ for the development of novel antitubercular agents.
84. **Matviuk T et al.,** <sup>144</sup> (2013) reported the discovery, synthesis and screening of a series of 3-(9H-fluoren-9-yl)pyrrolidine-2,5-dione derivatives as a novel class of potent inhibitors of *Mycobacterium tuberculosis* H37Rv strain as well as the enoyl acyl carrier protein reductase (ENR) InhA.
85. **Gasse C et al.,** <sup>145</sup> (2008) synthesized a series of N<sup>1</sup>-(4-substituted-benzyl)-pyrimidines as potential inhibitors of thymidine monophosphate kinase of *Mycobacterium tuberculosis* (TMPKmt) and performed *in vitro* antimycobacterial activity. The activity of the compounds was found to be potent showing k values in  $\mu\text{M}$  range and MIC<sub>50</sub> of 50 $\mu\text{g/ml}$  against *M. bovis*. The study also concluded that, thymidine monophosphate kinase (TMPKmt) as available target for designing antimycobacterial drugs.
86. **Kogler M et al.,** <sup>146</sup> (2011) synthesized a series of 5-substituted 2-deoxyuridine monophosphate analogues and evaluated them for their potential, as inhibitors of mycobacterial ThyX, a novel flavin dependant thymidylate synthase in *Mycobacterium tuberculosis*.



87. **Vanheusden V et al.,** <sup>147</sup> (2004) reported the discovery of a novel class of bicyclic thymidine analogues as selective and high-affinity inhibitors of *Mycobacterium tuberculosis* thymidine monophosphate kinase.
88. **Daele I V et al.,** <sup>148</sup> (2007) reported the rational design and synthesis of a series of 5'-thiourea-substituted  $\alpha$ -thymidine analogues. The compounds were assayed for their inhibitory potency on *Mycobacterium bovis* var. BCG growth by *in vitro*.
89. **Familiar O et al.,** <sup>149</sup> (2010) reported the design, synthesis and inhibitory activity against *Mycobacterium tuberculosis* thymidine monophosphate kinase of acyclic nucleoside analogues with a distal imidazoquinolinone.
90. **Poecke S V et al.,** <sup>150</sup> (2011) reported a series of new 3'- and 5'-modified thymidine analogues including  $\alpha$ - and  $\beta$ -derivatives possess inhibitory action on *Mycobacterium tuberculosis* thymidine monophosphate kinase (TMPKmt).
91. **Li de la S et al.,** <sup>45</sup> (2001) deposited the coordinates of the *TMPK Mtb* binary complex in the RCSB Protein Databank with accession number 1G3U. They reported that this is an essential enzyme to be targeted for designing of inhibitors against *Mycobacterium tuberculosis*.
92. **Gokulan K et al.,** <sup>39</sup> (2003) reported that the *lysA* gene of *M. tuberculosis* H37Rv has been established as essential for bacterial survival in immunocompromised mice, demonstrating that *de novo* biosynthesis of lysine is essential for *in vivo* viability.

93. **Huang C C *et al.***,<sup>40</sup> (2003) reported that there are at least three mycolic acid cyclopropane synthases (PcaA, CmaA1, and CmaA2) that are responsible for these site-specific modifications of mycolic acids. They conclude that these structures provide a foundation for rational-drug design, which may lead to the development of new inhibitors effective against persistent bacteria.
94. **Lee C E *et al.***,<sup>42</sup> (2007) reported the crystal structure of TrpD, a metabolic enzyme essential for lung colonization by *Mycobacterium tuberculosis*, in complex with its substrate phosphoribosylpyrophosphate.
95. **Sampathkumar P *et al.***,<sup>43</sup> (2007) reported that the structure of the *Mycobacterium tuberculosis* flavin dependant thymidylate synthase (MtbThyX).
96. **Xin H *et al.***,<sup>44</sup> (2007) reported the inhibition of the *Mycobacterium tuberculosis* enoyl acyl carrier protein reductase InhA by arylamides.
97. **Scherr N *et al.***,<sup>46</sup> (2007) reported the structural basis for the specific inhibition of protein kinase G, a virulence factor of *Mycobacterium tuberculosis*.
98. **Tretter E M *et al.***,<sup>47</sup> (2012) reported the mechanisms for defining supercoiling set point of DNA Gyrase Orthologs.
99. **Erdemli S B *et al.***,<sup>48</sup> (2012) reported the structure and mechanism of L, D-Transpeptidase 2, targeting the cell wall of *Mycobacterium tuberculosis*.
100. **Card G *et al.***,<sup>41</sup> (2005) reported the crystal structure of Rv1347c, a putative antibiotic resistance protein from *Mycobacterium tuberculosis* and the crystal structure of Rv1347C was also determined by multiwavelength anomalous

diffraction phasing from selenomethionine-substituted protein and refined at 2.2 Å resolution

101. **Raman K *et al.***, <sup>151</sup> (2008) reported a comprehensive *in silico* target identification pipeline, targetTB, for *Mycobacterium tuberculosis*.
102. **OECD Guidelines 423** <sup>152</sup> (2001) the test procedure deals with the guidelines for the testing of chemicals on animals to estimate the acute oral toxicity.
103. **Cheptea C *et al.***, <sup>153</sup> (2012) reported the synthesis and evaluation of acute toxicity and anti-tumour activity of thiazolidine-2, 3-disubstituted derivatives of 1'-acetamidyl-5'-nitro indazole.
104. **Pahari N *et al.***, <sup>154</sup> (2010) reported the synthesis of novel indole derivative from istatin and to evaluate its acute toxicity studies to estimate its safety dose level and evaluate its analgesic activity.
105. **Bhaumik A *et al.***, <sup>155</sup> (2014) reported the synthesis, characterization and evaluation of anticonvulsant activity of some novel 4-thiazolidinone derivatives using MES induced convulsions in mice.
106. **Kumar K K *et al.***, <sup>156</sup> (2011) reported the synthesis of quinoline coupled [1, 2, 3]-triazoles as a promising class of anti-tuberculosis agents by Luciferase Reporter Phage (LRP) assay.
107. **Collins L A *et al.***, <sup>157</sup> (1997) reported the high-throughput screening of compounds against *Mycobacterium tuberculosis* and *Mycobacterium avium* using Microplate Alamar Blue Assay (MABA) and compared with BACTEC 460 Assay System.

108. **Juan-Carlos P *et al.***, <sup>158</sup> (2002) reported a method for detecting multidrug-resistant *Mycobacterium tuberculosis* by using Resazurin Microtiter Assay Plate method (REMA).
109. **Cappoen D *et al.***, <sup>159</sup> (2014) reported a library of substituted 1,3-diaryltriazenes based on the acting component of the anti-trypanosomal drug, diminazene aceturate and evaluated for its potential as anti-tubercular agent.
110. **Prithwiraj D *et al.***, <sup>160</sup> (2011) reported the synthesis and SAR of a series of new cinnamic derivatives. They also concluded that, many compounds exhibited submicromolar minimum inhibitory concentrations against *Mycobacterium tuberculosis* strain (H37Rv).
111. **Ferreira M L *et al.***, <sup>161</sup> (2009) synthesized six Schiff base derivatives of D-mannitol, and evaluated for their *in vitro* antibacterial activity against *Mycobacterium tuberculosis* H37Rv using the Alamar Blue susceptibility test.
112. **Eldehna W M *et al.***, <sup>162</sup> (2015) synthesized three series of nicotinic acid hydrazides and evaluated for their potential *in vitro* antimycobacterial activity against *M. tuberculosis*.
113. **Primm T P *et al.***, <sup>163</sup> (2007) reviewed the recent advances in methodology and discussed the common issues in screening with mycobacteria, and consider potential future developments in the discovery of antimycobacterial drugs.
114. **Nagesh H N *et al.***, <sup>164</sup> (2013) designed and synthesized a series of nineteen new 6-(4-((substituted-1H-1,2,3-triazol-4-yl)methyl)piperazin-1-yl)phenanthridine

analogues and evaluated for their anti-tubercular activity against *Mycobacterium tuberculosis* H37Rv.

115. **Dutta N K *et al.***,<sup>165</sup> (2004) studied the *in vivo* potency of the non-steroidal anti-inflammatory drug diclofenac sodium against drug sensitive and drug resistant clinical isolates of *Mycobacterium tuberculosis*.

116. **Manna K *et al.***,<sup>166</sup> (2011) reported the synthesis, *in vitro* and *in vivo* antitubercular activity of indophenazine 1, 3, 5-trisubstituted pyrazoline derivatives bearing benzofuran nucleus.

117. **Hearn M J *et al.***,<sup>167</sup> (2009) reported the synthesis, *in vitro* and *in vivo* efficacy of some novel Schiff bases of isoniazid.

118. **Tyagi S *et al.***,<sup>168</sup> (2015) hypothesized that clofazimine shorten the duration of treatment for drug-susceptible TB of the first-line treatment regimen for experimental chemotherapy of tuberculosis.

119. **Sriram D *et al.***,<sup>169</sup> (2005) synthesized various 7-substituted ciprofloxacin derivatives and evaluated for antimycobacterial activity *in vitro* and *in vivo* against *Mycobacterium tuberculosis* and for inhibition of the super coiling activity of DNA gyrase from *Mycobacterium smegmatis*.

120. **Sriram D *et al.***,<sup>170</sup> (2005) synthesized various isoniazid derivatives by introducing the isoniazid pharmacophore into several molecules and screening for antimycobacterial activity.

## **2.4. Conclusion**

From the literature survey, various *in-silico* approaches have been reviewed in a detailed manner, which includes virtual screening like molecular docking studies, docking with multiple targets, pharmacophore modeling, homology modeling, molecular dynamic simulation studies, importance of *in-silico* toxicity assessment and *in-silico* ADME predictions.

In continuation, a detailed survey based on the importance of the heterocyclics in drug discovery was reviewed. The various synthetic strategies, including the challenges involved in the synthesis of heterocyclics were studied.

In pharmacological aspect, the importance of drug discovery against tuberculosis was witnessed. Further different types of critical targets available for *Mycobacterium tuberculosis* were studied. Finally different types of in-vitro and in-vivo screening methods available for the anti-tuberculosis activity was reviewed.

Overall, from the literature survey a research framework has been established in order to identify some potential lead molecules against *Mycobacterium tuberculosis*.

## CHAPTER 3

### RESEARCH ENVISAGED AND PLAN OF WORK

#### *3.1. Objective of the Present Study*

The literature survey reveals the significance of the research in the area of the development of new drugs for tuberculosis, capable of overcoming MDR and XDR-TB. The survey also indicates the importance of the small organic molecules which possess the heterocyclic nucleus such as thiazolidinones and some fused ring systems like thieno-pyrimidines, thieno-pyridines, thieno-thiazines and benzo-thiophenes as a core active moiety/pharmacophore. Considerable attention has been focused on these heterocyclic ring systems as they were reported to possess various biological activities such as tuberculostatic, anti-cancer, anti-tumour, hypoglycemic, anti-inflammatory, analgesic, anti-bacterial, antifungal, anticoagulant and antioxidant activities.

Thus the study directly aims to design and synthesize some heterocyclic analogues such as thiazolidinones and some fused ring systems like thieno-pyrimidines, thieno-pyridines, thieno-thiazines and benzo-thiophenes, which will prove to be effective against *Mycobacterium tuberculosis*.

### 3.2. Work Flow

- Based upon the review of literature, small heterocyclic nucleus such as thiazolidinones and some fused ring systems like thieno-pyrimidines, thienopyridines, thieno-thiazines, benzo-thiophenes were selected for computational design.
- An *in-house* chemical library comprising more than 2400 sketched molecules based upon the above selected heterocyclic nucleus was created.
- All the sketched molecules were subjected to preliminary docking (“Standard Precision Mode for reliably docking tens to hundreds of thousands of ligand with high accuracy”) against the pathophysiological target of *M. tuberculosis*.
- Based on the preliminary docking results, top 100 molecules with diverse heterocyclic nucleus were selected and further subjected to advanced docking (“XP-extra precision mode where further elimination of false positives is accomplished by more extensive sampling and advanced scoring, resulting in even higher enrichment”) against the same pathophysiological target of *M. tuberculosis*.
- Those 100 molecules were also subjected to *in silico* toxicity assessment and *in silico* Absorption, Distribution, Metabolism and Excretion (ADME) prediction.
- On the basis of XP mode docking results, *in silico* toxicity data, *in silico* ADME data and synthetic feasibility, top 30 molecules were considered for synthesis.
- The designed molecules were synthesized by using various organic synthetic reactions.



- Purification of the synthesized compounds was carried out by recrystallization.
- The purity of the synthesized compounds was confirmed by sharp melting points and Thin Layer Chromatography (TLC).
- Characterization of the synthesized compounds was done by spectral studies. X-ray crystallographic study for one of the synthetic derivative was performed.
- All the compounds were subjected to *in-vitro* anti-tubercular activity.
- Based upon the *in-vitro* results, synthesized compounds were further docked against multiple pathophysiological target enzymes of *M. tuberculosis* in order to validate the software and to correlate the *in-vitro* anti-tubercular results with the docking results and to find out the plausible mechanism by which the compounds would have exhibited the activity.
- Molecular Dynamic Simulation study was performed for the top three ranked ligands (based on *in-vitro* data), with its top scored receptor complex (based on the multiple docking study) in order to find out the stability of ligand-receptor complex.
- All the synthesized compounds which shows promising *in-vitro* antimycobacterial activity were subjected to acute toxicity studies in order to find out the toxicity induced mortality and other behavioral changes.
- Based upon the acute toxicity results, *in-vitro* anti-tubercular activity rankings with the support of multiple molecular docking studies including molecular dynamic simulation studies, top 3 compounds were selected and subjected for the *in-vivo* antitubercular activity.

# CHAPTER 4

## *In-Silico* Approach

### 5.1. *Materials*

- *In-house* chemical library comprising more than 2400 molecules based on heterocyclic nucleus thiazolidinones and some fused ring systems like thienopyrimidines, thienopyridines, thienothiazines, benzo-thiophenes was created by sketching the molecules using ChemDraw<sup>®</sup> Ultra, Version 8.0, April 23, 2003, CambridgeSoft Corporation, USA.
- The target enzyme InhA, “the enoyl acyl carrier protein reductase” (ENR) from *Mycobacterium tuberculosis*, is one of the key enzymes involved in the type II fatty acid biosynthesis, which is critical for the survival and growth of *Mycobacterium tuberculosis*. This target enzyme was selected from the *in-silico* target identification pipeline for *Mycobacterium tuberculosis* which comprises a total of 451 high-confidence targets. The crystal structure of the enzyme was downloaded from the Protein Data Bank (“An Information Portal to Biological Macromolecular Structures”) (PDB id – 2NSD).
- Other *Mtb* target enzymes used in the study such as Diaminopimelate Decarboxylase (PDB id – 1HKV), Cyclopropane Synthase (PDB id – 1L1E), Antibiotic Resistance Protein (PDB id – 1YK3), TrpD essential for lung colonization (PDB id – 1ZVW), Thymidylate Synthase X (PDB id – 2AF6), Thymidylate Kinase (PDB id – 1G3U), Protein Kinase G (PDB id – 2PZI), Gyrase TypeIIA Topoisomerase (PDB id – 3UC1), L, D Transpeptidase 2 (PDB id – 3VAE) were also downloaded from Protein Data Bank.

- All the ligands were prepared by using “LigPrep” v-2.5 (Schrodinger<sup>®</sup>) software to generate the low energy 3D conformers of the ligands.
- The protein was prepared using “Protein Preparation Wizard” from the Workflows of “Maestro” v-9.3.515 (Schrodinger<sup>®</sup>) platform.
- The binding sites (active sites) were analysed using “SiteMap” v-2.6 (Schrodinger<sup>®</sup>) software.
- Molecular docking was carried out using “Glide” v-5.8 (“Grid-Based Ligand Docking with Energies”) (Schrodinger<sup>®</sup>) software.
- *In-silico* ADME properties were predicted using “QikProp” v-3.5 (Schrodinger<sup>®</sup>) software.
- *In-silico* toxicity Assessment was performed using OSIRIS<sup>®</sup> Online Tool.
- Molecular Dynamic Studies were carried out using “Desmond” v-3.1 (Schrodinger<sup>®</sup>) software.
- All the computational works expecting *in-silico* toxicity assessments were performed by using “Maestro” v-9.3.515 (Schrodinger<sup>®</sup>) platform.

## **5.2. Experimental**

### **5.2.1. Molecular Docking**

#### ***Ligand Preparation***

All the ligands from *in-house* chemical library were built using “Maestro build panel”. They were prepared by using “LigPrep” v-2.5 (Schrodinger<sup>®</sup>) which uses “OPLS\_2005 (Optimized Potential for Liquid Simulation) force field and gave the

corresponding low energy 3D conformers of the ligands”. The ligand preparation involves the following tasks.

- Addition of hydrogen atoms.
- Neutralization of charged groups, then generation of ionization and tautomeric states with Epik.
- Generation of stereoisomers, particularly if stereochemical information is missing.
- Generation of low-energy ring conformations.
- Removal of any badly prepared structures.
- Optimization of the geometries.

In general, “LigPrep converts simple 2D structures to 3D structures by including tautomeric, stereochemical, and ionization variations, as well as energy minimization and flexible filters to generate fully customized ligand libraries that are optimized for further computational analyses”.<sup>102</sup>

### ***Protein Preparation***

The crystal structure of target enzyme InhA, “the enoyl acyl carrier protein reductase (ENR)” from *Mycobacterium tuberculosis* was downloaded from the Protein Data Bank (PDB id – 2NSD) and was prepared using “Protein Preparation Wizard” panel from the Workflows of Maestro.

In this course of action, the downloaded protein was processed in various aspects in order to make the protein perfect for docking. Initially, the protein was preprocessed with the aligning of the ionization and tautomeric states. Missing side chains and loops were also reoriented and corrected. Then all the water molecules were removed except the water molecules those coordinated to metals/bridged. Hydrogen

atoms were added and the geometry of all the hetero groups was corrected. Further, optimization of the hydrogen bond network was carried out using Hydrogen Bonds Assignment tool. Finally, with the default constraints (0.3 Å of RMSD and the OPLS\_2005 force field), energy minimization was carried out using Restrained Minimization tool.<sup>102</sup>

### ***Binding Site Analysis***

The active binding sites were searched by using SiteMap Version 2.6 (Schrodinger®). “SiteMap assigns numerical descriptors to evaluate the predicted binding sites by a series of physical parameters such as size, degree of enclosure/exposure, tightness, hydrophobic/hydrophilic character, and hydrogen bonding possibilities. An average of these measurements helps prioritize possible binding sites”.<sup>101</sup>

In this task, the prepared protein was subjected to binding site analysis with the default parameter settings to identify top-ranked potential receptor binding sites. Based on the SiteScore, one receptor binding site was chosen for docking.

### ***Receptor Grid Generation***

The prepared protein with its top ranked binding site was placed in the workspace and the receptor grid generation was done by using the Receptor Grid Generation panel. The grid was defined and represented by adjusting the size and position of the active site in order to accommodate the ligands for docking using the default box size (20×20×20Å<sup>3</sup>). Rotatable hydroxyl groups in the active site were picked and no constraints were selected. Other parameters were set by default.<sup>98</sup>

### ***Molecular docking***

Molecular docking is a process to find the best pose from the series of poses of ligand binding to the active site of the protein using a scoring method. The GLIDE software (version 5.8) provided by Schrödinger<sup>®</sup>, LLC suite offers three docking procedures viz., High throughput virtual screening (HTVS), Standard precision (SP) docking and Extra precision (XP) docking.

“Glide offers the full range of speed vs. accuracy options from the HTVS (high-throughput virtual screening) mode for efficiently enriching million compound libraries, to the SP (standard precision) mode for reliably docking tens to hundreds of thousands of ligand with high accuracy, to the XP (extra precision) mode where further elimination of false positives is accomplished by more extensive sampling and advanced scoring, resulting in even higher enrichment”.

### ***Glide docking***

Glide docking was performed by using the Ligand Docking panel. Initially the precision was set to Standard precision (SP) mode in order to rank the top 100 ligands from 2400 *in house* library ligands, which comprises diverse heterocyclic molecules based on thiazolidinones and some fused ring systems like thieno-pyrimidines, thienopyridines, benzo-thiophenes. For this, all the 2400 prepared ligands were generated as a single LigPrep out file. The docking task was performed by specifying the receptor grid base in the *receptor grid tool* and LigPrep out file in the *Ligands to be Docked* tool. With the other default parameter settings the Glide docking in Standard precision (SP) mode was performed. The best docking pose for every ligand was visualized by importing Pose viewer files after docking. Based upon the glide score, top 100 molecules were selected.

Further, docking for those 100 molecules was performed with the same receptor grid and those 100 molecules were selected from the *Project table* panel as selected entries. Docking precision mode was set to Extra precision (XP) mode. While setting Extra precision (XP) mode, *writing XP descriptors information* was checked in the docking tool. The G-Score and the energy minimized docking poses for all the ligands were analysed.<sup>97</sup>

### **5.2.2. *In-silico toxicity Assessment***

*In-silico* toxicity Assessment for those 100 molecules resulted from Standard Precision (SP) mode were predicted by using OSIRIS<sup>®</sup>, an JAVA based online tool. The tool predicts toxicity related parameters such as Mutagenicity, Tumorigenicity, Skin Irritancy and the Effects on Reproduction. The prediction is based on the fragment contribution group present in the structure of the molecule.

On accessing the OSIRIS Property Explorer, which is a JAVA applet, allows us to draw chemical structures. On drawing the chemical structures the toxicity risk parameters are calculated on-the-fly whenever a structure is valid. Prediction results are valued and color coded. Properties with high risks of undesired effects are shown in **red color**. Whereas a **green color** indicates **drug-conform** behaviour.<sup>78</sup>

### **5.2.3. *In-silico ADME predictions***

The ADMET properties of those 100 molecules were performed using QikProp program. The software program predicts the physically significant descriptors and pharmaceutically relevant properties such as “octanol/water log P, log S for aqueous solubility, log BB for brain/blood, Number of primary metabolites, CNS activity, % human oral absorption in GI, log K<sub>hsa</sub> for serum protein binding and log IC<sub>50</sub> for HERG K<sup>+</sup> Channel blockage, log K<sub>p</sub> for predicted skin permeability, Lipinski’s rule of

five violations and Jorgenson's rule of three violations". For this task, those top 100 LipPrep ligand molecules which resulted from Standard precision (SP) mode docking, were selected from the *Project table* panel as selected entries and were given as a source in *QikProp* panel. The obtained predicted properties were analysed.<sup>75</sup>

### **5.3. Results and Discussions**

The energy minimized 3D structures of 2400 ligand molecules were docked against InhA, the enoyl acyl carrier protein reductase (PDB ID-2NSD) in a standard precision mode (SP). The docking score of all the ligand molecules were found to be in the range of -1.2 to -12.6 kcal/mol. Based upon the docking score top 100 molecules with diverse heterocyclic nucleus were taken for Extra precision (XP) docking against the same target enzyme (PDB ID-2NSD).

The best docking pose of all the 100 ligand molecules were analyzed and various XP descriptors were reviewed. The docking scores/G-scores for 100 ligand molecules in XP mode docking ranges from -4.6 to -12.6 kcal/mol.

*In-silico* ADME property predictions of those 100 ligand molecules were analyzed for any violations in the range of critical parameters such as "CNS activity (CNS), total solvent accessible surface area (SASA), octanol/ water partition coefficient (QPlogPo/w), IC<sub>50</sub> value for blockage of HERG K<sup>+</sup> channels (QPlogHERG), brain blood partition co-efficient (QPlogBB), binding human serum albumin (QPlogKhsa), human oral absorption (PercentHumanOralAbsorption), violations of Lipinski's rule of five (RuleOfFive)". Some of the ligand molecules showed violations, while the majority of the ligand molecules were found to be within the range of recommended values for 95% of known drugs.



The *in-silico* toxicity assessment of those 100 ligand molecules gave better insights in the selection of the molecules for the synthesis. More than one third of the ligand molecules were found to be mutagenic in *in-silico* toxicity assessment. Some ligand molecules were found to have mutagenic and tumorigenic risk alerts, while some ligand molecules showed all the four toxicity risk alerts (ie), mutagenic, tumorigenic, skin irritancy and reproductive effect which were considered to be highly toxic based upon *in-silico* approach.

All those 100 ligand molecules were analyzed for their synthetic feasibility based upon their synthetic route, chemicals and reagents, green techniques and compound stability.

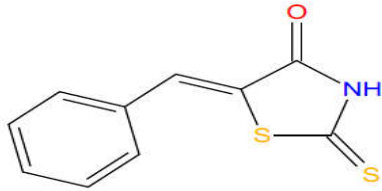
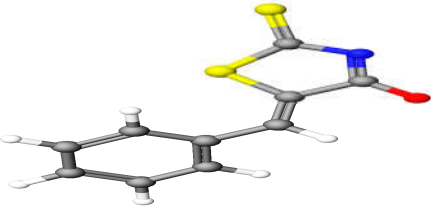
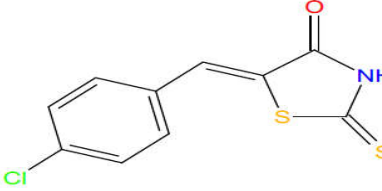
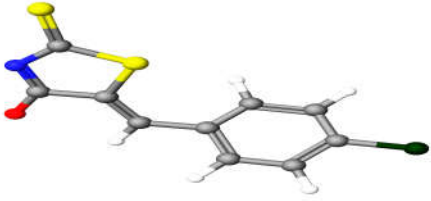
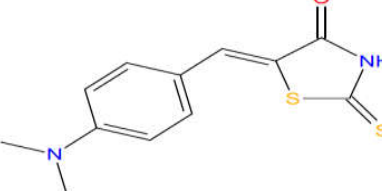
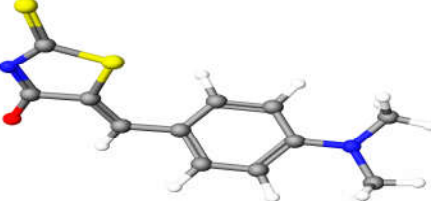
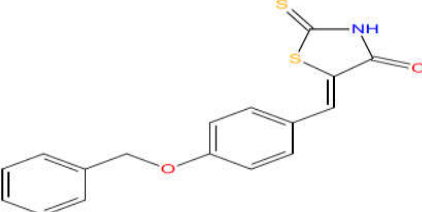
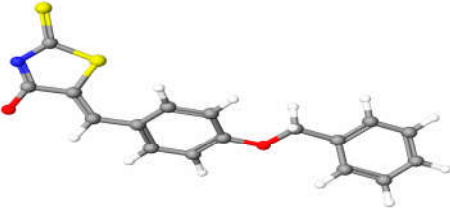
On considerations from the above *in-silico* approaches (molecular docking, *in-silico* toxicity assessment, *in-silico* ADME predictions) and synthetic feasibility, 30 ligand molecules with diverse heterocyclic nucleus were selected for the synthesis.

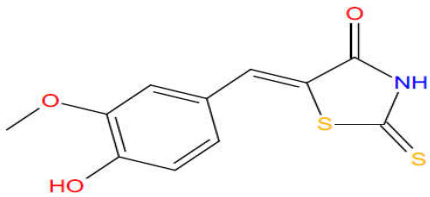
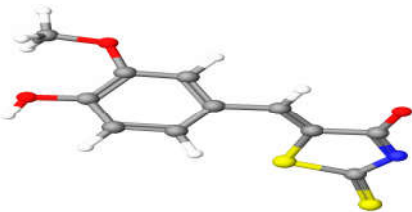
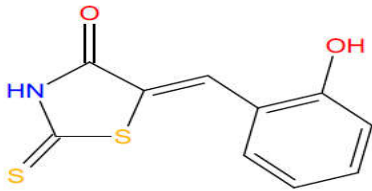
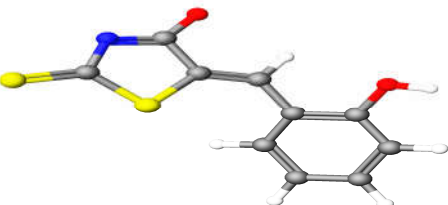
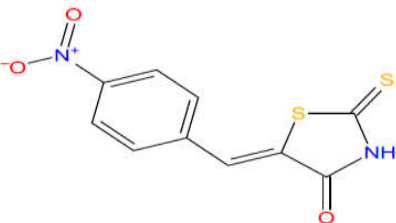
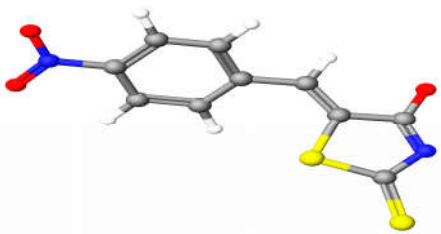
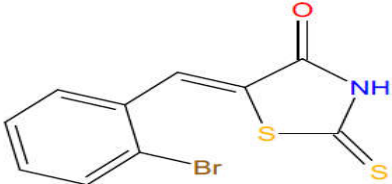
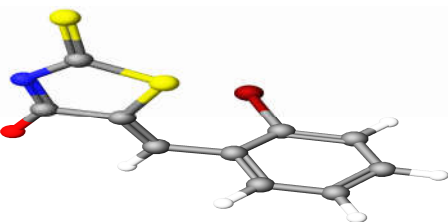
The ligand molecules selected for the synthesis are

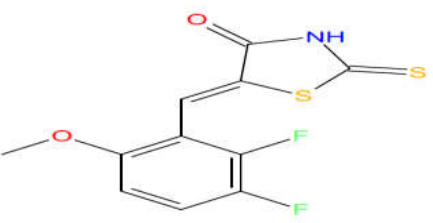

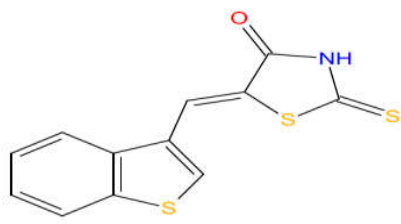
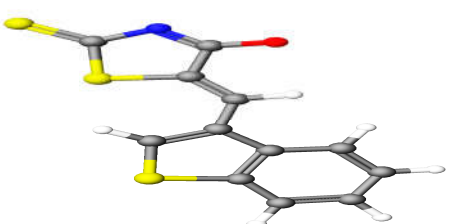
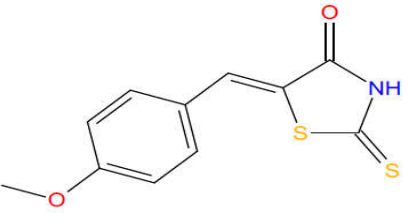

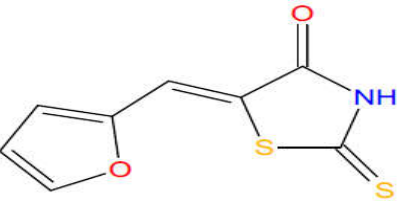
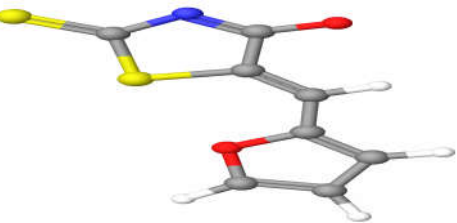
- 20 thiazolidinone analogues and
- 10 dioxolan based analogues comprising thieno-pyrimidine core (4 ligand molecules), thieno-pyridine core (2 ligand molecules), thieno-thiazine core (1 ligand molecule) and dihydro benzo-thiophene (3 ligand molecules).

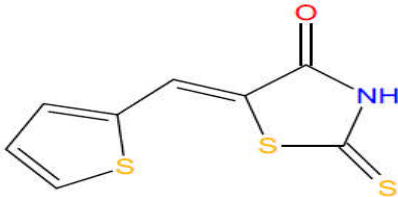
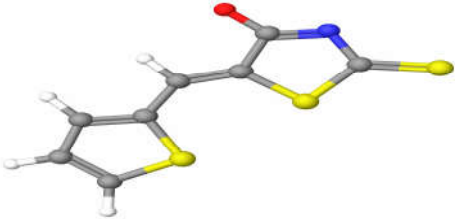
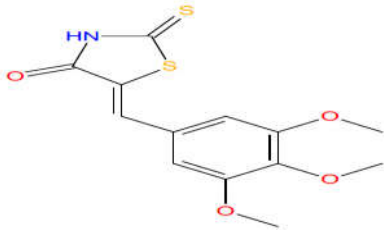

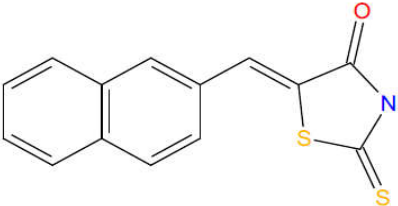
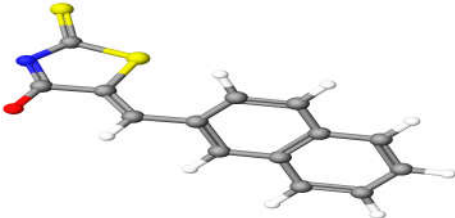
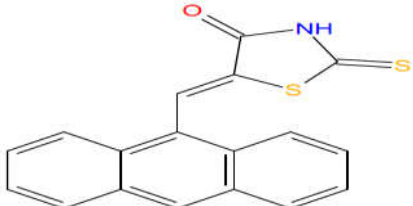
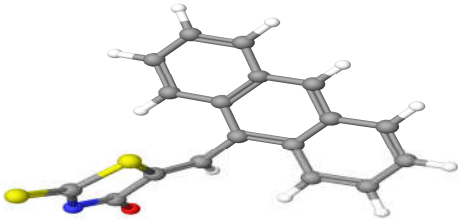
The 2D and energy minimized 3D structures of the selected molecules are shown in **Table 1**. 20 thiazolidinone analogues were re-coded as N1 to N20 for convenience. Other 10 compounds were retained with their same codes as used in the initial study.

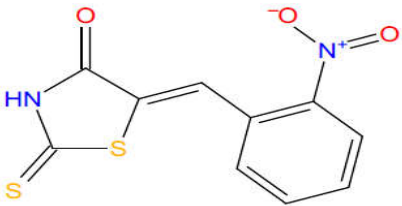
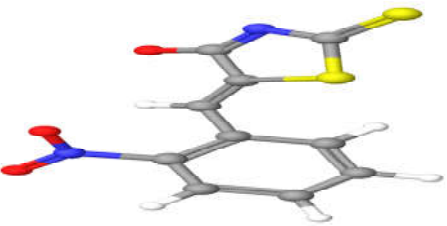
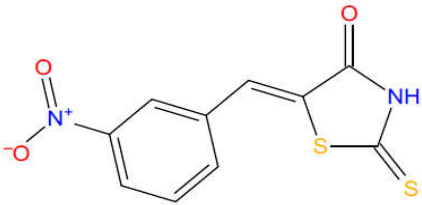
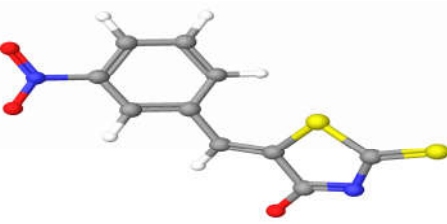
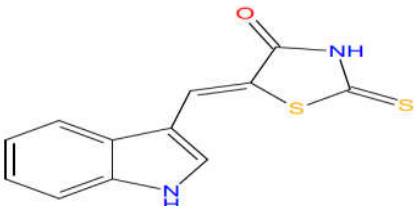
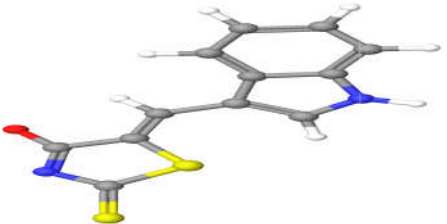
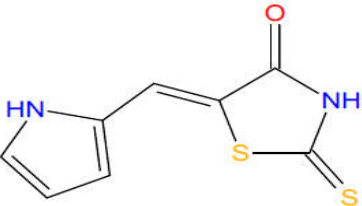
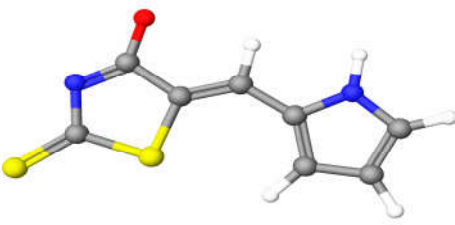
**Table 1: 2D and energy minimized 3D structures of the selected molecules**

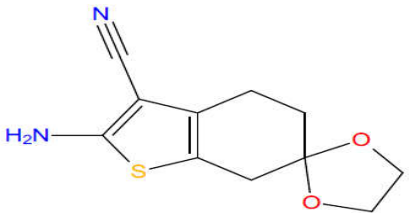

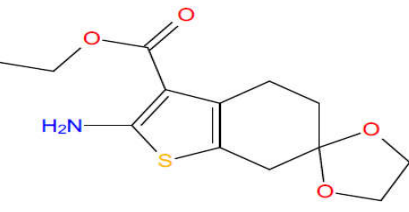
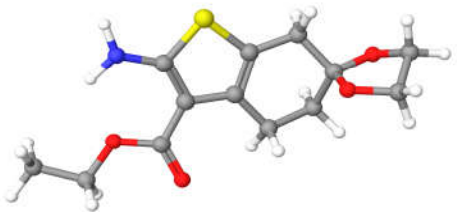
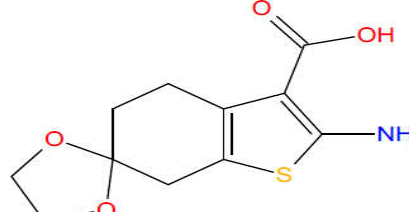
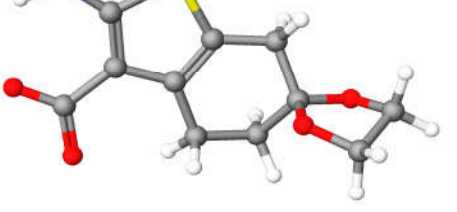
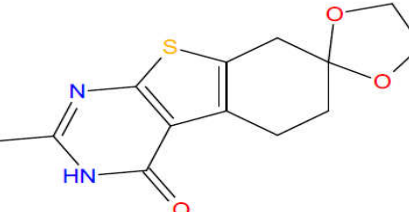

Ligand code	2D structure	Energy minimized 3D structure
N1		
N2		
N3		
N4		

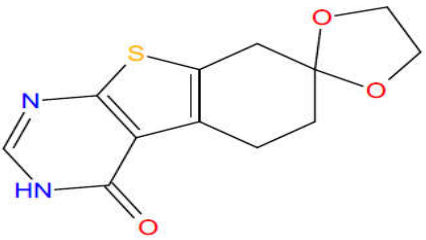
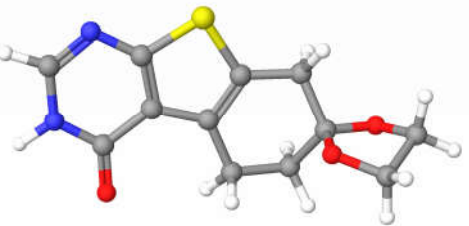
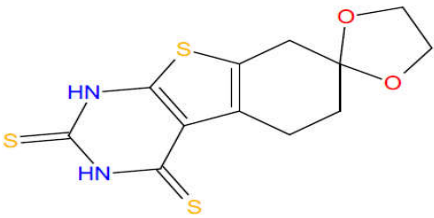
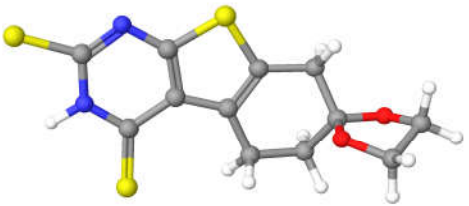
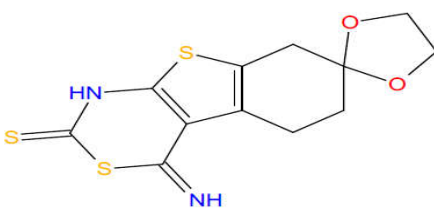
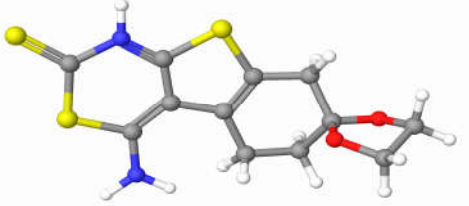
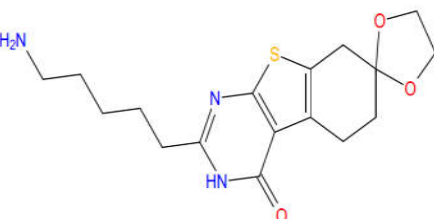
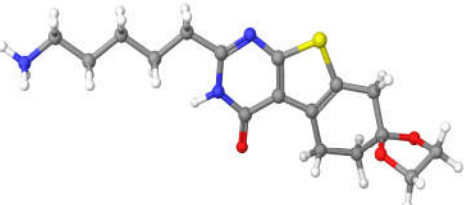
N5		
N6		
N7		
N8		

N9		
N10		
N11		
N12		

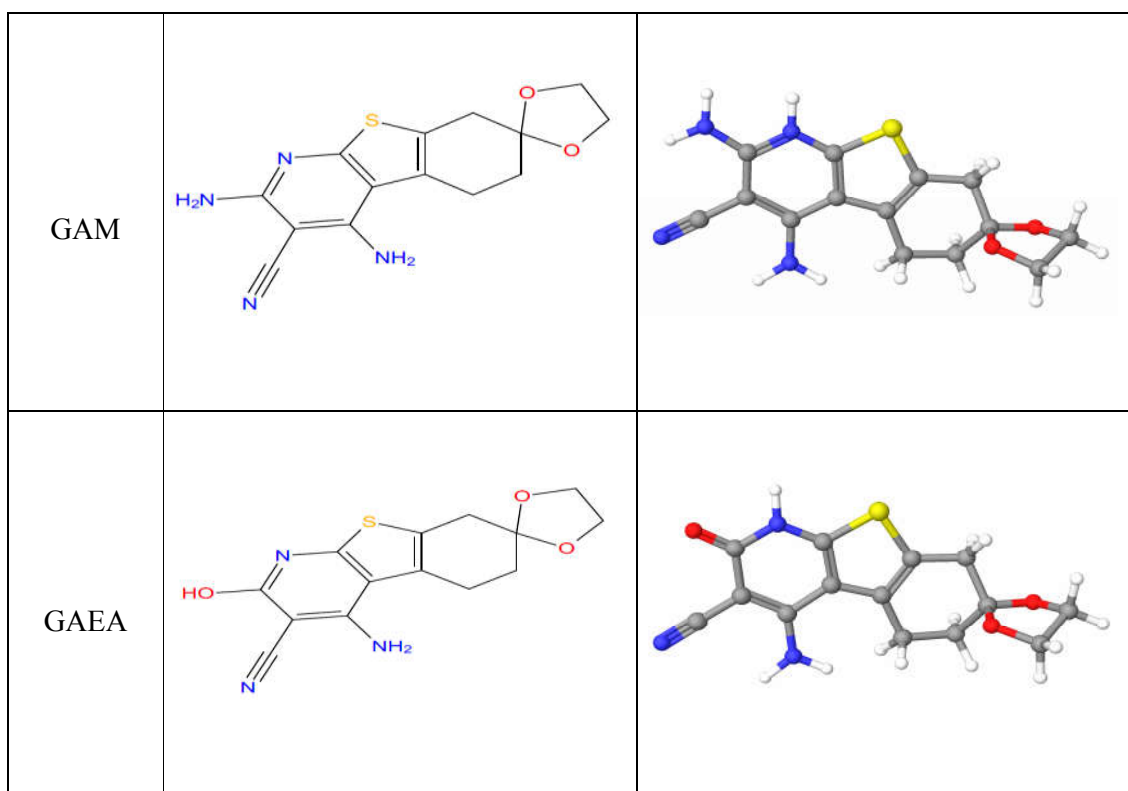
N13		
N14		
N15		
N16		

N17		
N18		
N19		
N20		

GA		
GAE		
GAT		
GAC		

GAC1		
GAC5		
GAC6		
GAC7		





### Rationality for selecting the above 30 ligand molecules for the synthesis

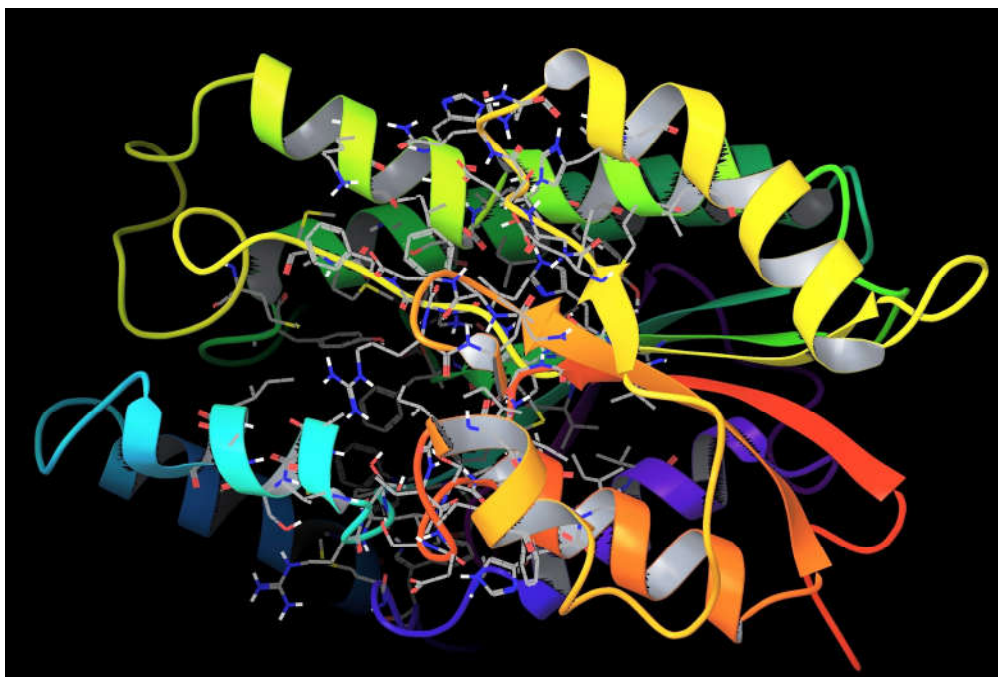
- Initially the selection was made based upon the best docking score/ G-score.
- The ligand molecules with less/no synthetic feasibility were omitted.
- The ligand molecules with good G-score and/or with some violations in *in-silico* ADME predictions and/or with higher level of toxicity in *in-silico* toxicity were omitted.
- Thus, the ligand molecules with considerable G-score, synthetic feasibility and with no violation in *in-silico* ADME predictions were considered to be the good criteria for selection. In case of *in-silico* toxicity assessment 27 ligand molecules were found to have no toxicity issues with the above criteria.

- In case of other 3 ligand molecules, one ligand molecule predicted to be mutagenic, one ligand molecule to be mutagenic and tumorigenic and one ligand molecule to be mutagenic, tumorigenic and irritant with the above selection criteria.
- The rationality behind the selection of those 3 ligand molecules was because of the low to moderate toxicity risk alert when compared to the rest of the ligand molecules which have all the four toxicity risk alerts with either good G-score or ADME profile. If those 3 ligand molecules were found to be having expected *in vitro* and *in vivo* antimycobacterial activity, structural fragment alteration would be considered for the predicted/ expected toxicity issues.

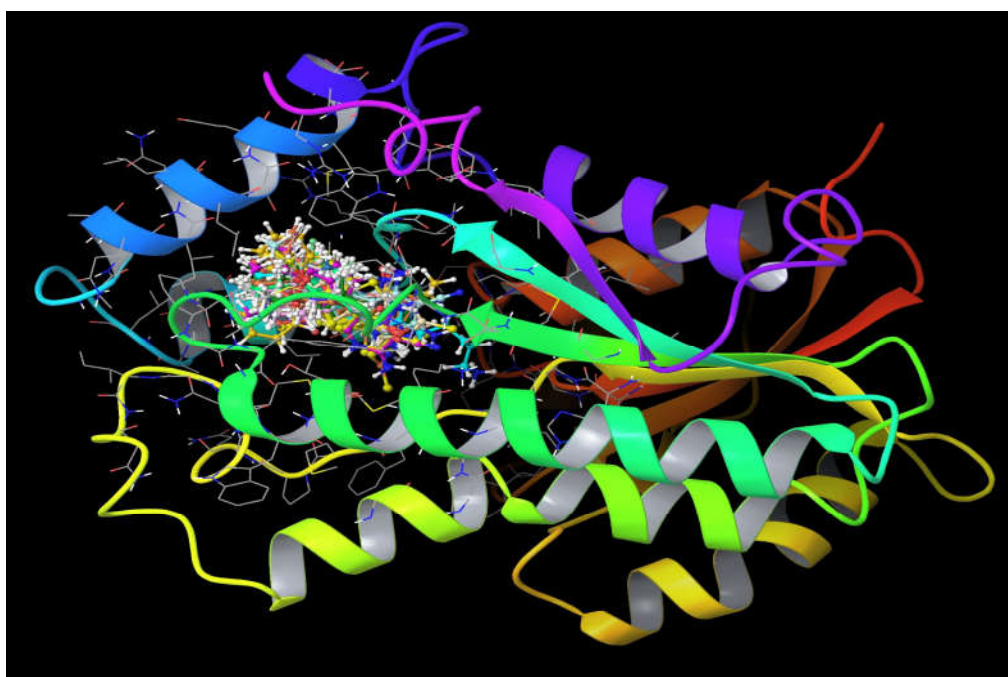
### **5.3.1. Molecular Docking Results**

The docking results of the above selected ligand molecules against the target enzyme InhA, “the enoyl acyl carrier protein reductase” (PDB id-2NSD) was summarized in **Table 2** . The overall glide docking scores of the docked ligands ranges from -10.62 to -5.83 for all the ligands on all the target enzymes.

As per the docking results, all the ligands showed better interactions with the active sites of target enzymes. The energy minimized 3D structure of prepared protein (PDB ID-2NSD) suitable for docking and the docked possess of all the ligands at the active site of target enzyme InhA is shown in **Figure 8 & 9** respectively. The major interactions by the ligands with enzyme InhA can be categorized as “hydrogen bonding, hydrophobic, electrostatic interactions,  $\pi$ - $\pi$ -stacking and  $\pi$ -cation-stacking”, which are critical for stabilizing the inhibitors inside the binding pocket of the receptor. The important interactions are shown in **Table 3**



**Figure 8: Energy minimized 3D structure of prepared protein (PDB ID-2NSD)**



**Figure 9: Docked poses of all the 30 ligands at the active site of target enzyme InhA**

The amino acid Tyr158 displays strong hydrogen bond interaction with the ligand molecules N1- N20 except N4 and N16 molecules. In case of dioxolane derivatives, strong hydrogen bond interaction was noticed with the amino acid residue Ile202. The inhibitors had successfully influenced hydrophobic effect in Ile202, Ala198, Met199, Ile215, Leu218, Val203, Met232, Pro193, Ile194, Phe149, Tyr158 and Met161. Other amino acids like Met 155, Ala157, Pro156, Ile21, Ile95, Met147, Ala191, and Trp222 also contribute to the hydrophobic interactions. Electrostatic interactions are also observed in the inhibitors having interactions with amino acids like Glu219, Lys165 and Asp148. Weak interactions like  $\pi$ - $\pi$ -stacking are also witnessed in most of the inhibitors with their aromatic group positioned near Phe149 and Tyr158. The ligand molecules with their ligand interactions are shown in **Figure 10**.

**Table 2: Docking results of the selected 30 analogs**

<b>Ligand</b>	<b>GScore<sup>a</sup></b>	<b>LipophilicEvdW<sup>b</sup></b>	<b>PhobEn<sup>c</sup></b>	<b>HBond<sup>d</sup></b>	<b>Electro<sup>e</sup></b>	<b>Sitemap<sup>f</sup></b>	<b>LowMW<sup>g</sup></b>	<b>RotPenalf<sup>h</sup></b>
N1	-8.34	-3.65	-2.14	-1.29	-0.33	-0.44	-0.5	0
N2	-9.09	-3.97	-2.59	-1.3	-0.29	-0.43	-0.5	0
N3	-8.7	-4.43	-1.75	-1.33	-0.38	-0.43	-0.5	0.11
N4	-10.62	-6.38	-2.7	-0.36	-0.12	-0.96	-0.41	0.3
N5	-8.78	-4.18	-1.71	-1.8	-0.27	-0.43	-0.5	0.11
N6	-8.14	-3.61	-1.91	-1.5	-0.28	-0.47	-0.5	0.13
N7	-8.09	-3.82	-1.83	-1.25	-0.36	-0.44	-0.5	0.11
N8	-8.88	-3.96	-2.58	-1.08	-0.33	-0.43	-0.5	0

<b>Ligand</b>	<b>GScore<sup>a</sup></b>	<b>LipophilicEvdW<sup>b</sup></b>	<b>PhobEn<sup>c</sup></b>	<b>HBond<sup>d</sup></b>	<b>Electro<sup>e</sup></b>	<b>Sitemap<sup>f</sup></b>	<b>LowMW<sup>g</sup></b>	<b>RotPenalf<sup>h</sup></b>
N9	-8.67	-4.12	-2.35	-0.73	-0.22	-0.86	-0.5	0.09
N10	-9.53	-4.51	-2.49	-1.29	-0.31	-0.43	-0.5	0
N11	-8.42	-3.85	-1.92	-1.48	-0.33	-0.46	-0.5	0.12
N12	-7.19	-2.83	-1.86	-1.25	-0.32	-0.44	-0.5	0
N13	-7.19	-3.11	-1.51	-1.31	-0.33	-0.43	-0.5	0
N14	-8.7	-4.73	-1.38	-1.5	-0.37	-0.34	-0.46	0.08
N15	-10.32	-5.07	-2.7	-1.33	-0.3	-0.43	-0.5	0
N16	-9.95	-6.01	-2.7	0	0.1	-0.91	-0.43	0
N17	-7.91	-3.75	-1.96	-1.05	-0.33	-0.43	-0.5	0.11

<b>Ligand</b>	<b>GScore<sup>a</sup></b>	<b>LipophilicEvdW<sup>b</sup></b>	<b>PhobEn<sup>c</sup></b>	<b>HBond<sup>d</sup></b>	<b>Electro<sup>e</sup></b>	<b>Sitemap<sup>f</sup></b>	<b>LowMW<sup>g</sup></b>	<b>RotPenalf<sup>h</sup></b>
N18	-8.35	-3.9	-2	-1.3	-0.32	-0.43	-0.5	0.11
N19	-8.74	-4.26	-1.71	-1.33	-0.55	-0.39	-0.5	0
N20	-5.83	-3.02	0	-1.51	-0.38	-0.43	-0.5	0
GA	-7.4	-3.67	-1.97	-0.6	-0.09	-0.57	-0.5	0
GAE	-7.98	-4.45	-1.88	-0.7	-0.1	-0.54	-0.5	0.19
GAT	-7.04	-3.51	-1.85	-0.35	-0.24	-0.59	-0.5	0
GAC	-8.68	-4.04	-1.94	-0.7	-0.1	-0.41	-0.5	0
GAC1	-8.62	-4.01	-1.9	-0.7	-0.12	-0.38	-0.5	0
GAC5	-6.42	-3.99	-1.11	0	-0.11	-0.75	-0.46	0

Ligand	GScore <sup>a</sup>	LipophilicEvdW <sup>b</sup>	PhobEn <sup>c</sup>	HBond <sup>d</sup>	Electro <sup>e</sup>	Sitemap <sup>f</sup>	LowMW <sup>g</sup>	RotPenal <sup>h</sup>
GAC6	-6.62	-4.13	-1.61	0	-0.04	-0.37	-0.46	0
GAC7	-8.76	-4.75	-1.69	-0.7	-0.09	-0.39	-0.33	0.2
GAM	-6.08	-4.16	-1.88	0	-0.06	-0.49	-0.49	0
GAEA	-7.27	-4.18	-2.01	0	-0.15	-0.43	-0.49	0
2NSD Internal Ligand	-8.66	-4.31	-1.98	-0.7	-0.28	-0.52	-0.5	0.36

<sup>a</sup>**GScore**: Sum of XP terms.

<sup>b</sup>**LipophilicEvdW**: Lipophilic term derived from hydrophobic grid potential at the hydrophobic ligand atoms.

<sup>c</sup>**PhobEn**: Hydrophobic enclosure reward.

<sup>d</sup>**HBond**: ChemScore H-bond pair term.

<sup>e</sup>**Electro**: Electrostatic rewards; includes C1oulomb and metal terms.

<sup>f</sup>**Sitemap**: SiteMap ligand-receptor non-H-bonding polar-hydrophobic terms.

<sup>g</sup>**LowMW**: Reward for ligands with low molecular weight.

<sup>h</sup>**RotPenal**: Rotatable bond penalty.



**Table 3: Residue interaction pattern for the synthesized compounds against target enzyme InhA**

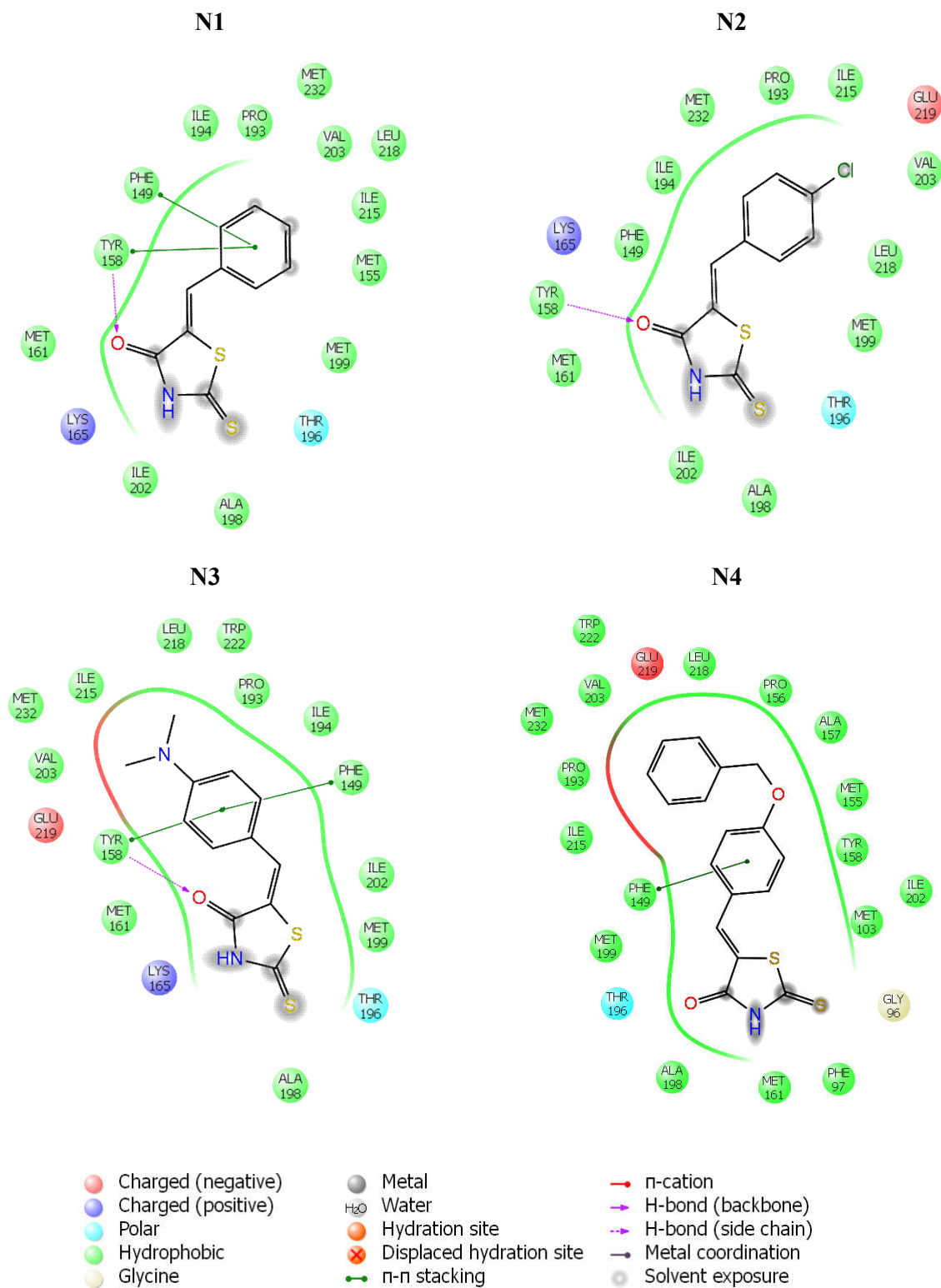
Compounds	Important Interactions of Ligands with the amino acids of the target enzyme InhA binding sites				
	Hydrogen Bonding	Hydrophobic	Positive Ionizable	Negative Ionizable	Polar
N1	Tyr158	Ile202, Ala198, Met199, Met155, Ile215, Leu218, Val203, Met232, Pro193, Ile194, Phe149, Tyr158, Met161, n-n stacking-Phe149, n-n stacking-Tyr158	Lys165	-	Thr196
N2	Tyr158	Ile202, Ala198, Met199, Leu218, Val203, Ile215, Pro193, Met232, Ile194, Phe149, Tyr158, Met161	Lys165	Glu219	Thr196
N3	Tyr158	Ala198, Met199, Ile202, Phe149, Ile194, Pro193, Trp222, Leu218, Ile215, Met232, Val203, Tyr158, Met161, n-n stacking- Phe149, Tyr158	Lys165	Glu219	Thr196
N4	-	Met161, Phe97, Met103, Ile202, Tyr158, Met155, Ala157, Pro156, Leu218, Trp222, Val203, Met232, Pro193, Ile215, Phe149, Met199, Ala198, n-n stacking-Phe149	Lys165	-	Thr196
N5	Tyr158	Val203, Ala157, Met103, Ile202, Leu218, Ile215, Pro193, Met232, Ile194, Phe149, Tyr158, Met161, Met199, Ala198	Lys165	Glu219	Thr196
N6	Tyr158	Met103, Val203, Ile215, Pro193, Phe149, Tyr158, Met161, Ile202, Met199, Ala198	Lys165	-	-

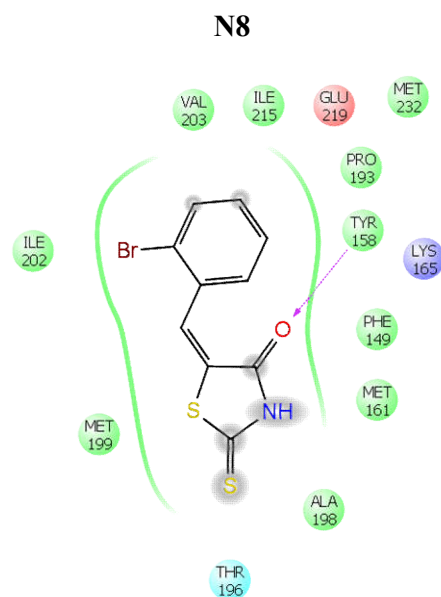
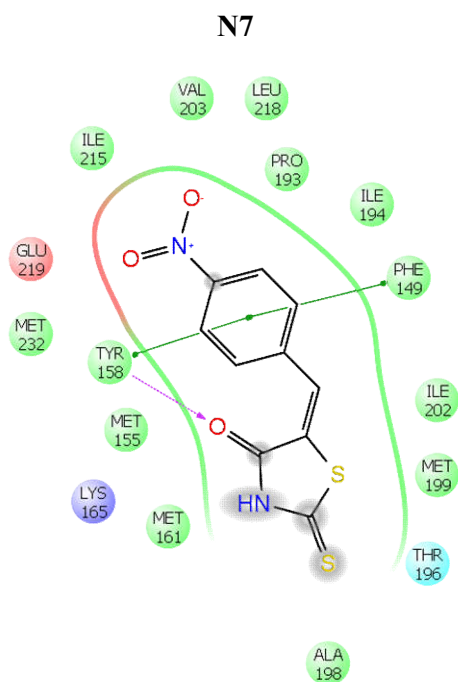
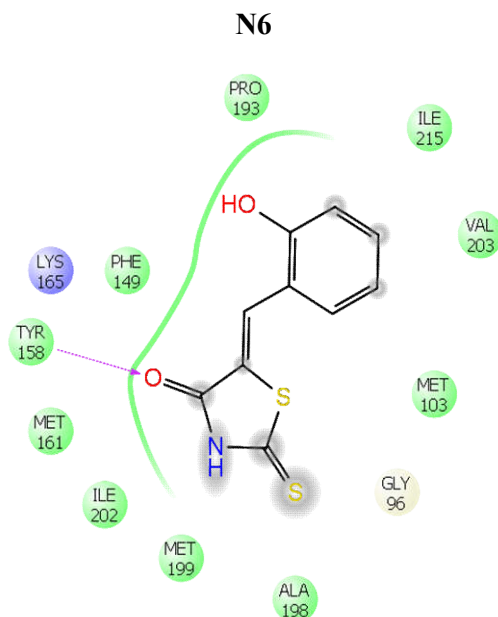
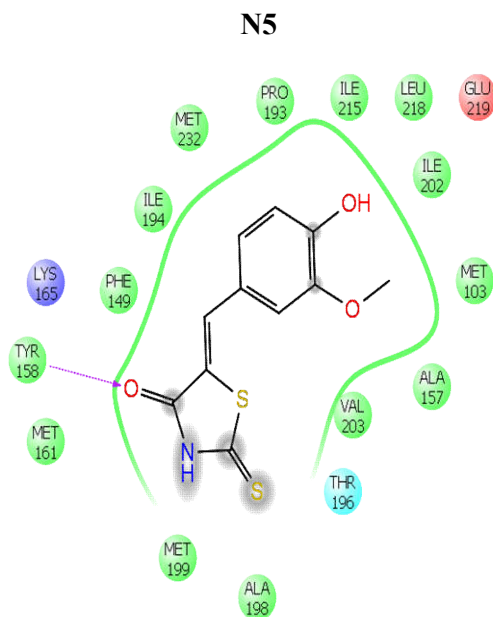
<b>N7</b>	Tyr158	Met199, Ile202, Phe149, Ile194, Pro193, Leu218, Val203, Ile215, Met232, Tyr158, Met155, Met161, Ala198, n-n stacking- Phe149, n-n stacking-Tyr158	Lys165	Glu219	Thr196
<b>N8</b>	Tyr158	Met161, Phe149, Tyr158, Pro193, Met232, Ile215, Val203, Ile202, Met199, Ala198	Lys165	Glu219	Thr196
<b>N9</b>	Tyr158	Met103, Met199, Ala157, Ile202, Val203, Ile215, Leu218, Met232, Pro193, Ile194, Met161, Tyr158, Phe149, Ala198	Lys165	Glu219	Thr196
<b>N10</b>	Tyr158	Ala198, Met199, Phe149, Ile202, Met103, Ala157, Val203, Ile215, Leu218, Pro193, Ile194, Tyr158, Met161	Lys165	-	Thr196
<b>N11</b>	Tyr158	Met199, Ile215, Val203, Met232, Pro193, Phe149, Tyr158, Met161, Ile202, Ala198	Lys165	Glu219	-
<b>N12</b>	Tyr158	Met199, Pro193, Val203, Leu218, Ile215, Met155, Phe149, Tyr158, Met161, Ile202, Ala198	Lys165	-	Thr196
<b>N13</b>	Tyr158	Met199, Pro193, Ile202, Met232, Val203, Leu218, Phe149, Tyr158, Met161, Ala198, n-n stacking- Phe149, n-n stacking- Tyr158	Lys165	-	Thr196
<b>N14</b>	Tyr158	Pro193, Met232, Ile215, Pro156, Val203, Leu218, Ile202, Met103, Ala157, Leu207, Tyr158, Phe149, Met161, Met199, Ala198, n-n stacking- Tyr158	Lys165	Glu219	-

<b>N15</b>	Tyr158	Met161, Tyr158, Phe149, Pro156, Ala157, Leu218, Val203, Ile215, Met232, Ile194, Ile202, Pro193, Ala198, Met199, n-n stacking- Phe149, n-n stacking-Tyr158	Lys165	Glu219	Thr196
<b>N16</b>	-	Tyr158, Ile202, Met103, Ala157, Leu207, Ile215, Val203, Leu218, Pro193, Trp222, Phe149, Met199, Ala198	-	Glu219	-
<b>N17</b>	Tyr158	Met199, Ala198, Met103, Ile202, Val203, Ile215, Pro193, Tyr158, Phe149, Met232, Met161	Lys165	Glu219	Thr196
<b>N18</b>	Tyr158	Met199, Ala198, Ile202, Ile194, Met232, Pro193, Val203, Ala157, Leu218, Pro156, Ile215, Phe149, Tyr158, Met161, n-n stacking-Tyr158	Lys165	-	Thr196
<b>N19</b>	Tyr158	Met199, Ala198, Met161, Phe149, Tyr158, Ile202, Met103, Ala157, Val203, Ile215, Leu218, Pro193, Ile194, n-n stacking-Tyr158	Lys165	-	Thr196
<b>N20</b>	Tyr158	Met199, Ala198, Met161, Ile202, Ile194, Val203, Leu218, Pro193, Met232, Phe149, Tyr158, n-n stacking-Phe149, n-n stacking-Tyr158	Lys165	-	Thr196
<b>GA</b>	Ile194	Met199, Ile202, Tyr158, Val203, Pro156, Ala157, Leu218, Met155, Ile215, Pro193, Ile194, Phe149, n-n stacking-Tyr158	-	-	-
<b>GAC</b>	Ile194	Met199, Ile202, Tyr158, Phe149, Met155, Leu218, Ile215, Pro156, Ala157, Val203, Pro193, Ile194, Met232, Ala198, Ile21, n-n stacking- Tyr158	-	Glu219	Thr196

<b>GAC1</b>	Ile194	Met199, Ile202, Tyr158, Phe149, Trp222, Met155, Leu218, Ile215, Pro156, Ala157, Val203, Pro193, Ile194, Met232, Ile21, n-n stacking- Tyr158	-	-	Thr196
<b>GAC5</b>	-	Met147, Met161, Met103, Ile202, Met199, Leu218, Pro156, Ala157, Ile215, Val203, Tyr158, Pro193, Phe149, Ile194, n-n stacking- Tyr158	Lys165	-	-
<b>GAC6</b>	Ile194	Ala198, Met199, Ile202, Tyr158, Trp222, Ile215, Leu218, Met232, Val203, Pro193, Phe149, Ile194, Ala191, Ile21	-	Glu219	Thr196
<b>GAC7</b>	Ile194, Ser94	Ile95, Phe149, Met161, Tyr158, Ile202, Trp222, Met155, Leu218, Ile215, Ala157, Val203, Pro193, Met199, Ile194, Met232, Met147, Ile21, n-n stacking- Tyr158	Lys165	Glu219	Thr196, Ser94
<b>GAE</b>	Ile194	Ile21, Met161, Met199, Ile202, Tyr158, Val203, Ile215, Leu218, Met155, Trp222, Met232, Pro193, Ile194, Phe149, Met147, Ala191, n-n stacking-Tyr158	-	Glu219, Asp148	-
<b>GAEA</b>	-	Ile21, Met199, Ile202, Val203, Tyr158, Met155, Ile215, Pro156, Ala157, Leu218, Pro193, Met232, Phe149, Ile194	-	-	Thr196
<b>GAM</b>	-	Met199, Ile202, Tyr158, Leu218, Met155, Ile215, Pro156, Ala157, Val203, Pro193, Phe149, Ile194, Ala191, Met147, Ile21, n-n stacking- Tyr158	Lys165	-	-
<b>GAT</b>	Ile194	Ile21, Met199, Ile202, Tyr158, Ile215, Val203, Pro156, Ala157, Met155, Leu218, Phe149, Ile194, Pro193, n-n stacking-Tyr158	-	-	-

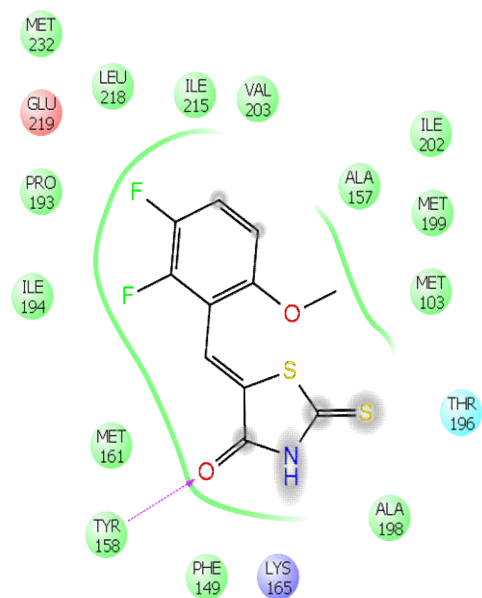
**Figure 10: Ligand Interaction Diagrams of all the 30 ligand molecules against active site of target enzyme InhA**



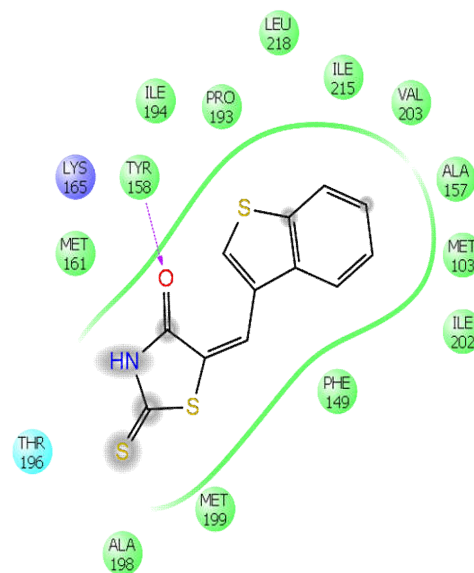


- |  |  |   |
|--|--|---|
| <span style="color: red;">●</span> Charged (negative)  | <span style="color: grey;">●</span> Metal                      | <span style="color: red;">→</span> π-cation               |
| <span style="color: blue;">●</span> Charged (positive) | <span style="color: grey;">H<sub>2</sub>O</span> Water         | <span style="color: purple;">→</span> H-bond (backbone)   |
| <span style="color: cyan;">●</span> Polar              | <span style="color: orange;">●</span> Hydration site           | <span style="color: purple;">→</span> H-bond (side chain) |
| <span style="color: green;">●</span> Hydrophobic       | <span style="color: orange;">X</span> Displaced hydration site | <span style="color: grey;">—</span> Metal coordination    |
| <span style="color: yellow;">●</span> Glycine          | <span style="color: green;">→</span> π-π stacking              | <span style="color: grey;">○</span> Solvent exposure      |

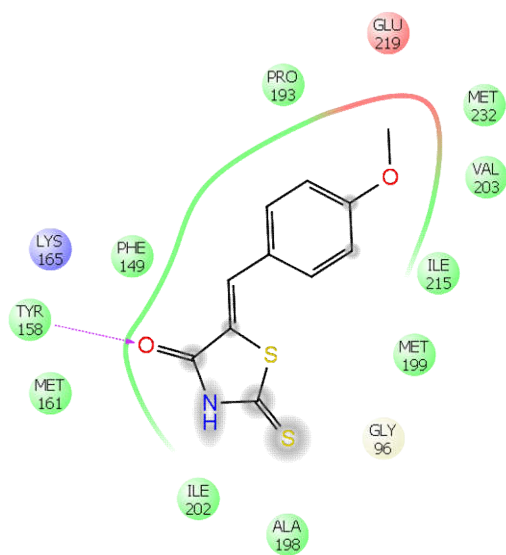
N9



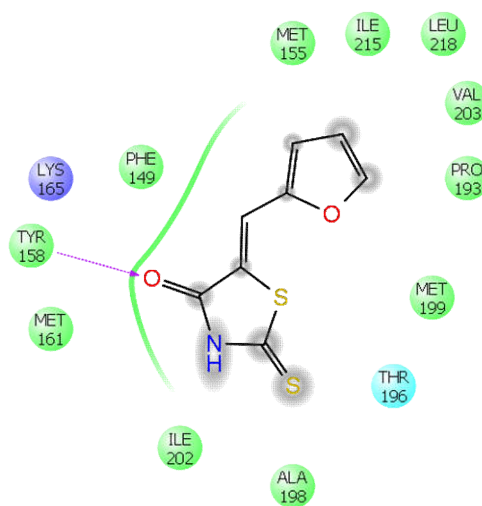
N10



N11

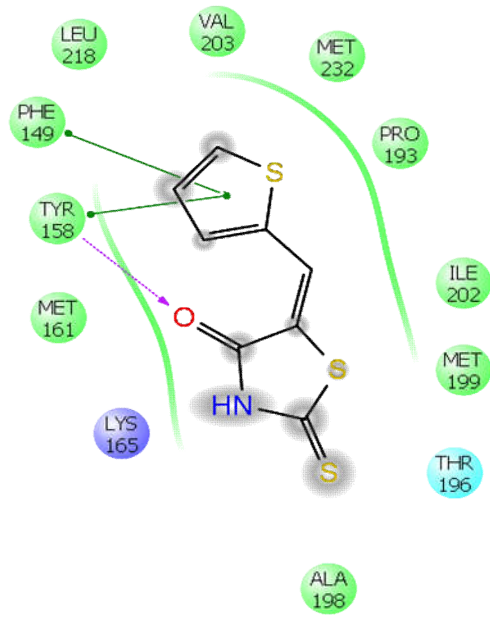


N12

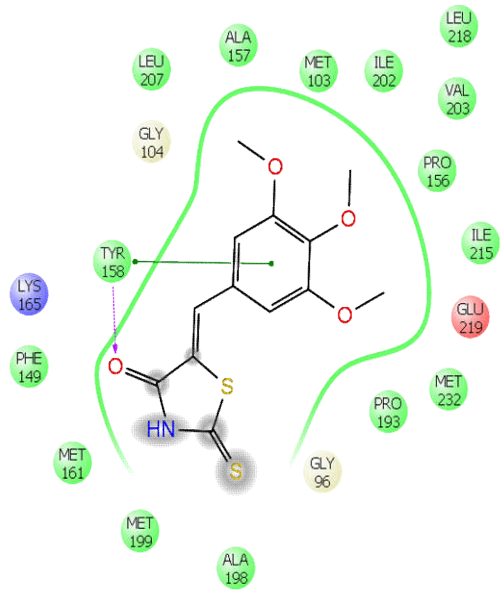


- |  |  |   |
|--|--|---|
| <span style="color: red;">●</span> Charged (negative)  | <span style="color: grey;">●</span> Metal                      | <span style="color: red;">→</span> n-cation               |
| <span style="color: blue;">●</span> Charged (positive) | <span style="color: grey;">●</span> H <sub>2</sub> O           | <span style="color: purple;">→</span> H-bond (backbone)   |
| <span style="color: cyan;">●</span> Polar              | <span style="color: orange;">●</span> Hydration site           | <span style="color: purple;">→</span> H-bond (side chain) |
| <span style="color: green;">●</span> Hydrophobic       | <span style="color: orange;">⊗</span> Displaced hydration site | <span style="color: grey;">→</span> Metal coordination    |
| <span style="color: yellow;">●</span> Glycine          | <span style="color: green;">—</span> n-n stacking              | <span style="color: grey;">○</span> Solvent exposure      |

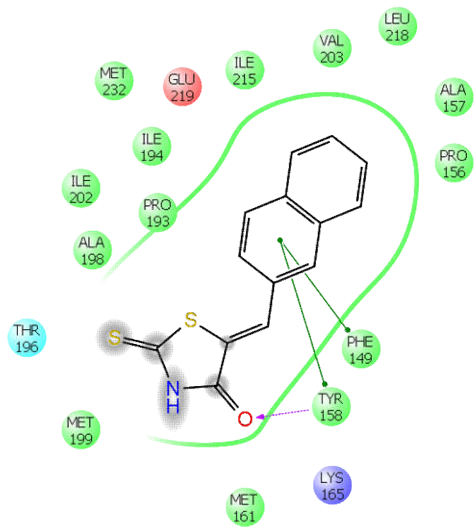
N13



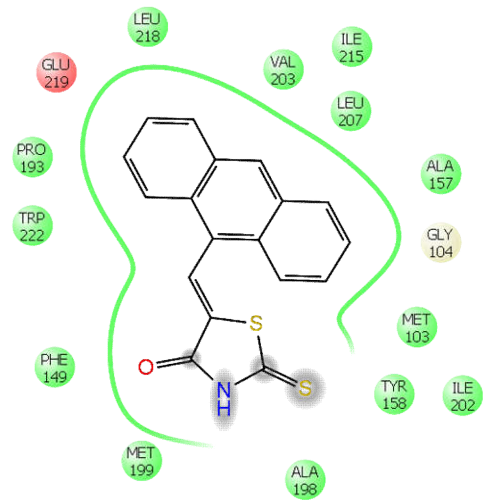
N14



N15



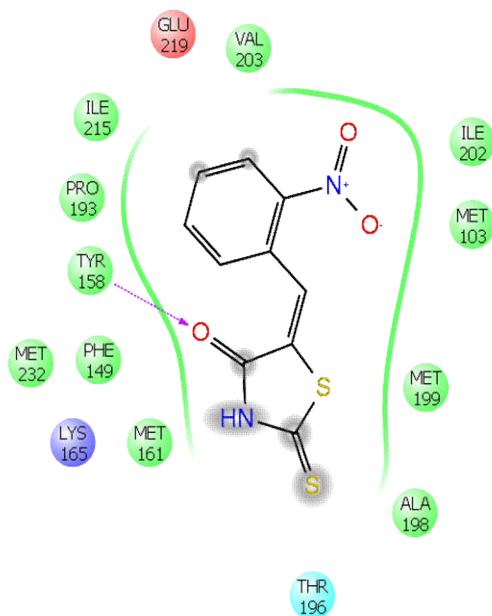
N16



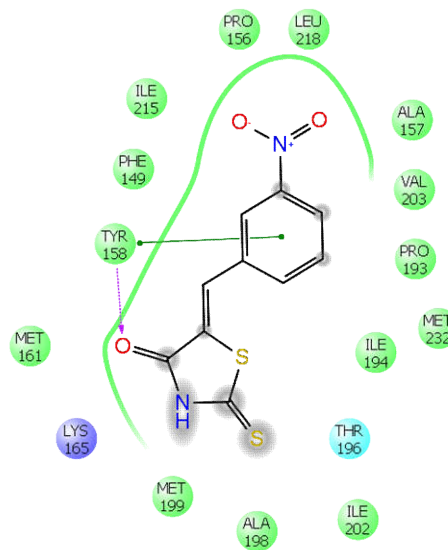
- |                      |                            |                       |
|----------------------|----------------------------|-----------------------|
| ● Charged (negative) | ● Metal                    | → π-cation            |
| ● Charged (positive) | H <sub>2</sub> O Water     | → H-bond (backbone)   |
| ● Polar              | ● Hydration site           | → H-bond (side chain) |
| ● Hydrophobic        | ● Displaced hydration site | → Metal coordination  |
| ● Glycine            | ● π-π stacking             | ○ Solvent exposure    |



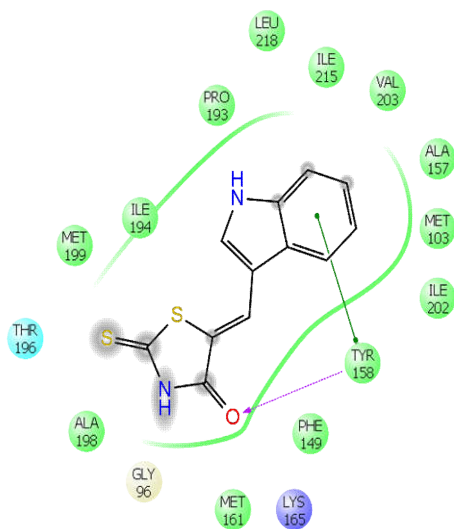
N17



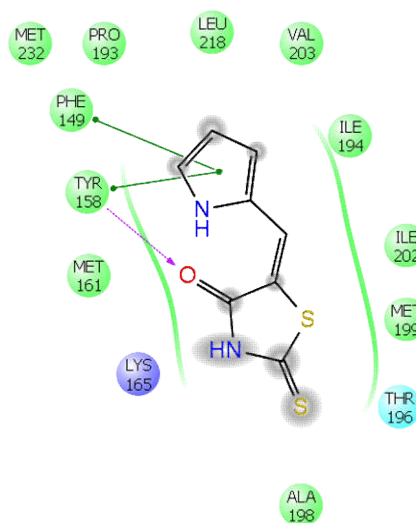
N18



N19

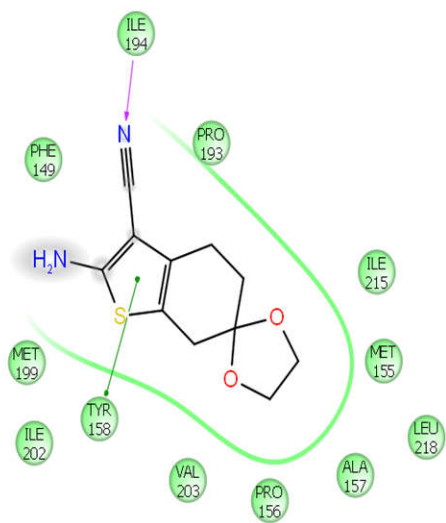


N20

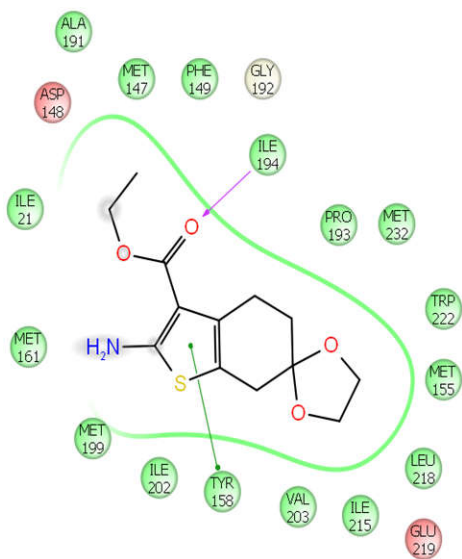


- |  |  |   |
|--|--|---|
| <span style="color: red;">●</span> Charged (negative)  | <span style="color: grey;">●</span> Metal                      | <span style="color: red;">→</span> n-cation               |
| <span style="color: blue;">●</span> Charged (positive) | <span style="color: grey;">H<sub>2</sub>O</span> Water         | <span style="color: purple;">→</span> H-bond (backbone)   |
| <span style="color: cyan;">●</span> Polar              | <span style="color: orange;">○</span> Hydration site           | <span style="color: purple;">→</span> H-bond (side chain) |
| <span style="color: green;">●</span> Hydrophobic       | <span style="color: orange;">○</span> Displaced hydration site | <span style="color: grey;">—</span> Metal coordination    |
| <span style="color: yellow;">●</span> Glycine          | <span style="color: green;">—</span> n-n stacking              | <span style="color: grey;">○</span> Solvent exposure      |

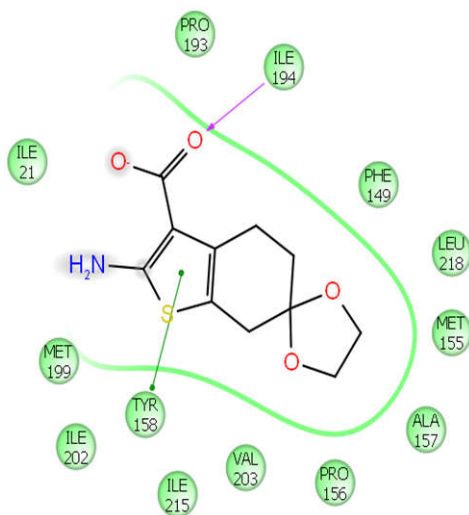
### GA



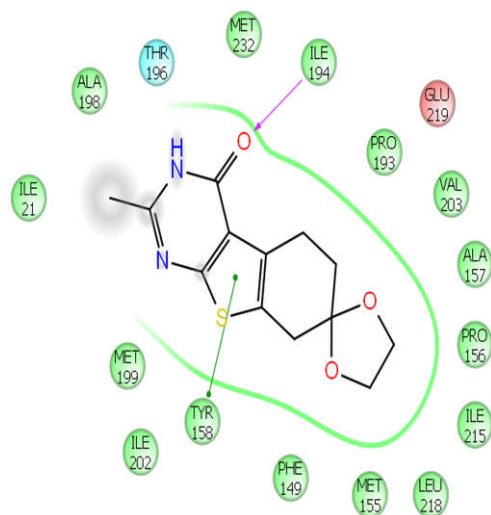
### GAE



### GAT



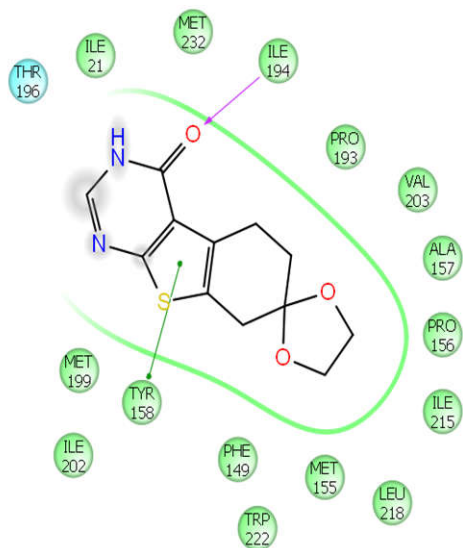
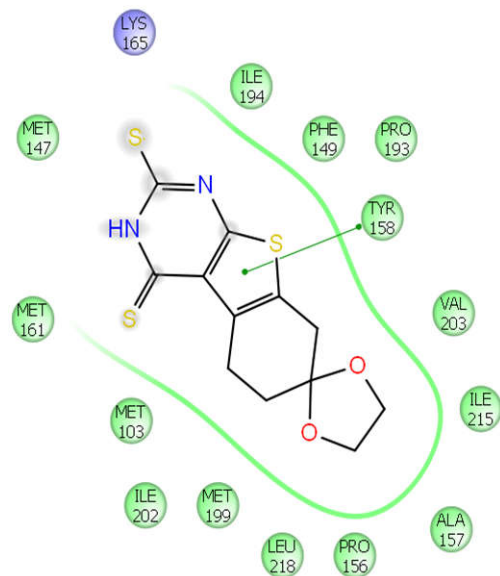
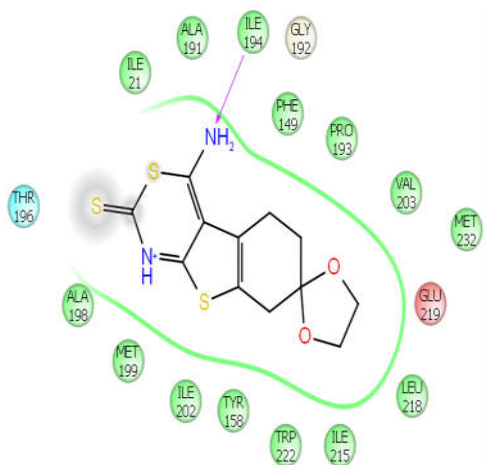
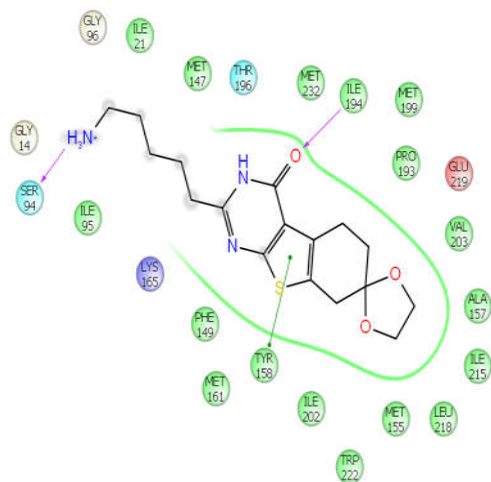
### GAC



- Charged (negative)
- Charged (positive)
- Polar
- Hydrophobic
- Glycine

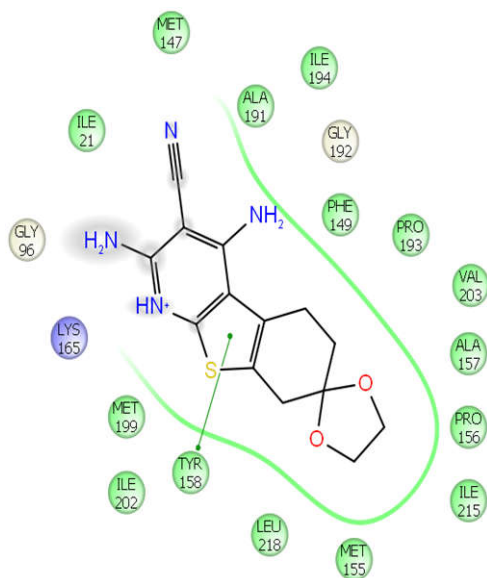
- Metal
- H<sub>2</sub>O Water
- Hydration site
- ⊗ Displaced hydration site
- n-n stacking

- n-cation
- H-bond (backbone)
- H-bond (side chain)
- Metal coordination
- Solvent exposure

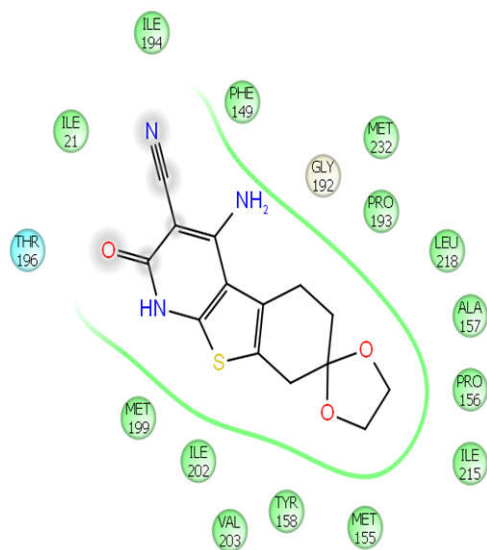
**GAC1****GAC5****GAC6****GAC7**

- |  |  |   |
|--|--|---|
| <span style="color: red;">●</span> Charged (negative)  | <span style="color: grey;">●</span> Metal                      | <span style="color: red;">→</span> n-cation               |
| <span style="color: blue;">●</span> Charged (positive) | <span style="color: grey;">●</span> H <sub>2</sub> O Water     | <span style="color: purple;">→</span> H-bond (backbone)   |
| <span style="color: cyan;">●</span> Polar              | <span style="color: orange;">●</span> Hydration site           | <span style="color: purple;">→</span> H-bond (side chain) |
| <span style="color: green;">●</span> Hydrophobic       | <span style="color: orange;">⊗</span> Displaced hydration site | <span style="color: grey;">→</span> Metal coordination    |
| <span style="color: yellow;">●</span> Glycine          | <span style="color: green;">→</span> n-n stacking              | <span style="color: grey;">○</span> Solvent exposure      |

### GAM



### GAEA



- |  |  |   |
|--|--|---|
| <span style="color: red;">●</span> Charged (negative)  | <span style="color: grey;">●</span> Metal                      | <span style="color: red;">→</span> n-cation               |
| <span style="color: blue;">●</span> Charged (positive) | <span style="color: grey;">H<sub>2</sub>O</span> Water         | <span style="color: purple;">→</span> H-bond (backbone)   |
| <span style="color: cyan;">●</span> Polar              | <span style="color: orange;">●</span> Hydration site           | <span style="color: purple;">→</span> H-bond (side chain) |
| <span style="color: green;">●</span> Hydrophobic       | <span style="color: orange;">⊗</span> Displaced hydration site | <span style="color: purple;">→</span> Metal coordination  |
| <span style="color: yellow;">●</span> Glycine          | <span style="color: green;">→</span> n-n stacking              | <span style="color: grey;">○</span> Solvent exposure      |

### **5.3.2. *In-Silico ADME Property Prediction Results***

*In-silico* ADME property prediction results of the selected 30 ligand molecules were summarized in **Table 4**. From the predicted results it was inferred that the obtained values for various critical ADME parameters such as “CNS activity (CNS), total solvent accessible surface area (SASA), octanol/ water partition co-efficient (QPlogPo/w), IC<sub>50</sub> value for blockage of HERG K<sup>+</sup> channels (QPlogHERG), brain blood partition co-efficient (QPlogBB), binding human serum albumin (QPlogKhsa), human oral absorption (PercentHumanOralAbsorption), violations of Lipinski’s rule of five (RuleOfFive) etc” were encouraging and in good agreement within the acceptable limit of 95% known drugs.

### **5.3.3. *In-Silico Toxicity Assessment Results***

The *in-silico* toxicity assessment results of the selected 30 ligand molecules were summarized in the **Table 5**. Except 3 ligand molecules, all the molecules were found to be non-toxic in the terms of mutagenicity, tumorigenicity, skin irritancy and reproductive effect based on the *in-silico* toxicity assessment study. The screen shot of the results were also given in the **Figure 11**.

**Table 4: *In-silico* ADME properties of the selected 30 ligand molecules**

<b>Ligand Molecules</b>	<b>CNS</b>	<b>mol_MW</b>	<b>SASA</b>	<b>QPlog Po/w</b>	<b>QPlog HERG</b>	<b>QPlogBB</b>	<b>QPlogKhsa</b>	<b>PercentHumanOral Absorption</b>	<b>RuleOfFive</b>
N1	0	221.29	427.89	2.28	-4.51	-0.06	-0.19	100	0
N2	1	255.74	451.95	2.91	-4.47	0.10	-0.08	100	0
N3	0	264.36	505.35	2.72	-4.61	-0.19	-0.03	100	0
N4	0	327.42	604.50	4.38	-6.34	-0.37	0.41	100	0
N5	0	267.32	476.51	1.98	-4.43	-0.53	-0.31	89.84	0
N6	0	237.29	437.44	1.77	-4.39	-0.52	-0.34	86.94	0
N7	-2	266.29	465.91	1.82	-4.48	-1.01	-0.22	78.54	0
N8	1	300.19	449.72	2.91	-4.40	0.08	-0.07	100	0
N9	1	287.30	484.17	2.78	-4.35	0.01	-0.09	100	0
N10	1	277.37	477.00	3.29	-4.74	0.04	0.08	100	0
N11	0	251.32	464.96	2.54	-4.44	-0.14	-0.17	100	0
N12	0	211.25	399.27	1.86	-4.20	-0.04	-0.42	95.25	0
N13	1	227.31	411.93	2.41	-4.17	0.04	-0.27	100	0
N14	0	311.37	529.05	2.75	-4.25	-0.29	-0.15	100	0
N15	0	271.35	497.01	3.38	-5.23	-0.10	0.17	100	0

N16	1	321.41	531.85	4.38	-5.31	0.09	0.58	100	0
N17	-1	266.29	461.07	1.90	-4.43	-0.89	-0.23	80.97	0
N18	-2	266.29	465.76	1.82	-4.48	-1.01	-0.22	78.55	0
N19	0	260.33	467.94	2.60	-4.79	-0.33	-0.05	94.77	0
N20	0	210.27	400.29	1.72	-4.09	-0.25	-0.38	90.29	0
GA	0	236.29	427.57	1.42	-3.17	-0.47	-0.23	85.42	0.00
GAE	0	283.34	509.08	2.86	-3.76	-0.30	0.20	100.00	0.00
GAT	-1	255.29	427.60	1.97	-1.18	-0.59	-0.32	75.00	0.00
GAC	0	278.33	487.25	1.99	-3.70	-0.11	-0.06	94.93	0.00
GAC1	0	264.30	442.48	1.55	-3.38	-0.14	-0.22	90.40	0.00
GAC5	2	312.42	502.00	3.03	-3.86	0.47	0.03	100.00	0.00
GAC6	1	312.42	483.86	2.59	-3.45	0.28	-0.06	100.00	0.00
GAC7	-1	349.45	649.59	2.04	-5.65	-0.90	0.12	73.43	0.00
GAEA	-2	303.34	492.15	0.81	-3.62	-1.02	-0.29	71.98	0.00
GAM	-2	302.35	501.89	1.13	-3.79	-1.06	-0.22	74.57	0.00

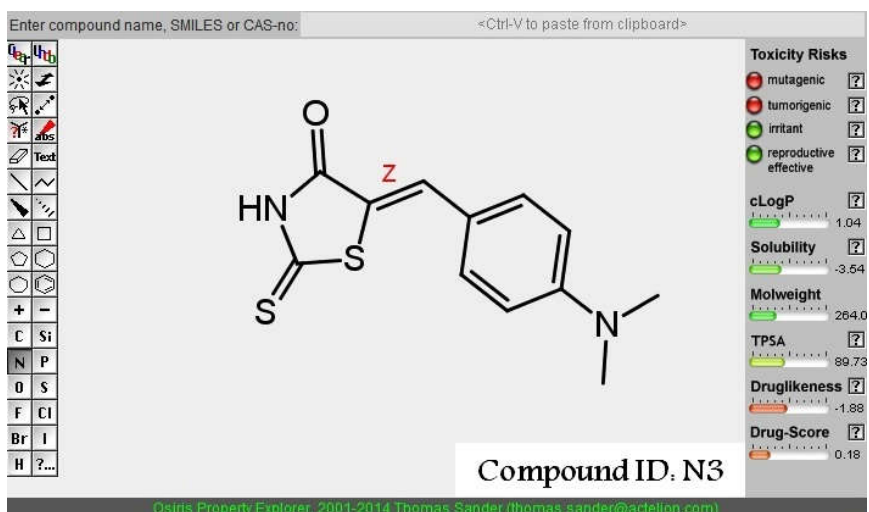
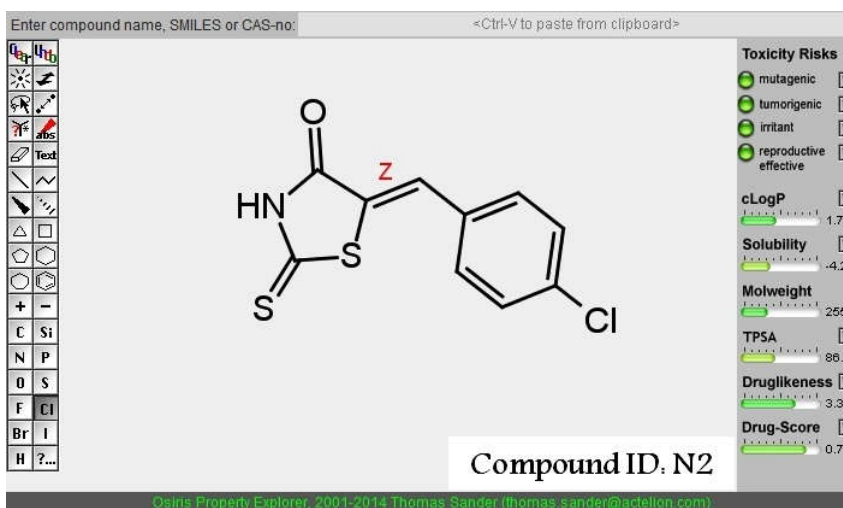
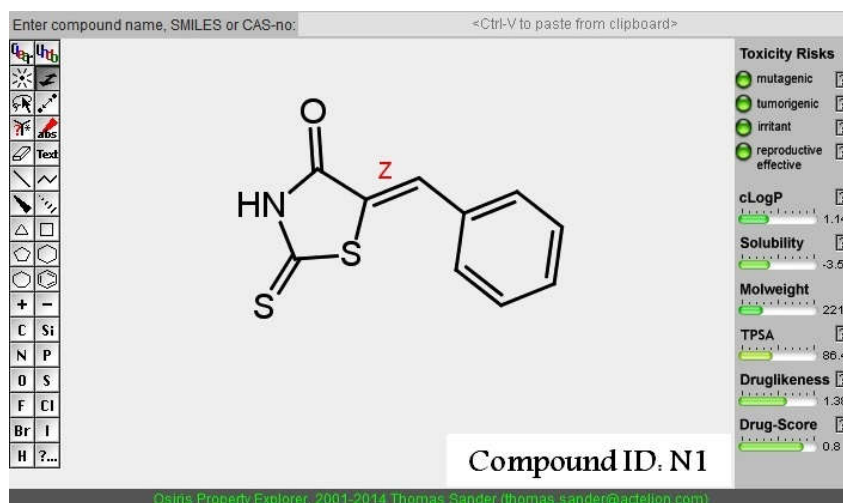
**Table 5: *In-silico* toxicity assessment results of the 30 ligand molecules**

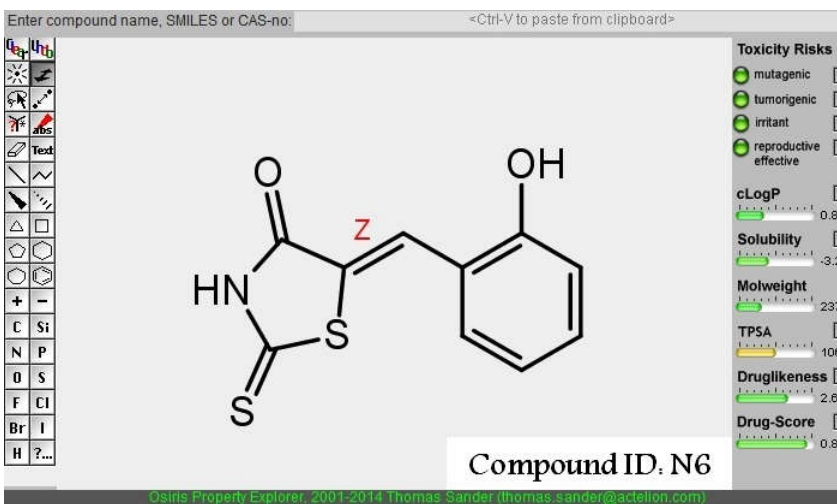
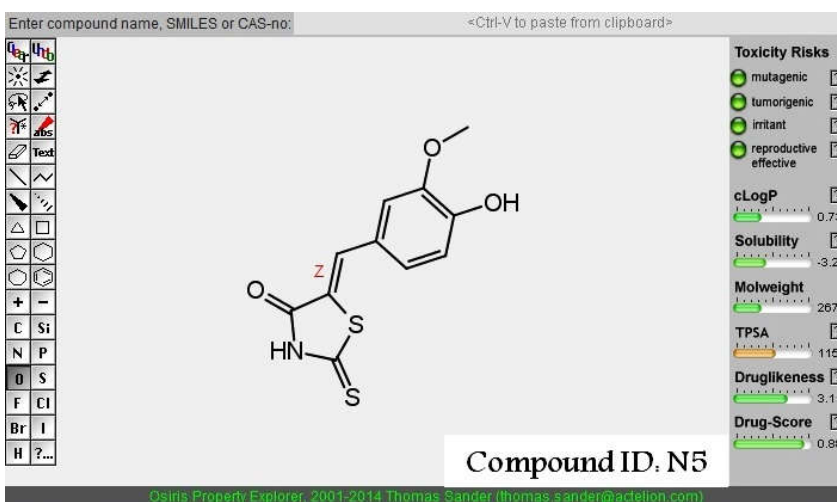
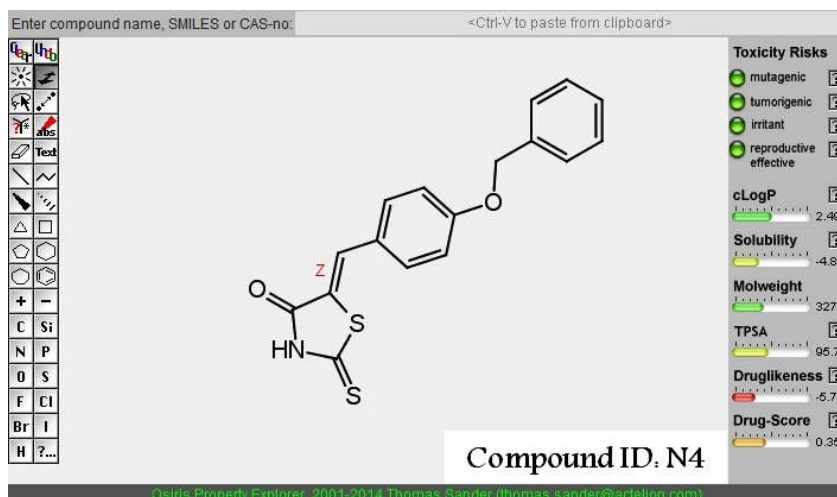
Compound ID	Mutagenicity	Tumorigenicity	Skin Irritancy	Reproductive Effect
N1	G	G	G	G
N2	G	G	G	G
N3	R	R	G	G
N4	G	G	G	G
N5	G	G	G	G
N6	G	G	G	G
N7	G	G	G	G
N8	G	G	G	G
N9	G	G	G	G
N10	G	G	G	G
N11	G	G	G	G
N12	R	G	G	G
N13	G	G	G	G
N14	G	G	G	G
N15	G	G	G	G
N16	R	R	R	G
N17	G	G	G	G
N18	G	G	G	G
N19	G	G	G	G
N20	G	G	G	G
GA	G	G	G	G
GAE	G	G	G	G
GAT	G	G	G	G
GAC	G	G	G	G
GAC1	G	G	G	G
GAC5	G	G	G	G
GAC6	G	G	G	G
GAC7	G	G	G	G
GAEA	G	G	G	G
GAM	G	G	G	G

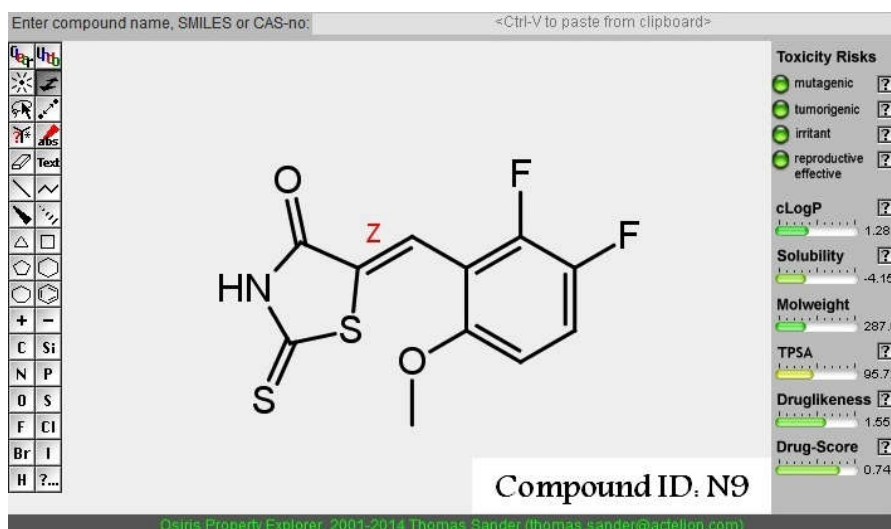
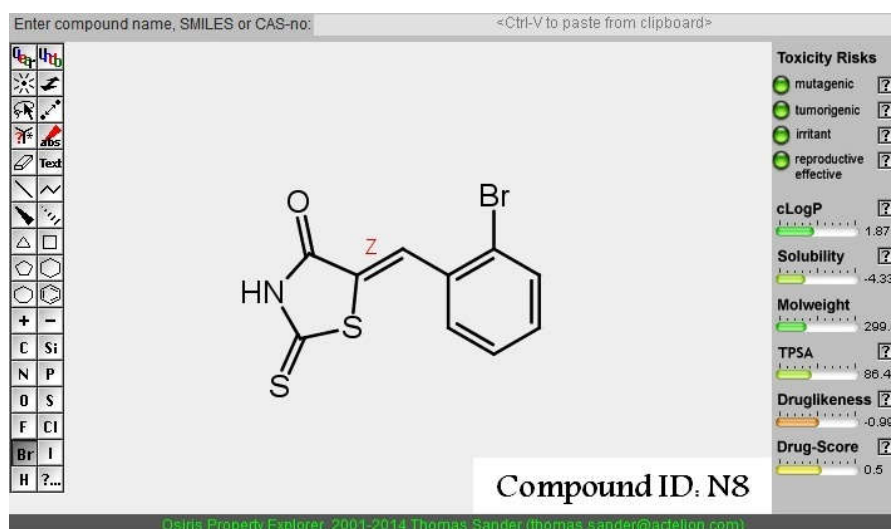
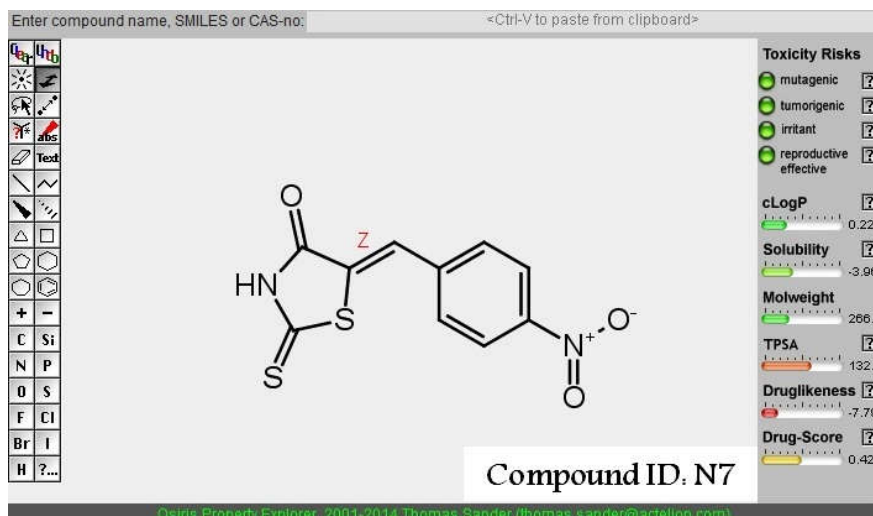
**G-Non-Toxic, R-Severe Toxicity**

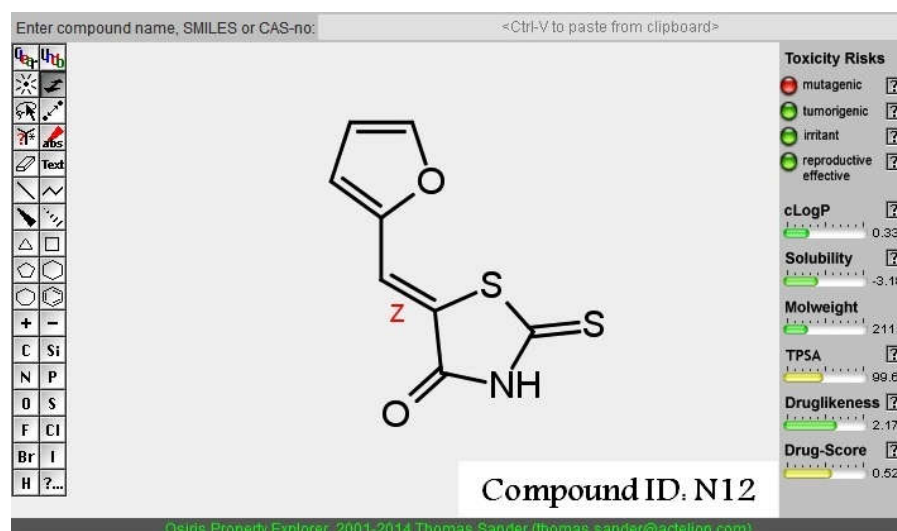
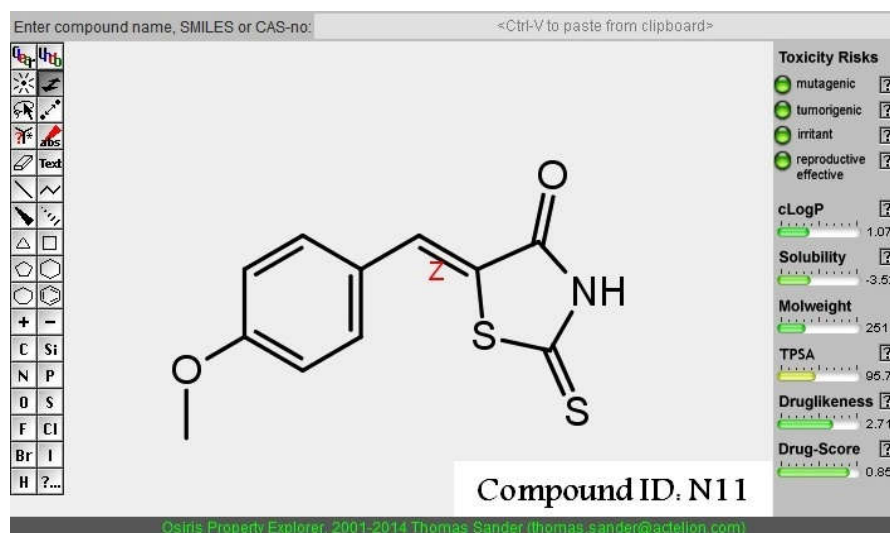
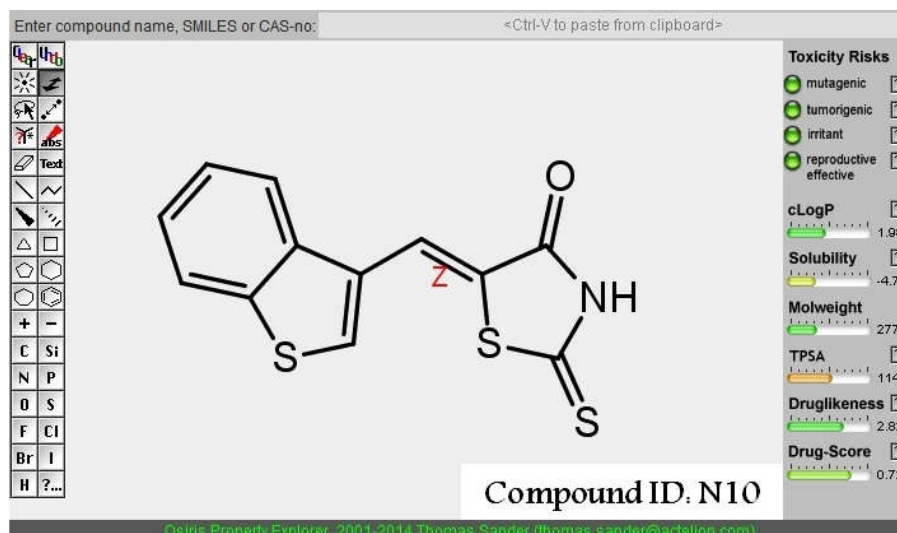


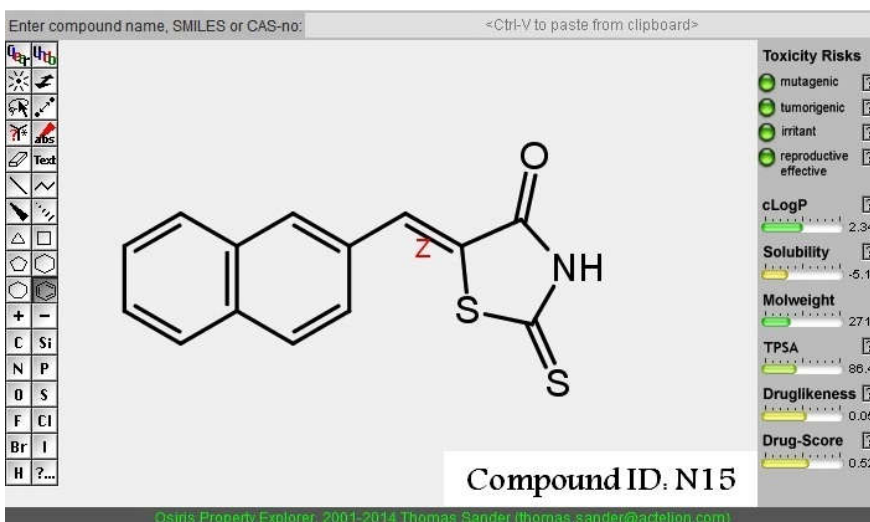
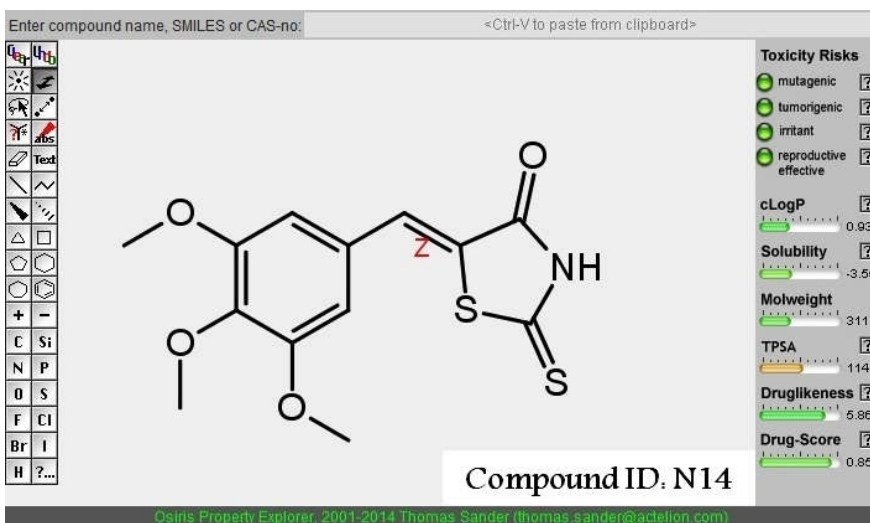
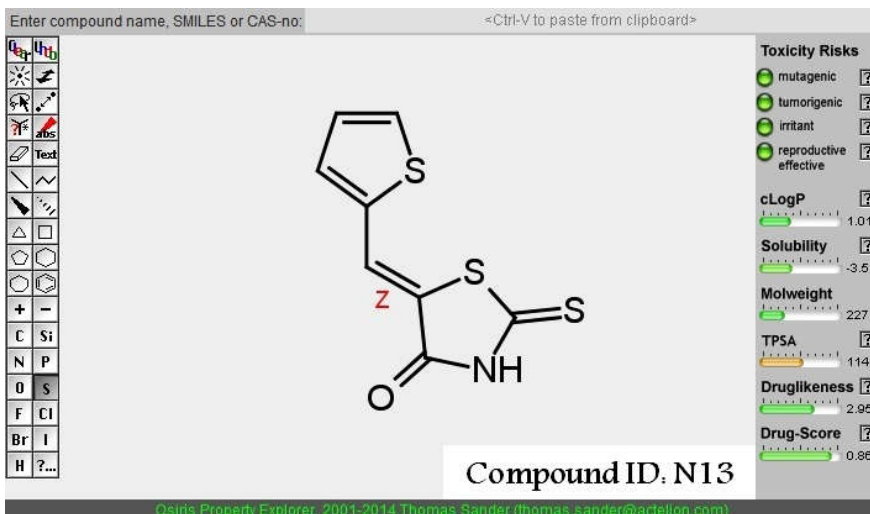
Figure 11: Screen shot of *In-silico* toxicity assessment results

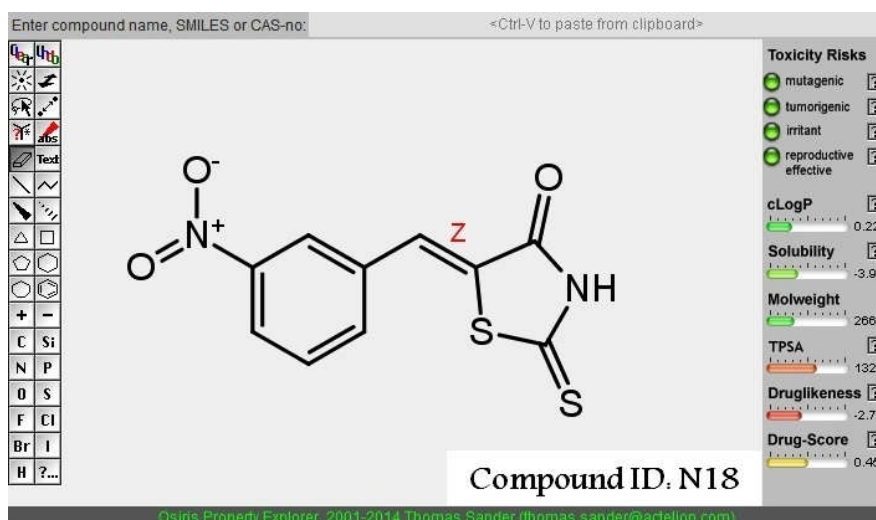
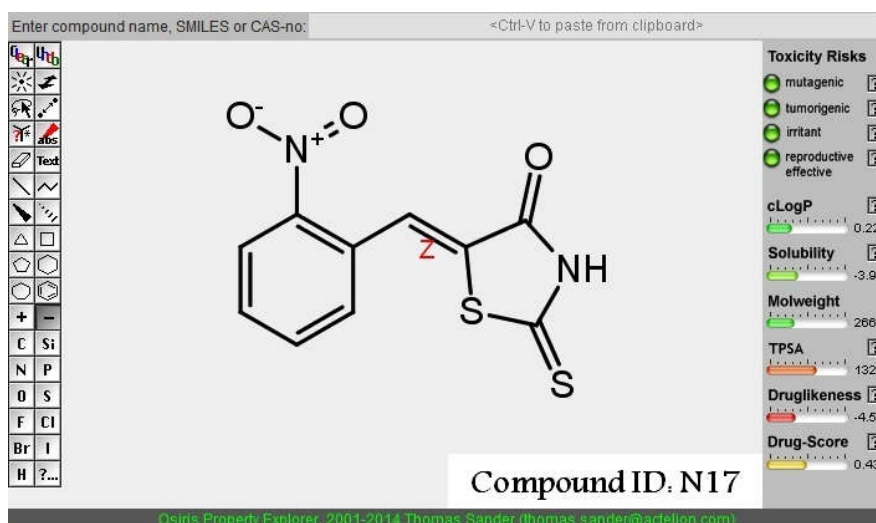
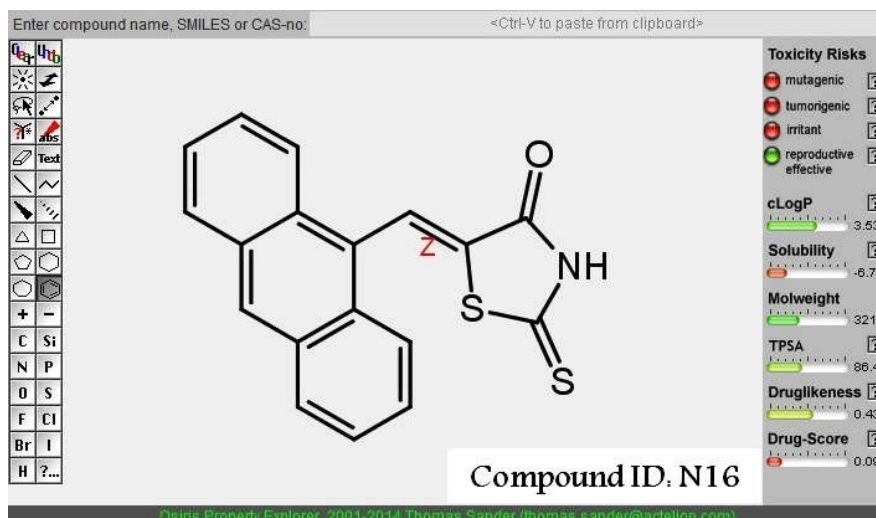


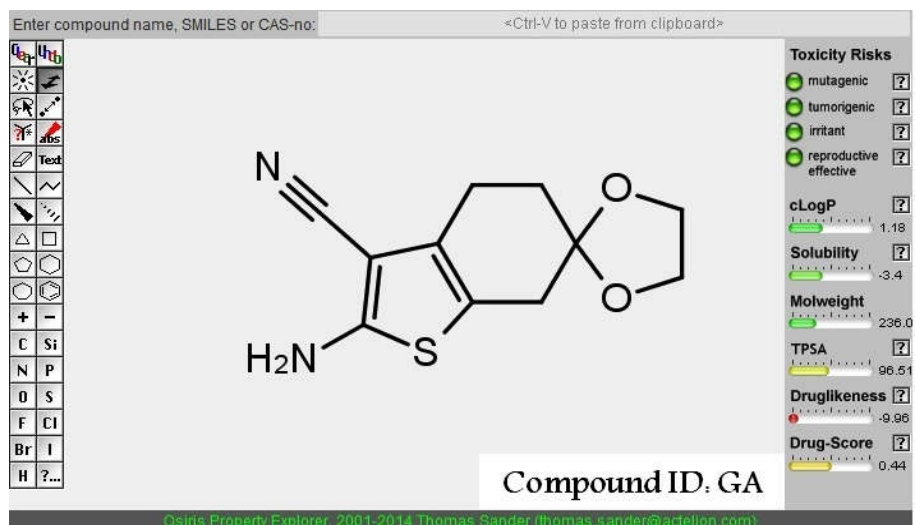
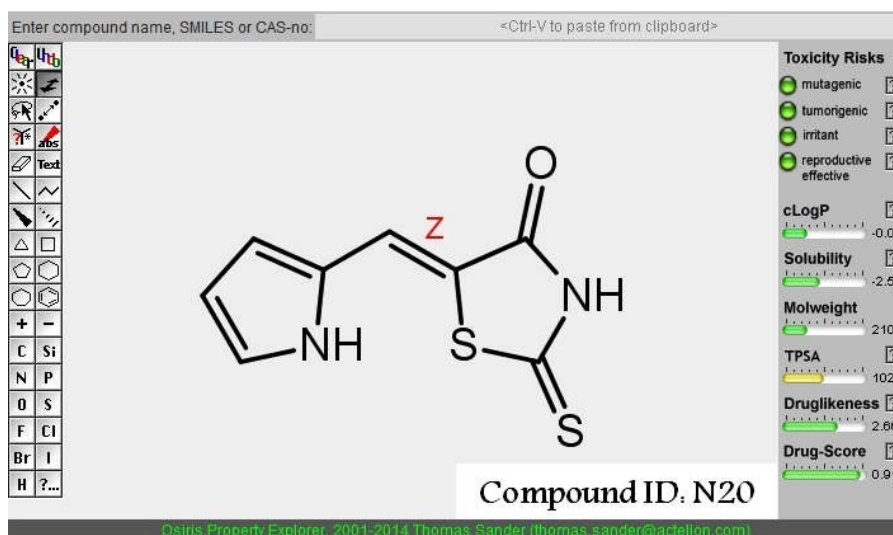
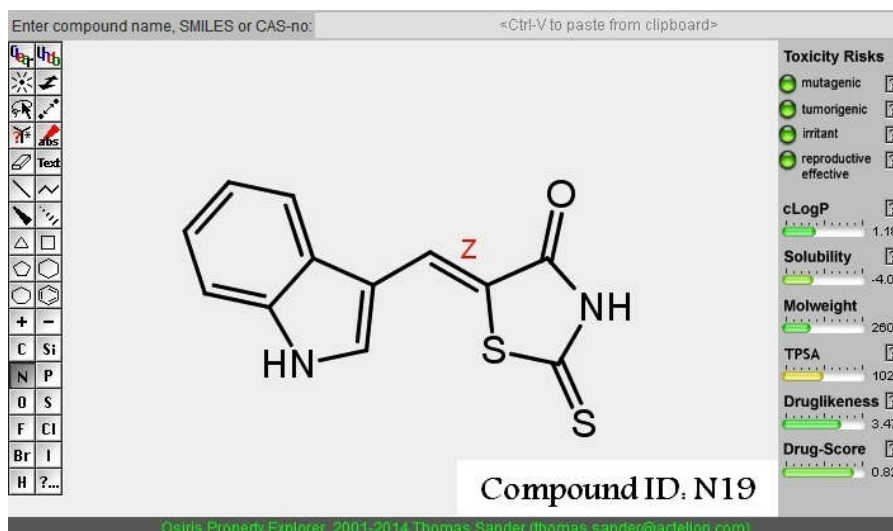


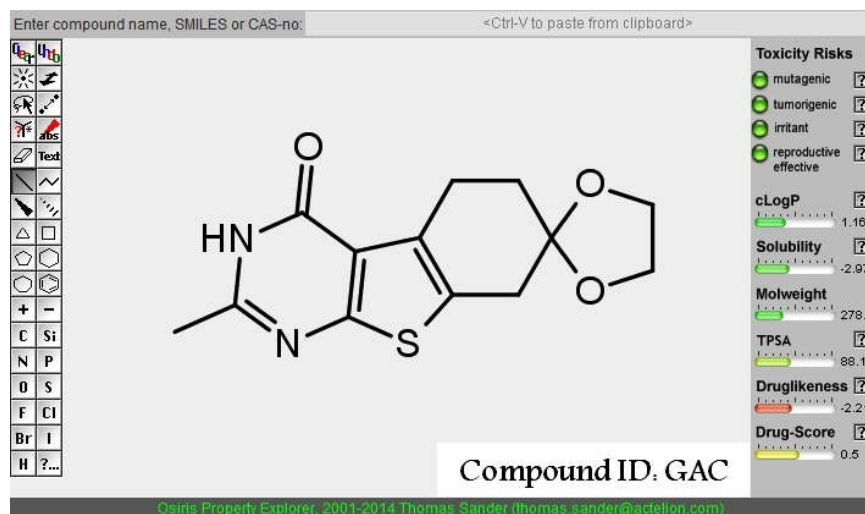
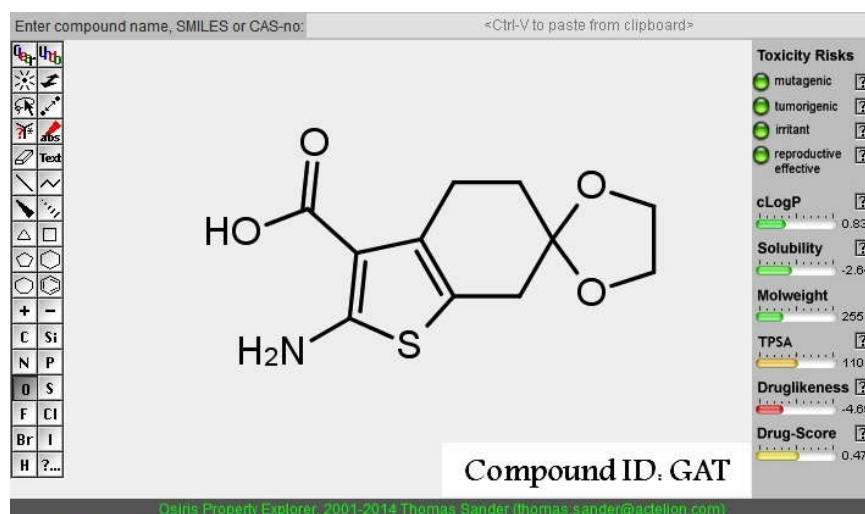
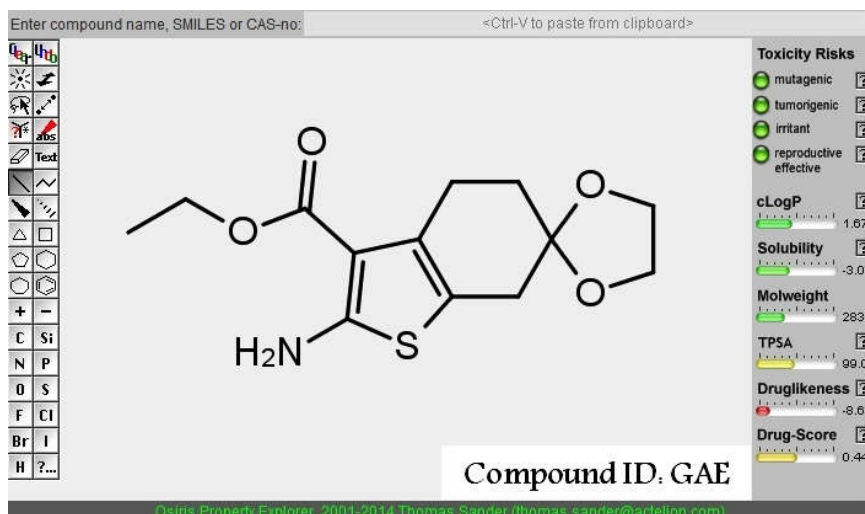




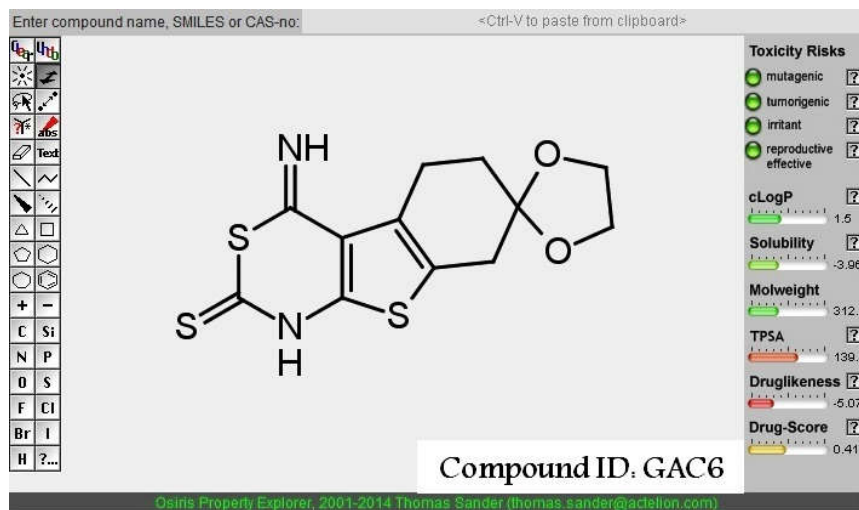
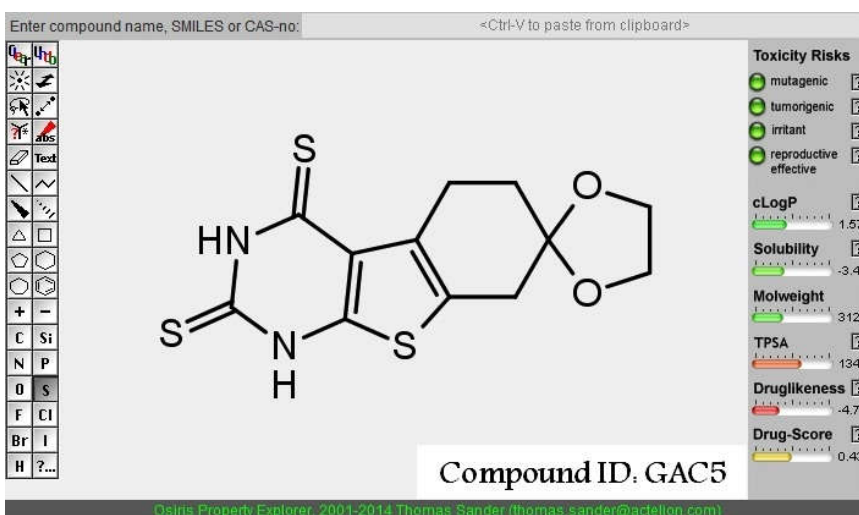
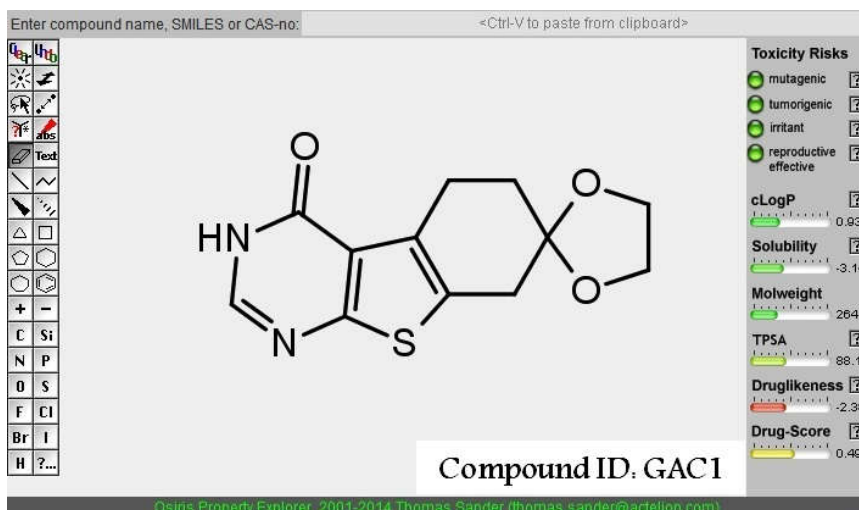


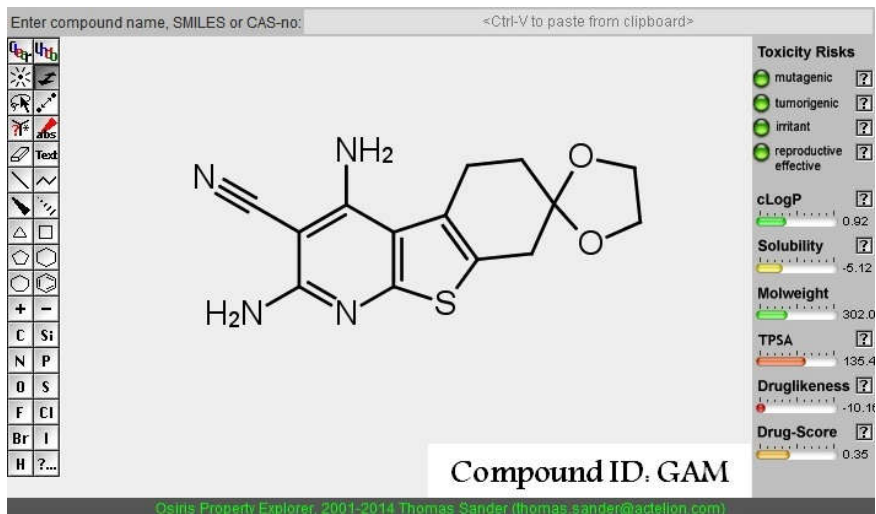
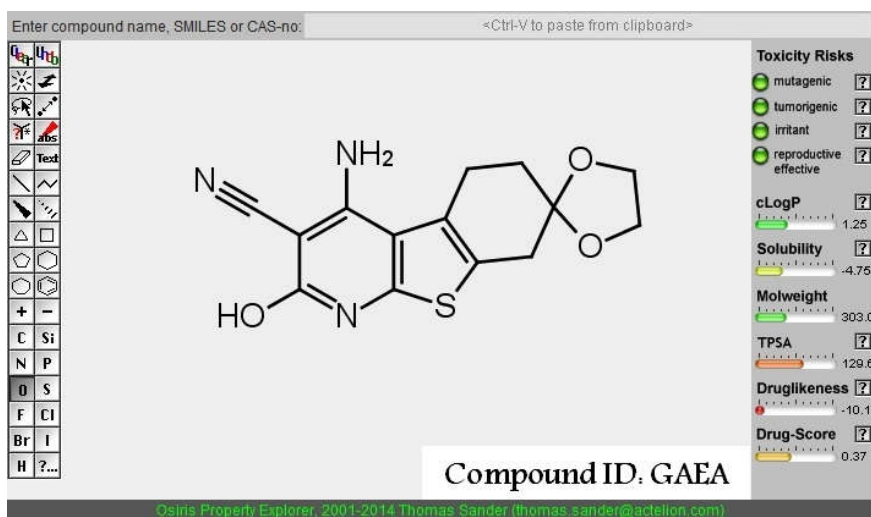
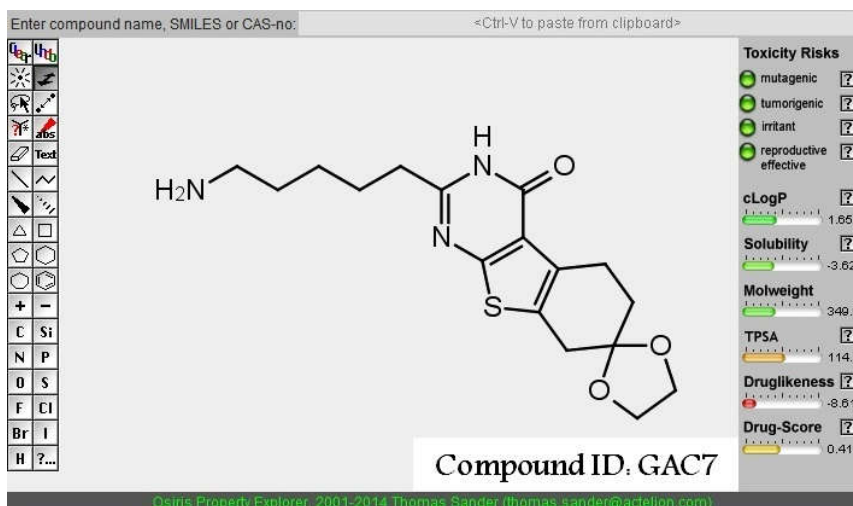












# CHAPTER 5

## CHEMISTRY

Based upon the results obtained from the *in-silico* approach 30 ligand molecules were selected for synthesis. The selected molecules belongs to the following class,

- 20 thiazolidinone analogues and
- 10 dioxolan based analogues comprising
  - ✓ thieno-pyrimidine core (4 ligand molecules),
  - ✓ thieno-pyridine core (2 ligand molecules),
  - ✓ thieno-thiazine core (1 ligand molecule) and
  - ✓ dihydro benzo-thiophene (3 ligand molecules).

### 5.1. Materials

- The chemicals required for the synthesis were procured from reputable manufacturers.
- The profile, identification and purity of the reactants were confirmed and used for the synthesis.
- The compounds were synthesized conventionally making use of a sequence of Organic Chemical Reactions. Completion of the reactions was monitored by TLC.
- The synthesized compounds were purified by re-crystallization using suitable solvents and the purity was confirmed by sharp melting points using open capillary tubes.
- The synthesized compounds were characterized by the following methods,

- ✓ IR Spectroscopy by Perkin-Elmer Spectrometer using KBr pellets.
  - ✓ <sup>1</sup>H-NMR Spectroscopy by 500 MHZ Bruker TopSpin using DMSO-d<sub>6</sub>.
  - ✓ <sup>13</sup>C-NMR Spectroscopy by 500 MHZ Bruker TopSpin using DMSO-d<sub>6</sub>.
  - ✓ MASS Spectroscopy by Perkin Elmer Clarus 600 (EI).
  - ✓ Elemental Analysis was performed by Perkin Elmer Model 240 degree c analyzer.
- X-ray crystallographic study for one of the synthetic derivative was performed by Bruker Kappa APEXII.

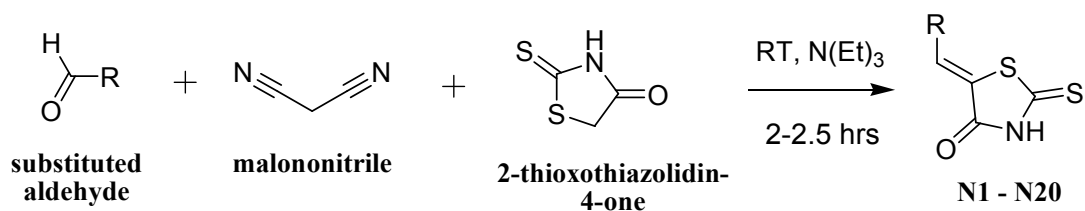
## 5.2. Experimental

**Scheme I:** Synthesis of 2-thioxo-1, 3-thiazolidin-4-one derivatives (20 Compounds).

**Scheme II:** Synthesis of 10 dioxolan based derivatives (10 Compounds).

### Synthetic Scheme I

Despite, various synthetic strategies available for the synthesis of thiazolidinone derivatives in literatures, a new approach was handled in order to synthesize 20 designed analogs bearing thiazolidinones. It is a simple and expedient sequential three component reaction of benzaldehyde, malononitrile and 2-thioxo-1, 3-thiazolidin-4-one in ethanol and in presence of triethylamine base under room temperature stirring to afford (*Z*)-5-benzylidene-2-thioxothiazolidin-4-one **N1**. The reaction proceeded smoothly with the elimination of malononitrile within 2hrs and the compound was isolated by simple filtration in good yield.



**Scheme I:** General scheme representing the synthesis of *substituted-2-thioxo-1, 3-thiazolidin-4-one derivatives*

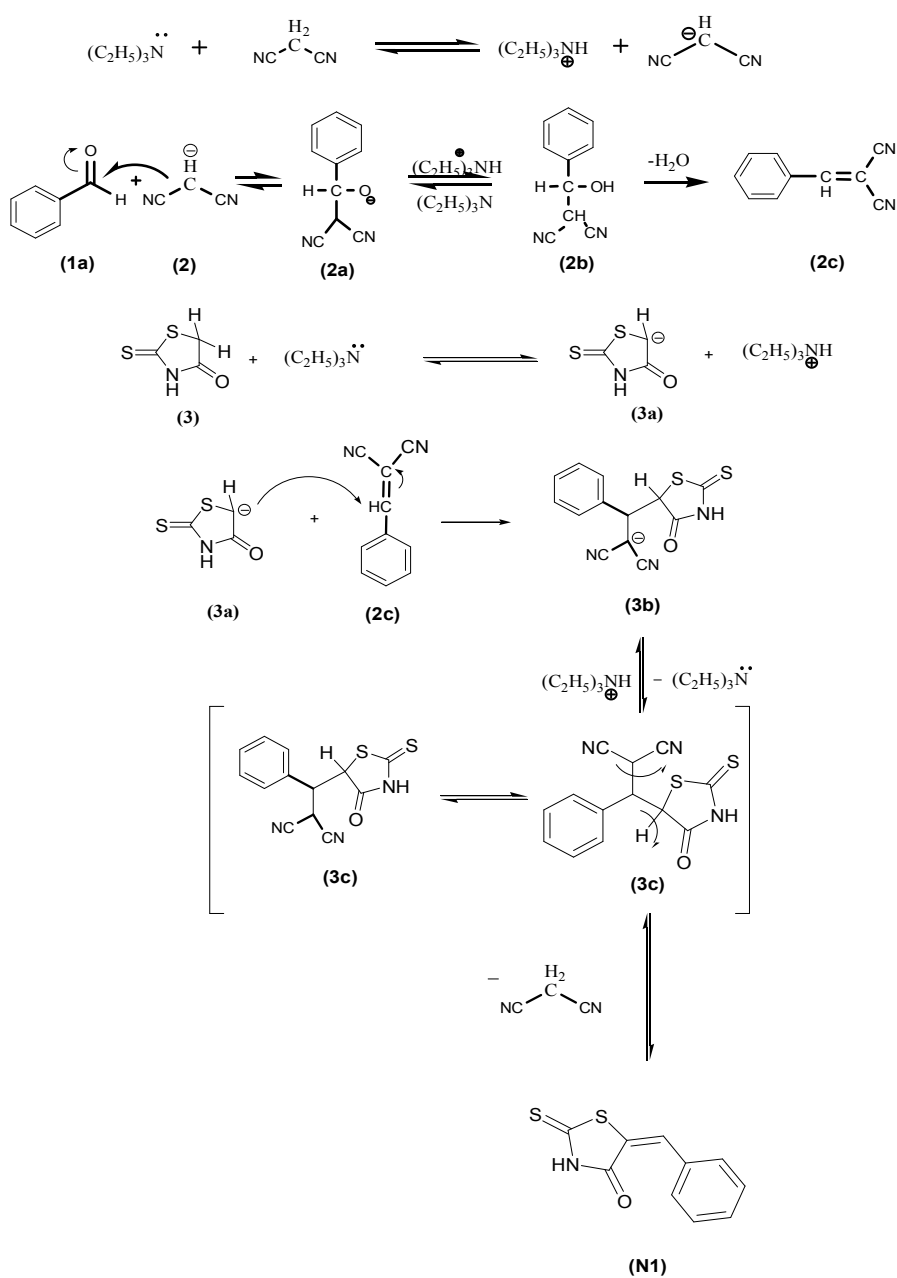
Thorough literature survey indicates that there has been no other report of using malononitrile as catalyst in the synthesis of thiazolidinone derivatives. However the use of malononitrile reagent as a catalyst has been reported in the literature. Wang X S *et al.*,<sup>124</sup> reported a highly selective methodology for synthesizing diarylallylidene malononitrile derivatives using malononitrile as catalyst.

The structure of **N1** was further verified by TLC, melting point and mixed melting point after independent synthesis via direct condensation of benzaldehyde with 2-thioxo-1, 3-thiazolidin-4-one in the presence of bases like triethylamine and sodium hydroxide. However, the independent synthetic method suffers from longer reaction times 12-24 hrs and requires aqueous workup procedures for the isolation of compound. Thus the use of malononitrile in the above reaction facilitates the reaction to take place quickly and allows the product to precipitate in the solution without any aqueous workups.

#### ***Plausible mechanism for the formation of Compound N1***

Initially, the reaction proceeded through the generation of malonyl adduct **2c** via the Knoevenagel condensation of benzaldehyde **1a** and malononitrile **2** in the presence of triethylamine base. The intermediate **2c** was isolated and its formation, proved by

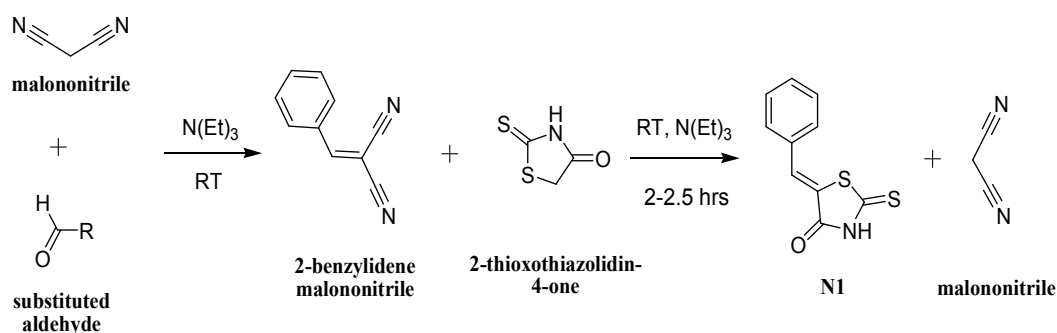
TLC. Compound **2c** a key intermediate undergone Michael Addition with **3a** to give **3c**, which upon elimination of malononitrile, leads to the formation of compound **N1**.



**Scheme-1a:** Plausible mechanism for the formation of Compound (*Z*)-5-benzylidene-2-thioxothiazolidin-4-one **N1**

***The synthetic protocol of compound N1:***

A mixture of malononitrile (1.1 mmol), benzaldehyde (1.0 mmol) and triethylamine (8-10 drops) in ethanol was stirred at room temperature. After the complete disappearance of both starting materials (monitored by TLC), 2-thioxo-1, 3-thiazolidin-4-one (1.0 mmol) was added and the stirring continued for 2 -2½hrs. After the completion of the reaction, the obtained solid was then separated by using vacuum filtration and washed with ethanol. The compound was recrystallized using methanol.



**Scheme-Ib:** Synthesis of the Compound (*Z*)-5-benzylidene-2-thioxothiazolidin-4-one **N1**

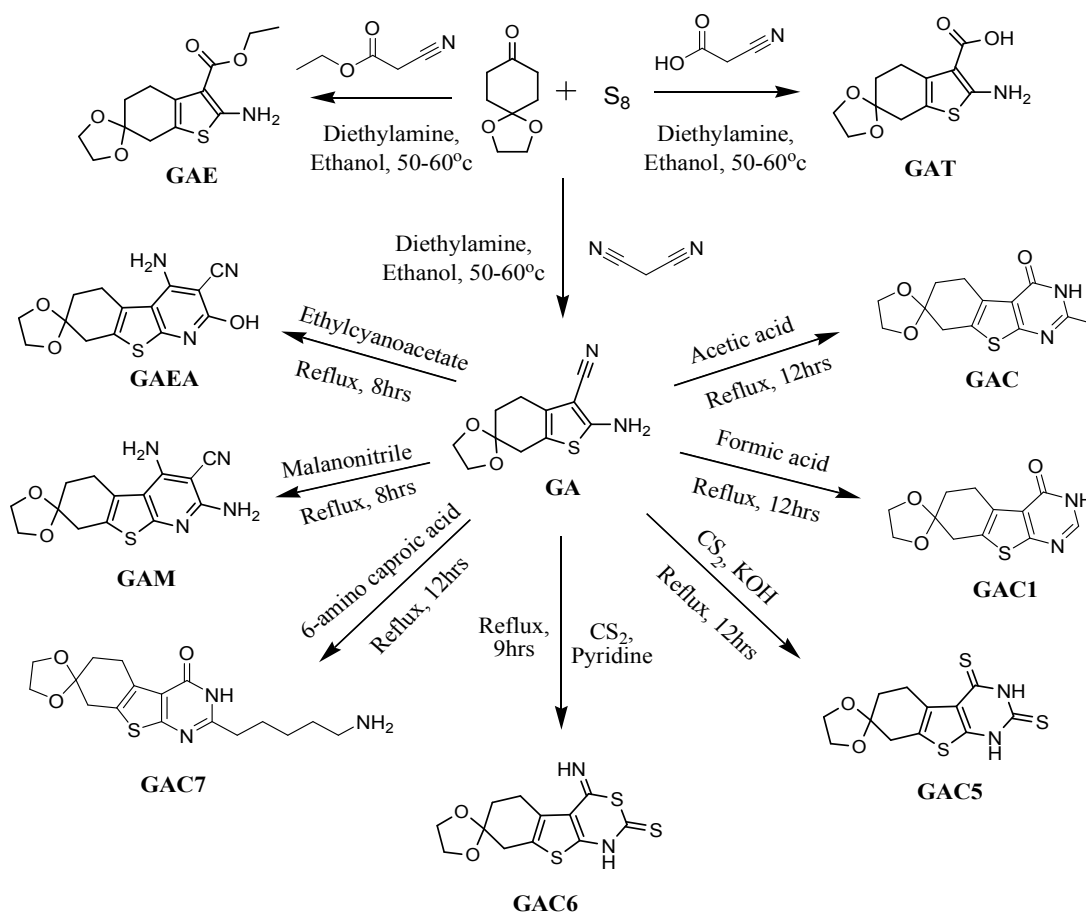
Similarly compounds N2-N20 were synthesized by changing the aldehydes such as 4-chloro-benzaldehyde, 4-dimethyl amino-benzaldehyde, 4-benzyloxy-benzaldehyde, Vanillin, Salicylaldehyde, 4-nitro-benzaldehyde, 2-bromo-benzaldehyde, 2,3-difluoro,6-methoxy-benzaldehyde, Thianaphthene-3-carboxaldehyde, Anisaldehyde, Furfural, 2-thiophene-carboxaldehyde, 3,4,5-trimethoxy-benzaldehyde, 2-naphthaldehyde, 9-anthraldehyde, 2-nitro-benzaldehyde, 3-nitro-benzaldehyde, Indole-3-carboxaldehyde, Pyrrole-2-carboxaldehyde respectively.

### ***Synthetic Scheme II***

Synthetic methodologies of 2-aminothiophenes are well established, one such is Gewald's amino-thiophene synthesis. Initially, based upon the above protocol, the three-component domino reactions of 1, 4-cyclohexanedione monoethylene acetal, malononitrile and sulfur in the presence of diethylamine was carried out. The reaction proceeded as expected with the formation of "2-amino-4, 7-dihydro-5H-spiro [benzo[b]thiophene-6, 2'-[1, 3] dioxolane]-3-carbonitrile" **GA**. Similarly, instead of malononitrile, ethyl cyanoacetate and cyano acetic acid were taken to synthesize compounds "ethyl 2-amino-4,7-dihydro-5H-spiro[benzo[b]thiophene-6,2'-[1,3]dioxolane]-3-carboxylate" **GAE** and "2-Amino-4, 7-dihydro-5H-spiro [benzo[b]thiophene-6, 2'-[1, 3] dioxolane]-3-carboxylic acid" **GAT** respectively.

Seven other compounds were synthesized from GA by modifications in the synthetic approach given by El-Gazzar ARBA *et al.*<sup>67</sup> The typical reactions with reaction conditions involved in the scheme are as follows,



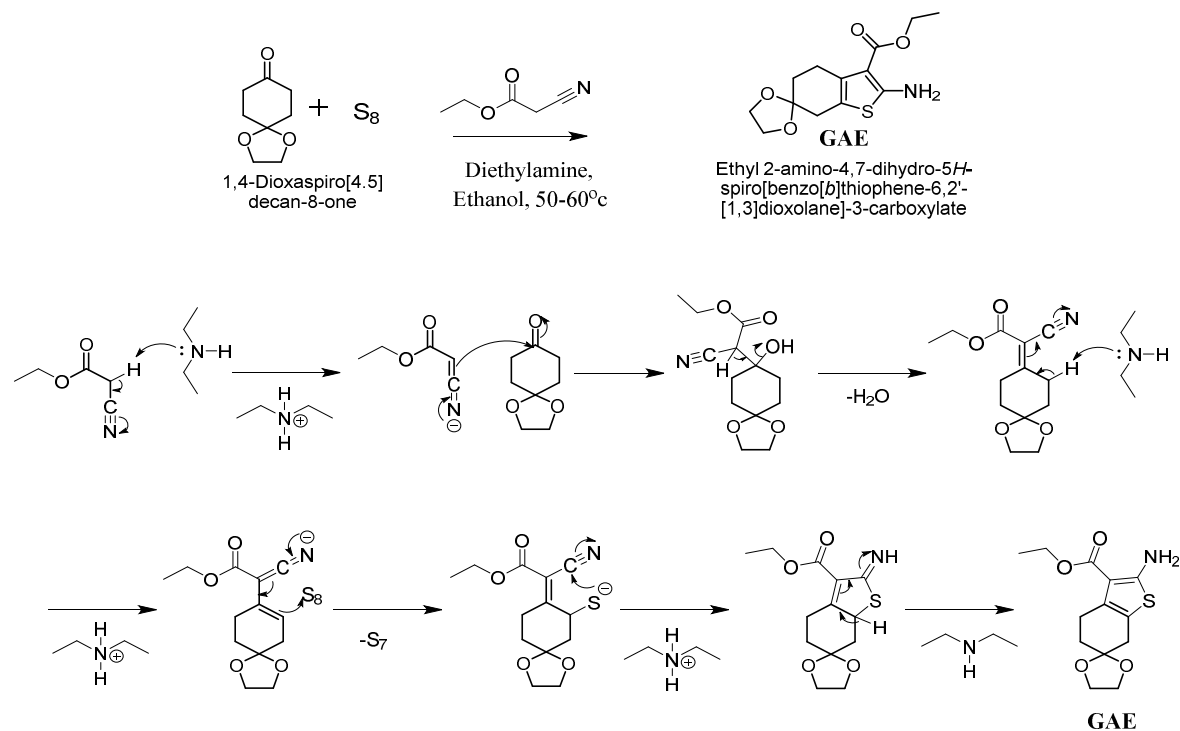


**Scheme II:** Synthesis of various dioxolan based derivatives

***Plausible mechanism for the formation of compound “Ethyl 2-amino-4, 7-dihydro-5H-spiro [benzo[b]thiophene-6, 2’-[1,3]dioxolane]-3-carboxylate” GAE:***

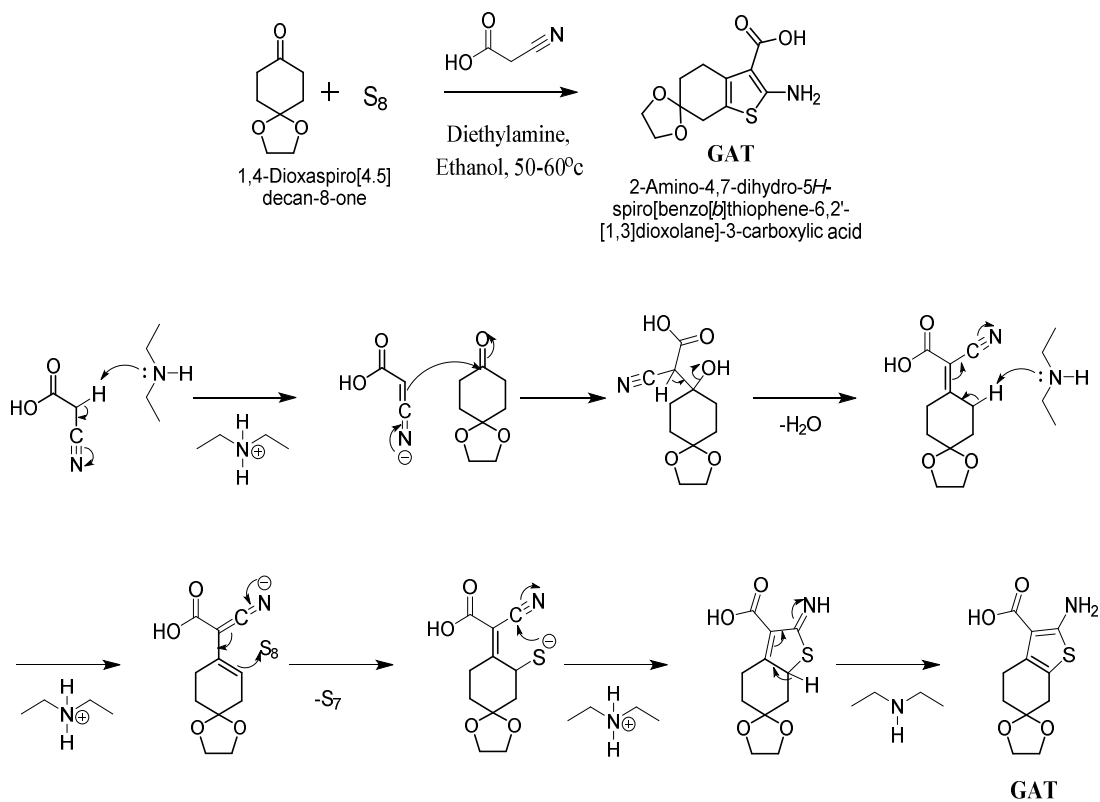
Initially, the reaction proceeded by the attack of diethyl amine towards the active methylene of ethyl cyanoacetate via Knoevenagel condensation. The base diethyl amine abstracts a proton from ethyl cyanoacetate and results in the formation of carbanion. The formed carbanion then attacks the carbonyl carbon of 1, 4-dioxaspiro [4, 5] decan-8-one, followed by the elimination of water molecule. Once again the base diethyl amine abstracts a proton from the addition product, which results in the intramolecular electron shift. This is then followed by the attack of sulphur atom, which

proceeded with the cyclization to form the title compound “*Ethyl 2-amino-4, 7-dihydro-5H-spiro [benzo[b]thiophene-6, 2’-[1, 3] dioxolane]-3-carboxylate*” **GAE**. The sequence of reactions is summarized in **Scheme IIa**.

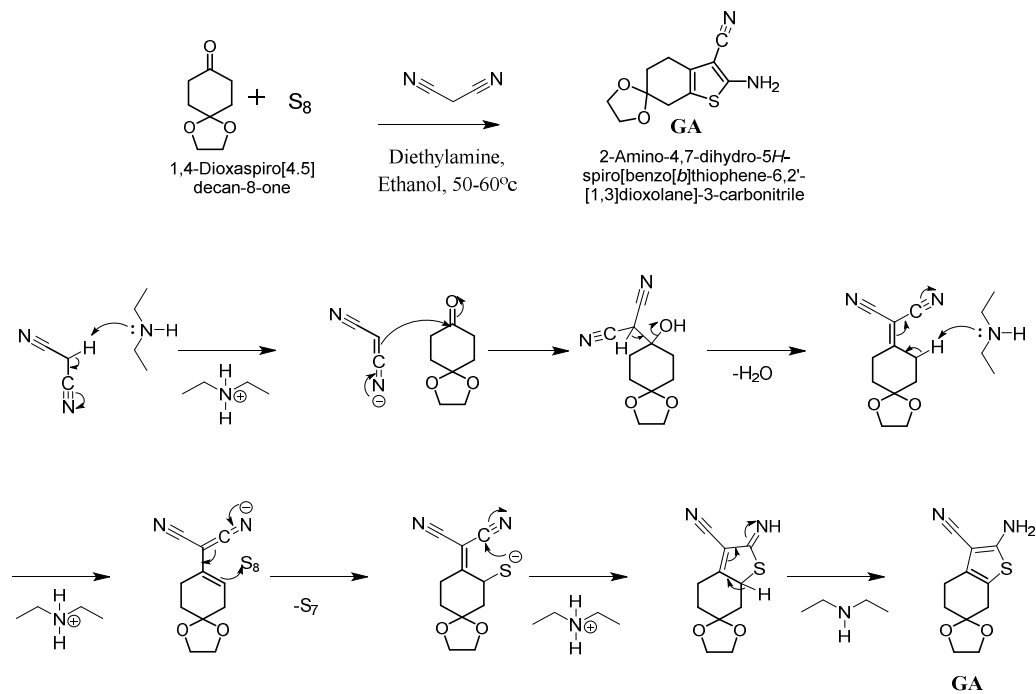


**Scheme IIa:** Synthesis and plausible mechanism for the formation of compound **GAE**

Similar mechanism is followed in the formation of compound “*2-Amino-4, 7-dihydro-5H-spiro [benzo[b]thiophene-6, 2’-[1, 3] dioxolane]-3-carboxylic acid*” **GAT** and in compound “*2-Amino-4, 7-dihydro-5H-spiro [benzo[b]thiophene-6, 2’-[1, 3] dioxolane]-3-carbonitrile*” **GA**. But instead of ethyl cyanoacetate, cyanoacetic acid and malononitrile was used in the reaction respectively. The sequences of reactions are summarized in **Scheme IIb** & **Scheme IIc** respectively.



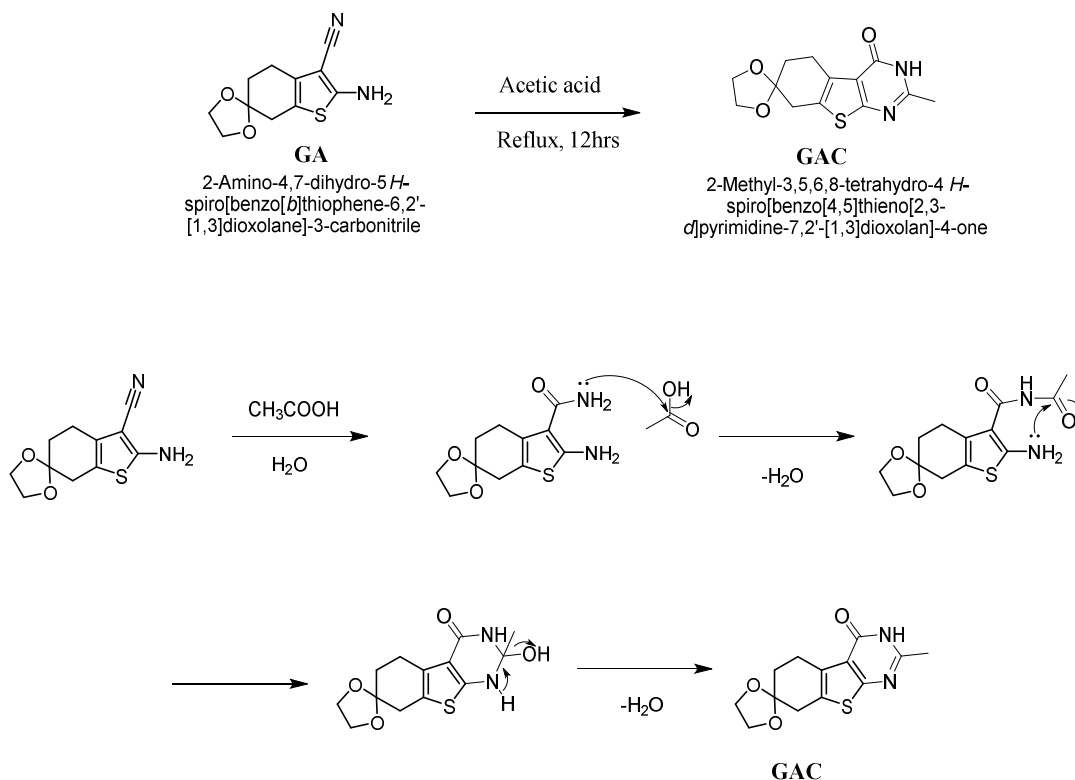
**.Scheme IIb:** Synthesis and plausible mechanism for the formation of compound **GAT**



**Scheme IIc:** Synthesis and plausible mechanism for the formation of compound **GA**

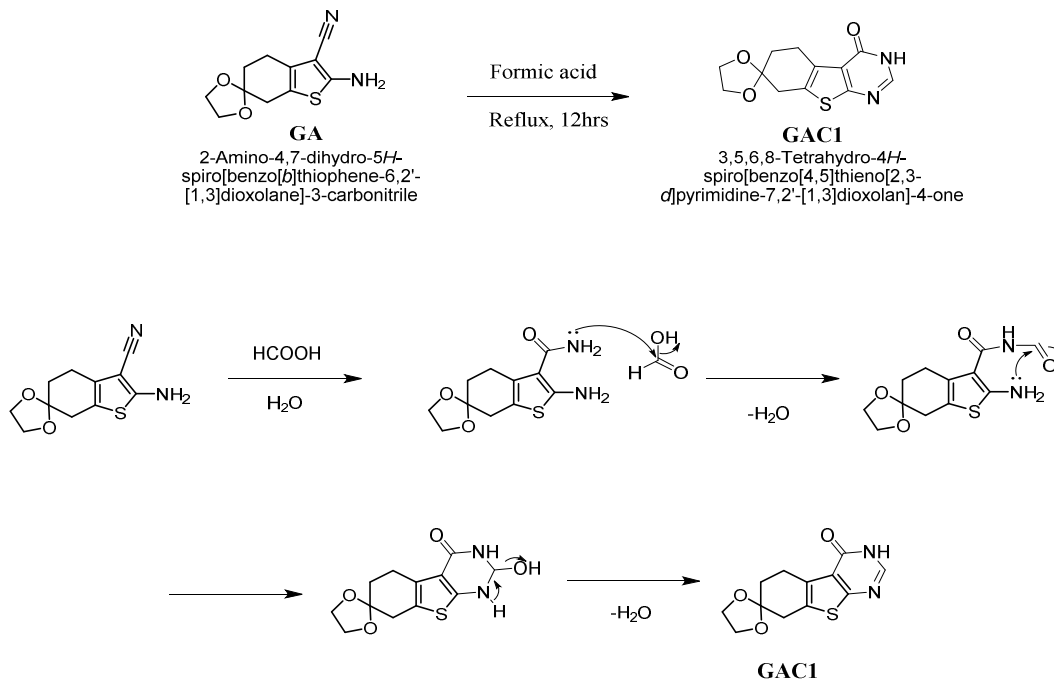
**Plausible mechanism for the formation of compound “2-Methyl-3,5,6,8-tetrahydro-4H-spiro[benzo[4,5]thieno[2,3-d]pyrimidine-7,2'-[1,3] dioxolan]-4-one” GAC:**

Compound **GAC** is formed by the reaction of compound **GA** and acetic acid. Initially, the lone pair of electrons in the amide NH<sub>2</sub> of compound **GA** attacks carboxylic carbon of the acid followed by the elimination of water molecule, for the formation of an amide intermediate. Now the extra lone pair of electrons in the amine NH<sub>2</sub> attacks the carbonyl carbon intra molecularly, as a result cyclization occurs, followed by the elimination of water molecule, leading to the formation of the title compound “2-Methyl-3,5,6,8-tetrahydro-4H-spiro[benzo[4,5]thieno[2,3-d]pyrimidine-7,2'-[1,3] dioxolan]-4-one” **GAC**. The sequence of reactions is summarized in **Scheme II**.

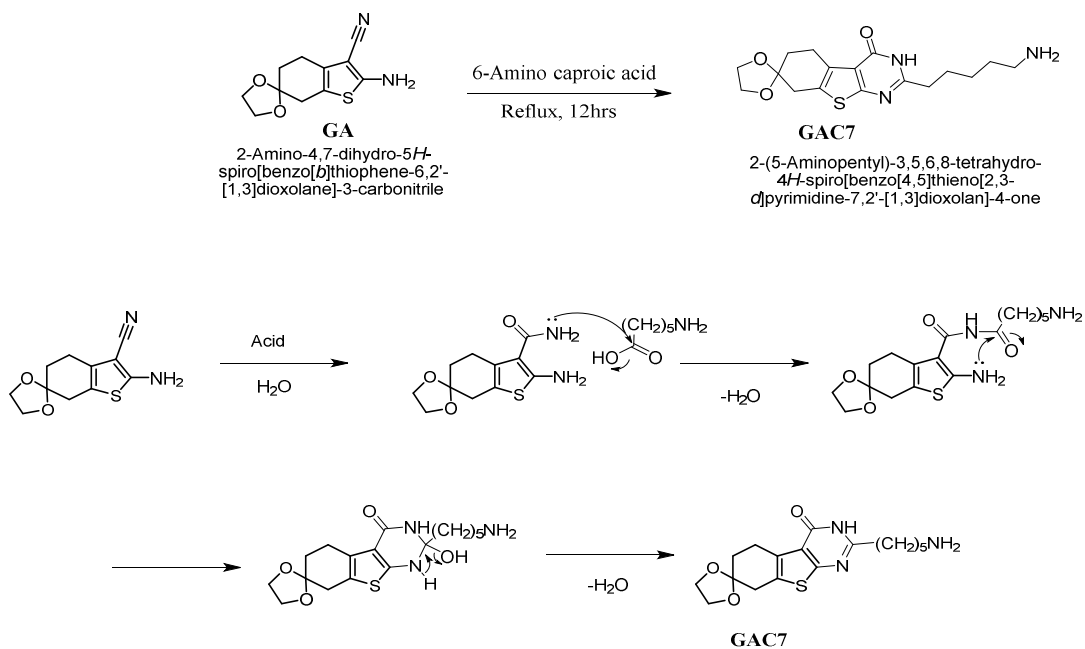


**Scheme II**: Synthesis and plausible mechanism for the formation of compound **GAC**

Compound “3,5,6,8-Tetrahydro-4H-spiro[benzo[4,5]thieno[2,3-d]pyrimidine-7,2'-[1,3]dioxolan]-4-one” **GAC1** and compound “2-(5-Aminopentyl)-3,5,6,8-tetrahydro-4H-spiro[benzo[4,5]thieno[2,3-d]pyrimidine-7,2'-[1,3]dioxolan]-4-one” **GAC7** are formed in the similar mechanism as like that of compound **GAC**. Instead of acetic acid, formic acid and 6-amino caproic acid was used for the formation of compound **GAC1** and compound **GAC7**, respectively. The sequences of reactions are summarized in **Scheme IIe** & **Scheme II f** respectively.



**Scheme IIe:** Synthesis and plausible mechanism for the formation of compound **GAC1**

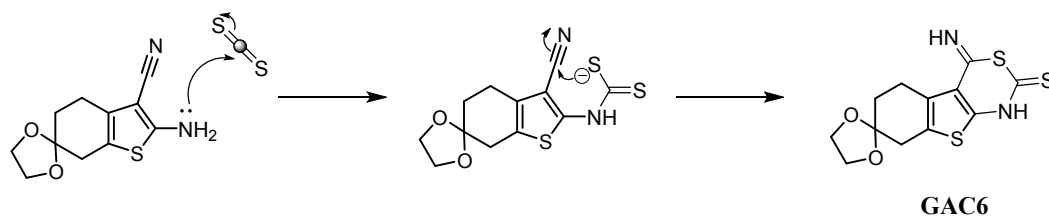
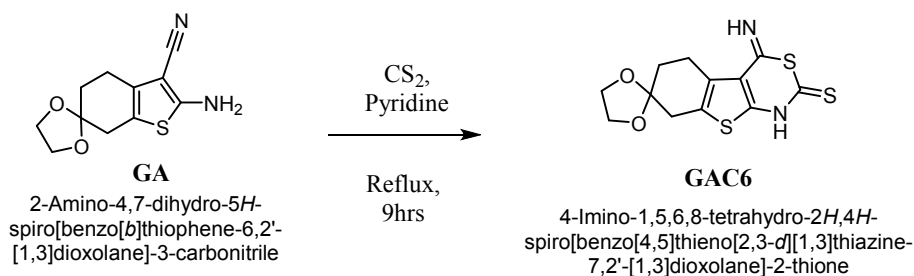


**Scheme III:** Synthesis and plausible mechanism for the formation of compound **GAC7**

*Plausible mechanism for the formation of compound “4-Imino-1,5,6,8-tetrahydro-2H,4H-spiro[benzo[4,5]thieno[2,3-d][1,3]thiazine-7,2'-[1,3]dioxolane]-2-thione”*

**GAC6:**

Formation of compound **GAC6** was achieved by the reaction between compound **GA** and carbon disulphide in the presence of pyridine. Initially, the reaction proceeded by the addition reaction mechanism between the amine nitrogen and CS<sub>2</sub> carbon. Then, the intramolecular cyclization occurs resulting in the formation of title compound **GAC6**. The sequences of reactions are summarized in **Scheme IIg**.

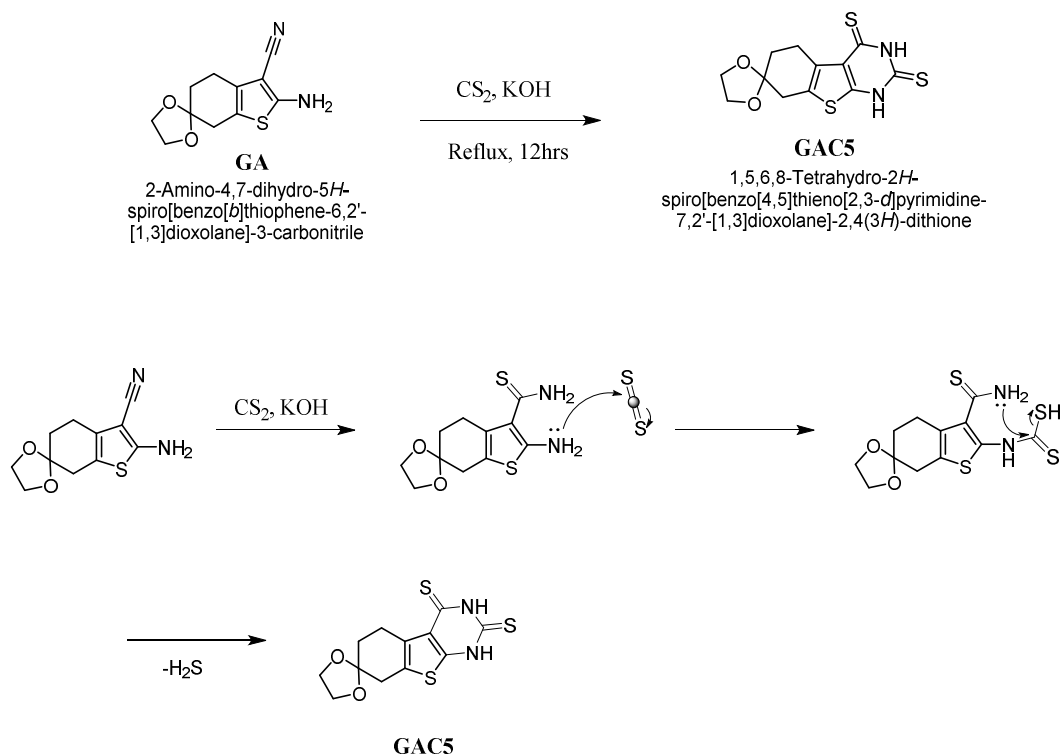


**Scheme IIg:** Synthesis and plausible mechanism for the formation of compound **GAC6**

*Plausible mechanism for the formation of compound “1,5,6,8-Tetrahydro-2H-spiro[benzo[4,5]thieno[2,3-*d*]pyrimidine-7,2'-1,3]dioxolane]-2,4(3H)-dithione”*

**GAC5:**

Formation of compound **GAC5** is as like that of the formation of compound **GAC6** but with elimination of  $\text{H}_2\text{S}$ . Initially, nitrile group present in the compound **GA** undergoes a base catalyzed oxidative hydration to form an amide derivative in the presence of potassium hydroxide. The amide intermediate is converted to thioamide intermediate upon reacting with carbon disulphide. This was achieved by an interconversion of carbonyl oxygen atoms with sulphur atoms. This intermediate once again reacts with the carbon disulphide in a similar manner like that of the formation of compound **GAC6**, resulting in the formation of compound **GAC5** with the elimination of  $\text{H}_2\text{S}$ . The sequences of reactions are summarized in **Scheme IIh**.

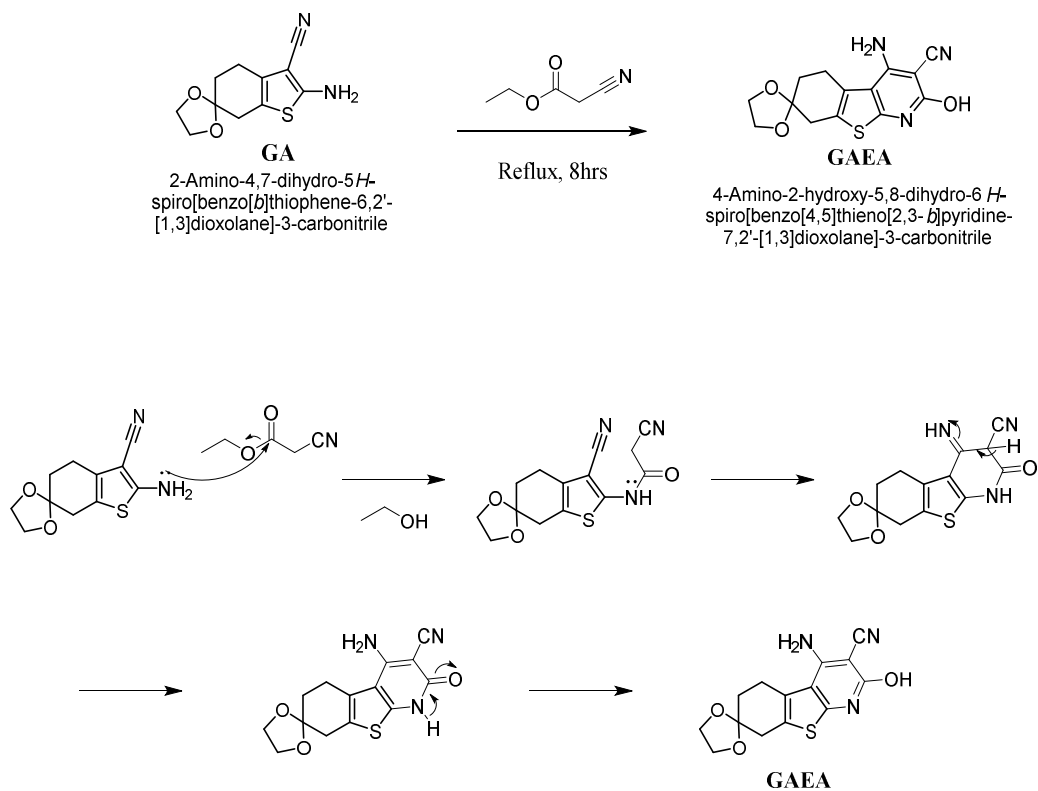


**Scheme IIIh:** Synthesis and plausible mechanism for the formation of compound **GAC5**

*Plausible mechanism for the formation of compound “4-Amino-2-hydroxy-5,8-dihydro-6H-spiro[benzo[4,5]thieno[2,3-b]pyridine-7,2'-[1,3]dioxolane]-3-carbonitrile” GAEA:*

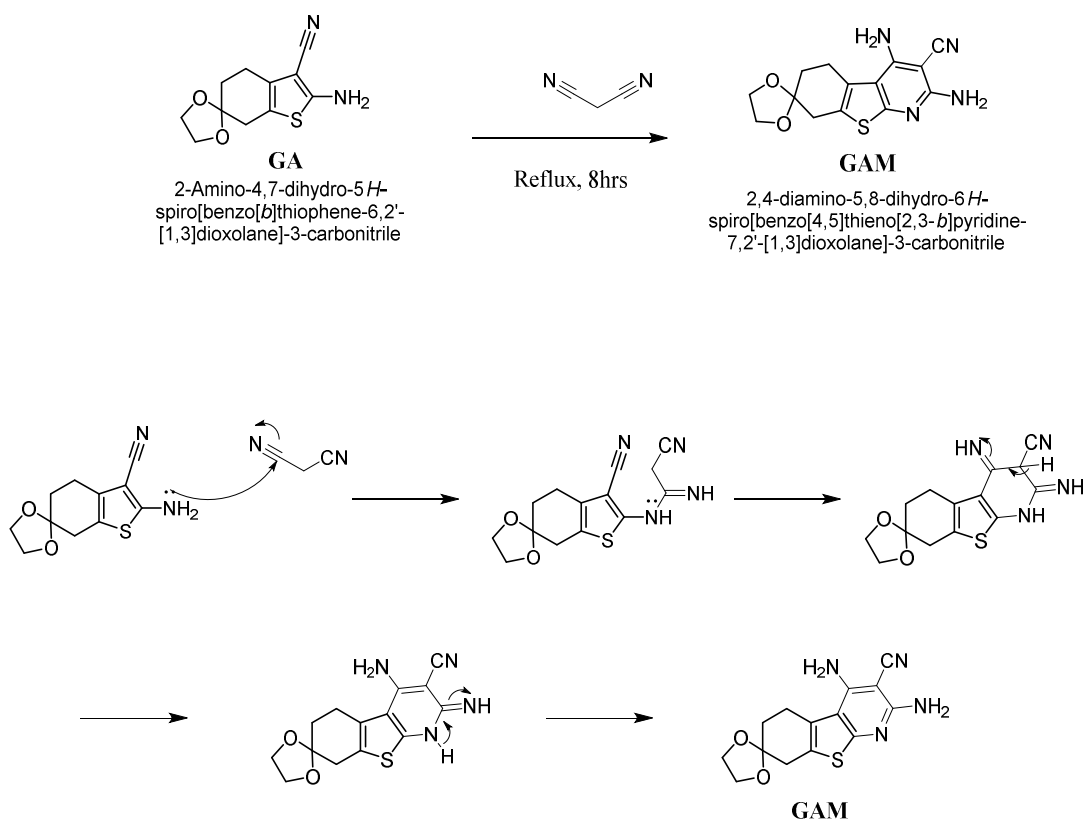
The formation of compound **GAEA** was achieved by the reaction of compound **GA** with ethyl cyanoacetate. Initially amine lone pair of electrons present in compound **GA** attacks the carbonyl carbon of ethyl cyanoacetate to give a reactive intermediate with the elimination of ethanol. This intermediate undergoes intramolecular cyclization, followed by a rearrangement *via* proton transfer leading to the formation of compound **GAEA**. The sequences of reactions are summarized in **Scheme IIIi**.





**Scheme III:** Synthesis and plausible mechanism for the formation of compound **GAEA**

Compound **GAM** is formed via similar mechanism like that of compound **GAEA**, instead of ethyl cyanoacetate, malononitrile is used. However, there is no elimination of ethanol as on the synthesis of **GAEA**. The sequences of reactions are summarized in **Scheme IIj**.



**Scheme IIj:** Synthesis and plausible mechanism for the formation of compound **GAM**

***Synthetic protocol of compound GA:***

A mixture of 1, 4-cyclohexanedione monoethylene acetal (0.01 mol), malononitrile (0.01 mol), sulfur (0.012 mol) and diethylamine (0.01 mol) was heated (60°C) under stirring in ethanol for 5 hours, and then the mixture was left at 0°C for 24 hours. The formed solid was collected by vacuum filtration and washed with ethanol. The compound was recrystallized using methanol.

***Synthetic protocol of compound GAE:***

A mixture of 1, 4-cyclohexanedione monoethylene acetal (0.01 mol), Ethyl cyanoacetate (0.01 mol), sulfur (0.012 mol) and diethylamine (0.01 mol) was heated (60°C) under stirring in ethanol for 5 hours, and then the mixture was left at 0°C for 24

hours. The formed solid was collected by vacuum filtration and washed with ethanol. The compound was recrystallized using methanol.

***Synthetic protocol of compound GAT:***

A mixture of 1, 4-cyclohexanedione monoethylene acetal (0.01 mol), Cyano acetic acid (0.01 mol), sulfur (0.012 mol) and diethylamine (0.01 mol) was heated (60°C) under stirring in ethanol for 5 hours, and then the mixture was left at 0°C for 24 hours. The formed solid was collected by vacuum filtration and washed with ethanol. The compound was recrystallized using methanol.

***Synthetic protocol of compound GAC:***

A mixture of compound **GA** “2-amino-4, 7-dihydro-5H-spiro [1-benzothiophene-6, 2’-[1, 3] dioxolane]-3-carbonitrile” (0.01 mol) and glacial acetic acid (30 mL) was stirred under reflux for 12 hours. The completion of the reaction was monitored under TLC analysis. The reaction mixture was allowed to cool to room temperature and was poured into water (100 mL). The solid thus-formed was collected by filtration, washed with ethanol (20 mL), dried and crystallized from dimethylformamide.

***Synthetic protocol of compound GAC1:***

A mixture of compound **GA** “2-amino-4, 7-dihydro-5H-spiro [1-benzothiophene-6, 2’-[1, 3] dioxolane]-3-carbonitrile” (0.01 mol) and formic acid (10 mL) and catalytic amount of concentrated hydrochloric acid was heated under reflux for 12 hours. The completion of the reaction was monitored under TLC analysis. The reaction mixture was allowed to cool to room temperature and then poured into water (100 mL). The solid thus-formed was collected by filtration, washed with ethanol (20 mL), dried and crystallized from dimethylformamide.

***Synthetic protocol of compound GAC5:***

A mixture of compound **GA** “2-amino-4, 7-dihydro-5H-spiro [1-benzothiophene-6, 2’-[1, 3] dioxolane]-3-carbonitrile” (0.01 mol) and carbon disulphide (excess 10 mL) was heated under reflux in ethanolic potassium hydroxide solution for 12 hours. The completion of the reaction was monitored under TLC analysis. The reaction mixture was allowed to cool to 0°C for 3 hours, the deposited precipitate was filtered off, washed with water (20 mL), dried and crystallized from dioxane.

***Synthetic protocol of compound GAC6:***

A mixture of compound **GA** “2-amino-4, 7-dihydro-5H-spiro [1-benzothiophene-6, 2’-[1, 3] dioxolane]-3-carbonitrile” (0.01 mol) and carbon disulphide (excess 10 mL) was heated under reflux on a waterbath (80°C) in 20 mL pyridine for 8 hours. The completion of the reaction was monitored under TLC analysis. The reaction mixture was allowed to cool to 0°C for 3 hours, the deposited precipitate was filtered off, washed with ethanol (20 mL), dried and crystallized from dioxane.

***Synthetic protocol of compound GAC7:***

A mixture of compound **GA** “2-amino-4, 7-dihydro-5H-spiro [1-benzothiophene-6, 2’-[1, 3] dioxolane]-3-carbonitrile” (0.01 mol) and 6-amino caproic acid (0.01 mol) and catalytic amount of concentrated hydrochloric acid was heated under reflux for 12 hours. The completion of the reaction was monitored under TLC analysis. The reaction mixture was allowed to cool to room temperature and was poured into water (100 mL). The solid thus-formed was collected by filtration, washed with ethanol (20 mL), dried and crystallized from dimethylformamide.

***Synthetic protocol of compound GAM:***

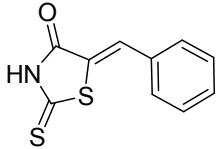
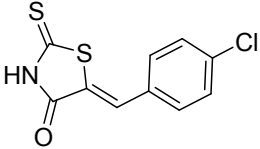
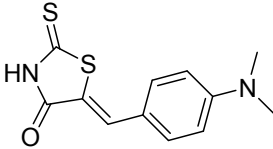
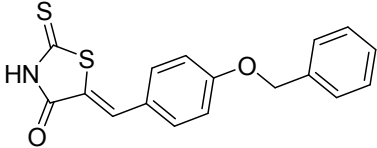
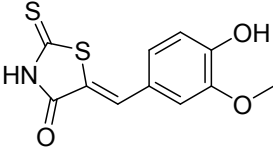
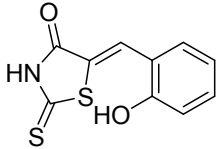
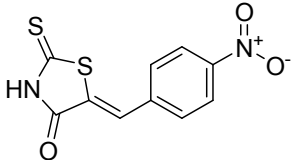
To a solution of **GA** “2-amino-4, 7-dihydro-5H-spiro [1-benzothiophene-6, 2'-[1, 3] dioxolane]-3-carbonitrile” (0.01 mol) in glacial acetic acid (50 mL), malononitrile (0.01 mol) was added. The reaction mixture was stirred under reflux for 8 hours, cooled to room temperature and was poured into cold water (100 mL). The obtained solid product was filtered off, washed with water, dried and crystallized from ethanol.

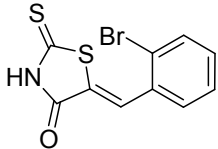
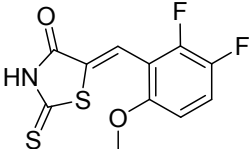
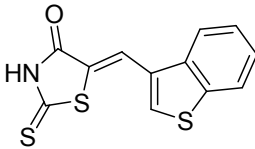
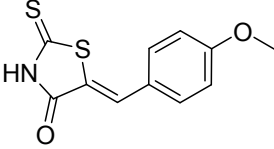
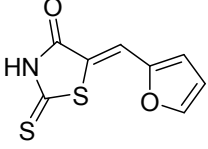
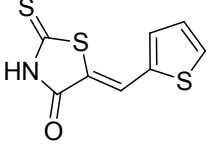
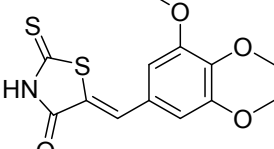
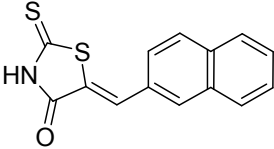
***Synthetic protocol of compound GAEA:***

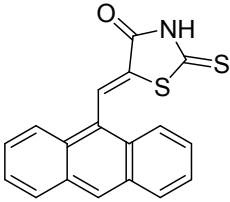
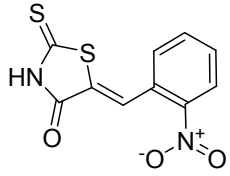
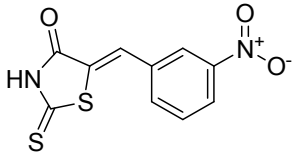
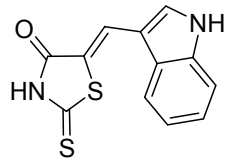
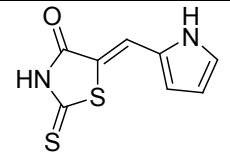
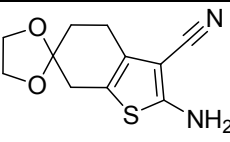
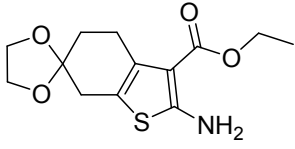
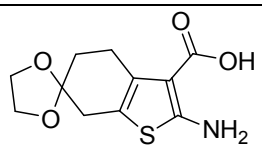
A mixture of **GA** “2-amino-4, 7-dihydro-5H-spiro [1-benzothiophene-6, 2'-[1, 3] dioxolane]-3-carbonitrile” (0.01 mol) and ethylcyanoacetate (0.01 mol) in dioxane (50 mL) containing a catalytic amount of triethylamine was stirred under reflux for 8 hours. The reaction mixture was allowed to cool and poured into cold water (100 mL) and neutralized with acetic acid. The obtained precipitate was filtered off, washed with water, dried and crystallized from dioxane.

### 5.3. Physical properties of the synthesized compounds

**Table 6:** List of synthesized compounds with their IUPAC name

Compounds	Structures	IUPAC name
N1		“(Z)-5-benzylidene-2-thioxothiazolidin-4-one”
N2		“(Z)-5-(4-chlorobenzylidene)-2-thioxothiazolidin-4-one”
N3		“(Z)-5-(4-(dimethylamino)benzylidene)-2-thioxothiazolidin-4-one”
N4		“(Z)-5-(4-(benzyloxy)benzylidene)-2-thioxothiazolidin-4-one”
N5		“(Z)-5-(4-hydroxy-3-methoxybenzylidene)-2-thioxothiazolidin-4-one”
N6		“(Z)-5-(2-hydroxybenzylidene)-2-thioxothiazolidin-4-one”
N7		“(Z)-5-(4-nitrobenzylidene)-2-thioxothiazolidin-4-one”

N8		“(Z)-5-(2-bromobenzylidene)-2-thioxothiazolidin-4-one”
N9		“(Z)-5-(2,3-difluoro-6-methoxybenzylidene)-2-thioxothiazolidin-4-one”
N10		“(Z)-5-((benzo[b]thiophen-3-yl)methylene)-2-thioxothiazolidin-4-one”
N11		“(Z)-5-(4-methoxybenzylidene)-2-thioxothiazolidin-4-one”
N12		“(Z)-5-((furan-2-yl)methylene)-2-thioxothiazolidin-4-one”
N13		“(Z)-5-((thiophen-2-yl)methylene)-2-thioxothiazolidin-4-one”
N14		“(Z)-5-(3,4,5-trimethoxybenzylidene)-2-thioxothiazolidin-4-one”
N15		“(Z)-5-((naphthalen-2-yl)methylene)-2-thioxothiazolidin-4-one”

N16		“(Z)-5-((anthracen-9-yl)methylene)-2-thioxothiazolidin-4-one”
N17		“(Z)-5-(2-nitrobenzylidene)-2-thioxothiazolidin-4-one”
N18		“(Z)-5-(3-nitrobenzylidene)-2-thioxothiazolidin-4-one”
N19		“(Z)-5-((1H-indol-3-yl)methylene)-2-thioxothiazolidin-4-one”
N20		“(Z)-5-((1H-pyrrol-2-yl)methylene)-2-thioxothiazolidin-4-one”
GA		“2-Amino-4,7-dihydro-5H-spiro[benzo[b]thiophene-6,2'-[1,3]dioxolane]-3-carbonitrile”
GAE		“Ethyl 2-amino-4,7-dihydro-5H-spiro[benzo[b]thiophene-6,2'-[1,3]dioxolane]-3-carboxylate”
GAT		“2-Amino-4,7-dihydro-5H-spiro[benzo[b]thiophene-6,2'-[1,3]dioxolane]-3-carboxylic acid”



GAC		“2-Methyl-3,5,6,8-tetrahydro-4H-spiro[benzo[4,5]thieno[2,3-d]pyrimidine-7,2'-[1,3]dioxolan]-4-one”
GAC1		“3,5,6,8-Tetrahydro-4H-spiro[benzo[4,5]thieno[2,3-d]pyrimidine-7,2'-[1,3]dioxolan]-4-one”
GAC5		“1,5,6,8-Tetrahydro-2H-spiro[benzo[4,5]thieno[2,3-d]pyrimidine-7,2'-1,3]dioxolane]-2,4(3H)-dithione”
GAC6		“4-Imino-1,5,6,8-tetrahydro-2H,4H-spiro[benzo[4,5]thieno[2,3-d][1,3]thiazine-7,2'-[1,3]dioxolane]-2-thione”
GAC7		“2-(5-Aminopentyl)-3,5,6,8-tetrahydro-4H-spiro[benzo[4,5]thieno[2,3-d]pyrimidine-7,2'-[1,3]dioxolan]-4-one”
GAEA		“4-Amino-2-hydroxy-5,8-dihydro-6H-spiro[benzo[4,5]thieno[2,3-b]pyridine-7,2'-[1,3]dioxolane]-3-carbonitrile”
GAM		“2,4-diamino-5,8-dihydro-6H-spiro[benzo[4,5]thieno[2,3-b]pyridine-7,2'-[1,3]dioxolane]-3-carbonitrile”

**Table 7: Melting Point, Percentage Yield and TLC Profile of the synthesized compounds**

Compounds	Melting point (°C)	Yield (%)	TLC Profile	
			R <sub>f</sub> value	Solvent system
N1	200-202	83	0.42	Ethyl acetate: Hexane (4:6)
N2	210-212	86	0.35	Ethyl acetate: Hexane (4:6)
N3	272-274	94	0.22	Ethyl acetate: Hexane (4:6)
N4	230-232	89	0.20	Ethyl acetate: Hexane (4:6)
N5	220-222	90	0.38	Ethyl acetate: Hexane (4:6)
N6	158-160	88	0.37	Ethyl acetate: Hexane (4:6)
N7	240-242	85	0.25	Ethyl acetate: Hexane (4:6)
N8	236-238	92	0.28	Ethyl acetate: Hexane (4:6)
N9	188-190	93	0.36	Ethyl acetate: Hexane (4:6)
N10	244-246	84	0.27	Ethyl acetate: Hexane (4:6)
N11	280-282	87	0.43	Ethyl acetate: Hexane (4:6)
N12	225-227	80	0.34	Ethyl acetate: Hexane (4:6)
N13	252-254	92	0.29	Ethyl acetate: Hexane (4:6)

N14	168-170	81	0.23	Ethyl acetate: Hexane (4:6)
N15	290-292	89	0.44	Ethyl acetate: Hexane (4:6)
N16	218-220	90	0.26	Ethyl acetate: Hexane (4:6)
N17	250-252	85	0.21	Ethyl acetate: Hexane (4:6)
N18	236-238	94	0.24	Ethyl acetate: Hexane (4:6)
N19	248-250	82	0.31	Ethyl acetate: Hexane (4:6)
N20	245-247	88	0.39	Ethyl acetate: Hexane (4:6)
GA	165-167	75	0.49	Ethyl acetate: Hexane (4:6)
GAE	81-83	62	0.40	Ethyl acetate: Hexane (4:6)
GAT	265-267	62	0.19	Ethyl acetate: Hexane (4:6)
GAC	159-161	61	0.41	Ethyl acetate: Hexane (4:6)
GAC1	145-147	66	0.46	Ethyl acetate: Hexane (4:6)
GAC5	260-262	71	0.33	Ethyl acetate: Hexane (4:6)
GAC6	258-260	73	0.47	Ethyl acetate: Hexane (4:6)
GAC7	122-124	68	0.32	Ethyl acetate: Hexane (4:6)
GAEA	162-164	67	0.30	Ethyl acetate: Hexane (4:6)
GAM	240-242	73	0.45	Ethyl acetate: Hexane (4:6)

**Table 8: Solubility data of the synthesized compounds**

<b>Compounds</b>	<b>Water</b>	<b>Methanol*</b>	<b>Ethanol*</b>	<b>Ethyl acetate</b>	<b>DMSO</b>	<b>DMF</b>
N1	I	S	S	S	S	S
N2	I	S	S	S	S	S
N3	I	S	S	S	S	S
N4	I	S	S	S	S	S
N5	I	S	S	S	S	S
N6	I	S	S	S	S	S
N7	I	S	S	S	S	S
N8	I	S	S	S	S	S
N9	I	S	S	S	S	S
N10	I	S	S	S	S	S
N11	I	S	S	S	S	S
N12	I	S	S	S	S	S
N13	I	S	S	S	S	S
N14	I	S	S	S	S	S
N15	I	S	S	S	S	S
N16	I	S	S	S	S	S
N17	I	S	S	S	S	S
N18	I	S	S	S	S	S
N19	I	S	S	S	S	S
N20	I	S	S	S	S	S
GA	I	S	S	S	S	S
GAE	I	S	S	S	S	S
GAT	I	S	S	S	S	S
GAC	I	S	S	S	S	S
GAC1	I	S	S	S	S	S
GAC5	I	S	S	S	S	S
GAC6	I	S	S	S	S	S
GAC7	I	S	S	S	S	S
GAEA	I	S	S	S	S	S
GAM	I	S	S	S	S	S

I-Insoluble, S-Soluble, \* = at 80°C

#### 5.4. Results and Discussions

A series of “5-substituted benzylidene-2-thioxo-1, 3-thiazolidin-4-one” derivatives (**N1- N20**) was synthesized by **Scheme I**. The synthesized compounds were characterized by IR,  $^1\text{H}$ , NMR,  $^{13}\text{C}$  NMR, Mass spectra and elemental analysis. The spectral data obtained for the synthesized compounds showed their respective peaks indicating their formation in the synthesis.

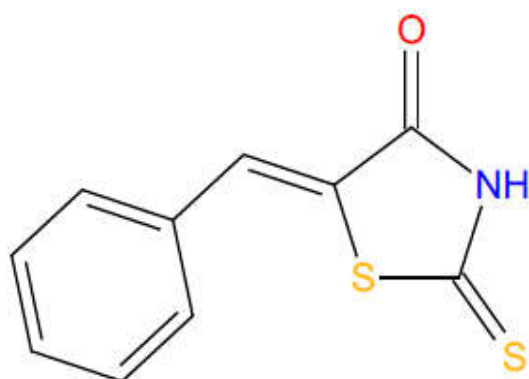
Formation of the final compounds (**N1-N20**) was confirmed by the absence of  $\text{CH}_2$  bands at around  $2950\text{ cm}^{-1}$  and the aldehyde peak with IR spectra and the appearance of peak at  $3556\text{-}3340$ ,  $1704\text{-}1566$ ,  $1798\text{-}1682\text{ cm}^{-1}$  confirms the presence of NH, C=O and C=S stretching, respectively. Furthermore the appearance of =CH peak in IR spectra in the region of  $3109\text{-}2839\text{ cm}^{-1}$  confirms the formation. Presence of alcoholic C-O, ether C-O, OH, C-NO<sub>2</sub>, CH<sub>2</sub> peaks were observed at their corresponding regions in the IR spectra confirming the structure of the final synthesized compounds.

This is also confirmed by the appearance of singlet at around  $\delta$  7.60 ppm for the formation of -CH= in  $^1\text{H}$  NMR spectra. The presence of multiplet at  $\delta$  6.76-8.08 ppm shows the presence of aromatic protons in the nuclear magnetic resonance. The heteroaromatic protons were also observed in the aromatic regions of  $^1\text{H}$  NMR spectra confirming the structure. The final compound also shows the presence of OCH<sub>3</sub>, N(CH<sub>3</sub>)<sub>2</sub> and OH groups which was confirmed by the presence of peaks in the NMR spectra at  $\delta$  3.74-3.84, 3.03-3.10, 5.03 and 10.13 ppm, respectively. The  $^{13}\text{C}$  NMR and elemental analysis were in accordance to the assumed structure. The appearance of their respective molecular ion peaks ( $\text{M}^+$ ) and also the isotopic peak ( $\text{M}^{+2}$ ) for the compound **N2** and **N8** in the mass spectroscopy confirms the formation. The Relative Stereochemistry of one the synthesized thiazolidinone derivative compound **N1** was further confirmed by X-ray Crystallography.

In **Scheme II**, a series of novel “2-amino-4,7-dihydro-5H-spiro [benzo[b] thiophene-6-2’-[1,3] dioxalane]-3-carbonitrile” derivatives (**GAC**, **GAC1**, **GAC5**, **GAC6**, **GAC7**, **GAEA** and **GAM**) and 1,4-dioxaspiro[4,5]decan-8-one derivatives (**GAE** and **GAT**) were synthesized. The spectral value of the synthesized compounds confirmed the structure. The IR peak for primary NH<sub>2</sub> group in the compound **GA** was present but when it had undergone cyclization to give subsequent products the peak was not observed. Apart from this, it was also found that the peak of CN was not observed in the next products further confirms its formation.

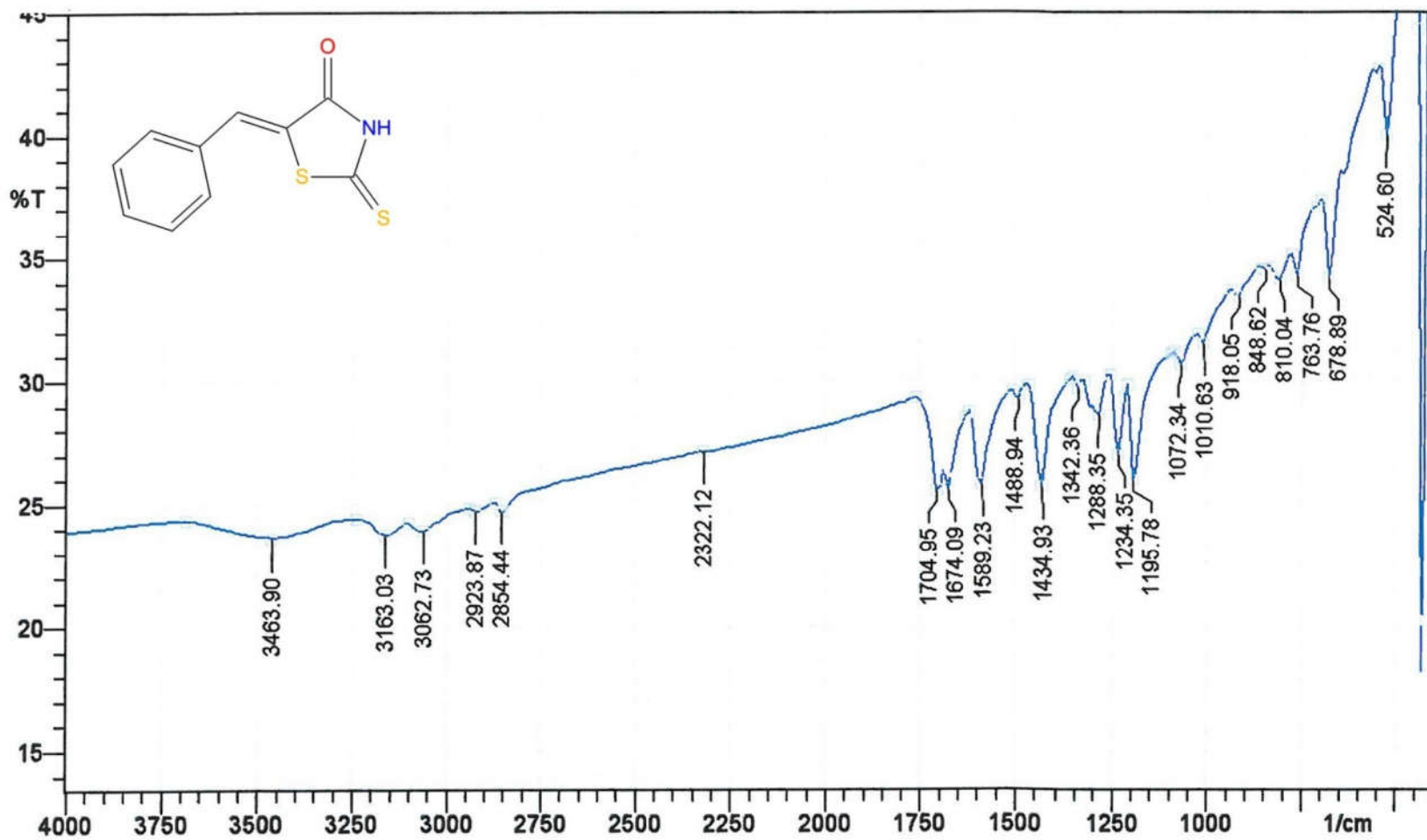
All the synthesized compounds showed the band for the aliphatic CH<sub>2</sub> protons peaks in the region of  $\delta$  1.05-3.97 in the NMR spectra. The primary NH peak of NH<sub>2</sub> that was present in the region of  $\delta$  7.02 in the compound **GA** was absent in the other compounds, which have undergone cyclization to form the compound (**GAC**, **GAC1**, **GAC5**, **GAC6**, **GAC7**, **GAEA** and **GAM**). In compound **GAC1** there was a peak in the region of  $\delta$  7.16 for pyrimidine CH which confirmed its formation. Two peaks were observed in the NMR spectra for the region of NH reduced pyrimidine NH. The appearance of the molecular ion peaks (M<sup>+</sup>) at 278, 264, 312, 312, 349, 303 and 302 confirms the formation of **GAC**, **GAC1**, **GAC5**, **GAC6**, **GAC7**, **GAEA** and **GAM**, respectively. The keto group that was present in the compound 1, 4-dioxaspiro[4, 5]decan-8-one was found to be absent in compound **GAE** and **GAT**. This confirms the formation of the compound. The IR spectrum of compound **GAE** and **GAT** shows the presence of ester and acid group by the appearance of peak in their respective region. Similarly, the peak for acid and aliphatic protons was noticed in the NMR spectra. The appearance of their respective molecular peaks (M<sup>+</sup>) in the mass spectroscopy confirms the formation. The <sup>13</sup>C NMR and elemental analysis were in accordance to the assigned structure. The spectral data of all the synthesized compounds including their spectra’s are as follows,

## Spectral Data of Compound N1



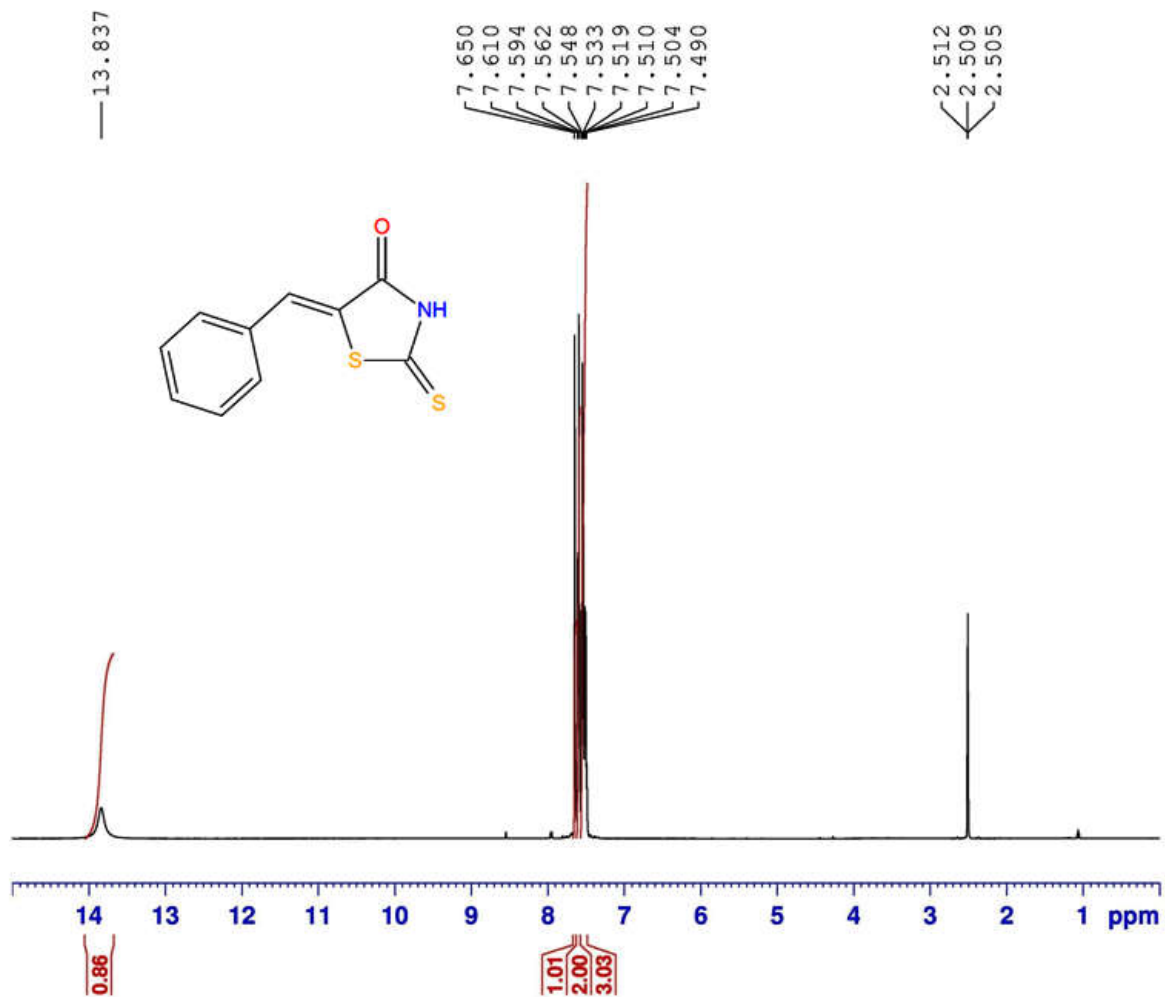
<b>IR (KBr, <math>\nu_{\max}</math>) <math>\text{cm}^{-1}</math></b>	1488.94 (Ar C-C), 1674.09 (C=O), 1704.95 (C=S), 2923.87 (=C-H), 3062.73 (Ar C-H), 3463.90 (N-H).
<b><math>^1\text{H}</math> NMR (DMSO-<math>\text{D}_6</math>) <math>\delta</math></b>	7.49-7.56 (m, 3H, Ar-H), 7.60 (d, 2H, Ar-H), 7.65 (s, 1H, =CH-), 13.83 (s, 1H, N-H).
<b><math>^{13}\text{C}</math> NMR (DMSO-<math>\text{D}_6</math>) <math>\delta</math></b>	116.17, 126.00, 129.91, 130.93, 131.19, 132.10, 133.44, 143.11, 169.81, 196.16.
<b>MASS SPECTROSCOPY</b>	221.05 ( $\text{M}^+$ ), 222.09 ( $\text{M}+1$ ), 134.11 ( <b>B</b> ).

Sample: N 1





N1.....Noorulla.



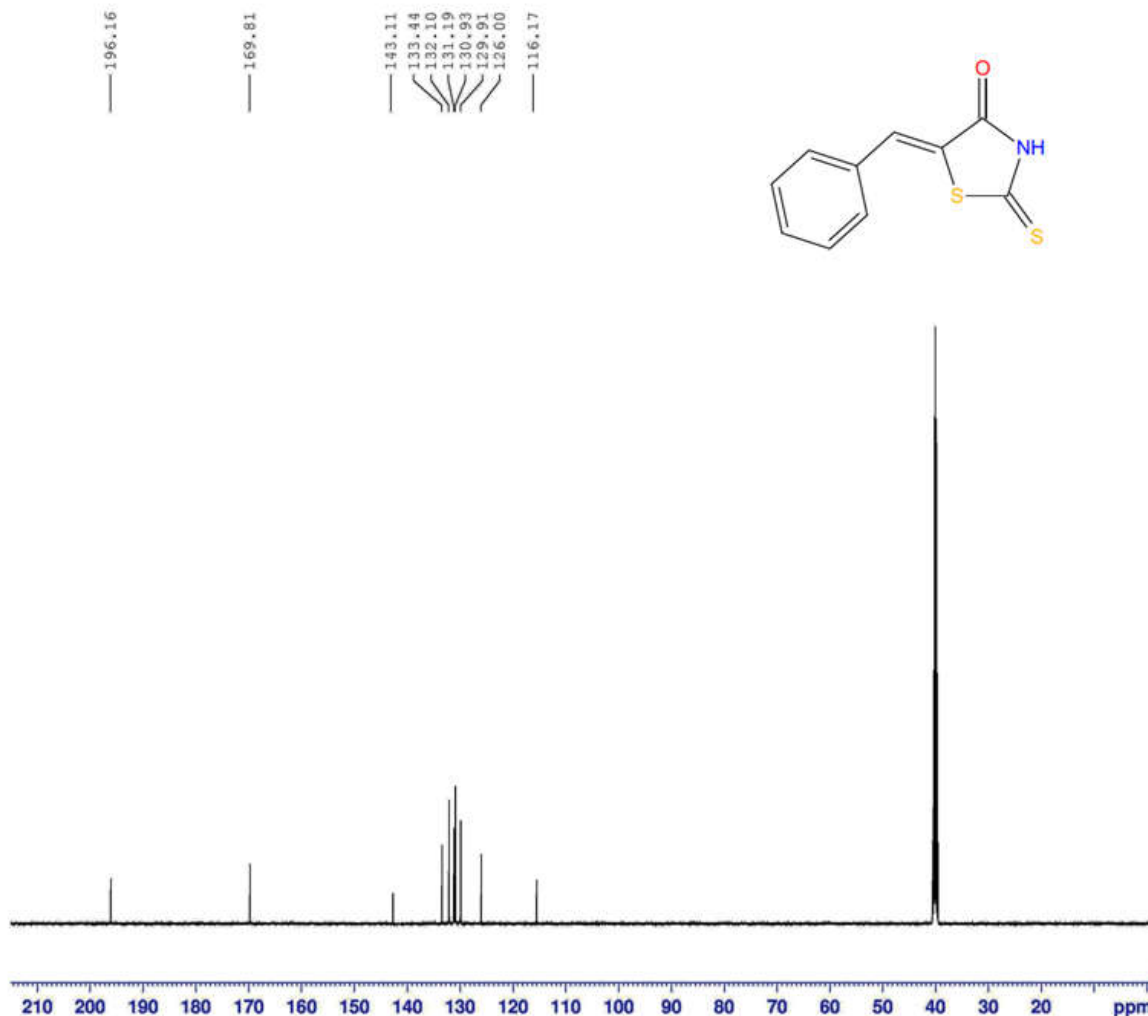
Current Data Parameters  
NAME N1  
EXPNO 11  
PROCNO 1

F2 - Acquisition Parameters  
Date\_ 20130911  
Time 2.51  
INSTRUM spect  
PROBHD 5 mm PABBO BB-  
PULPROG zg30  
TD 32768  
SOLVENT DMSO  
NS 32  
DS 2  
SWH 10330.578 Hz  
FIDRES 0.315264 Hz  
AQ 1.5860212 sec  
RG 203  
DW 48.400 usec  
DE 6.50 usec  
TE 299.7 K  
D1 1.00000000 sec  
TD0 1

===== CHANNEL f1 =====  
NUC1 1H  
P1 10.65 usec  
PL1 0 dB  
PL1W 23.53637505 W  
SFO1 500.1330885 MHz

F2 - Processing parameters  
SI 32768  
SF 500.1300000 MHz  
WDW EM  
SSB 0  
LB 0.30 Hz  
GB 0  
PC 1.00

N1.....Noorulla.



Current Data Parameters  
NAME N1  
EXPNO 12  
PROCNO 1

F2 - Acquisition Parameters  
Date\_ 20130911  
Time 3.37  
INSTRUM spect  
PROBHD 5 mm PABBO BB-  
PULPROG zgpg30  
TD 32768  
SOLVENT DMSO  
NS 1024  
DS 4  
SWH 29761.904 Hz  
FIDRES 0.908261 Hz  
AQ 0.5505524 sec  
RG 203  
DW 16.800 usec  
DE 6.50 usec  
TE 301.3 K  
D1 2.00000000 sec  
D11 0.03000000 sec  
TD0 1

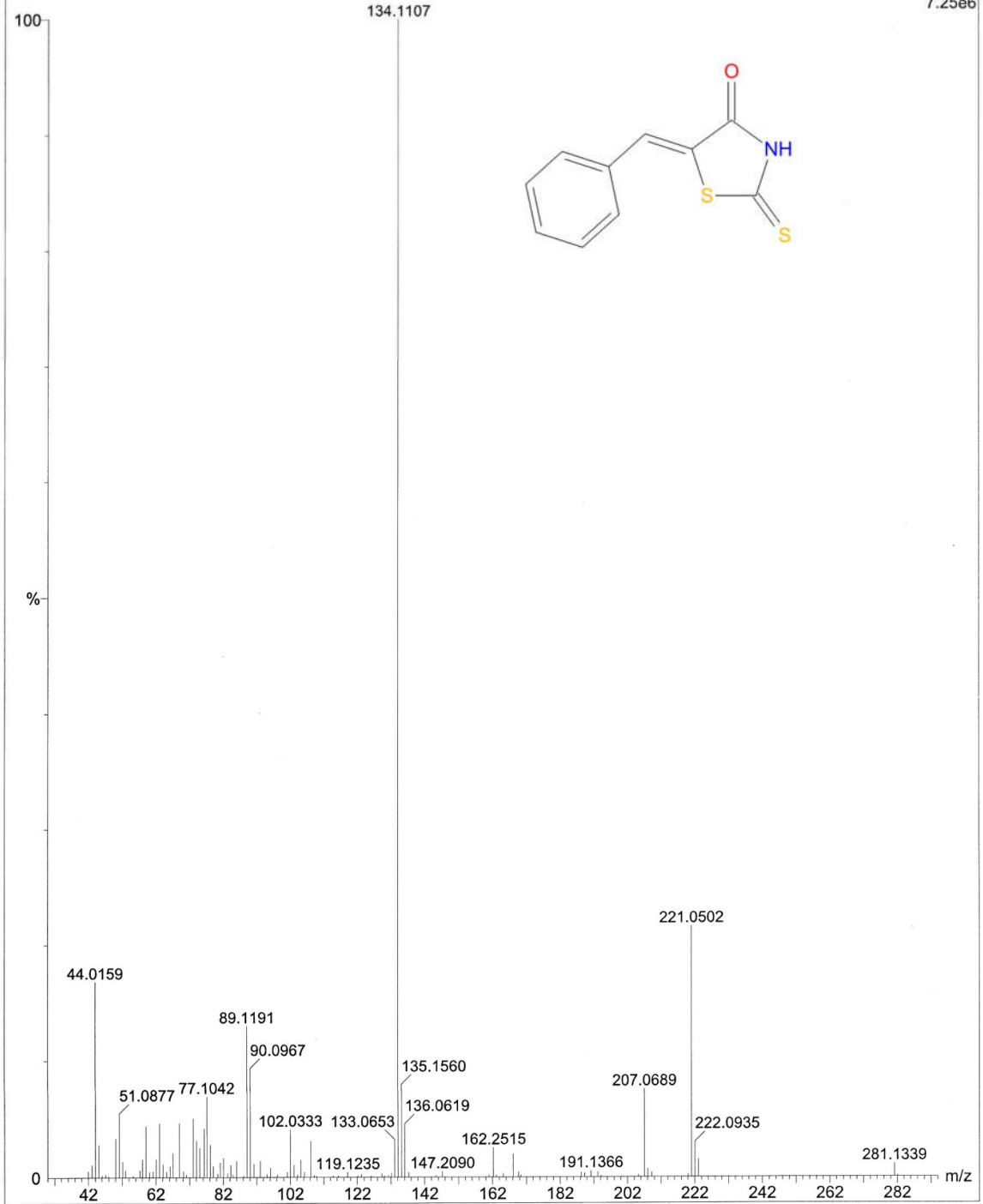
----- CHANNEL f1 -----  
NUC1 13C  
P1 7.80 usec  
PL1 0 dB  
PL1W 70.83519745 W  
SFO1 125.7703643 MHz

----- CHANNEL f2 -----  
CPDPRG2 waltz16  
NUC2 1H  
PCPD2 80.00 usec  
PL2 0 dB  
PL12 17.51 dB  
PL13 18.00 dB  
PL2W 23.53637505 W  
PL12W 0.41757989 W  
PL13W 0.37302643 W  
SFO2 500.1320005 MHz

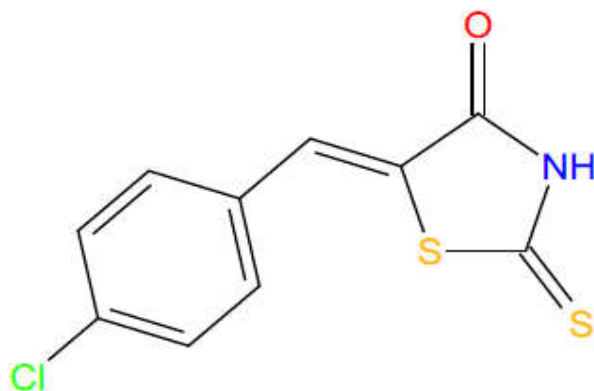
F2 - Processing parameters  
SI 32768  
SF 125.7577890 MHz  
WDW EM  
SSB 0  
LB 1.00 Hz  
GB 0  
PC 1.40

N1- 3807 (21.541)

Scan EI+  
7.25e6

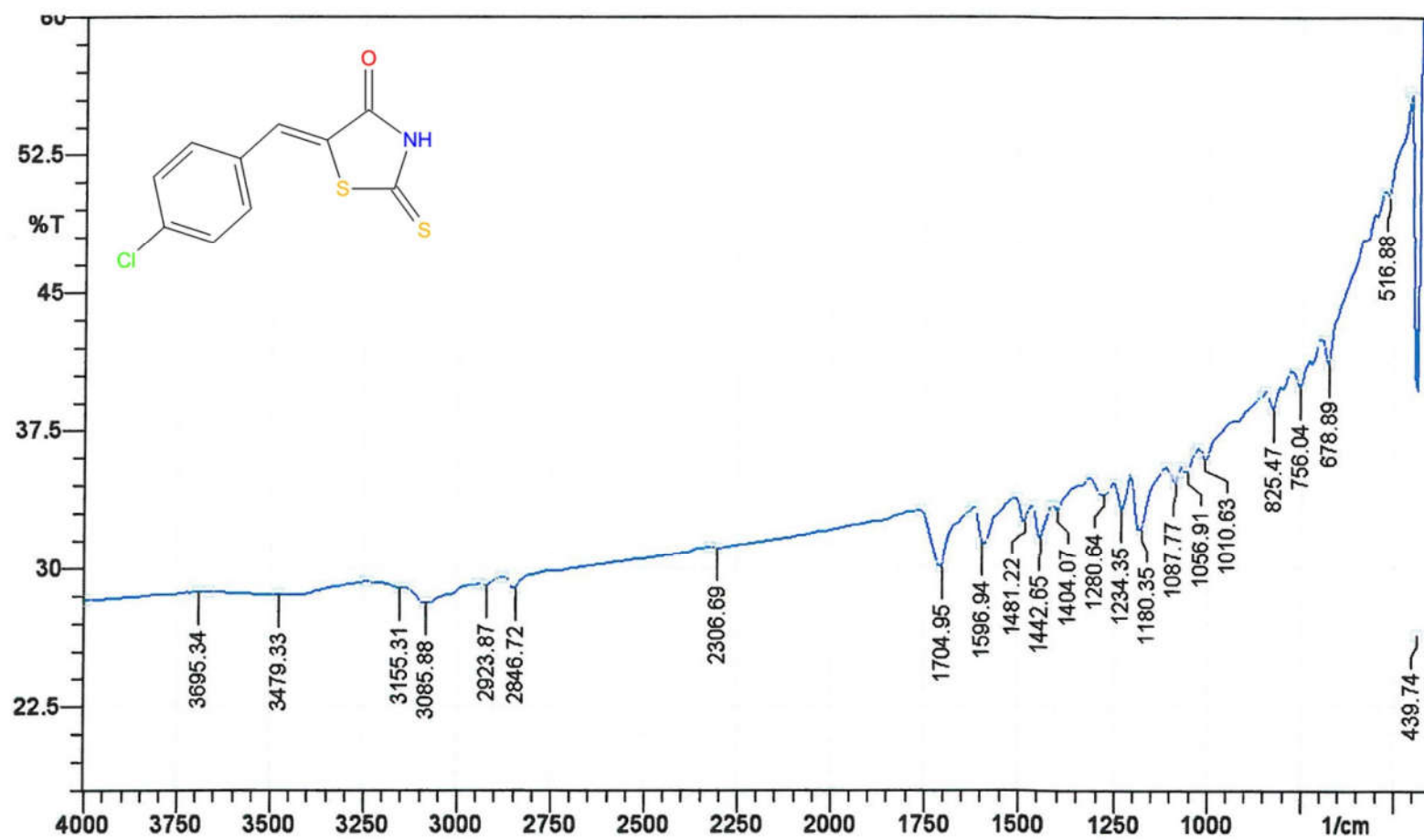


## Spectral Data of Compound N2

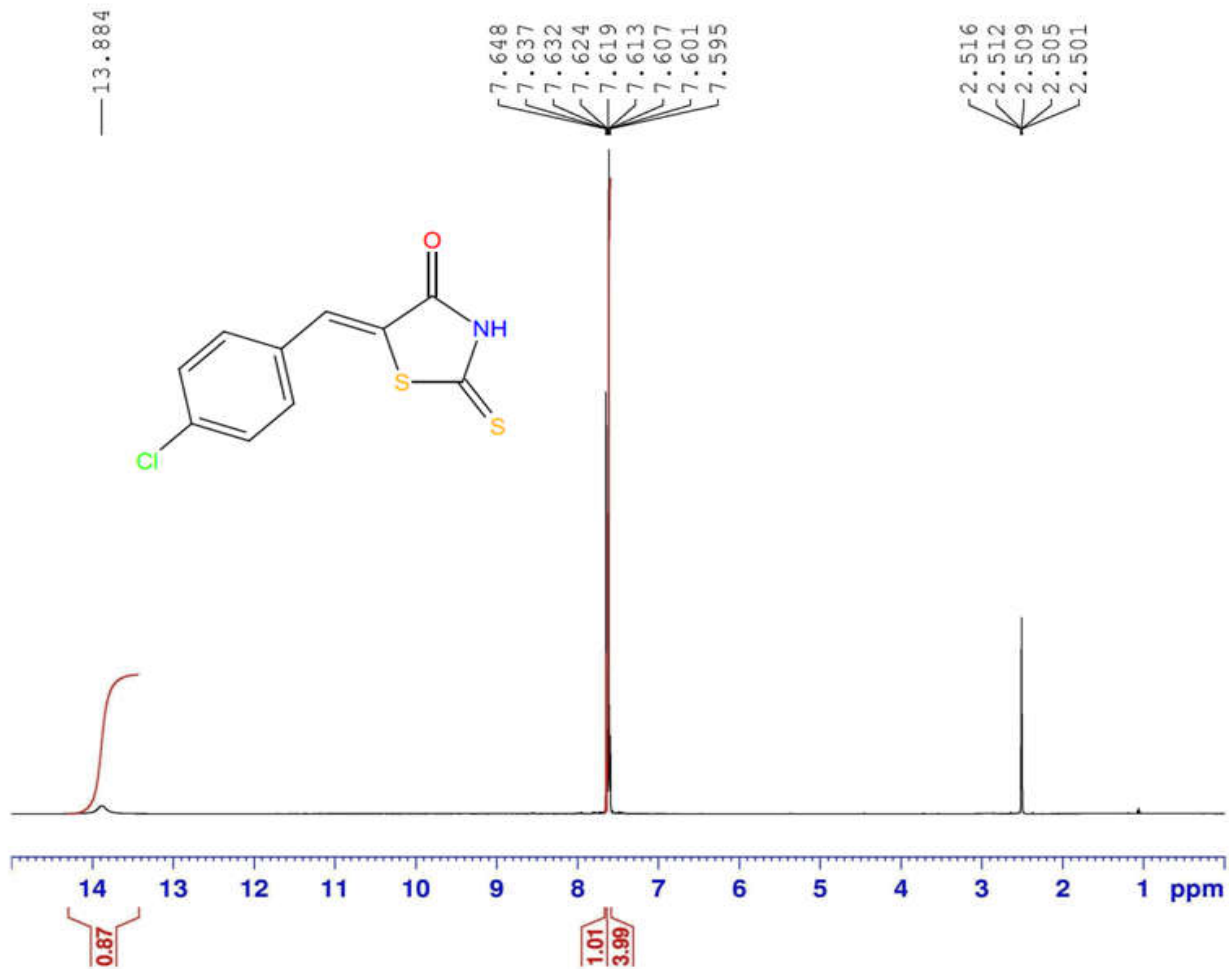


<b>IR (KBr, <math>\nu_{\max}</math>) <math>\text{cm}^{-1}</math></b>	825.47 (C-Cl), 1442.65 (Ar C-C), 1596.94 (C=O), 1704.95 (C=S), 2923.87 (=C-H), 3085.88 (Ar C-H), 3479.33 (N-H).
<b><math>^1\text{H}</math> NMR (DMSO-<math>\text{D}_6</math>) <math>\delta</math></b>	7.59-7.63 (m, 4H, Ar-H), 7.64 (s, 1H, =CH-), 13.88 (s, 1H, N-H).
<b><math>^{13}\text{C}</math> NMR (DMSO-<math>\text{D}_6</math>) <math>\delta</math></b>	115.14, 126.78, 129.98, 130.65, 132.36, 132.53, 135.82, 140.43, 169.78, 195.88
<b>MASS SPECTROSCOPY</b>	255.05 ( $\text{M}^+$ ), 257.07 ( $\text{M}+2$ ), 168.16 ( <b>B</b> ).

Sample: N 2



N2.....Noorulla.



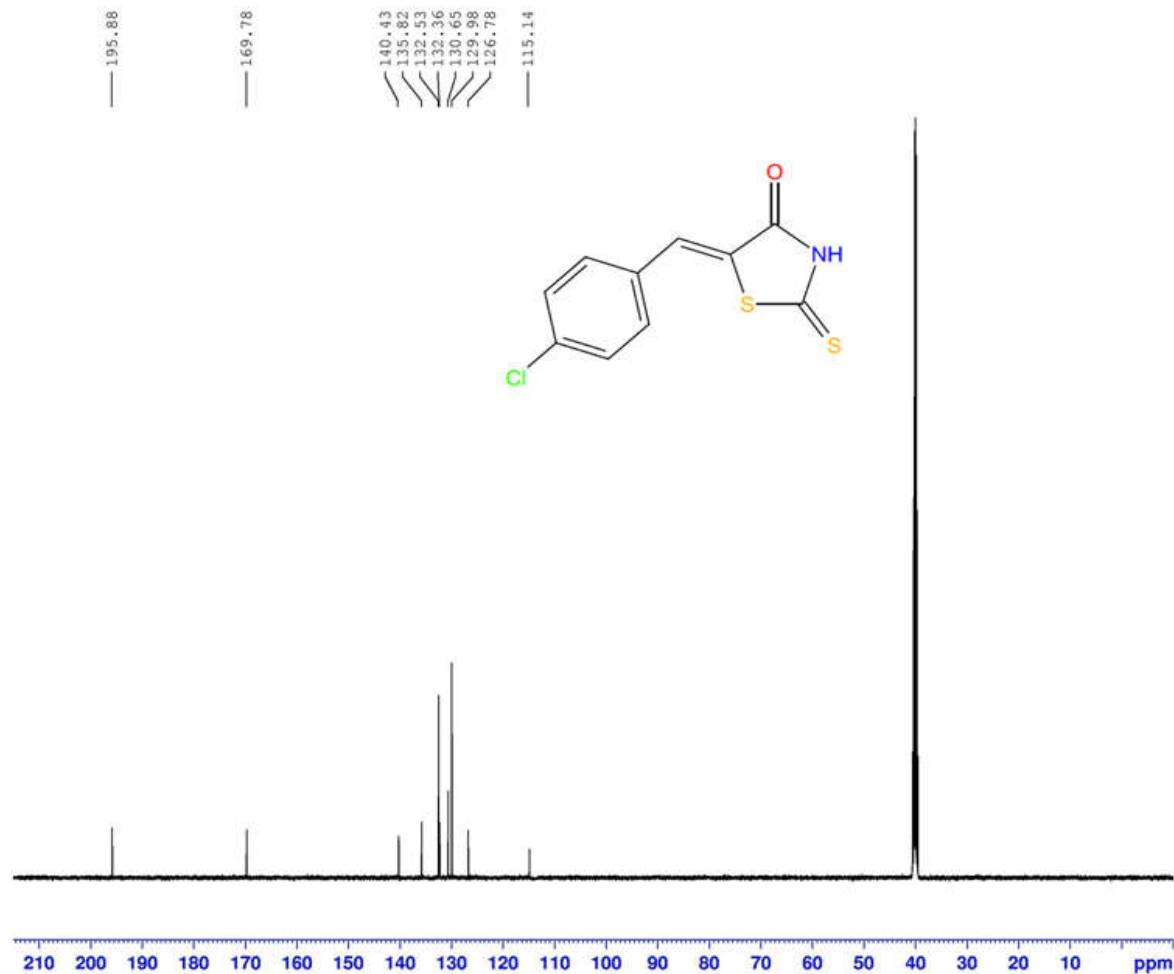
Current Data Parameters  
NAME N2  
EXPNO 5  
PROCNO 1

F2 - Acquisition Parameters  
Date\_ 20130911  
Time 0.26  
INSTRUM spect  
PROBHD 5 mm PABBO BB-  
PULPROG zg30  
TD 32768  
SOLVENT DMSO  
NS 32  
DS 2  
SWH 10330.578 Hz  
FIDRES 0.315264 Hz  
AQ 1.5860212 sec  
RG 203  
DW 48.400 usec  
DE 6.50 usec  
TE 298.3 K  
D1 1.00000000 sec  
TD0 1

===== CHANNEL f1 =====  
NUC1 1H  
P1 10.65 usec  
PL1 0 dB  
PL1W 23.53637505 W  
SFO1 500.1330885 MHz

F2 - Processing parameters  
SI 32768  
SF 500.1300000 MHz  
WDW EM  
SSB 0  
LB 0.30 Hz  
GB 0  
PC 1.00

N2.....Noorulla.



Current Data Parameters  
NAME N2  
EXPNO 6  
PROCNO 1

F2 - Acquisition Parameters  
Date\_ 20130911  
Time 1.11  
INSTRUM spect  
PROBHD 5 mm PABBO BB-  
PULPROG zgpg30  
TD 32768  
SOLVENT DMSO  
NS 1024  
DS 4  
SWH 29761.904 Hz  
FIDRES 0.908261 Hz  
AQ 0.5505524 sec  
RG 203  
DW 16.800 usec  
DE 6.50 usec  
TE 300.2 K  
D1 2.00000000 sec  
D11 0.03000000 sec  
TD0 1

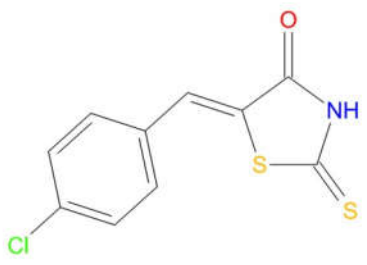
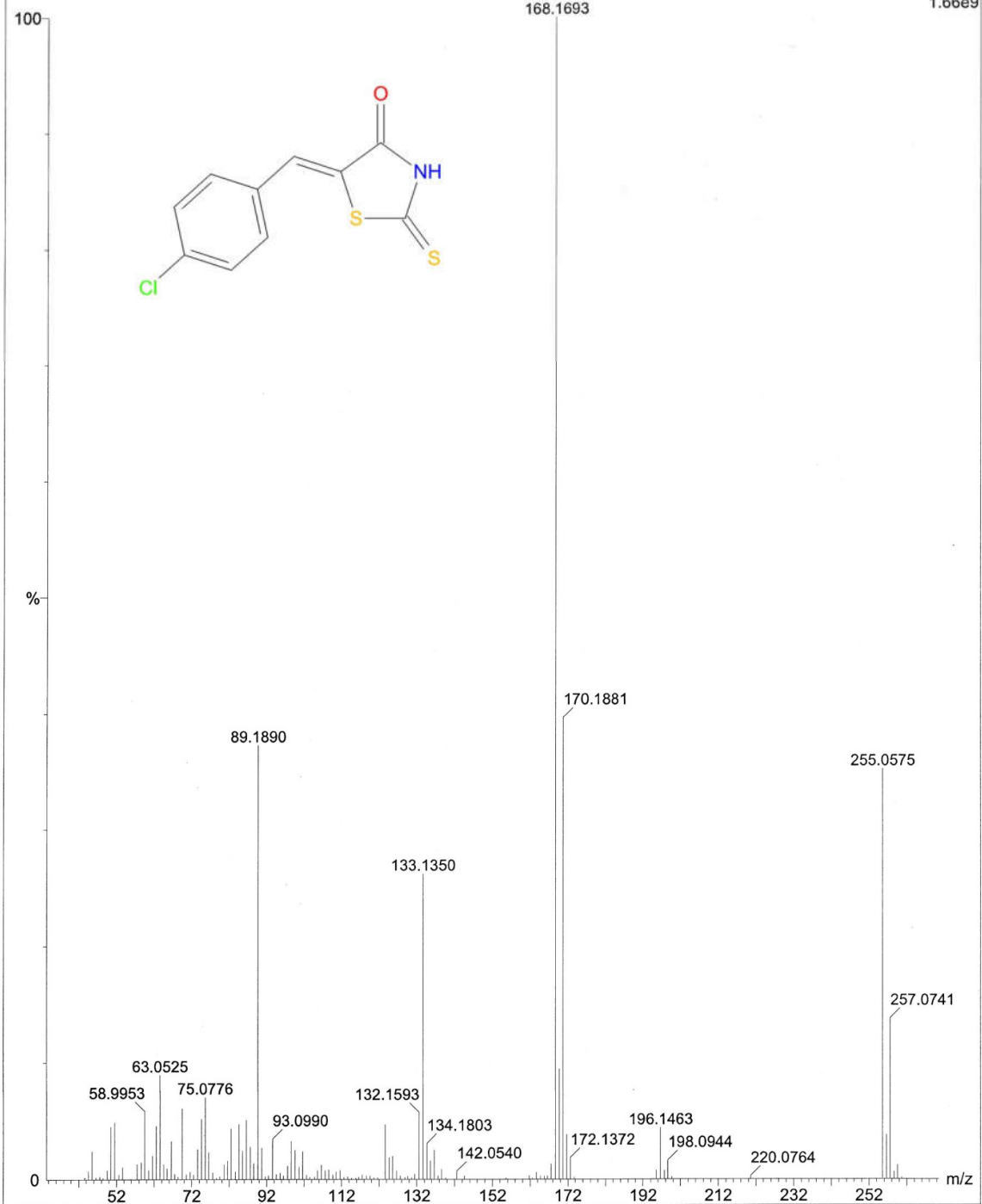
----- CHANNEL f1 -----  
NUC1 13C  
P1 7.80 usec  
PL1 0 dB  
PL1W 70.83519745 W  
SFO1 125.7703643 MHz

----- CHANNEL f2 -----  
CPDPRG2 waltz16  
NUC2 1H  
PCPD2 80.00 usec  
PL2 0 dB  
PL12 17.51 dB  
PL13 18.00 dB  
PL2W 23.53637505 W  
PL12W 0.41757989 W  
PL13W 0.37302643 W  
SFO2 500.1320005 MHz

F2 - Processing parameters  
SI 32768  
SF 125.7577890 MHz  
WDW EM  
SSB 0  
LB 1.00 Hz  
GB 0  
PC 1.40

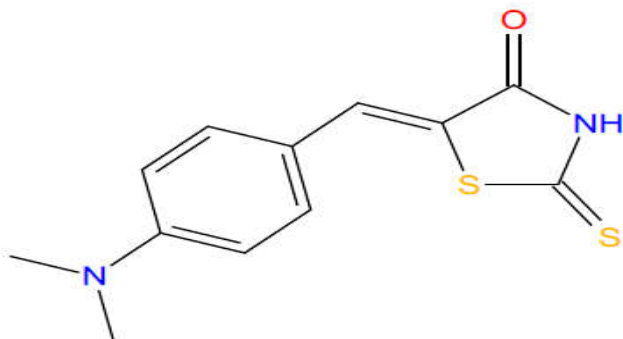
N2- 4162 (23.317)

Scan EI+  
1.66e9





### Spectral Data of Compound N3



**IR (KBr,  $\nu_{\max}$ )  $\text{cm}^{-1}$**

1249.78 (amine C-N), 1442.65 (Ar C-C), 1612.37 (C=O), 1681.80 (C=S), 2854.44 (alkane C-H), 2916.16 (=C-H), 3039.59 (Ar C-H), 3457.06 (N-H).

**$^1\text{H}$  NMR (DMSO- $\text{D}_6$ )  $\delta$**

3.03 (s, 3H, N-CH<sub>3</sub>), 3.10 (s, 3H, N-CH<sub>3</sub>), 6.81-6.85 (q, 2H, Ar-H), 7.41 (d, 1H, Ar-H), 7.51 (s, 1H, =CH-), 7.83 (d, 1H, Ar-H), 13.54 (s, 1H, N-H).

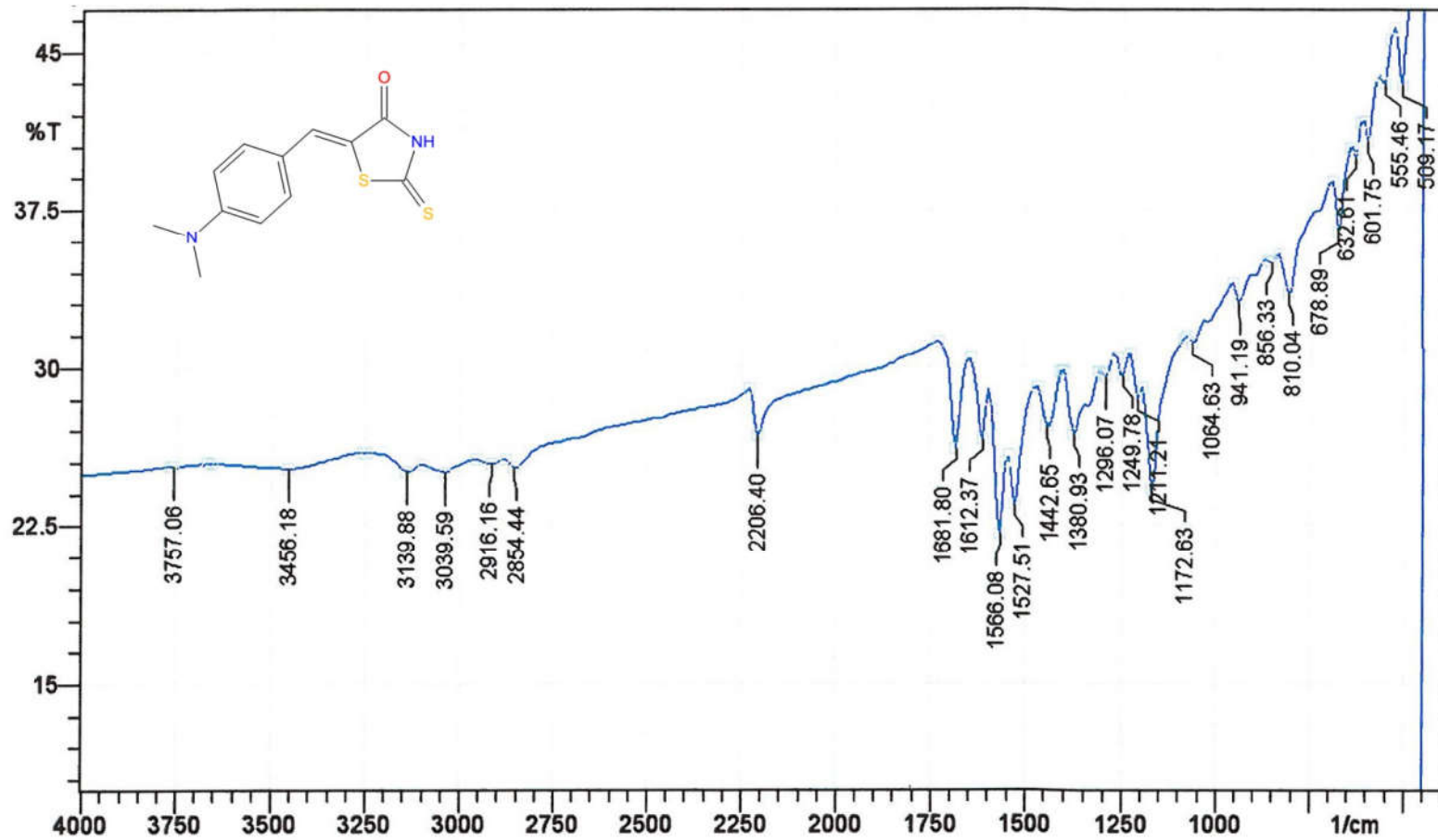
**$^{13}\text{C}$  NMR (DMSO- $\text{D}_6$ )  $\delta$**

68.19, 69.15, 115.99, 117.83, 119.23, 120.26, 133.36, 133.73, 134.06, 152.25, 169.88, 195.47.

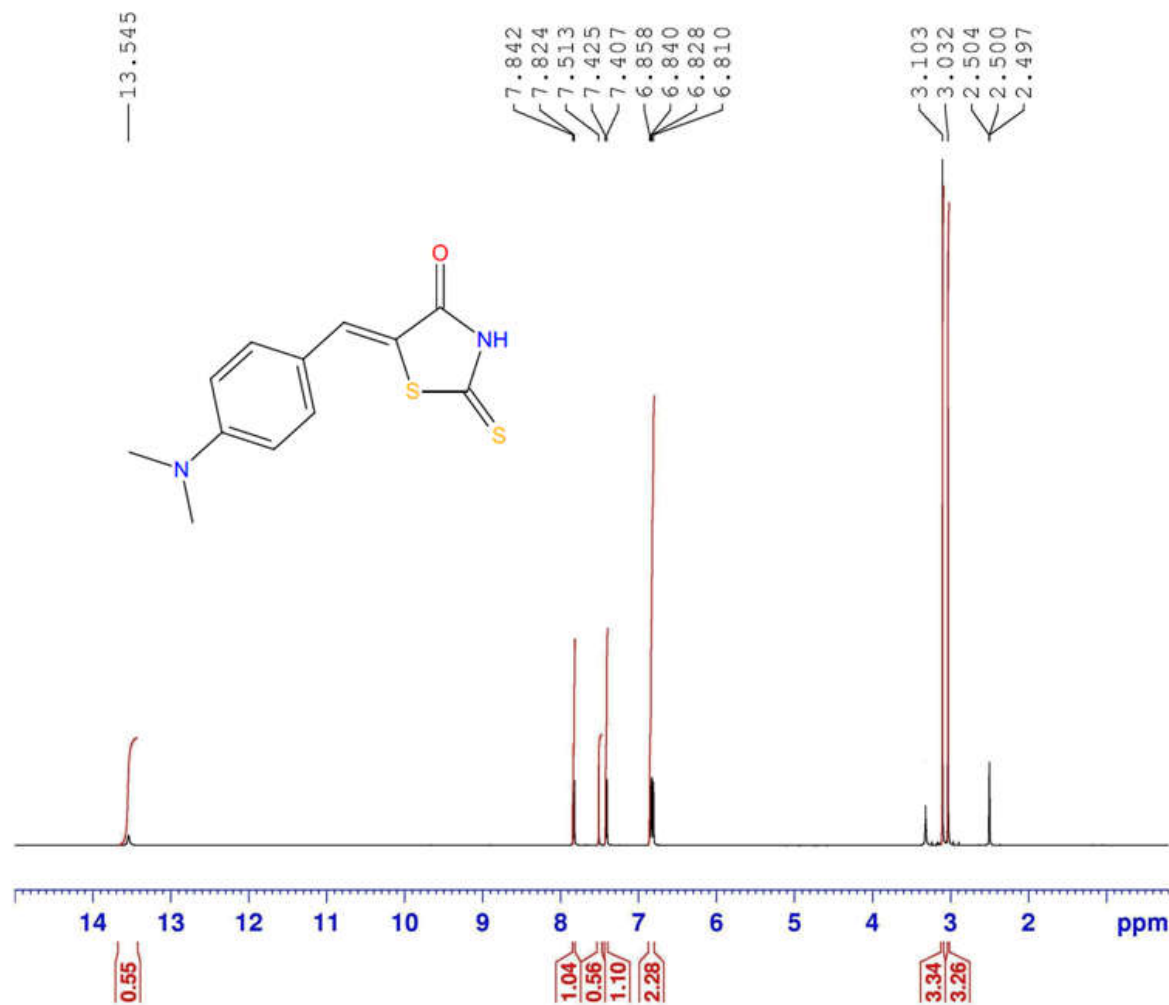
**MASS SPECTROSCOPY**

264.16 ( $\text{M}^+$ ), 177.21 (**B**).

Sample: N 3



N3.....Noorulla.



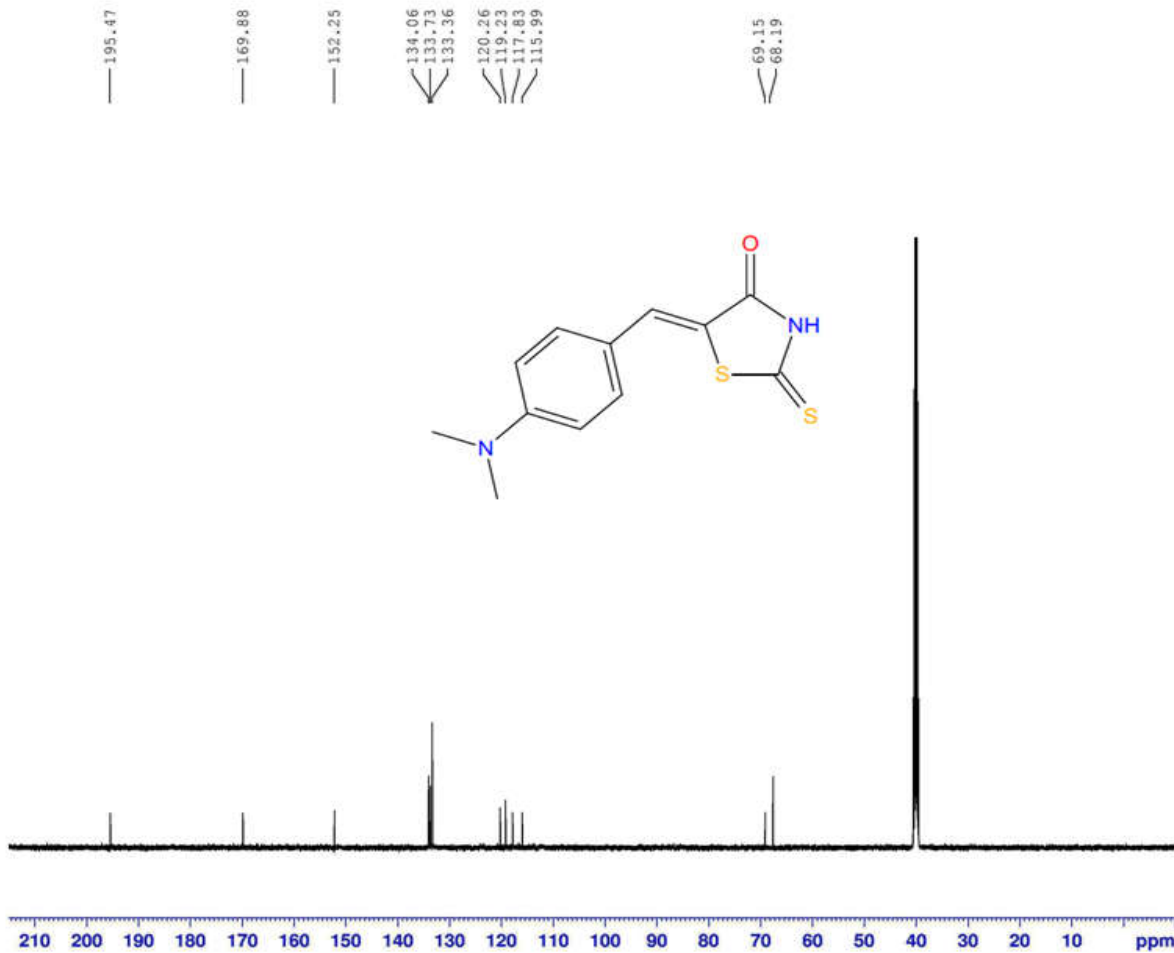
Current Data Parameters  
NAME N3  
EXPNO 7  
PROCNO 1

F2 - Acquisition Parameters  
Date\_ 20130911  
Time 1.14  
INSTRUM spect  
PROBHD 5 mm PABBO BB-  
PULPROG zg30  
TD 32768  
SOLVENT DMSO  
NS 32  
DS 2  
SWH 10330.578 Hz  
FIDRES 0.315264 Hz  
AQ 1.5860212 sec  
RG 203  
DW 48.400 usec  
DE 6.50 usec  
TE 298.9 K  
D1 1.00000000 sec  
TD0 1

----- CHANNEL f1 -----  
NUC1 1H  
P1 10.65 usec  
PL1 0 dB  
PL1W 23.53637505 W  
SFO1 500.1330885 MHz

F2 - Processing parameters  
SI 32768  
SF 500.1300042 MHz  
WDW EM  
SSB 0  
LB 0.30 Hz  
GB 0  
PC 1.00

N3.....Noorulla.



Current Data Parameters  
NAME N3  
EXPNO 8  
PROCNO 1

F2 - Acquisition Parameters  
Date\_ 20130911  
Time 1.59  
INSTRUM spect  
PROBHD 5 mm PABBO BB-  
PULPROG zgpg30  
TD 32768  
SOLVENT DMSO  
NS 1024  
DS 4  
SWH 29761.904 Hz  
FIDRES 0.908261 Hz  
AQ 0.5505524 sec  
RG 203  
DW 16.800 usec  
DE 6.50 usec  
TE 300.7 K  
D1 2.00000000 sec  
D11 0.03000000 sec  
TD0 1

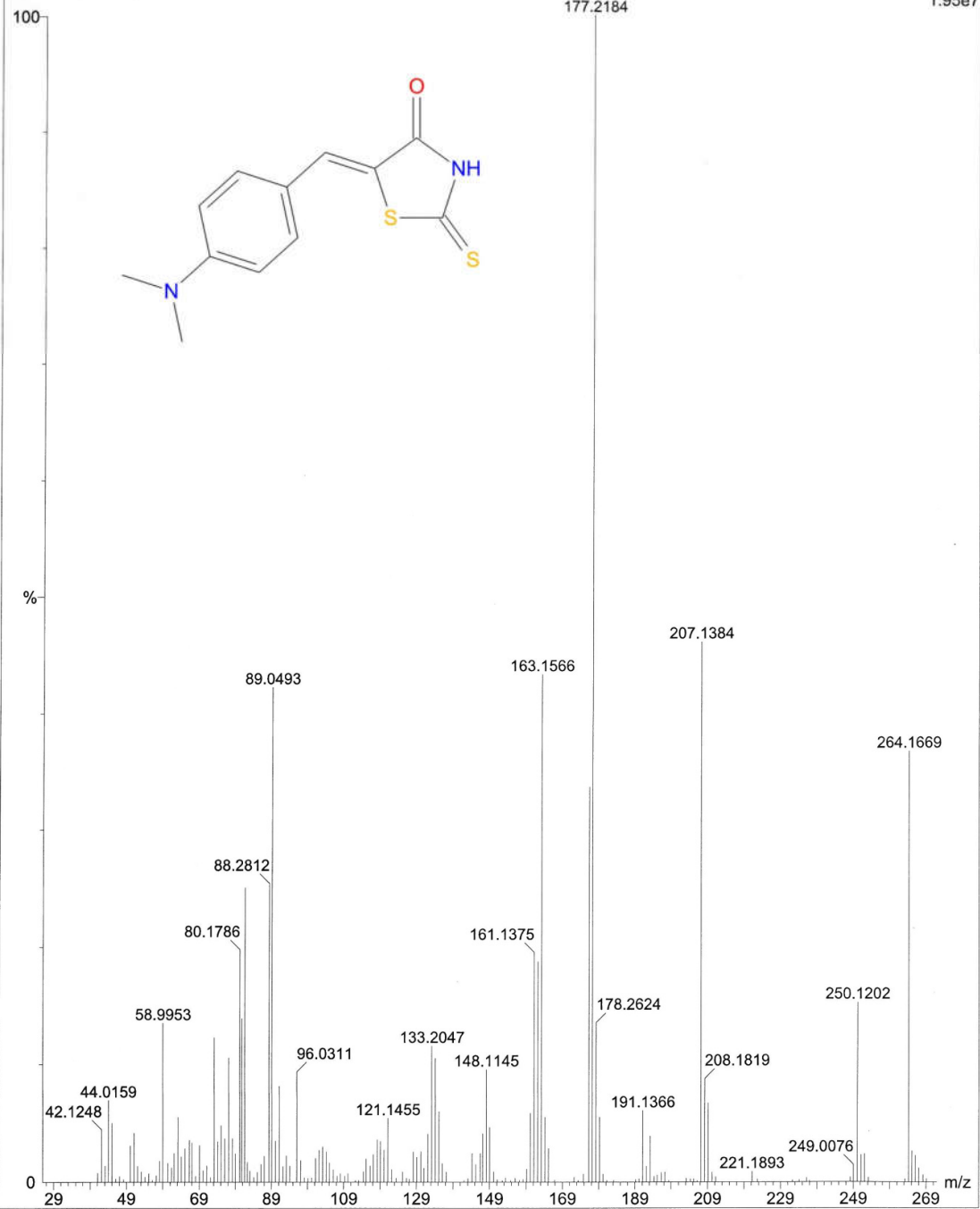
===== CHANNEL f1 =====  
NUC1 13C  
P1 7.80 usec  
PL1 0 dB  
PL1W 70.83519745 W  
SFO1 125.7703643 MHz

===== CHANNEL f2 =====  
CPDPRG2 waltz16  
NUC2 1H  
PCPD2 80.00 usec  
PL2 0 dB  
PL12 17.51 dB  
PL13 18.00 dB  
PL2W 23.53637505 W  
PL12W 0.41757989 W  
PL13W 0.37302643 W  
SFO2 500.1320005 MHz

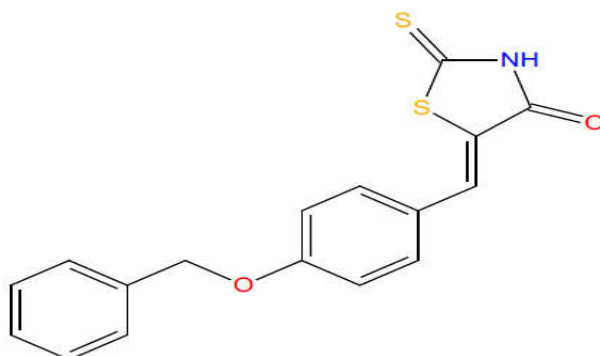
F2 - Processing parameters  
SI 32768  
SF 125.7577890 MHz  
WDW EM  
SSB 0  
LB 1.00 Hz  
GB 0  
PC 1.40

N3-4869 (26.853)

Scan EI+  
1.95e7

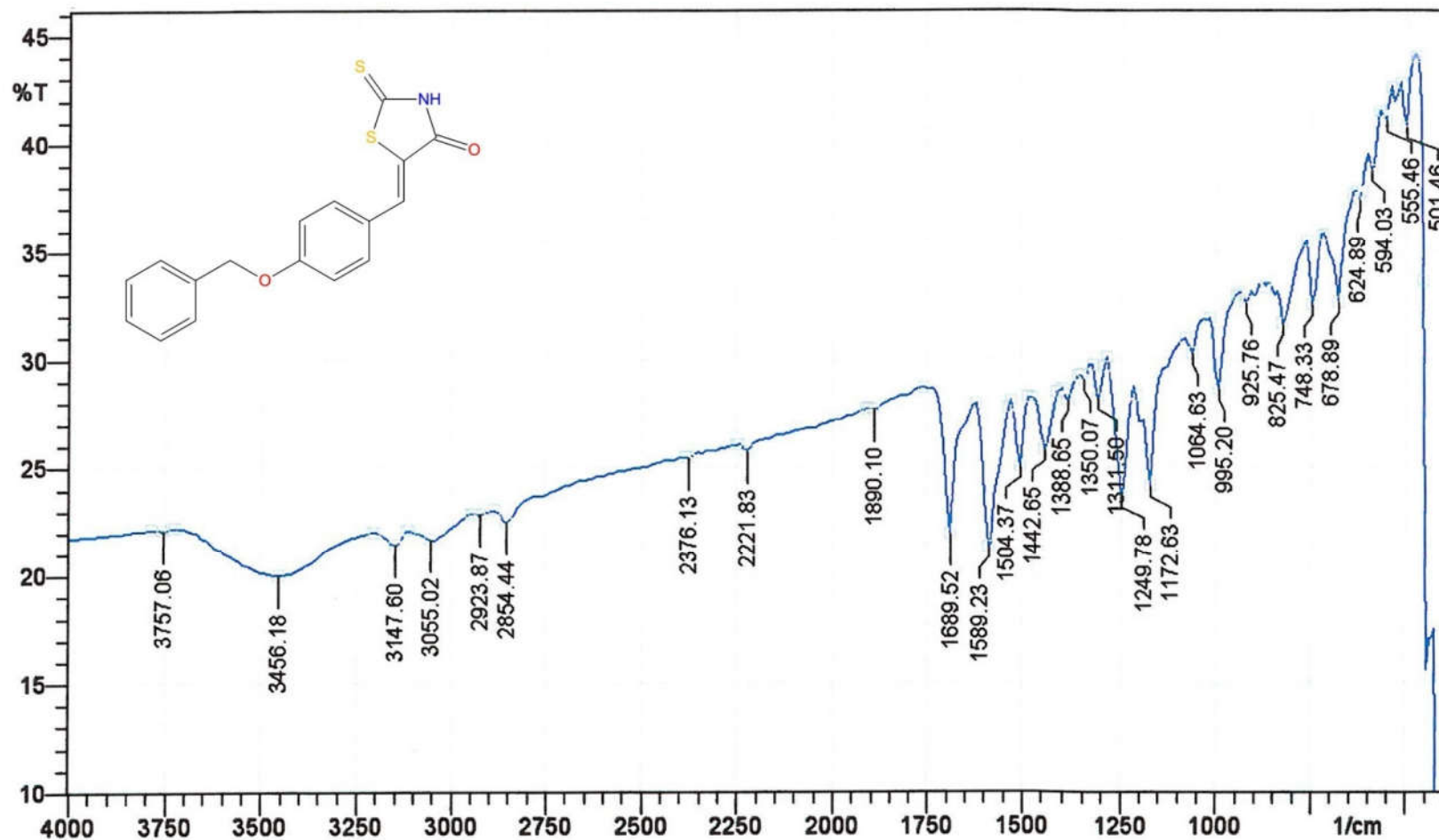


## Spectral Data of Compound N4

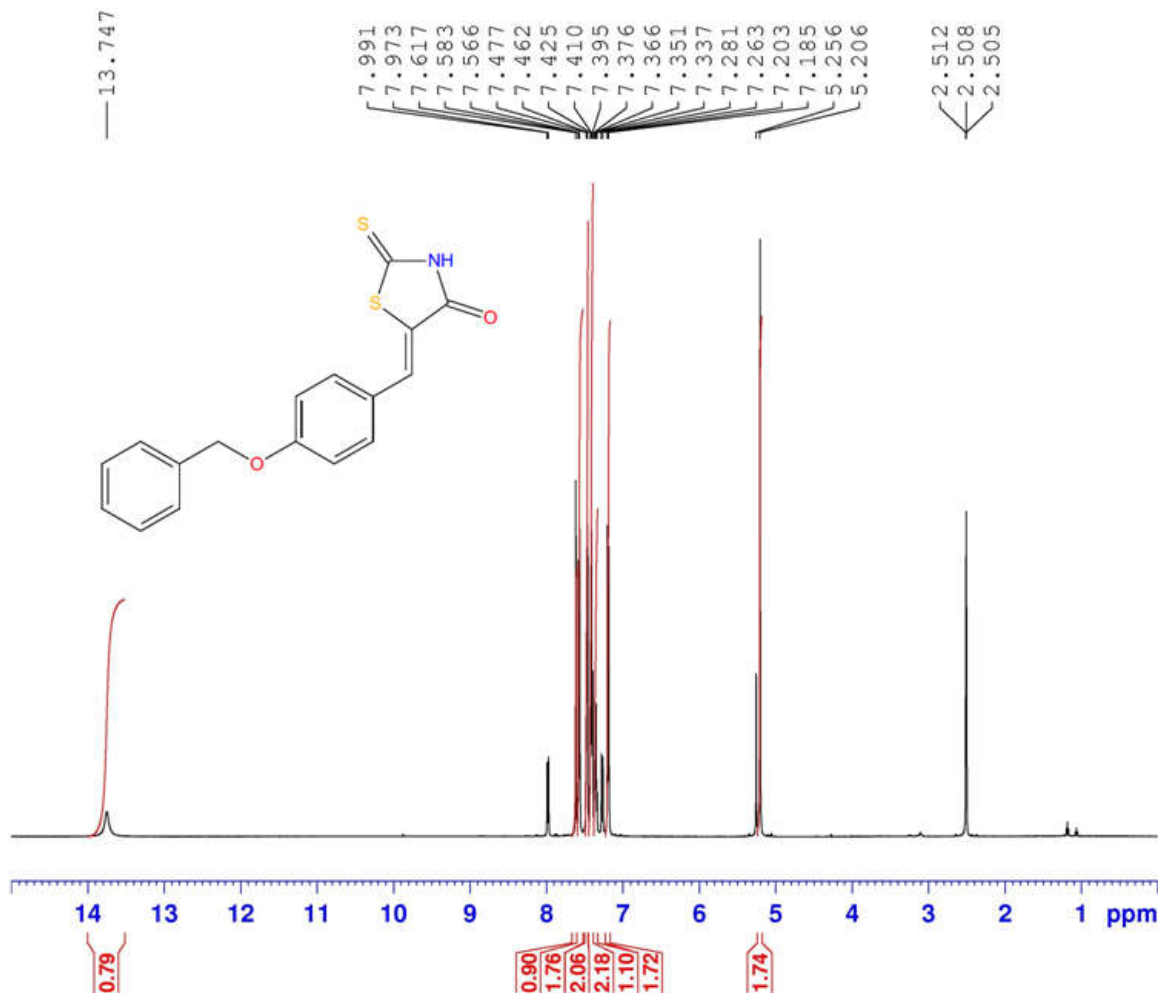


<b>IR (KBr, <math>\nu_{\max}</math>) <math>\text{cm}^{-1}</math></b>	1249.78 (ether C-O), 1442.65 (Ar C-C), 1589.23 (C=O), 1689.52 (C=S), 2854.44 (alkane C-H), 2923.87 (=C-H), 3055.02 (Ar C-H), 3456.18 (N-H).
<b><math>^1\text{H}</math> NMR (DMSO-<math>\text{D}_6</math>) <math>\delta</math></b>	5.22 (d, 2H, $\text{CH}_2$ ), 7.19 (d, 2H, Ar-H), 7.33-7.37 (q, 1H, Ar-H), 7.41 (t, 2H, Ar-H), 7.47 (d, 2H, Ar-H), 7.57 (d, 2H, Ar-H), 7.61 (s, 1H, =CH-), 13.74 (s, 1H, NH).
<b><math>^{13}\text{C}</math> NMR (DMSO-<math>\text{D}_6</math>) <math>\delta</math></b>	70.04, 115.26, 126.16, 128.28, 128.43, 128.51, 128.66, 128.97, 129.01, 132.27, 133.14, 133.82, 136.51, 136.91, 141.24, 160.90, 163.89, 169.92, 195.98
<b>MASS SPECTROSCOPY</b>	327.17 ( $\text{M}^+$ ), 328.07 ( $\text{M}+1$ ), 91.14 ( <b>B</b> ).

Sample: N 4



N4.....Noorulla.



Current Data Parameters  
NAME N4  
EXPNO 9  
PROCNO 1

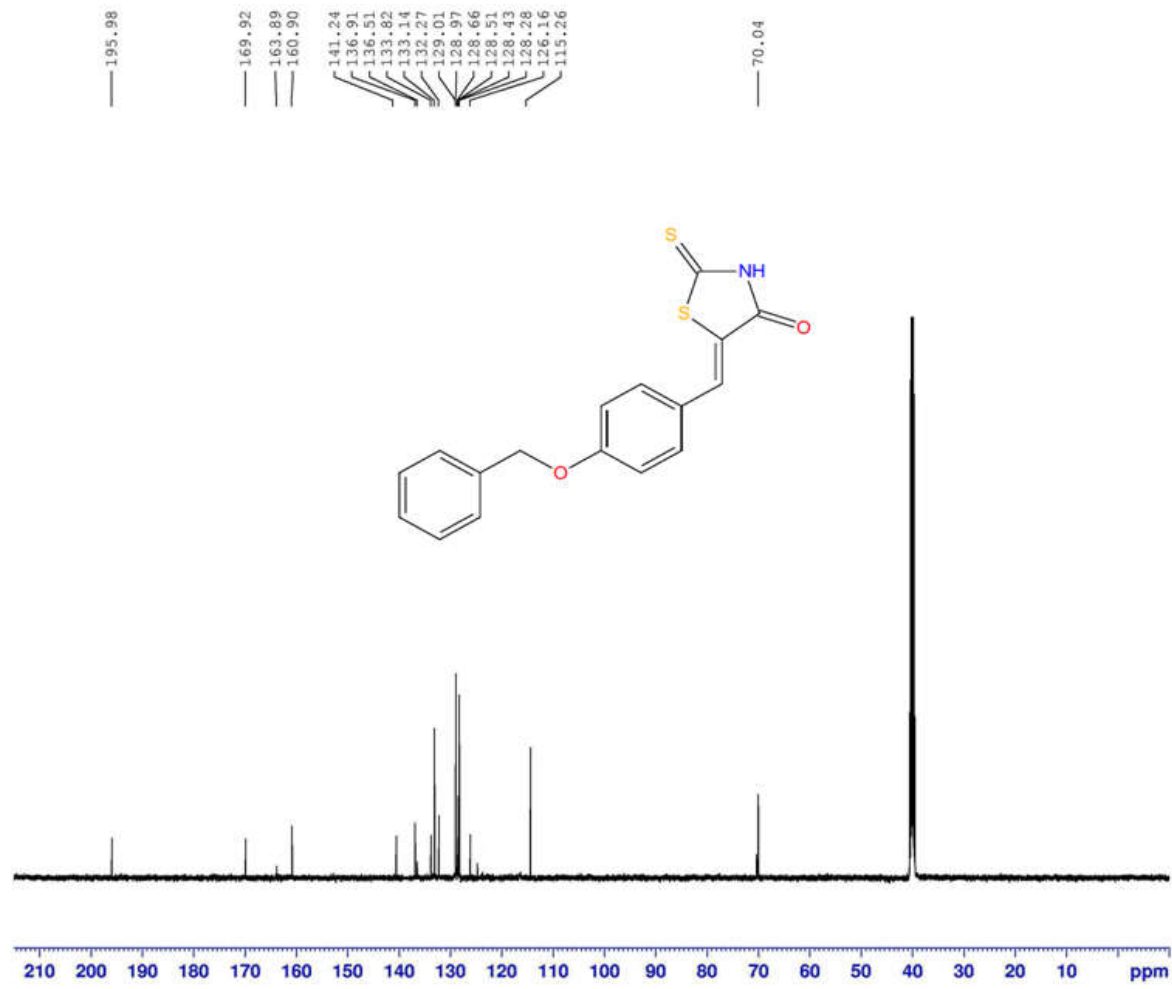
F2 - Acquisition Parameters  
Date\_ 20130911  
Time 2.03  
INSTRUM spect  
PROBHD 5 mm PABBO BB-  
PULPROG zg30  
TD 32768  
SOLVENT DMSO  
NS 32  
DS 2  
SWH 10330.578 Hz  
FIDRES 0.315264 Hz  
AQ 1.5860212 sec  
RG 203  
DW 48.400 usec  
DE 6.50 usec  
TE 299.4 K  
D1 1.00000000 sec  
TD0 1

===== CHANNEL f1 =====  
NUC1 1H  
P1 10.65 usec  
PL1 0 dB  
PL1W 23.53637505 W  
SF01 500.1330885 MHz

F2 - Processing parameters  
SI 32768  
SF 500.1300000 MHz  
WDW EM  
SSB 0  
LB 0.30 Hz  
GB 0  
PC 1.00



N4.....Noorulla.



Current Data Parameters  
NAME N4  
EXPNO 10  
PROCNO 1

F2 - Acquisition Parameters  
Date\_ 20130911  
Time 2.48  
INSTRUM spect  
PROBHD 5 mm PABBO BB-  
PULPROG zgpg30  
TD 32768  
SOLVENT DMSO  
NS 1024  
DS 4  
SWH 29761.904 Hz  
FIDRES 0.908261 Hz  
AQ 0.5505524 sec  
RG 203  
DW 16.800 usec  
DE 6.50 usec  
TE 301.0 K  
D1 2.0000000 sec  
D11 0.0300000 sec  
TD0 1

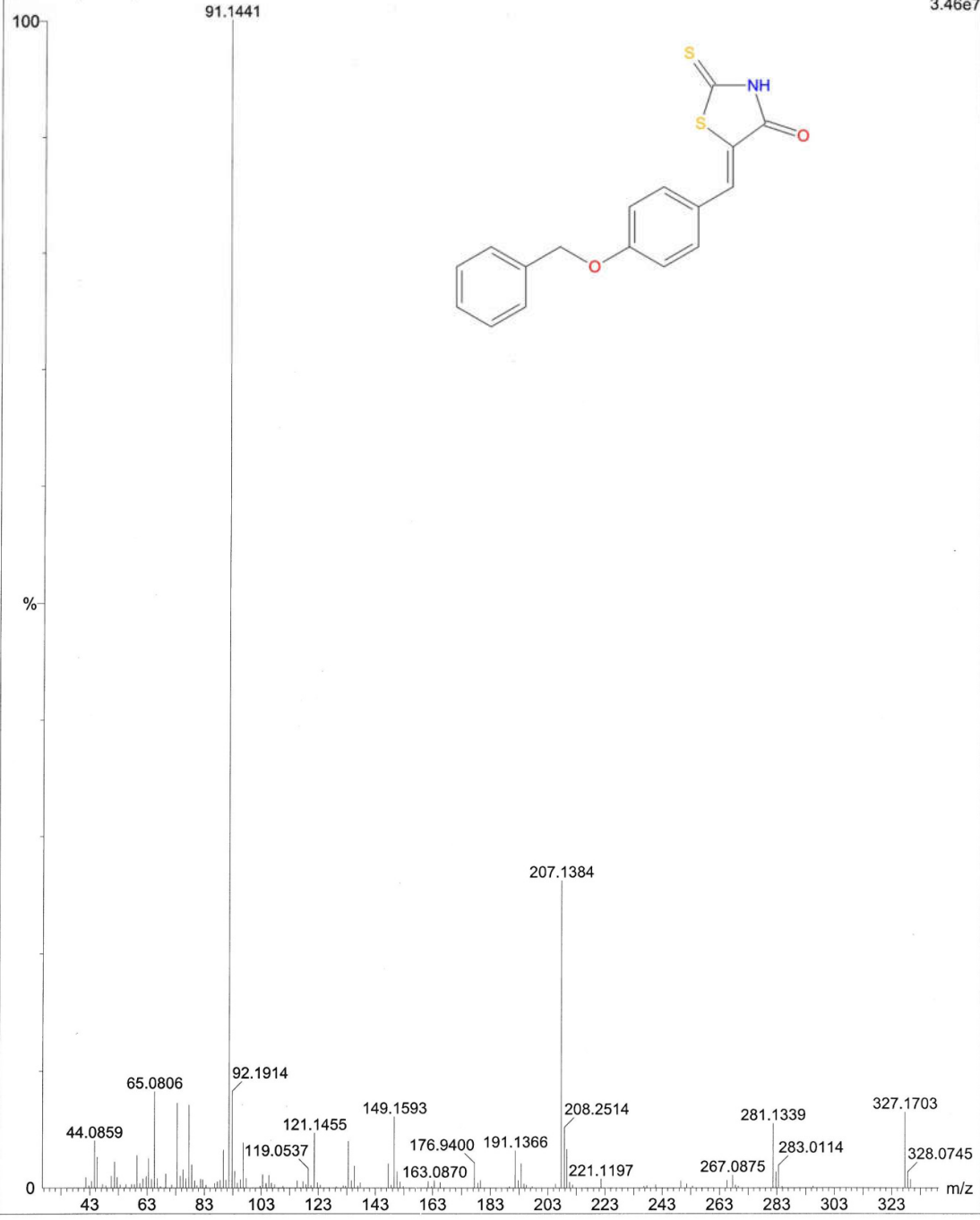
===== CHANNEL f1 =====  
NUC1 13C  
P1 7.80 usec  
PL1 0 dB  
PL1W 70.83519745 W  
SFO1 125.7703643 MHz

===== CHANNEL f2 =====  
CPDPRG2 waltz16  
NUC2 1H  
PCPD2 80.00 usec  
PL2 0 dB  
PL12 17.51 dB  
PL13 18.00 dB  
PL2W 23.53637505 W  
PL12W 0.41757989 W  
PL13W 0.37302643 W  
SFO2 500.1320005 MHz

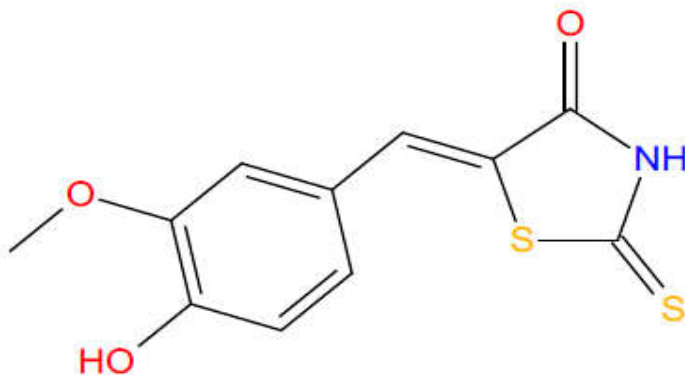
F2 - Processing parameters  
SI 32768  
SF 125.7577890 MHz  
WDW EM  
SSB 0  
LB 1.00 Hz  
GB 0  
PC 1.40

N4-5857 (31.795)

Scan EI+  
3.46e7



## Spectral Data of Compound N5



**IR (KBr,  $\nu_{\max}$ )  $\text{cm}^{-1}$**

1280.64 (alcoholic C-O), 1442.65 (Ar C-C), 1589.23 (C=O),  
1712.66 (C=S), 2854.44 (alkane C-H), 2923.87 (=C-H), 3008.73 (Ar  
C-H), 3340.46 (N-H), 3610.48 (O-H).

**$^1\text{H}$  NMR (DMSO- $\text{D}_6$ )  $\delta$**

3.82 (s, 3H, O- $\text{CH}_3$ ), 6.93 (d, 1H, Ar-H), 7.06 (d, 1H, Ar-H), 7.11 (s,  
1H, Ar-H), 7.54 (s, 1H, =CH-), 10.13 (s, 1H, Ar-OH), 13.62 (s, 1H,  
N-H).

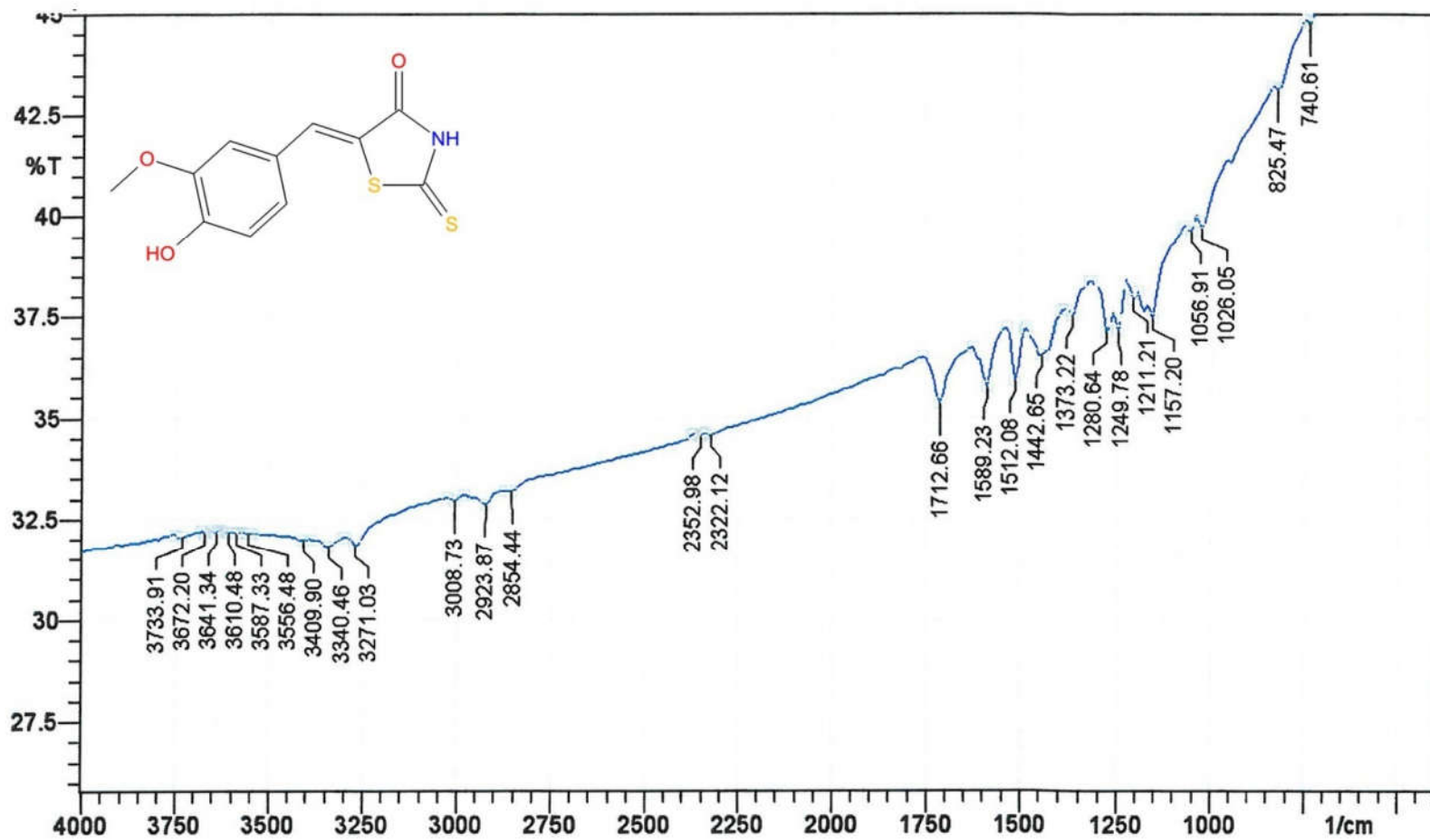
**$^{13}\text{C}$  NMR (DMSO- $\text{D}_6$ )  $\delta$**

56.11, 114.73, 121.06, 124.86, 125.55, 133.25, 134.90, 137.44,  
148.59, 169.88, 195.90.

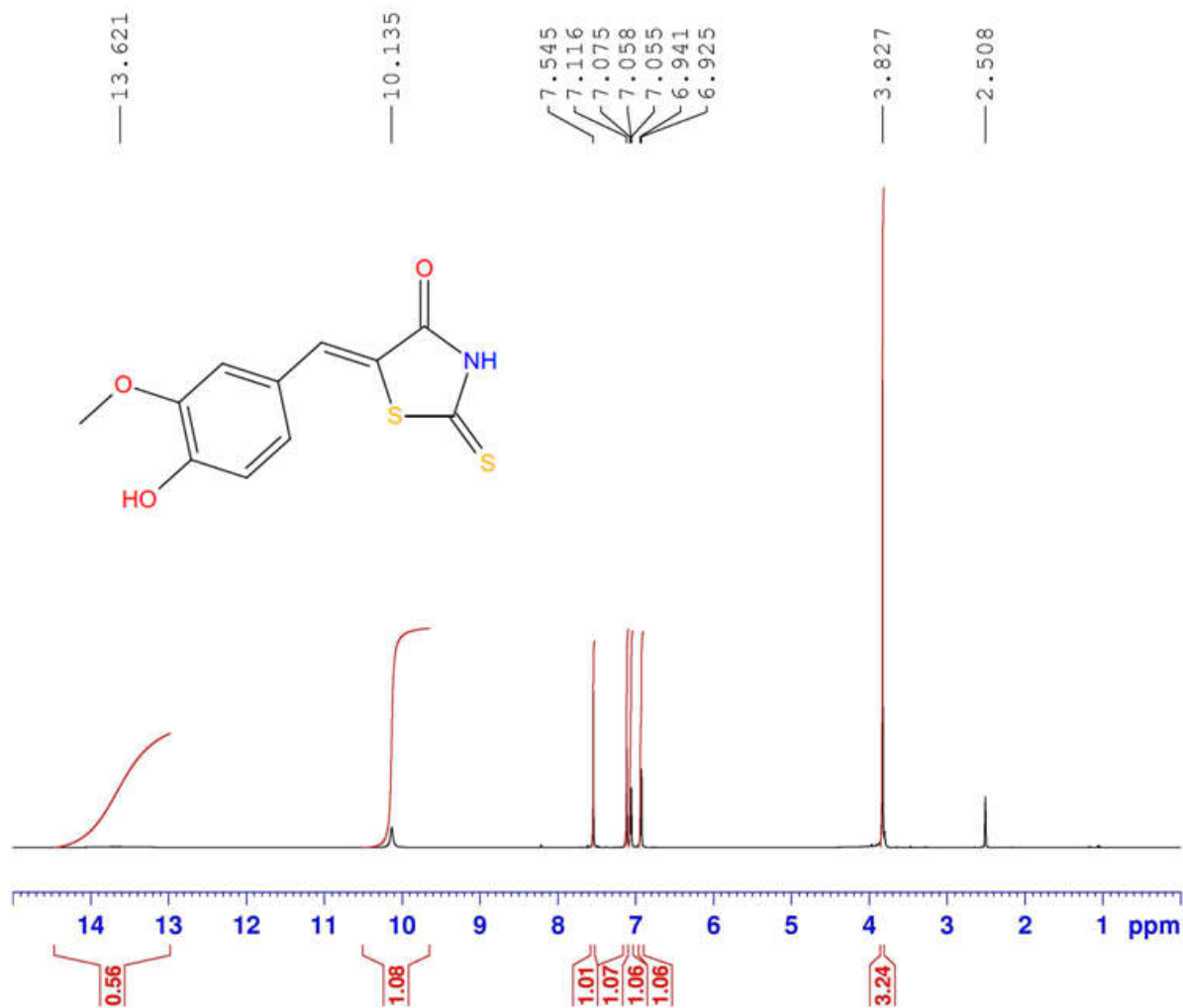
**MASS SPECTROSCOPY**

267.15 ( $\text{M}^+$ ), 268.13 ( $\text{M}+1$ ), 180.21 (**B**).

Sample: N 5



N5.....Noorulla.



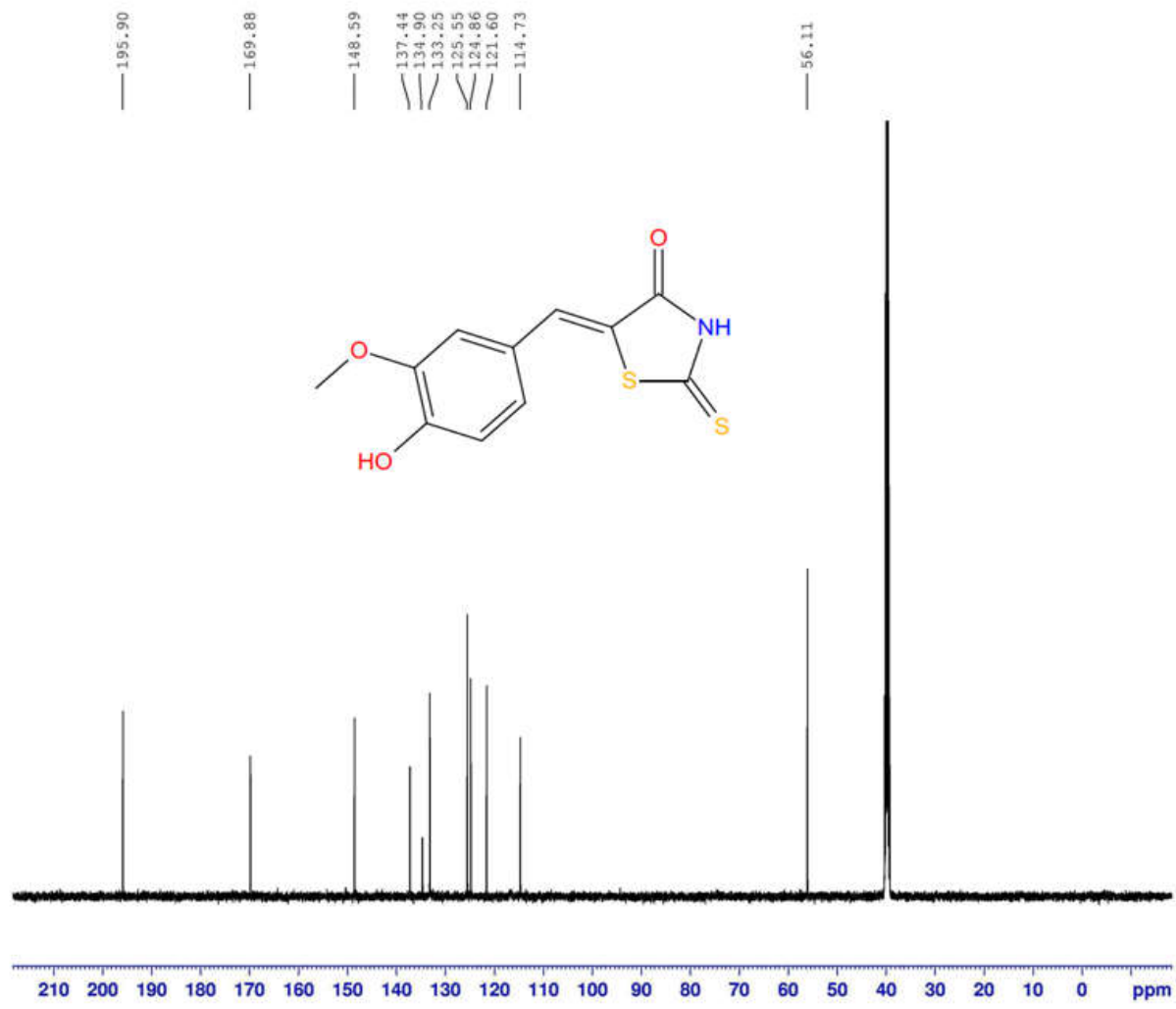
Current Data Parameters  
NAME N5  
EXPNO 13  
PROCNO 1

F2 - Acquisition Parameters  
Date\_ 20130911  
Time 3.40  
INSTRUM spect  
PROBHD 5 mm PABBO BB-  
PULPROG zg30  
TD 32768  
SOLVENT DMSO  
NS 32  
DS 2  
SWH 10330.578 Hz  
FIDRES 0.315264 Hz  
AQ 1.5860212 sec  
RG 57  
DW 48.400 usec  
DE 6.50 usec  
TE 300.0 K  
D1 1.00000000 sec  
TD0 1

===== CHANNEL f1 =====  
NUC1 1H  
P1 10.65 usec  
PL1 0 dB  
PL1W 23.53637505 W  
SFO1 500.1330885 MHz

F2 - Processing parameters  
SI 32768  
SF 500.1300000 MHz  
WDW EM  
SSB 0  
LB 0.30 Hz  
GB 0  
PC 1.00

N5.....Noorulla.



Current Data Parameters  
NAME N5  
EXPNO 14  
PROCNO 1

F2 - Acquisition Parameters  
Date\_ 20130911  
Time 4.25  
INSTRUM spect  
PROBHD 5 mm PABBO BB-  
PULPROG zgpg30  
TD 32768  
SOLVENT DMSO  
NS 1024  
DS 4  
SWH 29761.904 Hz  
FIDRES 0.908261 Hz  
AQ 0.5505524 sec  
RG 203  
DW 16.800 usec  
DE 6.50 usec  
TE 301.4 K  
D1 2.00000000 sec  
D11 0.03000000 sec  
TD0 1

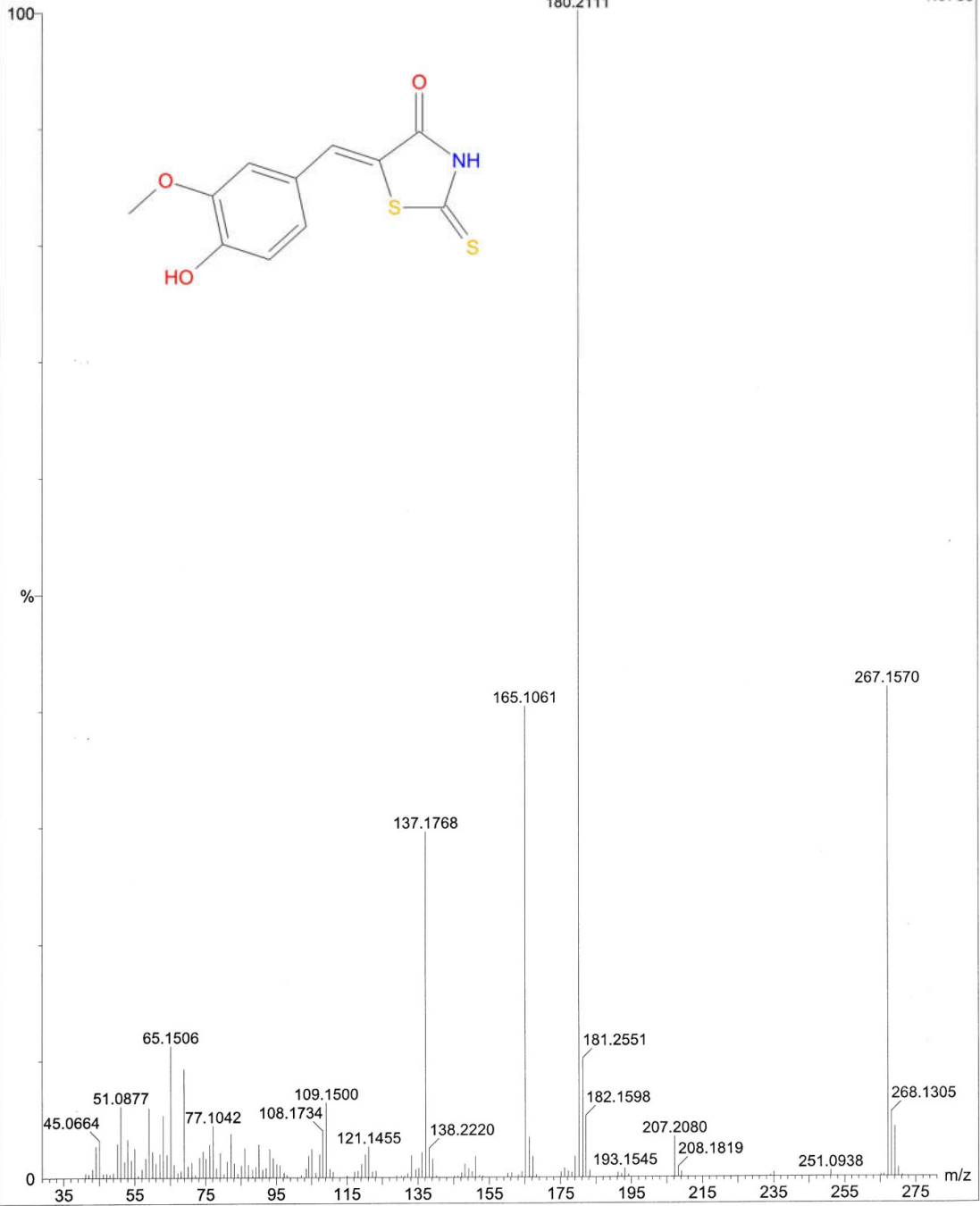
----- CHANNEL f1 -----  
NUC1 13C  
P1 7.80 usec  
PL1 0 dB  
PL1W 70.83519745 W  
SFO1 125.7703643 MHz

----- CHANNEL f2 -----  
CPDPRG2 waitz16  
NUC2 1H  
PCPD2 80.00 usec  
PL2 0 dB  
PL12 17.51 dB  
PL13 18.00 dB  
PL2W 23.53637505 W  
PL12W 0.41757989 W  
PL13W 0.37302643 W  
SFO2 500.1320005 MHz

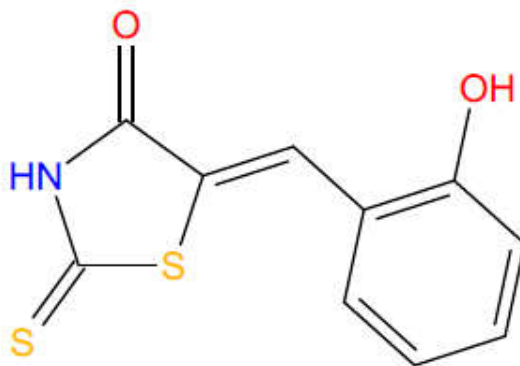
F2 - Processing parameters  
SI 32768  
SF 125.7577890 MHz  
WDW EM  
SSB 0  
LB 1.00 Hz  
GB 0  
PC 1.40

N5-4579 (25.403)

Scan EI+  
1.07e8



## Spectral Data of Compound N6



**IR (KBr,  $\nu_{\max}$ )  $\text{cm}^{-1}$**

1280.64 (alcoholic C-O), 1442.65 (Ar C-C), 1653.52 (C=O),  
1743.52 (C=S), 2862.15 (=C-H), 3116.74 (Ar C-H), 3340.46 (N-H),  
3633.62 (O-H).

**$^1\text{H}$  NMR (DMSO- $\text{D}_6$ )  $\delta$**

5.03 (s, 1H, O-H), 7.02-7.04 (q, 1H, Ar-H), 7.17-7.22 (m, 2H, Ar-H),  
7.30-7.34 (m, 1H, Ar-H), 7.44 (d, 1H, =CH-), 13.32 (s, 1H, N-H).

**$^{13}\text{C}$  NMR (DMSO- $\text{D}_6$ )  $\delta$**

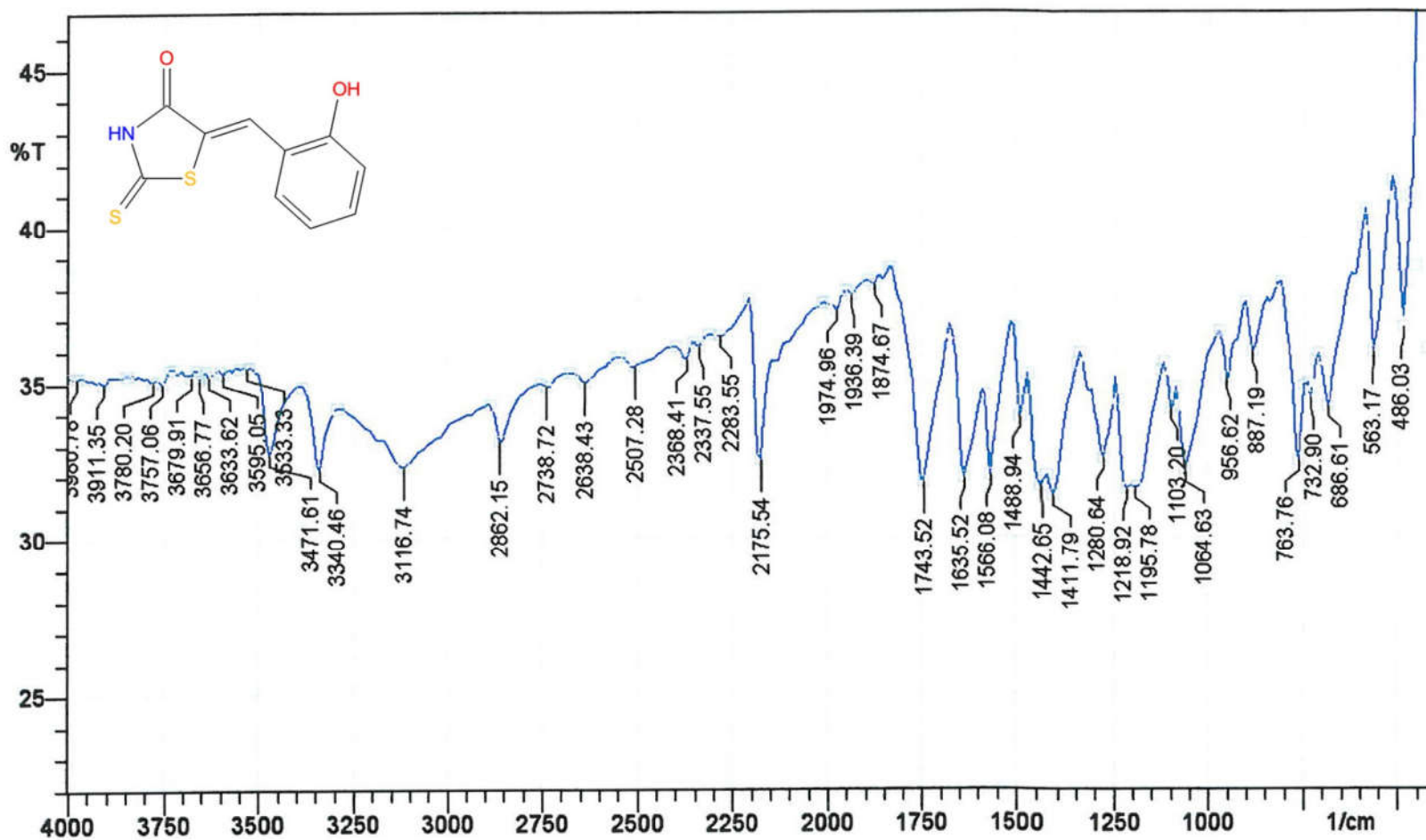
116.65, 120.22, 120.81, 125.54, 128.92, 129.77, 130.89, 149.68,  
176.34, 203.70.

**MASS SPECTROSCOPY**

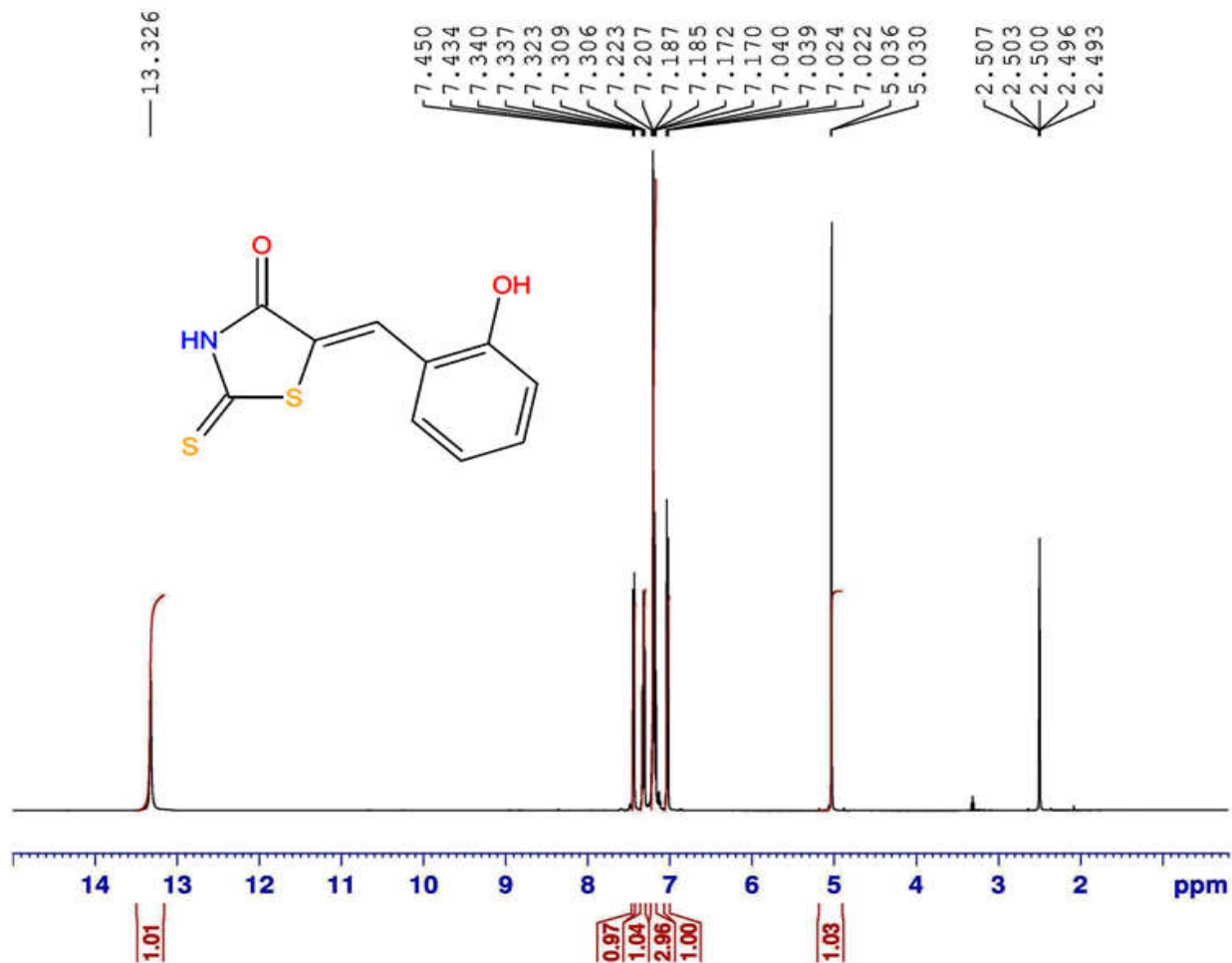
237.26 ( $\text{M}^+$ ), 178.19 (**B**).



Sample: N 6



N6.....Noorulla.



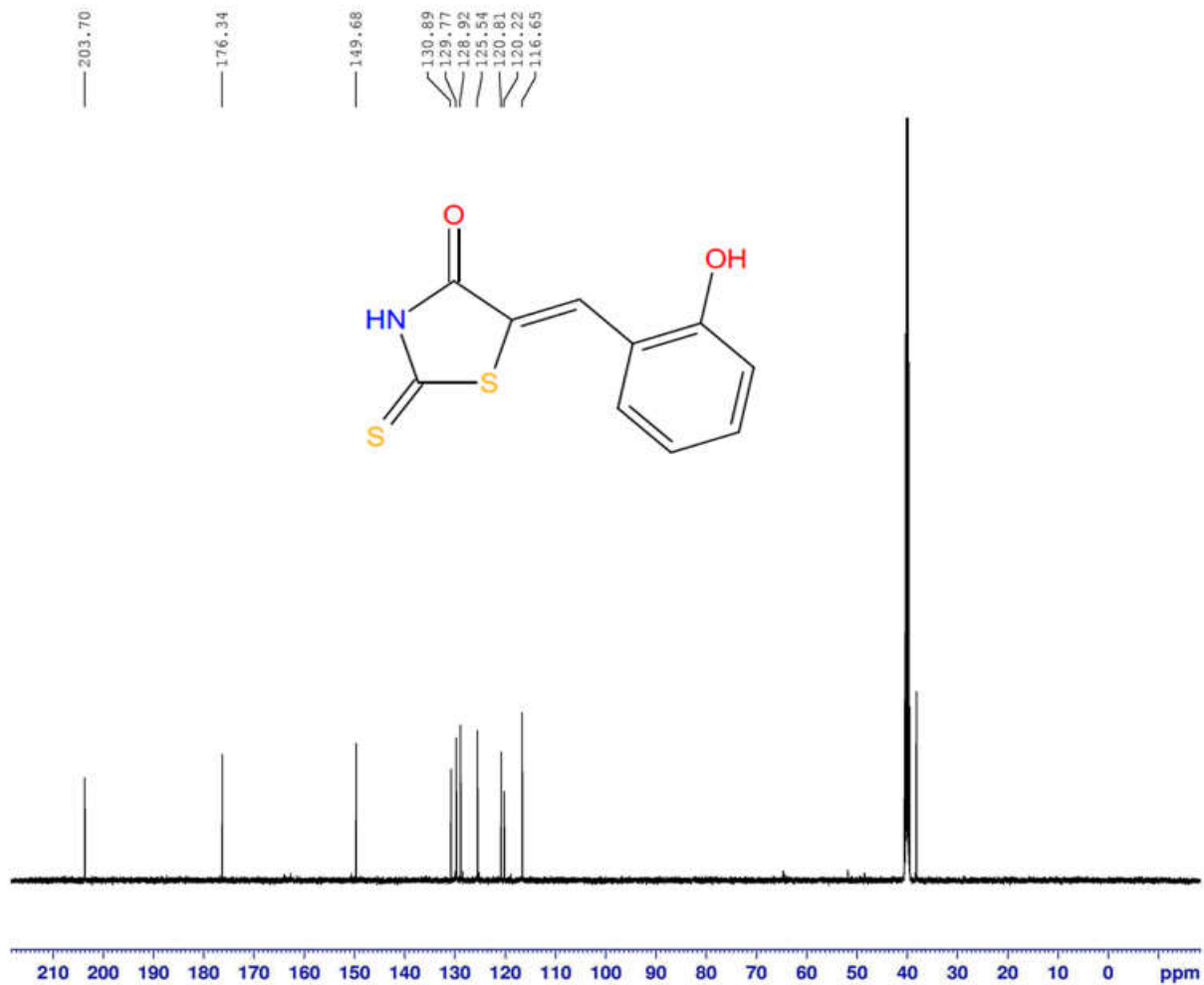
Current Data Parameters  
NAME N6  
EXPNO 15  
PROCNO 1

F2 - Acquisition Parameters  
Date\_ 20130911  
Time 4.28  
INSTRUM spect  
PROBHD 5 mm PABBO BB-  
PULPROG zg30  
TD 32768  
SOLVENT DMSO  
NS 32  
DS 2  
SWH 10330.578 Hz  
FIDRES 0.315264 Hz  
AQ 1.5860212 sec  
RG 203  
DW 48.400 usec  
DE 6.50 usec  
TE 300.1 K  
D1 1.00000000 sec  
TD0 1

----- CHANNEL f1 -----  
NUC1 1H  
P1 10.65 usec  
PL1 0 dB  
PL1W 23.53637505 W  
SFO1 500.1330885 MHz

F2 - Processing parameters  
SI 32768  
SF 500.1300044 MHz  
WDW EM  
SSB 0  
LB 0.30 Hz  
GB 0  
PC 1.00

N6.....Noorulla.



Current Data Parameters  
NAME N6  
EXPNO 16  
PROCNO 1

F2 - Acquisition Parameters  
Date\_ 20130911  
Time 5.13  
INSTRUM spect  
PROBHD 5 mm PABBO BB-  
PULPROG zgpg30  
TD 32768  
SOLVENT DMSO  
NS 1024  
DS 4  
SWH 29761.904 Hz  
FIDRES 0.908261 Hz  
AQ 0.5505524 sec  
RG 203  
DW 16.800 usec  
DE 6.50 usec  
TE 301.4 K  
D1 2.0000000 sec  
D11 0.03000000 sec  
TD0 1

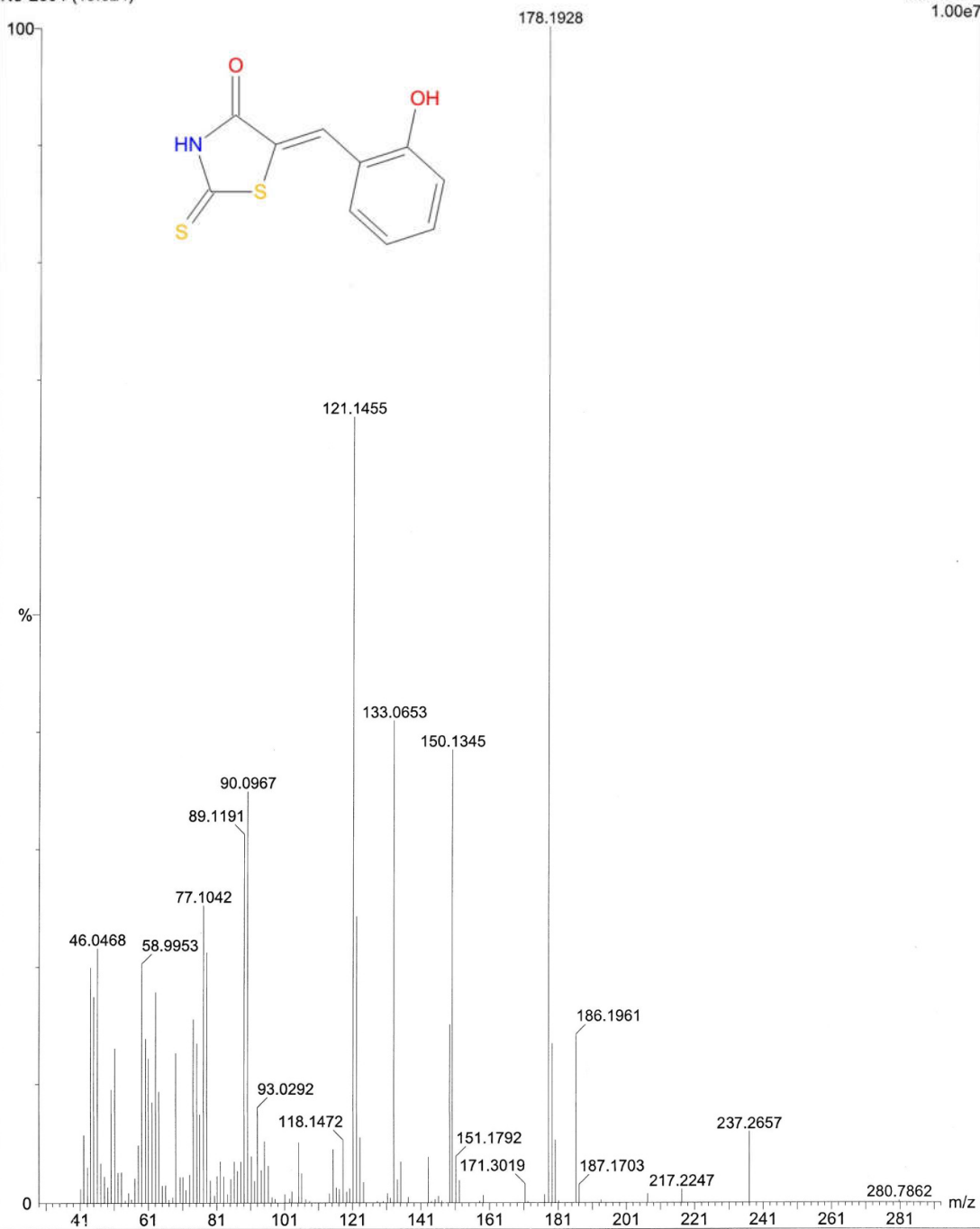
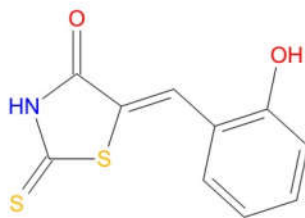
===== CHANNEL f1 =====  
NUC1 13C  
P1 7.80 usec  
PL1 0 dB  
PL1W 70.83519745 W  
SFO1 125.7703643 MHz

===== CHANNEL f2 =====  
CPDPRG2 waltz16  
NUC2 1H  
PCPD2 80.00 usec  
PL2 0 dB  
PL12 17.51 dB  
PL13 18.00 dB  
PL2W 23.53637505 W  
PL12W 0.41757989 W  
PL13W 0.37302643 W  
SFO2 500.1320005 MHz

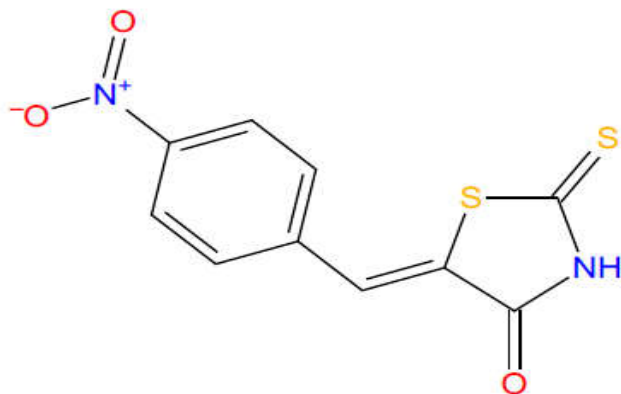
F2 - Processing parameters  
SI 32768  
SF 125.7577890 MHz  
WDW EM  
SSB 0  
LB 1.00 Hz  
GB 0  
PC 1.40

N6-2604 (15.524)

Scan EI+  
1.00e7



## Spectral Data of Compound N7



**IR (KBr,  $\nu_{\max}$ )  $\text{cm}^{-1}$**

1342.36 (nitro N-O), 1411.79 (Ar C-C), 1604.66 (C=O), 1720.38 (C=S), 2923.87 (=C-H), 3016.45 (Ar C-H), 3440.76 (N-H).

**$^1\text{H}$  NMR (DMSO- $\text{D}_6$ )  $\delta$**

7.73 (s, 1H, =CH-), 7.86 (t, 2H, Ar-H), 8.32-8.34 (m, 2H, Ar-H), 14.00 (s, 1H, NH).

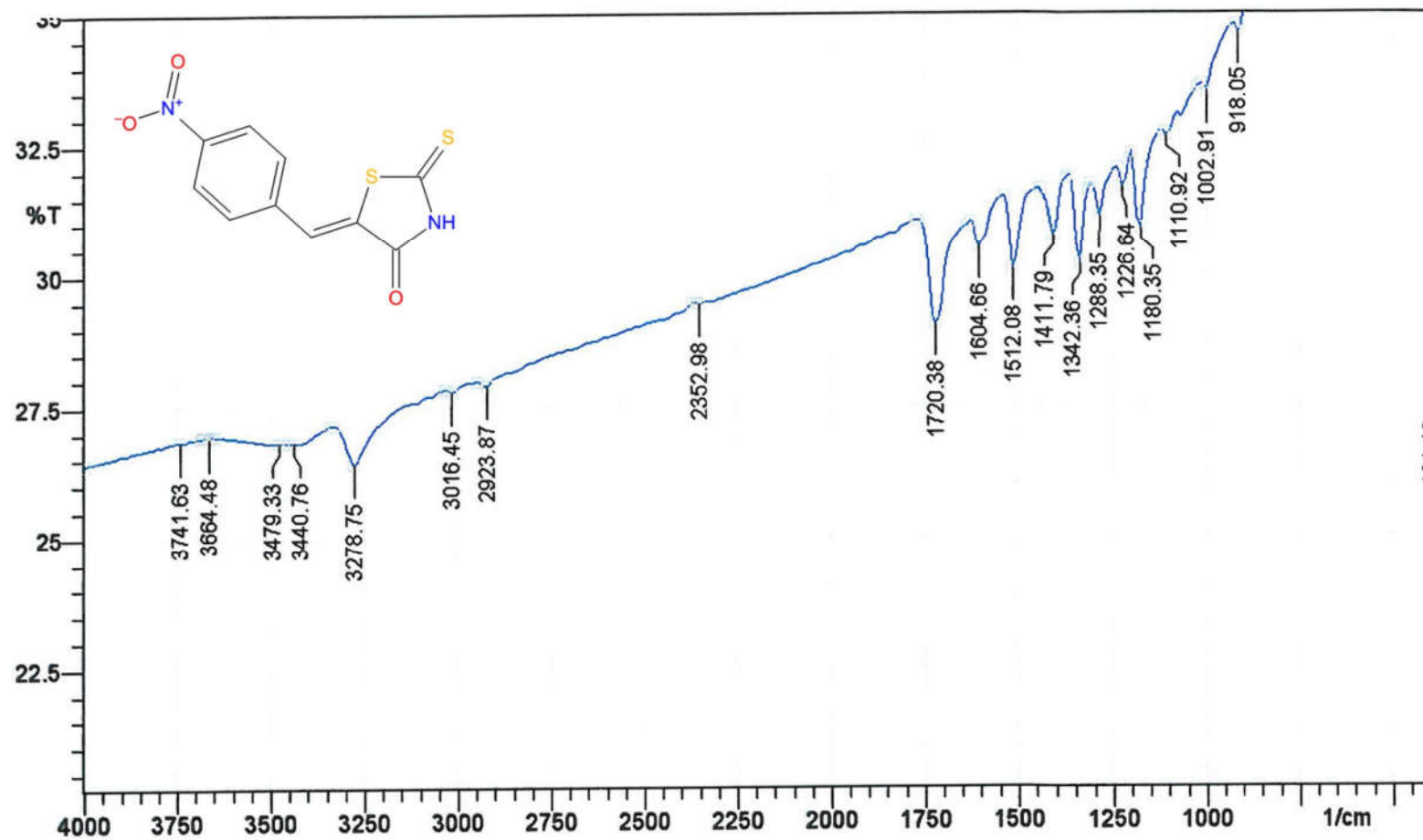
**$^{13}\text{C}$  NMR (DMSO- $\text{D}_6$ )  $\delta$**

116.96, 124.79, 129.03, 130.44, 131.76, 135.33, 139.67, 147.99, 169.70, 195.73.

**MASS SPECTROSCOPY**

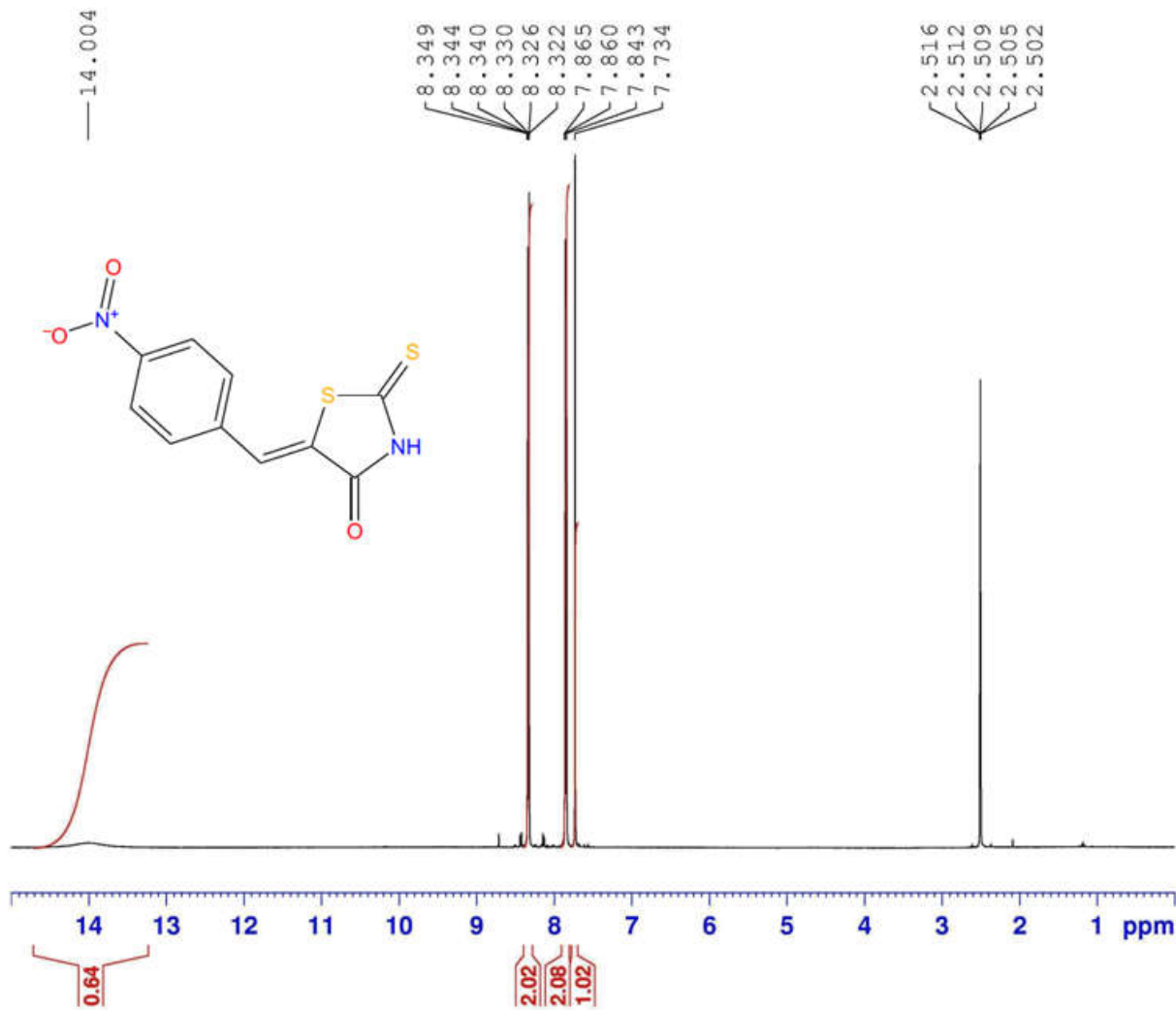
266.11 ( $\text{M}^+$ ), 267.15 ( $\text{M}+1$ ), 179.16 (**B**).

Sample: N 7



401.16

N7.....Noorulla.



Current Data Parameters  
NAME N7  
EXPNO 17  
PROCNO 1

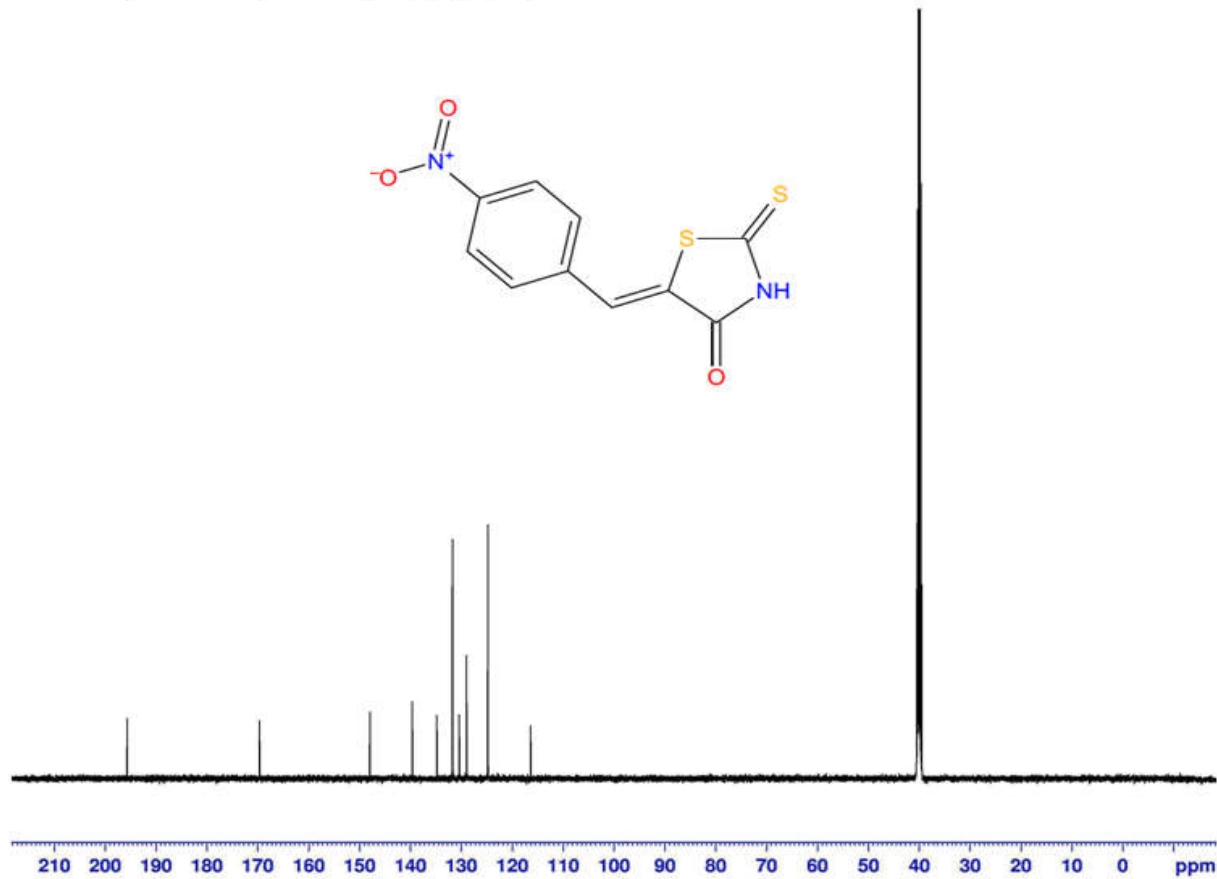
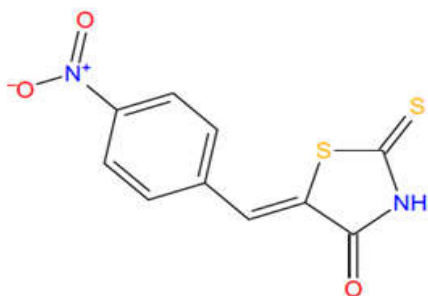
F2 - Acquisition Parameters  
Date\_ 20130911  
Time 5.17  
INSTRUM spect  
PROBHD 5 mm PABBO BB-  
PULPROG zg30  
TD 32768  
SOLVENT DMSO  
NS 32  
DS 2  
SWH 10330.578 Hz  
FIDRES 0.315264 Hz  
AQ 1.5860212 sec  
RG 203  
DW 48.400 usec  
DE 6.50 usec  
TE 300.0 K  
D1 1.00000000 sec  
TD0 1

===== CHANNEL f1 =====  
NUC1 1H  
P1 10.65 usec  
PL1 0 dB  
PL1W 23.53637505 W  
SFO1 500.1330885 MHz

F2 - Processing parameters  
SI 32768  
SF 500.1300000 MHz  
WDW EM  
SSB 0  
LB 0.30 Hz  
GB 0  
PC 1.00

N7.....Noorulla.

— 195.73 — 169.70 — 147.99 —  
139.67 135.33 131.76 130.44 129.03 124.79 — 116.96



Current Data Parameters  
NAME N7  
EXPNO 18  
PROCNO 1

F2 - Acquisition Parameters  
Date\_ 20130911  
Time 6.02  
INSTRUM spect  
PROBHD 5 mm PABBO BB-  
PULPROG zgpg30  
TD 32768  
SOLVENT DMSO  
NS 1024  
DS 4  
SWH 29761.904 Hz  
FIDRES 0.908261 Hz  
AQ 0.5505524 sec  
RG 203  
DW 16.800 usec  
DE 6.50 usec  
TE 301.3 K  
D1 2.0000000 sec  
D11 0.0300000 sec  
TD0 1

----- CHANNEL f1 -----  
NUC1 13C  
P1 7.80 usec  
PL1 0 dB  
PL1W 70.83519745 W  
SFO1 125.7703643 MHz

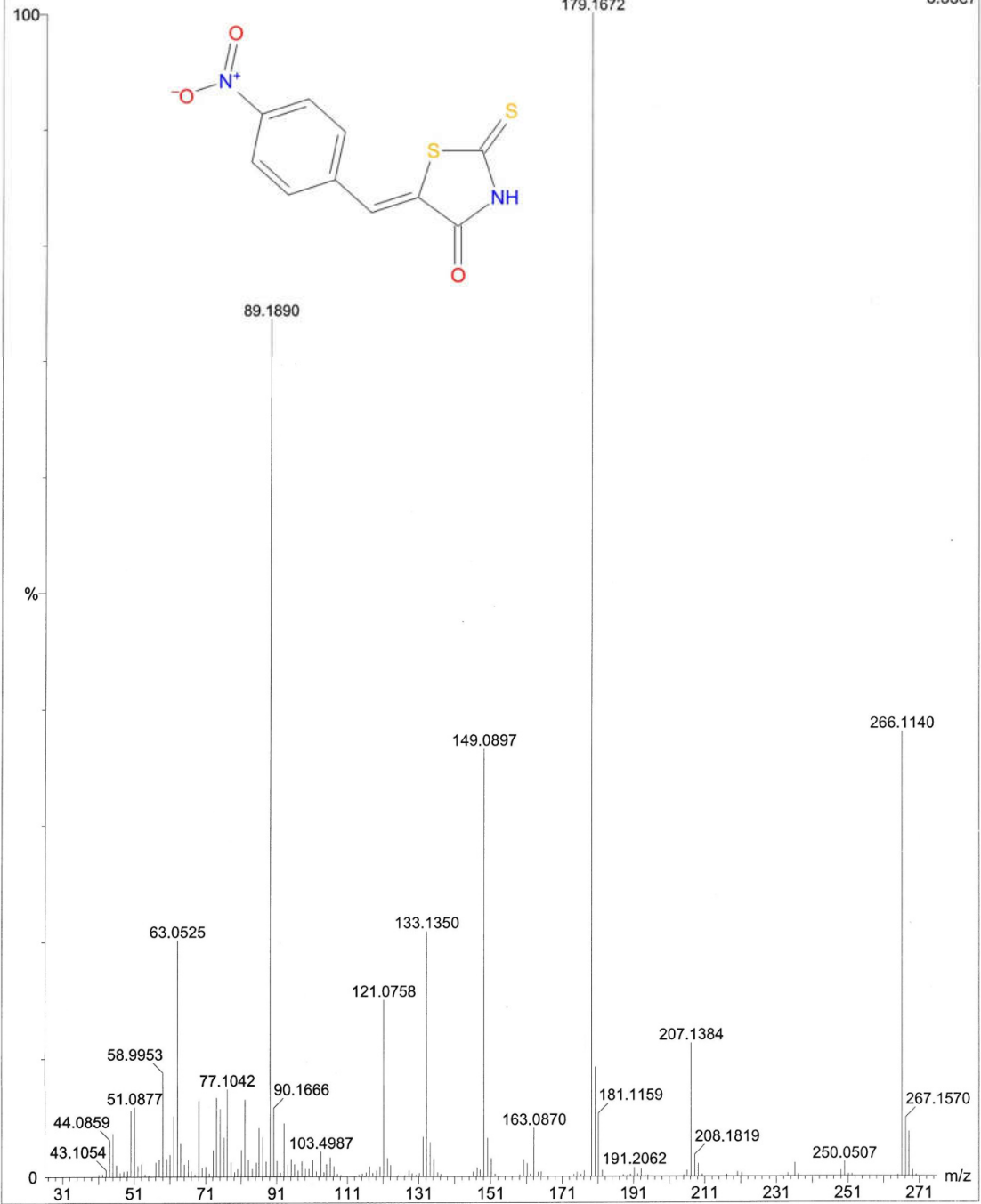
----- CHANNEL f2 -----  
CPDPRG2 waltz16  
NUC2 1H  
PCPD2 80.00 usec  
PL2 0 dB  
PL12 17.51 dB  
PL13 18.00 dB  
PL2W 23.53637505 W  
PL12W 0.41757989 W  
PL13W 0.37302643 W  
SFO2 500.1320005 MHz

F2 - Processing parameters  
SI 32768  
SF 125.7577890 MHz  
WDW EM  
SSB 0  
LB 1.00 Hz  
GB 0  
PC 1.40

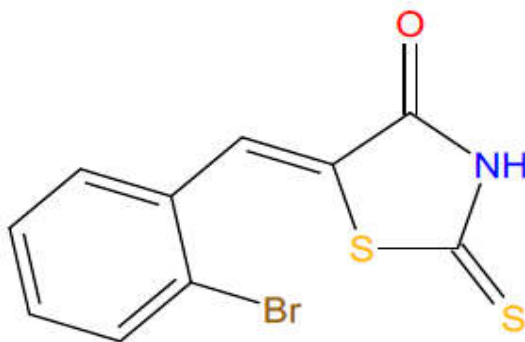


N7-4615 (25.583)

Scan EI+  
8.33e7



## Spectral Data of Compound N8



**IR (KBr,  $\nu_{\max}$ )  $\text{cm}^{-1}$**

604.87 (C-Br), 1450.36 (Ar C-C), 1604.66 (C=O), 1728.09 (C=S),  
2923.87 (=C-H), 3109.02 (Ar C-H), 3440.76 (N-H).

**$^1\text{H}$  NMR (DMSO- $\text{D}_6$ )  $\delta$**

7.40-7.45 (m, 1H, Ar-H), 7.51-7.59 (m, 2H, Ar-H), 7.72 (s, 1H, =C-H),  
7.81 (t, 1H, Ar-H), 13.96 (s, 1H, N-H)

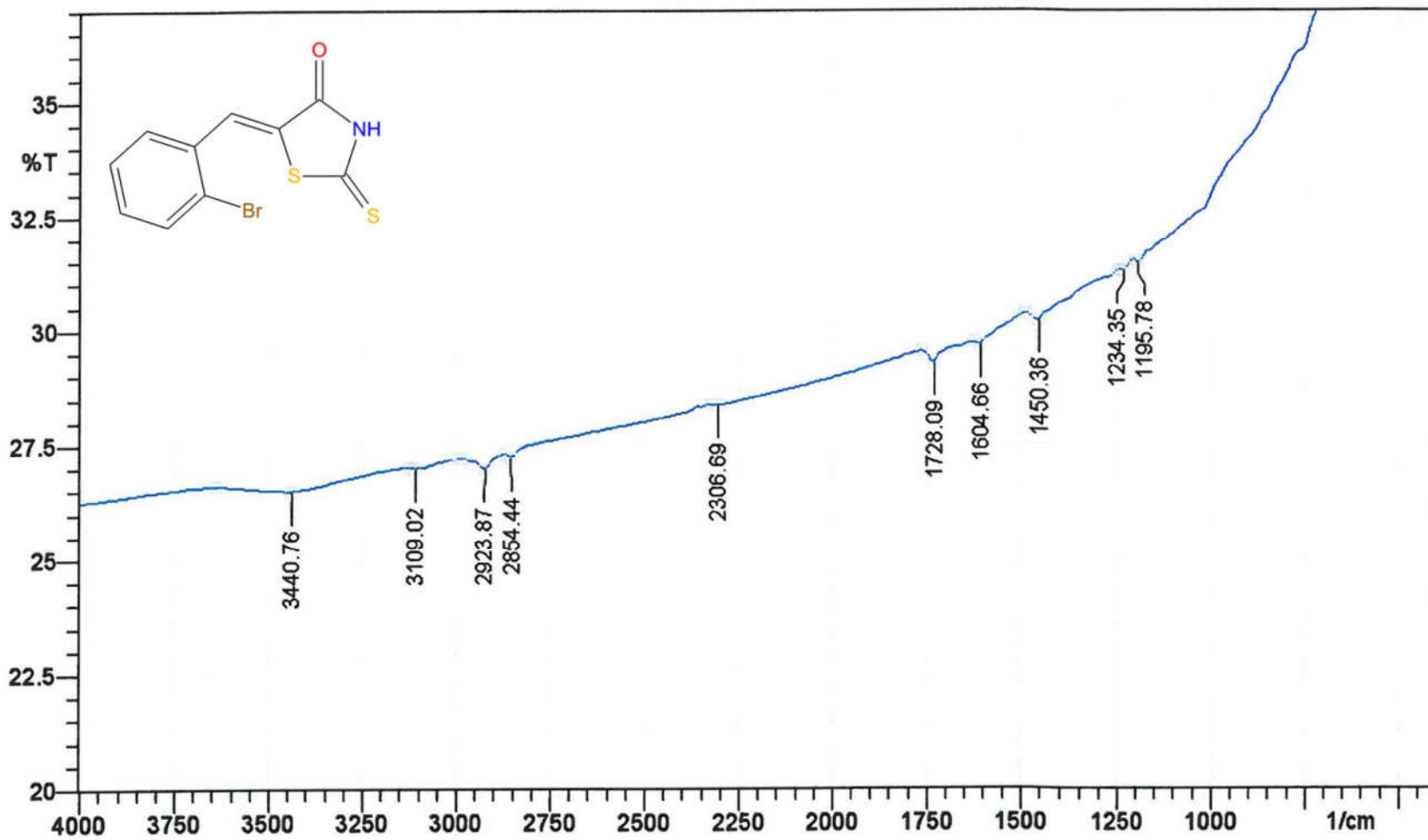
**$^{13}\text{C}$  NMR (DMSO- $\text{D}_6$ )  $\delta$**

117.18, 128.86, 129.11, 129.40, 132.21, 132.54, 133.71, 142.54,  
169.05, 195.58.

**MASS SPECTROSCOPY**

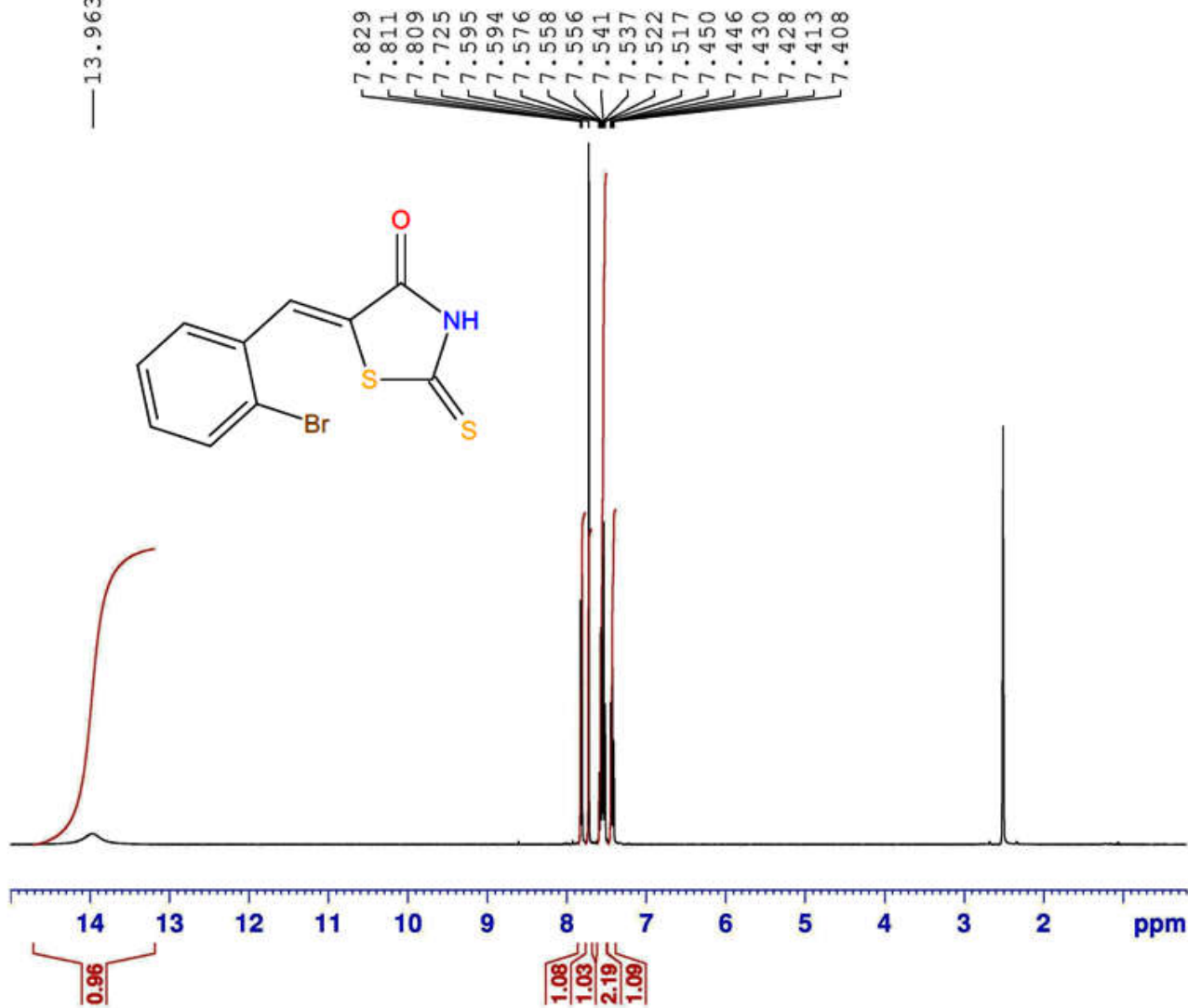
300.01 ( $\text{M}^+$ ), 302.21 ( $\text{M}+2$ ), 89.16 (**B**).

Sample: N 8



N8.....Noorulla

—13.963



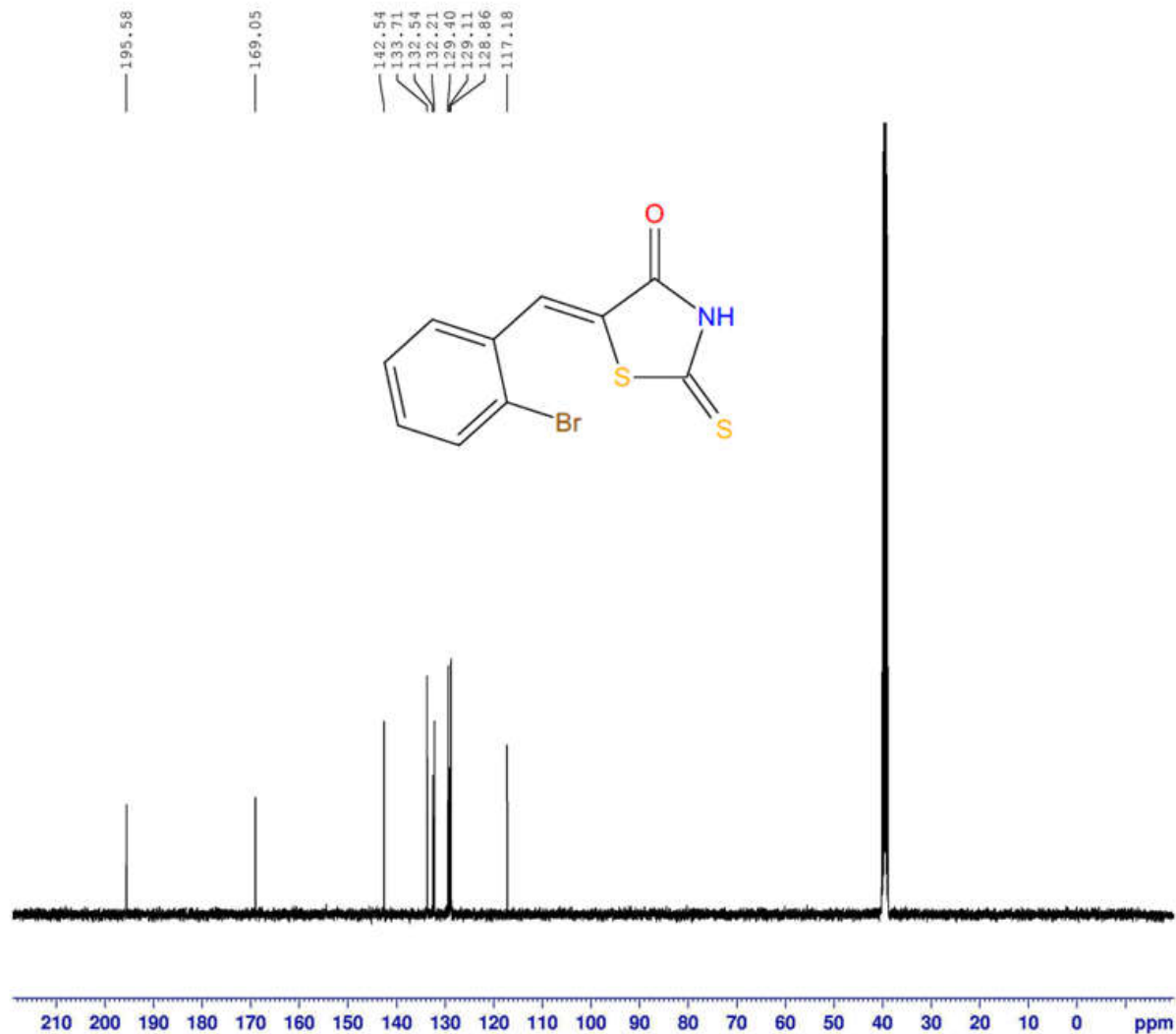
Current Data Parameters  
NAME N8  
EXPNO 211  
PROCNO 1

F2 - Acquisition Parameters  
Date\_ 20150726  
Time 4.13  
INSTRUM spect  
PROBHD 5 mm PABBO BB/  
PULPROG zg30  
TD 65536  
SOLVENT DMSO  
NS 16  
DS 2  
SWH 8223.685 Hz  
FIDRES 0.125483 Hz  
AQ 3.9846387 sec  
RG 156.91  
DW 60.800 usec  
DE 6.50 usec  
TE 297.4 K  
D1 1.00000000 sec  
TD0 1

===== CHANNEL f1 =====  
NUC1 1H  
P1 14.25 usec  
PLW1 14.00000000 W  
SFO1 400.2604718 MHz

F2 - Processing parameters  
SI 65536  
SF 400.2580010 MHz  
WDW EM  
SSB 0  
LB 0.30 Hz  
GB 0  
PC 1.00

N8.....Noorulla



Current Data Parameters  
NAME N8  
EXPNO 213  
PROCNO 1

F2 - Acquisition Parameters  
Date\_ 20150726  
Time 7.34  
INSTRUM spect  
PROBHD 5 mm PABBO BB/  
PULPROG zgpg30  
TD 65536  
SOLVENT DMSO  
NS 600  
DS 4  
SWH 24038.461 Hz  
FIDRES 0.366798 Hz  
AQ 1.3631988 sec  
RG 199.6  
DW 20.800 usec  
DE 6.50 usec  
TE 299.0 K  
D1 2.00000000 sec  
D11 0.03000000 sec  
TD0 1

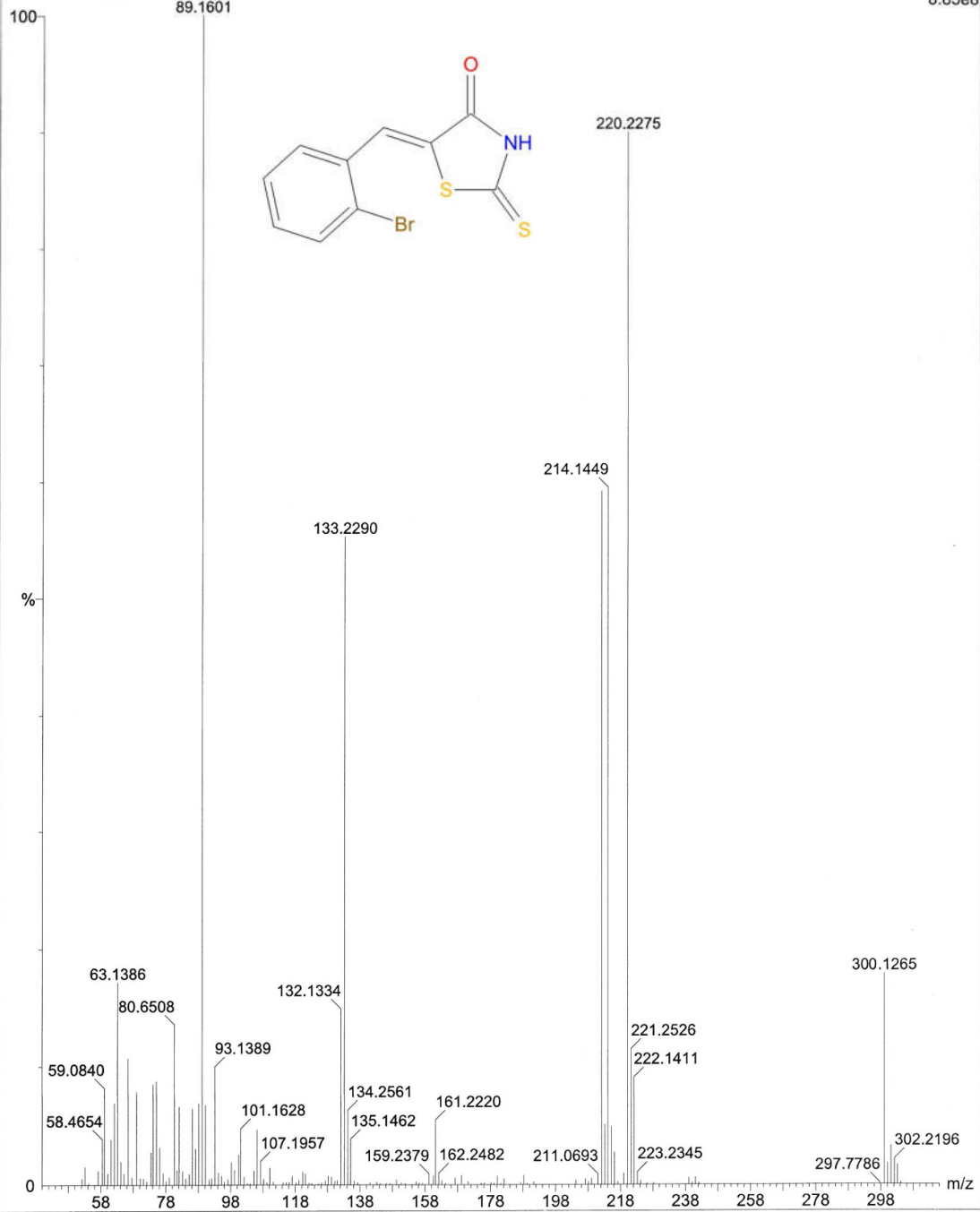
===== CHANNEL f1 =====  
NUC1 13C  
P1 9.80 usec  
PLW1 58.00000000 W  
SFO1 100.6550182 MHz

===== CHANNEL f2 =====  
CPDPRG2 waltz16  
NUC2 1H  
PCPD2 90.00 usec  
PLW2 14.00000000 W  
PLW12 0.35097000 W  
PLW13 0.28428999 W  
SFO2 400.2596010 MHz

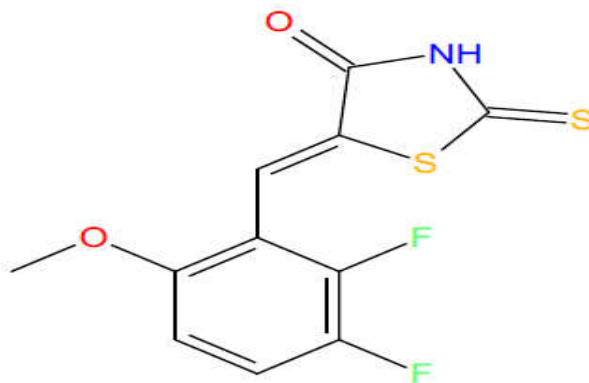
F2 - Processing parameters  
SI 32768  
SF 100.6450043 MHz  
WDW EM  
SSB 0  
LB 1.00 Hz  
GB 0  
PC 1.40

N8-4108 (23.047)

Scan EI+  
8.85e8



## Spectral Data of Compound N9



**IR (KBr,  $\nu_{\max}$ )  $\text{cm}^{-1}$**

1080.06 (C-F), 1203.49 (ether C-O), 1434.93 (Ar C-C), 1581.51 (C=O), 1697.23 (C=S), 2854.44 (alkane C-H), 3109.02 (=C-H), 3147.60 (Ar C-H), 3556.48 (N-H).

**$^1\text{H}$  NMR (DMSO- $\text{D}_6$ )  $\delta$**

3.91 (s, 3H, O- $\text{CH}_3$ ), 6.95-6.98 (m, 1H, Ar-H), 7.51 (s, 1H, =CH-), 7.54-7.62 (q, 1H, Ar-H), 13.78 (s, 1H, N-H).

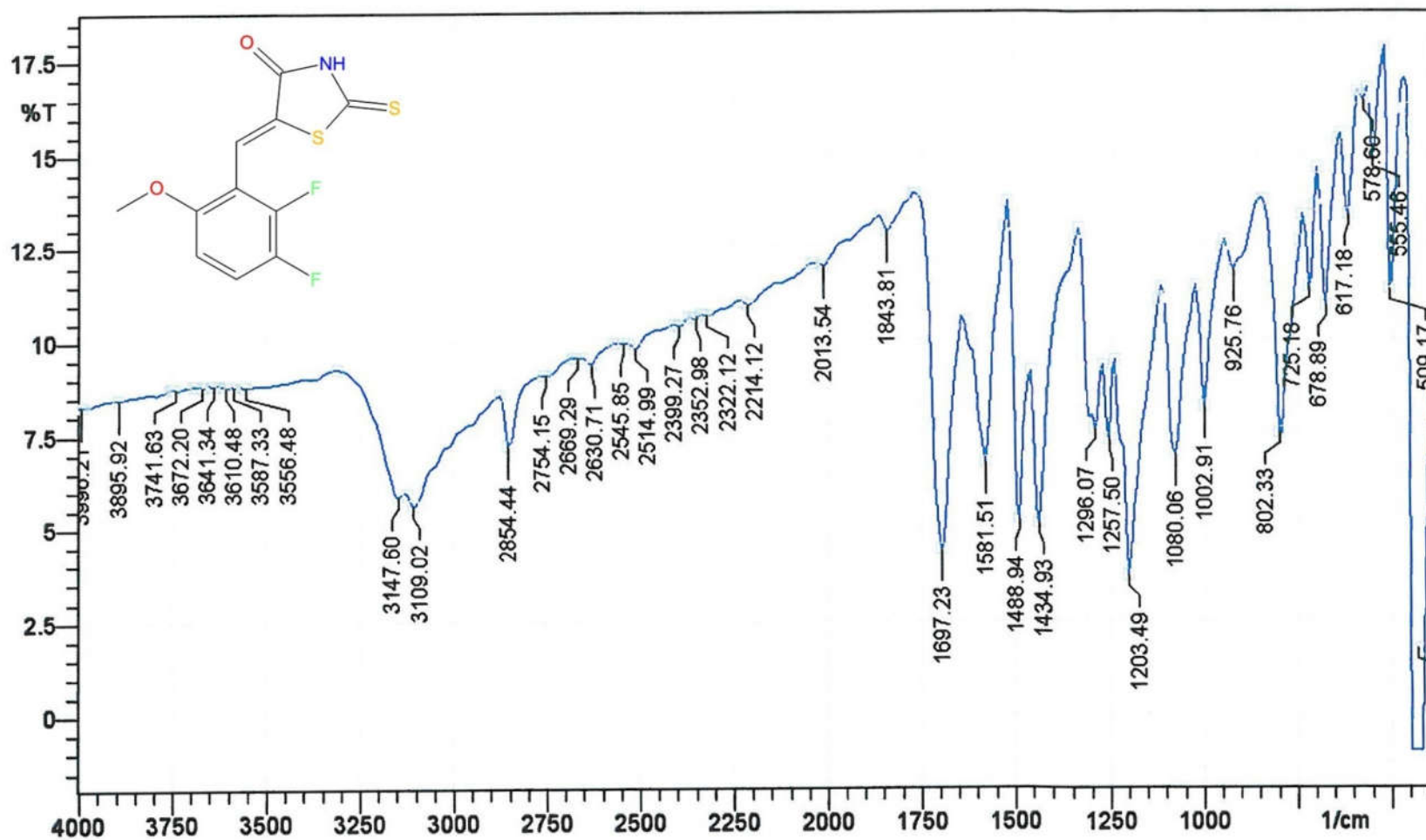
**$^{13}\text{C}$  NMR (DMSO- $\text{D}_6$ )  $\delta$**

56.20, 111.46, 119.83, 120.01, 120.20, 120.25, 120.28, 130.44, 142.92, 169.07, 196.44.

**MASS SPECTROSCOPY**

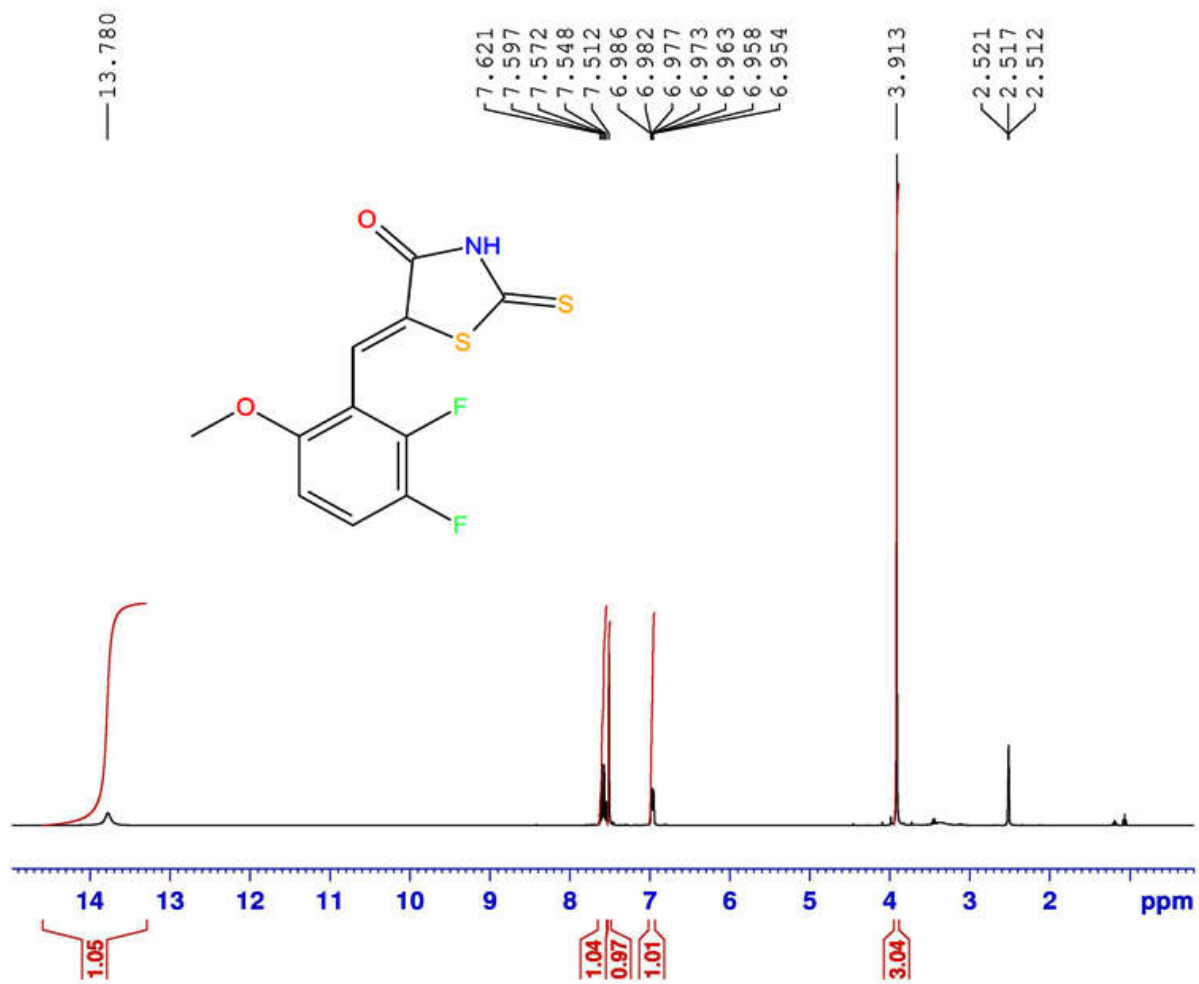
287.18 ( $\text{M}^+$ ), 288.21 ( $\text{M}+1$ ), 200.26 (**B**).

Sample: N 9





N9.....Noorulla



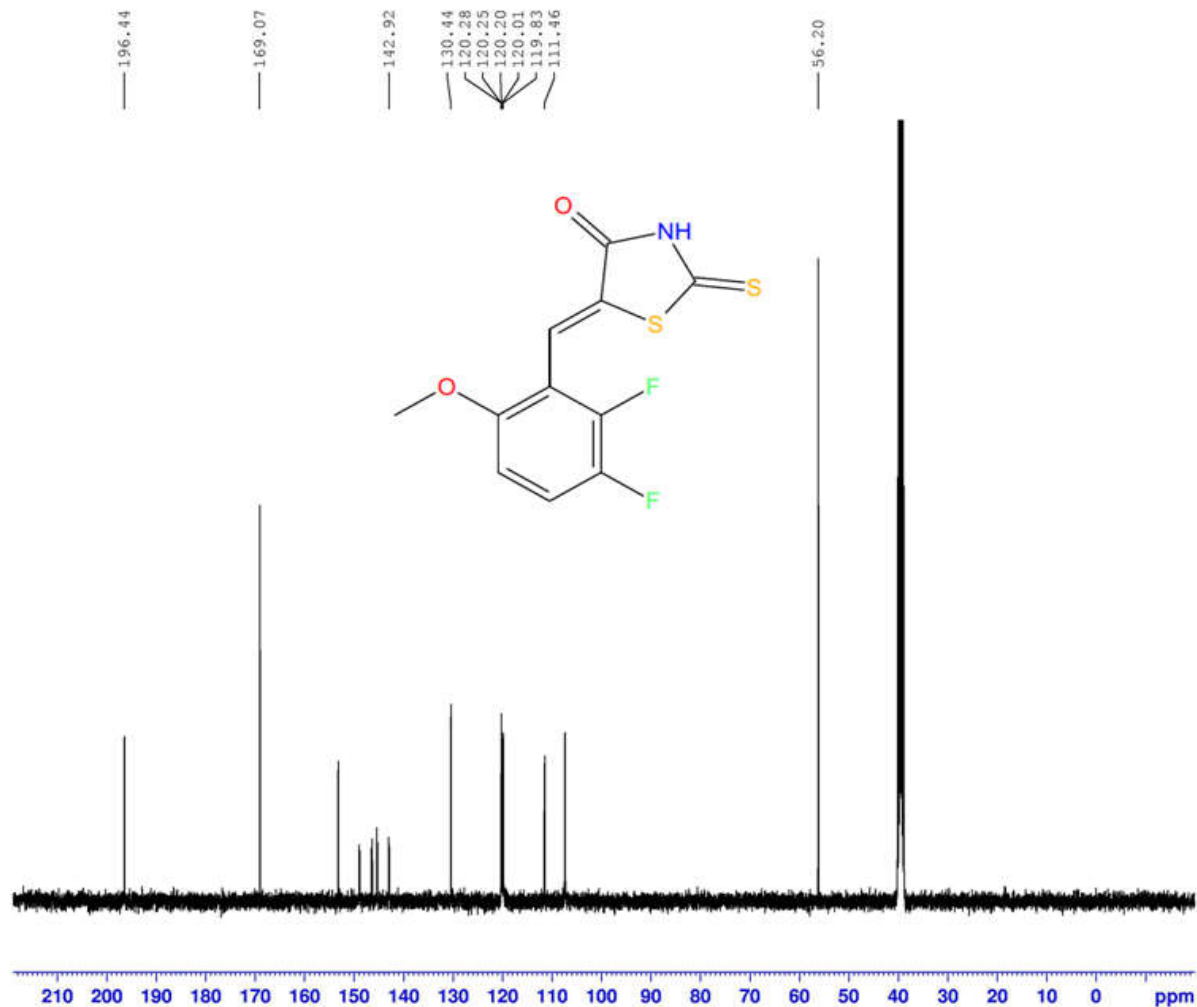
Current Data Parameters  
NAME N9  
EXPNO 212  
PROCNO 1

F2 - Acquisition Parameters  
Date\_ 20150726  
Time 4.16  
INSTRUM spect  
PROBHD 5 mm PABBO BB/  
PULPROG zg30  
TD 65536  
SOLVENT DMSO  
NS 16  
DS 2  
SWH 8223.685 Hz  
FIDRES 0.125483 Hz  
AQ 3.9846387 sec  
RG 127.79  
DW 60.800 usec  
DE 6.50 usec  
TE 297.4 K  
D1 1.00000000 sec  
TD0 1

===== CHANNEL f1 =====  
NUC1 1H  
P1 14.25 usec  
PLW1 14.00000000 W  
SF01 400.2604718 MHz

F2 - Processing parameters  
SI 65536  
SF 400.2579985 MHz  
WDW EM  
SSB 0  
LB 0.30 Hz  
GB 0  
PC 1.00

N9.....Noorulla



Current Data Parameters  
NAME N9  
EXPNO 214  
PROCNO 1

F2 - Acquisition Parameters  
Date\_ 20150726  
Time 8.10  
INSTRUM spect  
PROBHD 5 mm PABBO BB/  
PULPROG zgpg30  
TD 65536  
SOLVENT DMSO  
NS 600  
DS 4  
SWH 24038.461 Hz  
FIDRES 0.366798 Hz  
AQ 1.3631988 sec  
RG 199.6  
DW 20.800 usec  
DE 6.50 usec  
TE 299.0 K  
D1 2.00000000 sec  
D11 0.03000000 sec  
TD0 1

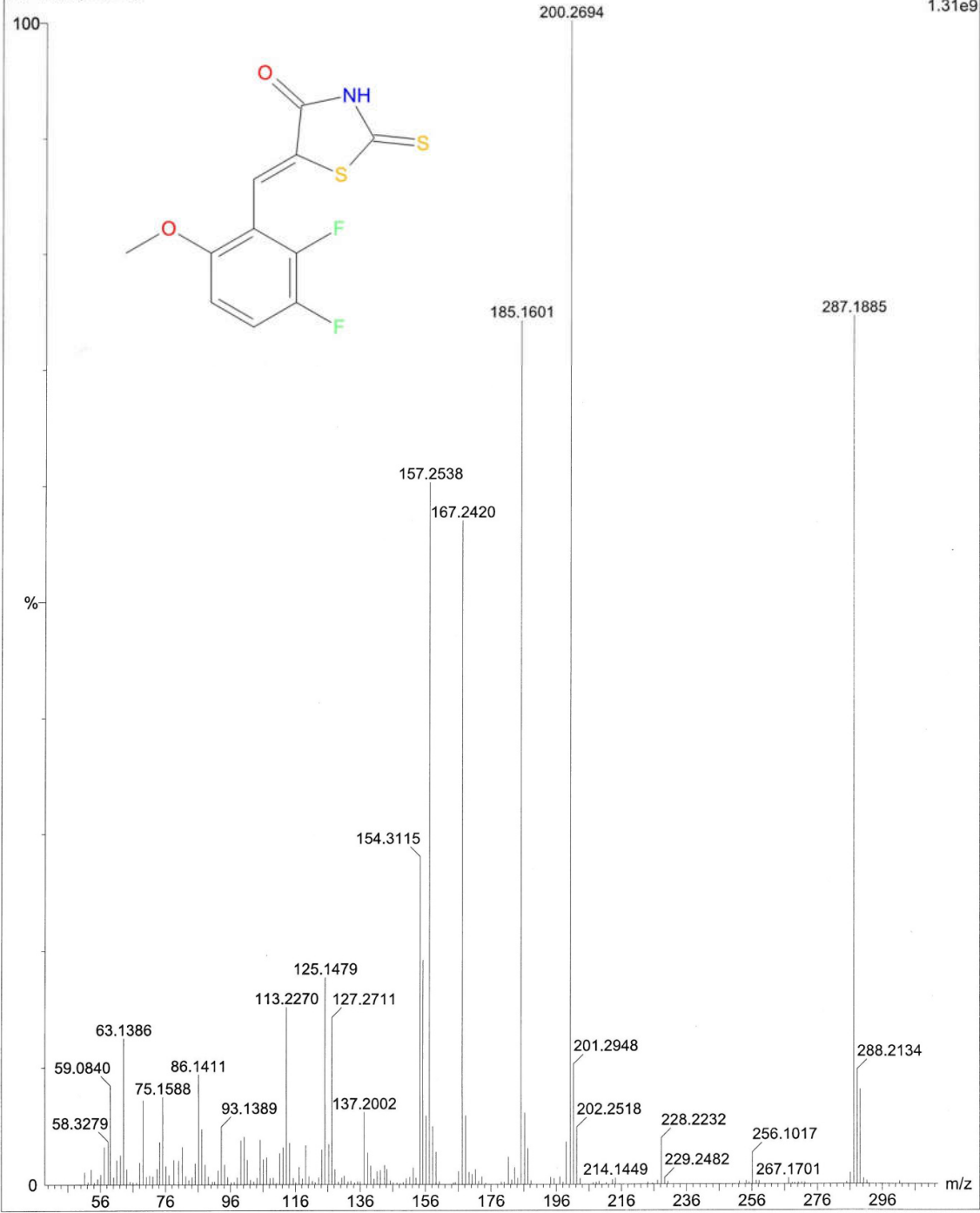
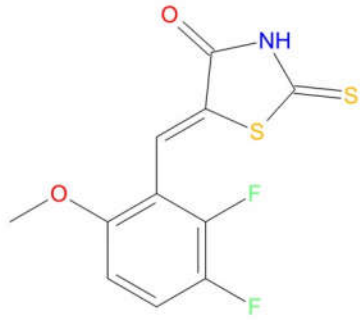
===== CHANNEL f1 =====  
NUC1 13C  
P1 9.80 usec  
PLW1 58.00000000 W  
SFO1 100.6550182 MHz

===== CHANNEL f2 =====  
CPDPRG2 waltz16  
NUC2 1H  
PCPD2 90.00 usec  
PLW2 14.00000000 W  
PLW12 0.35097000 W  
PLW13 0.28428999 W  
SFO2 400.2596010 MHz

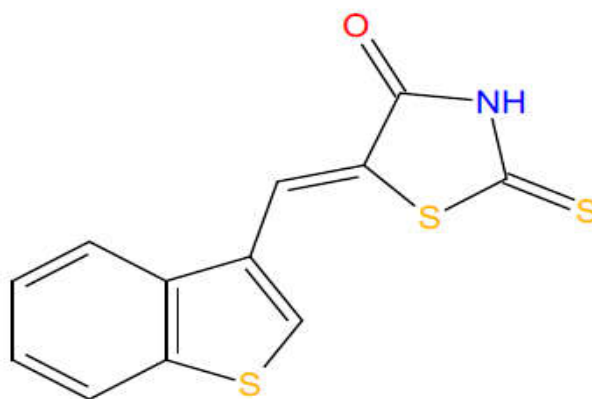
F2 - Processing parameters  
SI 32768  
SF 100.6450043 MHz  
WDW EM  
SSB 0  
LB 1.00 Hz  
GB 0  
PC 1.40

N9-4013 (22.571)

Scan E1+  
1.31e9



## Spectral Data of Compound N10



**IR (KBr,  $\nu_{\max}$ )  $\text{cm}^{-1}$**

1427.22 (Ar C-C), 1589.23 (C=O), 1697.23 (C=S), 2839.01 (=C-H),  
3062.73 (Ar C-H), 3456.18 (N-H).

**$^1\text{H}$  NMR (DMSO- $\text{D}_6$ )  $\delta$**

7.50-7.55 (m, 2H, Ar-H), 7.88 (s, 1H, =CH-), 8.09-8.16 (m, 3H, Ar-H), 13.87 (s, 1H, N-H).

**$^{13}\text{C}$  NMR (DMSO- $\text{D}_6$ )  $\delta$**

114.01, 125.34, 125.64, 125.71, 125.94, 126.65, 127.74, 138.72,  
139.12, 151.00, 169.08, 195.38.

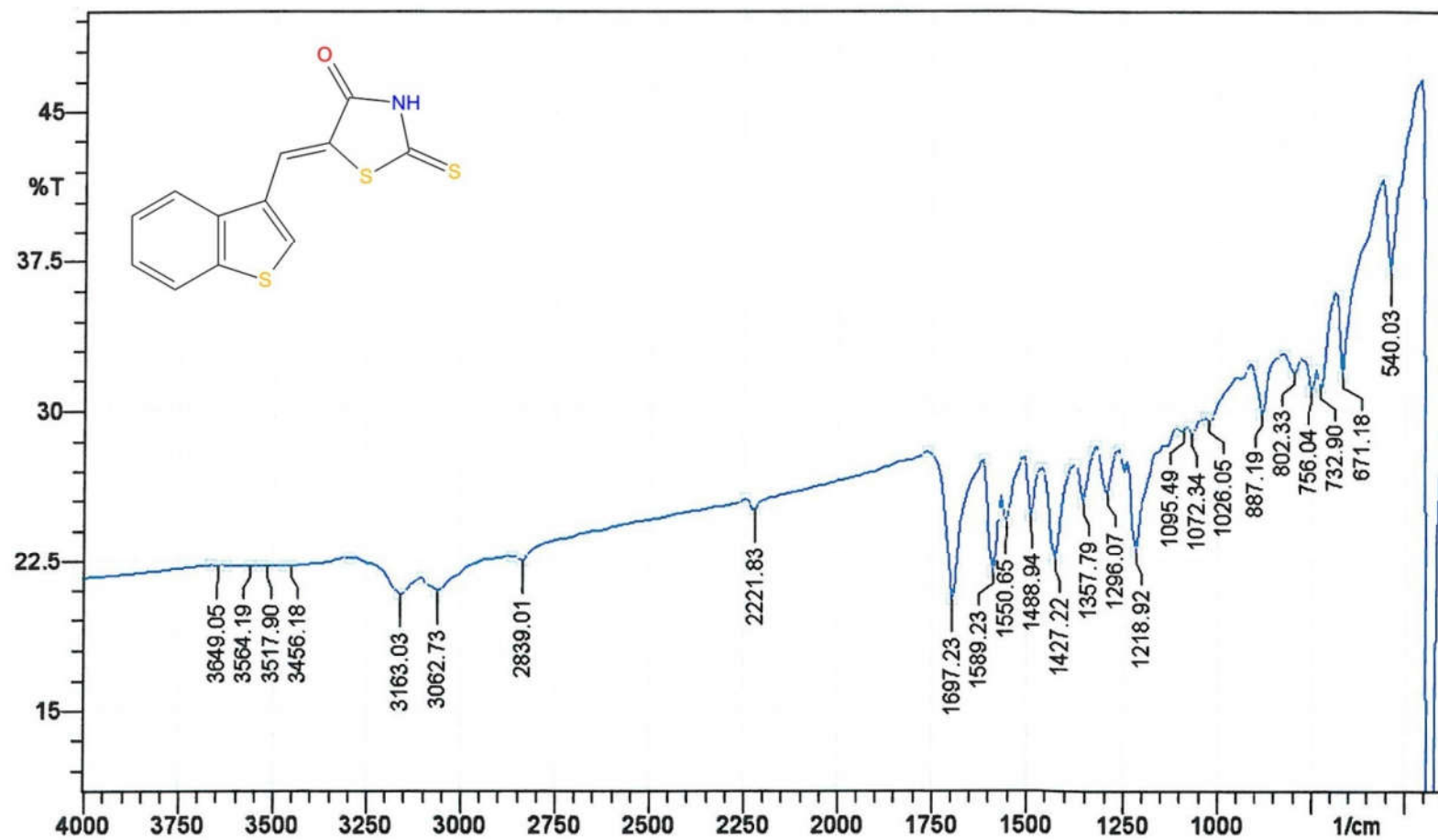
**MASS SPECTROSCOPY**

277.14 ( $\text{M}^+$ ), 278.23 ( $\text{M}+1$ ), 190.15 ( $\text{B}$ ).

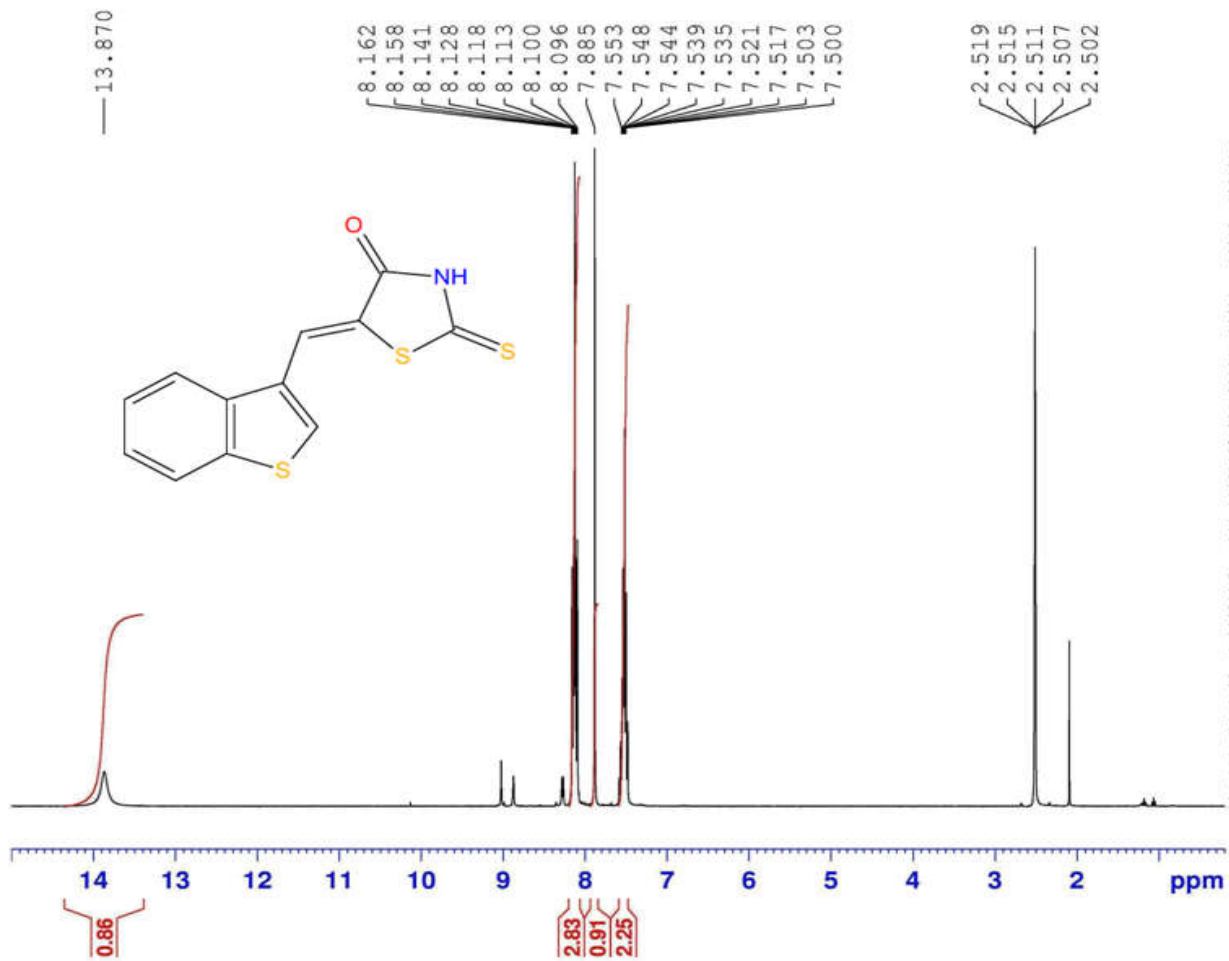
**ELEMENTAL ANALYSIS**

Anal. Calcd. For N10: C, 51.96; H, 2.54; N, 5.05; Obsd. C, 52.11; H, 2.53; N, 5.04.

Sample: N 10



N10.....Noorulla



Current Data Parameters  
NAME N10  
EXPNO 215  
PROCNO 1

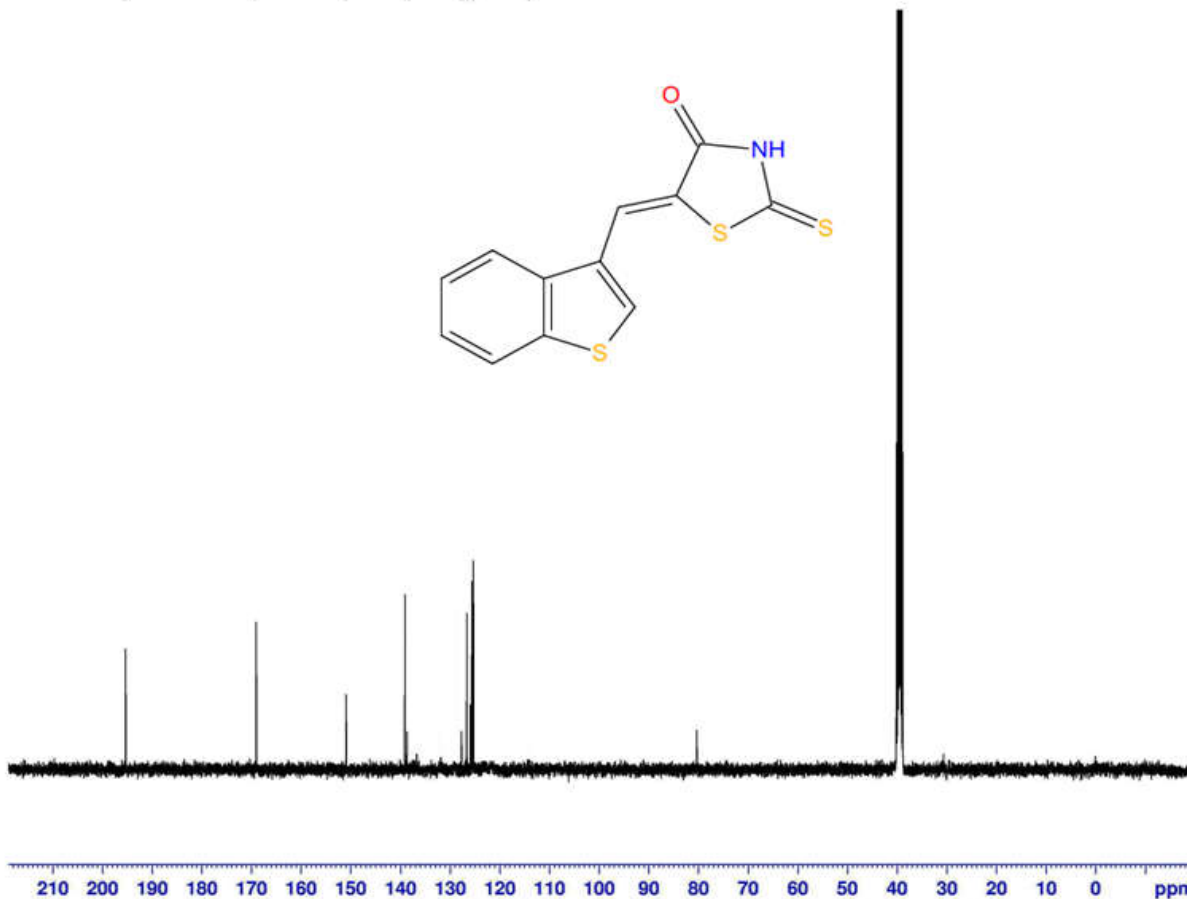
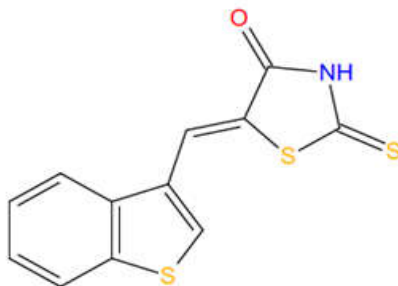
F2 - Acquisition Parameters  
Date\_ 20150726  
Time 8.13  
INSTRUM spect  
PROBHD 5 mm PABBO BB/  
PULPROG zg30  
TD 65536  
SOLVENT DMSO  
NS 16  
DS 2  
SWH 8223.685 Hz  
FIDRES 0.125483 Hz  
AQ 3.9846387 sec  
RG 175.97  
DW 60.800 usec  
DE 6.50 usec  
TE 298.3 K  
D1 1.00000000 sec  
TD0 1

===== CHANNEL f1 =====  
NUC1 1H  
P1 14.25 usec  
PLW1 14.00000000 W  
SFO1 400.2604718 MHz

F2 - Processing parameters  
SI 65536  
SF 400.2580009 MHz  
WDW EM  
SSB 0  
LB 0.30 Hz  
GB 0  
PC 1.00

N10.....Noorulla

195.38  
169.08  
151.00  
139.12  
138.72  
127.74  
126.65  
125.94  
125.71  
125.64  
125.34  
114.01



Current Data Parameters  
NAME N10  
EXPNO 216  
PROCNO 1

F2 - Acquisition Parameters  
Date\_ 20150726  
Time 8.48  
INSTRUM spect  
PROBHD 5 mm PABBO BB/  
PULPROG zgpg30  
TD 65536  
SOLVENT DMSO  
NS 600  
DS 4  
SWH 24038.461 Hz  
FIDRES 0.366798 Hz  
AQ 1.3631988 sec  
RG 199.6  
DW 20.800 usec  
DE 6.50 usec  
TE 299.1 K  
D1 2.00000000 sec  
D11 0.03000000 sec  
TD0 1

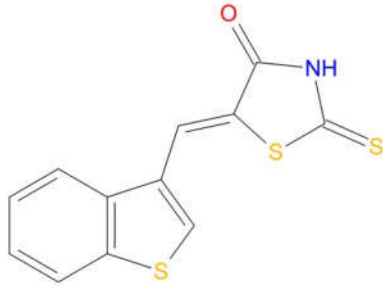
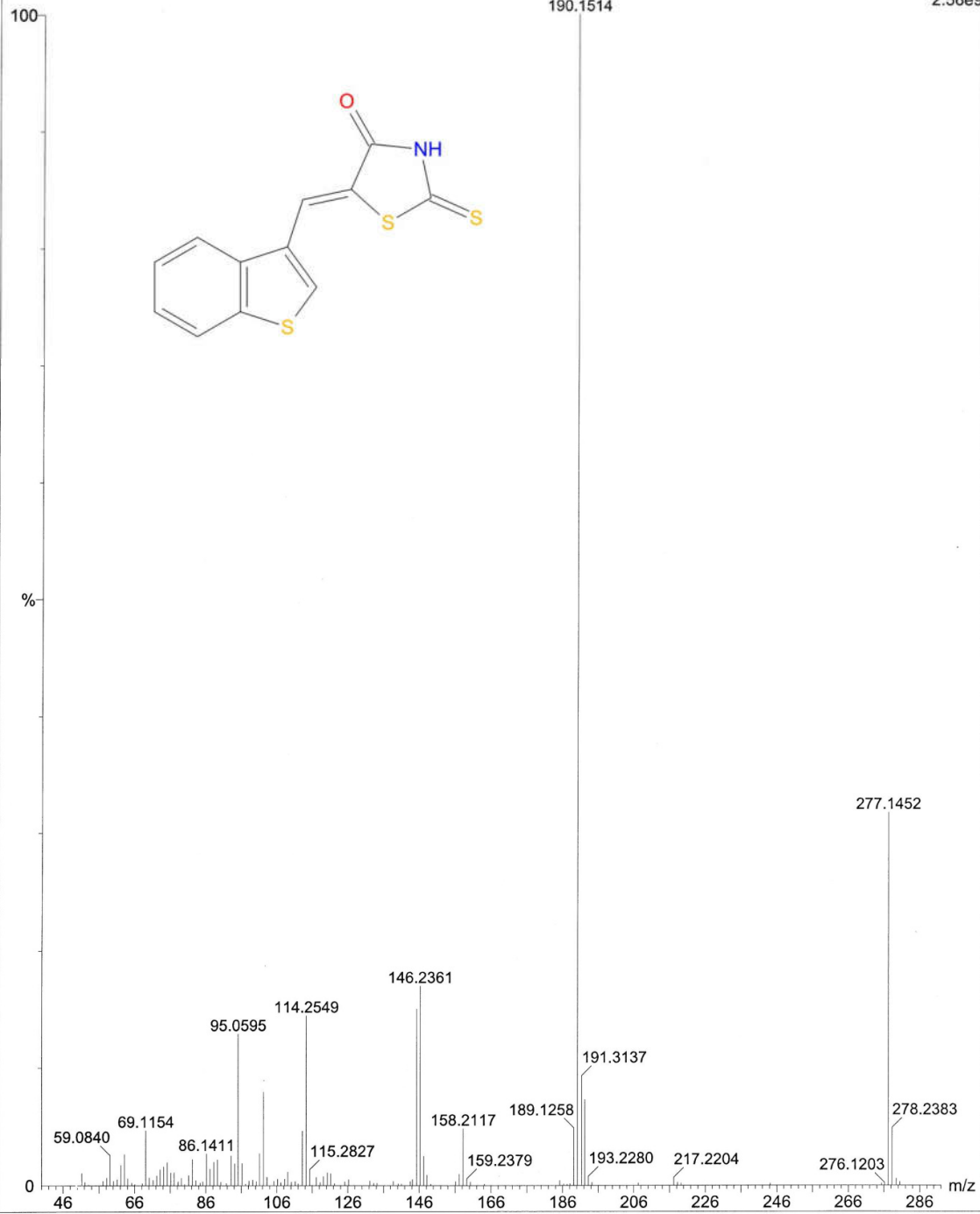
===== CHANNEL f1 =====  
NUC1 13C  
P1 9.80 usec  
PLW1 58.00000000 W  
SFO1 100.6550182 MHz

===== CHANNEL f2 =====  
CPDPRG2 waltz16  
NUC2 1H  
PCPD2 90.00 usec  
PLW2 14.00000000 W  
PLW12 0.35097000 W  
PLW13 0.28428999 W  
SFO2 400.2596010 MHz

F2 - Processing parameters  
SI 32768  
SF 100.6450043 MHz  
WDW EM  
SSB 0  
LB 1.00 Hz  
GB 0  
PC 1.40

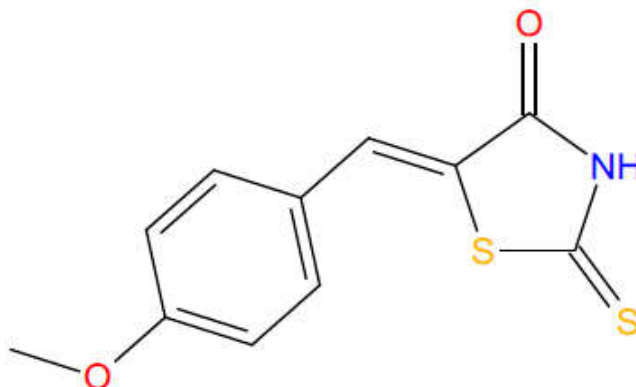
N10-4689 (25.953)

Scan EI+  
2.56e9





## Spectral Data of Compound N11



### IR (KBr, $\nu_{\max}$ ) $\text{cm}^{-1}$

1257.50 (ether C-O), 1442.65 (Ar C-C), 1689.52 (C=O), 1751.24 (C=S), 2923.87 (alkane C-H), 3008.73 (=C-H), 3132.17 (Ar C-H), 3471.61 (N-H).

### $^1\text{H}$ NMR (DMSO- $\text{D}_6$ ) $\delta$

3.84 (s, 3H, O-CH<sub>3</sub>), 7.10 (d, 2H, Ar-H), 7.56 (d, 2H, Ar-H), 7.60 (s, 1H, =CH-), 13.74 (s, 1H, NH).

### $^{13}\text{C}$ NMR (DMSO- $\text{D}_6$ ) $\delta$

55.53, 115.06, 122.19, 125.45, 128.05, 131.86, 132.66, 133.59, 144.24, 169.39, 195.47.

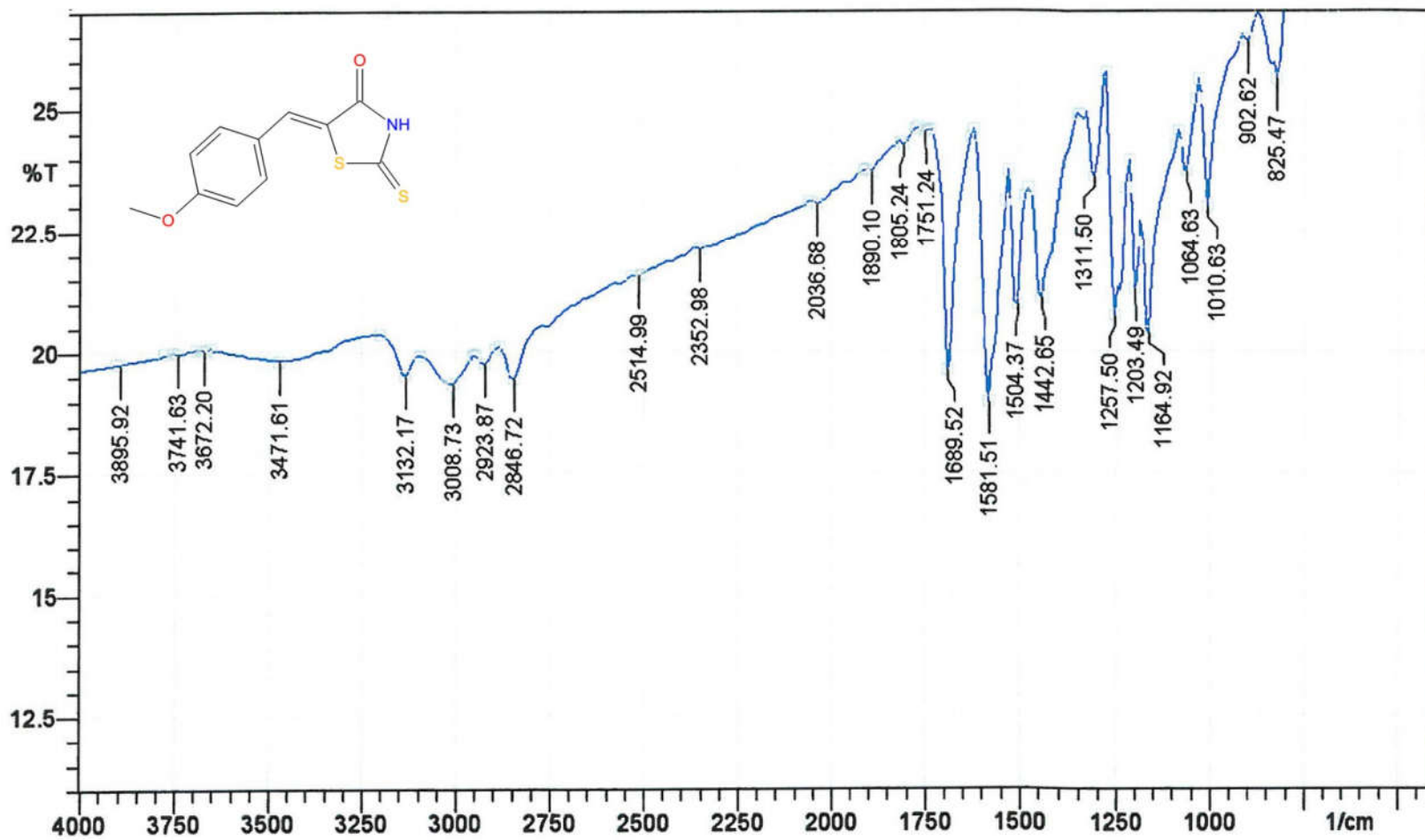
### MASS SPECTROSCOPY

251.25 ( $\text{M}^+$ ), 252.27 ( $\text{M}+1$ ), 164.30 (**B**).

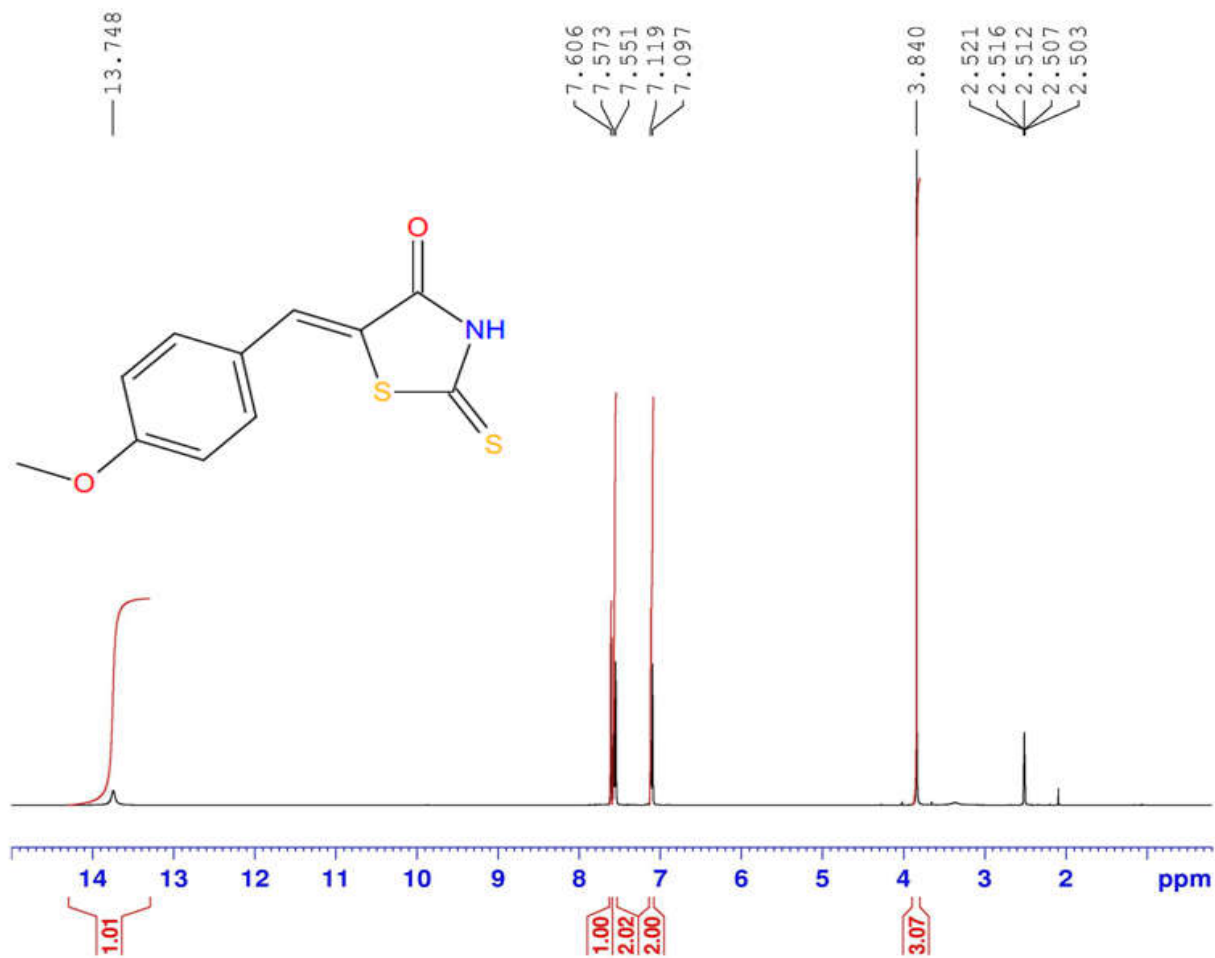
### ELEMENTAL ANALYSIS

Anal. Calcd. For N11: C, 52.57; H, 3.61; N, 5.57; Obsd. C, 52.39; H, 3.62; N, 5.56.

Sample: N 11



N11.....Noorulla



Current Data Parameters  
NAME N11  
EXPNO 217  
PROCNO 1

F2 - Acquisition Parameters  
Date\_ 20150726  
Time 8.51  
INSTRUM spect  
PROBHD 5 mm PABBO BB/  
PULPROG zg30  
TD 65536  
SOLVENT DMSO  
NS 16  
DS 2  
SWH 8223.685 Hz  
FIDRES 0.125483 Hz  
AQ 3.9846387 sec  
RG 127.79  
DW 60.800 usec  
DE 6.50 usec  
TE 298.3 K  
D1 1.00000000 sec  
TD0 1

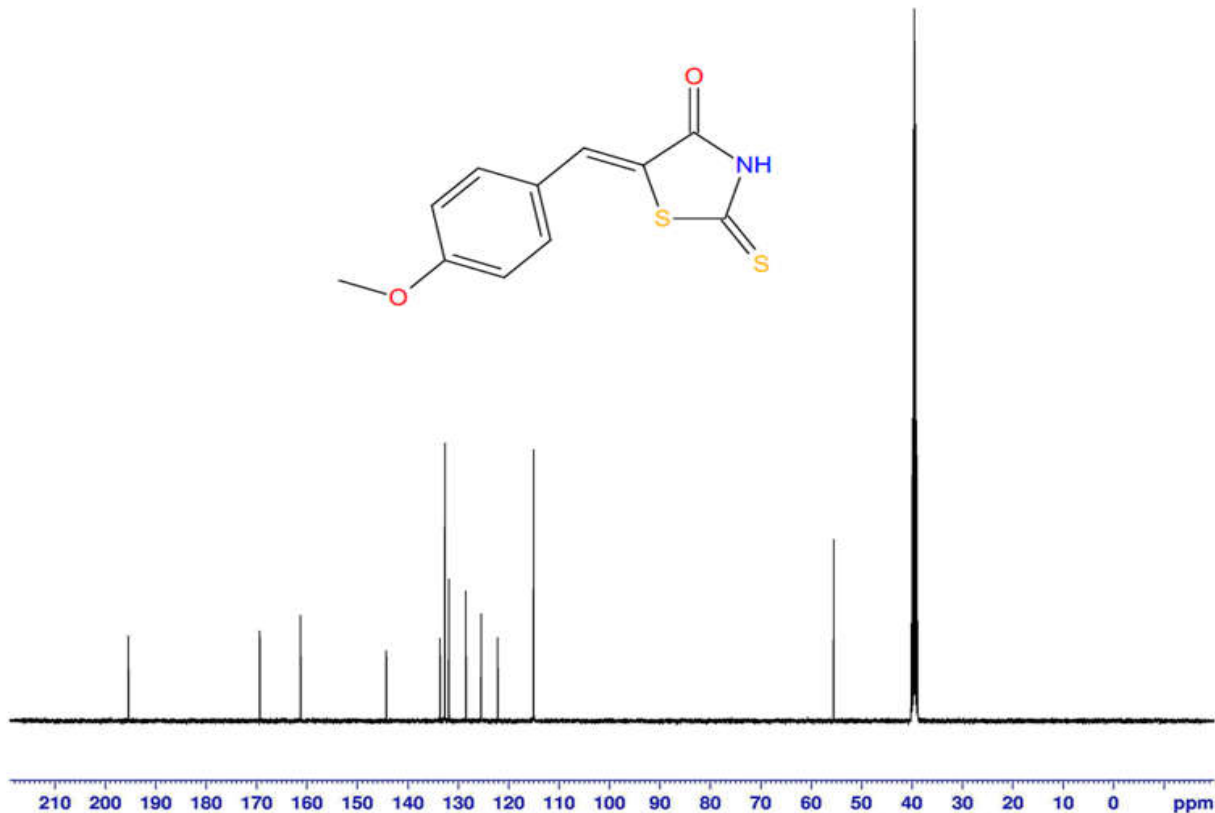
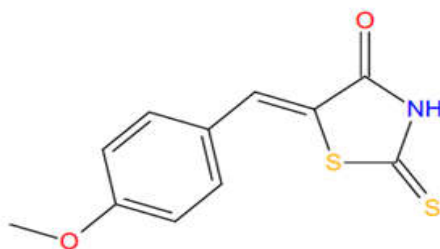
===== CHANNEL f1 =====  
NUC1 1H  
P1 14.25 usec  
PLW1 14.00000000 W  
SFO1 400.2604718 MHz

F2 - Processing parameters  
SI 65536  
SF 400.2580005 MHz  
WDW EM  
SSB 0  
LB 0.30 Hz  
GB 0  
PC 1.00

N11.....Noorulla

195.47  
169.39  
144.24  
133.59  
132.66  
131.86  
128.05  
125.45  
122.19  
115.06

55.53



Current Data Parameters  
NAME N11  
EXPNO 218  
PROCNO 1

F2 - Acquisition Parameters  
Date\_ 20150726  
Time 9.26  
INSTRUM spect  
PROBHD 5 mm PABBO BB/  
PULPROG zgpg30  
TD 65536  
SOLVENT DMSO  
NS 600  
DS 4  
SWH 24038.461 Hz  
FIDRES 0.366798 Hz  
AQ 1.3631988 sec  
RG 156.91  
DW 20.800 usec  
DE 6.50 usec  
TE 299.0 K  
D1 2.0000000 sec  
D11 0.0300000 sec  
TD0 1

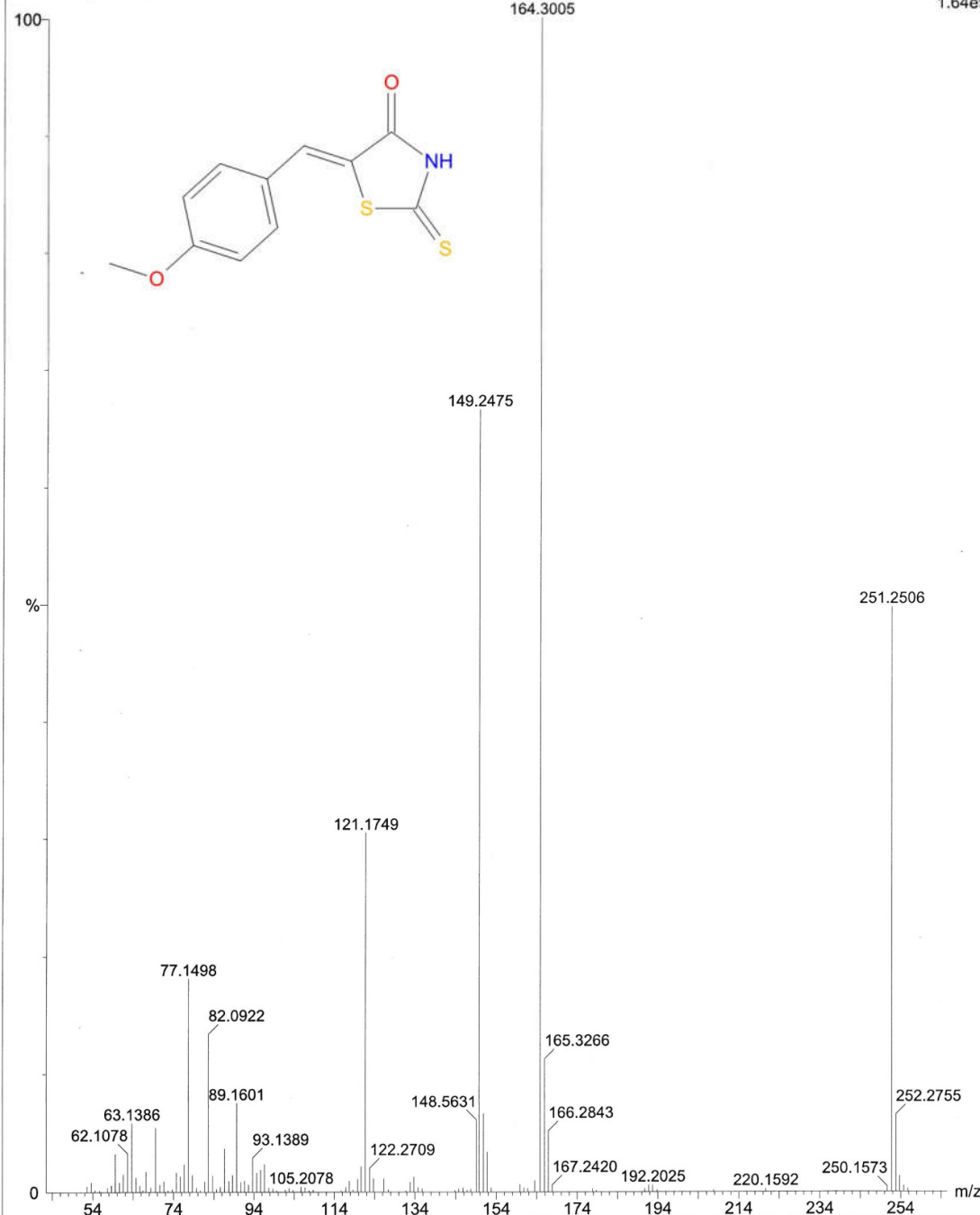
===== CHANNEL f1 =====  
NUC1 13C  
P1 9.80 usec  
PLW1 58.0000000 W  
SFO1 100.6550182 MHz

===== CHANNEL f2 =====  
CPDPRG2 waltz16  
NUC2 1H  
PCPD2 90.00 usec  
PLW2 14.0000000 W  
PLW12 0.35097000 W  
PLW13 0.28428999 W  
SFO2 400.2596010 MHz

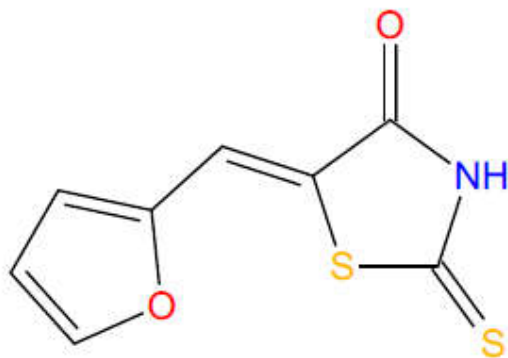
F2 - Processing parameters  
SI 32768  
SF 100.6450043 MHz  
WDW EM  
SSB 0  
LB 1.00 Hz  
GB 0  
PC 1.40

N11-4249 (23.752)

Scan EI+  
1.64e9



## Spectral Data of Compound N12



**IR (KBr,  $\nu_{\max}$ )  $\text{cm}^{-1}$**

1442.65 (Ar C-C), 1689.52 (C=O), 1797.52 (C=S), 2923.87 (=C-H),  
3031.88 (Ar C-H), 3456.18 (N-H).

**$^1\text{H}$  NMR (DMSO- $\text{D}_6$ )  $\delta$**

6.76-6.78 (q, 1H, hetero Ar-H), 7.18 (d, 1H, hetero Ar-H), 7.49 (s,  
1H, =CH-), 8.11 (d, 1H, hetero Ar-H), 13.69 (s, 1H, NH).

**$^{13}\text{C}$  NMR (DMSO- $\text{D}_6$ )  $\delta$**

113.89, 119.85, 122.42, 129.54, 135.72, 148.29, 168.98, 196.47.

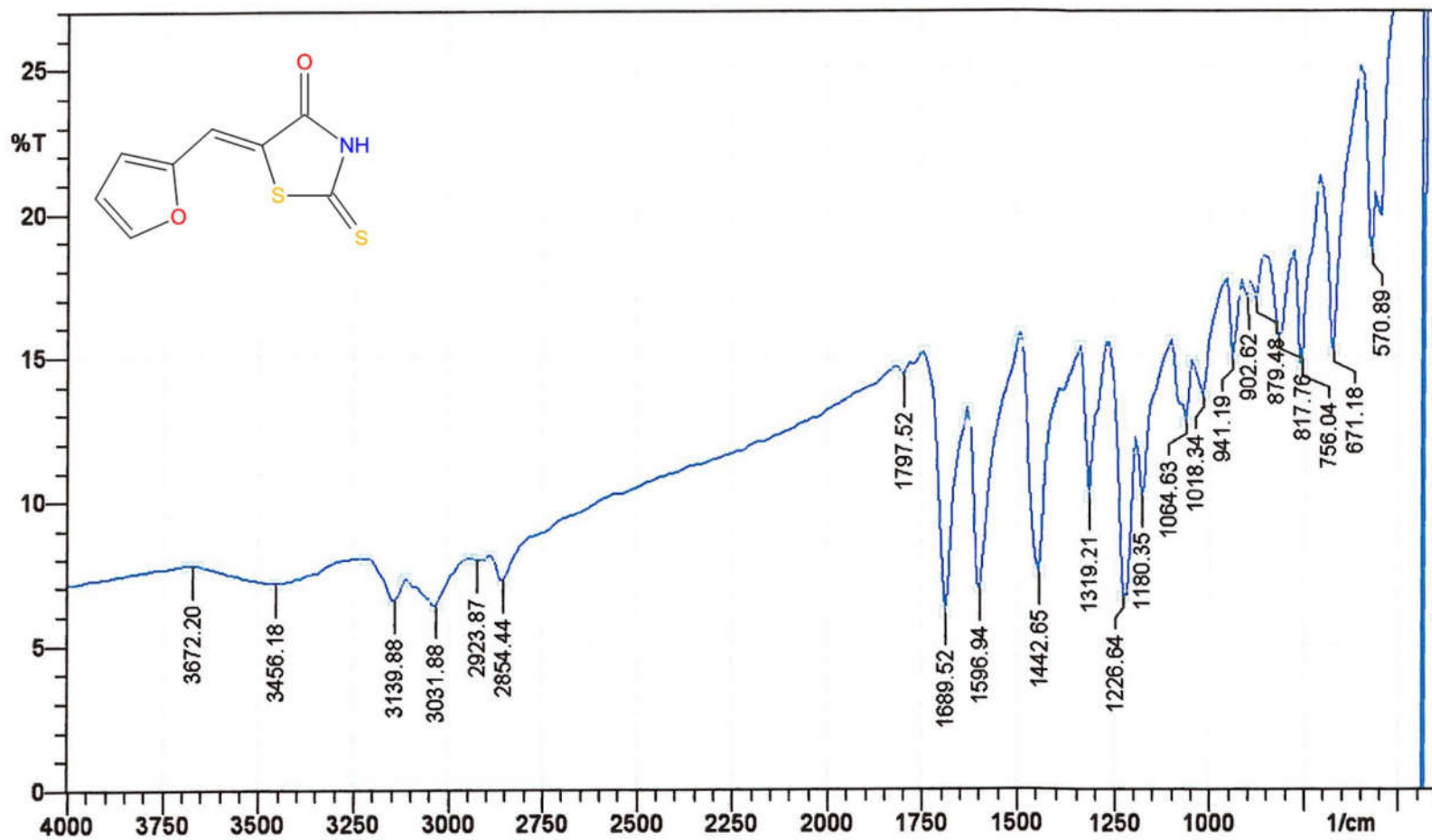
**MASS SPECTROSCOPY**

211.20 ( $\text{M}^+$ ), 212.29 ( $\text{M}+1$ ), 124.12 (**B**).

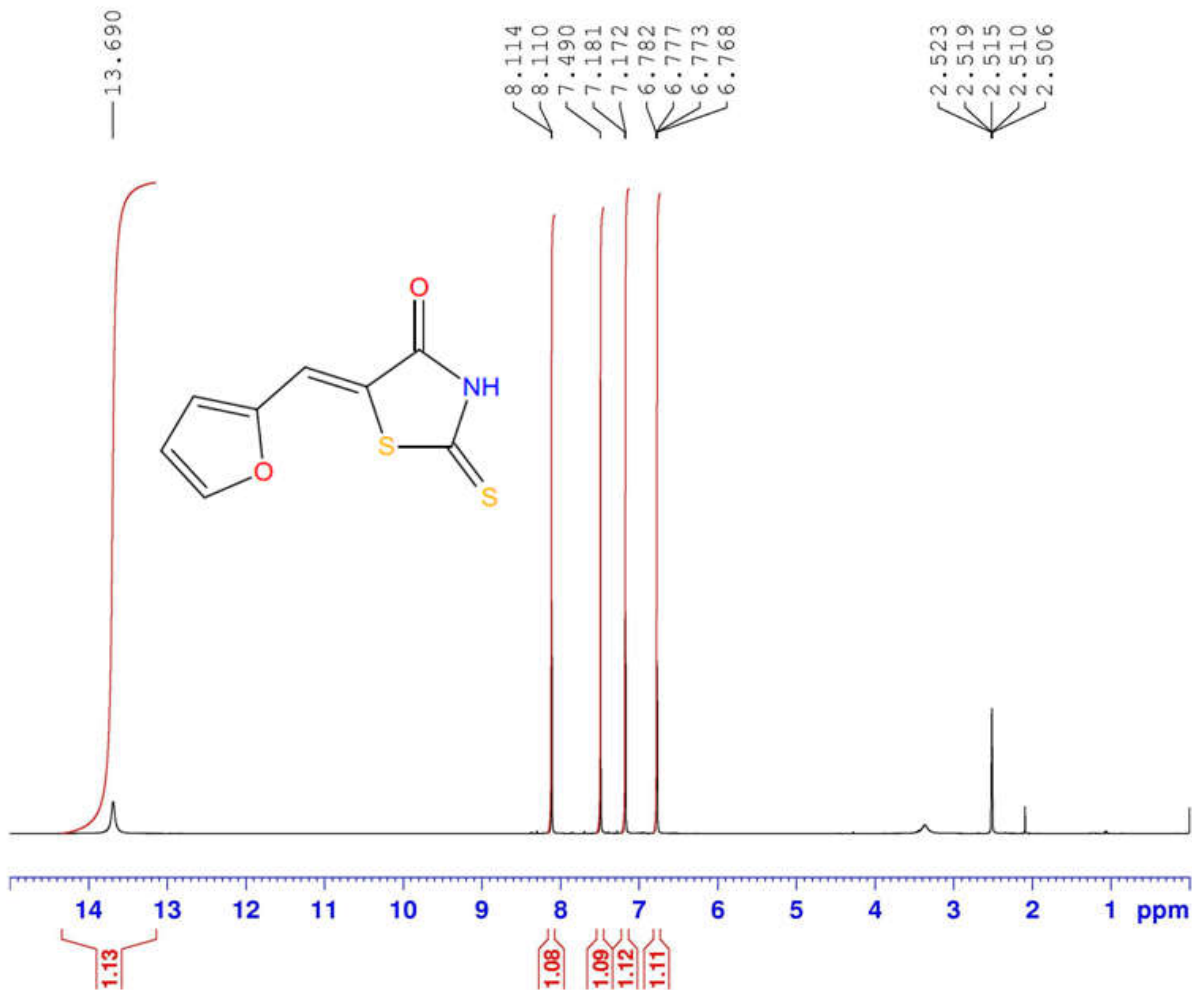
**ELEMENTAL ANALYSIS**

Anal. Calcd. For N12: C, 45.48; H, 2.39; N, 6.63; Obsd. C, 45.39; H,  
2.38; N, 6.64.

Sample: N 12



N12.....Noorulla



Current Data Parameters  
NAME N12  
EXPNO 219  
PROCNO 1

F2 - Acquisition Parameters  
Date\_ 20150726  
Time 9.30  
INSTRUM spect  
PROBHD 5 mm PABBO BB/  
PULPROG zg30  
TD 65536  
SOLVENT DMSO  
NS 16  
DS 2  
SWH 8223.685 Hz  
FIDRES 0.125483 Hz  
AQ 3.9846387 sec  
RG 143.73  
DW 60.800 usec  
DE 6.50 usec  
TE 298.3 K  
D1 1.00000000 sec  
TD0 1

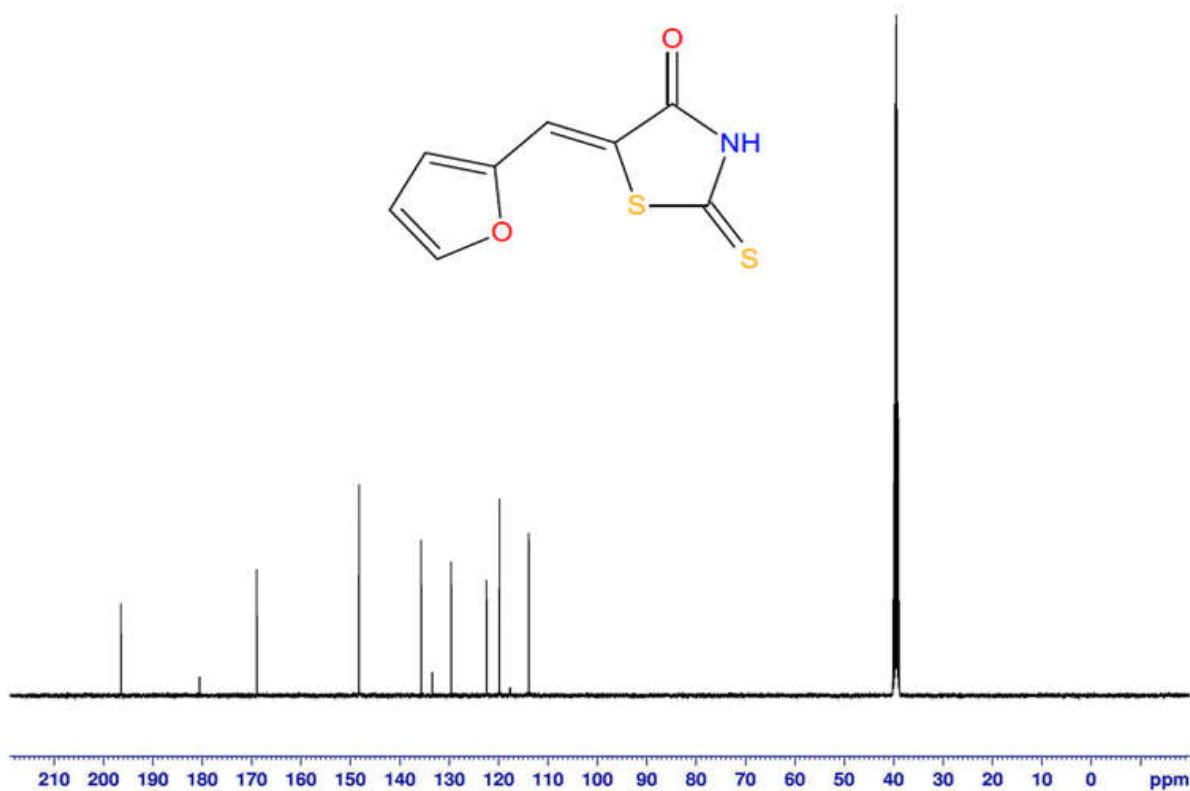
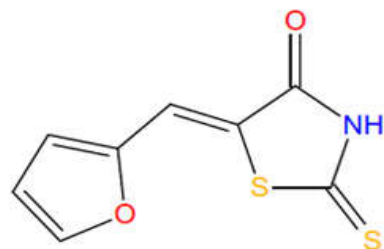
===== CHANNEL f1 =====  
NUC1 1H  
P1 14.25 usec  
PLW1 14.00000000 W  
SFO1 400.2604718 MHz

F2 - Processing parameters  
SI 65536  
SF 400.2579995 MHz  
WDW EM  
SSB 0  
LB 0.30 Hz  
GB 0  
PC 1.00



N12.....Noorulla

—196.47  
—168.98  
—148.29  
—135.72  
—129.54  
—122.42  
—119.85  
—113.89



Current Data Parameters  
NAME N12  
EXPNO 220  
PROCNO 1

F2 - Acquisition Parameters  
Date\_ 20150726  
Time 10.05  
INSTRUM spect  
PROBHD 5 mm PABBO BB/  
PULPROG zgpg30  
TD 65536  
SOLVENT DMSO  
NS 600  
DS 4  
SWH 24038.461 Hz  
FIDRES 0.366798 Hz  
AQ 1.3631988 sec  
RG 175.97  
DW 20.800 usec  
DE 6.50 usec  
TE 299.0 K  
D1 2.00000000 sec  
D11 0.03000000 sec  
TD0 1

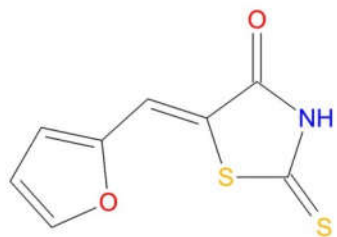
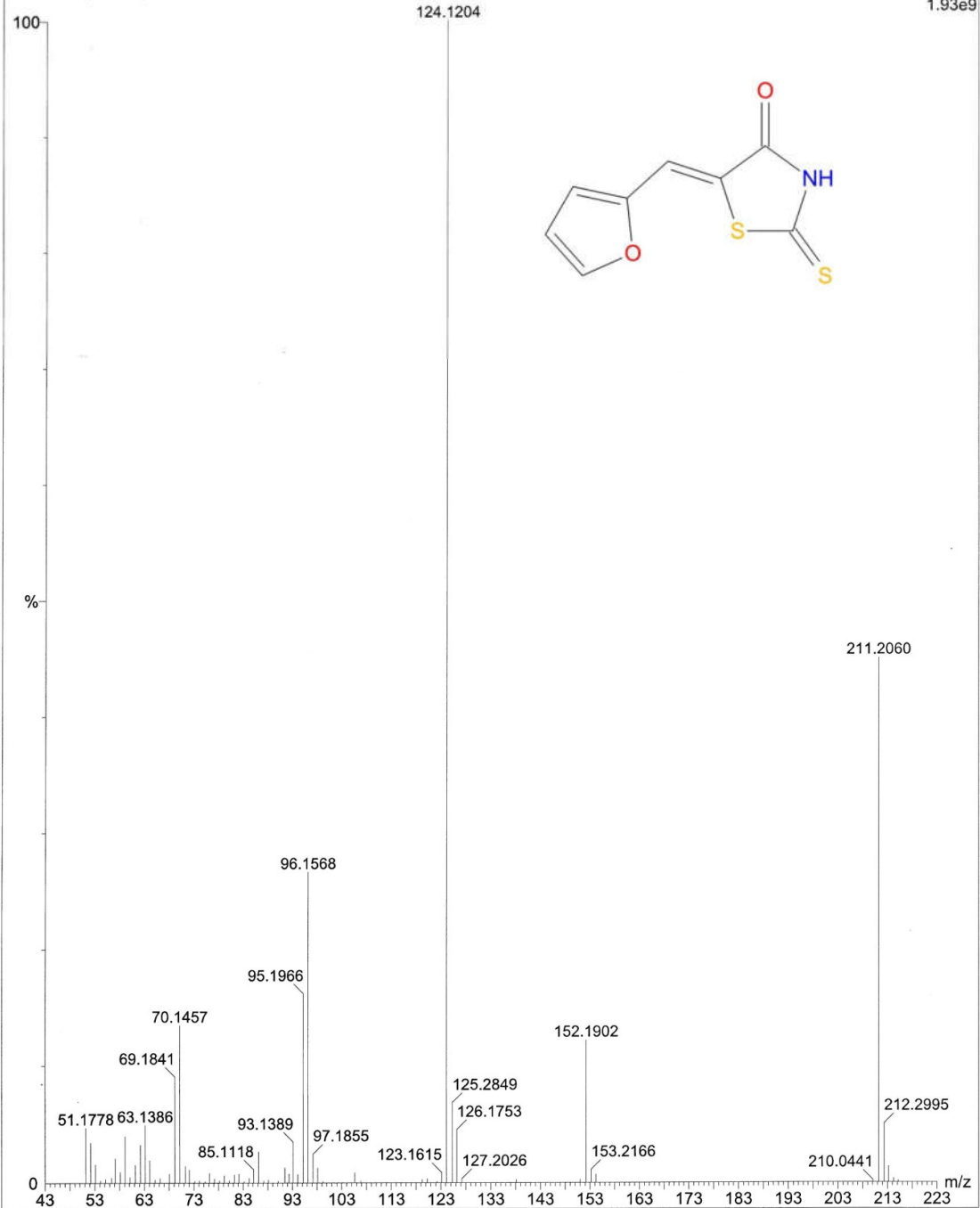
===== CHANNEL f1 =====  
NUC1 13C  
P1 9.80 usec  
PLW1 58.00000000 W  
SFO1 100.6550182 MHz

===== CHANNEL f2 =====  
CPDPRG2 waltz16  
NUC2 1H  
PCPD2 90.00 usec  
PLW2 14.00000000 W  
PLW12 0.35097000 W  
PLW13 0.28428999 W  
SFO2 400.2596010 MHz

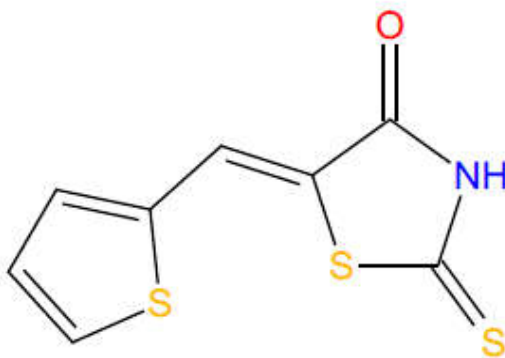
F2 - Processing parameters  
SI 32768  
SF 100.6450043 MHz  
WDW EM  
SSB 0  
LB 1.00 Hz  
GB 0  
PC 1.40

N12-3428 (19.645)

Scan EI+  
1.93e9



## Spectral Data of Compound N13



**.IR (KBr,  $\nu_{\max}$ )  $\text{cm}^{-1}$**

1434.93 (Ar C-C), 1681.80 (C=O), 1797.52 (C=S), 3078.16 (=C-H),  
3139.88 (Ar C-H), 3556.48 (N-H).

**$^1\text{H}$  NMR (DMSO- $\text{D}_6$ )  $\delta$**

7.29-7.32 (q, 1H, hetero Ar-H), 7.71 (d, 1H, hetero Ar -H), 7.92 (s,  
1H, =CH-), 8.08 (d, 1H, hetero Ar -H), 13.79 (s, 1H, NH).

**$^{13}\text{C}$  NMR (DMSO- $\text{D}_6$ )  $\delta$**

122.96, 124.77, 129.27, 134.30, 135.38, 137.42, 169.00, 194.59.

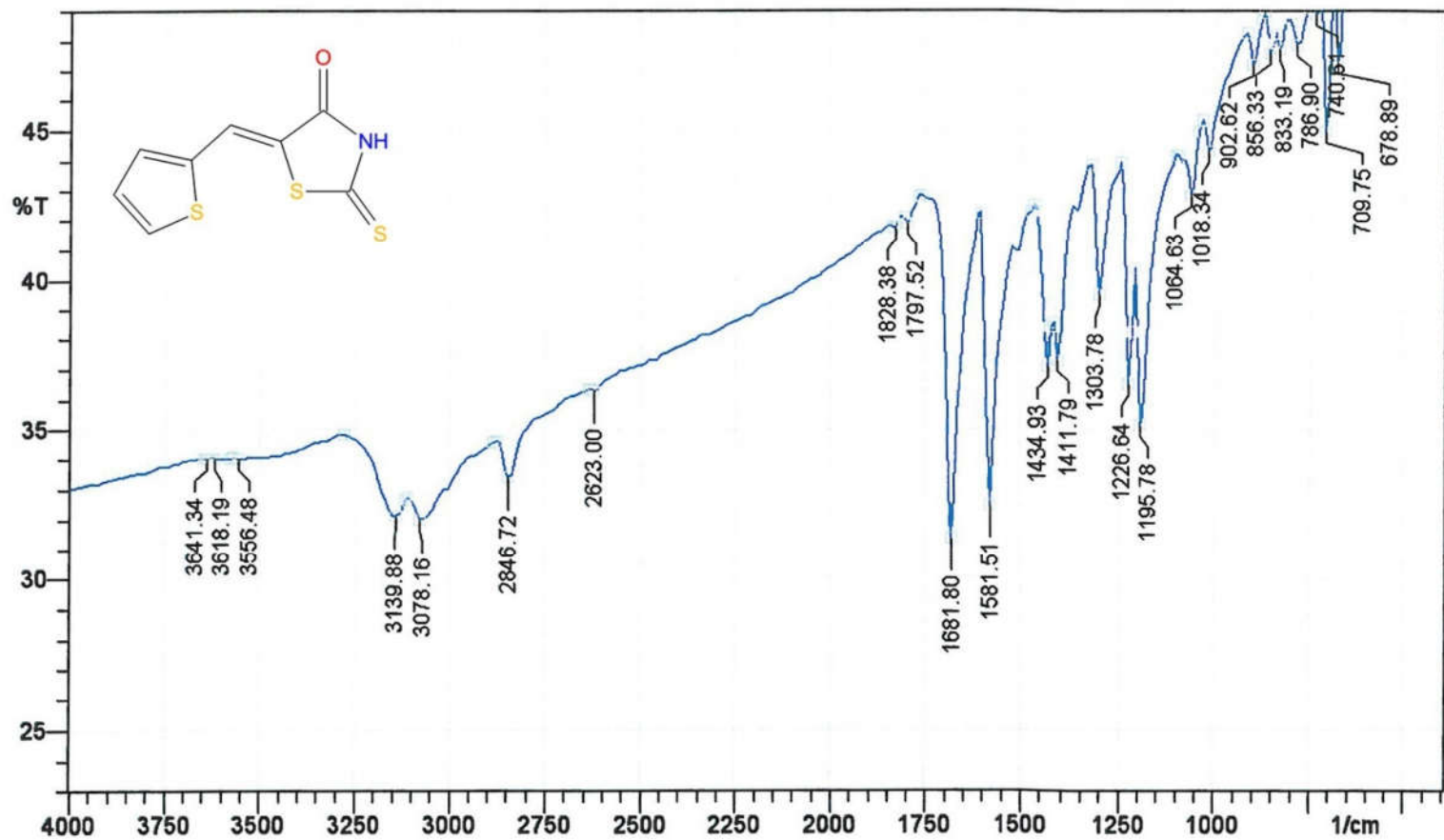
**MASS SPECTROSCOPY**

227.10 ( $\text{M}^+$ ), 229.04 ( $\text{M}+2$ ), 140.17 (**B**).

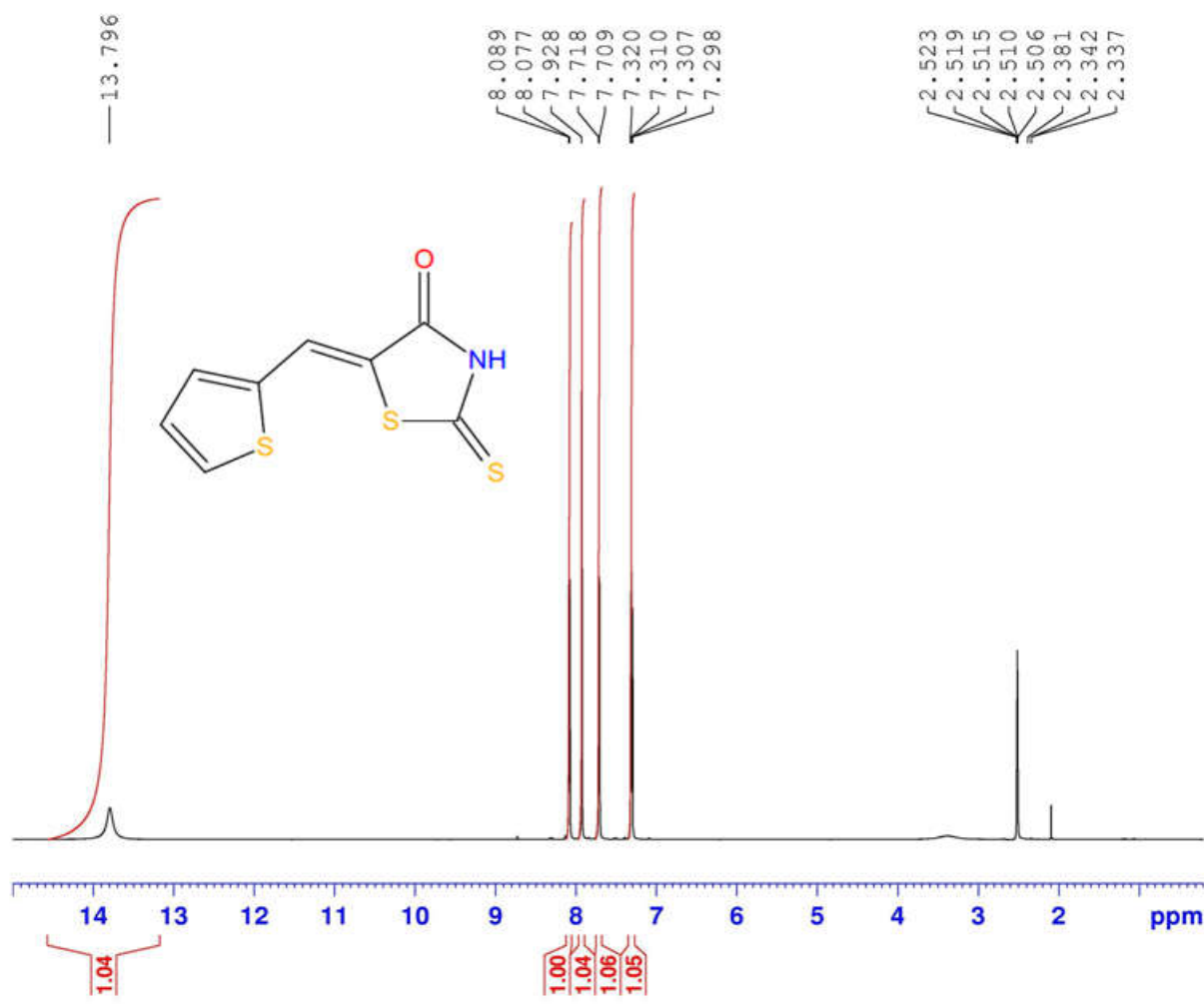
**ELEMENTAL ANALYSIS**

Anal. Calcd. For N13: C, 42.27; H, 2.22; N, 6.16; Obsd. C, 42.49; H,  
2.21; N, 6.17.

Sample: N 13



N13.....Noorulla



Current Data Parameters  
NAME N13  
EXPNO 221  
PROCNO 1

F2 - Acquisition Parameters  
Date\_ 20150726  
Time 10.08  
INSTRUM spect  
PROBHD 5 mm PABBO BB/  
PULPROG zg30  
TD 65536  
SOLVENT DMSO  
NS 16  
DS 2  
SWH 8223.685 Hz  
FIDRES 0.125483 Hz  
AQ 3.9846387 sec  
RG 143.73  
DW 60.800 usec  
DE 6.50 usec  
TE 298.2 K  
D1 1.00000000 sec  
TD0 1

===== CHANNEL f1 =====  
NUC1 1H  
P1 14.25 usec  
PLW1 14.00000000 W  
SFO1 400.2604718 MHz

F2 - Processing parameters  
SI 65536  
SF 400.2579993 MHz  
WDW EM  
SSB 0  
LB 0.30 Hz  
GB 0  
PC 1.00

N13.....Noorulla

194.59

169.00

137.42

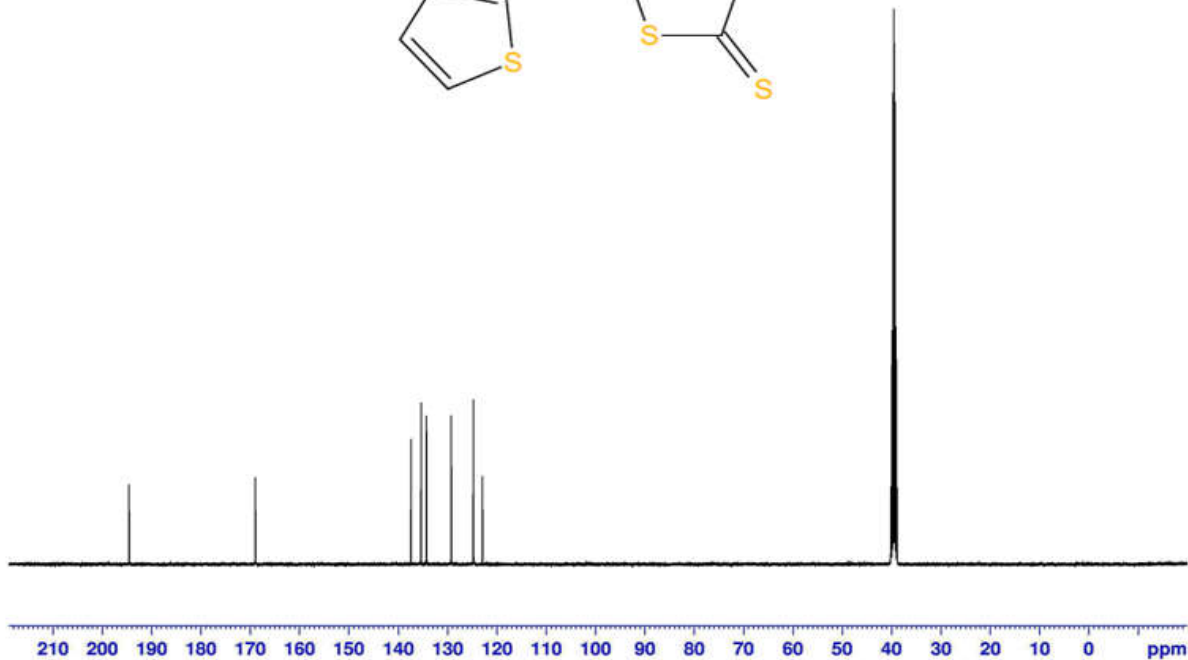
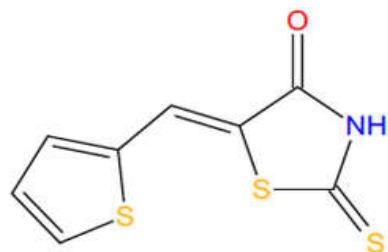
135.38

134.30

129.27

123.77

122.96



Current Data Parameters  
NAME N13  
EXPNO 222  
PROCNO 1

F2 - Acquisition Parameters  
Date\_ 20150726  
Time 10.42  
INSTRUM spect  
PROBHD 5 mm PABBO BB/  
PULPROG zgpg30  
TD 65536  
SOLVENT DMSO  
NS 600  
DS 4  
SWH 24038.461 Hz  
FIDRES 0.366798 Hz  
AQ 1.3631988 sec  
RG 199.6  
DW 20.800 usec  
DE 6.50 usec  
TE 298.9 K  
D1 2.00000000 sec  
D11 0.03000000 sec  
TD0 1

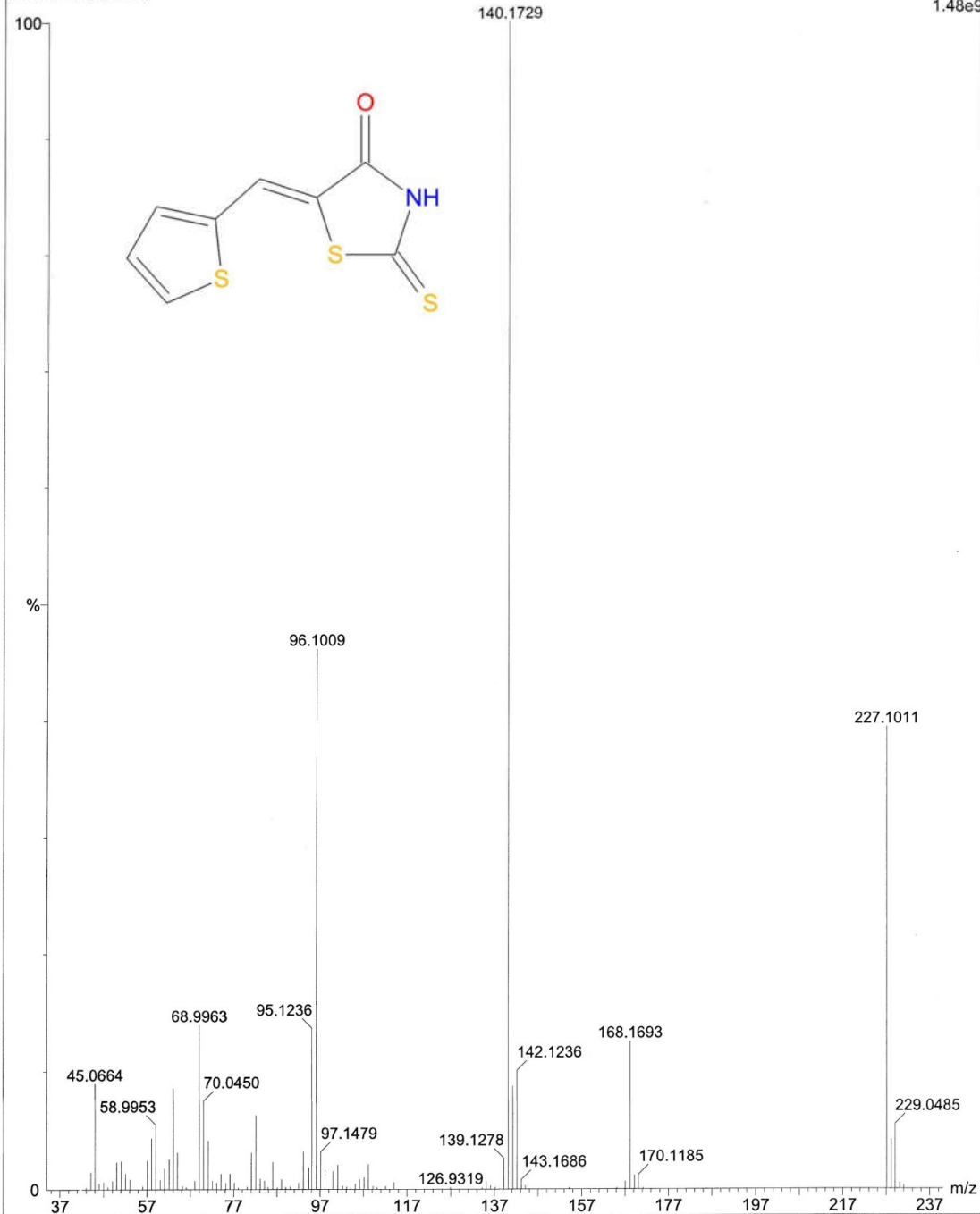
===== CHANNEL f1 =====  
NUC1 13C  
P1 9.80 usec  
PLW1 58.00000000 W  
SFO1 100.6550182 MHz

===== CHANNEL f2 =====  
CPDPRG2 waltz16  
NUC2 1H  
PCPD2 90.00 usec  
PLW2 14.00000000 W  
PLW12 0.35097000 W  
PLW13 0.28428999 W  
SFO2 400.2596010 MHz

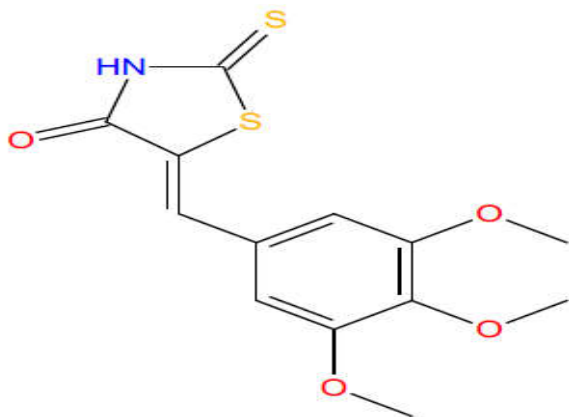
F2 - Processing parameters  
SI 32768  
SF 100.6450043 MHz  
WDW EM  
SSB 0  
LB 1.00 Hz  
GB 0  
PC 1.40

N13-3914 (22.076)

Scan EI+  
1.48e9



## Spectral Data of Compound N14



### IR (KBr, $\nu_{\max}$ ) $\text{cm}^{-1}$

1249.78 (ether C-O), 1496.65 (Ar C-C), 1689.52 (C=O), 1766.67 (C=S), 2839.01 (alkane C-H), 2939.30 (=C-H), 3008.73 (Ar C-H), 3471.61 (N-H).

### $^1\text{H}$ NMR (DMSO- $\text{D}_6$ ) $\delta$

3.74 (s, 3H, O- $\text{CH}_3$ ), 3.83 (d, 6H, O- $\text{CH}_3$ ), 6.88 (s, 2H, Ar-H), 7.58 (s, 1H, =CH-), 13.82 (s, 1H, N-H)

### $^{13}\text{C}$ NMR (DMSO- $\text{D}_6$ ) $\delta$

55.98, 60.19, 60.42, 114.37, 124.23, 126.34, 128.39, 132.01, 139.74, 142.91, 153.23, 169.23, 195.42.

### MASS SPECTROSCOPY

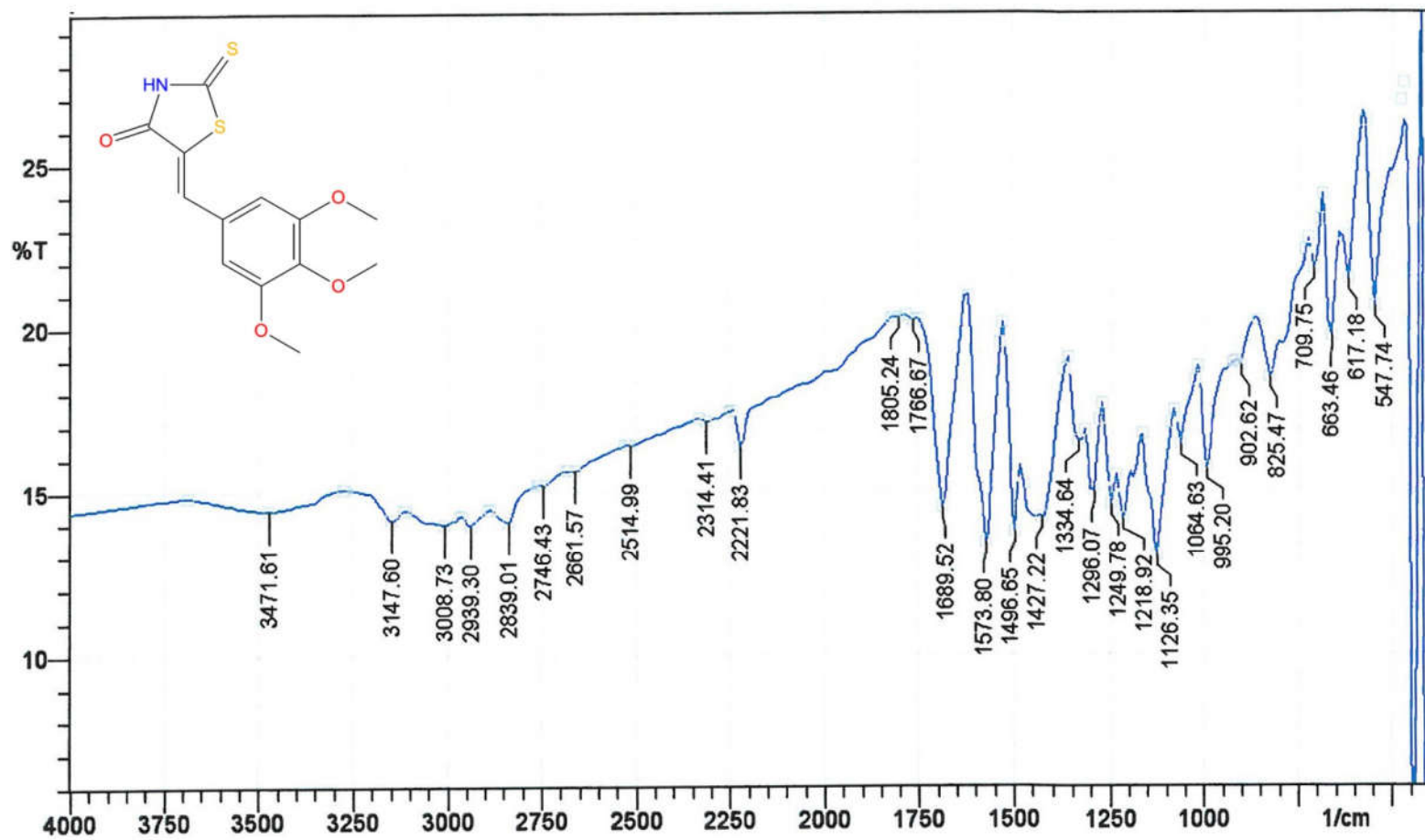
311.10 ( $\text{M}^+$ ), 209.08 (**B**).

### ELEMENTAL ANALYSIS

Anal. Calcd. For N14: C, 50.14; H, 4.21; N, 4.50; Obsd. C, 49.98; H, 4.22; N, 4.49.



Sample: N 14



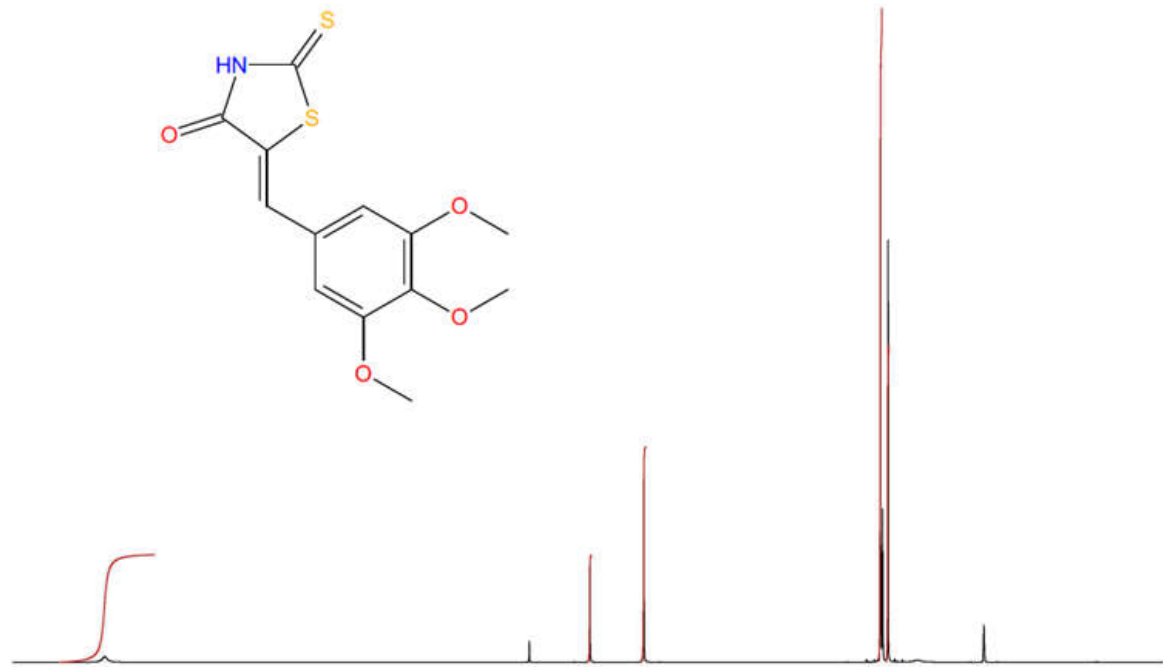
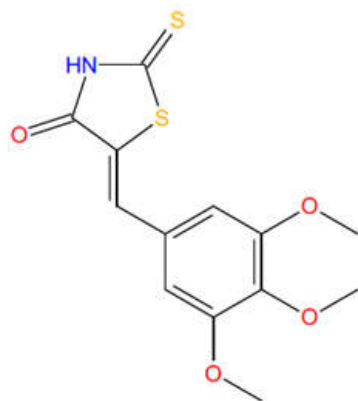
N14.....Noorulla

—13.820

—7.580

—6.886

3.844  
3.818  
3.746  
2.522  
2.518  
2.513  
2.509  
2.505

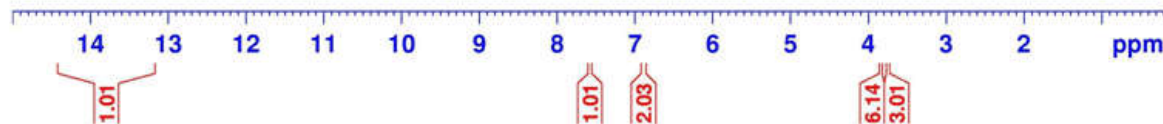


Current Data Parameters  
NAME N14  
EXPNO 226  
PROCNO 1

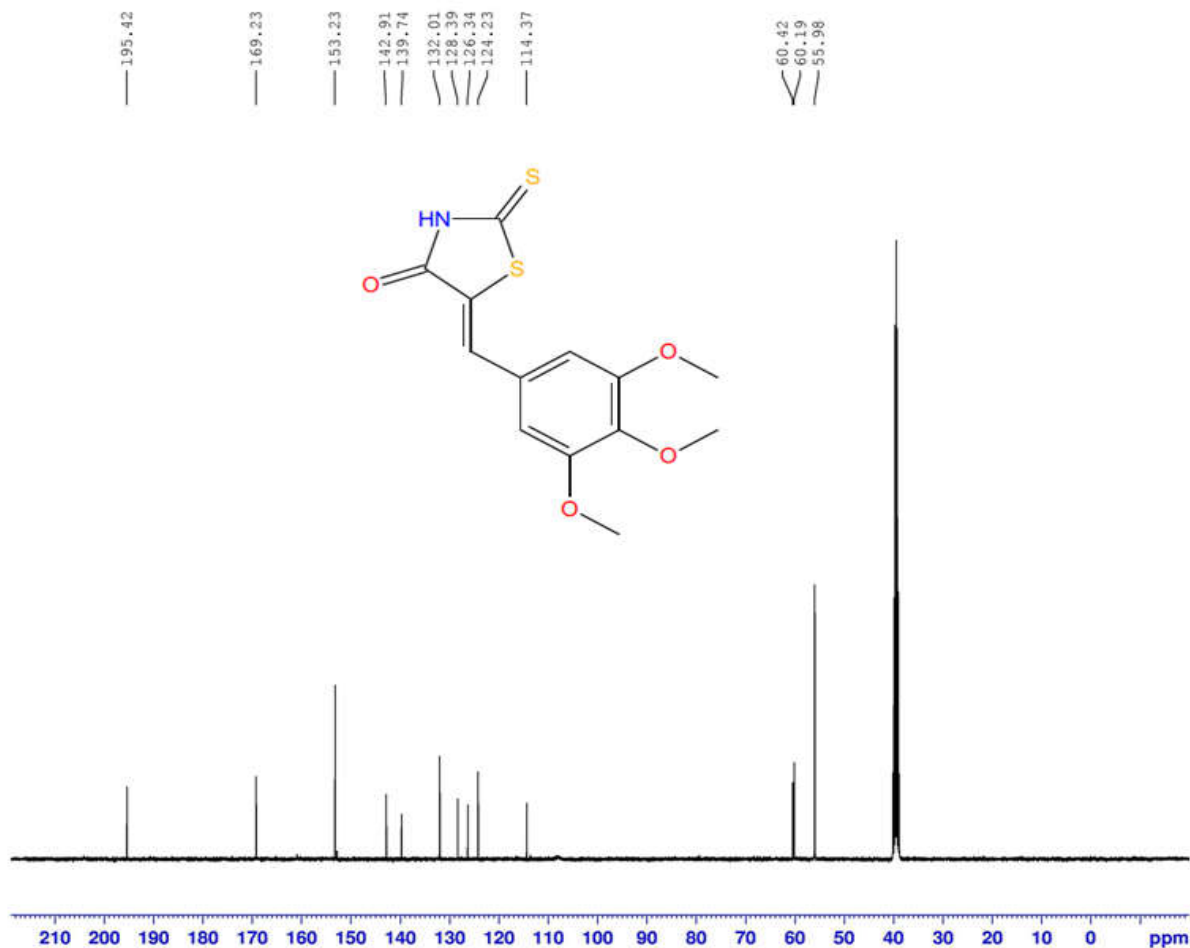
F2 - Acquisition Parameters  
Date\_ 20150727  
Time 5.50  
INSTRUM spect  
PROBHD 5 mm PABBO BB/  
PULPROG zg30  
TD 65536  
SOLVENT DMSO  
NS 16  
DS 2  
SWH 8223.685 Hz  
FIDRES 0.125483 Hz  
AQ 3.9846387 sec  
RG 88.69  
DW 60.800 usec  
DE 6.50 usec  
TE 298.1 K  
D1 1.00000000 sec  
TD0 1

===== CHANNEL f1 =====  
NUC1 1H  
P1 14.25 usec  
PLW1 14.00000000 W  
SF01 400.2604718 MHz

F2 - Processing parameters  
SI 65536  
SF 400.2580000 MHz  
WDW EM  
SSB 0  
LB 0.30 Hz  
GB 0  
PC 1.00



N14.....Noorulla



Current Data Parameters  
NAME N14  
EXPNO 227  
PROCNO 1

F2 - Acquisition Parameters  
Date\_ 20150727  
Time 6.25  
INSTRUM spect  
PROBHD 5 mm PABBO BB/  
PULPROG zgpg30  
TD 65536  
SOLVENT DMSO  
NS 600  
DS 4  
SWH 24038.461 Hz  
FIDRES 0.366798 Hz  
AQ 1.3631988 sec  
RG 199.6  
DW 20.800 usec  
DE 6.50 usec  
TE 298.9 K  
D1 2.00000000 sec  
D11 0.03000000 sec  
TD0 1

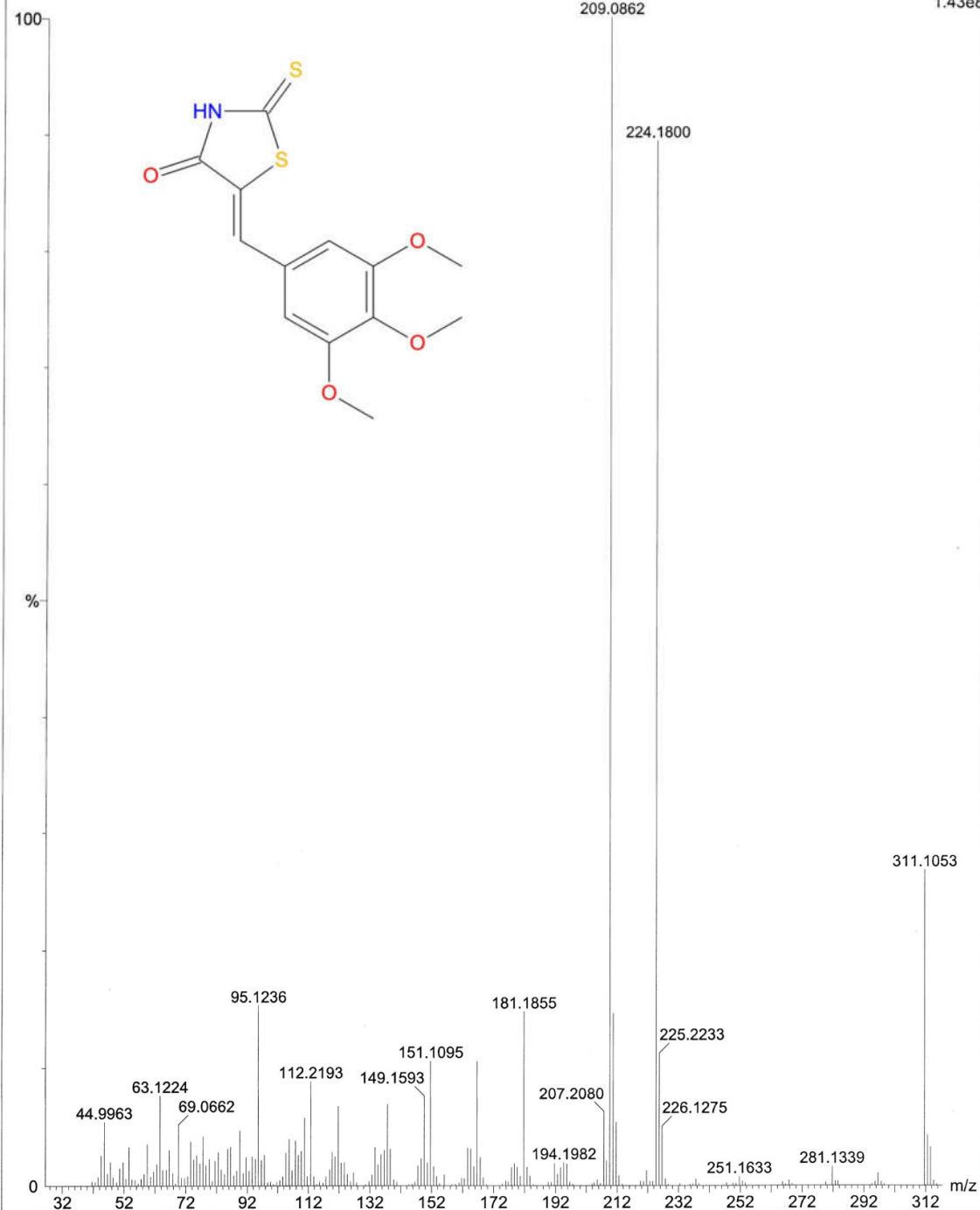
===== CHANNEL f1 =====  
NUC1 13C  
P1 9.80 usec  
PLW1 58.00000000 W  
SFO1 100.6550182 MHz

===== CHANNEL f2 =====  
CPDPRG2 waltz16  
NUC2 1H  
PCPD2 90.00 usec  
PLW2 14.00000000 W  
PLW12 0.35097000 W  
PLW13 0.28428999 W  
SFO2 400.2596010 MHz

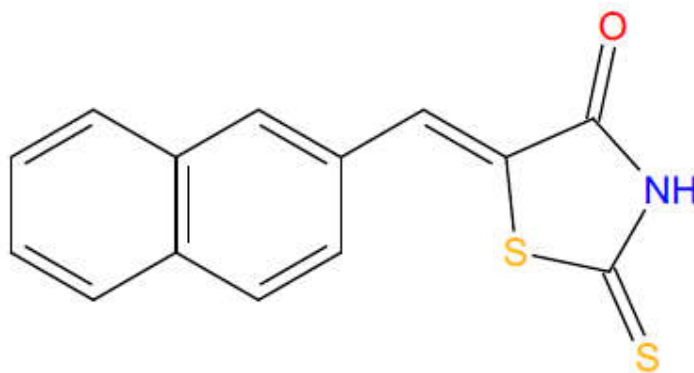
F2 - Processing parameters  
SI 32768  
SF 100.6450043 MHz  
WDW EM  
SSB 0  
LB 1.00 Hz  
GB 0  
PC 1.40

N14-4913 (27.073)

Scan EI+  
1.43e8



## Spectral Data of Compound N15



**IR (KBr,  $\nu_{\max}$ )  $\text{cm}^{-1}$**

1427.22 (Ar C-C), 1704.95 (C=O), 1789.81 (C=S), 2923.87 (=C-H),  
3070.45 (Ar C-H), 3448.47 (.N-H)

**$^1\text{H}$  NMR (DMSO- $\text{D}_6$ )  $\delta$**

7.60-7.69 (m, 3H, Ar-H), 7.79 (s, 1H, =CH-), 7.98 (t, 1H, Ar-H),  
8.06 (t, 2H, Ar-H), 8.19 (s, 1H, Ar-H), 13.88 (s, 1H, N-H).

**$^{13}\text{C}$  NMR (DMSO- $\text{D}_6$ )  $\delta$**

116.12, 127.20, 127.71, 128.21, 128.84, 129.08, 129.56, 130.55,  
131.49, 131.60, 132.76, 140.62, 169.45, 195.73.

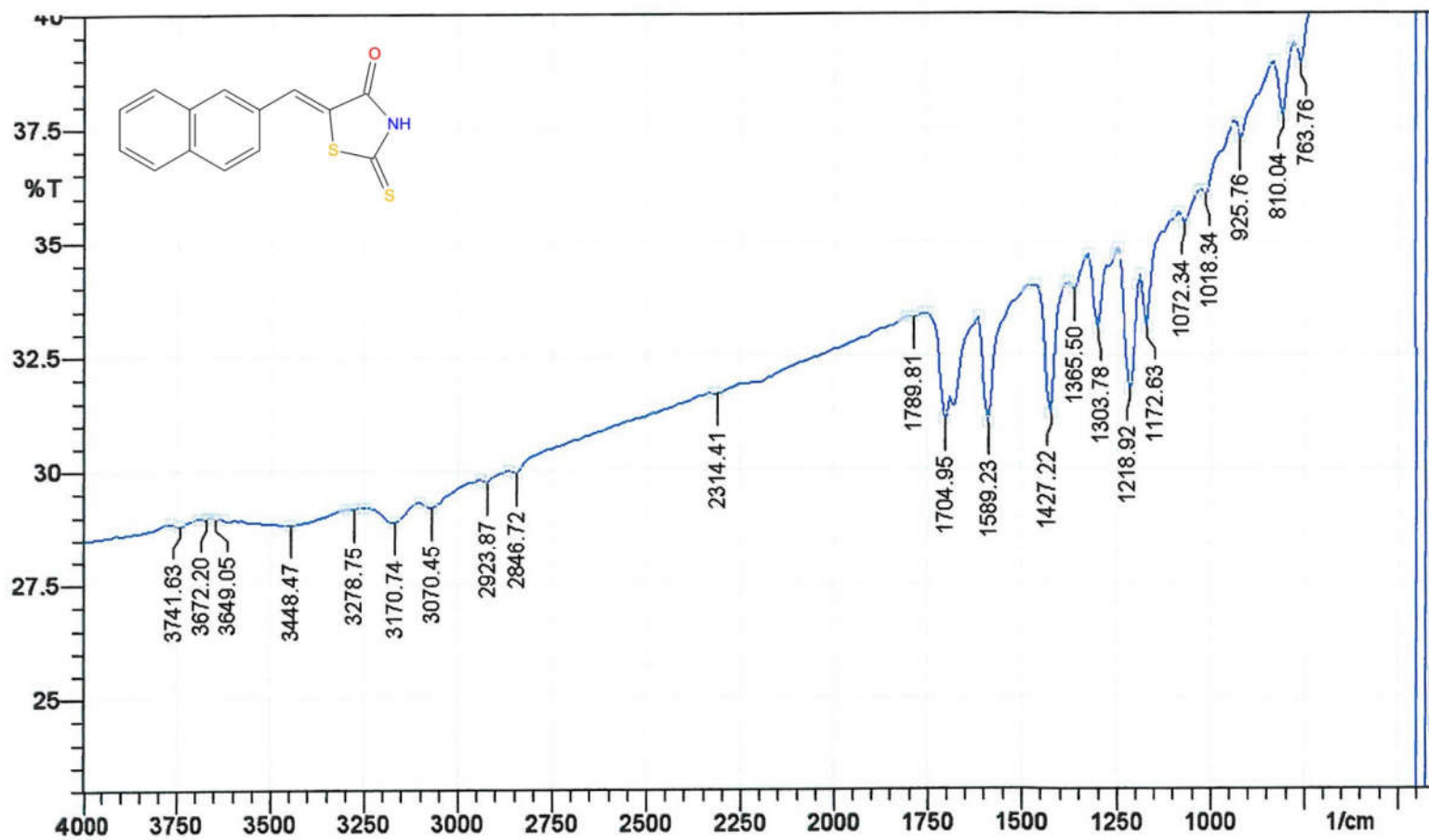
**MASS SPECTROSCOPY**

271.12 ( $\text{M}^+$ ), 272.16 ( $\text{M}+1$ ), 184.17 (**B**).

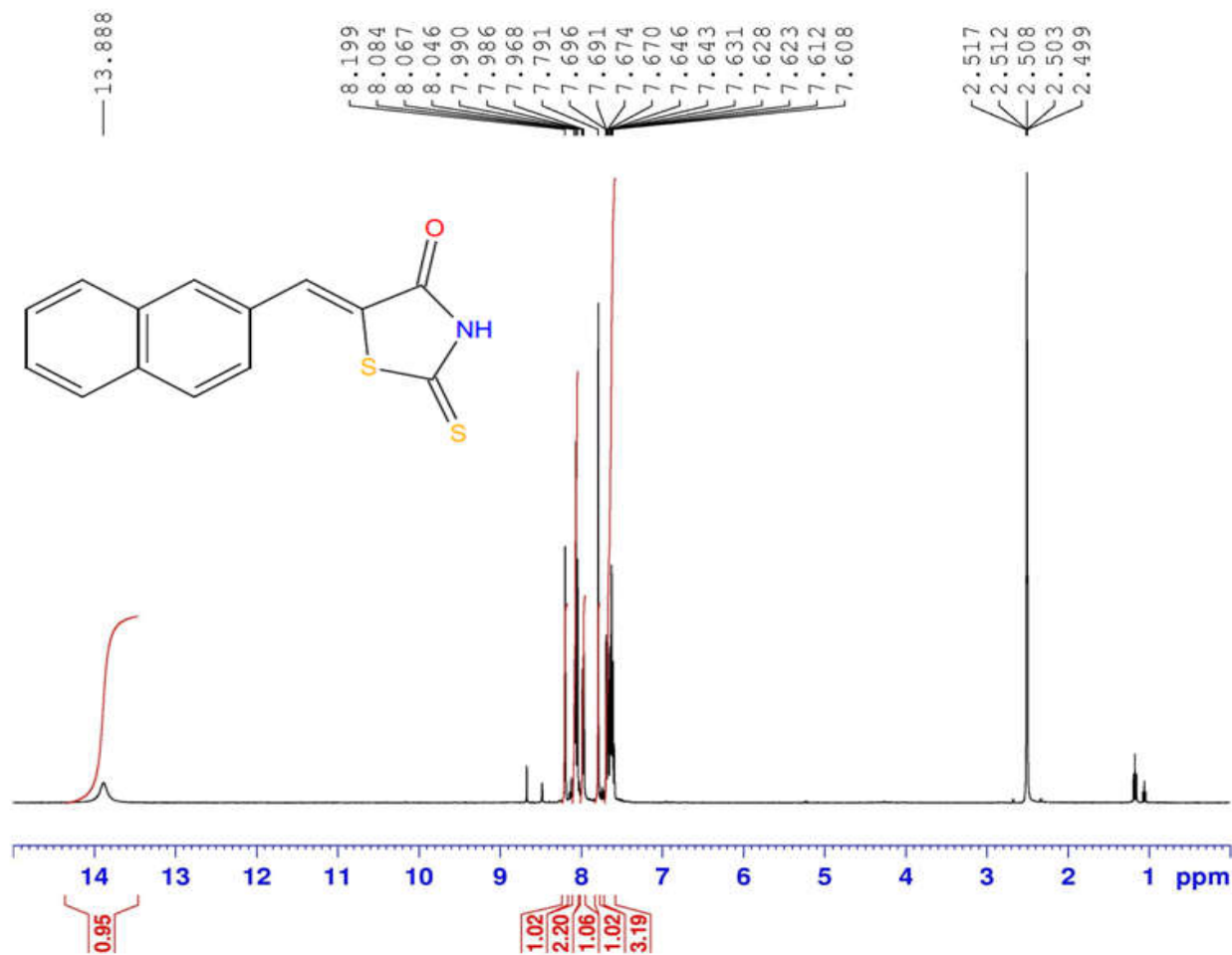
**ELEMENTAL ANALYSIS**

Anal. Calcd. For N15: C, 61.97; H, 3.34; N, 5.16; Obsd. C, 61.79; H,  
3.35; N, 5.15.

Sample: N 15



N15.....Noorulla



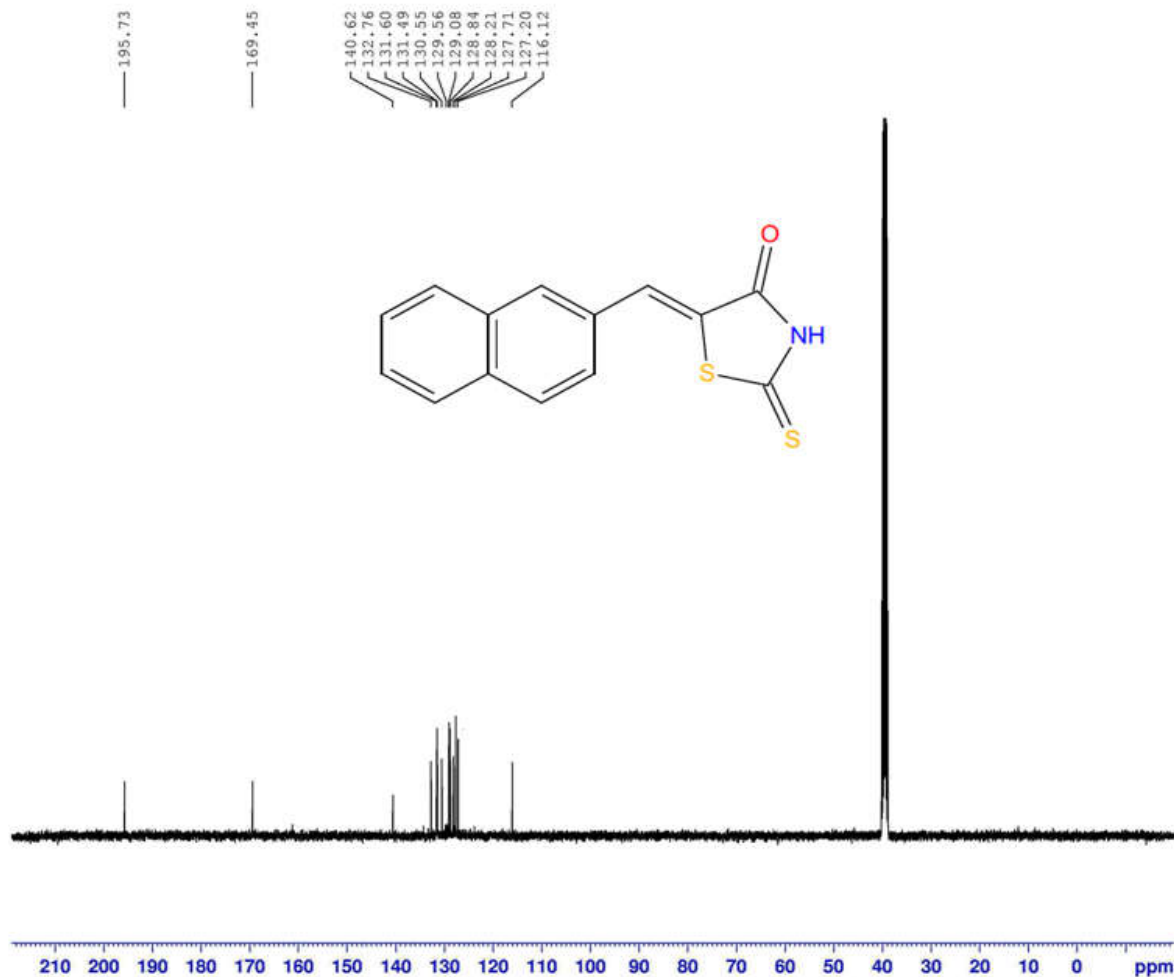
Current Data Parameters  
NAME N15  
EXPNO 228  
PROCNO 1

F2 - Acquisition Parameters  
Date\_ 20150727  
Time 6.29  
INSTRUM spect  
PROBHD 5 mm PABBO BB/  
PULPROG zg30  
TD 65536  
SOLVENT DMSO  
NS 16  
DS 2  
SWH 8223.685 Hz  
FIDRES 0.125483 Hz  
AQ 3.9846387 sec  
RG 199.6  
DW 60.800 usec  
DE 6.50 usec  
TE 298.2 K  
D1 1.00000000 sec  
TD0 1

===== CHANNEL f1 =====  
NUC1 1H  
P1 14.25 usec  
PLW1 14.00000000 W  
SF01 400.2604718 MHz

F2 - Processing parameters  
SI 65536  
SF 400.2580022 MHz  
WDW EM  
SSB 0  
LB 0.30 Hz  
GB 0  
PC 1.00

N15.....Noorulla



Current Data Parameters  
NAME N15  
EXPNO 229  
PROCNO 1

F2 - Acquisition Parameters  
Date\_ 20150727  
Time 7.03  
INSTRUM spect  
PROBHD 5 mm PABBO BB/  
PULPROG zgpg30  
TD 65536  
SOLVENT DMSO  
NS 600  
DS 4  
SWH 24038.461 Hz  
FIDRES 0.366798 Hz  
AQ 1.3631988 sec  
RG 199.6  
DW 20.800 usec  
DE 6.50 usec  
TE 299.0 K  
D1 2.00000000 sec  
D11 0.03000000 sec  
TD0 1

===== CHANNEL f1 =====  
NUC1 13C  
P1 9.80 usec  
PLW1 58.00000000 W  
SFO1 100.6550182 MHz

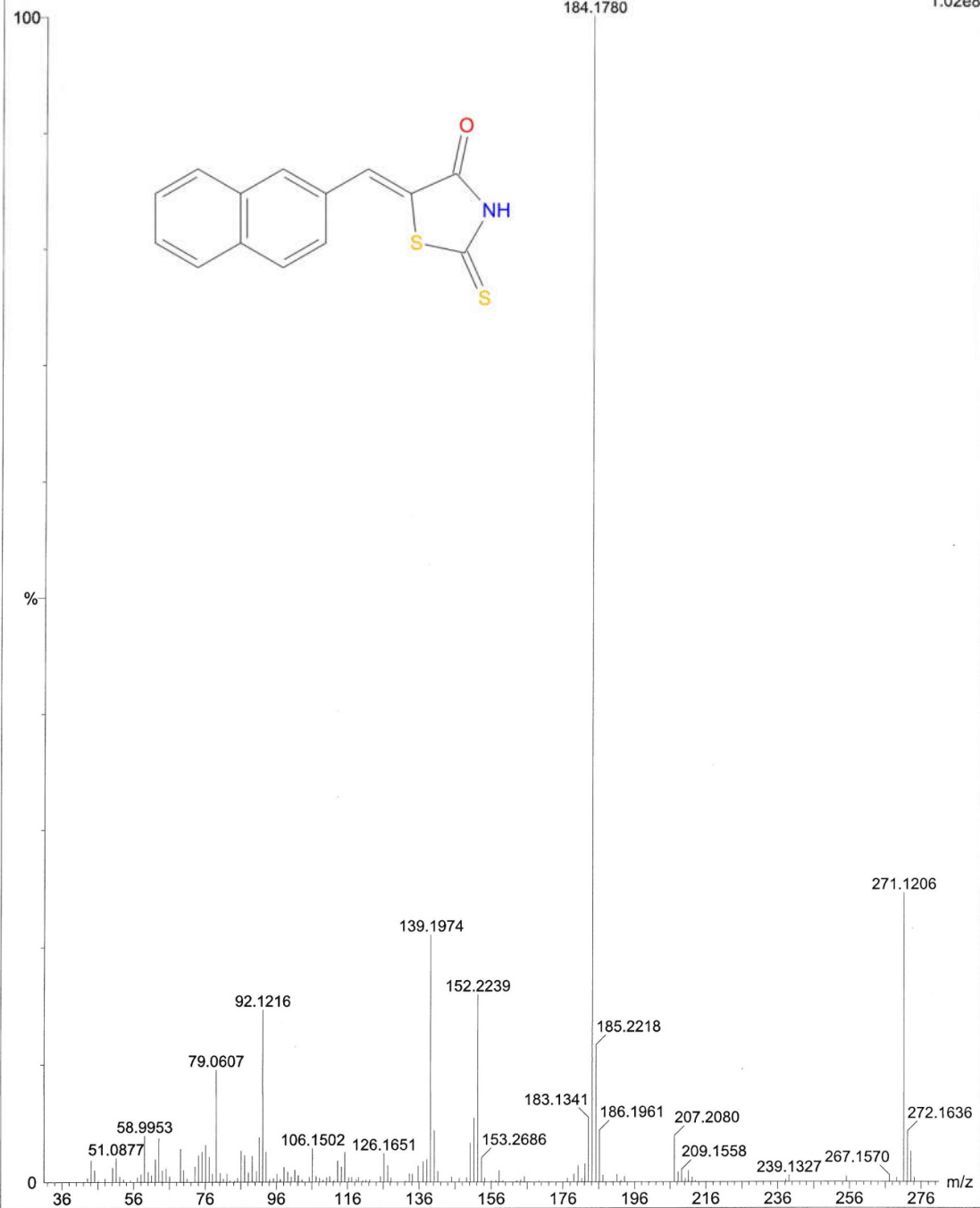
===== CHANNEL f2 =====  
CPDPRG2 waltz16  
NUC2 1H  
PCPD2 90.00 usec  
PLW2 14.00000000 W  
PLW12 0.35097000 W  
PLW13 0.28428999 W  
SFO2 400.2596010 MHz

F2 - Processing parameters  
SI 32768  
SF 100.6450043 MHz  
WDW EM  
SSB 0  
LB 1.00 Hz  
GB 0  
PC 1.40

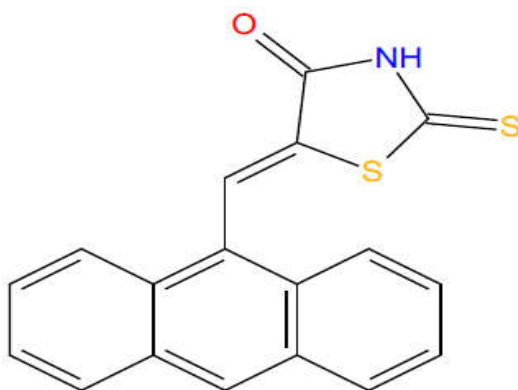


N15-4828 (26.648)

Scan EI+  
1.02e8

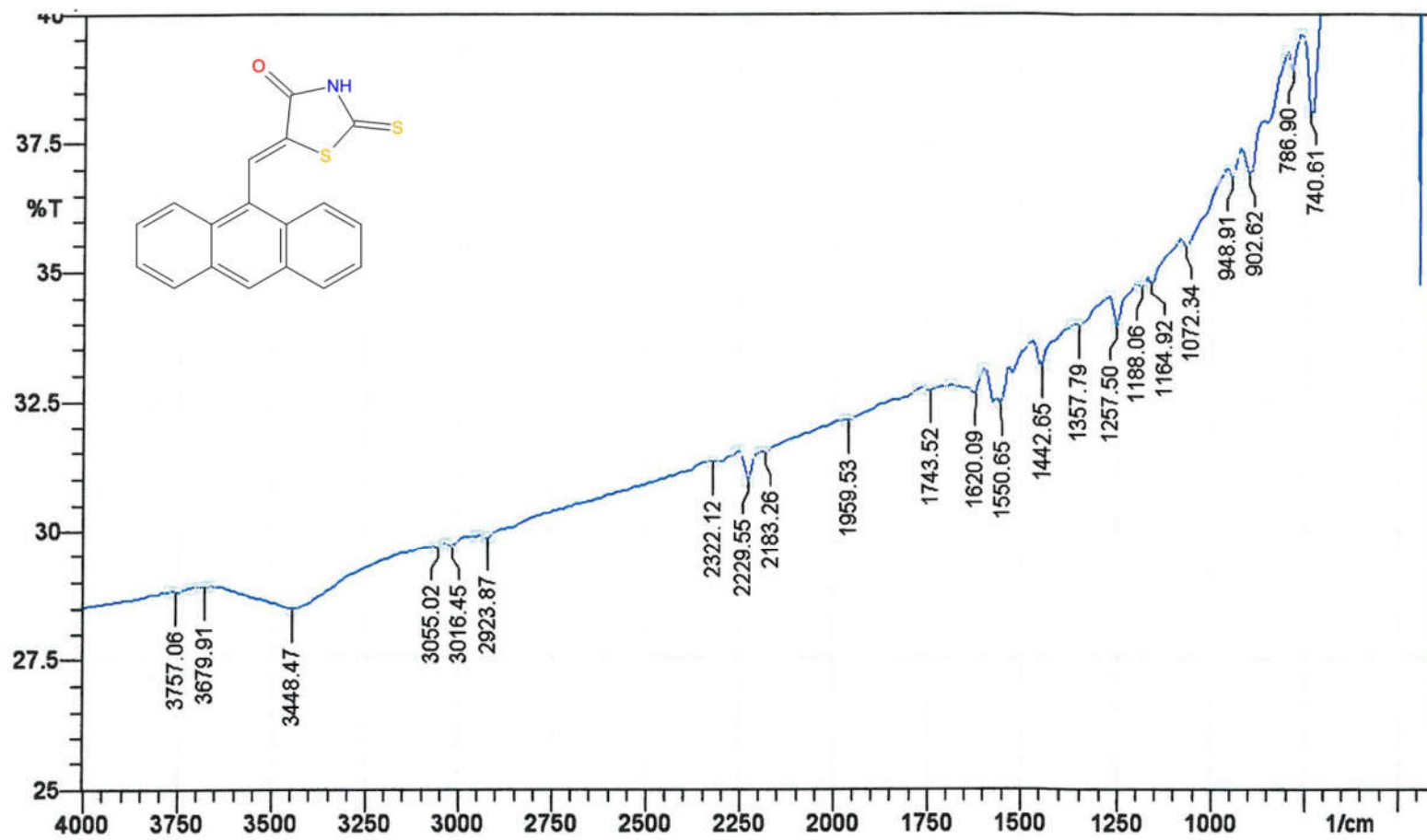


## Spectral Data of Compound N16

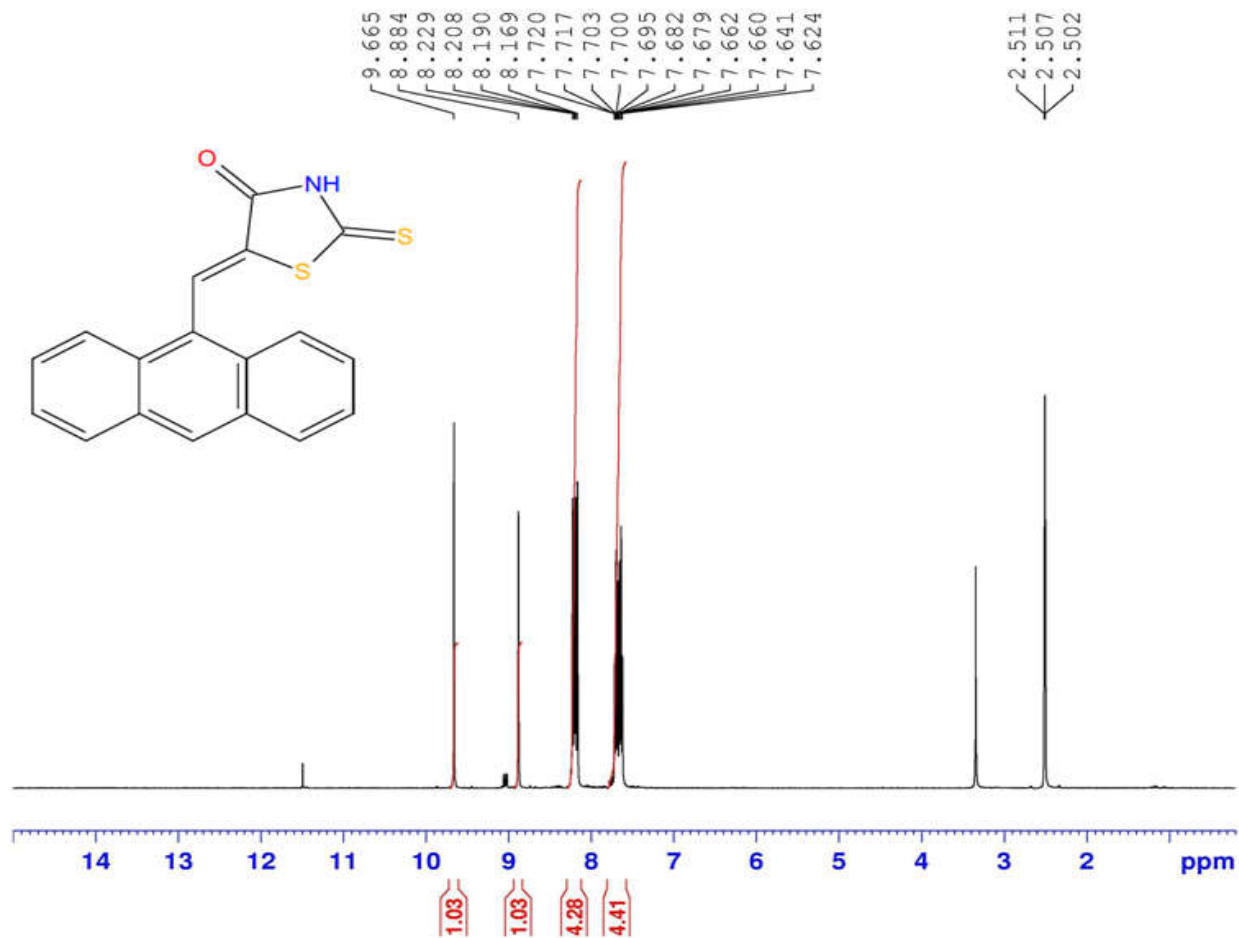


<b>IR (KBr, <math>\nu_{\max}</math>) <math>\text{cm}^{-1}</math></b>	1442.65 (Ar C-C), 1620.09 (C=O), 1743.52 (C=S), 3016.45 (=C-H), 3055.02 (Ar C-H), 3448.47 (N-H).
<b><math>^1\text{H}</math> NMR (DMSO-<math>\text{D}_6</math>) <math>\delta</math></b>	7.62-7.72 (m, 4H, Ar-H), 8.16-8.22 (q, 4H, Ar-H), 8.88 (s, 1H, =CH-), 9.66 (s, 1H, Ar-H).
<b><math>^{13}\text{C}</math> NMR (DMSO-<math>\text{D}_6</math>) <math>\delta</math></b>	113.88, 123.97, 125.05, 125.36, 126.33, 126.55, 128.34, 128.89, 129.56, 129.77, 129.84, 130.93, 131.90, 139.48, 163.07, 195.82.
<b>MASS SPECTROSCOPY</b>	321.23 ( $\text{M}^+$ ), 159.04 ( <b>B</b> ).
<b>ELEMENTAL ANALYSIS</b>	Anal. Calcd. For N16: C, 67.26; H, 3.45; N, 4.36; Obsd. C, 67.01; H, 3.44; N, 4.37.

Sample: N 16



N16.....Noorulla



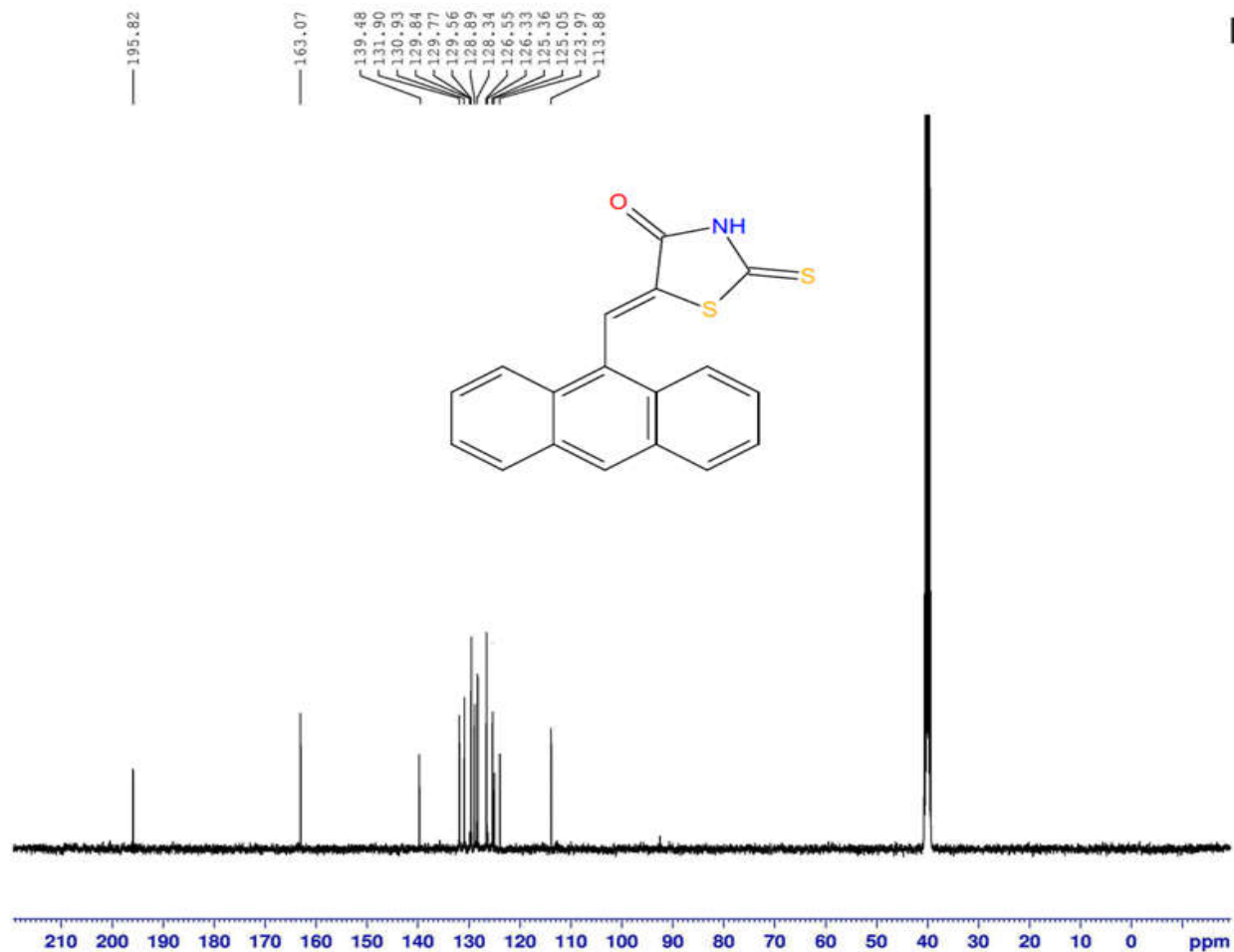
Current Data Parameters  
NAME N16  
EXPNO 230  
PROCNO 1

F2 - Acquisition Parameters  
Date\_ 20150727  
Time 7.07  
INSTRUM spect  
PROBHD 5 mm PABBO BB/  
PULPROG zg30  
TD 65536  
SOLVENT DMSO  
NS 16  
DS 2  
SWH 8223.685 Hz  
FIDRES 0.125483 Hz  
AQ 3.9846387 sec  
RG 175.97  
DW 60.800 usec  
DE 6.50 usec  
TE 298.3 K  
D1 1.00000000 sec  
TD0 1

----- CHANNEL f1 -----  
NUC1 1H  
P1 14.25 usec  
PLW1 14.00000000 W  
SFO1 400.2604718 MHz

F2 - Processing parameters  
SI 65536  
SF 400.2580026 MHz  
WDW EM  
SSB 0  
LB 0.30 Hz  
GB 0  
PC 1.00

N16.....Noorulla



Current Data Parameters  
NAME N16  
EXPNO 231  
PROCNO 1

F2 - Acquisition Parameters  
Date\_ 20150727  
Time 7.41  
INSTRUM spect  
PROBHD 5 mm PABBO BB/  
PULPROG zgpg30  
TD 65536  
SOLVENT DMSO  
NS 600  
DS 4  
SWH 24038.461 Hz  
FIDRES 0.366798 Hz  
AQ 1.3631988 sec  
RG 199.6  
DW 20.800 usec  
DE 6.50 usec  
TE 298.9 K  
D1 2.00000000 sec  
D11 0.03000000 sec  
TD0 1

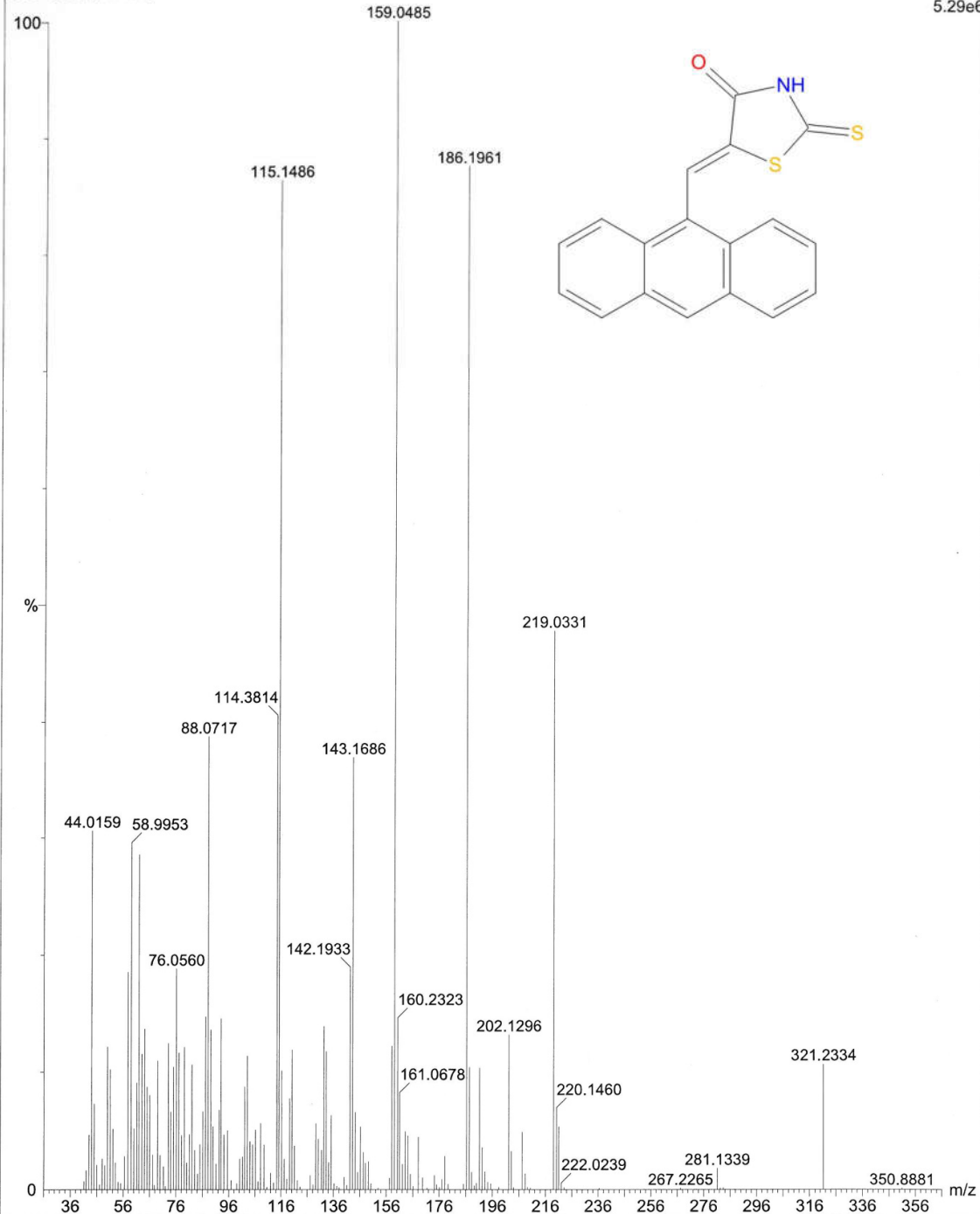
===== CHANNEL f1 =====  
NUC1 13C  
P1 9.80 usec  
PLW1 58.00000000 W  
SFO1 100.6550182 MHz

===== CHANNEL f2 =====  
CPDPRG2 waltz16  
NUC2 1H  
PCPD2 90.00 usec  
PLW2 14.00000000 W  
PLW12 0.35097000 W  
PLW13 0.28428999 W  
SFO2 400.2596010 MHz

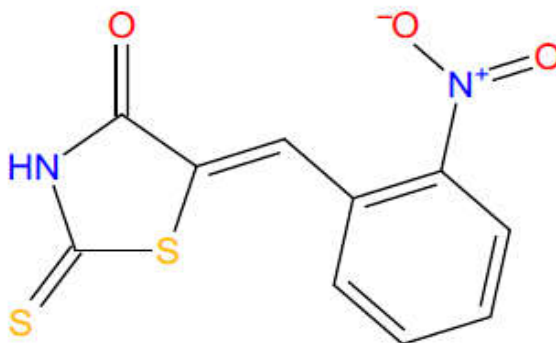
F2 - Processing parameters  
SI 32768  
SF 100.6449540 MHz  
WDW EM  
SSB 0  
LB 2.00 Hz  
GB 0  
PC 1.40

N16-3658 (20.796)

Scan EI+  
5.29e6



## Spectral Data of Compound N17



**IR (KBr,  $\nu_{\max}$ )  $\text{cm}^{-1}$**

1458.08 (Ar C-C), 1527.51 (nitro N-O), 1697.23 (C=O), 1735.81 (C=S), 2923.87 (=C-H), 3093.59 (Ar C-H), 3409.90 (N-H).

**$^1\text{H}$  NMR (DMSO- $\text{D}_6$ )  $\delta$**

7.70-7.76 (m, 2H, Ar-H), 7.87-7.91 (q, 2H, Ar-H), 8.20-8.22 (q, 1H, =CH-), 13.96 (s, 1H, N-H).

**$^{13}\text{C}$  NMR (DMSO- $\text{D}_6$ )  $\delta$**

117.18, 127.80, 128.72, 129.36, 130.31, 131.21, 134.56, 147.92, 168.60, 195.73.

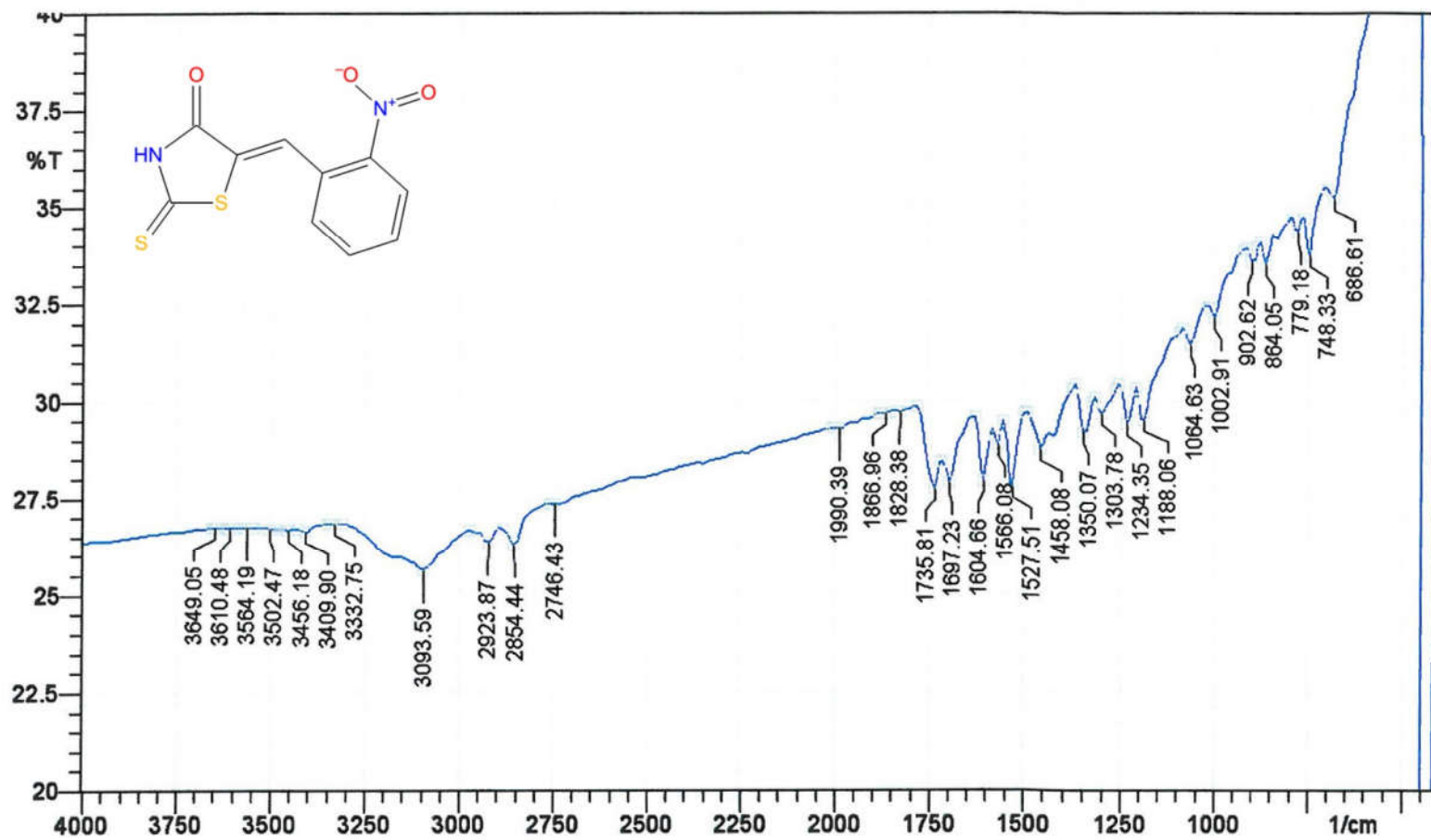
**MASS SPECTROSCOPY**

266.04 ( $\text{M}^+$ ), 267.08 ( $\text{M}+1$ ), 89.04 ( $\text{B}$ ).

**ELEMENTAL ANALYSIS**

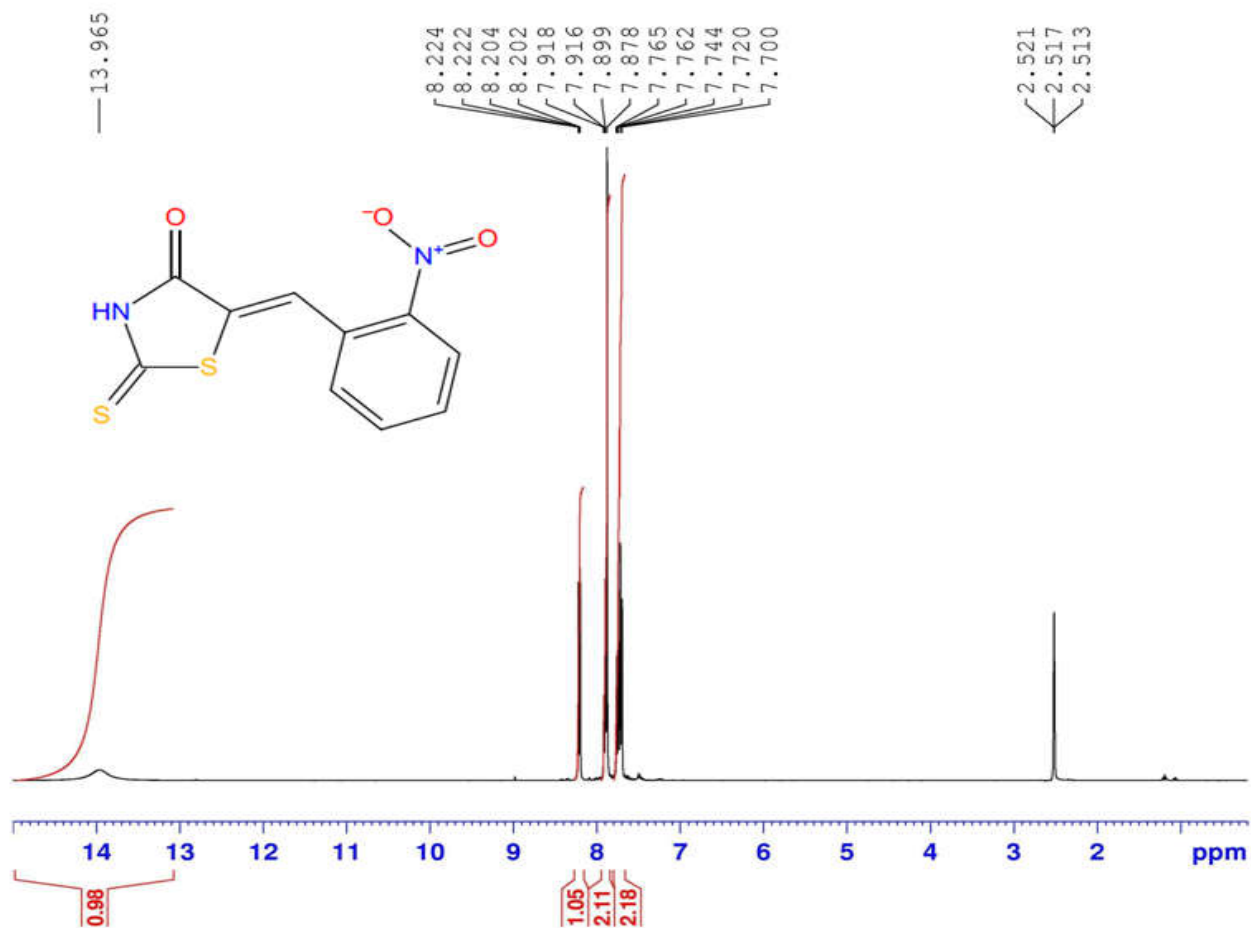
Anal. Calcd. For N17: C, 45.10; H, 2.27; N, 10.52; Obsd. C, 45.29; H, 2.26; N, 10.51.

Sample: N 17





N17.....Noorulla



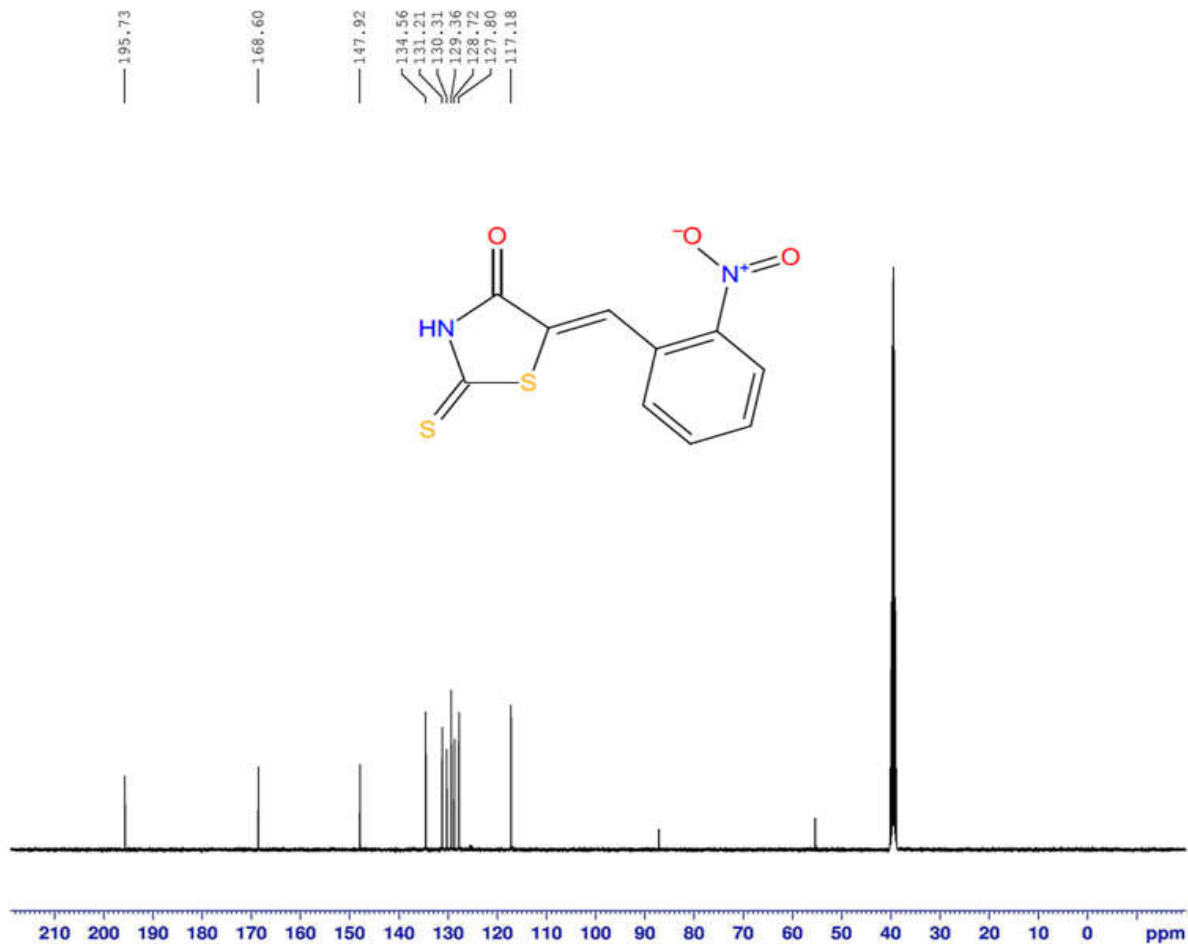
Current Data Parameters  
NAME N17  
EXPNO 232  
PROCNO 1

F2 - Acquisition Parameters  
Date\_ 20150727  
Time 7.44  
INSTRUM spect  
PROBHD 5 mm PABBO BB/  
PULPROG zg30  
TD 65536  
SOLVENT DMSO  
NS 16  
DS 2  
SWH 8223.685 Hz  
FIDRES 0.125483 Hz  
AQ 3.9846387 sec  
RG 143.73  
DW 60.800 usec  
DE 6.50 usec  
TE 298.3 K  
D1 1.0000000 sec  
TD0 1

===== CHANNEL f1 =====  
NUC1 1H  
P1 14.25 usec  
PLW1 14.0000000 W  
SFO1 400.2604718 MHz

F2 - Processing parameters  
SI 65536  
SF 400.2579985 MHz  
WDW EM  
SSB 0  
LB 0.30 Hz  
GB 0  
PC 1.00

N17.....Noorulla



Current Data Parameters  
NAME N17  
EXPNO 233  
PROCNO 1

F2 - Acquisition Parameters  
Date\_ 20150727  
Time 8.19  
INSTRUM spect  
PROBHD 5 mm PABBO BB/  
PULPROG zgpg30  
TD 65536  
SOLVENT DMSO  
NS 600  
DS 4  
SWH 24038.461 Hz  
FIDRES 0.366798 Hz  
AQ 1.3631988 sec  
RG 199.6  
DW 20.800 usec  
DE 6.50 usec  
TE 298.9 K  
D1 2.0000000 sec  
D11 0.0300000 sec  
TD0 1

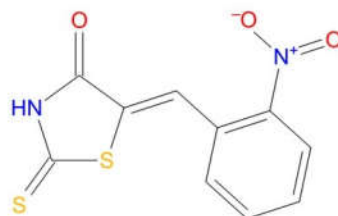
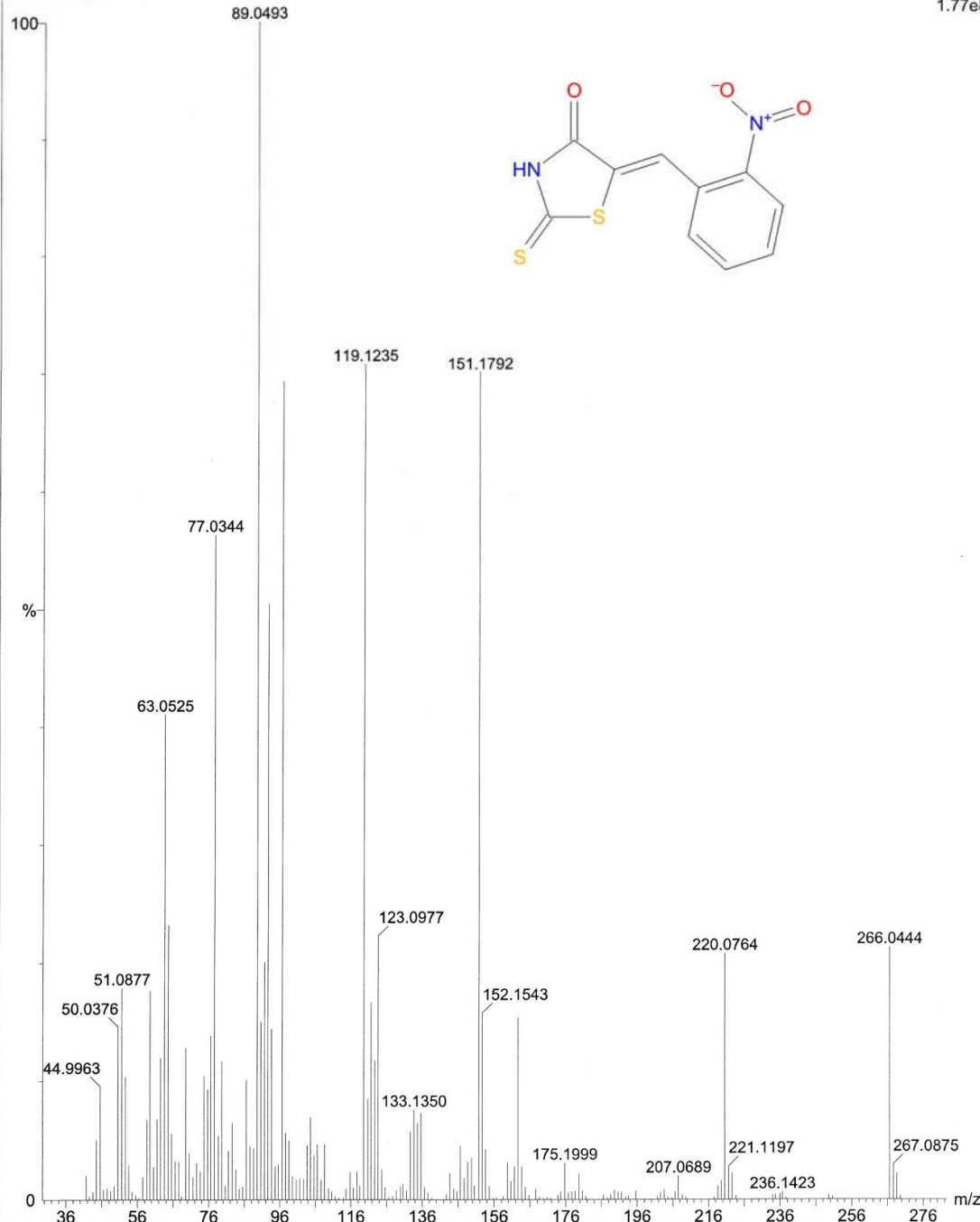
===== CHANNEL f1 =====  
NUC1 13C  
P1 9.80 usec  
PLW1 58.0000000 W  
SFO1 100.6550182 MHz

===== CHANNEL f2 =====  
CPDPRG2 waltz16  
NUC2 1H  
PCPD2 90.00 usec  
PLW2 14.0000000 W  
PLW12 0.35097000 W  
PLW13 0.28428999 W  
SFO2 400.2596010 MHz

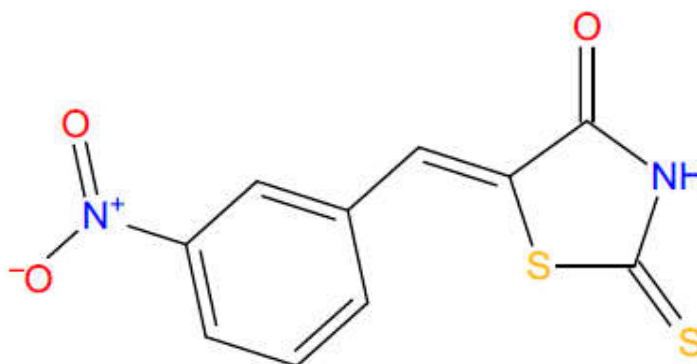
F2 - Processing parameters  
SI 32768  
SF 100.6450043 MHz  
WDW EM  
SSB 0  
LB 1.00 Hz  
GB 0  
PC 1.40

N17-4427 (24.642)

Scan EI+  
1.77e8



## Spectral Data of Compound N18



**IR (KBr,  $\nu_{\max}$ )  $\text{cm}^{-1}$**

1419.50 (Ar C-C), 1527.51 (nitro N-O), 1697.23 (C=O), 1797.52 (C=S), 3008.73 (=C-H), 3093.59 (Ar C-H), 3348.18 (N-H).

**$^1\text{H}$  NMR (DMSO- $\text{D}_6$ )  $\delta$**

7.76 (s, 1H, =CH-), 7.82 (t, 1H, Ar-H), 8.00 (d, 1H, Ar-H), 8.28-8.30 (q, 1H, Ar-H), 8.43 (t, 1H, Ar-H), 13.96 (br-s, 1H, N-H).

**$^{13}\text{C}$  NMR (DMSO- $\text{D}_6$ )  $\delta$**

120.38, 124.47, 124.64, 128.37, 129.23, 130.94, 134.80, 135.68, 170.13, 195.58.

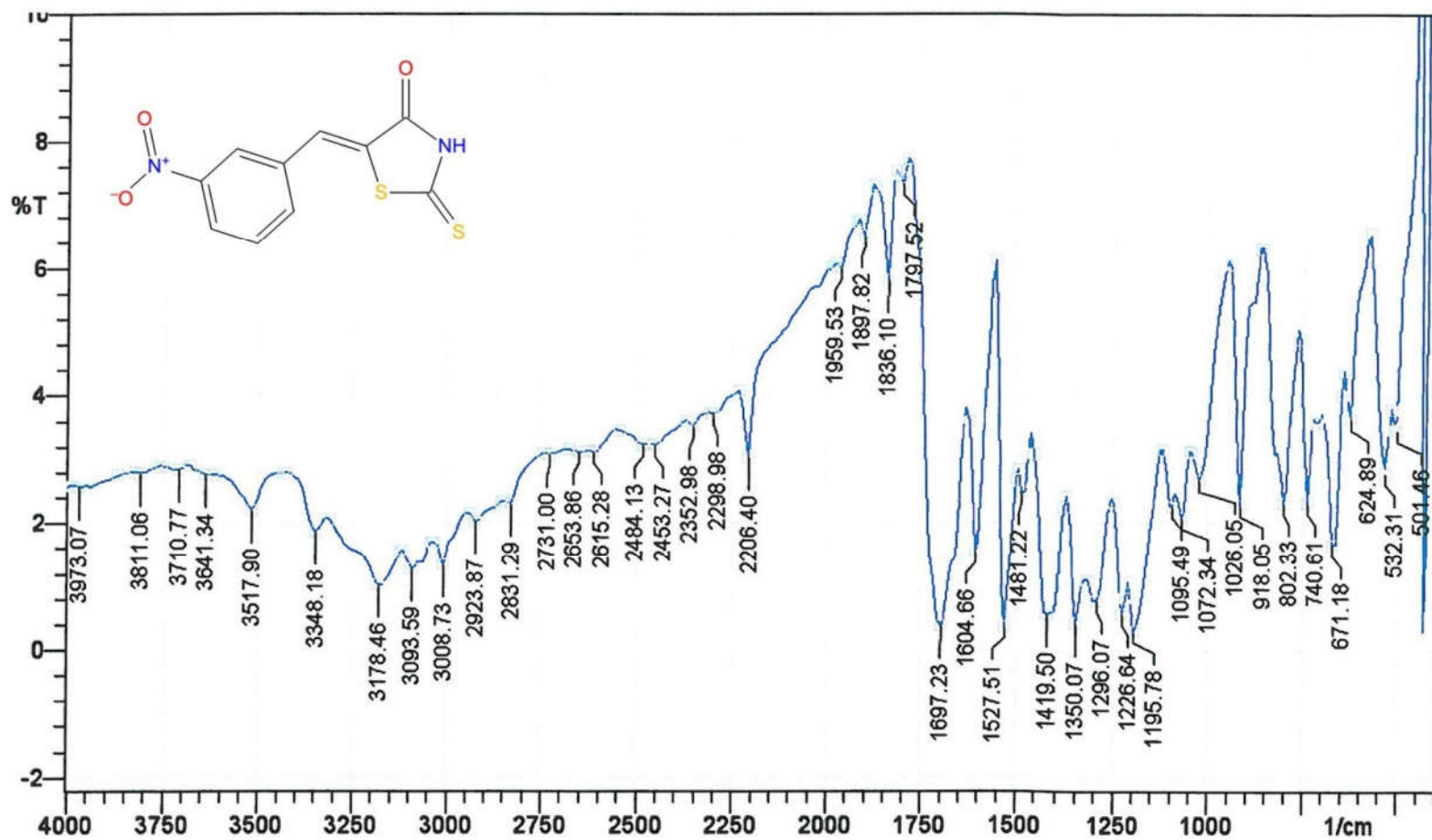
**MASS SPECTROSCOPY**

266.11 ( $\text{M}^+$ ), 267.15 ( $\text{M}+1$ ), 179.23 (**B**).

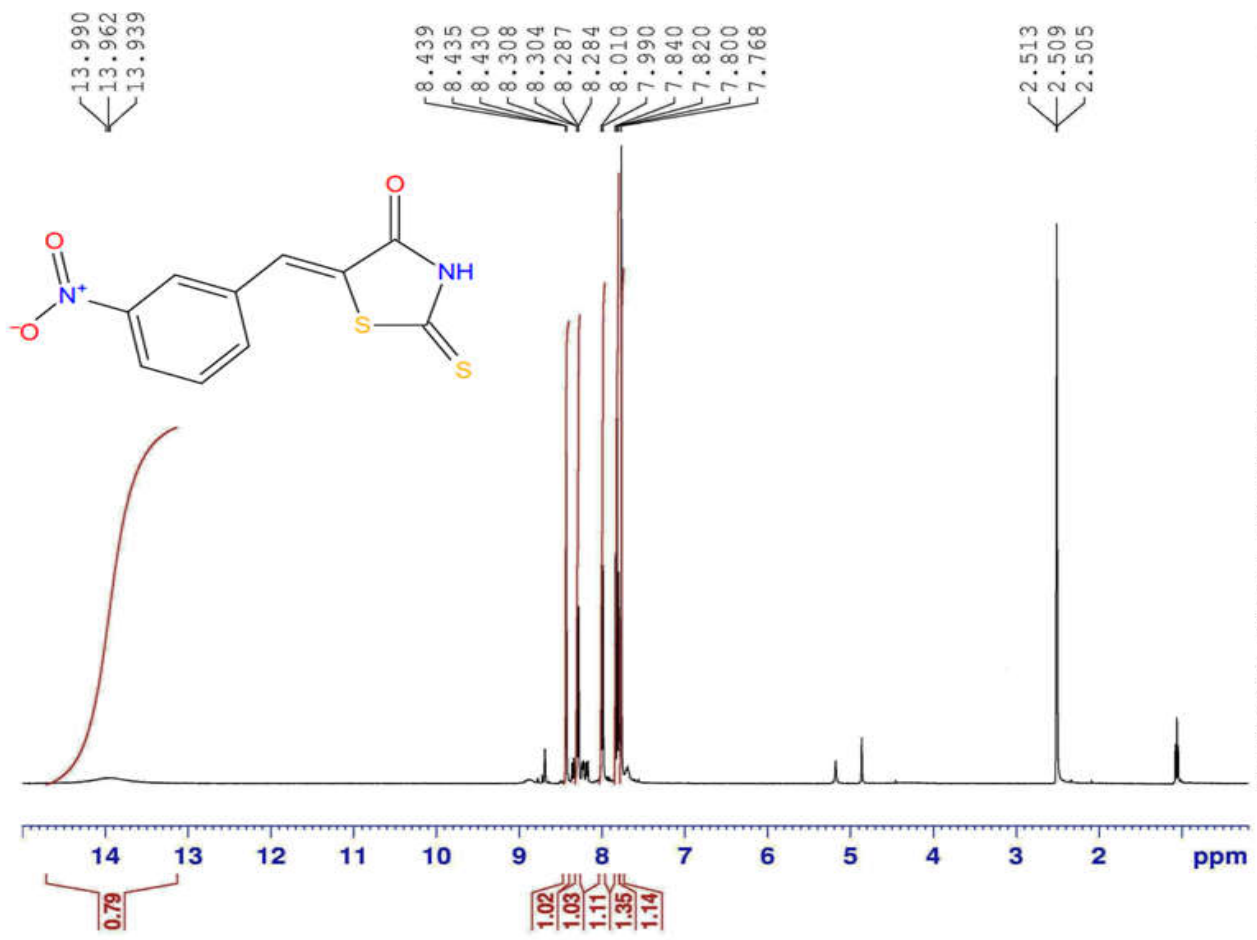
**ELEMENTAL ANALYSIS**

Anal. Calcd. For N18: C, 45.10; H, 2.27; N, 10.52; Obsd. C, 44.98; H, 2.28; N, 10.53.

Sample: N 18



N18.....Noorulla



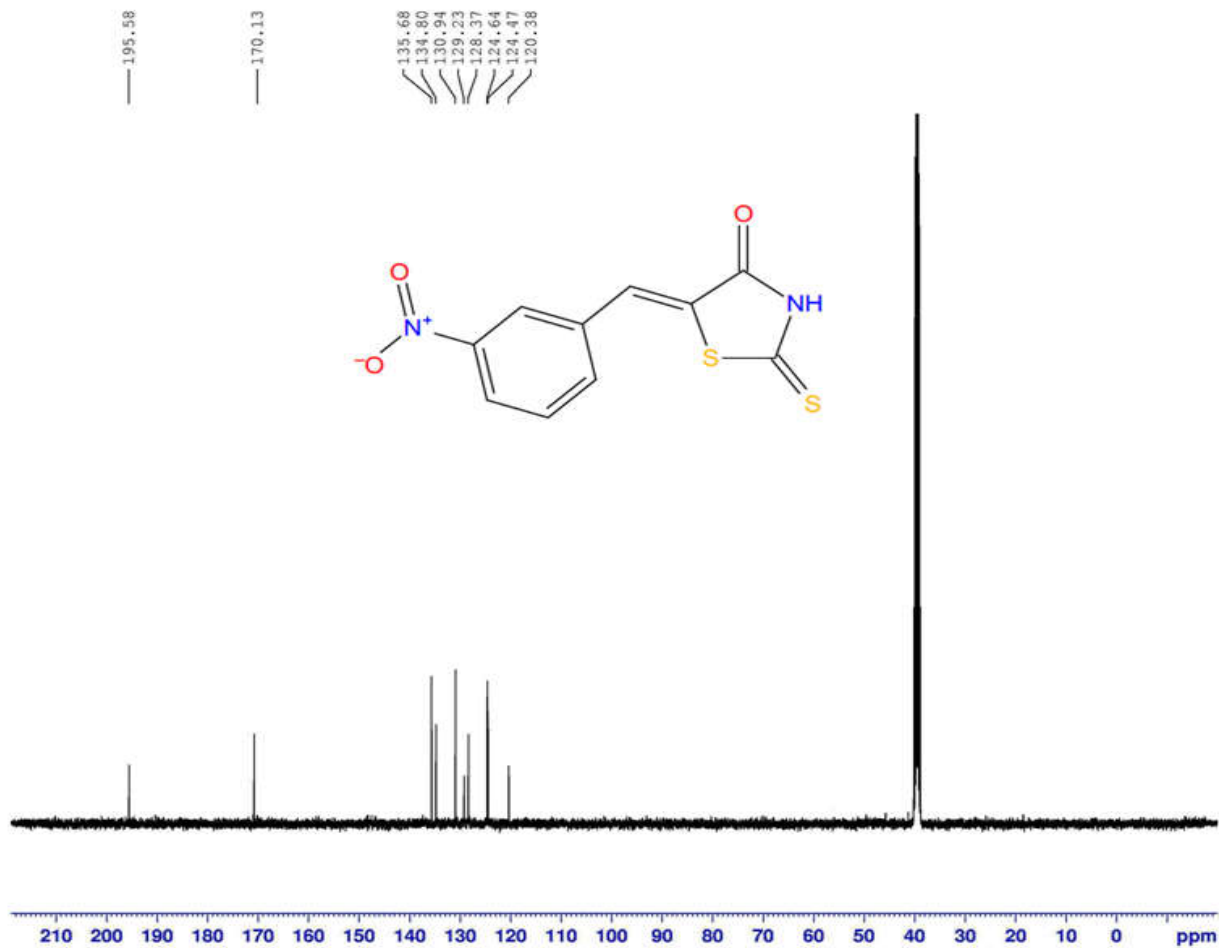
Current Data Parameters  
NAME N18  
EXPNO 234  
PROCNO 1

F2 - Acquisition Parameters  
Date\_ 20150727  
Time 8.23  
INSTRUM spect  
PROBHD 5 mm PABBO BB/  
PULPROG zg30  
TD 65536  
SOLVENT DMSO  
NS 16  
DS 2  
SWH 8223.685 Hz  
FIDRES 0.125483 Hz  
AQ 3.9846387 sec  
RG 175.97  
DW 60.800 usec  
DE 6.50 usec  
TE 298.3 K  
D1 1.00000000 sec  
TD0 1

===== CHANNEL f1 =====  
NUC1 1H  
P1 14.25 usec  
PLW1 14.00000000 W  
SFQ1 400.2604718 MHz

F2 - Processing parameters  
SI 65536  
SF 400.2580018 MHz  
WDW EM  
SSB 0  
LB 0 0.30 Hz  
GB 0  
PC 1.00

N18.....Noorulla



Current Data Parameters  
NAME N18  
EXPNO 235  
PROCNO 1

F2 - Acquisition Parameters  
Date\_ 20150727  
Time 8.57  
INSTRUM spect  
PROBHD 5 mm PABBO BB/  
PULPROG zgpg30  
TD 65536  
SOLVENT DMSO  
NS 600  
DS 4  
SWH 24038.461 Hz  
FIDRES 0.366798 Hz  
AQ 1.3631988 sec  
RG 199.6  
DW 20.800 usec  
DE 6.50 usec  
TE 299.0 K  
D1 2.00000000 sec  
D11 0.03000000 sec  
TD0 1

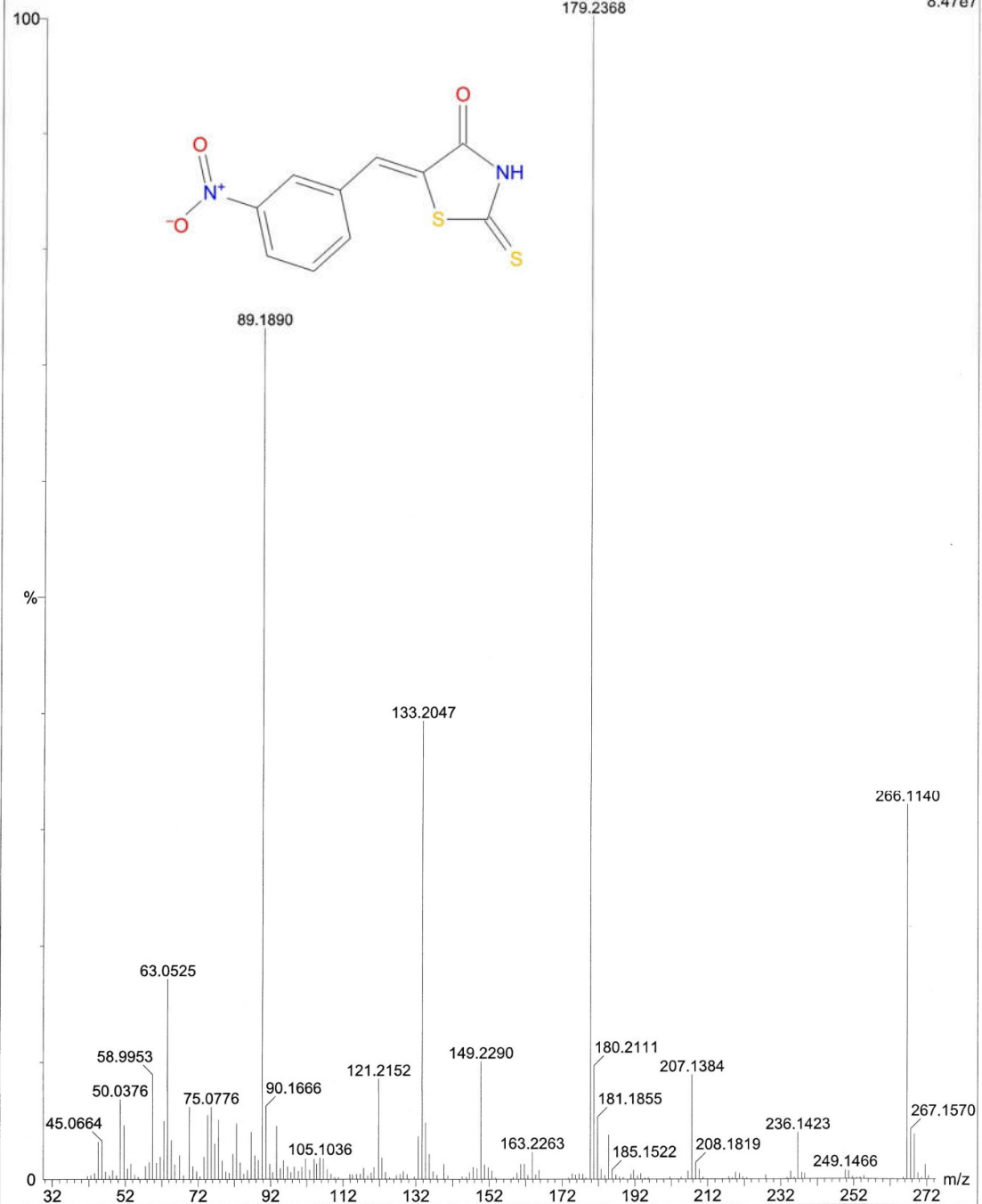
===== CHANNEL f1 =====  
NUC1 13C  
P1 9.80 usec  
PLW1 58.00000000 W  
SFO1 100.6550182 MHz

===== CHANNEL f2 =====  
CPDPRG2 waltz16  
NUC2 1H  
PCPD2 90.00 usec  
PLW2 14.00000000 W  
PLW12 0.35097000 W  
PLW13 0.28428999 W  
SFO2 400.2596010 MHz

F2 - Processing parameters  
SI 32768  
SF 100.6450043 MHz  
WDW EM  
SSB 0  
LB 1.00 Hz  
GB 0  
PC 1.40

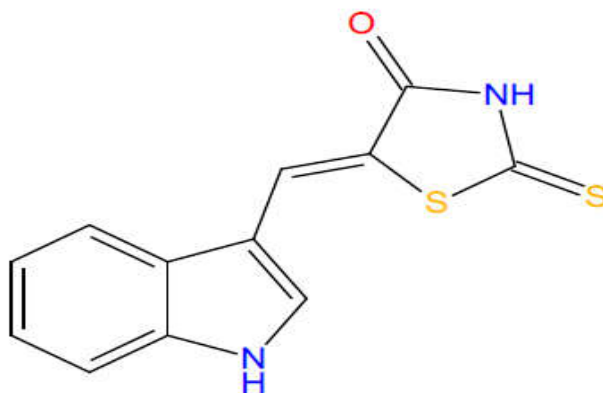
N18-4544 (25.227)

Scan EI+  
8.47e7





## Spectral Data of Compound N19



**IR (KBr,  $\nu_{\max}$ )  $\text{cm}^{-1}$**

1434.93 (Ar C-C), 1566.08 (C=O), 1681.80 (C=S), 3039.59 (=C-H),  
3116.74 (Ar C-H), 3456.18 (N-H).

**$^1\text{H}$  NMR (DMSO- $\text{D}_6$ )  $\delta$**

7.20-7.29 (m, 2H, Ar-H), 7.51 (d, 1H, =CH-), 7.83 (d, 1H, hetero  
Ar-H), 7.93 (d, 2H, Ar-H), 12.31 (s, 1H, indole N-H), 13.56 (s, 1H,  
N-H).

**$^{13}\text{C}$  NMR (DMSO- $\text{D}_6$ )  $\delta$**

112.50, 117.86, 118.44, 121.37, 123.25, 124.76, 126.74, 130.01,  
136.37, 140.20, 169.10, 194.61.

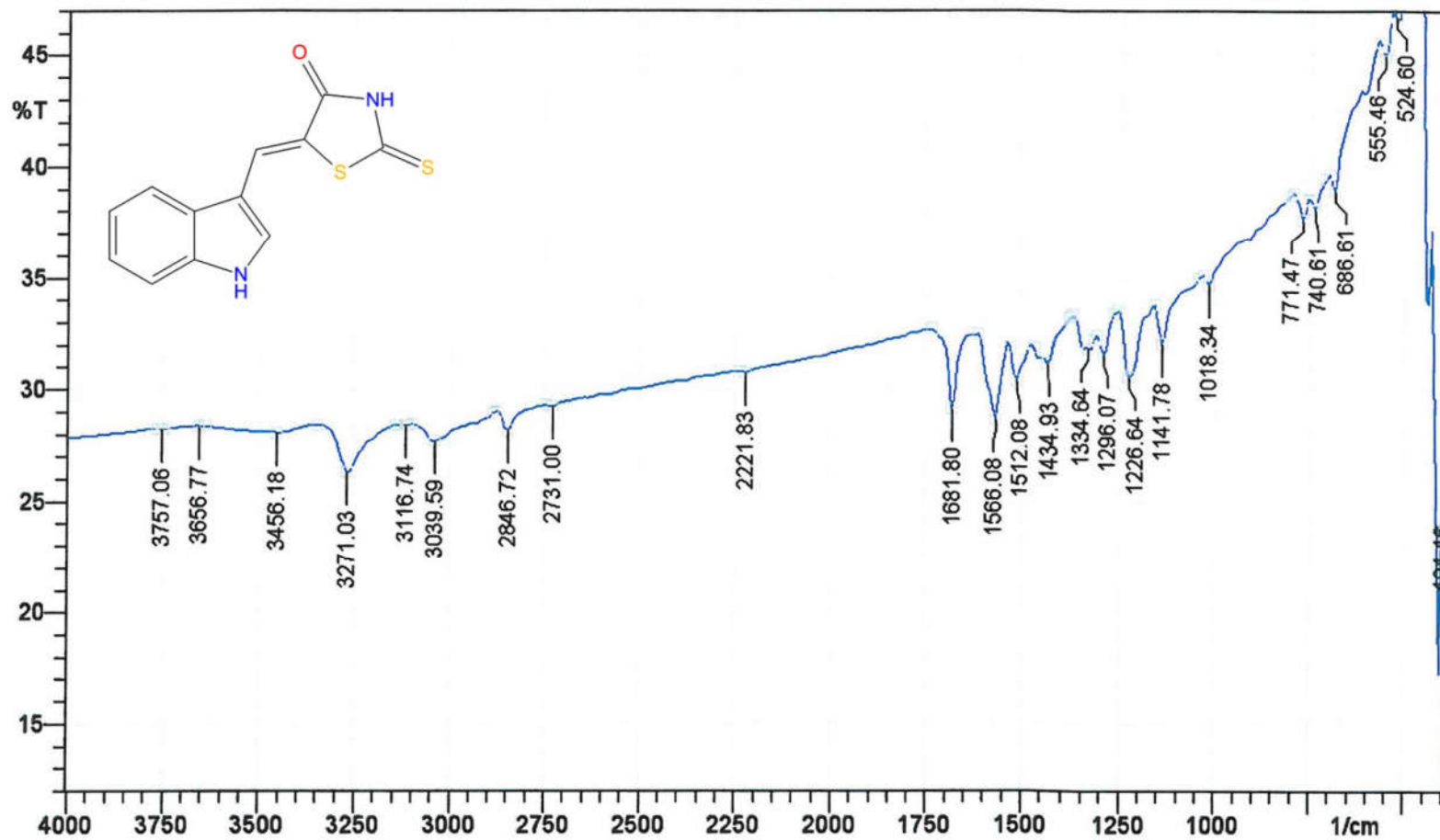
**MASS SPECTROSCOPY**

260.20 ( $\text{M}^+$ ), 207.13 (**B**).

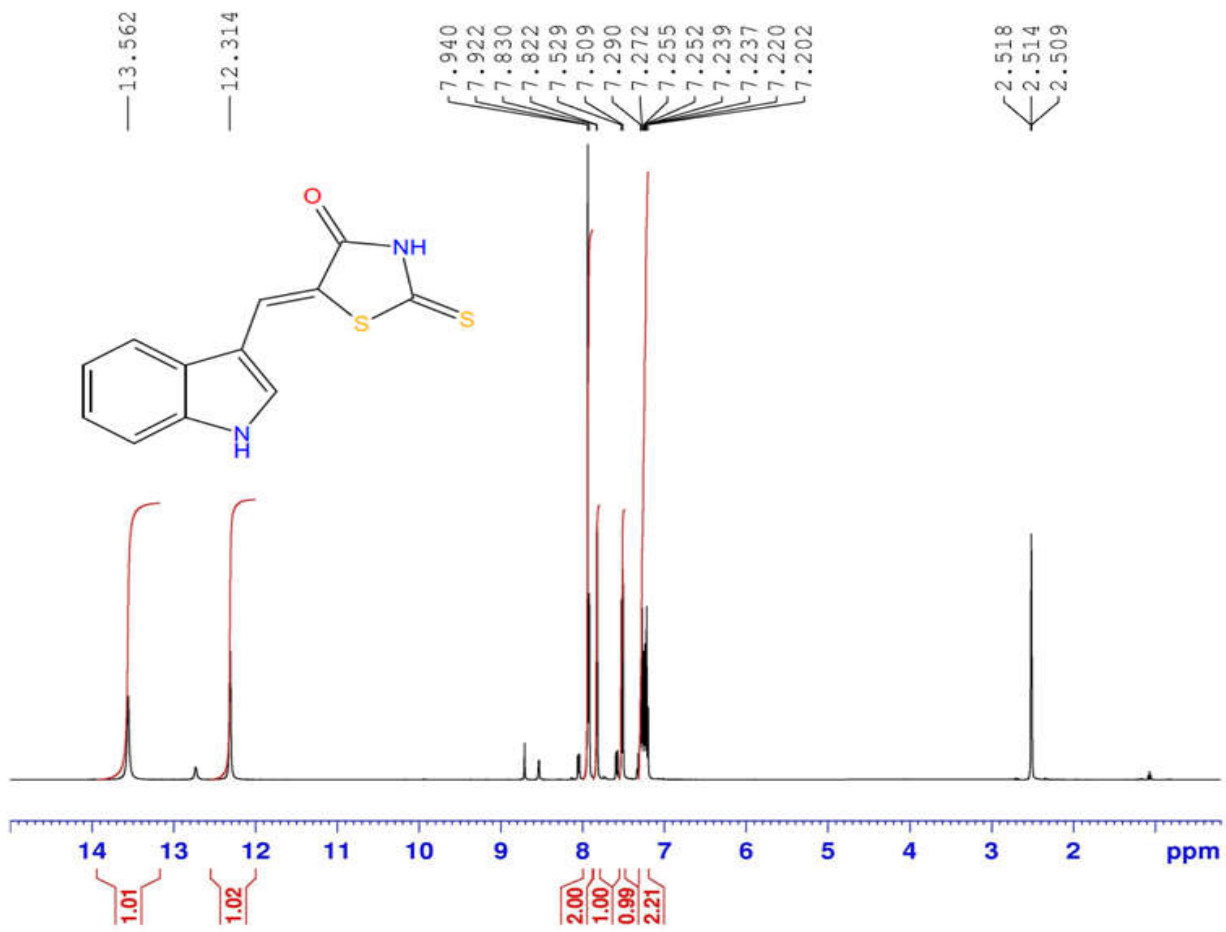
**ELEMENTAL ANALYSIS**

Anal. Calcd. For N19: C, 55.36; H, 3.10; N, 10.76; Obsd. C, 55.21;  
H, 3.11; N, 10.75.

Sample: N 19



N19.....Noorulla



Current Data Parameters  
NAME N19  
EXPNO 236  
PROCNO 1

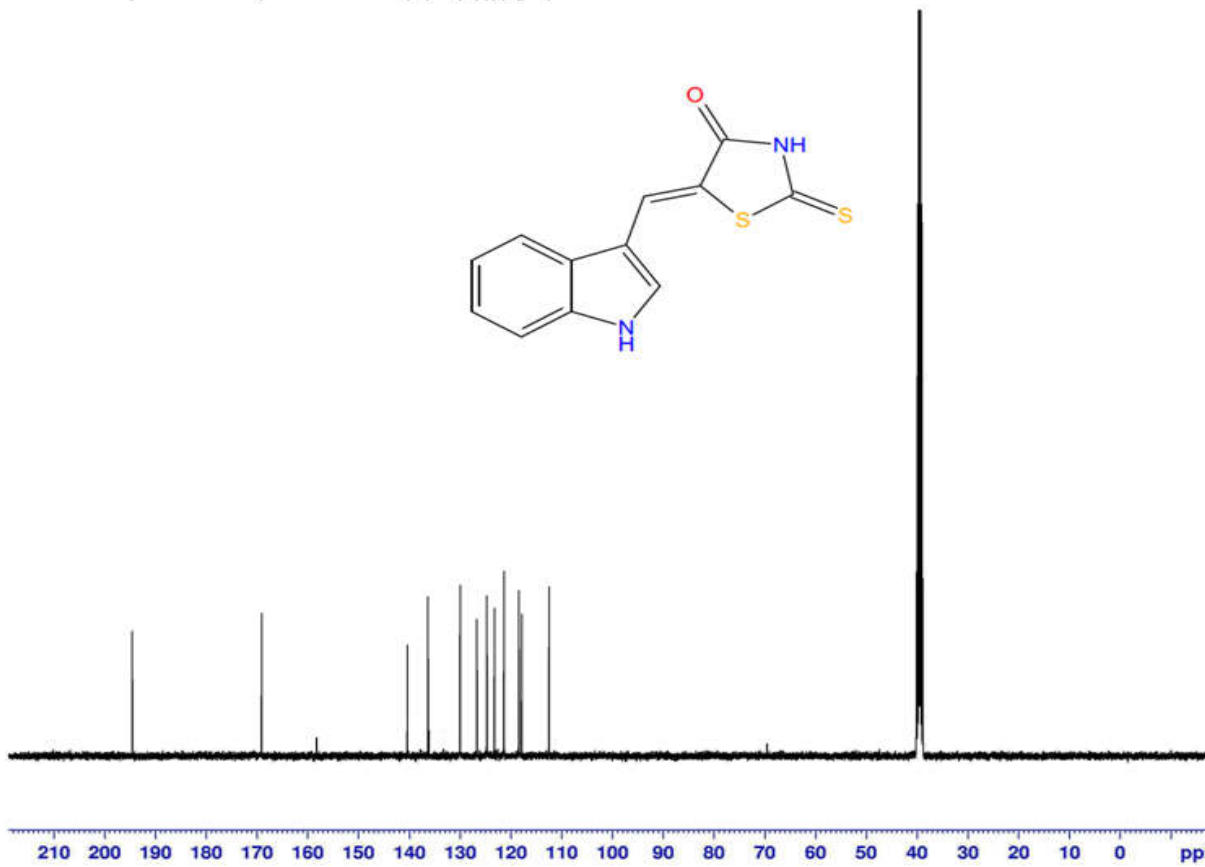
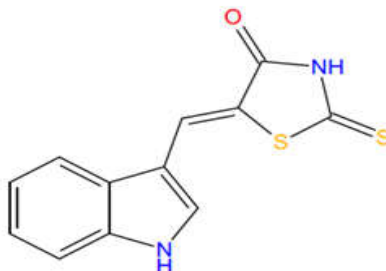
F2 - Acquisition Parameters  
Date\_ 20150727  
Time 9.00  
INSTRUM spect  
PROBHD 5 mm PABBO BB/  
PULPROG zg30  
TD 65536  
SOLVENT DMSO  
NS 16  
DS 2  
SWH 8223.685 Hz  
FIDRES 0.125483 Hz  
AQ 3.9846387 sec  
RG 156.91  
DW 60.800 usec  
DE 6.50 usec  
TE 298.3 K  
D1 1.00000000 sec  
TD0 1

===== CHANNEL f1 =====  
NUC1 1H  
P1 14.25 usec  
PLW1 14.00000000 W  
SFO1 400.2604718 MHz

F2 - Processing parameters  
SI 65536  
SF 400.2580000 MHz  
WDW EM  
SSB 0  
LB 0.30 Hz  
GB 0  
PC 1.00

N19.....Noorulla

194.61  
169.10  
140.20  
136.37  
130.01  
126.74  
124.76  
123.25  
121.37  
118.44  
117.86  
112.50



Current Data Parameters  
NAME N19  
EXPNO 237  
PROCNO 1

F2 - Acquisition Parameters  
Date\_ 20150727  
Time 9.35  
INSTRUM spect  
PROBHD 5 mm PABBO BB/  
PULPROG zgpg30  
TD 65536  
SOLVENT DMSO  
NS 600  
DS 4  
SWH 24038.461 Hz  
FIDRES 0.366798 Hz  
AQ 1.3631988 sec  
RG 199.6  
DW 20.800 usec  
DE 6.50 usec  
TE 299.1 K  
D1 2.00000000 sec  
D11 0.03000000 sec  
TD0 1

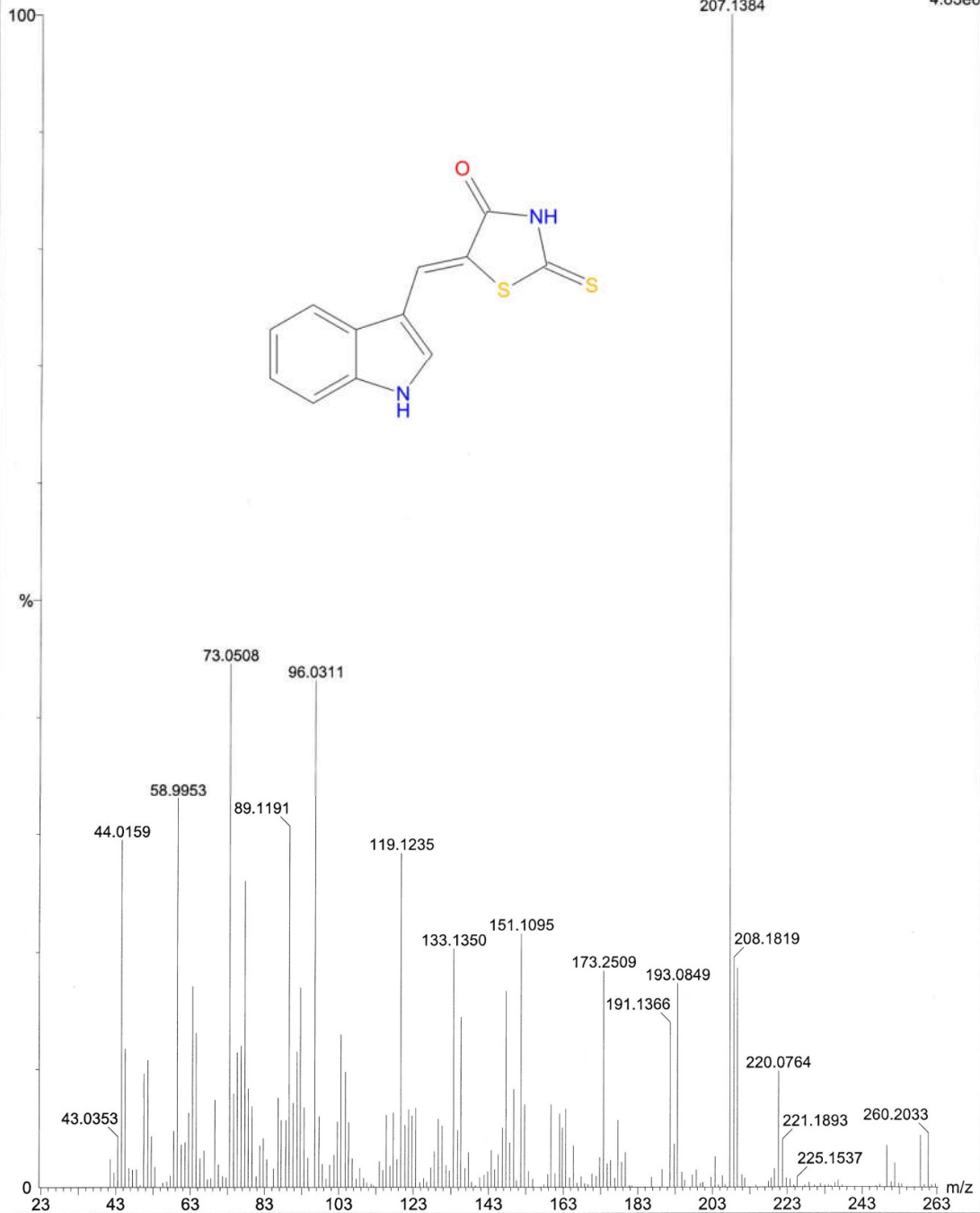
===== CHANNEL f1 =====  
NUC1 13C  
P1 9.80 usec  
PLW1 58.00000000 W  
SFO1 100.6550182 MHz

===== CHANNEL f2 =====  
CPDPRG2 waltz16  
NUC2 1H  
PCPD2 90.00 usec  
PLW2 14.00000000 W  
PLW12 0.35097000 W  
PLW13 0.28428999 W  
SFO2 400.2596010 MHz

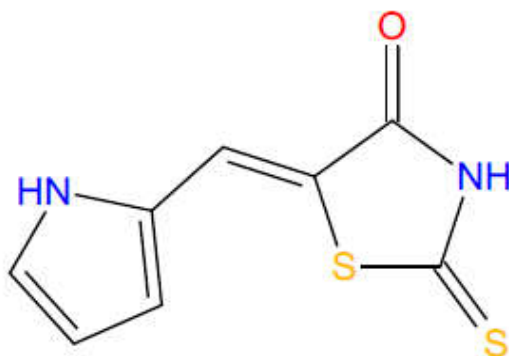
F2 - Processing parameters  
SI 32768  
SF 100.6450043 MHz  
WDW EM  
SSB 0  
LB 1.00 Hz  
GB 0  
PC 1.40

N19-5456 (29.789)

Scan EI+  
4.83e6



## Spectral Data of Compound N20



**IR (KBr,  $\nu_{\max}$ )  $\text{cm}^{-1}$**

1442.65 (Ar C-C), 1596.94 (C=O), 1704.95 (C=S), 2923.87(=C-H),  
3085.88 (Ar C-H), 3479.33 (N-H).

**$^1\text{H}$  NMR (DMSO- $\text{D}_6$ )  $\delta$**

6.39-6.41 (q, 1H, Hetero Ar-H), 6.53 (s, 1H, hetero Ar-H), 7.27-7.29  
(m, 1H, hetero Ar-H), 7.52 (s, 1H, =CH-), 11.80 (s, 1H, pyrrole  
NH), 13.53 (s, 1H, NH)

**$^{13}\text{C}$  NMR (DMSO- $\text{D}_6$ )  $\delta$**

114.97, 121.94, 125.71, 127.21, 132.95, 139.34, 169.18, 194.77.

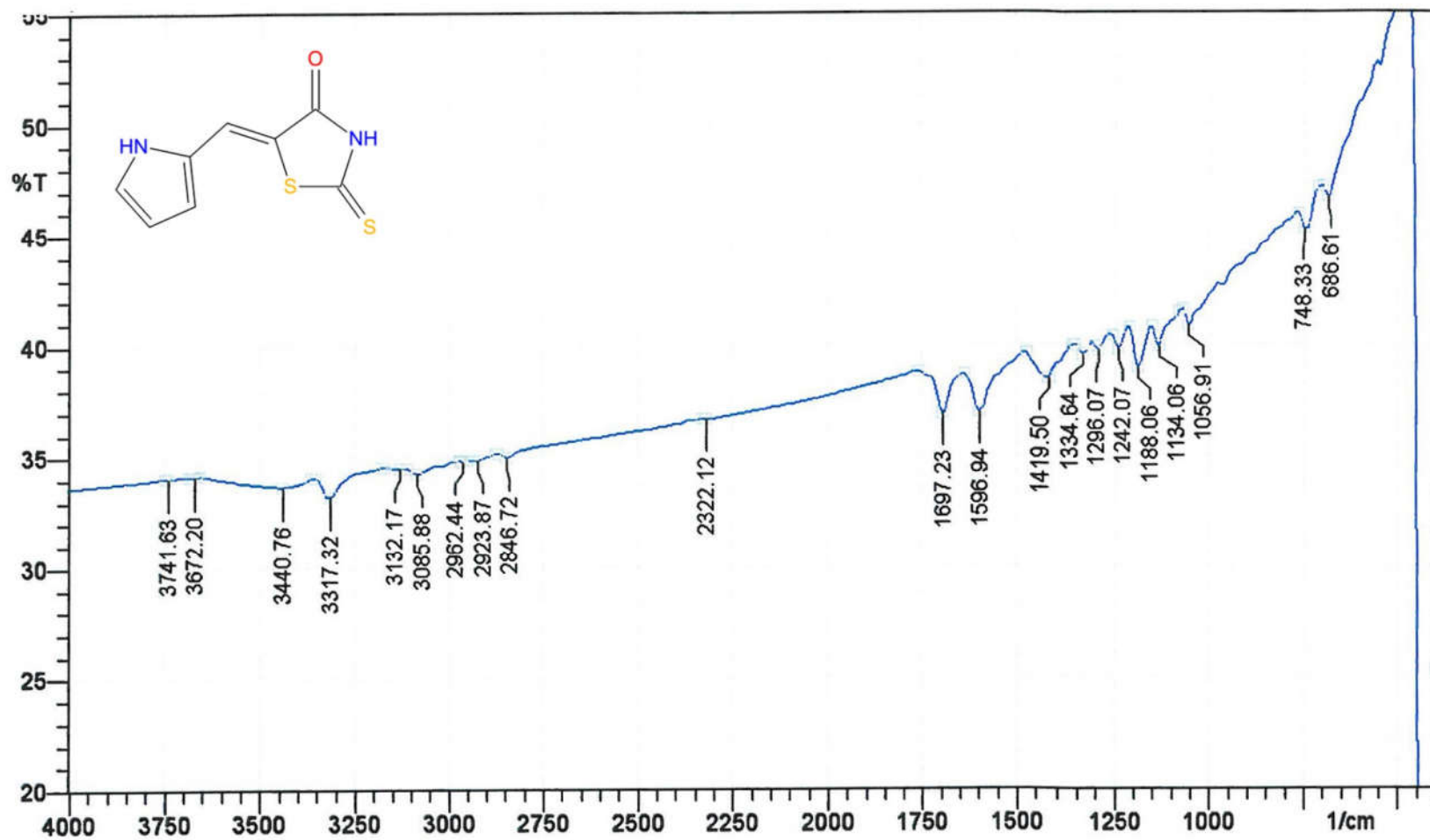
**MASS SPECTROSCOPY**

210.12 ( $\text{M}^+$ ), 211.17 ( $\text{M}+1$ ), 123.16 (**B**).

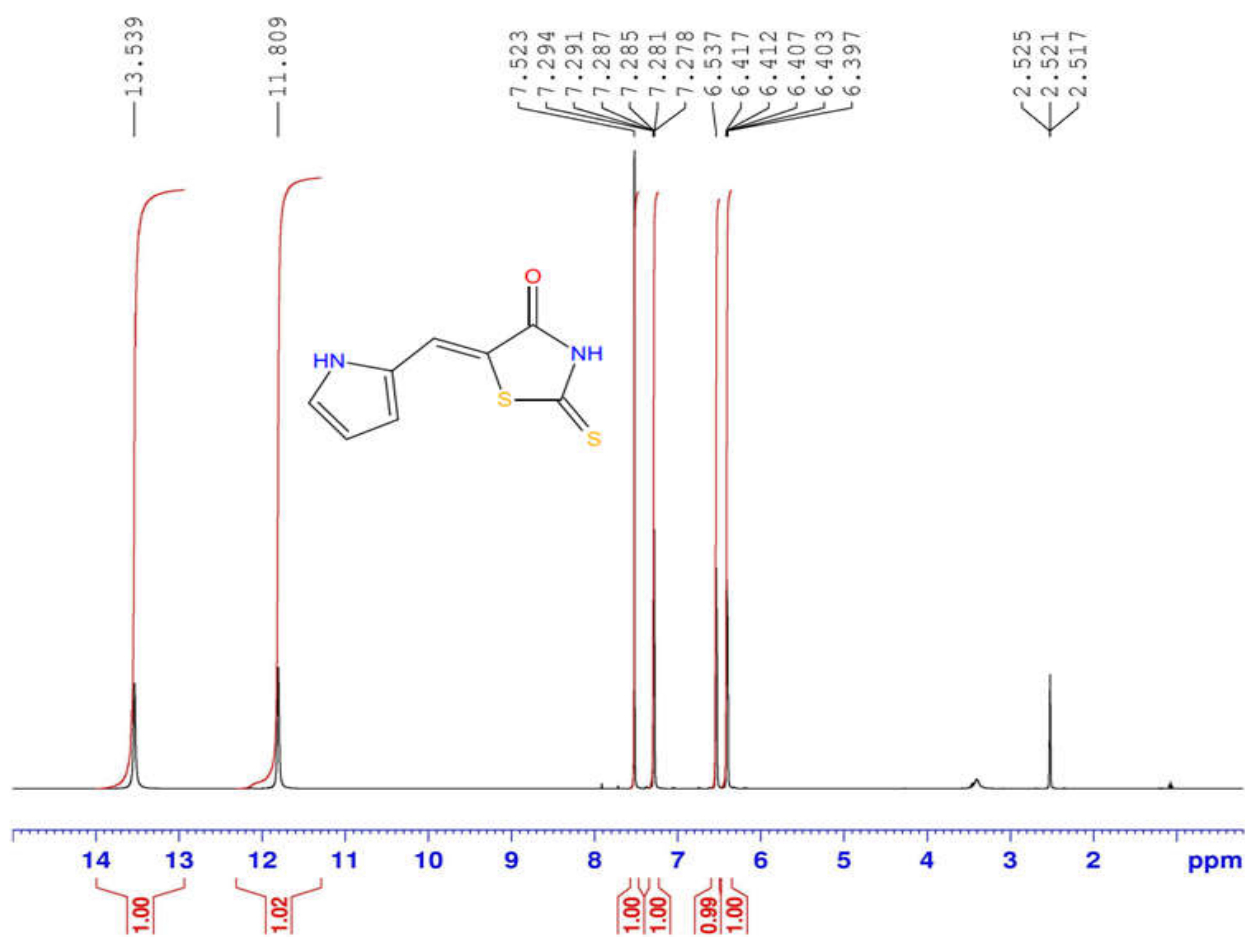
**ELEMENTAL ANALYSIS**

Anal. Calcd. For N20: C, 45.69; H, 2.88; N, 13.32; Obsd. C, 45.58;  
H, 2.89; N, 13.31.

Sample: N 20



N20.....Noorulla



Current Data Parameters  
NAME N20  
EXPNO 238  
PROCNO 1

F2 - Acquisition Parameters  
Date\_ 20150727  
Time 9.38  
INSTRUM spect  
PROBHD 5 mm PABBO BB/  
PULPROG zg30  
TD 65536  
SOLVENT DMSO  
NS 16  
DS 2  
SWH 8223.685 Hz  
FIDRES 0.125483 Hz  
AQ 3.9846387 sec  
RG 112.69  
DW 60.800 usec  
DE 6.50 usec  
TE 298.5 K  
D1 1.00000000 sec  
TDO 1

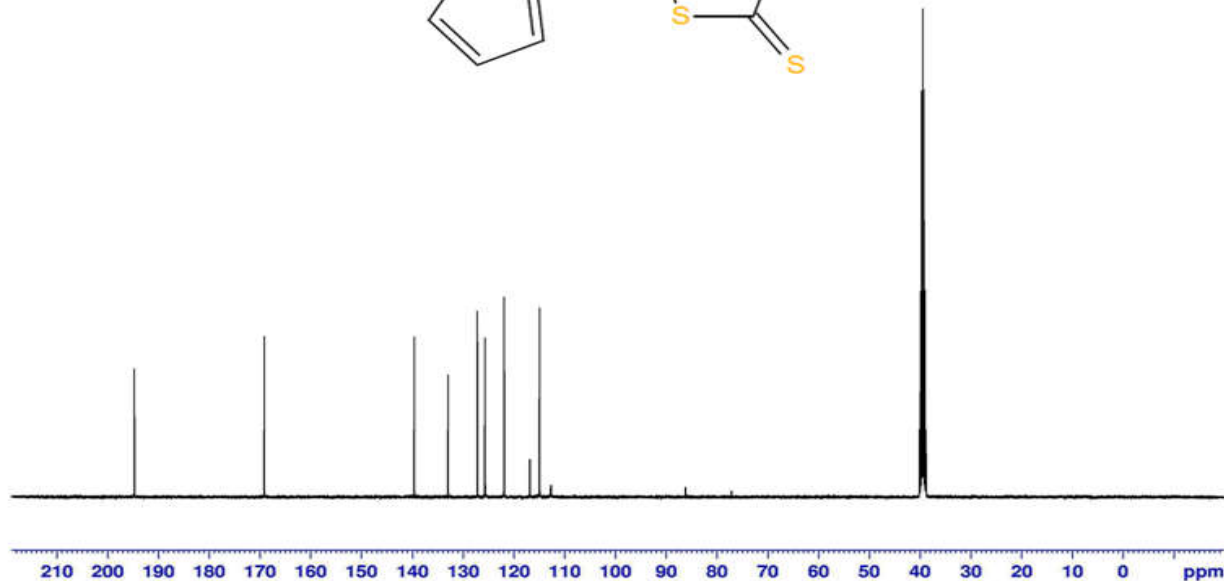
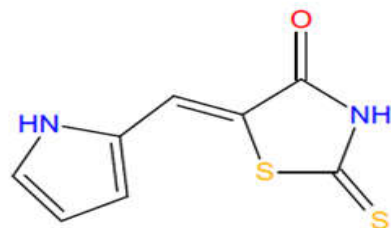
===== CHANNEL f1 =====  
NUC1 1H  
P1 14.25 usec  
PLW1 14.00000000 W  
SFO1 400.2604718 MHz

F2 - Processing parameters  
SI 65536  
SF 400.2579971 MHz  
WDW EM  
SSB 0  
LB 0.30 Hz  
GB 0  
PC 1.00



N20.....Noorulla

— 194.77 —  
— 169.18 —  
— 139.34 —  
— 132.95 —  
— 127.21 —  
— 125.71 —  
— 121.94 —  
— 114.97 —



Current Data Parameters  
NAME N20  
EXPNO 239  
PROCNO 1

F2 - Acquisition Parameters  
Date\_ 20150727  
Time 10.13  
INSTRUM spect  
PROBHD 5 mm PABBO BB/  
PULPROG zgpg30  
TD 65536  
SOLVENT DMSO  
NS 600  
DS 4  
SWH 24038.461 Hz  
FIDRES 0.366798 Hz  
AQ 1.3631988 sec  
RG 199.6  
DW 20.800 usec  
DE 6.50 usec  
TE 299.0 K  
D1 2.00000000 sec  
D11 0.03000000 sec  
TD0 1

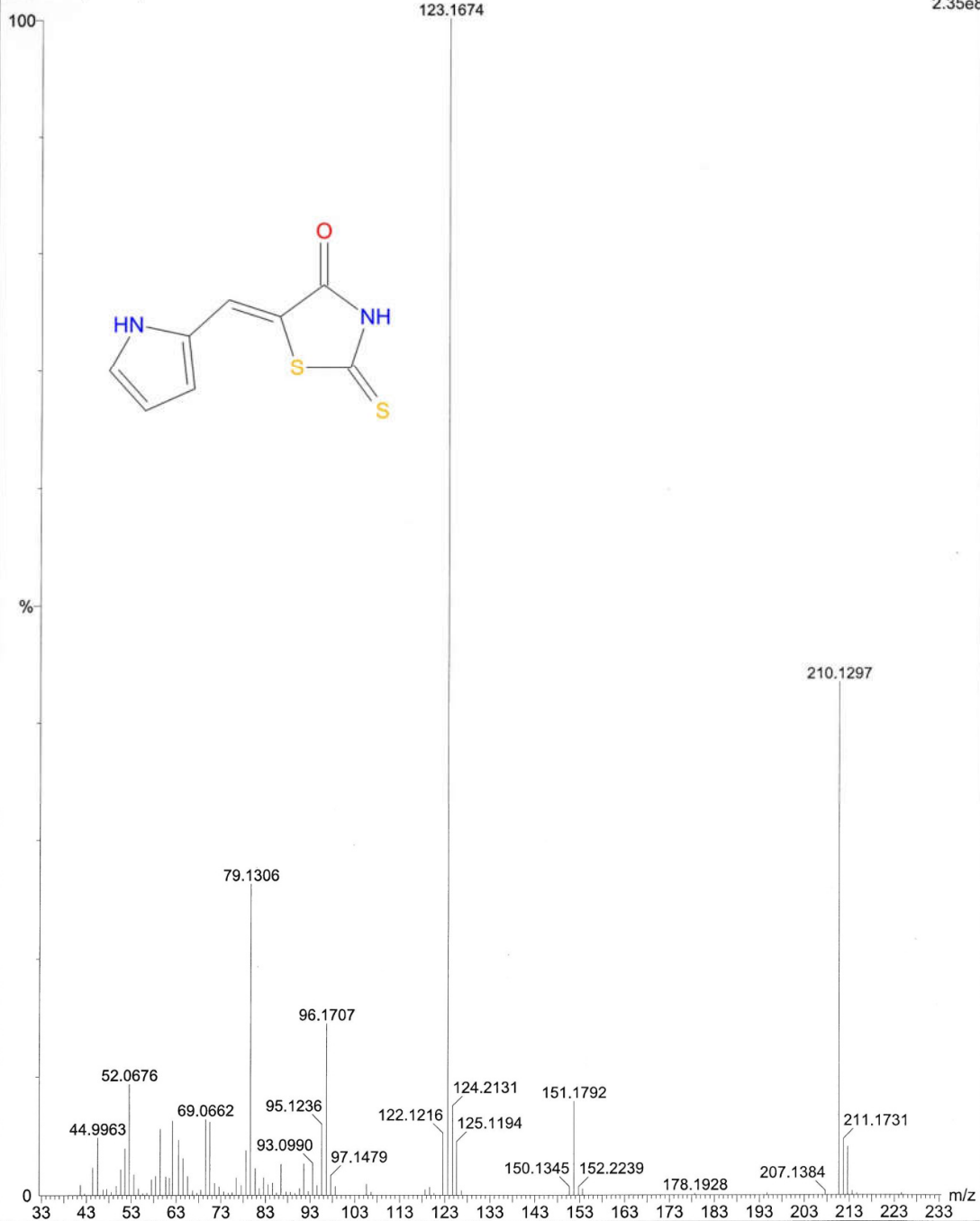
===== CHANNEL f1 =====  
NUC1 13C  
P1 9.80 usec  
PLW1 58.00000000 W  
SFO1 100.6550182 MHz

===== CHANNEL f2 =====  
CPDPRG2 waltz16  
NUC2 1H  
PCPD2 90.00 usec  
PLW2 14.00000000 W  
PLW12 0.35097000 W  
PLW13 0.28428999 W  
SFO2 400.2596010 MHz

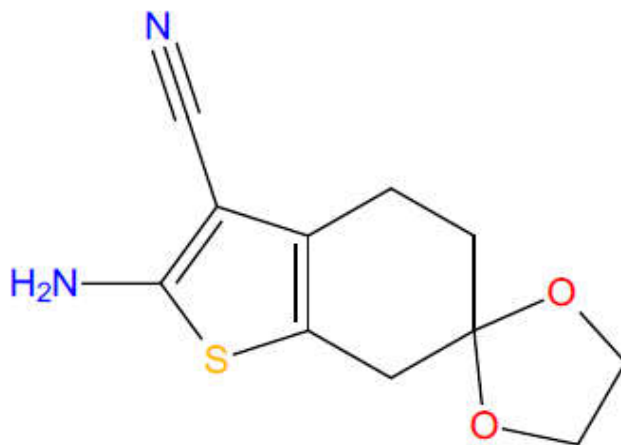
F2 - Processing parameters  
SI 32768  
SF 100.6450043 MHz  
WDW EM  
SSB 0  
LB 1.00 Hz  
GB 0  
PC 1.40

N20-3759 (21.301)

Scan EI+  
2.35e8

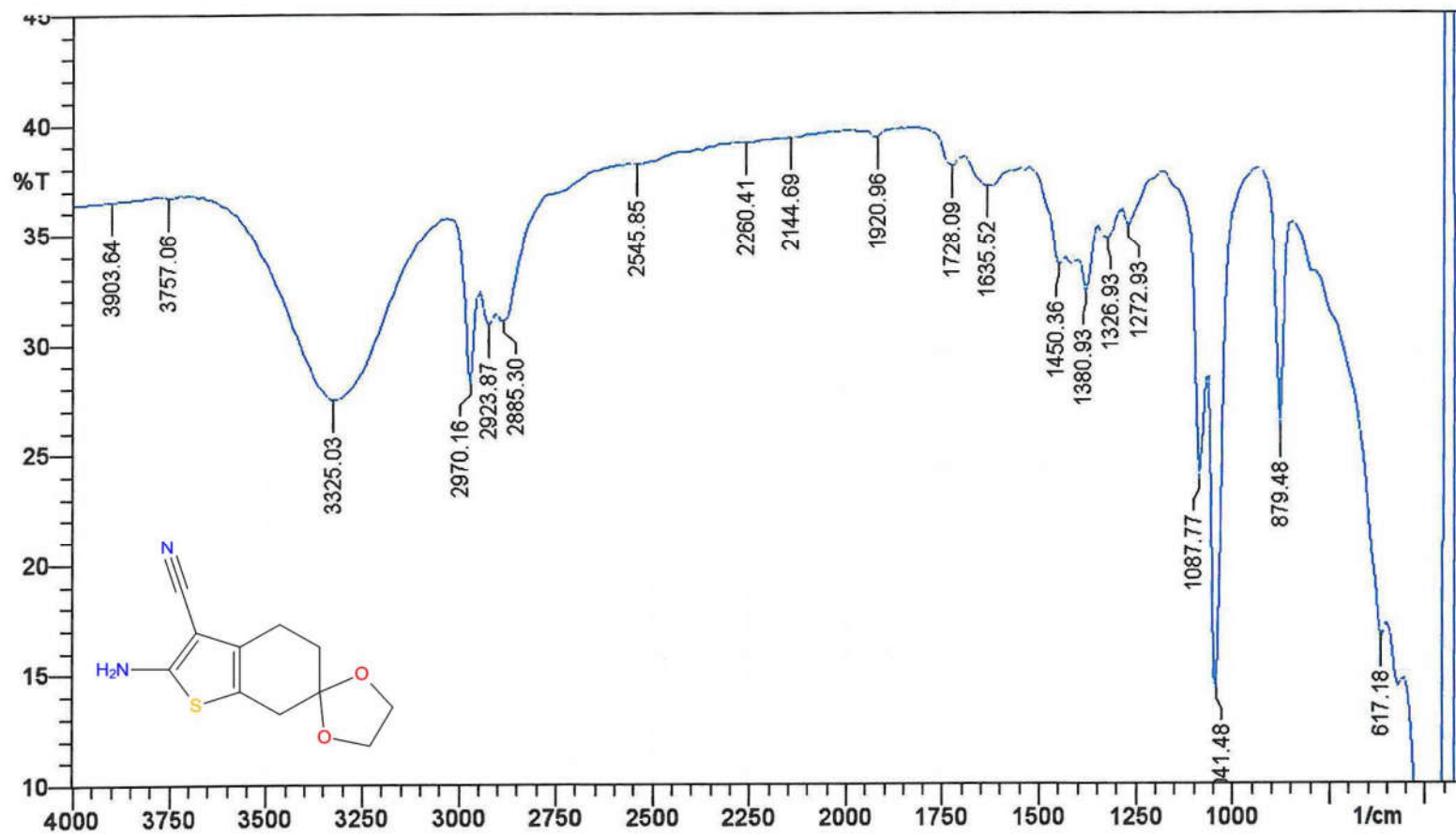


## Spectral Data of Compound GA

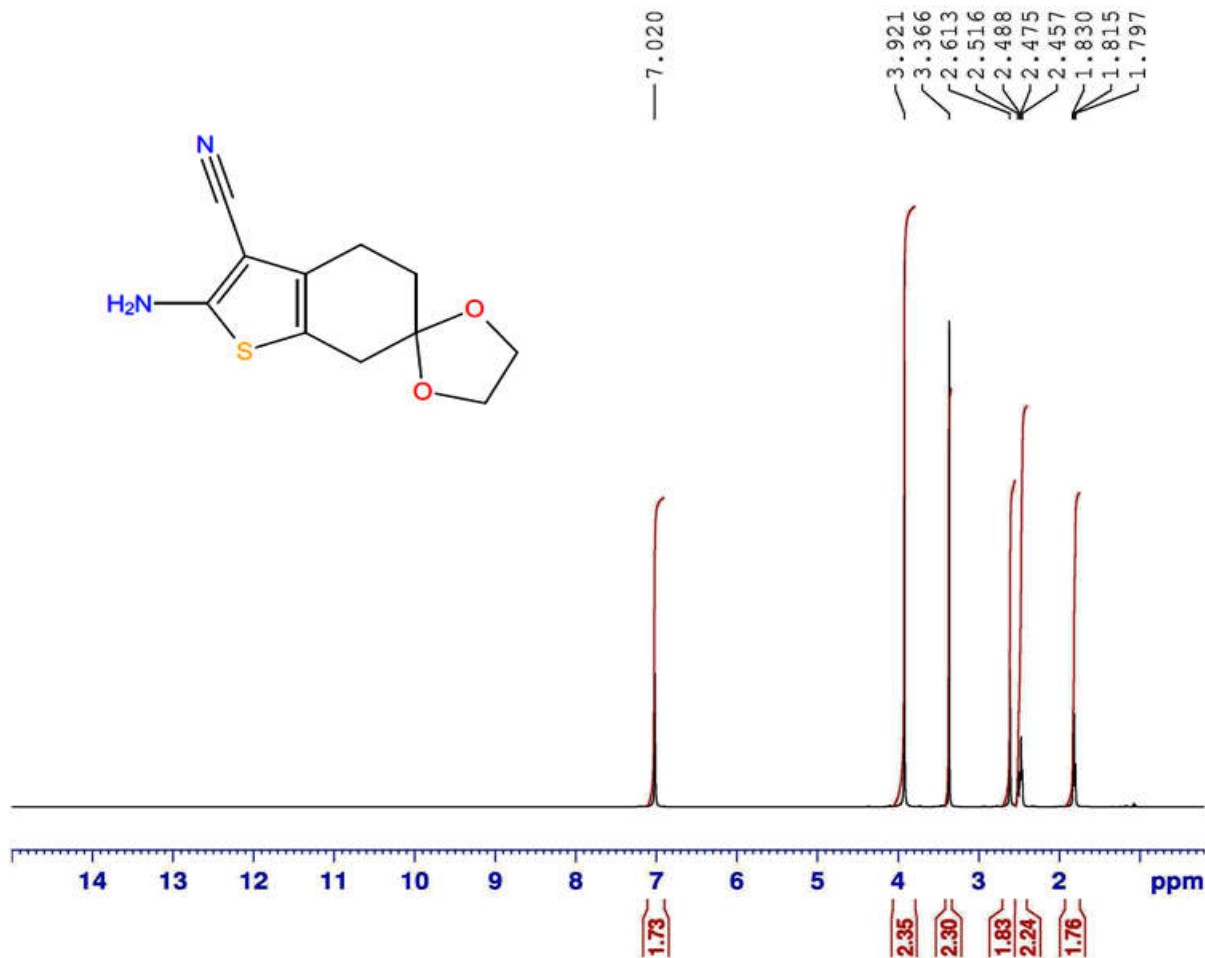
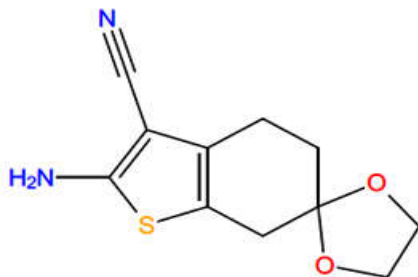


<b>IR (KBr, <math>\nu_{\max}</math>) <math>\text{cm}^{-1}</math></b>	3325.03 (amine N-H), 2970.16 (aliphatic C-H), 2260.41 (nitrile C≡N), 1272.93 (C-O-C), 1326.93 (amine C-N), 617.18 (C-S).
<b><math>^1\text{H NMR}</math> (DMSO-<math>\text{D}_6</math>) <math>\delta</math></b>	1.81 (t, 2H, CH <sub>2</sub> ), 2.45-2.51 (q, 2H, CH <sub>2</sub> ), 2.61 (s, 2H, CH <sub>2</sub> ), 3.36 (s, 2H, CH <sub>2</sub> ), 3.92 (s, 2H, CH <sub>2</sub> ), 7.02 (s, 2H, NH <sub>2</sub> ).
<b><math>^{13}\text{C NMR}</math> (DMSO-<math>\text{D}_6</math>) <math>\delta</math></b>	22.77, 24.46, 27.58, 30.55, 34.05, 63.93, 107.54, 114.23, 116.05, 130.13, 163.51.
<b>MASS SPECTROSCOPY</b>	236.17 ( $\text{M}^+$ ), 237.12 ( $\text{M}+1$ ), 150.09 ( <b>B</b> ).

Sample: GA



GA .....Noorulla



Current Data Parameters  
NAME GA  
EXPNO 1  
PROCNO 1

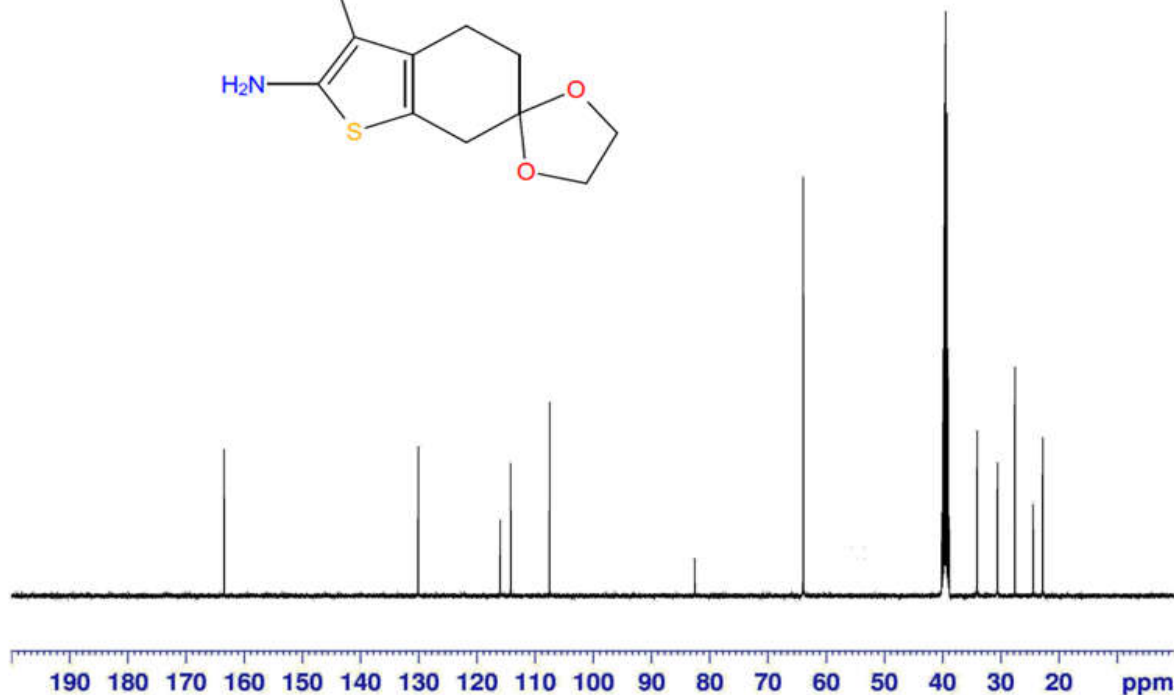
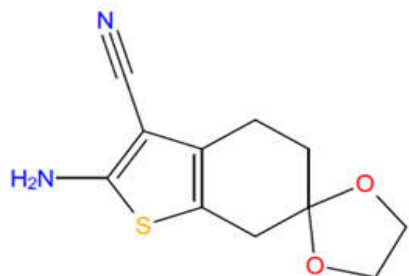
F2 - Acquisition Parameters  
Date\_ 20151205  
Time 20.30  
INSTRUM spect  
PROBHD 5 mm PABBO BB/  
PULPROG zg30  
TD 65536  
SOLVENT DMSO  
NS 16  
DS 2  
SWH 8223.685 Hz  
FIDRES 0.125483 Hz  
AQ 3.9846387 sec  
RG 77.73  
DW 60.800 usec  
DE 6.50 usec  
TE 298.5 K  
D1 1.00000000 sec  
TD0 1

===== CHANNEL f1 =====  
NUC1 1H  
P1 14.25 usec  
PLW1 14.00000000 W  
SFO1 400.2604718 MHz

F2 - Processing parameters  
SI 65536  
SF 400.2580000 MHz  
WDW EM  
SSB 0  
LB 0.30 Hz  
GB 0  
PC 1.00

GA.....Noorulla

163.51  
130.13  
116.05  
114.23  
107.54  
63.93  
34.05  
30.55  
27.58  
24.46  
22.77



Current Data Parameters  
NAME GA  
EXPNO 3  
PROCNO 1

F2 - Acquisition Parameters  
Date\_ 20151205  
Time 21.14  
INSTRUM spect  
PROBHD 5 mm PABBO BB/  
PULPROG zgpg30  
TD 65536  
SOLVENT DMSO  
NS 512  
DS 4  
SWH 24038.461 Hz  
FIDRES 0.366798 Hz  
AQ 1.3631988 sec  
RG 156.91  
DW 20.800 usec  
DE 6.50 usec  
TE 300.2 K  
D1 2.00000000 sec  
D11 0.03000000 sec  
TD0 1

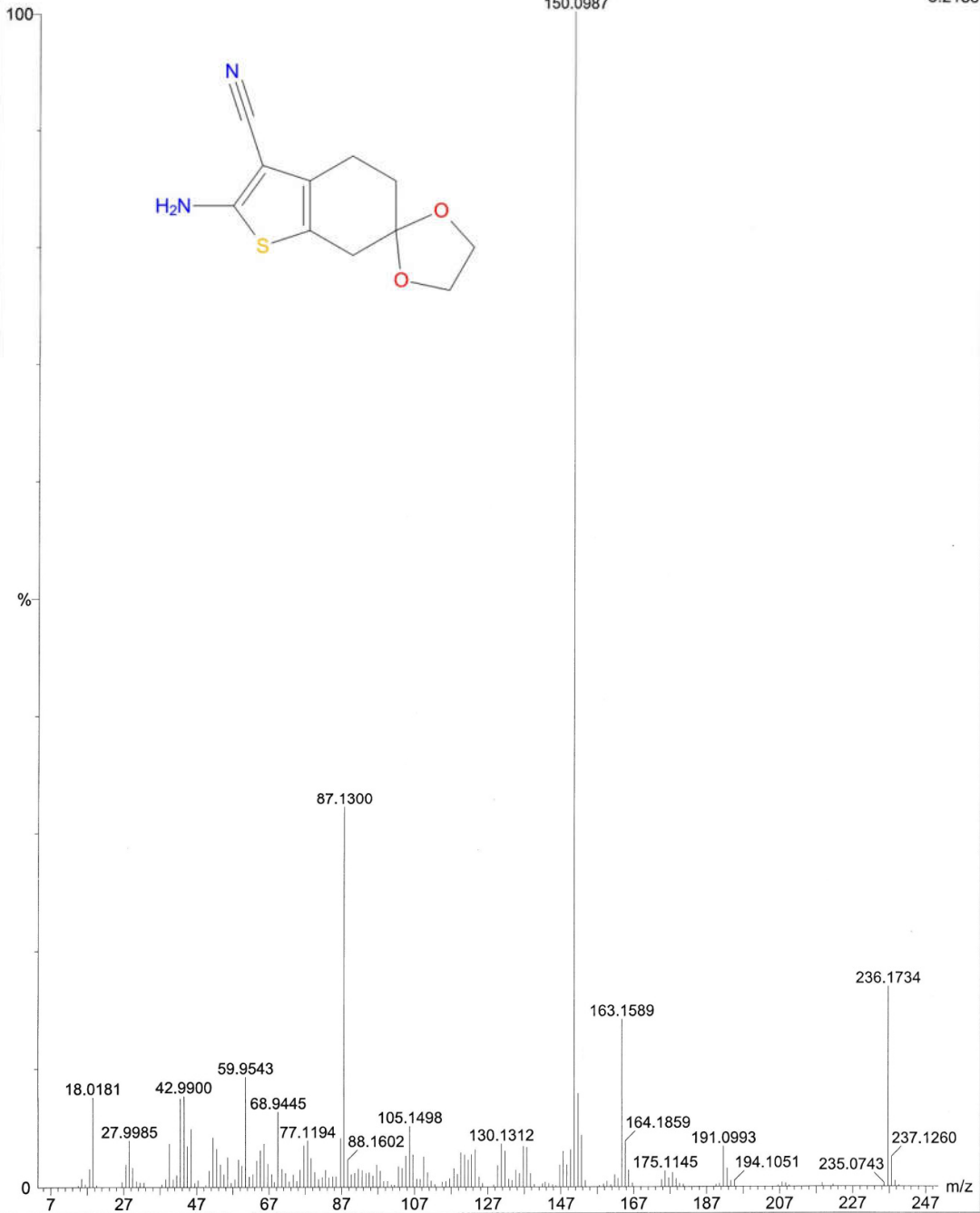
===== CHANNEL f1 =====  
NUC1 13C  
P1 9.80 usec  
PLW1 58.00000000 W  
SFO1 100.6550182 MHz

===== CHANNEL f2 =====  
CPDPRG2 waltz16  
NUC2 1H  
PCPD2 90.00 usec  
PLW2 14.00000000 W  
PLW12 0.35097000 W  
PLW13 0.28428999 W  
SFO2 400.2596010 MHz

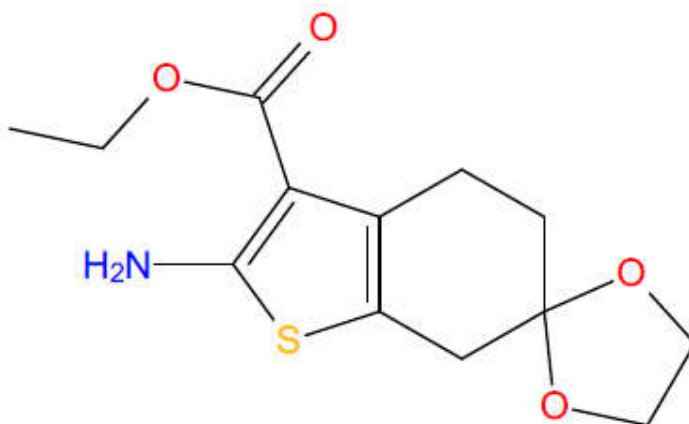
F2 - Processing parameters  
SI 32768  
SF 100.6450043 MHz  
WDW EM  
SSB 0  
LB 1.00 Hz  
GB 0  
PC 1.40

GA-3565 (20.631)

Scan EI+  
3.21e8



## Spectral Data of Compound GAE



**IR (KBr,  $\nu_{\max}$ )  $\text{cm}^{-1}$**

3502.47 (amine N-H), 2947.01 (aliphatic C-H), 1728.09 (ester C=O), 1373.22 (ester C-O), 609.46 (C-S).

**$^1\text{H}$  NMR (DMSO- $\text{D}_6$ )  $\delta$**

1.25 (t, 3H,  $\text{CH}_3$ ), 1.77 (t, 2H,  $\text{CH}_2$ ), 2.61 (s, 2H,  $\text{CH}_2$ ), 2.74 (t, 2H,  $\text{CH}_2$ ), 3.36 (s, 2H,  $\text{CH}_2$ ), 3.91 (s, 4H,  $\text{CH}_2$ ), 7.24 (s, 2H,  $\text{NH}_2$ ).

**$^{13}\text{C}$  NMR (DMSO- $\text{D}_6$ )  $\delta$**

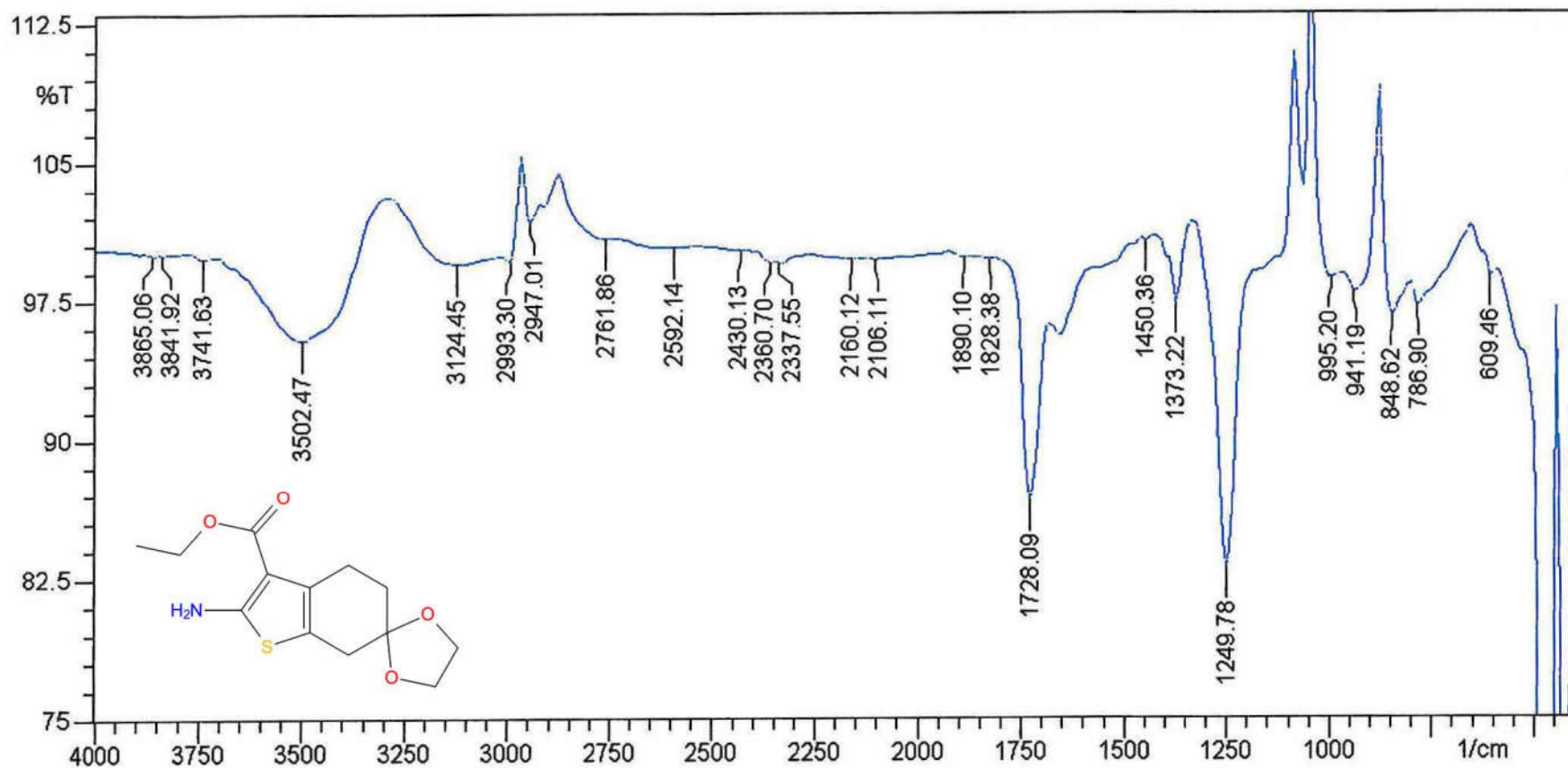
14.33, 18.51, 20.64, 22.85, 25.06, 30.95, 34.28, 58.67, 63.84, 107.45, 112.78, 130.35, 163.44.

**MASS SPECTROSCOPY**

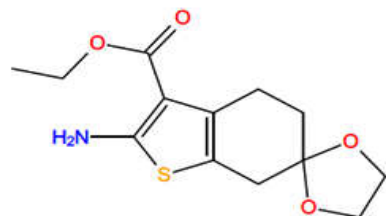
283.15 ( $\text{M}^+$ ), 207.13 (**B**).



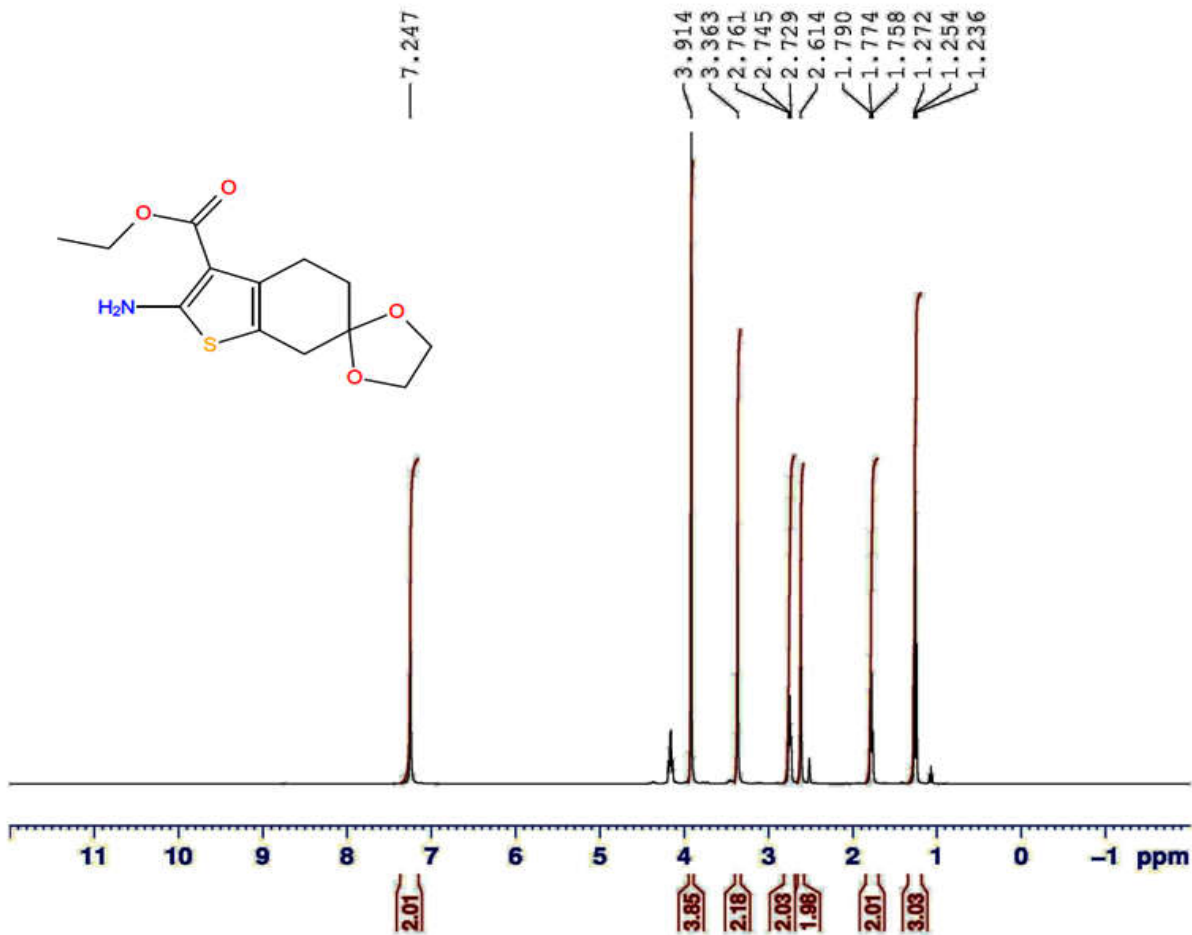
Sample: GAE



GAE.....Noorulla



—7.247



Current Data Parameters  
NAME GAE  
EXPNO 5  
PROCNO 1

F2 - Acquisition Parameters  
Date\_ 20151205  
Time 21.54  
INSTRUM spect  
PROBHD 5 mm PABBO BB/  
PULPROG zg30  
TD 65536  
SOLVENT DMSO  
NS 32  
DS 2  
SWH 8223.685 Hz  
FIDRES 0.125483 Hz  
AQ 3.9846387 sec  
RG 63.11  
DW 60.800 usec  
DE 6.50 usec  
TE 299.6 K  
D1 1.00000000 sec  
TD0 1

----- CHANNEL f1 -----  
NUC1 1H  
P1 14.25 usec  
PLW1 14.00000000 W  
SFO1 400.2604718 MHz

F2 - Processing parameters  
SI 65536  
SF 400.2580000 MHz  
WDW EM  
SSB 0  
LB 0.30 Hz  
GB 0  
PC 1.00

GAE.....Noorulla

163.44

130.35

112.78

107.45

63.84

58.67

34.28

30.95

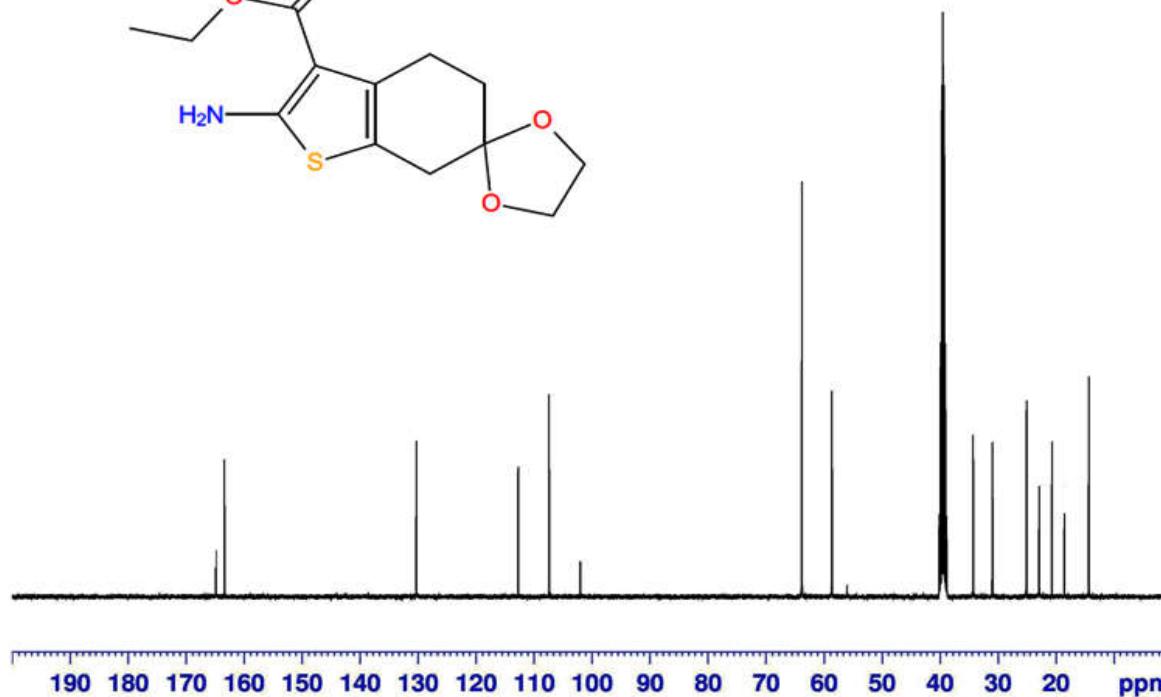
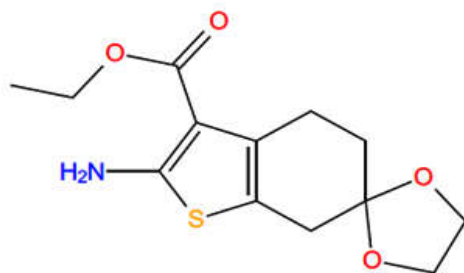
25.06

22.85

20.64

18.51

14.33



Current Data Parameters  
NAME GAE  
EXPNO 6  
PROCNO 1

F2 - Acquisition Parameters  
Date\_ 20151205  
Time 23.47  
INSTRUM spect  
PROBHD 5 mm PABBO BB/  
PULPROG zgpg30  
TD 65536  
SOLVENT DMSO  
NS 512  
DS 4  
SWH 24038.461 Hz  
FIDRES 0.366798 Hz  
AQ 1.3631988 sec  
RG 63.11  
DW 20.800 usec  
DE 6.50 usec  
TE 301.5 K  
D1 2.00000000 sec  
D11 0.03000000 sec  
TD0 1

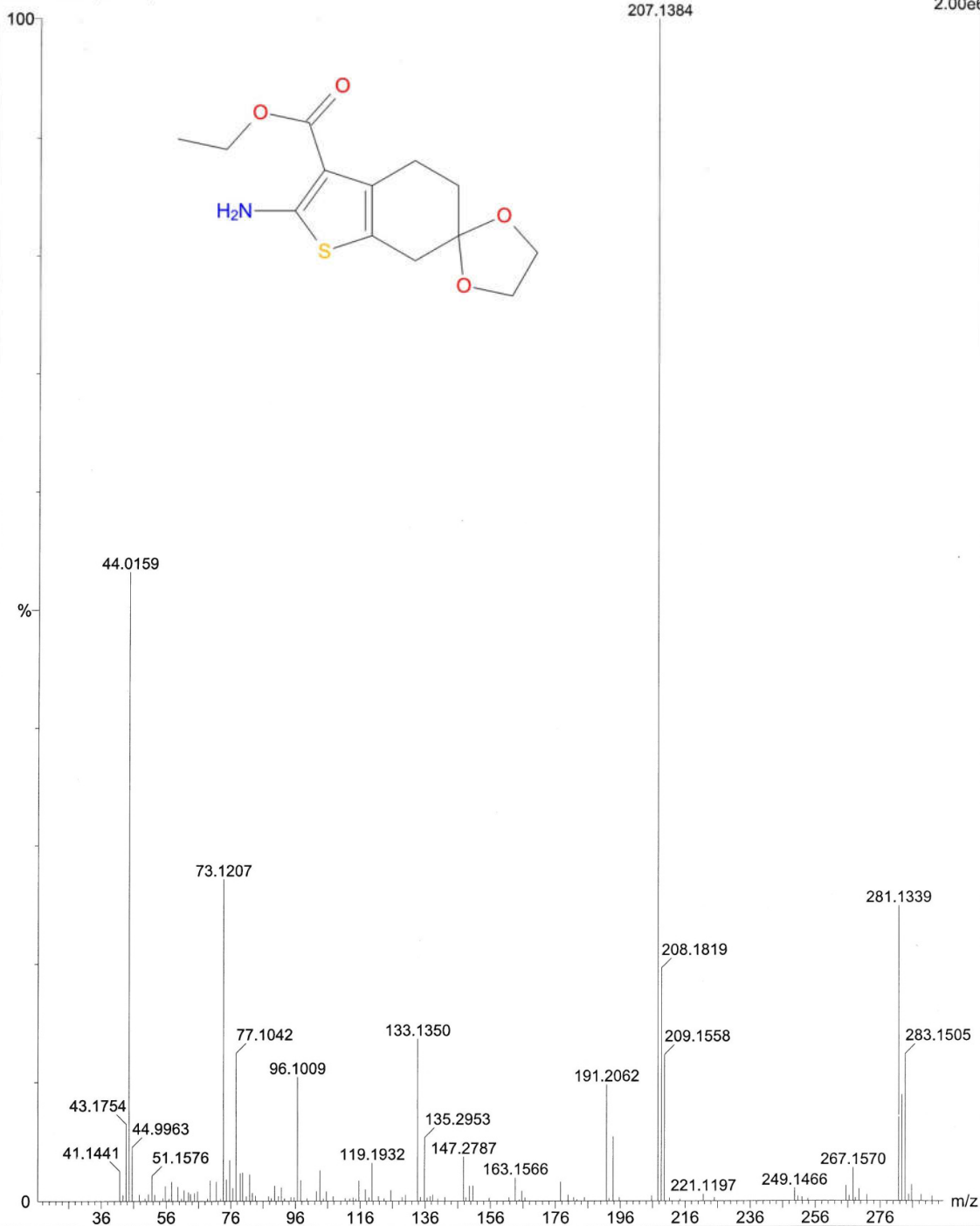
==== CHANNEL f1 =====  
NUC1 13C  
P1 9.80 usec  
PLW1 58.00000000 W  
SFO1 100.6550182 MHz

==== CHANNEL f2 =====  
CPDPRG2 waltz16  
NUC2 1H  
PCPD2 90.00 usec  
PLW2 14.00000000 W  
PLW12 0.35097000 W  
PLW13 0.28428999 W  
SFO2 400.2596010 MHz

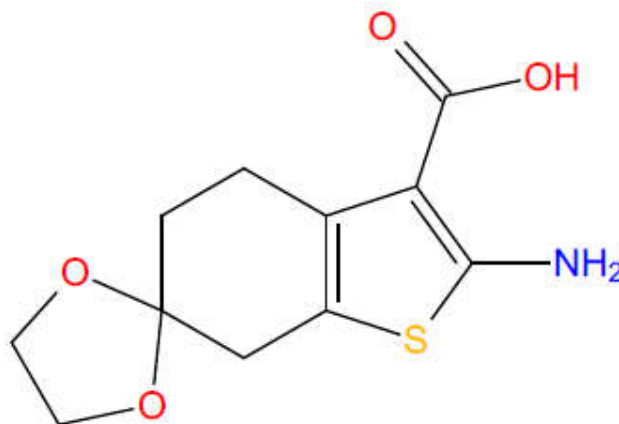
F2 - Processing parameters  
SI 32768  
SF 100.6450043 MHz  
WDW EM  
SSB 0  
LB 1.00 Hz  
GB 0  
PC 1.40

GAE- 4508 (25.047)

Scan EI+  
2.00e6

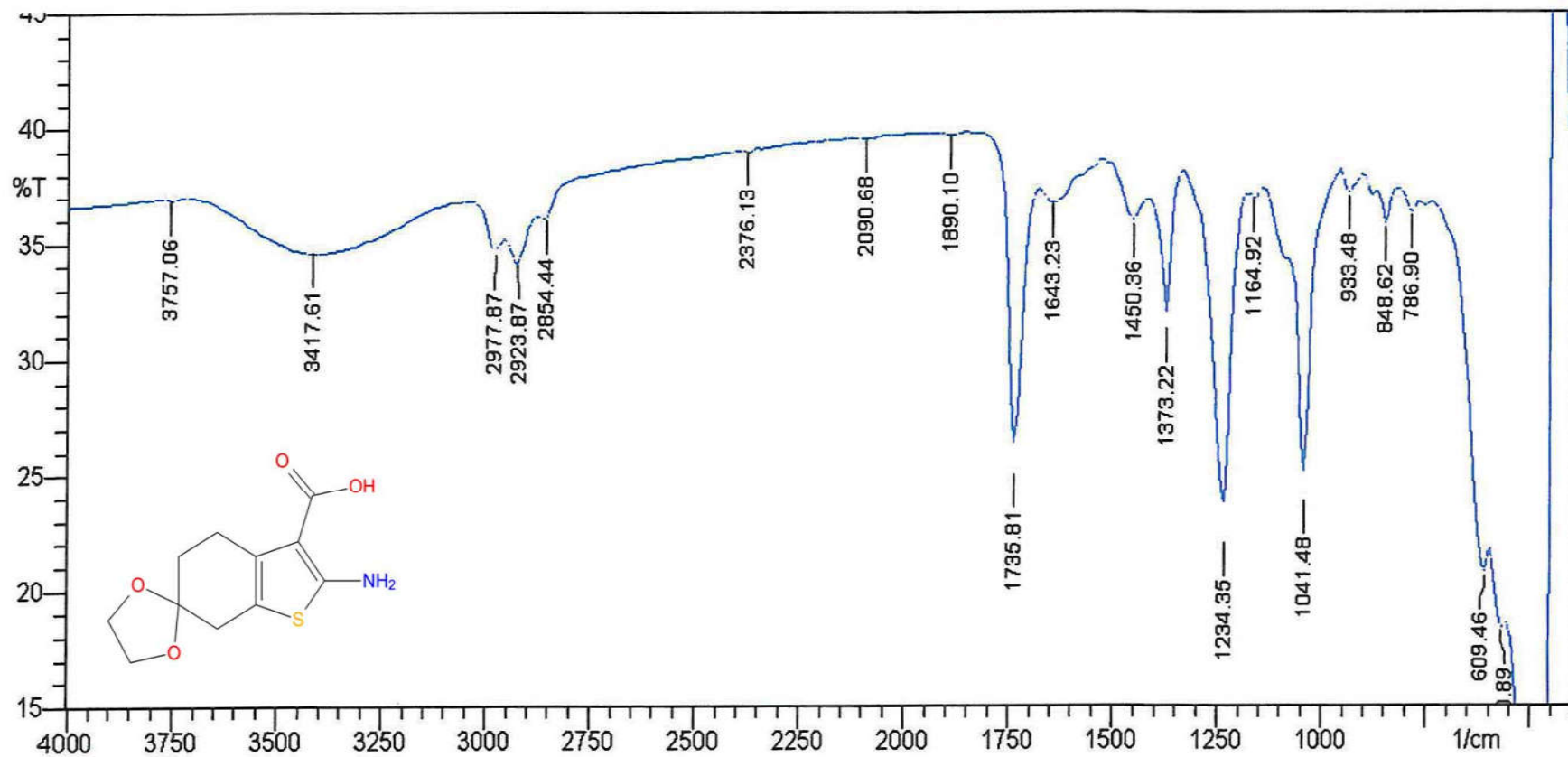


## Spectral Data of Compound GAT

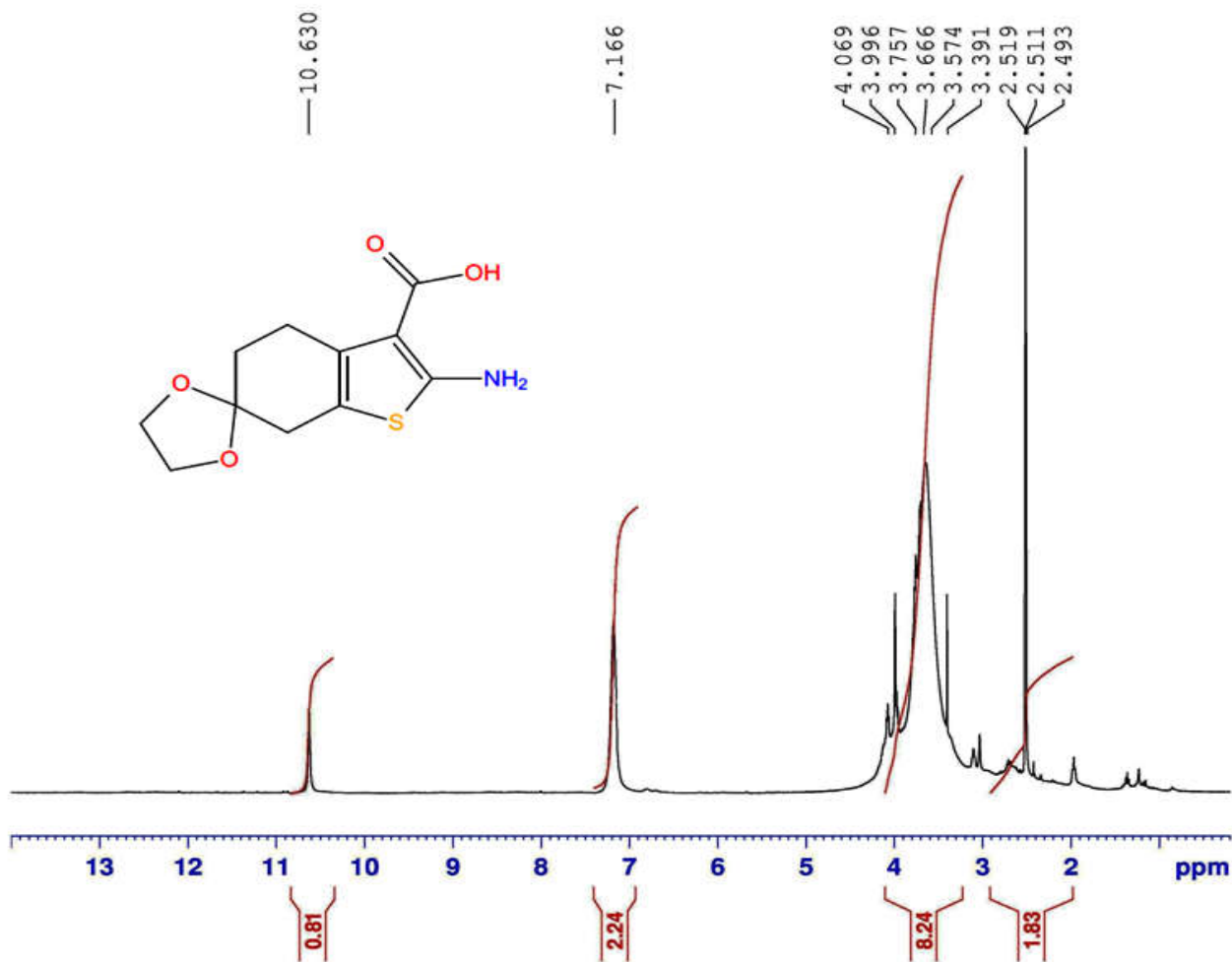


<b>IR (KBr, <math>\nu_{\max}</math>) <math>\text{cm}^{-1}</math></b>	3417.61 (amine N-H), 2923.87 (aliphatic C-H), 1164.92 (C-O-C), 1735.81 (carboxylic C=O), 1164.92 (carboxylic C-O), 2977.87 (carboxylic O-H), 609.46 (C-S).
<b><math>^1\text{H}</math> NMR (DMSO-<math>\text{D}_6</math>) <math>\delta</math></b>	2.51 (t, 2H, $\text{CH}_2$ ), 3.39-4.06 (m, 8H, $\text{CH}_2$ ), 7.16 (s, 2H, $\text{NH}_2$ ), 10.63 (s, 1H, carboxylic O-H).
<b><math>^{13}\text{C}</math> NMR (DMSO-<math>\text{D}_6</math>) <math>\delta</math></b>	13.42, 18.54, 24.93, 31.53, 33.45, 70.04, 121.23, 128.48, 134.87, 138.28, 168.53.
<b>MASS SPECTROSCOPY</b>	255.19 ( $\text{M}^+$ ), 256.17 ( $\text{M}+1$ ), 178.19 ( <b>B</b> ).
<b>ELEMENTAL ANALYSIS</b>	Anal. Calcd. For GAT: C, 51.75; H, 5.13; N, 5.49; Obsd. C, 51.83; H, 5.12; N, 5.48.

Sample: GAT



GAT.....Noorulla



Current Data Parameters  
NAME GAT  
EXPNO 6  
PROCNO 1

F2 - Acquisition Parameters  
Date\_ 20151205  
Time 23.15  
INSTRUM spect  
PROBHD 5 mm PABBO BB/  
PULPROG zg30  
TD 65536  
SOLVENT DMSO  
NS 64  
DS 2  
SWH 8223.685 Hz  
FIDRES 0.125483 Hz  
AQ 3.9846387 sec  
RG 112.69  
DW 60.800 usec  
DE 6.50 usec  
TE 300.5 K  
D1 1.00000000 sec  
TD0 1

===== CHANNEL f1 =====  
NUC1 1H  
P1 14.25 usec  
PLW1 14.00000000 W  
SFO1 400.2604718 MHz

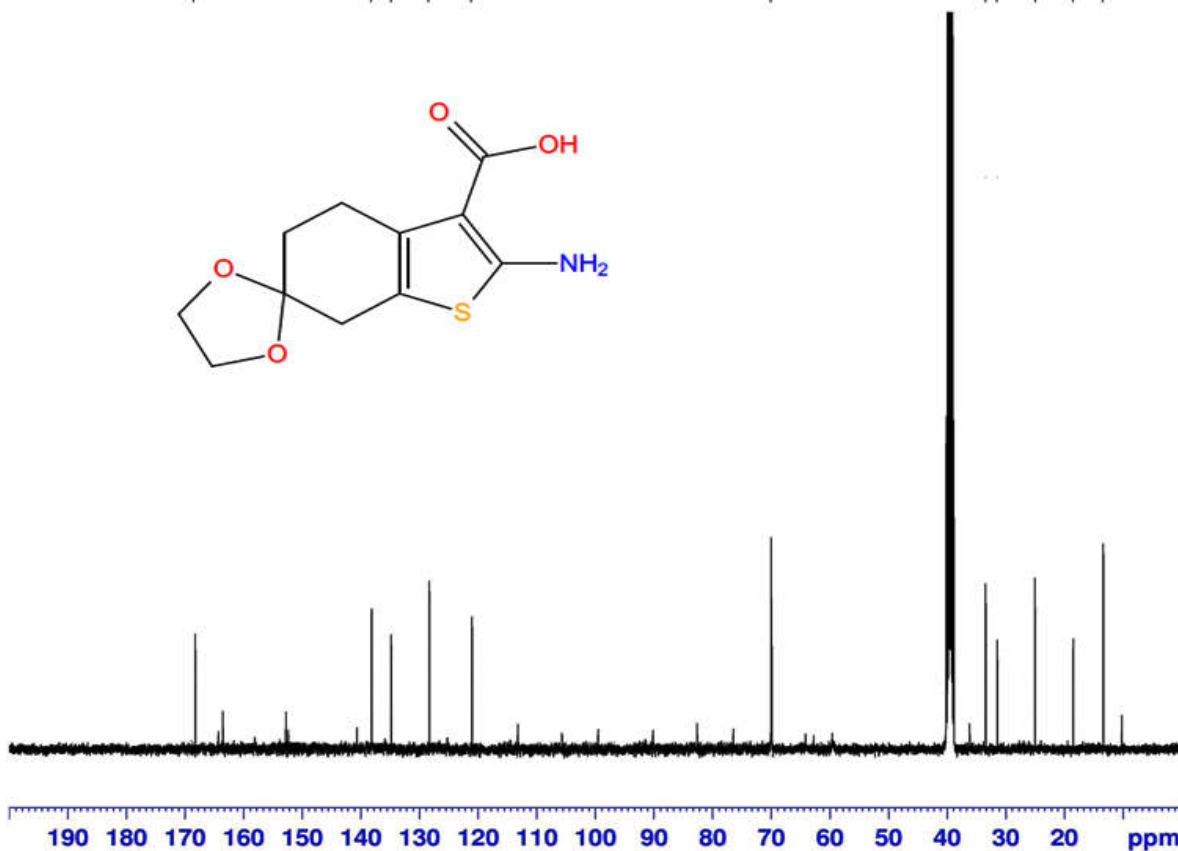
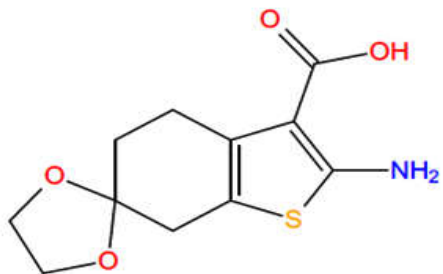
F2 - Processing parameters  
SI 65536  
SF 400.2580000 MHz  
WDW EM  
SSB 0  
LB 0.30 Hz  
GB 0  
PC 1.00

GAT.....Noorulla

168.53  
138.28  
134.87  
128.48  
121.23

70.04

33.45  
31.53  
24.93  
18.54  
13.42



Current Data Parameters  
NAME GAT  
EXPNO 7  
PROCNO 1

F2 - Acquisition Parameters  
Date\_ 20151206  
Time\_ 2.04  
INSTRUM spect  
PROBHD 5 mm PABBO BB/  
PULPROG zgpg30  
TD 65536  
SOLVENT DMSO  
NS 1024  
DS 4  
SWH 24038.461 Hz  
FIDRES 0.366798 Hz  
AQ 1.3631988 sec  
RG 199.6  
DW 20.800 usec  
DE 6.50 usec  
TE 302.0 K  
D1 2.00000000 sec  
D11 0.03000000 sec  
TD0 1

===== CHANNEL f1 =====  
NUC1 13C  
P1 9.80 usec  
PLW1 58.00000000 W  
SFO1 100.6550182 MHz

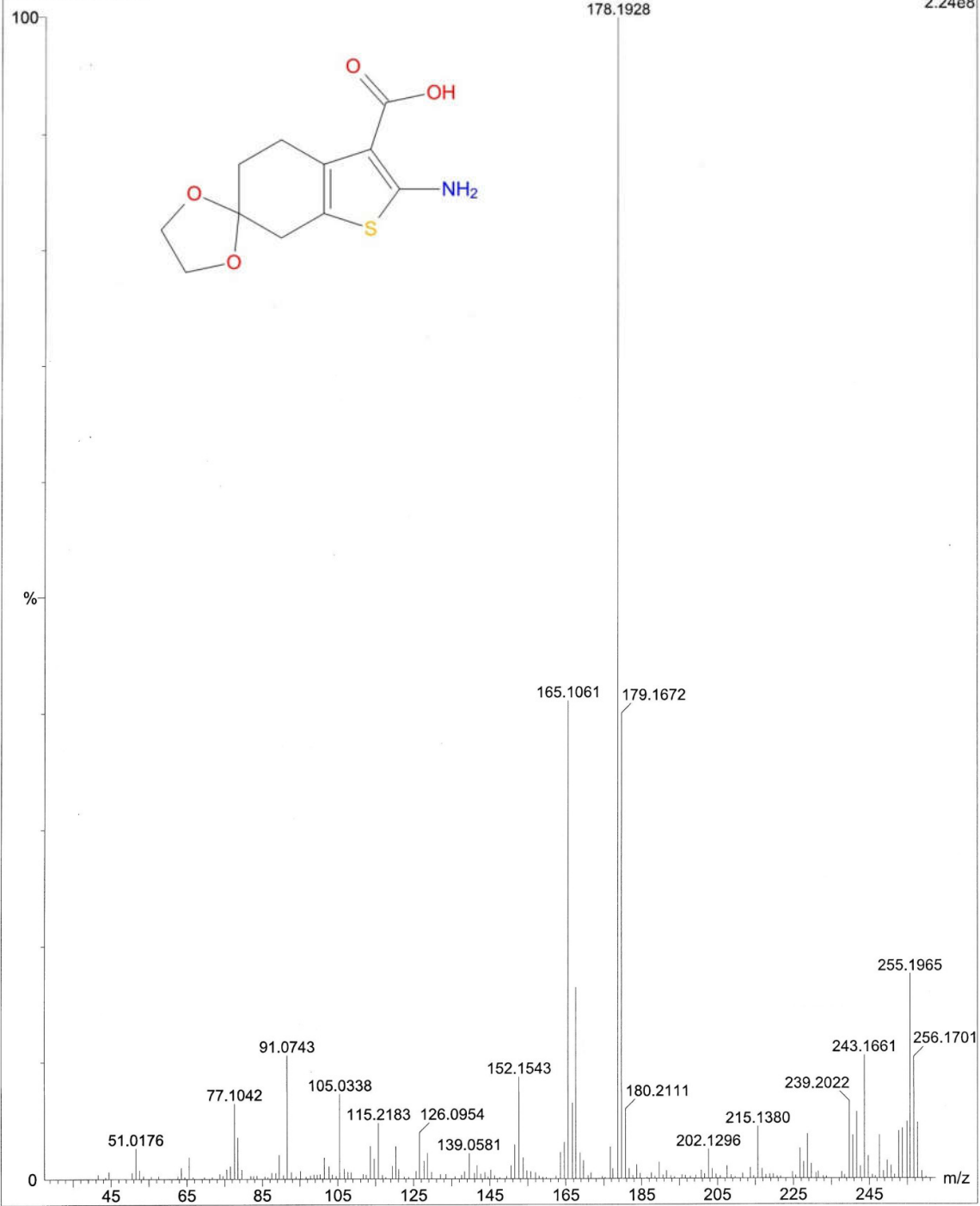
===== CHANNEL f2 =====  
CPDPRG2 waltz16  
NUC2 1H  
PCPD2 90.00 usec  
PLW2 14.00000000 W  
PLW12 0.35097000 W  
PLW13 0.28428999 W  
SFO2 400.2596010 MHz

F2 - Processing parameters  
SI 32768  
SF 100.6450043 MHz  
WDW EM  
SSB 0  
LB 1.00 Hz  
GB 0  
PC 1.40

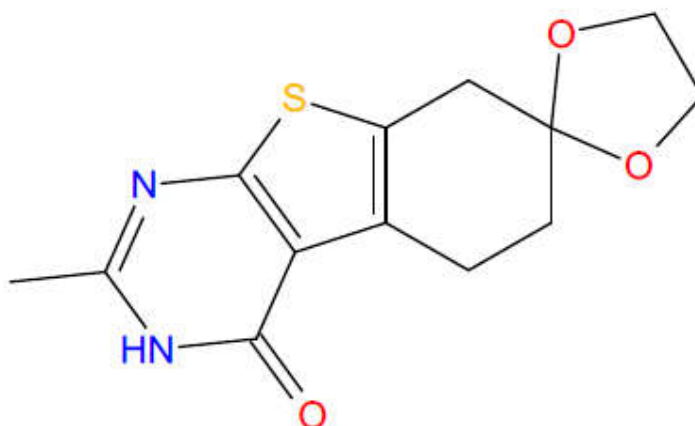


GAT-1328 (24.147)

Scan E1+  
2.24e8



## Spectral Data of Compound GAC



**IR (KBr,  $\nu_{\max}$ )  $\text{cm}^{-1}$**

3679.91 (amide N-H), 2923.87 (aliphatic C-H), 1635.52 (amide C=O), 1164.92 (C-O-C), 756.04 (C-S).

**$^1\text{H}$  NMR (DMSO- $\text{D}_6$ )  $\delta$**

1.79-1.88 (m, 4H,  $\text{CH}_2$ ), 2.18 (s, 3H,  $\text{CH}_3$ ), 2.59-2.65 (q, 4H,  $\text{CH}_2$ ), 2.78 (s, 2H,  $\text{CH}_2$ ), 11.59 (s, 1H, N-H).

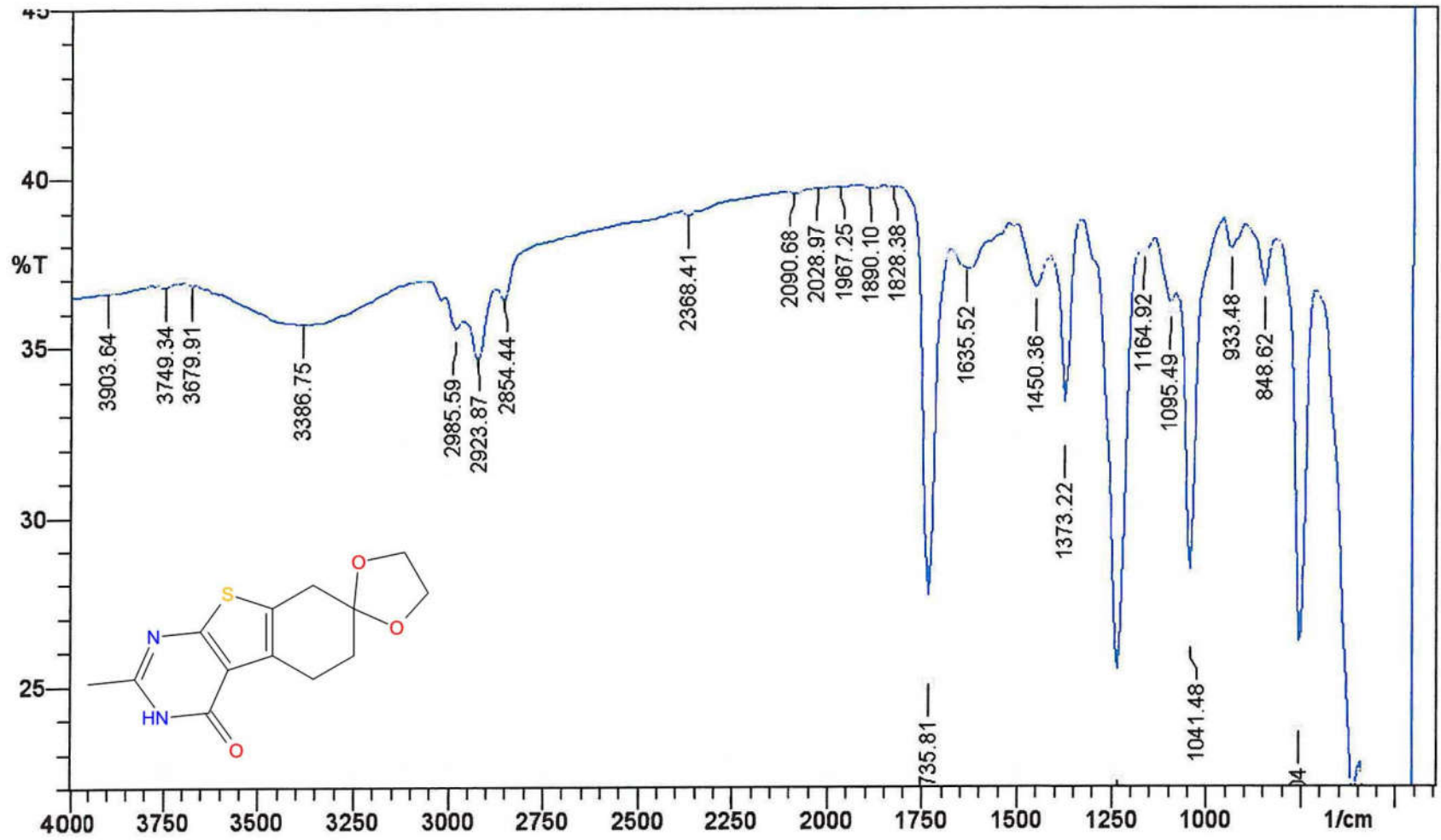
**$^{13}\text{C}$  NMR (DMSO- $\text{D}_6$ )  $\delta$**

22.41, 22.77, 30.48, 30.55, 33.75, 34.06, 63.93, 64.01, 124.72, 129.53, 130.13, 131.12, 168.23.

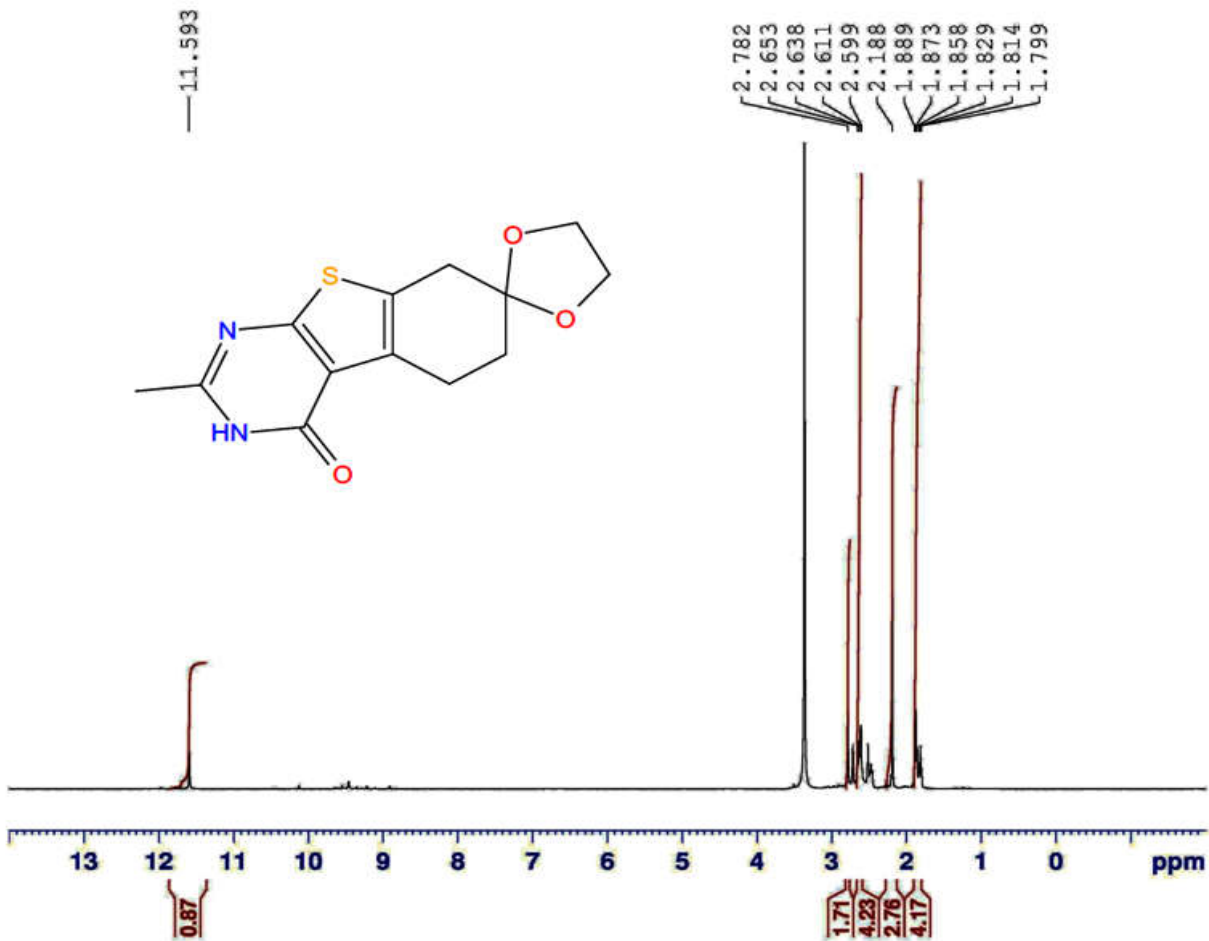
**MASS SPECTROSCOPY**

278.15 ( $\text{M}^+$ ), 279.10 ( $\text{M}+1$ ), 150.09 (**B**).

Sample: GAC



GAC.....Noorulla



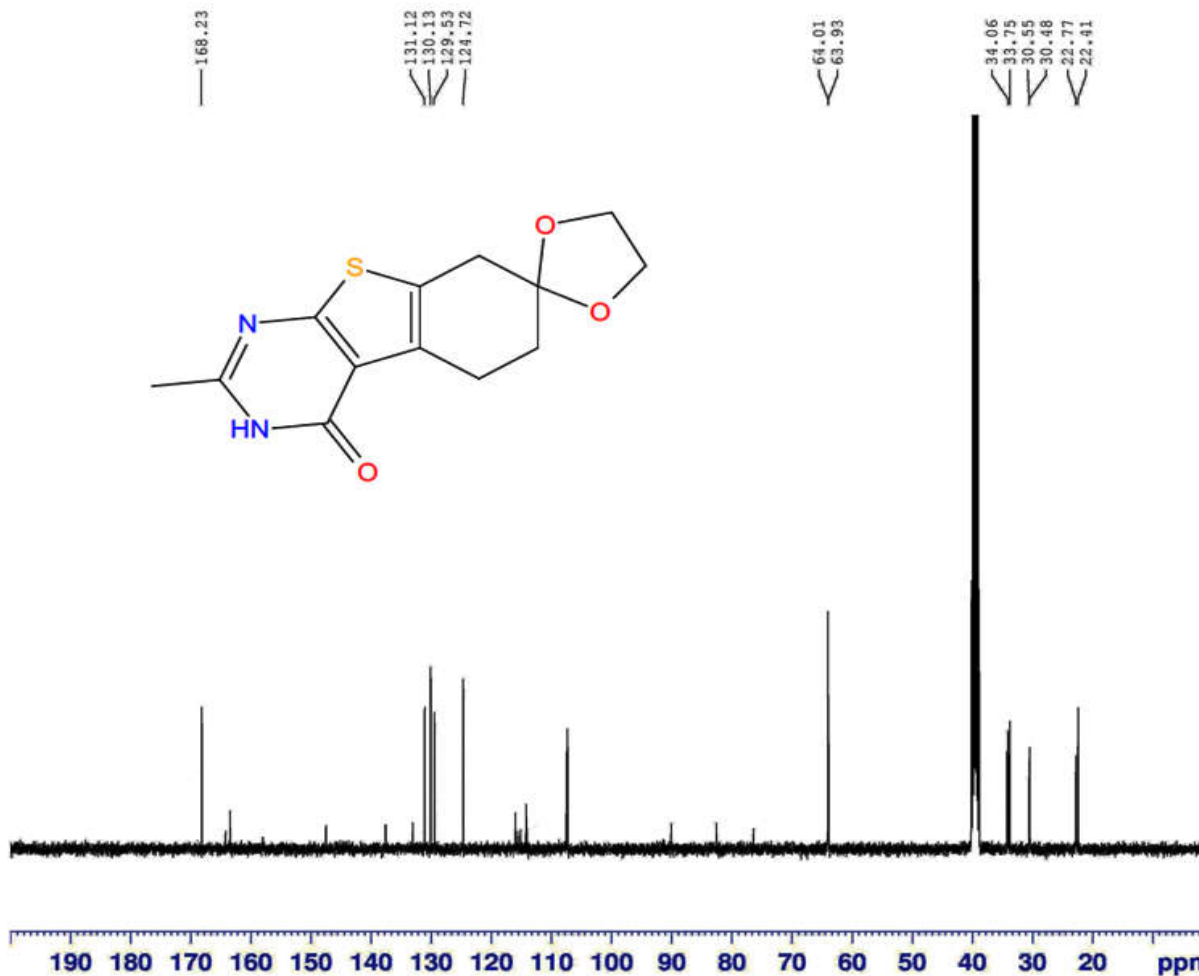
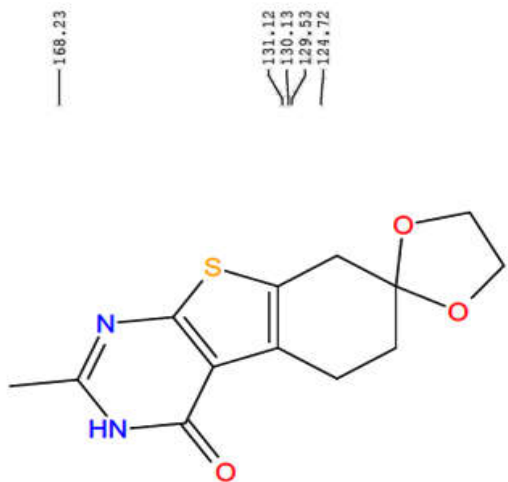
Current Data Parameters  
NAME GAC  
EXPNO 2  
PROCNO 1

F2 - Acquisition Parameters  
Date\_ 20151205  
Time 21.33  
INSTRUM spect  
PROBHD 5 mm PABBO BB/  
PULPROG zg30  
TD 65536  
SOLVENT DMSO  
NS 16  
DS 2  
SWH 8223.685 Hz  
FIDRES 0.125483 Hz  
AQ 3.9846387 sec  
RG 98.85  
DW 60.800 usec  
DE 6.50 usec  
TE 299.4 K  
D1 1.00000000 sec  
TD0 1

----- CHANNEL f1 -----  
NUC1 1H  
P1 14.25 usec  
PLW1 14.00000000 W  
SFO1 400.2604718 MHz

F2 - Processing parameters  
SI 65536  
SF 400.2580000 MHz  
WDW EM  
SSB 0  
LB 0.30 Hz  
GB 0  
PC 1.00

GAC.....Noorulla



Current Data Parameters  
NAME GAC  
EXPNO 5  
PROCNO 1

F2 - Acquisition Parameters  
Date\_ 20151205  
Time 23.08  
INSTRUM spect  
PROBHD 5 mm PABBO BB/  
PULPROG zgpg30  
TD 65536  
SOLVENT DMSO  
NS 600  
DS 4  
SWH 24038.461 Hz  
FIDRES 0.366798 Hz  
AQ 1.3631988 sec  
RG 63.11  
DW 20.800 usec  
DE 6.50 usec  
TE 301.3 K  
D1 2.00000000 sec  
D11 0.03000000 sec  
TD0 1

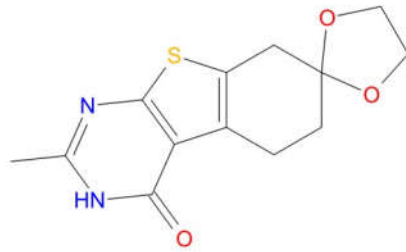
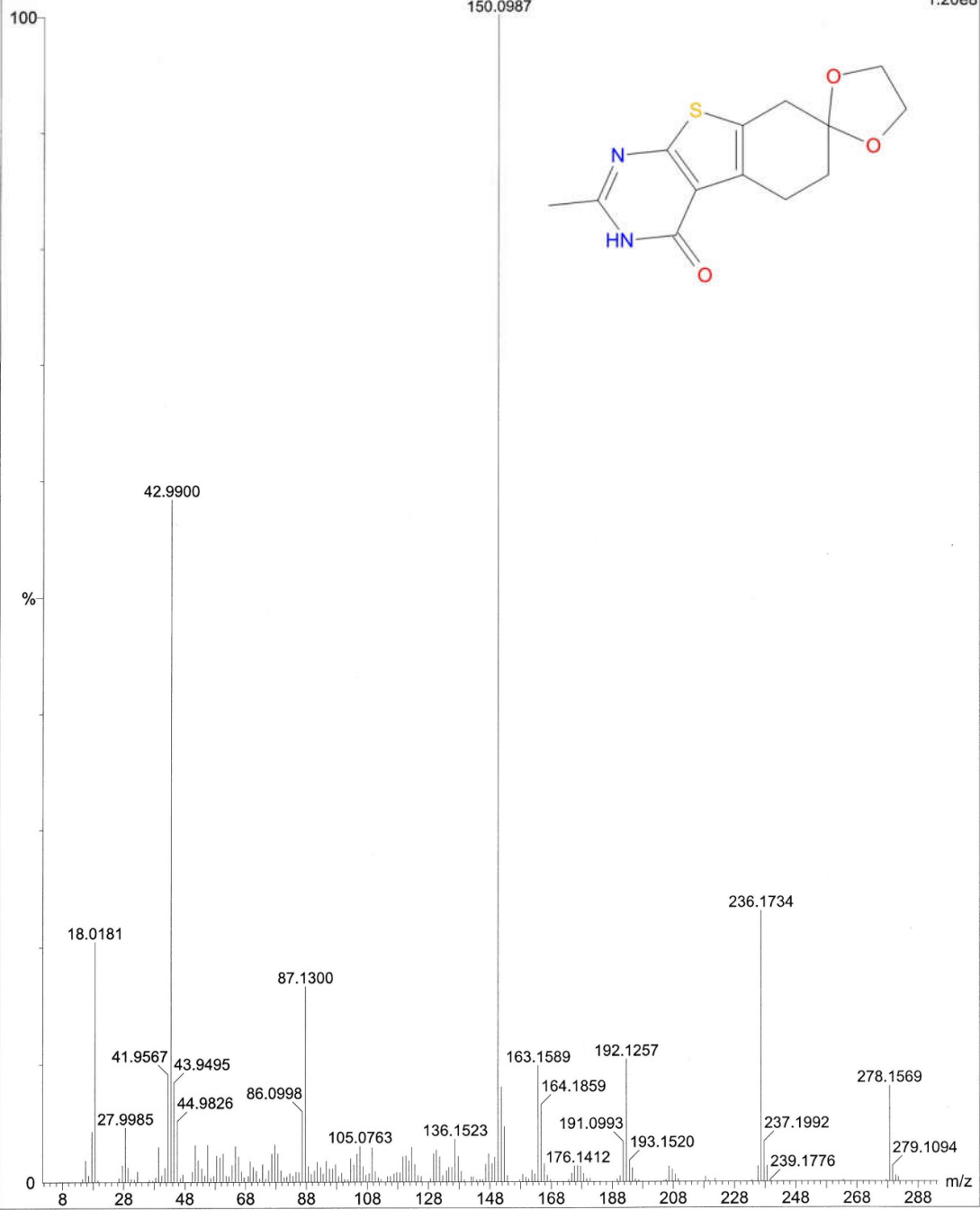
===== CHANNEL f1 =====  
NUC1 13C  
P1 9.80 usec  
PLW1 58.00000000 W  
SFO1 100.6550182 MHz

===== CHANNEL f2 =====  
CPDPRG2 waltz16  
NUC2 1H  
PCPD2 90.00 usec  
PLW2 14.00000000 W  
PLW12 0.35097000 W  
PLW13 0.28428999 W  
SFO2 400.2596010 MHz

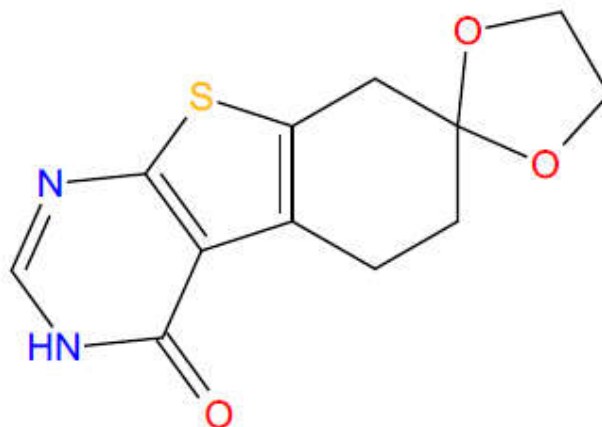
F2 - Processing parameters  
SI 32768  
SF 100.6450043 MHz  
WDW EM  
SSB 0  
LB 1.00 Hz  
GB 0  
PC 1.40

GAC-3976 (22.686)

Scan EI+  
1.20e8



## Spectral Data of Compound GAC1



**IR (KBr,  $\nu_{\max}$ )  $\text{cm}^{-1}$**

3749.34 (amide N-H), 2923.87 (aliphatic C-H), 1249.78 (C-O-C),  
1643.23 (amide C=O), 617.18 (C-S).

**$^1\text{H}$  NMR (DMSO- $\text{D}_6$ )  $\delta$**

2.51-2.59 (m, 2H,  $\text{CH}_2$ ), 3.32-3.53 (m, 8H,  $\text{CH}_2$ ), 7.16 (s, 1H,  
pyrimidine C-H).

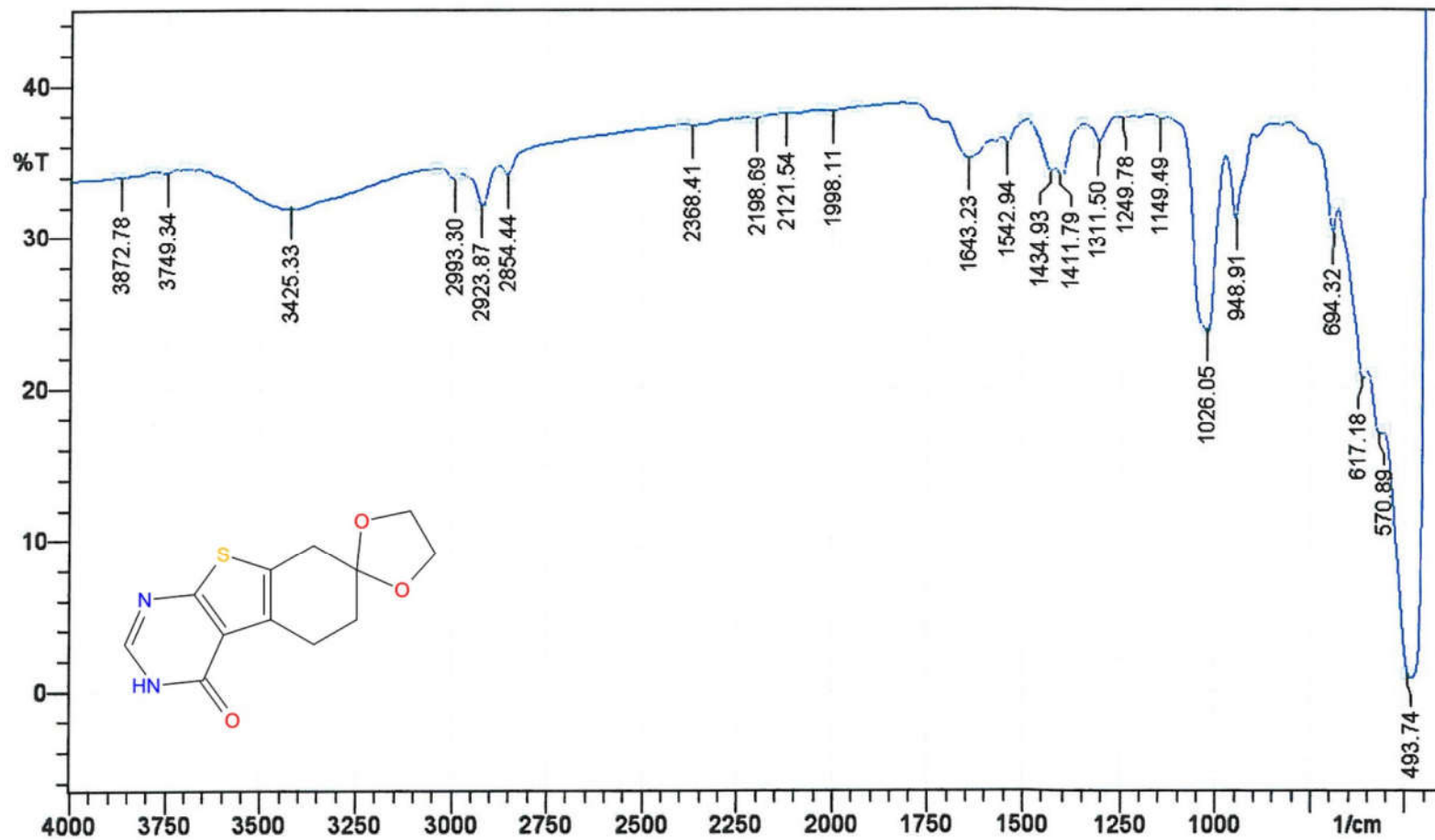
**$^{13}\text{C}$  NMR (DMSO- $\text{D}_6$ )  $\delta$**

22.66, 22.76, 23.24, 30.54, 34.04, 50.71, 113.03, 124.36, 130.35,  
130.78, 146.54, 164.15.

**MASS SPECTROSCOPY**

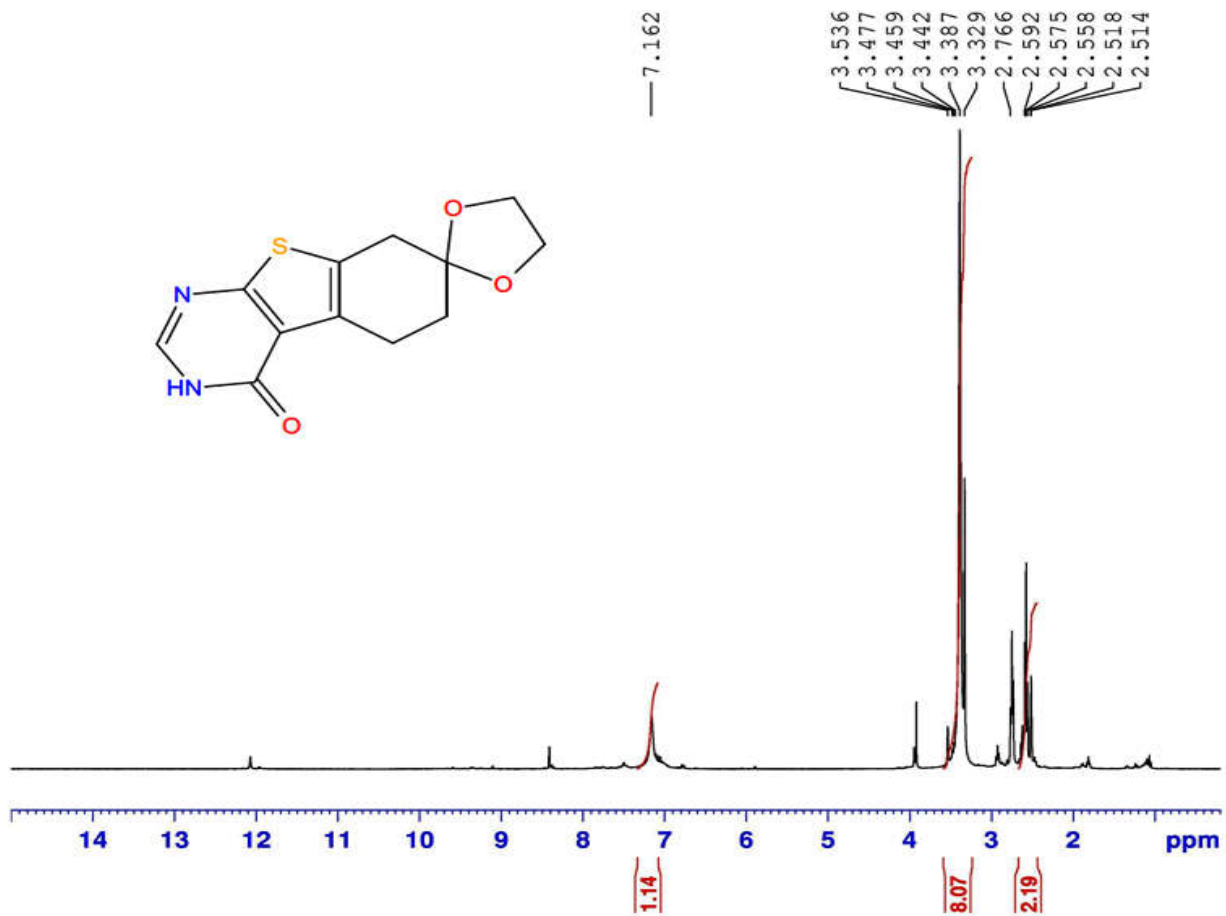
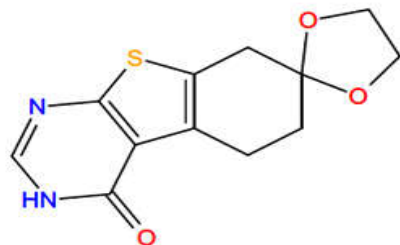
264.16 ( $\text{M}^+$ ), 177.21 (**B**).

Sample: GAC1





GAC1.....Noorulla



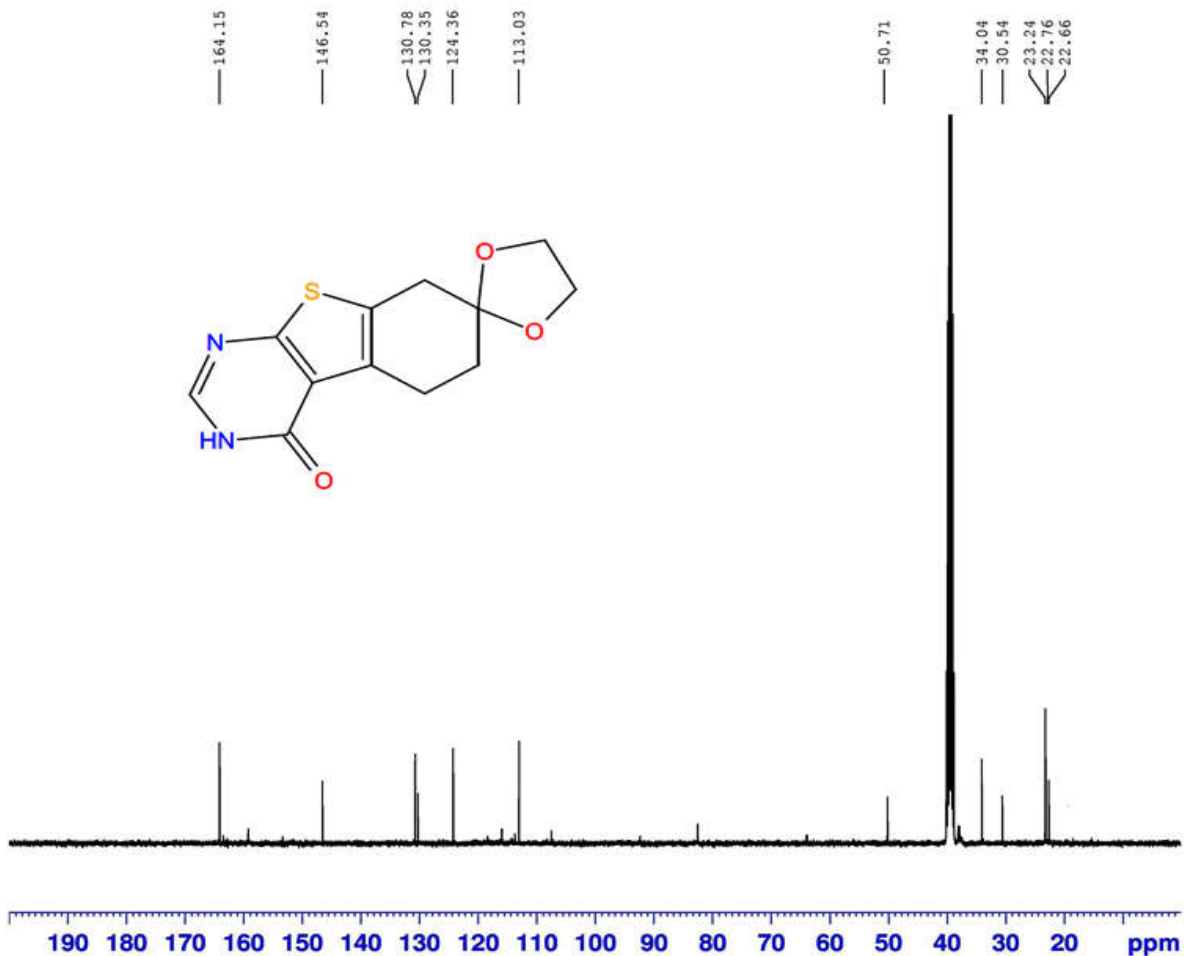
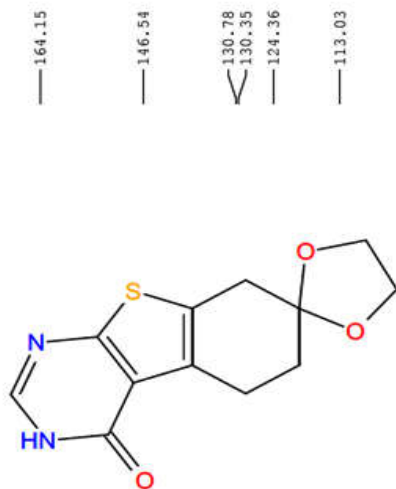
Current Data Parameters  
NAME GAC1  
EXPNO 10  
PROCNO 1

F2 - Acquisition Parameters  
Date\_ 20151206  
Time 10.02  
INSTRUM spect  
PROBHD 5 mm PABBO BB/  
PULPROG zg30  
TD 65536  
SOLVENT DMSO  
NS 16  
DS 2  
SWH 8223.685 Hz  
FIDRES 0.125483 Hz  
AQ 3.9846387 sec  
RG 98.85  
DW 60.800 usec  
DE 6.50 usec  
TE 298.6 K  
D1 1.00000000 sec  
TD0 1

===== CHANNEL f1 =====  
NUC1 1H  
P1 14.25 usec  
PLW1 14.00000000 W  
SFO1 400.2604718 MHz

F2 - Processing parameters  
SI 65536  
SF 400.2580000 MHz  
WDW EM  
SSB 0  
LB 0.30 Hz  
GB 0  
PC 1.00

GAC1.....Noorulla



Current Data Parameters  
NAME GAC1  
EXPNO 11  
PROCNO 1

F2 - Acquisition Parameters  
Date\_ 20151206  
Time 11.29  
INSTRUM spect  
PROBHD 5 mm PABBO BB/  
PULPROG zgpg30  
TD 65536  
SOLVENT DMSO  
NS 1500  
DS 4  
SWH 24038.461 Hz  
FIDRES 0.366798 Hz  
AQ 1.3631988 sec  
RG 143.73  
DW 20.800 usec  
DE 6.50 usec  
TE 299.2 K  
D1 2.00000000 sec  
D11 0.03000000 sec  
TD0 1

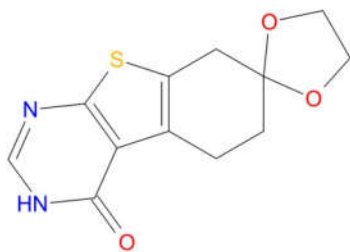
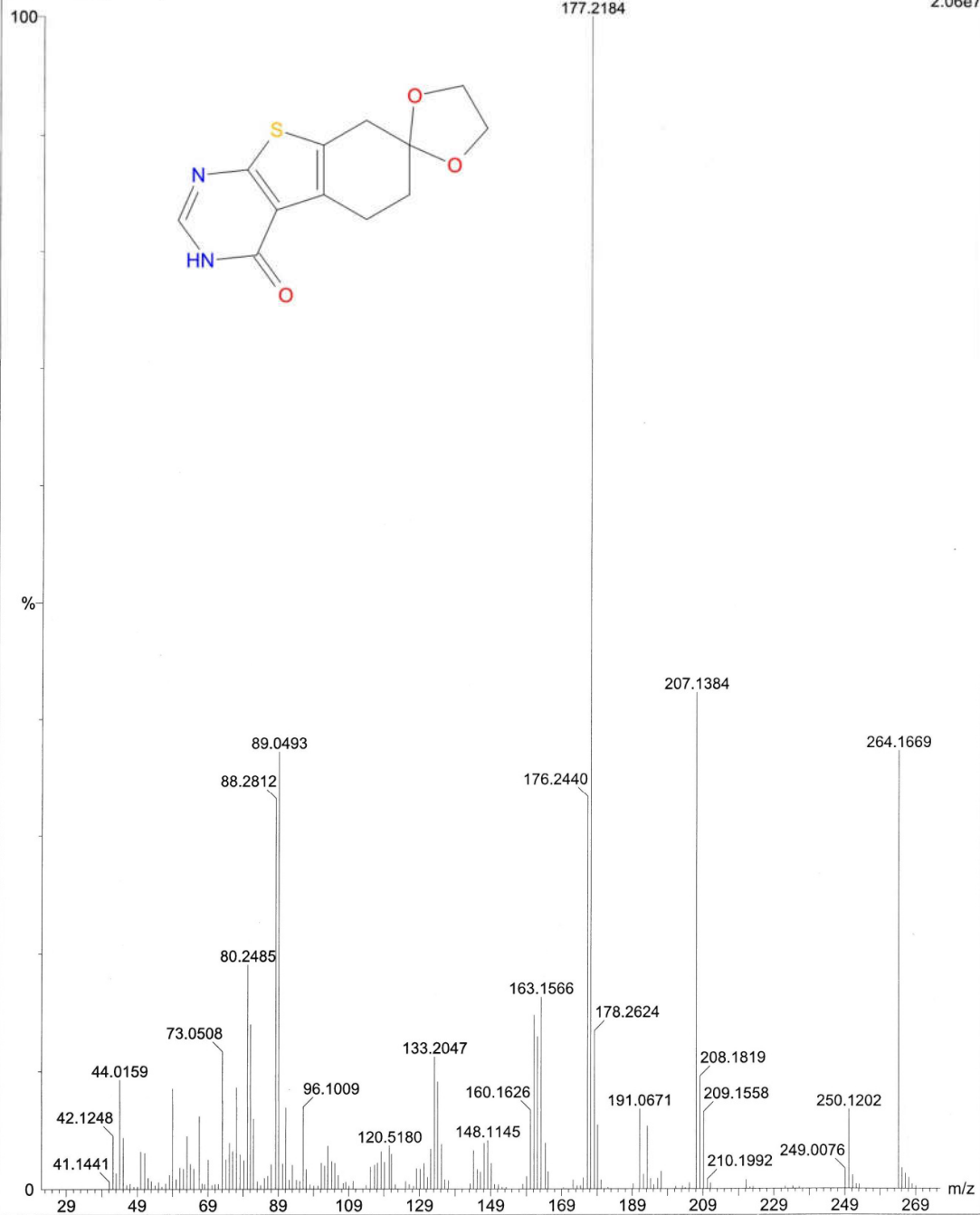
===== CHANNEL f1 =====  
NUC1 13C  
P1 9.80 usec  
PLW1 58.00000000 W  
SFO1 100.6550182 MHz

===== CHANNEL f2 =====  
CPDPRG2 waltz16  
NUC2 1H  
PCPD2 90.00 usec  
PLW2 14.00000000 W  
PLW12 0.35097000 W  
PLW13 0.28428999 W  
SFO2 400.2596010 MHz

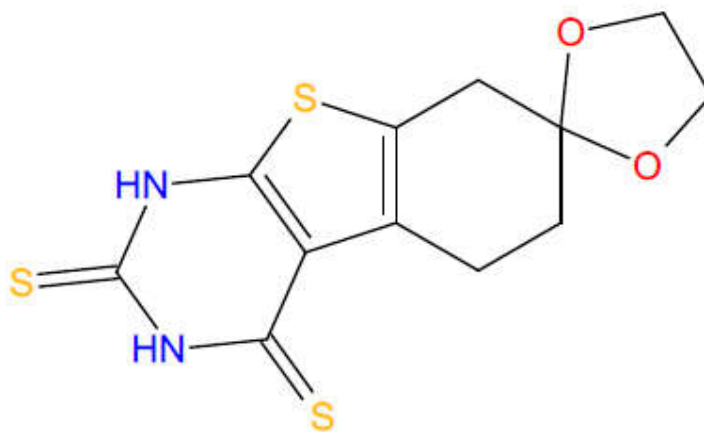
F2 - Processing parameters  
SI 32768  
SF 100.6450043 MHz  
WDW EM  
SSB 0  
LB 1.00 Hz  
GB 0  
PC 1.40

GAC1- 4293(26.913)

Scan EI+  
2.06e7



## Spectral Data of Compound GAC5



**IR (KBr,  $\nu_{\max}$ )  $\text{cm}^{-1}$**

3425.33 (amine N-H), 2923.87 (aliphatic C-H), 1735.81 (C=S),  
1149.49 (C-O-C), 617.18 (C-S).

**$^1\text{H}$  NMR (DMSO- $\text{D}_6$ )  $\delta$**

1.84 (t, 2H,  $\text{CH}_2$ ), 2.85 (s, 2H,  $\text{CH}_2$ ), 3.14 (t, 2H,  $\text{CH}_2$ ), 3.97 (s, 4H,  
 $\text{CH}_2$ ), 8.61 (s, 1H, N-H), 13.23 (s, 1H, N-H).

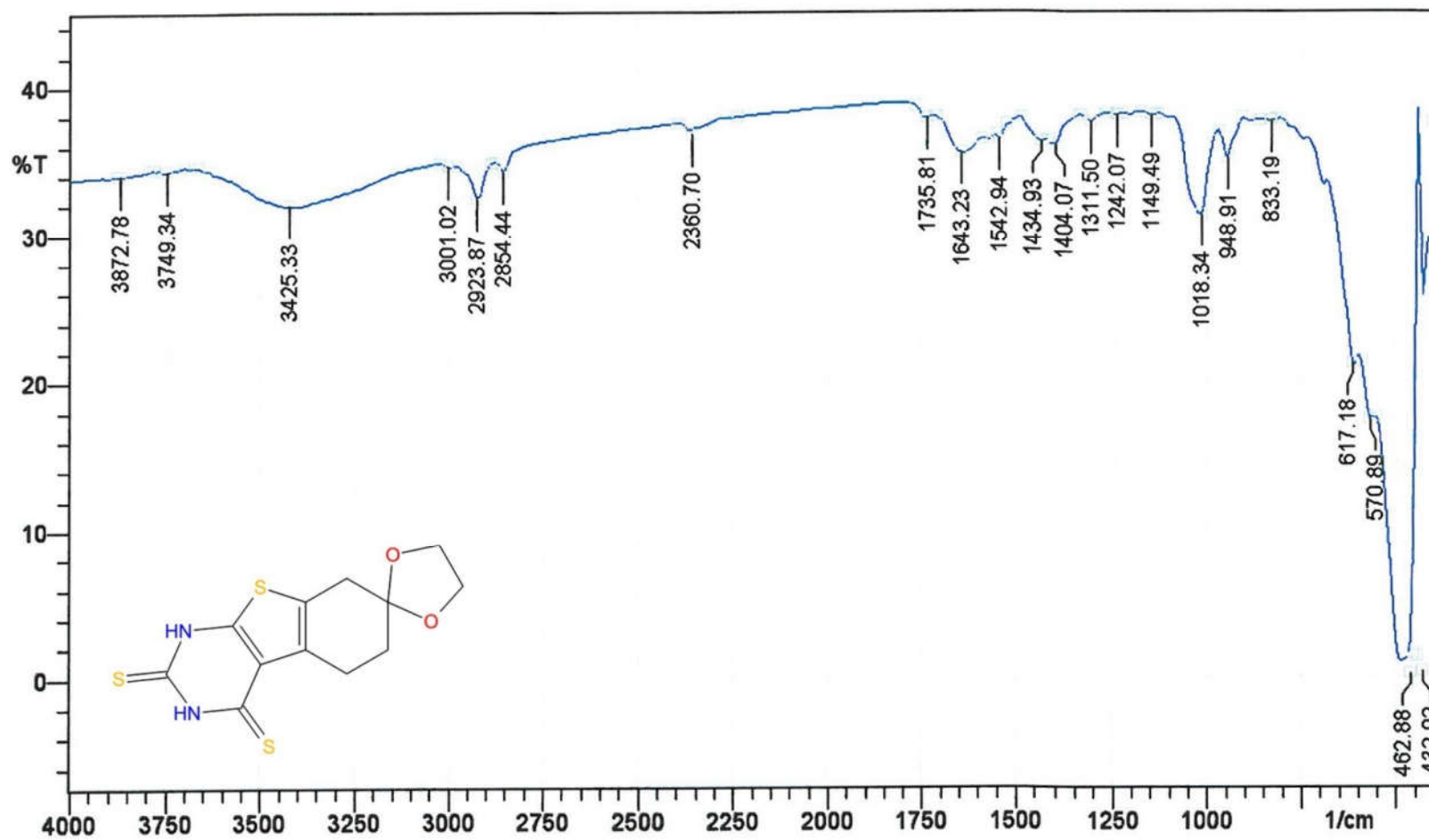
**$^{13}\text{C}$  NMR (DMSO- $\text{D}_6$ )  $\delta$**

21.33, 23.29, 25.87, 30.33, 34.74, 63.99, 124.11, 124.55, 127.16,  
131.14, 169.25, 181.57.

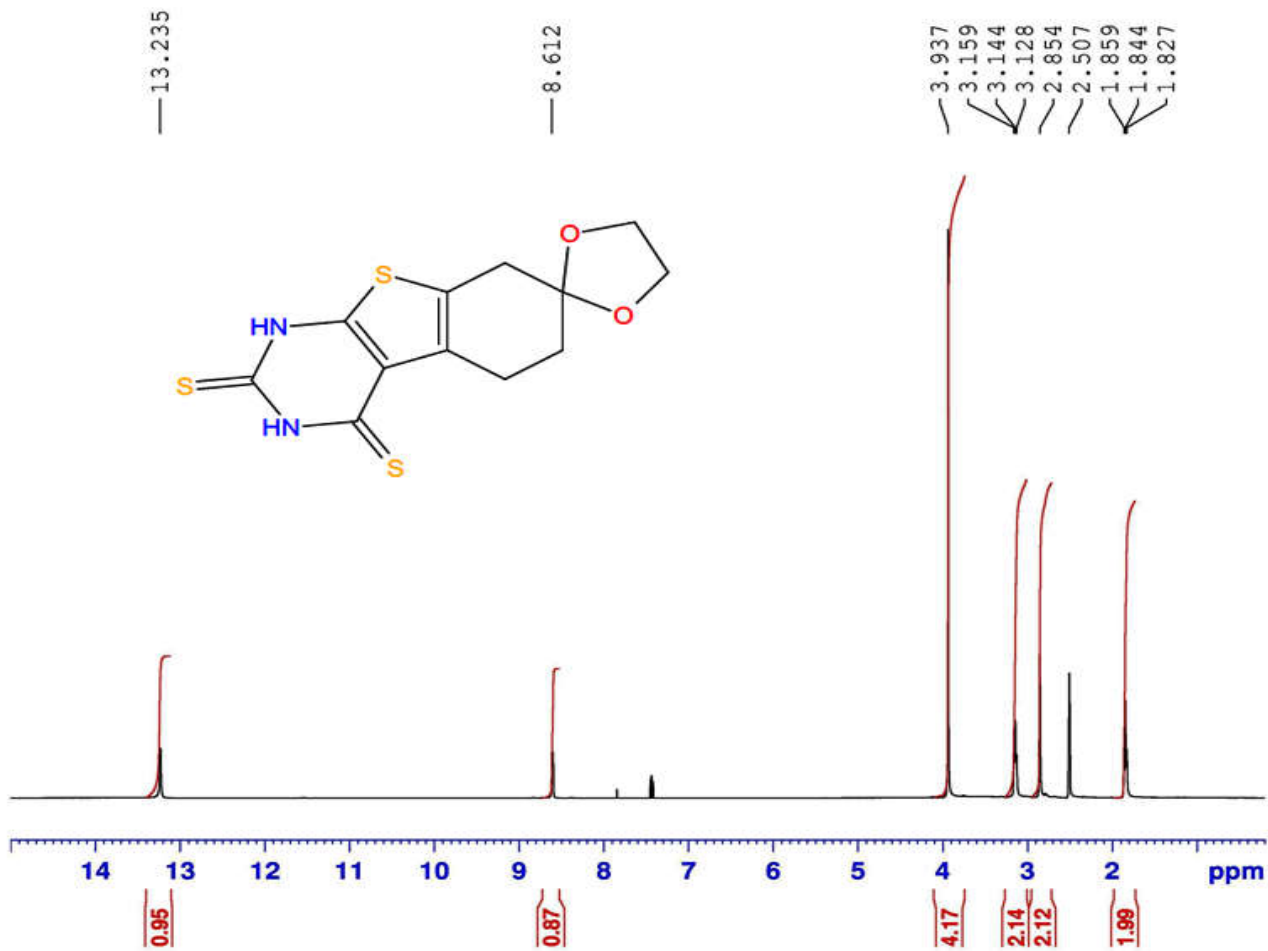
**MASS SPECTROSCOPY**

312.28 ( $\text{M}^+$ ), 165.17 (**B**).

Sample: GAC5



GAC5.....Noorulla



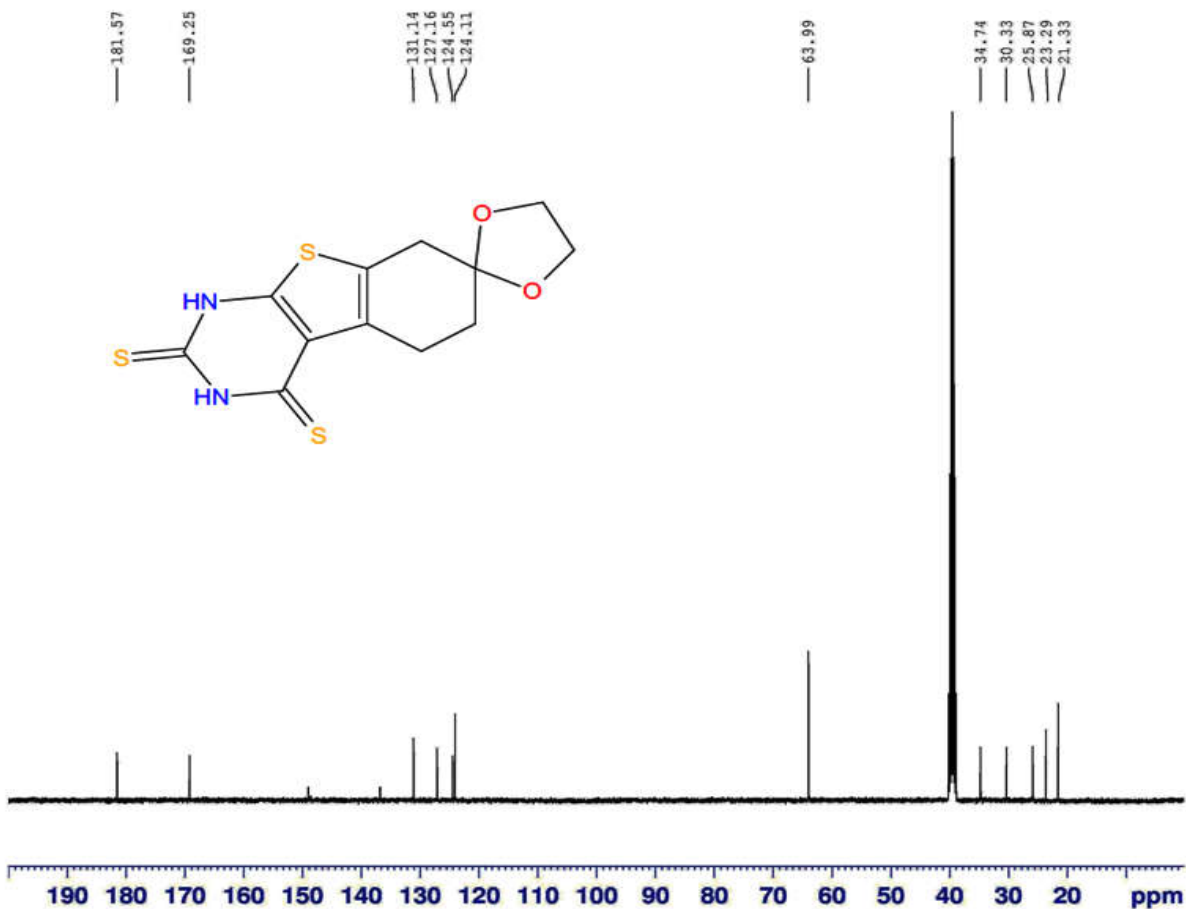
Current Data Parameters  
NAME GAC5  
EXPNO 25  
PROCNO 1

F2 - Acquisition Parameters  
Date\_ 20151213  
Time 3.36  
INSTRUM spect  
PROBHD 5 mm PABBO BB/  
PULPROG zg30  
TD 65536  
SOLVENT DMSO  
NS 32  
DS 2  
SWH 8223.685 Hz  
FIDRES 0.125483 Hz  
AQ 3.9846387 sec  
RG 127.79  
DW 60.800 usec  
DE 6.50 usec  
TE 302.0 K  
D1 1.00000000 sec  
TD0 1

===== CHANNEL f1 =====  
NUC1 1H  
P1 14.25 usec  
PLW1 14.00000000 W  
SFO1 400.2604718 MHz

F2 - Processing parameters  
SI 65536  
SF 400.2580031 MHz  
WDW EM  
SSB 0  
LB 0.30 Hz  
GB 0  
PC 1.00

GAC5 .....Noorulla



Current Data Parameters  
NAME GAC5  
EXPNO 27  
PROCNO 1

F2 - Acquisition Parameters  
Date\_ 20151213  
Time 5.28  
INSTRUM spect  
PROBHD 5 mm PABBO BB/  
PULPROG zgpg30  
ID 65536  
SOLVENT DMSO  
NS 600  
DS 4  
SWH 24038.461 Hz  
FIDRES 0.366798 Hz  
AQ 1.3631988 sec  
RG 175.97  
DW 20.800 usec  
DE 6.50 usec  
TE 300.9 K  
D1 2.00000000 sec  
D11 0.03000000 sec  
TD0 1

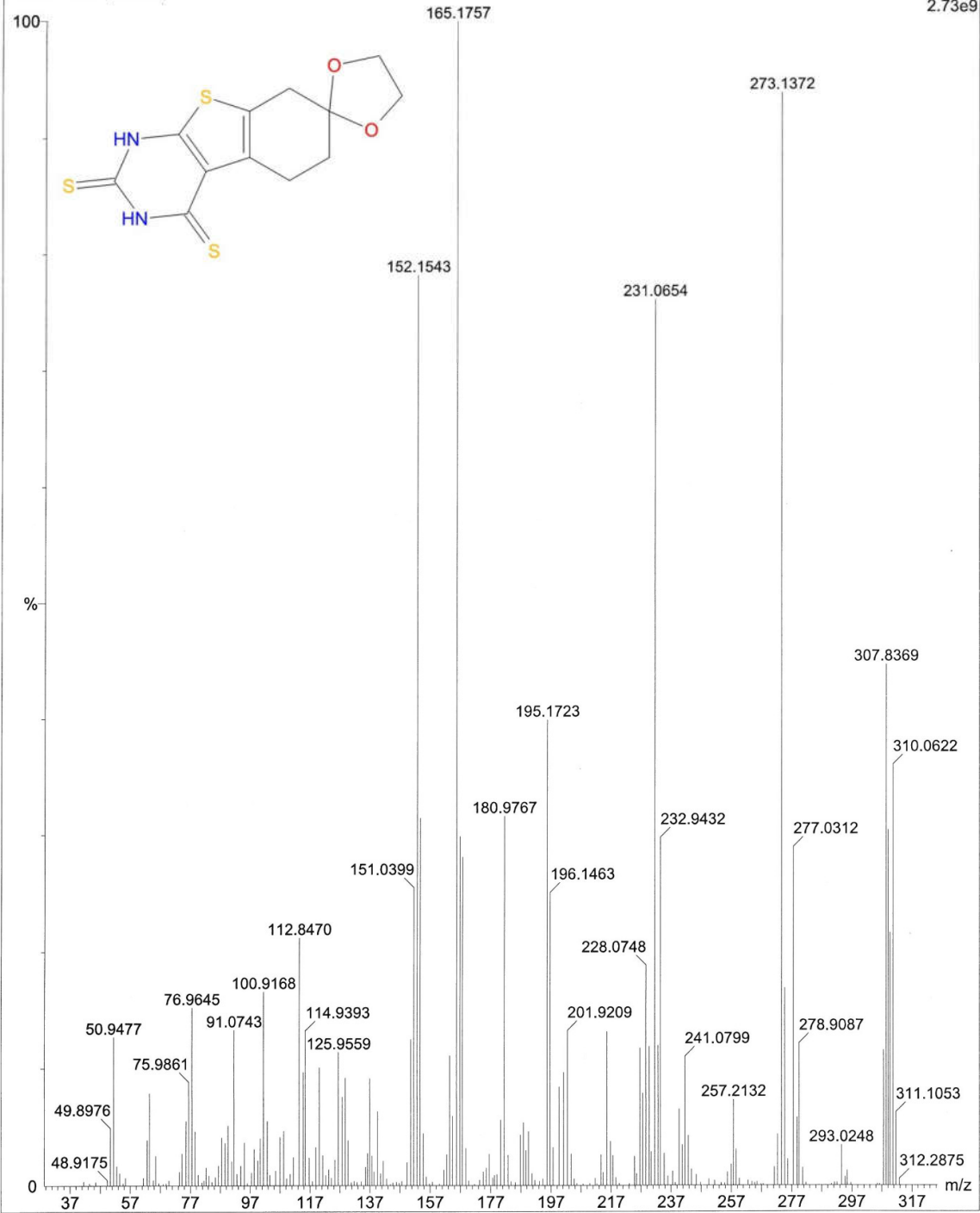
===== CHANNEL f1 =====  
NUC1 13C  
P1 9.80 usec  
PLW1 58.00000000 W  
SFO1 100.6550182 MHz

===== CHANNEL f2 =====  
CPDPRG2 waltz16  
NUC2 1H  
PCPD2 90.00 usec  
PLW2 14.00000000 W  
PLW12 0.35097000 W  
PLW13 0.28428999 W  
SFO2 400.2596010 MHz

F2 - Processing parameters  
SI 32768  
SF 100.6450043 MHz  
WDW EM  
SSB 0  
LB 1.00 Hz  
GB 0  
PC 1.40

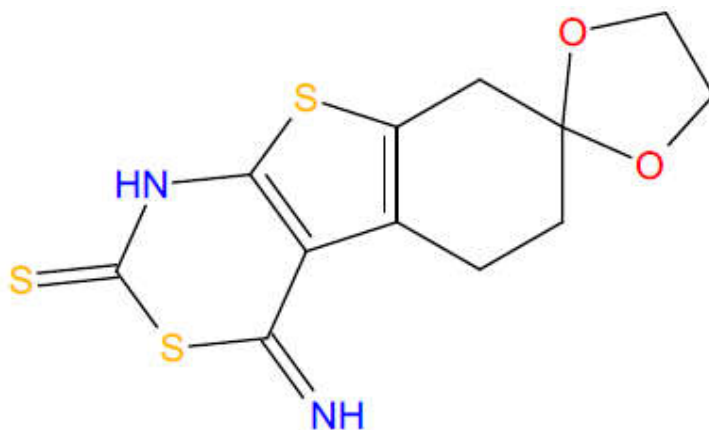
GAC5-4125 (23.132)

Scan EI+  
2.73e9





## Spectral Data of Compound GAC6



**IR (KBr,  $\nu_{\max}$ )  $\text{cm}^{-1}$**

3402.18 (amine N-H), 2923.87 (aliphatic C-H), 1735.81 (C=S),  
1149.49 (C-O-C), 617.18 (C-S).

**$^1\text{H}$  NMR (DMSO- $\text{D}_6$ )  $\delta$**

1.84 (t, 2H,  $\text{CH}_2$ ), 2.85 (s, 2H,  $\text{CH}_2$ ), 3.14 (t, 2H,  $\text{CH}_2$ ), 3.93 (s, 4H,  
 $\text{CH}_2$ ), 7.00 (s, 1H, N-H), 13.26 (s, 1H, N-H).

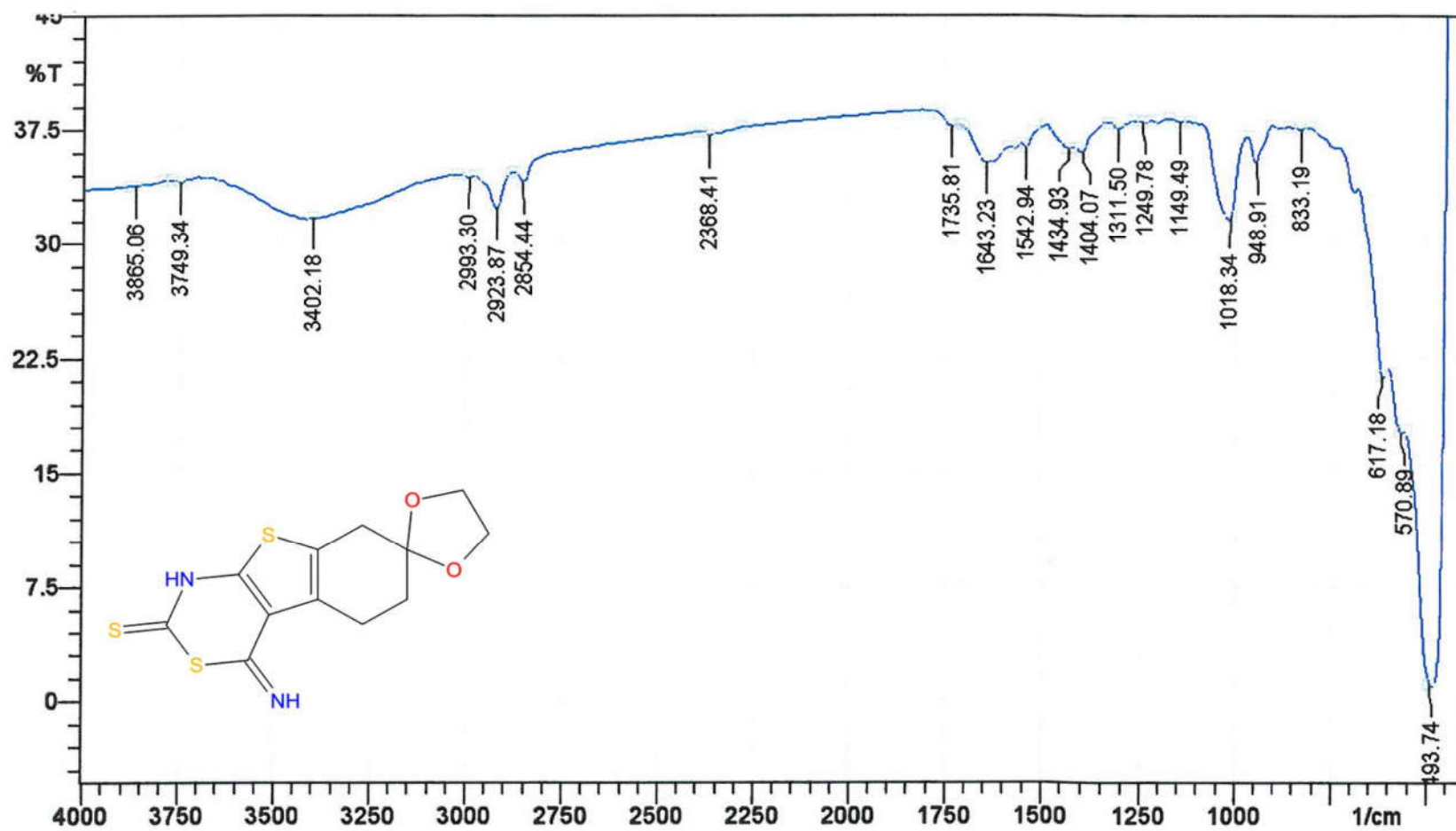
**$^{13}\text{C}$  NMR (DMSO- $\text{D}_6$ )  $\delta$**

25.86, 30.32, 30.55, 34.07, 34.73, 64.00, 106.76, 124.57, 127.21,  
131.16, 169.19, 181.64.

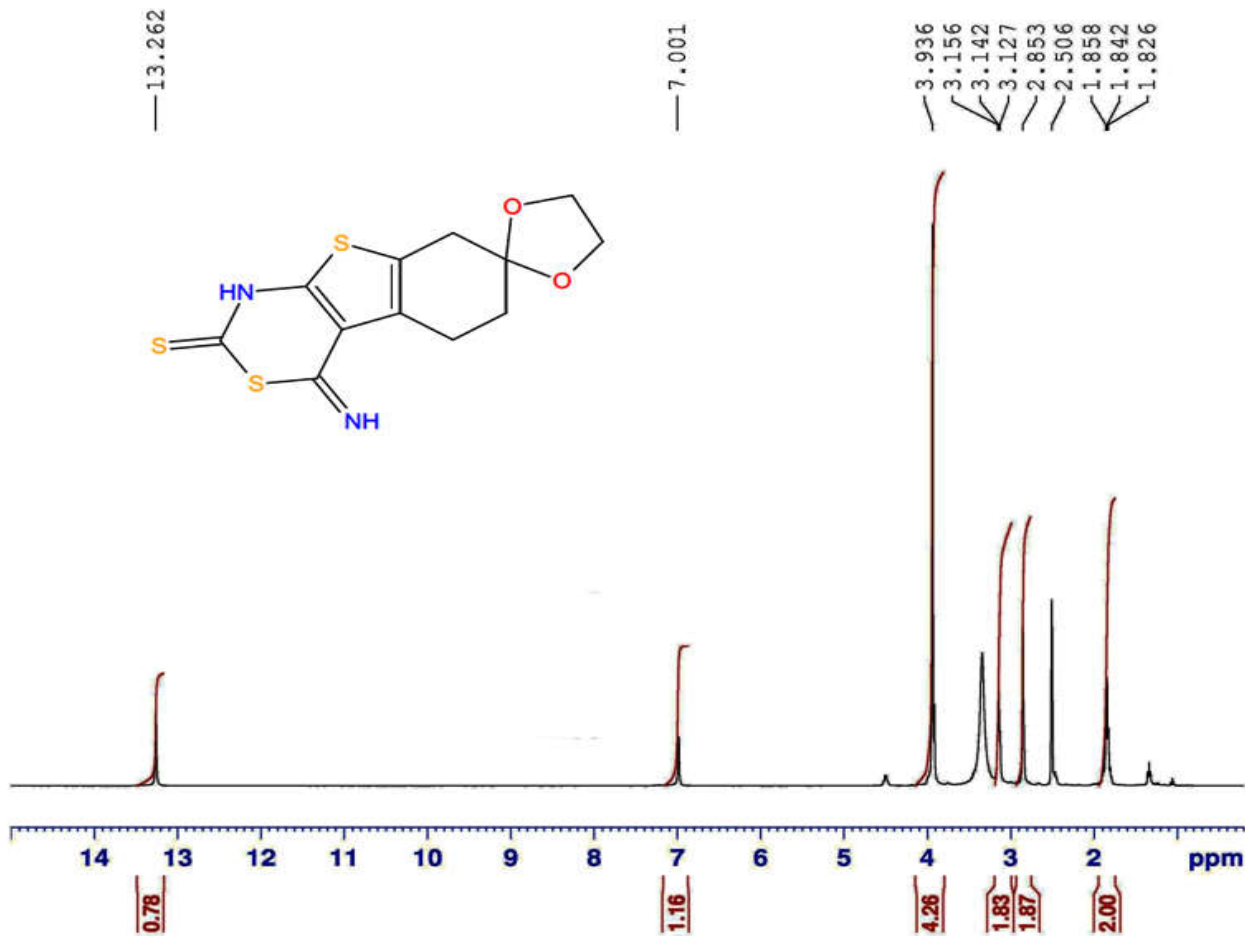
**MASS SPECTROSCOPY**

312.21 ( $\text{M}^+$ ), 153.19 (**B**).

Sample: GAC 6



GAC6.....Noorulla



Current Data Parameters  
NAME GAC6  
EXPNO 26  
PROCNO 1

F2 - Acquisition Parameters  
Date\_ 20151213  
Time 3.41  
INSTRUM spect  
PROBHD 5 mm PABBO BB/  
PULPROG zg30  
TD 65536  
SOLVENT DMSO  
NS 32  
DS 2  
SWH 8223.685 Hz  
FIDRES 0.125483 Hz  
AQ 3.9846387 sec  
RG 127.79  
DW 60.800 usec  
DE 6.50 usec  
TE 301.9 K  
D1 1.00000000 sec  
TD0 1

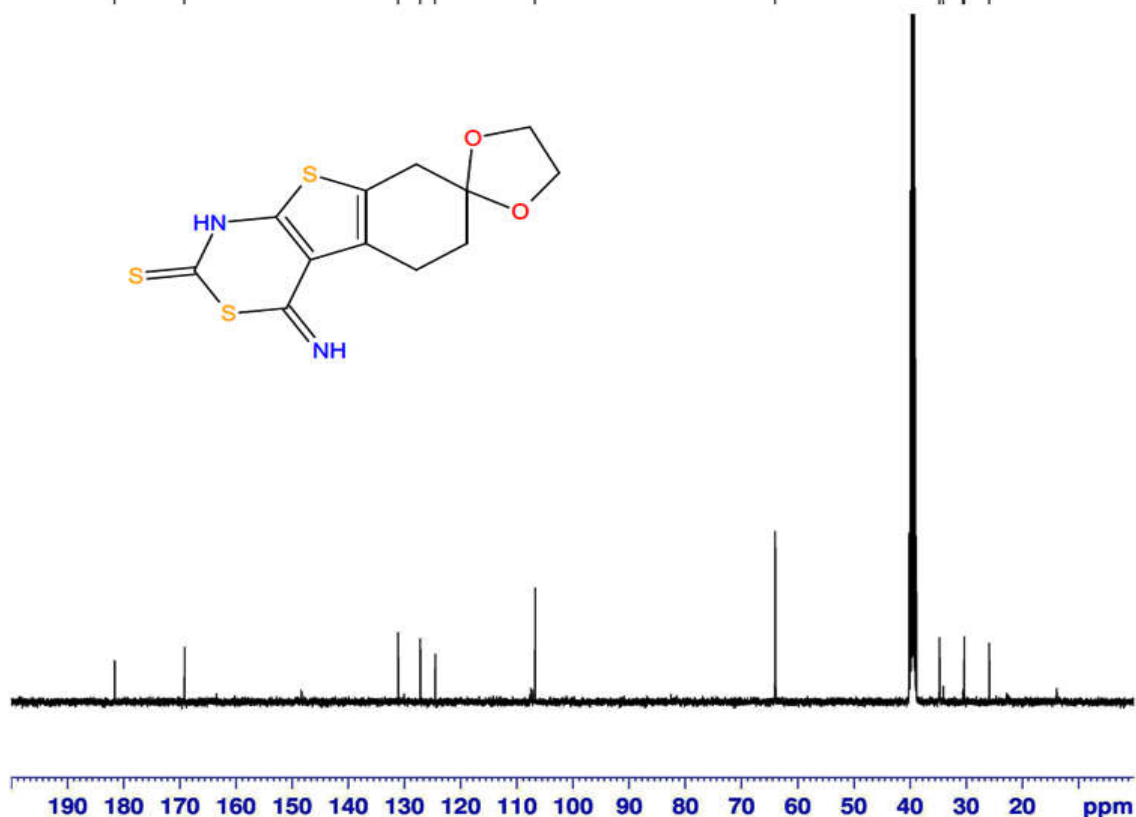
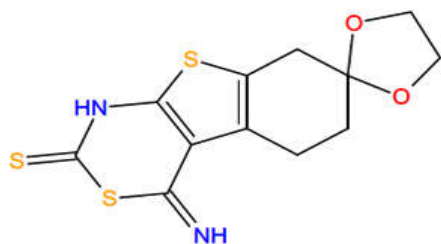
----- CHANNEL f1 -----  
NUC1 1H  
P1 14.25 usec  
PLW1 14.00000000 W  
SFO1 400.2604718 MHz

F2 - Processing parameters  
SI 65536  
SF 400.2580037 MHz  
WDW EM  
SSB 0  
LB 0.30 Hz  
GB 0  
PC 1.00

GAC6.....Noorulla

181.64  
169.19  
131.16  
127.21  
124.57  
106.76  
64.00

34.73  
34.07  
30.55  
30.32  
25.86



Current Data Parameters  
NAME GAC6  
EXPNO 28  
PROCNO 1

F2 - Acquisition Parameters  
Date\_ 20151213  
Time 6.05  
INSTRUM spect  
PROBHD 5 mm PABBO BB/  
PULPROG zgpg30  
TD 65536  
SOLVENT DMSO  
NS 600  
DS 4  
SWH 24038.461 Hz  
FIDRES 0.366798 Hz  
AQ 1.3631988 sec  
RG 175.97  
DW 20.800 usec  
DE 6.50 usec  
TE 300.5 K  
D1 2.00000000 sec  
D11 0.03000000 sec  
TD0 1

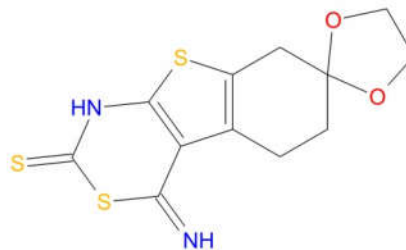
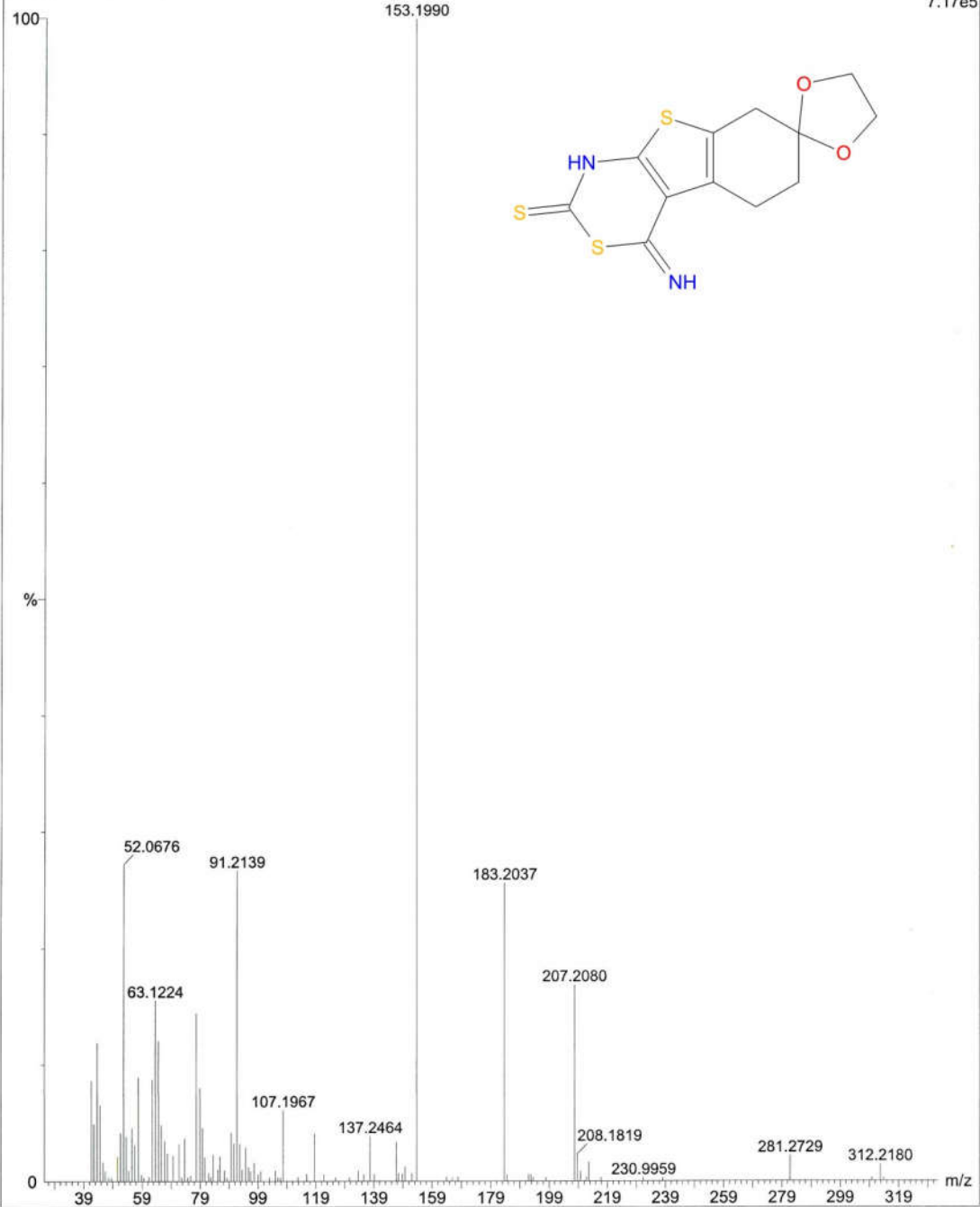
===== CHANNEL f1 =====  
NUC1 13C  
P1 9.80 usec  
PLW1 58.00000000 W  
SFO1 100.6550182 MHz

===== CHANNEL f2 =====  
CPDPRG2 waltz16  
NUC2 1H  
PCPD2 90.00 usec  
PLW2 14.00000000 W  
PLW12 0.35097000 W  
PLW13 0.28428999 W  
SFO2 400.2596010 MHz

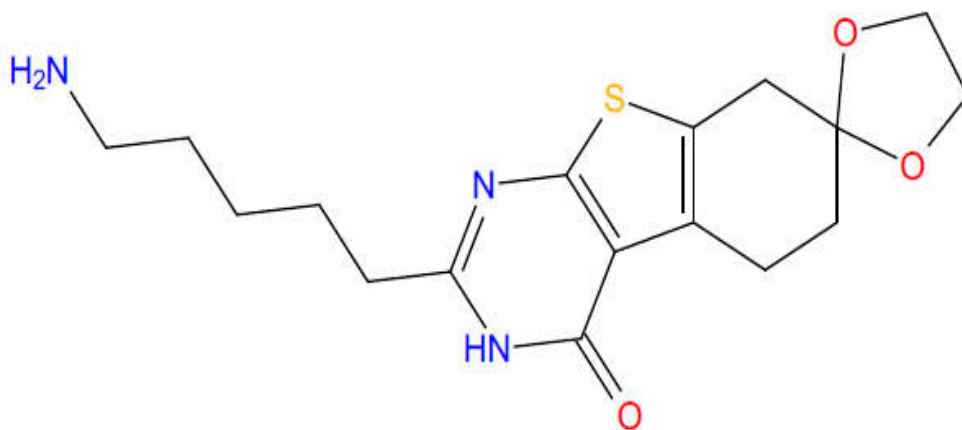
F2 - Processing parameters  
SI 32768  
SF 100.6450043 MHz  
WDW EM  
SSB 0  
LB 1.00 Hz  
GB 0  
PC 1.40

GAC6-3513 (20.070)

Scan EI+  
7.17e5



## Spectral Data of Compound GAC7



**IR (KBr,  $\nu_{\max}$ )  $\text{cm}^{-1}$**

3749.34 (amide N-H), 3355.89 (amine N-H), 2923.87 (aliphatic C-H), 1620.09 (amide C=O), 1242.07 (amine C-N), 1218.92 (C-O-C).

**$^1\text{H}$  NMR (DMSO- $\text{D}_6$ )  $\delta$**

1.05-1.11 (m, 6H,  $\text{CH}_2$ ), 1.89 (t, 2H,  $\text{CH}_2$ ), 2.35 (t, 2H,  $\text{CH}_2$ ), 2.51 (s, 4H,  $\text{CH}_2$ ), 2.56-2.61 (q, 2H,  $\text{CH}_2$ ), 2.66 (s, 2H,  $\text{CH}_2$ ), 2.75 (t, 2H,  $\text{CH}_2$ ), 6.98 (s, 2H,  $\text{NH}_2$ ), 7.15 (s, 1H, N-H).

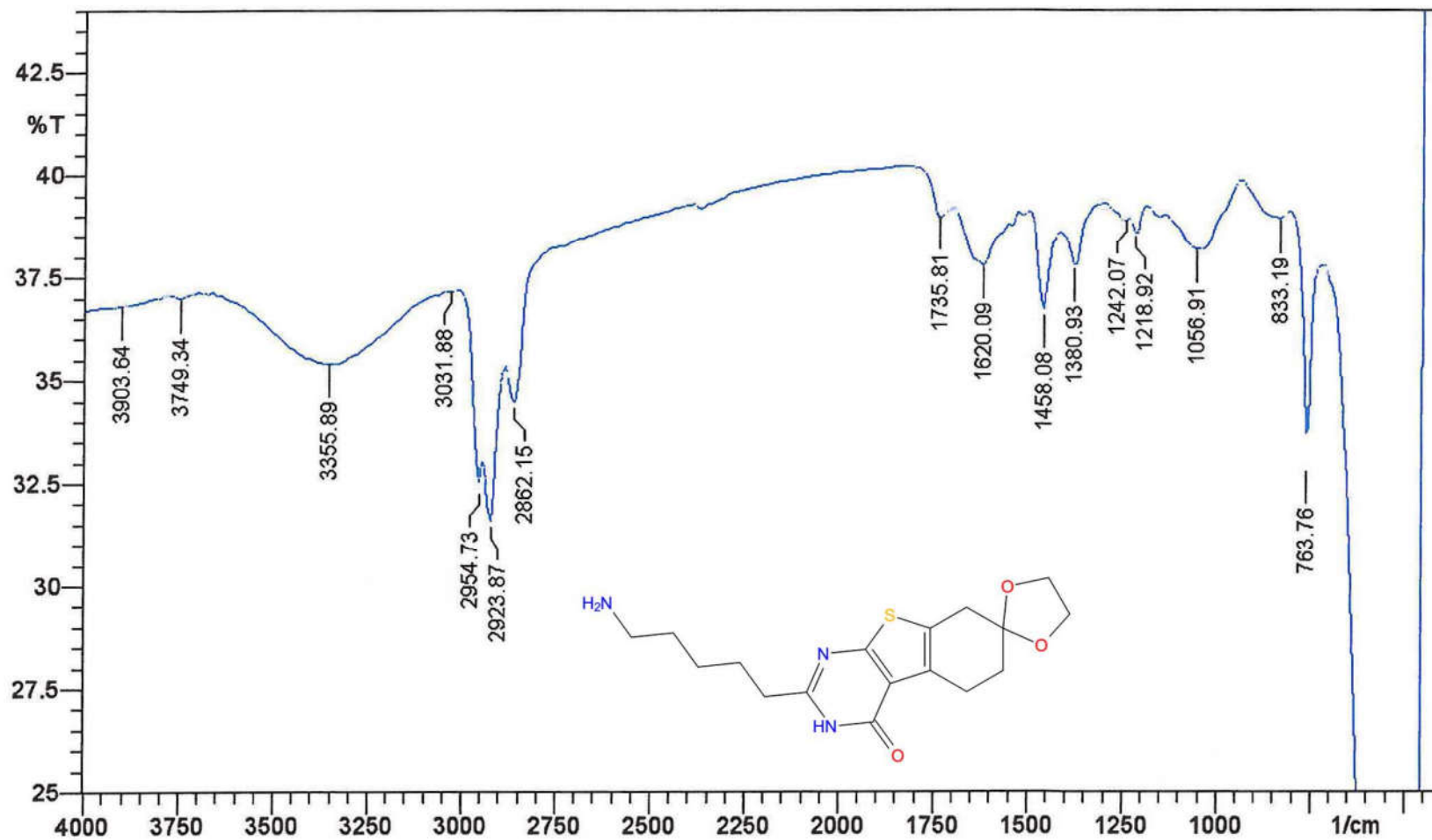
**$^{13}\text{C}$  NMR (DMSO- $\text{D}_6$ )  $\delta$**

15.33, 18.52, 22.16, 22.76, 23.24, 29.01, 33.55, 34.05, 37.68, 38.10, 55.05, 113.04, 113.95, 115.94, 116.09, 130.39, 163.39.

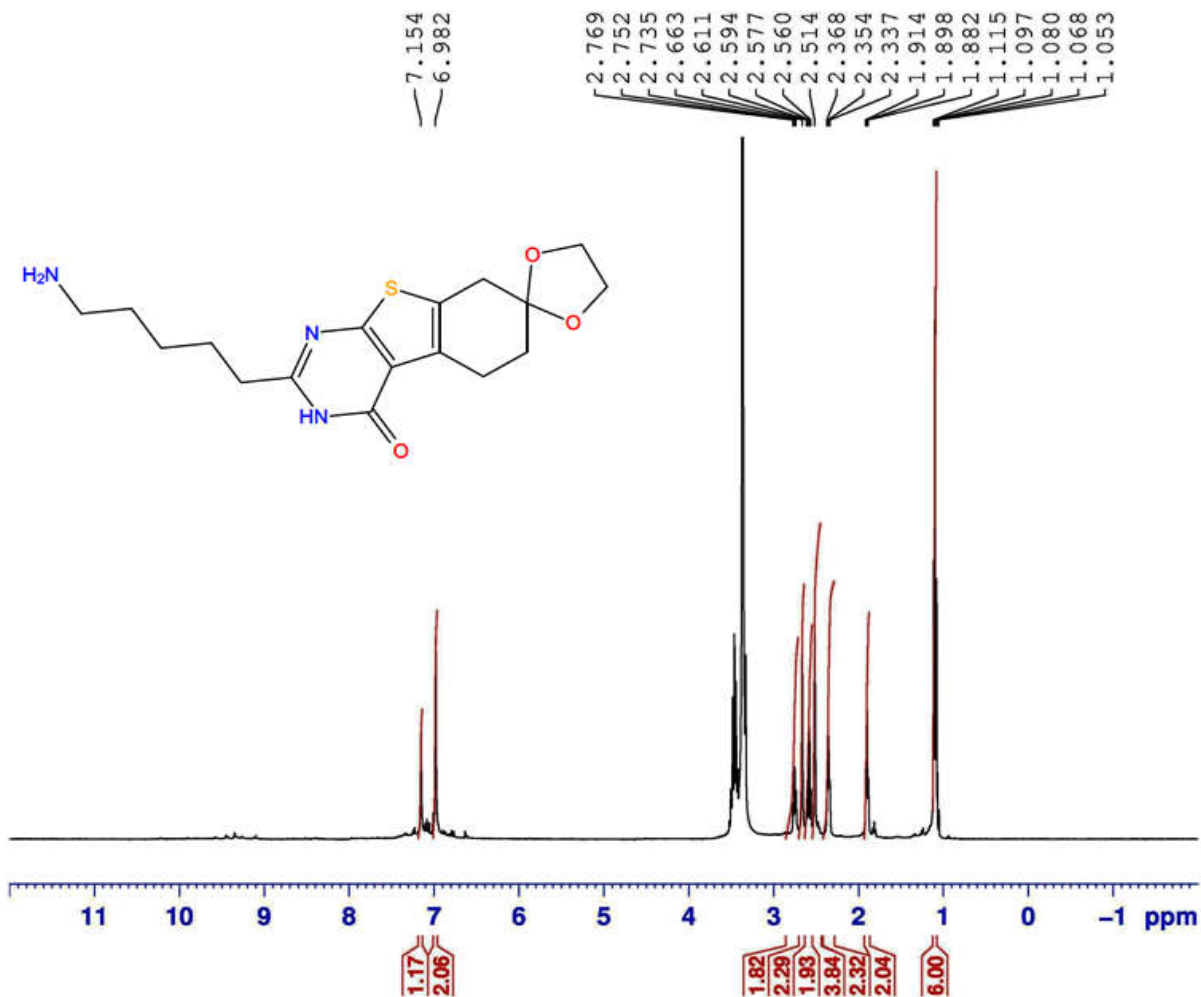
**MASS SPECTROSCOPY**

349.07 ( $\text{M}^+$ ), 78.01 (**B**).

Sample: GAC 7



GAC7.....Noorulla



Current Data Parameters  
NAME GAC7  
EXPNO 8  
PROCNO 1

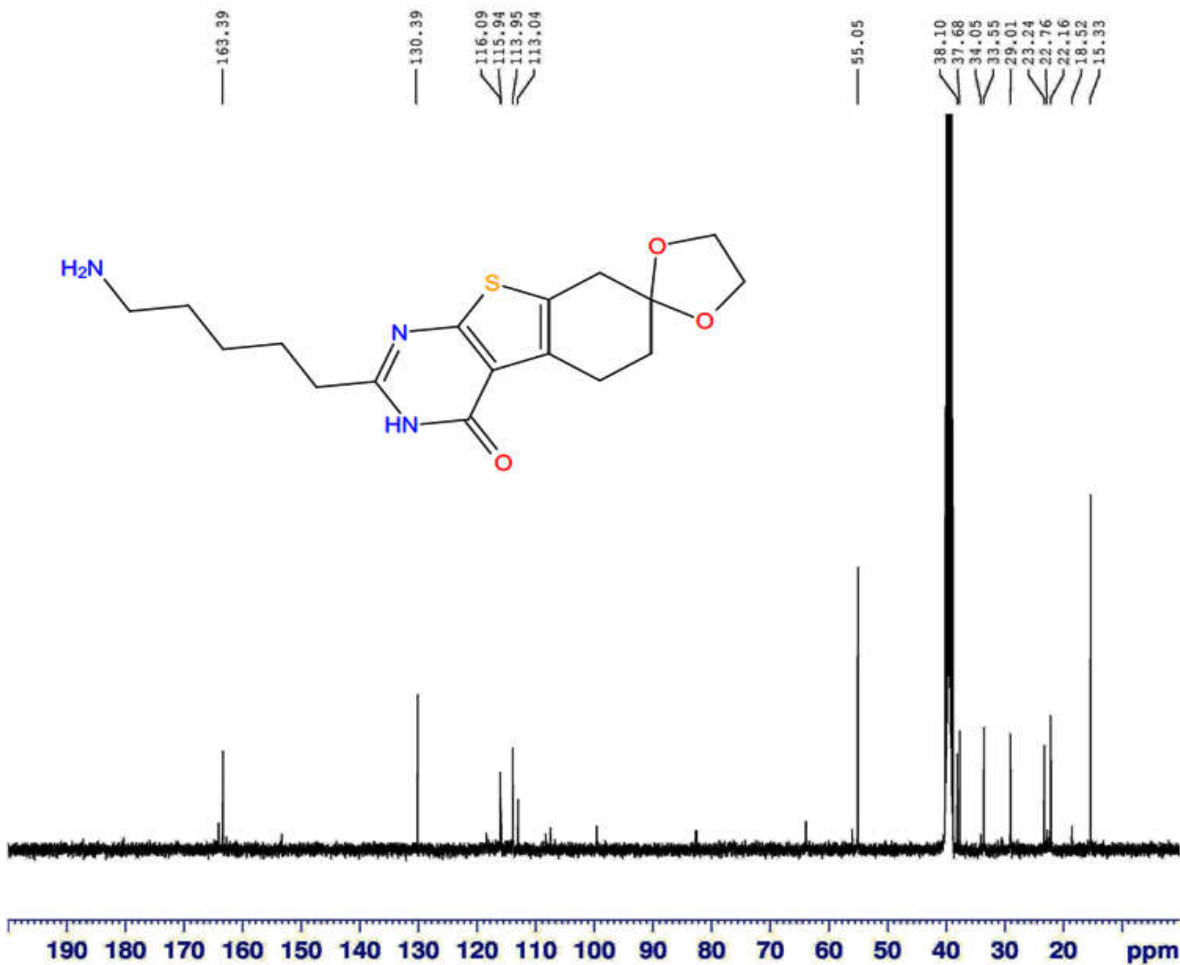
F2 - Acquisition Parameters  
Date\_ 20151206  
Time 4.00  
INSTRUM spect  
PROBHD 5 mm PABBO BB/  
PULPROG zg30  
TD 65536  
SOLVENT DMSO  
NS 16  
DS 2  
SWH 8223.685 Hz  
FIDRES 0.125483 Hz  
AQ 3.9846387 sec  
RG 98.85  
DW 60.800 usec  
DE 6.50 usec  
TE 300.9 K  
D1 1.00000000 sec  
TD0 1

===== CHANNEL f1 =====  
NUC1 1H  
P1 14.25 usec  
PLW1 14.00000000 W  
SF01 400.2604718 MHz

F2 - Processing parameters  
SI 65536  
SF 400.2580000 MHz  
WDW EM  
SSB 0  
LB 0.30 Hz  
GB 0  
PC 1.00



GAC7.....Noorulla



Current Data Parameters  
NAME GAC7  
EXPNO 9  
PROCNO 1

F2 - Acquisition Parameters  
Date\_ 20151206  
Time 5.58  
INSTRUM spect  
PROBHD 5 mm PABBO BB/  
PULPROG zgpg30  
TD 65536  
SOLVENT DMSO  
NS 1500  
DS 4  
SWH 24038.461 Hz  
FIDRES 0.366798 Hz  
AQ 1.3631988 sec  
RG 199.6  
DW 20.800 usec  
DE 6.50 usec  
TE 300.5 K  
D1 2.0000000 sec  
D11 0.0300000 sec  
TD0 1

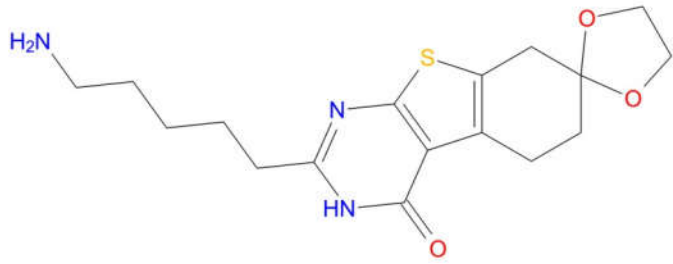
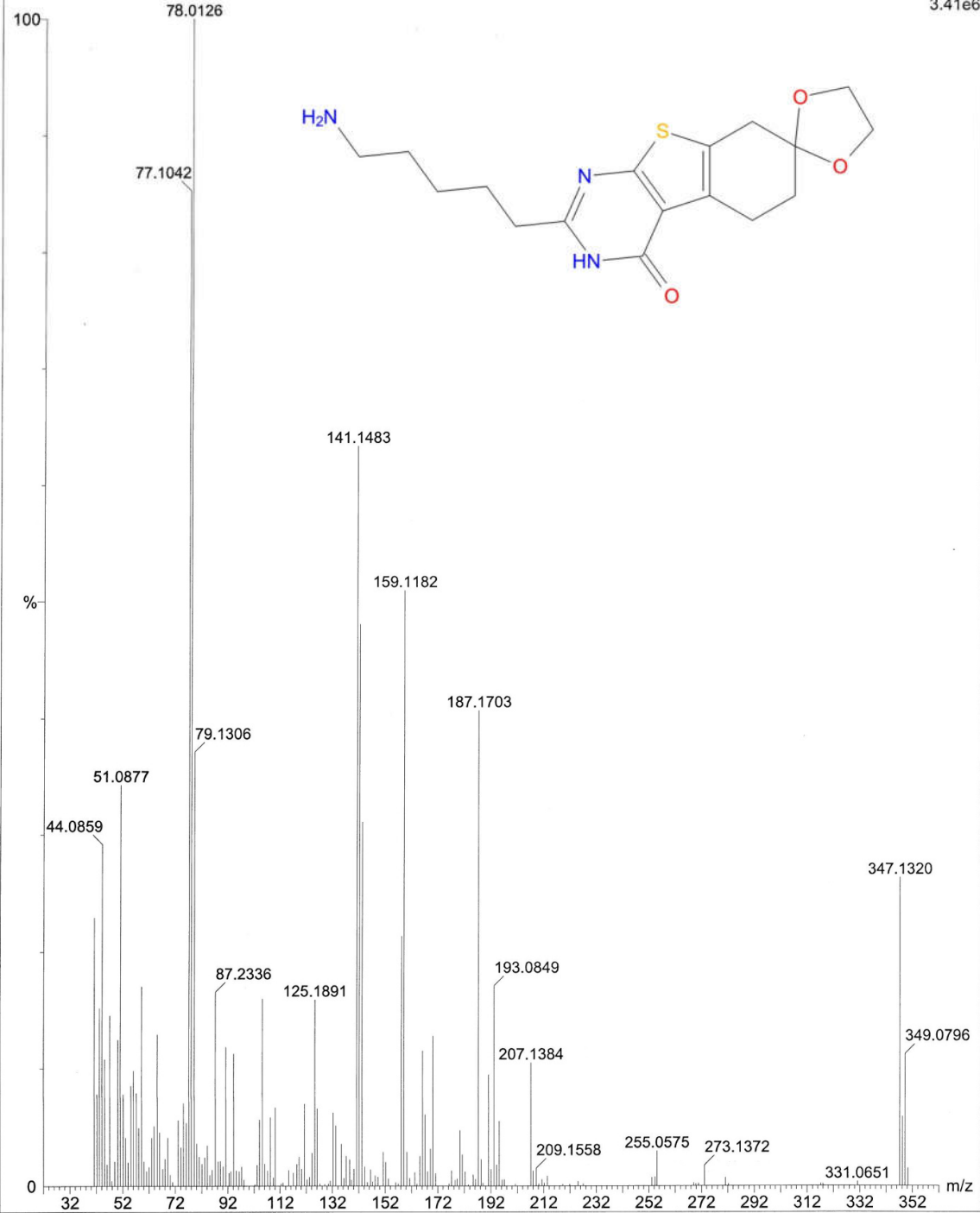
===== CHANNEL f1 =====  
NUC1 13C  
P1 9.80 usec  
PLW1 58.00000000 W  
SFO1 100.6550182 MHz

===== CHANNEL f2 =====  
CPDPRG2 waltz16  
NUC2 1H  
PCPD2 90.00 usec  
PLW2 14.00000000 W  
PLW12 0.35097000 W  
PLW13 0.28428999 W  
SFO2 400.2596010 MHz

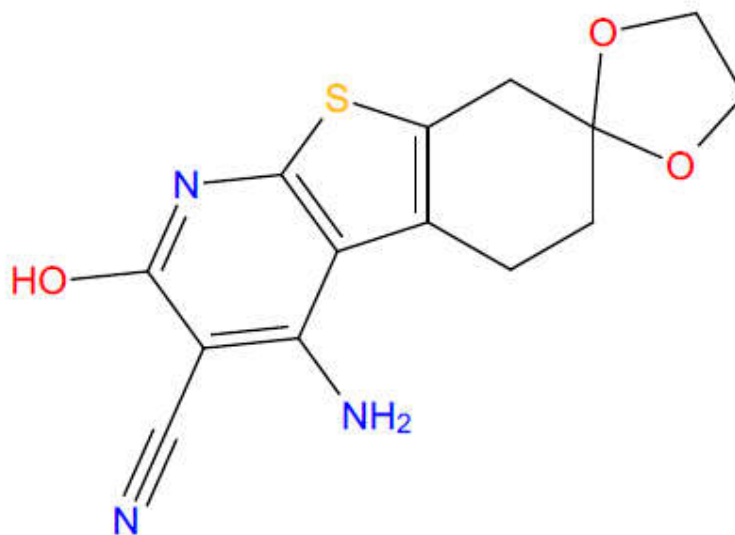
F2 - Processing parameters  
SI 32768  
SF 100.6450043 MHz  
WDW EM  
SSB 0  
LB 1.00 Hz  
GB 0  
PC 1.40

GAC7- 2585 (15.429)

Scan EI+  
3.41e6



## Spectral Data of Compound GAEA



**IR (KBr,  $\nu_{\max}$ )  $\text{cm}^{-1}$**

3425.33 (amine N-H), 2923.87 (aliphatic C-H), 2368.41 (nitrile C≡N), 1095.49 (C-O-C), 3456.18 (alcoholic O-H).

**$^1\text{H}$  NMR (DMSO- $\text{D}_6$ )  $\delta$**

1.81 (t, 2H, CH<sub>2</sub>), 2.46-2.51 (m, 2H, CH<sub>2</sub>), 2.61 (s, 2H, CH<sub>2</sub>), 3.92 (s, 4H, CH<sub>2</sub>), 7.01 (s, 2H, NH<sub>2</sub>).

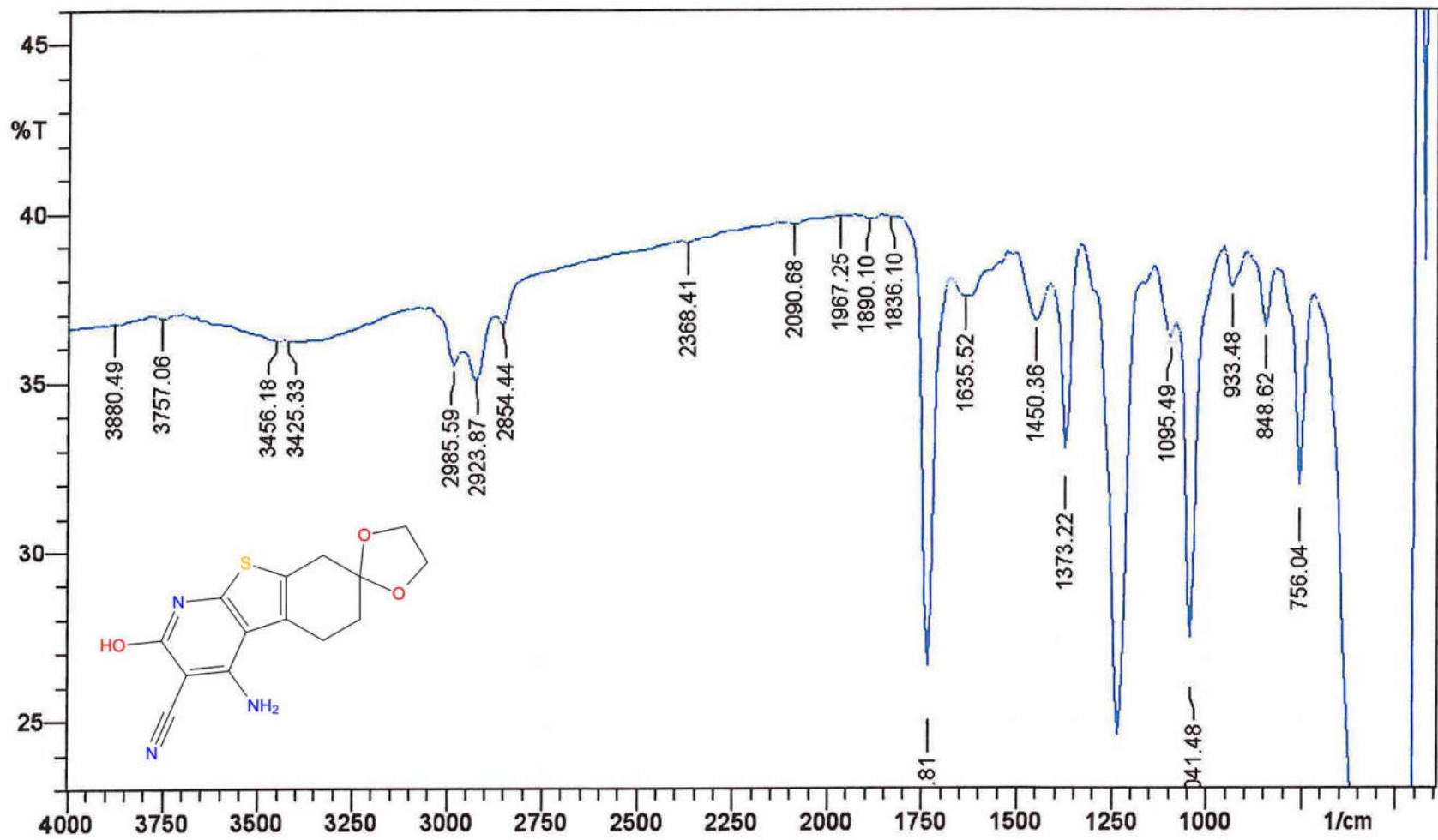
**$^{13}\text{C}$  NMR (DMSO- $\text{D}_6$ )  $\delta$**

22.77, 24.32, 26.81, 30.55, 34.05, 63.93, 66.33, 82.59, 107.54, 114.24, 116.04, 121.59, 124.45, 130.13.

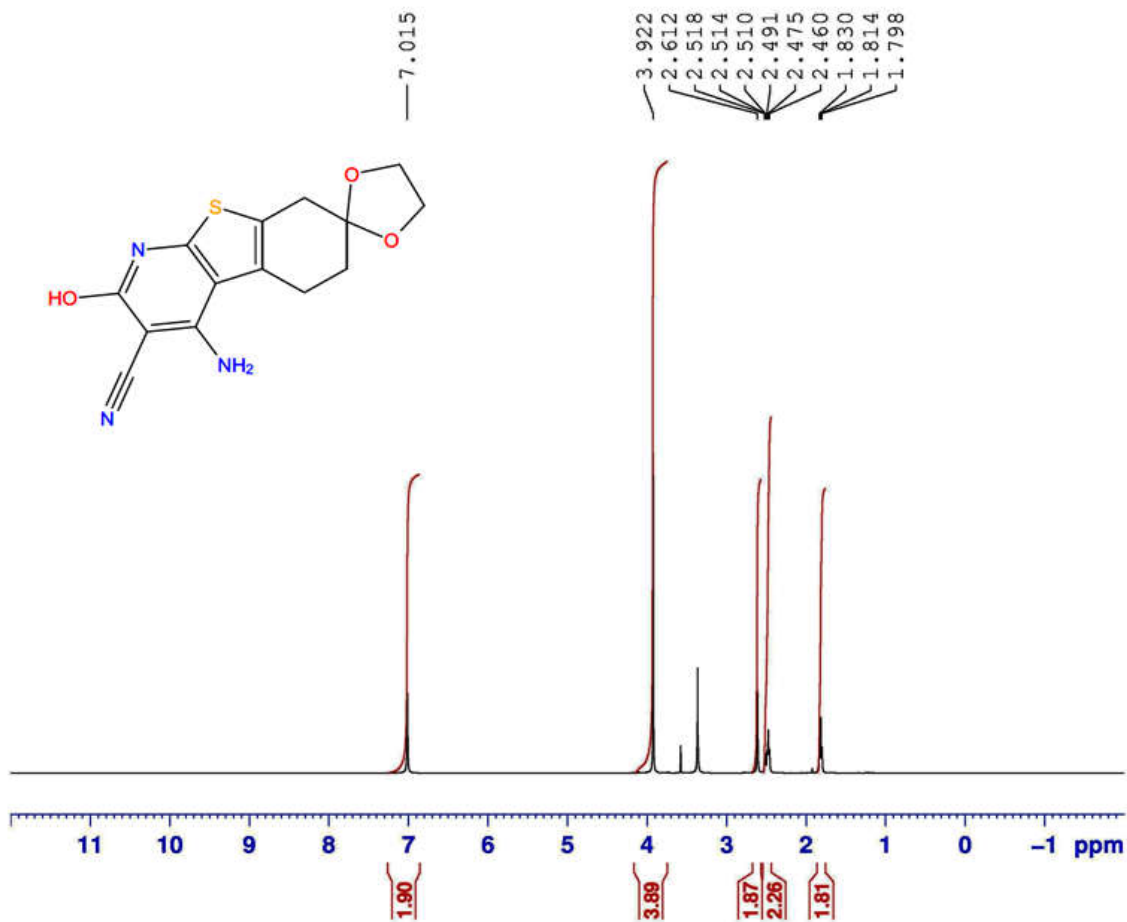
**MASS SPECTROSCOPY**

303.01 ( $\text{M}^+$ ), 207.06 (**B**).

Sample: GAEA



GAEA.....Noorulla



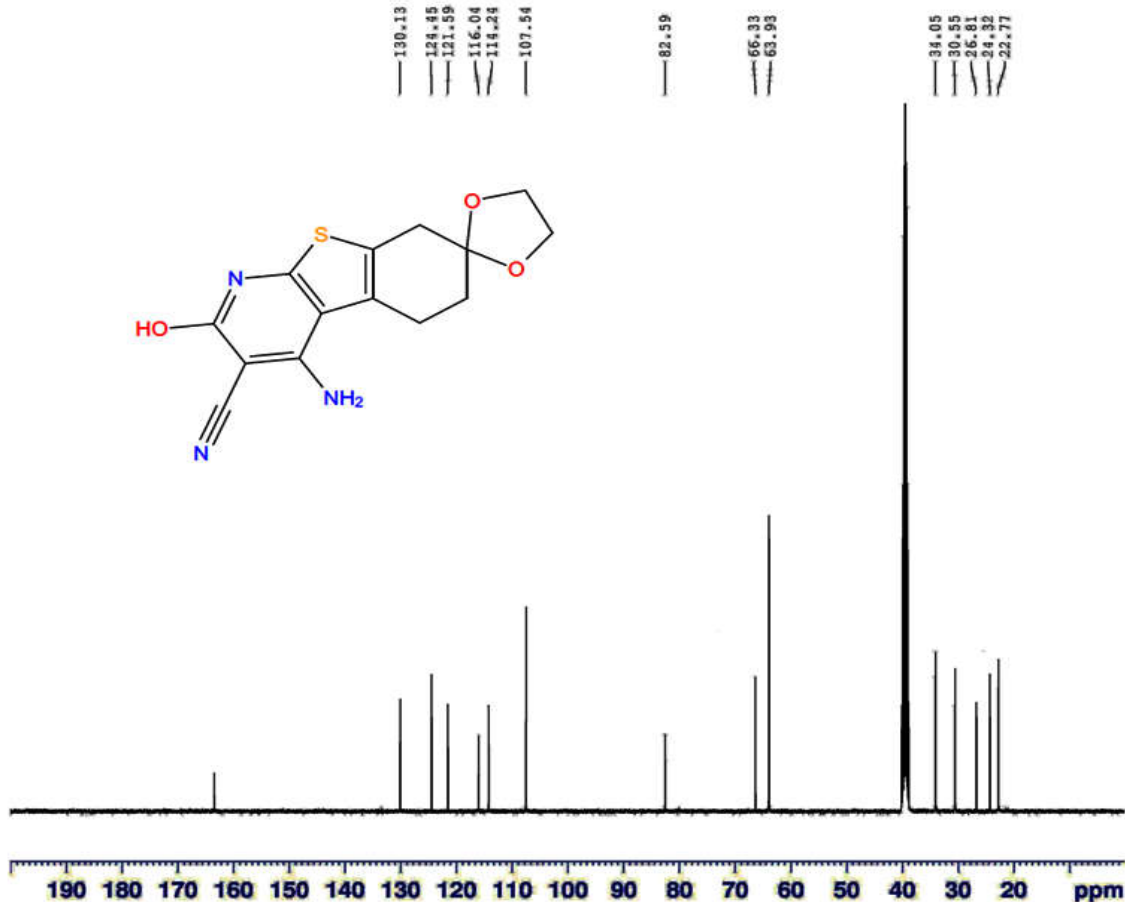
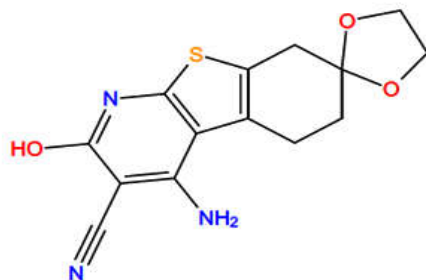
Current Data Parameters  
NAME GAEA  
EXPNO 1  
PROCNO 1

F2 - Acquisition Parameters  
Date\_ 20151205  
Time 21.30  
INSTRUM spect  
PROBHD 5 mm PABBO BB/  
PULPROG zg30  
TD 65536  
SOLVENT DMSO  
NS 16  
DS 2  
SWH 8223.685 Hz  
FIDRES 0.125483 Hz  
AQ 3.9846387 sec  
RG 77.73  
DW 60.800 usec  
DE 6.50 usec  
TE 299.4 K  
D1 1.00000000 sec  
TD0 1

==== CHANNEL f1 =====  
NUC1 1H  
P1 14.25 usec  
PLW1 14.00000000 W  
SFO1 400.2604718 MHz

F2 - Processing parameters  
SI 65536  
SF 400.2580000 MHz  
WDW EM  
SSB 0  
LB 0.30 Hz  
GB 0  
PC 1.00

GAEA.....Noorulla



Current Data Parameters  
NAME GAEA  
EXPNO 4  
PROCNO 1

F2 - Acquisition Parameters  
Date\_ 20151205  
Time 22.31  
INSTRUM spect  
PROBHD 5 mm PABBO BB/  
PULPROG zgpg30  
TD 65536  
SOLVENT DMSO  
NS 600  
DS 4  
SWH 24038.461 Hz  
FIDRES 0.366798 Hz  
AQ 1.3631988 sec  
RG 175.97  
DW 20.800 usec  
DE 6.50 usec  
TE 301.0 K  
D1 2.0000000 sec  
D11 0.03000000 sec  
TD0 1

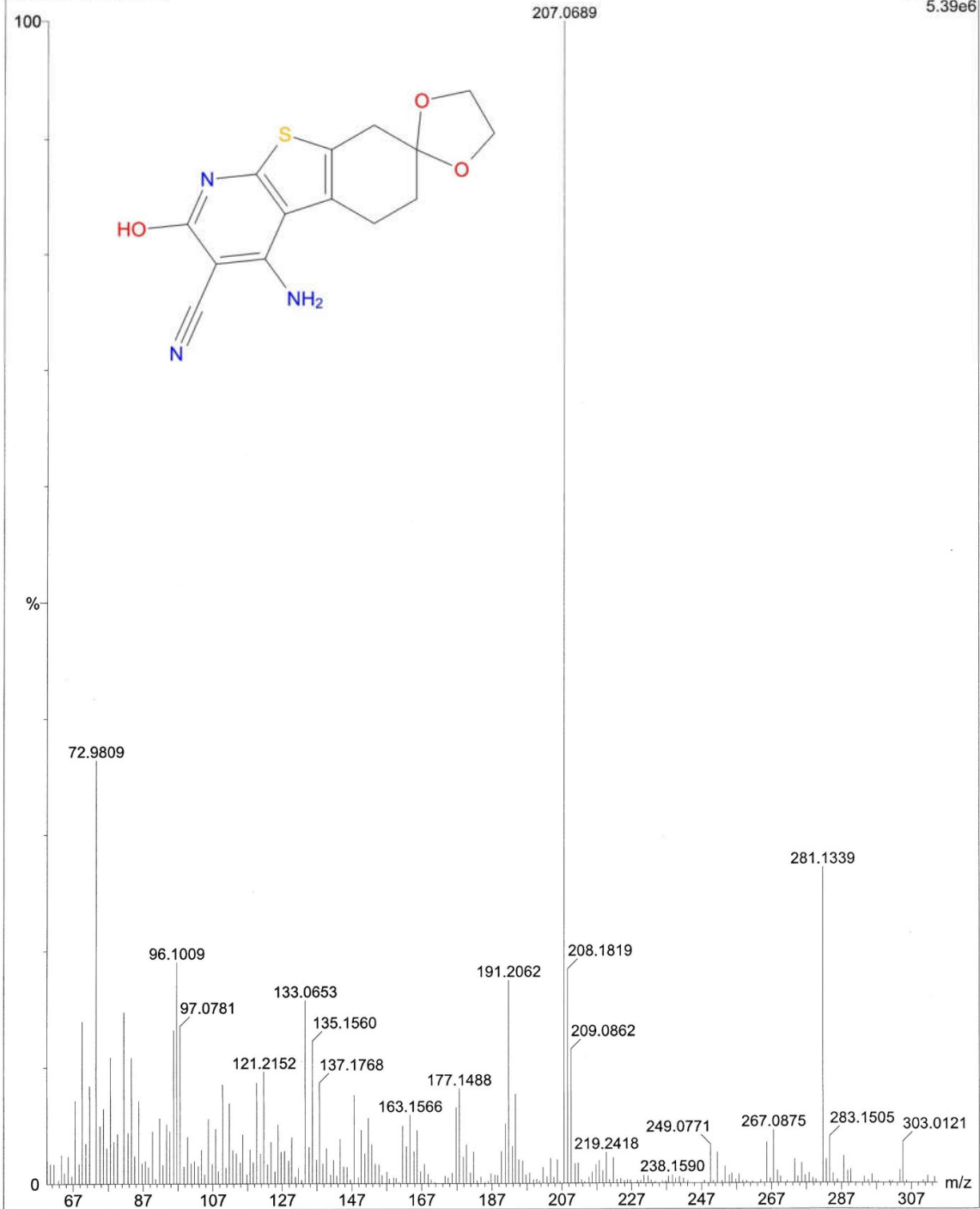
===== CHANNEL f1 =====  
NUC1 13C  
P1 9.80 usec  
PLW1 58.0000000 W  
SFO1 100.6250182 MHz

===== CHANNEL f2 =====  
CPDPRG2 waltz16  
NUC2 1H  
PCPD2 90.00 usec  
PLW2 14.0000000 W  
PLW12 0.35097000 W  
PLW13 0.28428999 W  
SFO2 400.2596010 MHz

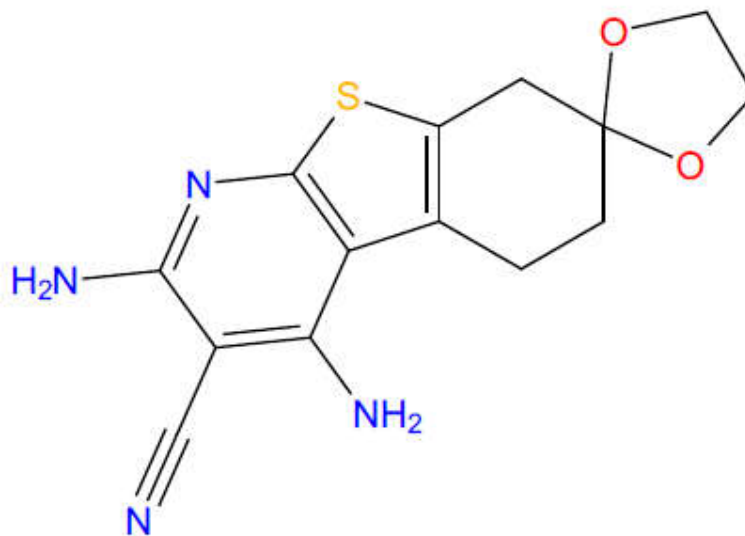
F2 - Processing parameters  
SI 32768  
SF 100.6450043 MHz  
WDW EM  
SSB 0  
LB 1.00 Hz  
GB 0  
PC 1.40

GAEA-4944 (27.228)

Scan EI+  
5.39e6



## Spectral Data of Compound GAM



**IR (KBr,  $\nu_{\max}$ )  $\text{cm}^{-1}$**

3379.04 (amine N-H), 2923.87 (aliphatic C-H), 2252.69 (nitrile C $\equiv$ N), 1087.77 (C-O-C), 1249.78 (amine C-N).

**$^1\text{H}$  NMR (DMSO- $\text{D}_6$ )  $\delta$**

1.87-2.86 (m, 6H, CH<sub>2</sub>), 2.51-2.78 (m, 4H, CH<sub>2</sub>), 7.20-7.84 (m, 4H, NH<sub>2</sub>).

**$^{13}\text{C}$  NMR (DMSO- $\text{D}_6$ )  $\delta$**

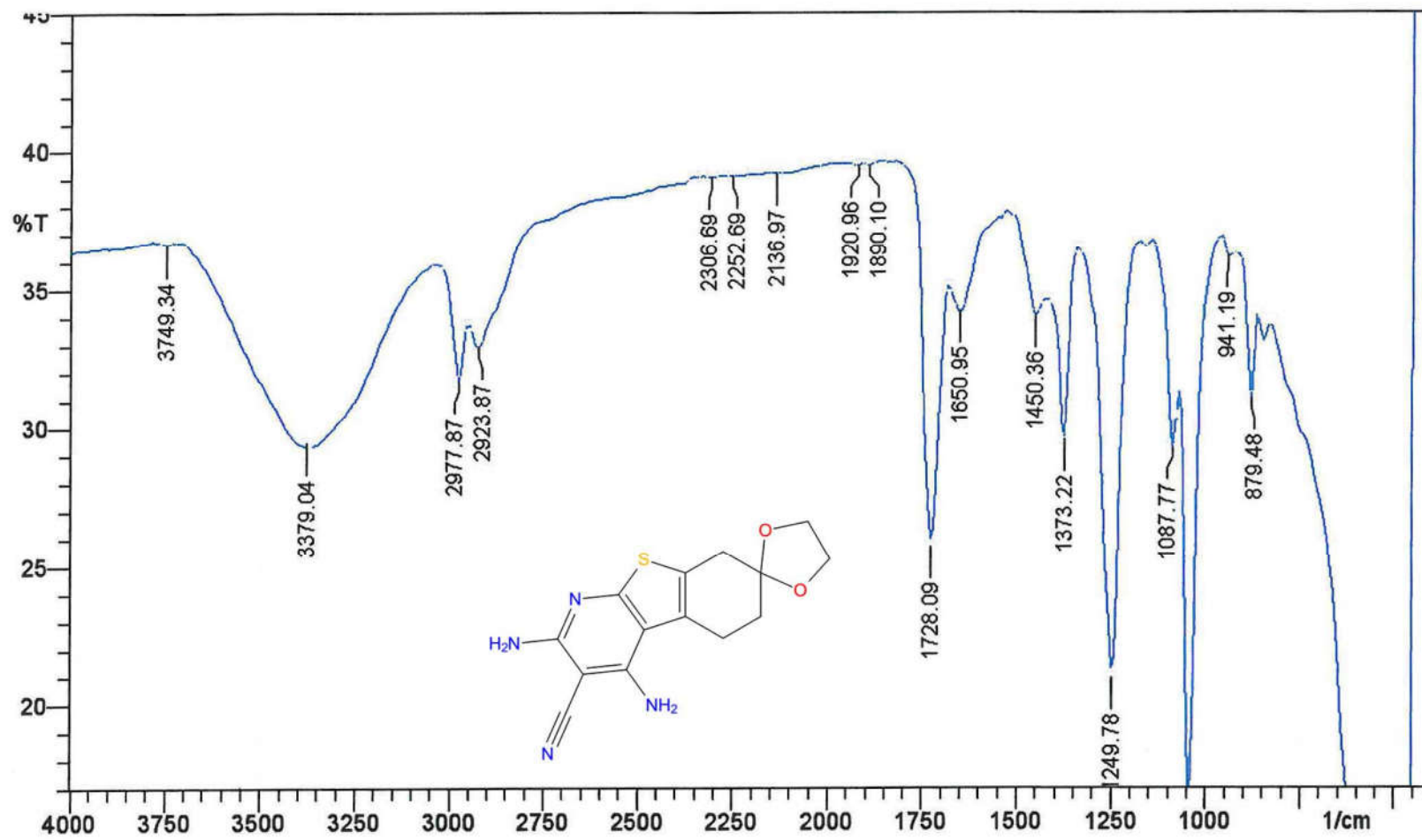
17.47, 21.02, 22.41, 26.63, 30.47, 57.10, 64.01, 107.37, 108.29, 115.05, 123.36, 132.10, 139.56.

**MASS SPECTROSCOPY**

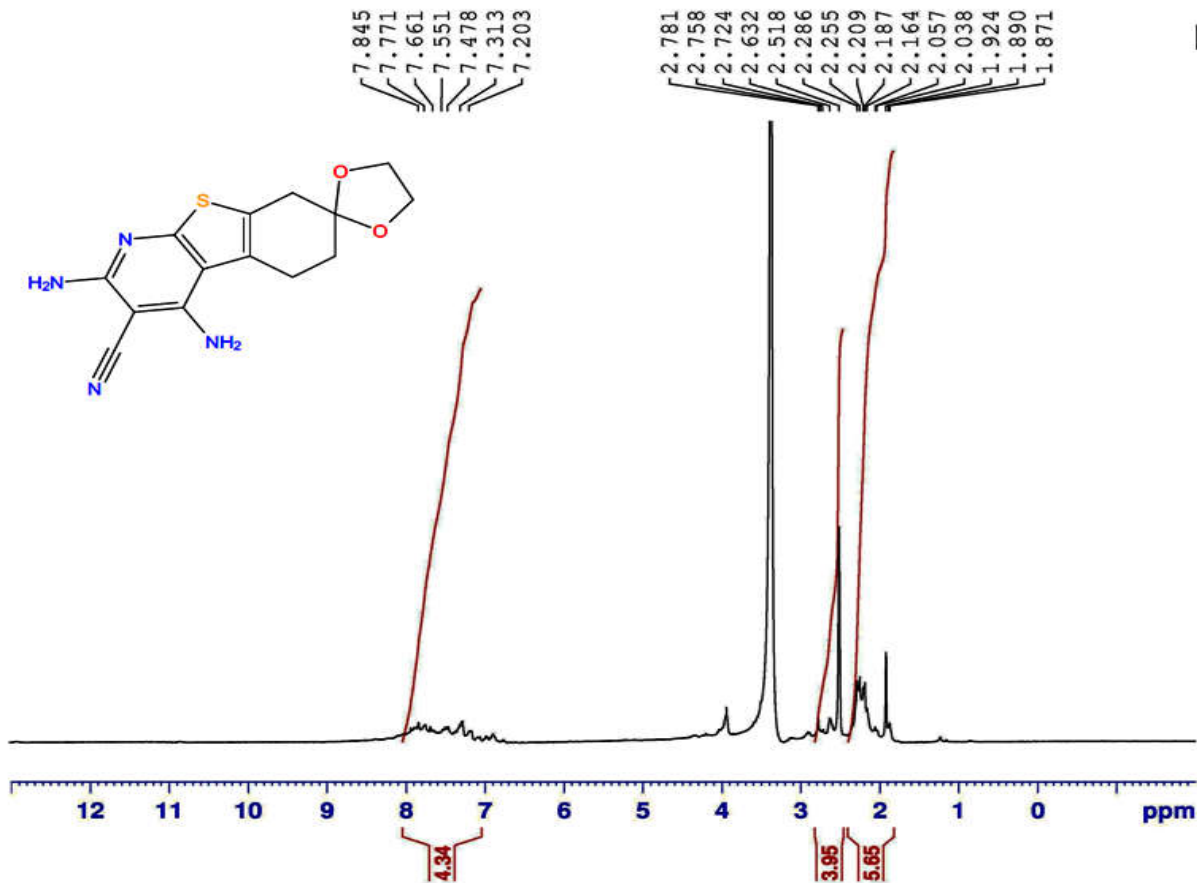
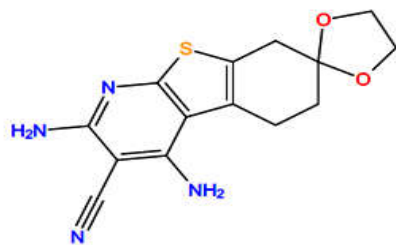
302.38 ( $\text{M}^+$ ), 303.35 ( $\text{M}+1$ ), 55.07 ( $\text{B}$ ).



Sample: GAM



GAM.....Noorulla



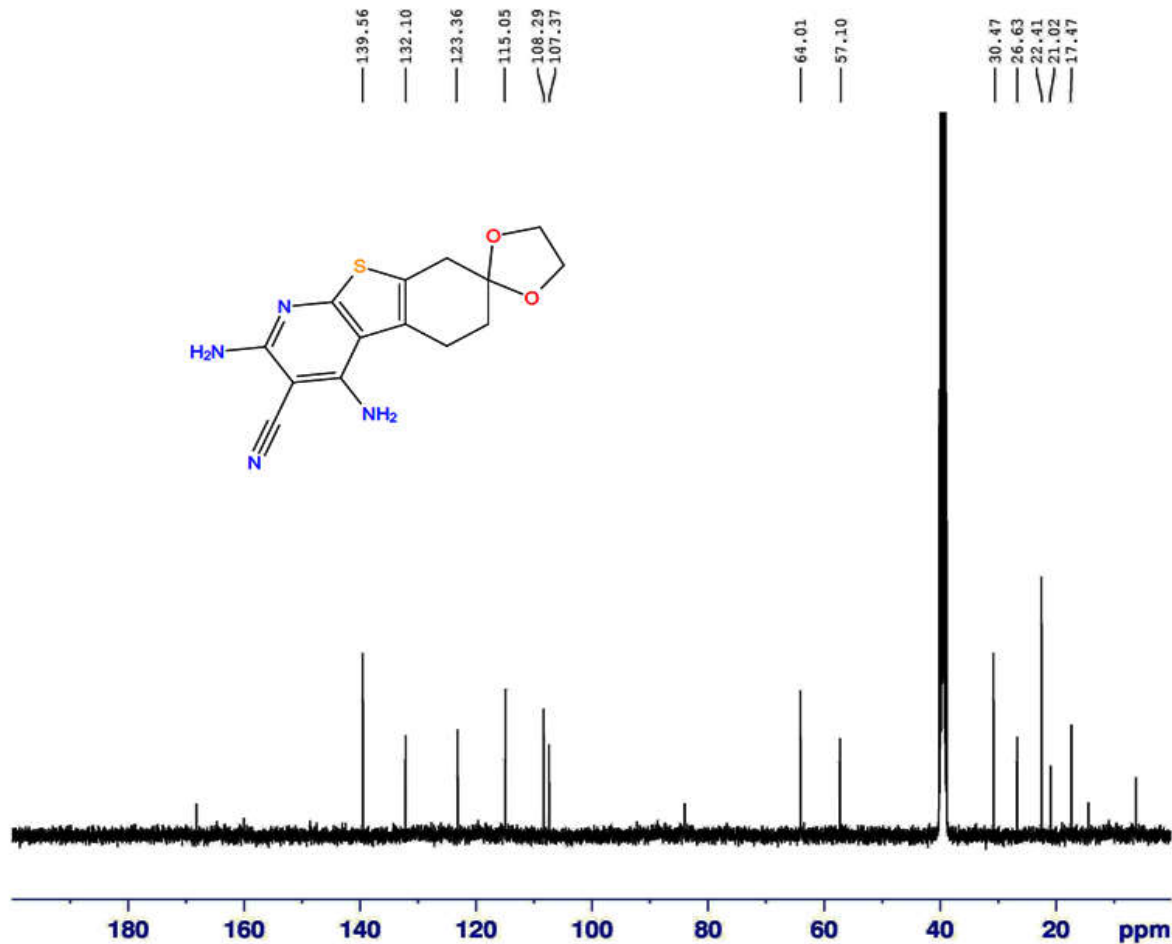
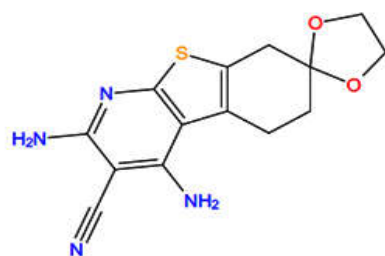
Current Data Parameters  
NAME GAM  
EXPNO 2  
PROCNO 1

F2 - Acquisition Parameters  
Date\_ 20151205  
Time 20.33  
INSTRUM spect  
PROBHD 5 mm PABBO BB/  
PULPROG zg30  
TD 65536  
SOLVENT DMSO  
NS 16  
DS 2  
SWH 8223.685 Hz  
FIDRES 0.125483 Hz  
AQ 3.9846387 sec  
RG 127.79  
DW 60.800 usec  
DE 6.50 usec  
TE 298.5 K  
D1 1.00000000 sec  
TD0 1

===== CHANNEL f1 =====  
NUC1 1H  
P1 14.25 usec  
PLW1 14.00000000 W  
SF01 400.2604718 MHz

F2 - Processing parameters  
SI 65536  
SF 400.2580000 MHz  
WDW EM  
SSB 0  
LB 0.30 Hz  
GB 0  
PC 1.00

GAM.....Noorulla



Current Data Parameters  
NAME GAM5  
EXPNO 7  
PROCNO 1

F2 - Acquisition Parameters  
Date\_ 20151206  
Time 1.04  
INSTRUM spect  
PROBHD 5 mm PABBO BB/  
PULPROG zgpg30  
TD 65536  
SOLVENT DMSO  
NS 1024  
DS 4  
SWH 24038.461 Hz  
FIDRES 0.366798 Hz  
AQ 1.3631988 sec  
RG 199.6  
DW 20.800 usec  
DE 6.50 usec  
TE 301.8 K  
D1 2.00000000 sec  
D11 0.03000000 sec  
TD0 1

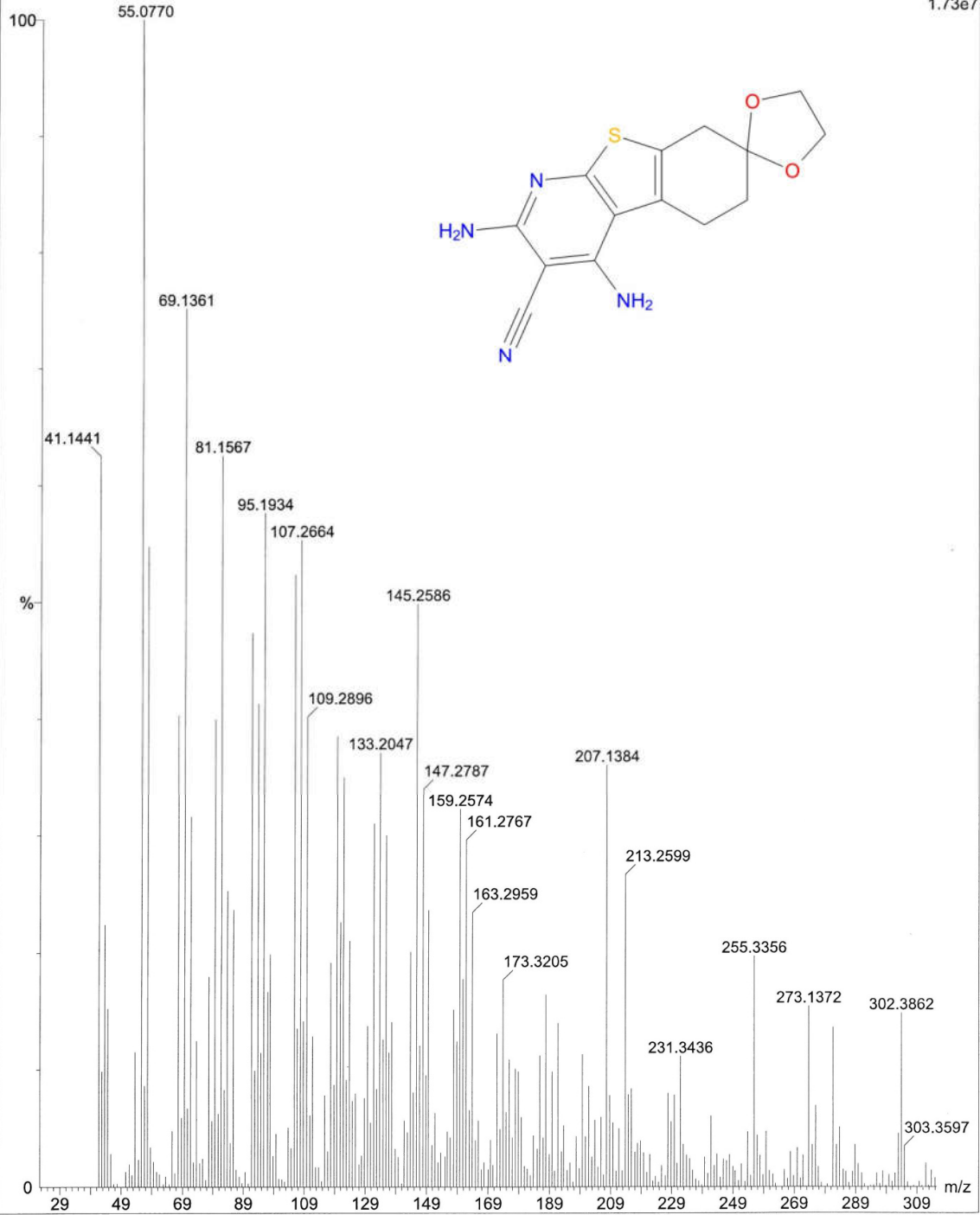
===== CHANNEL f1 =====  
NUC1 13C  
P1 9.80 usec  
PLW1 58.00000000 W  
SFO1 100.6550182 MHz

===== CHANNEL f2 =====  
CPDPRG2 waltz16  
NUC2 1H  
PCPD2 90.00 usec  
PLW2 14.00000000 W  
PLW12 0.35097000 W  
PLW13 0.28428999 W  
SFO2 400.2596010 MHz

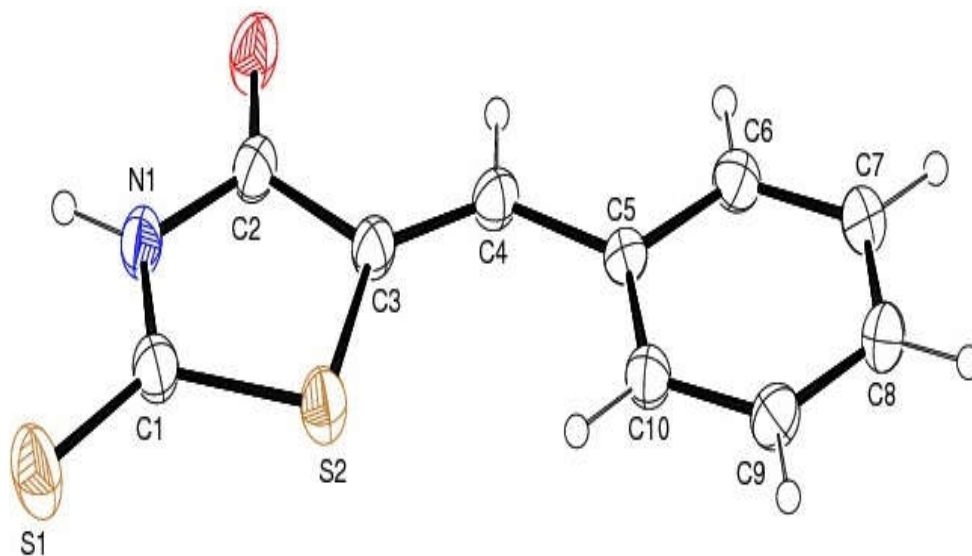
F2 - Processing parameters  
SI 32768  
SF 100.6450043 MHz  
WDW EM  
SSB 0  
LB 1.00 Hz  
GB 0  
PC 1.40

GAM-5451 (29.764)

Scan EI+  
1.73e7



The relative stereochemistry of the synthesized compound **N1** was established through single-crystal X-ray analysis (**Figure 12**)



**Figure12:** ORTEP diagram of compound **N1**

## CHAPTER 6

### *In-Vitro* Anti-Mycobacterial Assay

All the 30 synthesized compounds N1-N20, GA, GAC, GAC1, GAC5, GAC6, GAC7, GAE, GAEA, GAM and GAT were subjected to *in-vitro* anti-mycobacterial assay in order to find out their *in-vitro* potency of inhibiting tuberculosis. The desired study was performed by using “Microplate Alamar Blue assay” (MABA) method.<sup>171</sup>

#### **6.1. Materials**

- The *in-vitro* antimycobacterial activity of the synthesized compounds was performed using Microplate Alamar Blue assay (MABA) against *Mtb* (H37RV, ATCC No: 27294).
- Pyrazinamide, Ciprofloxacin and streptomycin were used as reference drugs. The results were based upon the minimum inhibitory concentration (MIC)

#### **6.2. Experimental**

- 1) The anti mycobacterial activity of compounds were assessed against *M. tuberculosis* using “Microplate Alamar Blue assay” (MABA).
- 2) This methodology is non-toxic, uses a thermally stable reagent and shows good correlation with proportional and BACTEC radiometric method.
- 3) Briefly, 200µl of sterile deionized water was added to all outer perimeter wells of sterile 96 wells plate to minimized evaporation of medium in the test wells during incubation.
- 4) The 96 wells plate received 100 µl of the Middlebrook 7H9 broth and serial dilution of compounds were made directly on plate.
- 5) The final drug concentrations tested were 100 to 0.2 µg/ml.

- 6) Plates were covered and sealed with parafilm and incubated at 37°C for five days.
- 7) After this time, 25µl of freshly prepared 1:1 mixture of Almar Blue reagent and 10% tween 80 was added to the plate and incubated for 24 hrs.
- 8) A blue color in the well was interpreted as no bacterial growth, and pink color was scored as growth.
- 9) The MIC was defined as lowest drug concentration which prevented the color change from blue to pink.

### ***6.3. Results and Discussions***

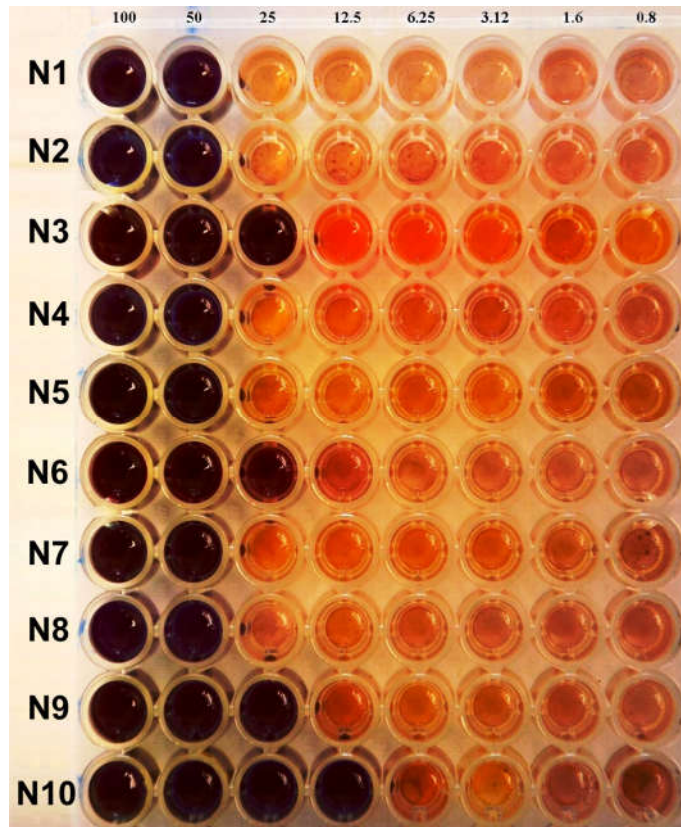
All the synthesized compounds were screened for their *in-vitro* antimycobacterial activity against MTB (H37RV, ATCC No: 27294) using Almar Blue assay (MABA). Pyrazinamide, Ciprofloxacin and streptomycin were used as reference drugs. The results as minimum inhibitory concentration (MIC) (**Figure 13**) are presented in **Table 9**.

When screened against MTB the synthesized compounds **N1-N20, GA, GAC, GAC1, GAC5, GAC6, GAC7, GAE, GAEA, GAM and GAT** showed moderate to potent *in vitro* activity against MTB with MIC range **0.05-50 µg/ml**. Compounds **N18, N11 and N20** displayed most potent *in-vitro* activity with MICs **0.05, 0.1, 0.2 µg/ml** concentrations respectively. Further, compounds **N14, N17, N19, N13, N15, N16 and N12** showed potent *in-vitro* activity with MIC range **0.4 to 1.6 µg/ml** concentrations, while the other compounds showed moderate to good activity. Based on the *in-vitro* antimycobacterial results, it is clear that the synthesized thiazolidinone derivatives show remarkable activity when compared with standard drugs and the synthesized dioxolane derivatives.

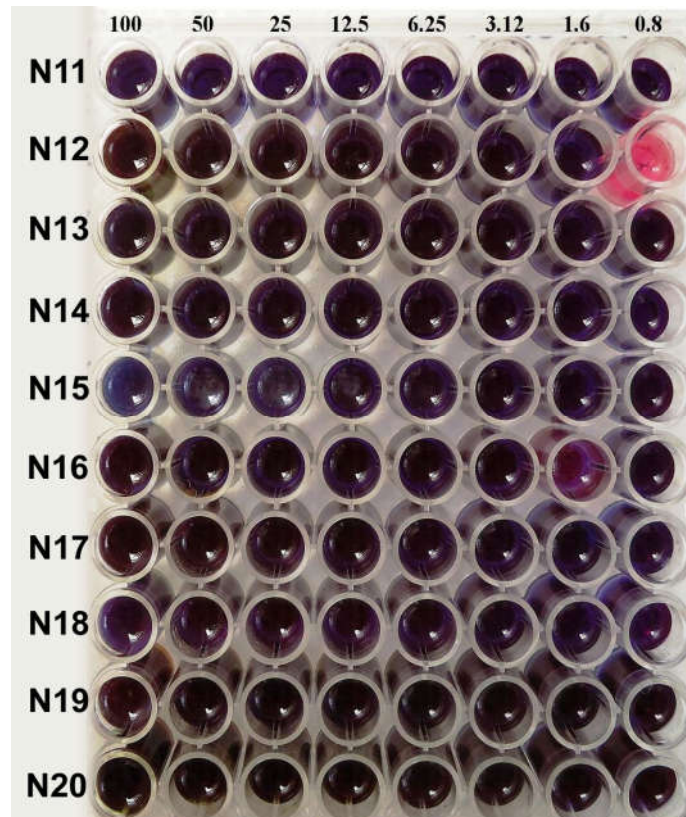
The influence of the different chemical groups on the observed antimycobacterial activity against MTB deserves comment. Incorporation of nitro group at 3<sup>rd</sup> position of the phenyl ring (**Compound N18**) led to show potent inhibition of *M tuberculosis* at 0.05 µg/ml concentration, while nitro position at 2<sup>nd</sup> and 4<sup>th</sup> position of the phenyl ring (**Compound N17 and N7**) led to reduction of the activity 8 and 100 times respectively. Introduction of mono-methoxy group at 4<sup>th</sup> position of the phenyl ring (**Compound N11**) also exhibited potent inhibition at 0.1 µg/ml concentration, while tri-methoxy group at 3<sup>rd</sup>, 4<sup>th</sup> and 5<sup>th</sup> positions (**Compound N14**) reduced the activity 8 times. The phenyl substitution (**Compound N1**) showed moderate activity at 50 µg/ml concentration whereas there is a tenfold increase in activity in case of naphthalen and anthracen aromatic hydrocarbon substitution (**Compound N15 and N16**). Conversely five membered heterocyclic rings in the place of six membered rings (**Compound N10, N12, N13, N19 and N20**) increased the activity remarkably. Furthermore halogen substitution of the phenyl ring (**Compound N2, N8 and N9**) showed moderate activity.



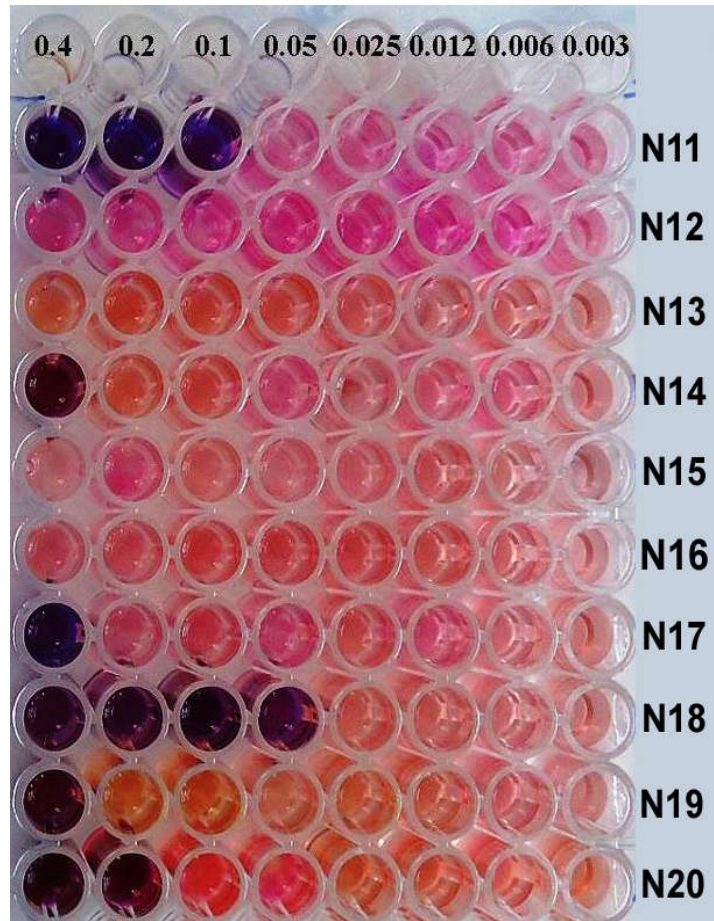
A)



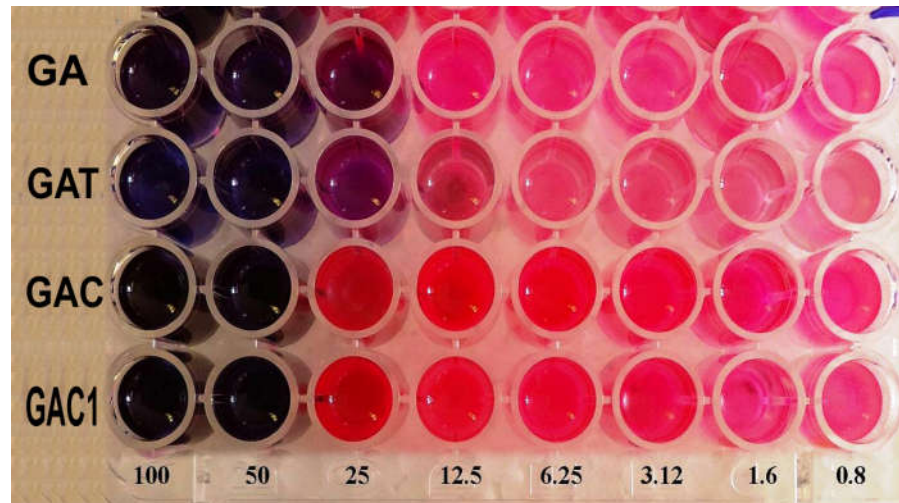
B)

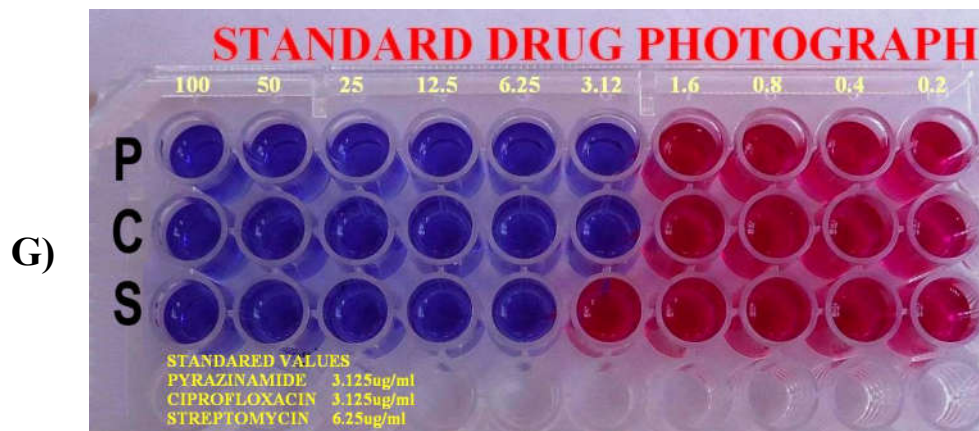
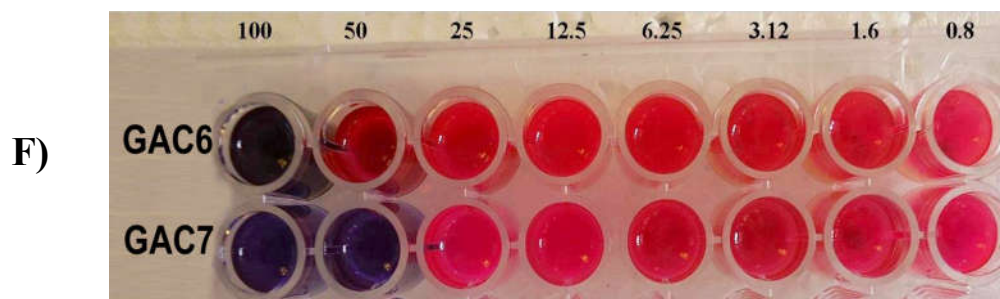
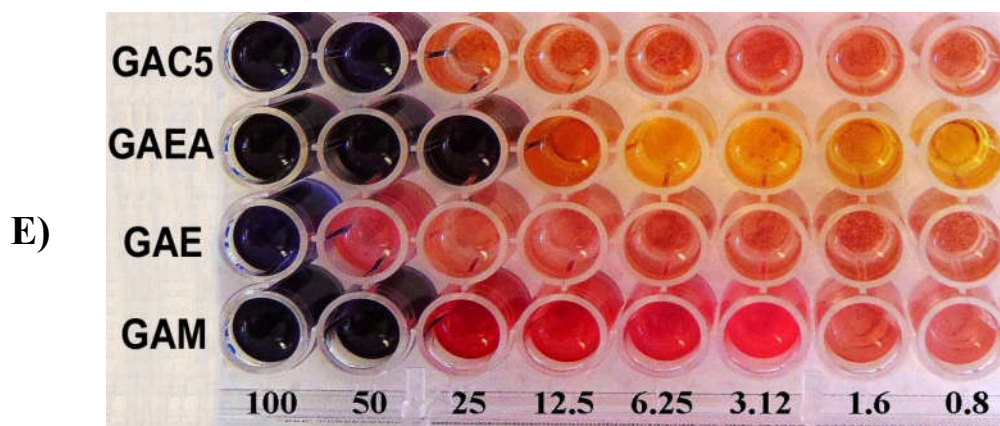


C)



D)





**Figure13:** A) Antimycobacterial activity of compounds N1-N10 tested at 100-0.8 µg/ml concentrations. B) Antimycobacterial activity of compounds N11-N20 tested at 100-0.8 µg/ml concentrations. C) Antimycobacterial activity of compounds N11-N20 tested at 0.4-0.003 µg/ml concentrations. D) Antimycobacterial activity of compounds GA, GAT, GAC and GAC1 tested at 100-0.8 µg/ml concentrations. E) Antimycobacterial activity of compounds GAC5, GAEA, GAE and GAM tested at 100-0.8 µg/ml concentrations. F) Antimycobacterial activity of compounds GAC6 and GAC7 tested at 100-0.8 µg/ml concentrations. G) Antimycobacterial activity of standard drugs Pyrazinamide, Ciprofloxacin and Streptomycin.

**Table 9: Ranking of the compounds based on the *in-vitro* antimycobacterial activity**

Rank	Compounds	MIC* ( $\mu\text{g/ml}$ )	Rank	Compounds	MIC* ( $\mu\text{g/ml}$ )
1	N18	0.05	16	N6	25
2	N11	0.1	17	GA	25
3	N20	0.2	18	N5	50
4	N17	0.4	19	GAM	50
5	N19	0.4	20	GAC1	50
6	N14	0.4	21	GAC5	50
7	N13	0.8	22	GAC	50
8	N15	0.8	23	N8	50
9	N16	0.8	24	N7	50
10	N12	1.6	25	N4	50
11	N10	12.25	26	N2	50
12	GAT	12.25	27	N1	50
13	GAEA	25	28	GAC7	50
14	N9	25	29	GAE	100
15	N3	25	30	GAC6	100

\*MIC-based on the “as lowest drug concentration which prevented the color change from blue to pink”.

# CHAPTER 7

## MULTIPLE *DOCKING* ANALYSIS AND MOLECULAR DYNAMIC SIMULATION STUDIES

### 7.1. Multiple Docking Analysis

As per the initial docking results, all the ligands showed better interactions with the active sites of target enzymes. On comparing the *in-vitro* antitubercular activity results with the docking results of the compounds against target enzyme InhA (PDB id – 2NSD), there is no good agreement with the results. Hence, to correlate the *in-vitro* antimycobacterial activity results with the docking results and to find out the plausible mechanism by which the compounds would have exhibited the activity, multiple docking analyses was performed. The study was also supported by the literature Zhou Z *et al.*,<sup>95</sup> (2007). They studied the “importance of docking into multiple receptor structures in decreasing the docking errors, when screening a diverse set of active compounds”.

#### 7.1.1. Materials

- The compounds which showed *in-vitro* antimycobacterial activity at less than 12.5 µg/ml concentrations were selected for the multiple docking analyses. A total of 12 compounds were selected, and the compounds codes were as follows, **N10, N11 to N20** and **GAT**.
- The multiple *Mtb* target enzymes used in the study are Thymidylate Kinase (PDB id – 1G3U), Diaminopimelate Decarboxylase (PDB id – 1HKV), Cyclopropane Synthase (PDB id – 1L1E), Antibiotic Resistance Protein (PDB id – 1YK3), TrpD essential for lung colonization (PDB id – 1ZVW), Thymidylate Synthase X (PDB id – 2AF6), Protein Kinase G (PDB id – 2PZI),

Gyrase TypeIIA Topoisomerase (PDB id – 3UC1), L, D Transpeptidase 2 (PDB id – 3VAE) were also downloaded from Protein Data Bank.

- All the computational works including softwares used in the multiple docking studies were in the similar manner as in the initial docking study for target enzyme InhA (PDB id – 2NSD).

### **7.1.2. Experimental**

- The LigPrep structures of the compounds (**N10, N11 to N20 and GAT**) for the multiple docking studies were selected from the *Project table* panel as selected entries.
- Protein preparation task and the binding site analysis for the above enzymes were performed in the similar manner as performed for the initial target enzyme InhA (PDB id – 2NSD).
- All the docking studies of the compounds (**N10, N11 to N20 and GAT**) against the multiple target enzymes were performed in Glide Extra precision (XP) mode, and the protocol was followed in the similar manner as in the initial study.

### **7.1.3. Results and Discussions**

The overall glide docking scores of all the studied compounds (**N10, N11 to N20 and GAT**) ranges from -10.31 to -2.53 kcal/mol on all the target enzymes and were summarized in **Table 10**. On comparing the multiple docking results of the studied compounds with their *in-vitro* antitubercular activity results/ranks, top-ranked compounds of the *in-vitro* antitubercular activity shows deviation from the docking score rankings in all the studied target enzymes.

**Table 10:** Glide docking scores of selected compounds (N10, N11 to N20 and GAT) against multiple target enzymes

Entry	Glide docking scores in kcal/mol																	
	1G3U		1HKV		1L1E		1YK3		1ZVW		2AF6		2PZI		3UCI		3VAE	
	G-scores	R	G-scores	R	G-scores	R	G-scores	R	G-scores	R	G-scores	R	G-scores	R	G-scores	R	G-scores	R
<b>N10</b>	-3.5	11	-1.83	9	-6.23	7	-5.44	2	-4.72	5	-3.31	12	-7.48	3	-4.47	4	-4.38	9
<b>N11</b>	-7.62	1	-1.35	10	-5.69	10	-5.21	3	-4.76	4	-3.82	5	-6.76	8	-3.18	12	-3.22	12
<b>N12</b>	-7.3	3	-3.15	1	-4.35	12	-4.67	11	-3.51	12	-3.74	6	-7.29	4	-3.91	7	-5.41	4
<b>N13</b>	-6.75	5	-2.8	3	-6.42	4	-4.85	7	-3.76	11	-3.57	10	-6.91	6	-4.03	6	-3.24	11
<b>N14</b>	-4.49	8	-2.61	5	-6.38	6	-5.19	5	-4.62	6	-4.77	1	-5.18	11	-3.55	9	-4.74	7
<b>N15</b>	-5.33	6	-3.01	2	-6.4	5	-5.2	4	-4.79	3	-3.41	11	-7.66	2	-3.55	10	-4.07	10
<b>N16</b>	-3.39	10	-1.97	8	-5.94	9	-6.58	1	-5.33	2	-3.84	4	-8.89	1	-3.89	8	-6.33	1
<b>N17</b>	-4.29	9	-2.31	6	-4.76	11	-4.77	9	-4.33	8	-3.68	8	-5.87	9	-4.28	3	-6.33	2
<b>N18</b>	-6.88	4	-1.76	11	-7.09	3	-4.68	10	-3.81	9	-3.67	9	-5.16	12	-4.22	2	-4.5	8
<b>N19</b>	-5.26	7	-0.64	12	-8.33	1	-4.28	12	-5.64	1	-4.44	2	-6.93	5	-5.42	1	-5	6
<b>N20</b>	-7.44	2	-2.74	4	-6.01	8	-4.83	8	-3.79	10	-4.03	3	-6.89	7	-4.18	5	-5.13	5
<b>GAT</b>	-2.53	12	-1.98	7	-7.16	2	-5.19	6	-4.45	7	-3.7	7	-5.45	10	-3.48	11	-5.77	3

**G-Scores-** Glide docking Scores, **R-** Ranking of compounds based on their docking scores.

In order to rationalize the correlation between the *in-vitro* antitubercular activity and multi-target docking results a cross observational analysis was performed. The top-ranked three compounds (**N18, N11 and N20**) of *in-vitro* antitubercular activity were cross observed with their docking ranks on all the studied target enzymes for their deviations in their ranks. The results are given in **Table 11**.

**Table 11:** Cross observational analysis of top three ranked compounds with docking ranks

Target Enzymes (PDB id)	Ranking positions based on docking scores		
	N18 <sup>a</sup>	N11 <sup>a</sup>	N20 <sup>a</sup>
<b>Thymidylate Kinase (1G3U)</b>	4	1	2
<b>Diaminopimelate Decarboxylase (1HKV)</b>	11	10	4
<b>Cyclopropane Synthase (1L1E)</b>	3	10	8
<b>Antibiotic Resistance Protein (1YK3)</b>	10	3	8
<b>TrpD essential for lung colonization (1ZVW)</b>	9	4	10
<b>Thymidylate Synthase X (2AF6)</b>	9	5	3
<b>Protein Kinase G (2PZI)</b>	12	8	7
<b>Gyrase TypeIIA Topoisomerase (3UC1)</b>	2	12	5
<b>L, D Transpeptidase 2 (3VAE)</b>	8	12	5

<sup>a</sup> - top three ranked compounds (**N18-1<sup>st</sup>, N11-2<sup>nd</sup> and N20-3<sup>rd</sup>**) in *in-vitro* antitubercular activity.

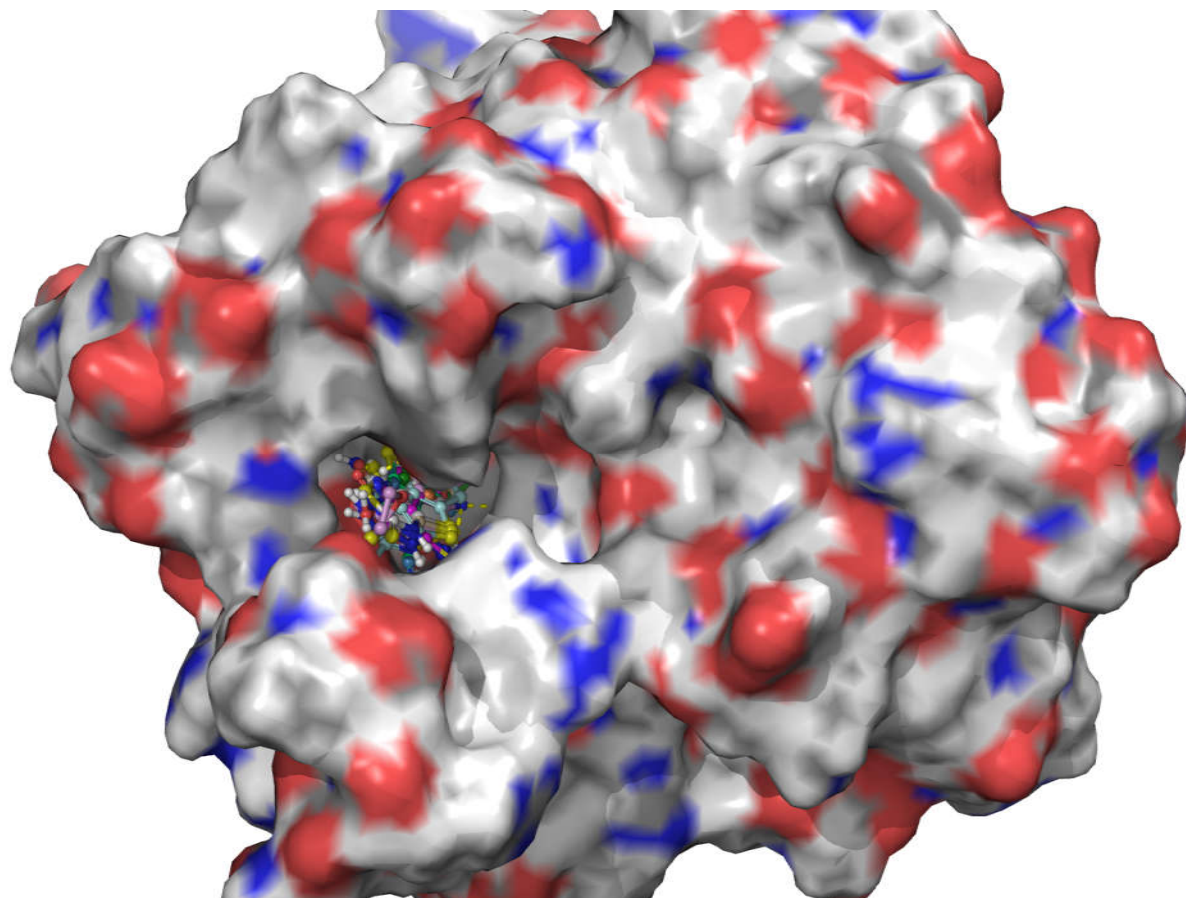
Based upon the results, the docking pose ranking of all the three compounds (**N18, N11 and N20**) showed marginal deviation in thymidylate kinase (PDB id – 1G3U) target enzyme at 4<sup>th</sup>, 1<sup>st</sup> and 2<sup>nd</sup> ranks respectively when compared with docking



pose rankings of other studied target enzymes. Additionally top three ranked *in-vitro* antitubercular compounds lies within top four positions in thymidylate kinase (PDB id – 1G3U) target enzyme. Thus the study warrants the elimination of false negatives and rationalizes that the enzyme **thymidylate kinase** would be the plausible target for the tested compounds for their *in-vitro* antitubercular activity.

The docked poses of all the studied compounds (**N10, N11 to N20** and **GAT**) at the active site of thymidylate kinase target is shown in **Figure 14**. The major interactions by the ligands with thymidylate kinase can be categorized as hydrogen bonding, hydrophobic, electrostatic interactions,  $\pi$ - $\pi$ -stacking and  $\pi$ -cation-stacking, which are critical for stabilizing the inhibitors inside the binding pocket of the receptor. The important interactions are shown in **Table 12**.

The amino acid Asn100 displays strong hydrogen bond interaction with the inhibitors. Arg74 and Tyr39 participate in hydrogen bond interaction in only one inhibitor each, along with Asn100. Other amino acids like Asp163, Arg95, Lys13 and Gly59 also contribute to the hydrogen bonding in some inhibitors. The inhibitors had successfully influenced hydrophobic effect in Tyr39, Tyr103, Tyr165, Pro37, Phe70 and Leu52. Other amino acids like Ala67, Ala35, Ala49, Met66, Val63 and Phe36 also contribute to the hydrophobic interactions. Electrostatic interactions are predominant in inhibitors having interactions with amino acids like Arg74, Arg95, Arg160, Glu166, Asp9 and Asp163. Other weak interactions like  $\pi$ -cation-stacking and  $\pi$ - $\pi$ -stacking are witnessed in most of the inhibitors with their aromatic group positioned near Arg95, Tyr103 and Phe70. The docked compounds with their ligand interactions are shown in **Figure 15**.



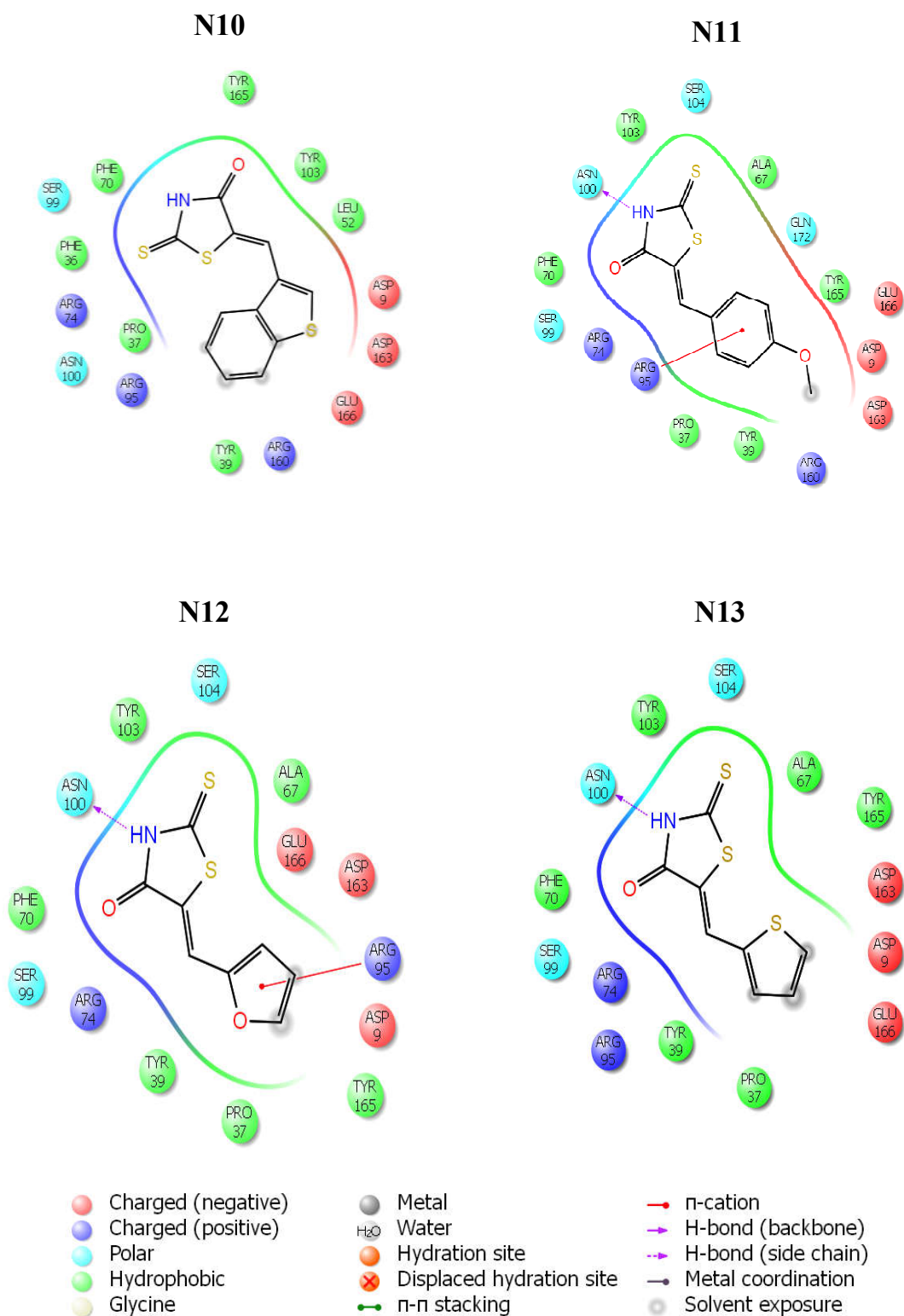
**Figure 14:** The docked poses of the all the studied compounds (N10, N11 to N20 and GAT) at the active site of thymidylate kinase

**Table 12:** Residue interaction pattern for all the studied compounds (N10, N11 to N20 and GAT) against thymidylate kinase

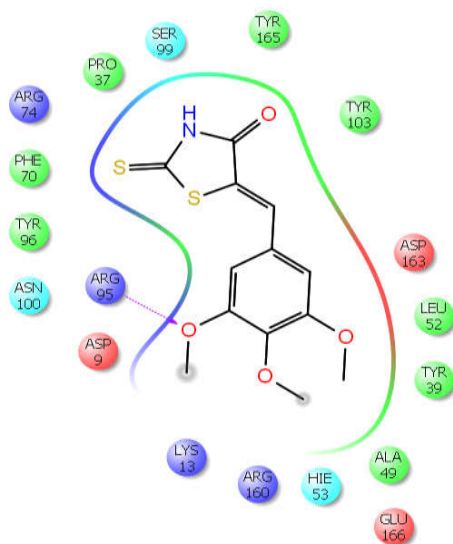
Compounds	Important Interactions of Ligands with amino acids of binding site of thymidylate kinase (1G3U)				
	Hydrogen Bonding	Hydrophobic	Positive Ionizable	Negative Ionizable	Polar
N10	-	Phe70, Phe36, Pro37, Tyr39, Leu52, Tyr103, Tyr165	Asp9, Asp163, Glu166	Arg74, Arg95, Arg160	Ser99, Asn100
N11	Asn100, $\pi$ -cation-stacking-Arg95	Tyr103, Phe70, Pro37, Tyr39, Tyr165, Ala67	Asp9, Asp163, Glu166	Arg74, Arg95, Arg160	Ser99, Asn100, Ser104, Gln172
N12	Asn100, $\pi$ -cation-stacking-Arg95	Tyr103, Phe70, Pro37, Tyr39, Tyr165, Ala67	Asp9, Asp163, Glu166	Arg74, Arg95	Ser99, Asn100, Ser104
N13	Asn100	Tyr103, Phe70, Pro37, Tyr39, Tyr165, Ala67	Asp9, Asp163, Glu166	Arg74, Arg95	Ser99, Asn100, Ser104
N14	Arg95	Pro37, Phe70, Tyr96, Ala49, Tyr39, Leu52, Tyr103, Tyr165	Asp9, Asp163, Glu166	Arg74, Arg95, Lys13, Arg160	Ser99, Asn100, Hie53
N15	Asn100, $\pi$ -cation-stacking-Arg95	Phe70, Phe36, Pro37, Tyr39, Leu52, Tyr103, Tyr16, Ala67	Asp9, Asp163, Glu166	Arg74, Arg95, Arg160	Ser99, Asn100, Ser104

<b>N16</b>	Lys13	Phe70, Tyr103, Tyr39, Pro37, Ala35, Ala49, Leu52, Tyr165	Asp9, Asp163, Asp94	Lys13, Arg95, Arg14, Arg160	Ser99, Hie53
<b>N17</b>	-	Phe70, Tyr96, Pro37, Phe36, Tyr39, Tyr103, Tyr165	Asp9, Asp163, Glu166	Arg74, Arg95, Arg160	Ser99, Asn100, Ser104
<b>N18</b>	Asn100, Tyr39, $\pi$ - cation- stacking- Arg95	Tyr103, Phe36, Phe70, Pro37, Tyr39, Ala67, Tyr165	Asp9, Asp163, Glu166	Arg74, Arg95, Arg160	Ser99, Asn100, Ser104, Gln172
<b>N19</b>	Asn100, $\pi$ -cation- stacking- Arg95	Phe70, Phe36, Pro37, Tyr39, Tyr103, Ala67, Tyr165	Asp9, Asp163, Glu166	Arg74, Arg95, Arg160	Ser99, Asn100, Ser104
<b>N20</b>	Asn100	Phe70, Pro37, Tyr165, Tyr103, Met66, Val63, Ala67	-	Arg74, Arg95, Arg107	Ser99, Asn100, Ser104
<b>GAT</b>	Arg74, Asn100	Phe36, Pro37, Tyr39, Tyr165, Leu52, Tyr103, Phe70, Ala67, $\pi$ - $\pi$ -stacking- Phe70	Arg74, Arg95	Glu166, Asp9, Asp163	Ser99, Asn100

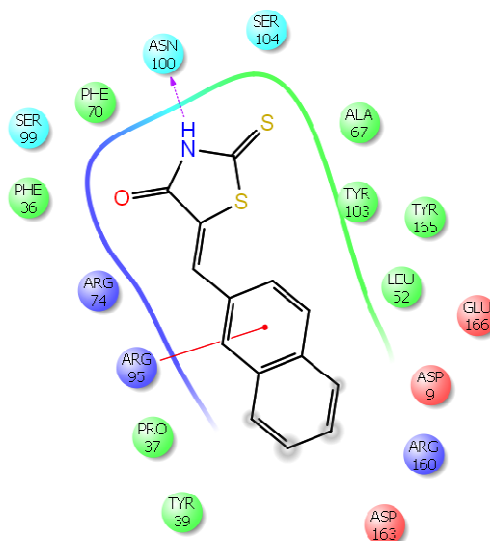
**Figure 15:** Ligand interaction diagrams of all the studied compounds (N10, N11 to N20 and GAT) against the binding site of target enzyme thymidylate kinase (1G3U)



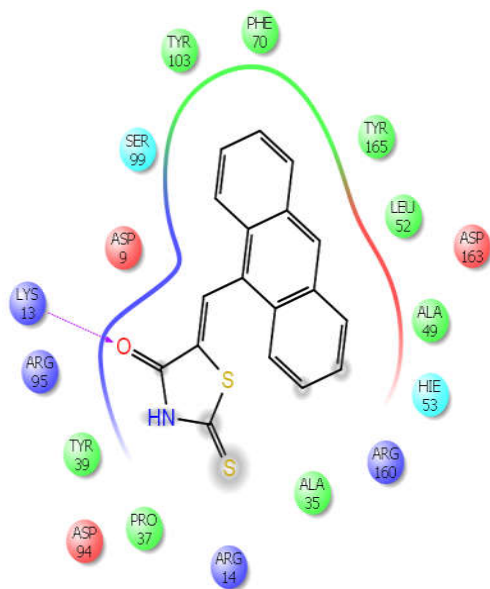
**N14**



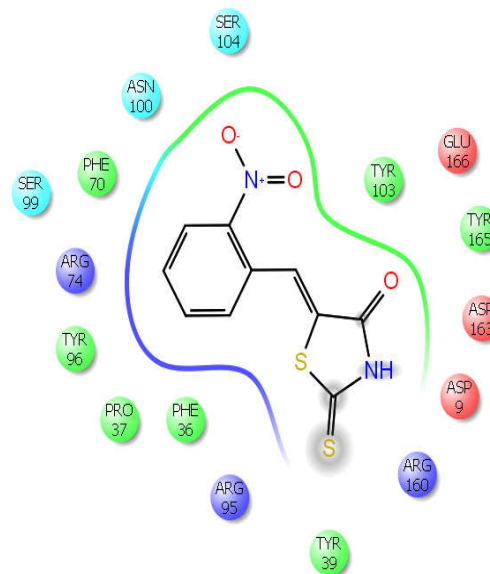
**N15**



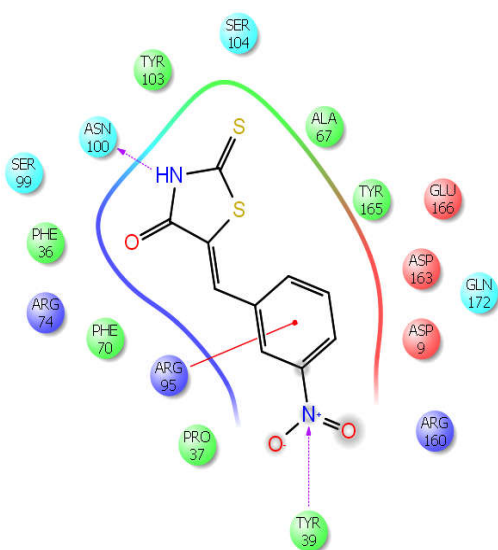
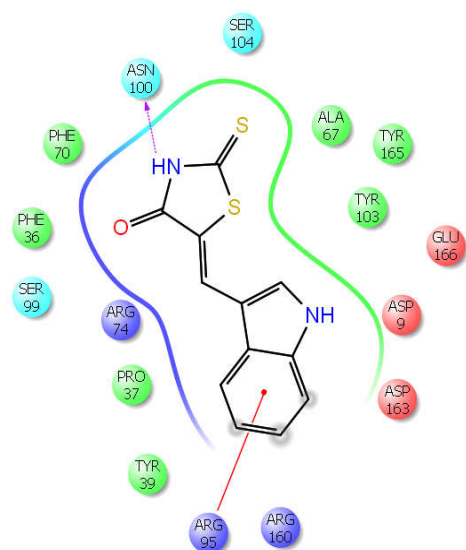
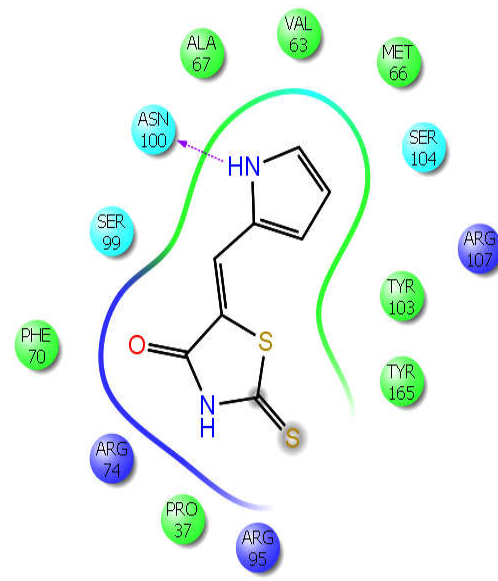
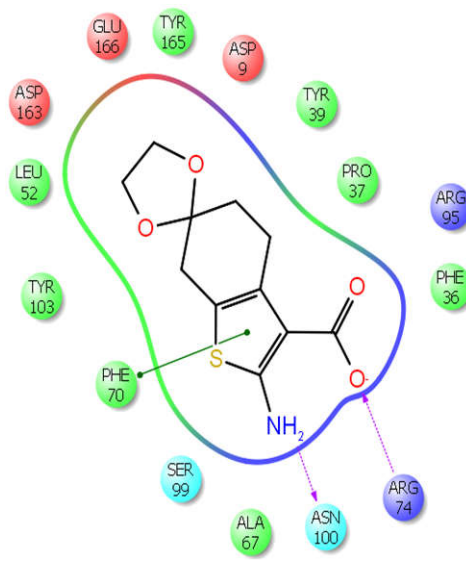
**N16**



**N17**



- |  |  |   |
|--|--|---|
| <span style="color: red;">●</span> Charged (negative)  | <span style="color: grey;">●</span> Metal                      | <span style="color: red;">→</span> n-cation               |
| <span style="color: blue;">●</span> Charged (positive) | <span style="color: grey;">●</span> H <sub>2</sub> O Water     | <span style="color: purple;">→</span> H-bond (backbone)   |
| <span style="color: cyan;">●</span> Polar              | <span style="color: orange;">●</span> Hydration site           | <span style="color: purple;">→</span> H-bond (side chain) |
| <span style="color: green;">●</span> Hydrophobic       | <span style="color: orange;">⊗</span> Displaced hydration site | <span style="color: blue;">→</span> Metal coordination    |
| <span style="color: yellow;">●</span> Glycine          | <span style="color: green;">→</span> n-n stacking              | <span style="color: grey;">○</span> Solvent exposure      |

**N18****N19****N20****GAT**

- Charged (negative)
- Charged (positive)
- Polar
- Hydrophobic
- Glycine

- Metal
- H<sub>2</sub>O Water
- Hydration site
- ⊗ Displaced hydration site
- n-n stacking

- n-cation
- H-bond (backbone)
- H-bond (side chain)
- Metal coordination
- Solvent exposure

## ***7.2. Molecular Dynamic Simulation***

The Extra Precision (XP) docking results gave an idea, about the rational binding modalities of the ligand molecules at the target site and also helped in the determination of the amino acid residues which are engaged with the ligand recognition. However, a molecular dynamic simulation study was performed for the ligand-receptor complex in order to further explore the binding modalities of the ligand. Hence, top-ranked 3 ligand-receptor complexes were selected for the study. The aim of molecular dynamic simulation was to acquire a more suitable ligand-receptor model, which is close to the natural conditions and to further investigate the binding modalities of the ligand, in the view of the fact that even smaller variances are also accountable by the molecular dynamic simulation.

### ***7.2.1. Materials***

- Desmond v3.1 (Schrodinger<sup>®</sup>) software was used to perform molecular dynamics simulation studies.
- The ligands **N18-1G3U**, **N11-1G3U** and **N20-1G3U** (-thymidylate kinase) complex (top-ranked docking ligand-receptor complex) were chosen for the study.

### ***7.2.1. Experimental***

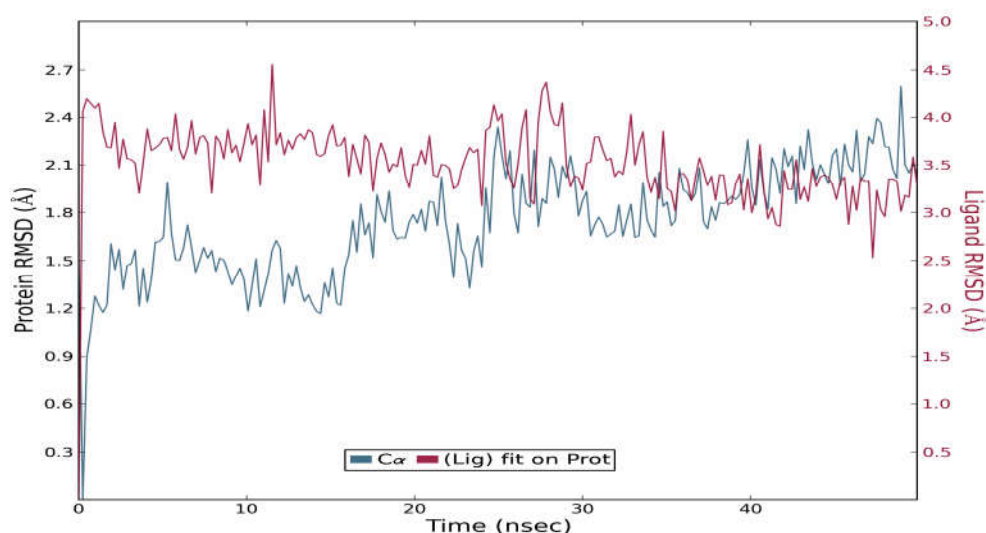
- The explicit molecular dynamics study of the ligand–receptor was carried out using Desmond<sup>®</sup> (Schrodinger<sup>®</sup>) and analyzed with Maestro's trajectory Visualizer.
- It was performed to assess the change in the structure of the binding site and active site.



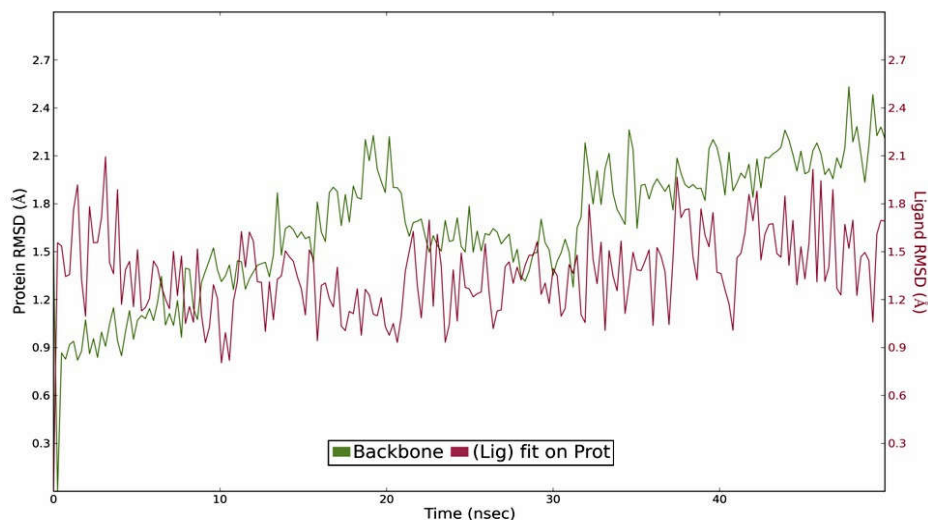
- The cell shape was orthorhombic. The water molecules were modeled with TIP3P. Ion neutralizer option was selected to balance the charge of the system.
- After a short minimization step and equilibrium run, the main MD simulation was performed. NVT ensemble with set temperature of 300K was used.
- The time step was set as 50ns. Desmond (Schrodinger<sup>®</sup>) uses, by default, a cutoff distance of 9Å and Ewald summation for long range columbic interactions. OPLS 2005 force field was used.

### 7.2.3. Results and Discussions

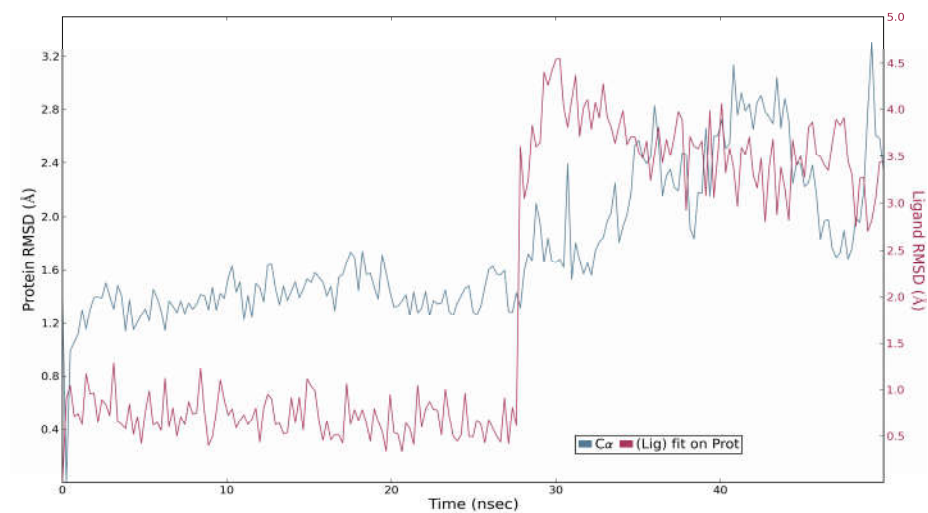
The conformational stability of the studied ligand-receptor complexes (**N18-1G3U**, **N11-1G3U** and **N20-1G3U**) in the simulation procedure was assessed by carrying out a 50ns (nanoseconds) molecular dynamic simulation using Desmond (Schrodinger<sup>®</sup>) and analyzed with Maestro's trajectory Visualizer. The trajectories were stable throughout the MD simulation run. The trajectory stability was checked and was substantiated by the analysis of protein-ligand RMSD (Root Mean Square Deviation). The RMSD evolution of the studied ligand-receptor complexes are shown in **Figure 16**, **17 & 18**.



**Figure 16:** Plot showing Protein-Ligand (**N18-1G3U**) RMSD evolution



**Figure 17:** Plot showing Protein-Ligand (N11-1G3U) RMSD evolution



**Figure 18:** Plot showing Protein-Ligand (N20-1G3U) RMSD evolution

**Figure 16, 17 & 18** reveals that the protein RMSD values (left Y-axis) of **N18-1G3U**, **N11-1G3U** and **N20-1G3U** complexes have some acceptable fluctuations which did not exceeded  $\sim 2.5\text{\AA}$ ,  $\sim 2.6\text{\AA}$  and  $\sim 3.2\text{\AA}$  respectively, throughout the MD simulation run. All the ligand complexes end with the protein RMSD values at below  $\sim 2.4\text{\AA}$ , at end of the simulation run. This indicates that the protein is stable without any notable conformational changes during the simulation run.

In case of ligand RMSD (right Y-axis) of **N18-1G3U**, **N11-1G3U** and **N20-1G3U** complexes, some acceptable fluctuations were observed and at the end of simulation run, the ligand RMSD values were found to be  $\sim 3.3\text{\AA}$ ,  $\sim 2.1\text{\AA}$ ,  $\sim 3.4\text{\AA}$  respectively. This shows the ligands in the protein-ligand complexes were found to be more stable, in which ligand in **N11-1G3U** complex found to be with greater stability as it has very low RMSD deviations of only  $\sim 2.1\text{\AA}$ , when compared to the other two ligand RMSD values. Moreover the observed ligand RMSD values of all the ligand complexes are smaller than their Protein RMSD values, which indicate the stability of the ligand with respect to the protein and its binding pocket.

At the end of the MD simulation, position and orientation of ligand in the introduced binding site were changed and this important observation indicates useful application of MD simulation after docking of ligands in the binding site.

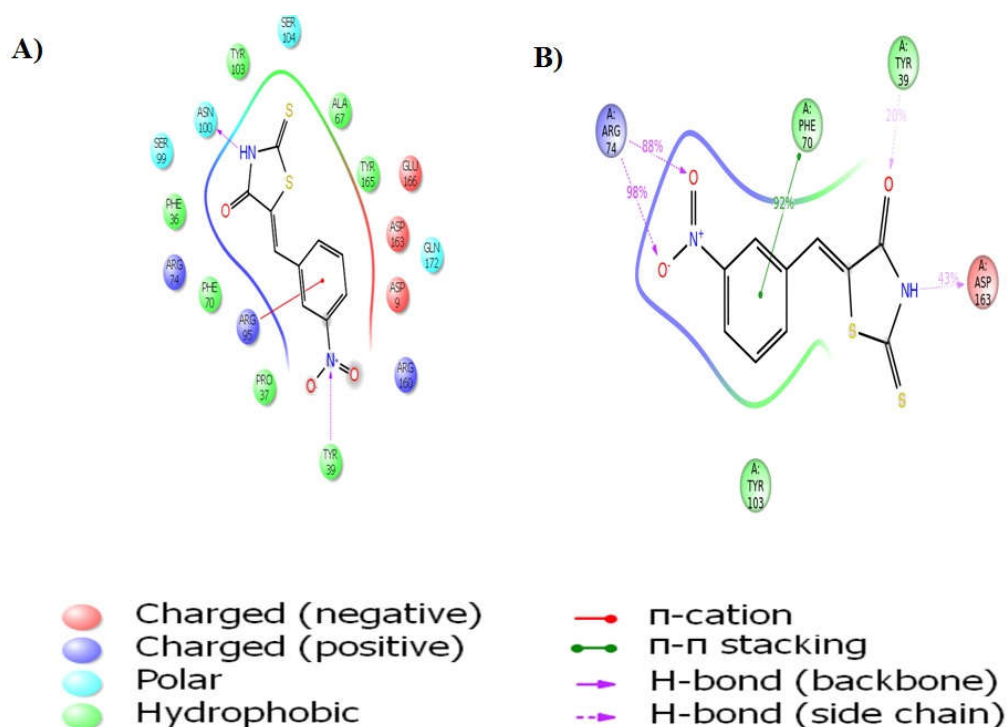
Explorative run of the MD simulation on the **N18-1G3U** complex revealed that except for Arg95, Asp163, Tyr39, Tyr103 and Phe70 the rest of residues of the active site determined by docking were changed. The residues such as Arg95, Asp163 and Phe70 are newly positioned in proximity of ligand and participated in the interaction. At the end of MD simulation a two new hydrogen bonding was found to exist between docked molecule and Arg95 and Asp163. Compound **N18** is also stabilized by an extra hydrophobic  $\pi$ - $\pi$ -stacking interaction with the retained Phe70 which does not exist before MD simulation. On the other end, the hydrophobic interactions (Phe36, Pro37, Ala67 and Tyr165) and electrostatic interactions (Asp9, Glu166, Arg74 and Arg160) with the ligand were vanished. Along with this one hydrogen bond interaction (Asn100) with the ligand was also vanished. conclusively, the difference in the orientation of ligand **N18** in binding modes after MD simulation was also noticed.

Explorative run of the MD simulation on the **N11-1G3U** complex revealed that except for Asn100, Arg95, Tyr165 and Phe70 the rest of residues of the active site determined by docking were changed. The residues such as Tyr103 and Arg74 are newly positioned in proximity of ligand and participated in the interaction. At the end of MD simulation a new hydrogen bonding was found to exist between docked molecule and Arg74. compound **N11** is also stabilized by an extra hydrophobic  $\pi$ - $\pi$ -stacking interaction with Tyr103 which does not exist before MD simulation. On the other end, the hydrophobic interactions (Ala67, Pro37 and Tyr39) and electrostatic interactions (Arg160, Glu66, Asp9 and Asp163) with the ligand were vanished. Finally, the difference in the orientation of ligand **N11** in binding modes after MD simulation was also noticed.

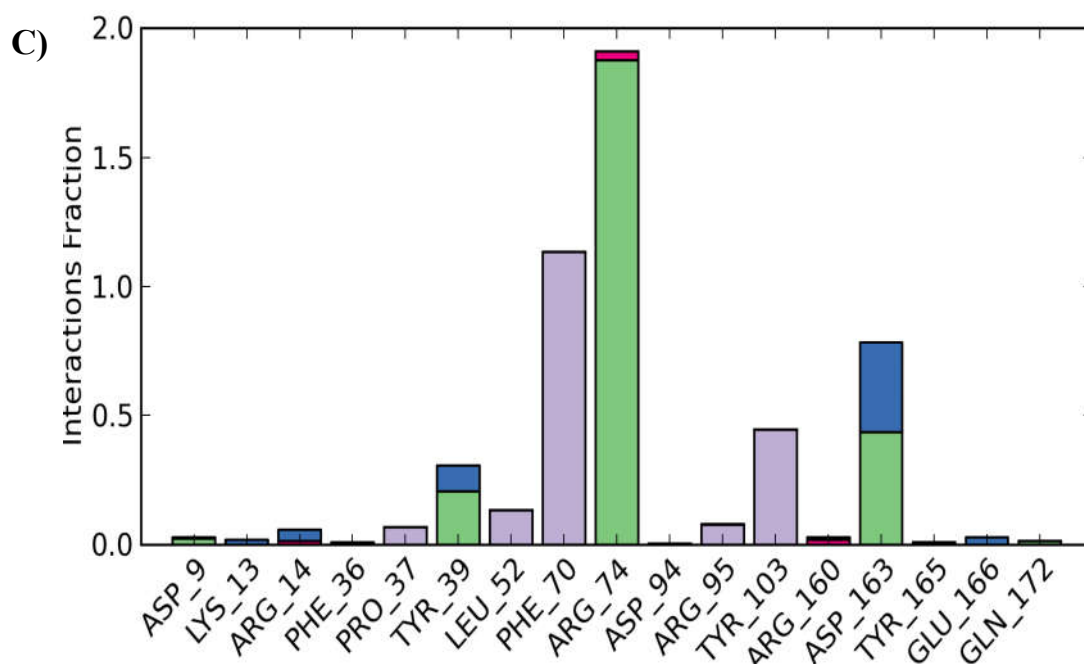
Explorative run of the MD simulation on the **N20-1G3U** complex revealed that except Asn100, Arg95, Arg74, Tyr103, Arg107, Ser104 and Phe70 the rest of residues of the active site determined by docking were changed. The residues such as Arg74, Ser104, Lys13, Tyr103, and Arg95 are newly positioned in proximity of ligand and participated in the interaction. At the end of MD simulation a two new hydrogen bonding was found to exist between docked molecule and Arg74 and Ser104. Compound **N20** is also stabilized by an extra hydrophobic  $\pi$ - $\pi$ -stacking interaction with the retained Tyr103, and two extra  $\pi$ -cation stacking interaction with the Lys13 and Arg95, which does not exist before MD simulation. On the other end, the hydrophobic interactions (Pro37, Tyr165, Met66, Val63 and Ala67) with the ligand were vanished. At last, the change in the orientation of ligand **N20** in binding modes after MD simulation was also noticed.

These results revealed that MD simulation obligate ligand to optimize its orientation and distance to binding site for maximum interaction with receptor. On

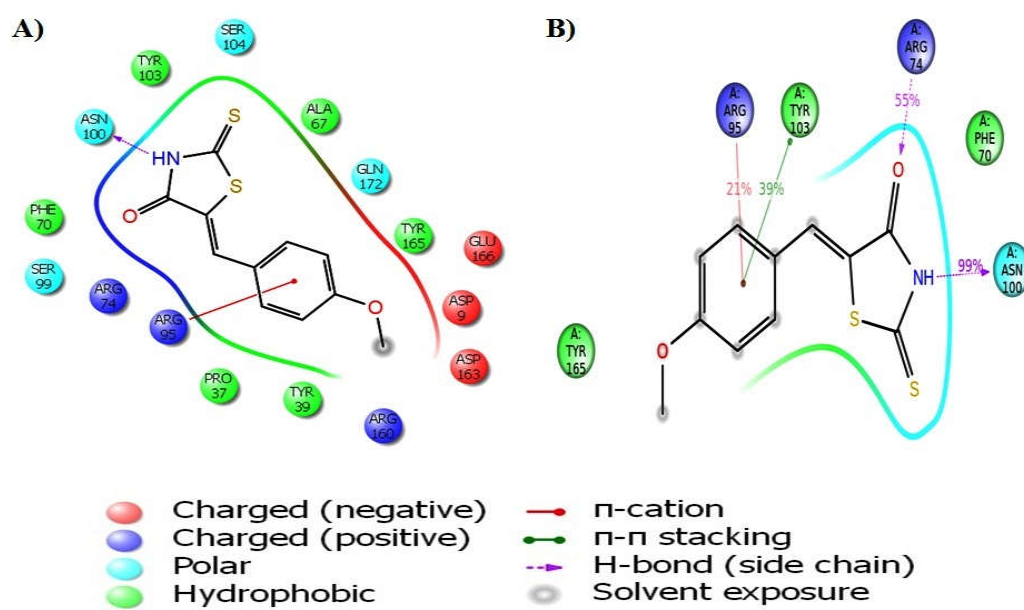
docking of compounds **N18**, **N11** and **N20** against **1G3U**, the lowest energy confirmation did not show any observed changes due to the absence of appropriate orientation and distance as was observed at the MD simulation. Ligand interaction pattern with percentage of contacts (interactions that occur more than 20.0% of the simulation time) of the ligands **N18**, **N11** and **N20** against **1G3U** & BAR representation of the conserved binding site residues which influenced compounds **N18**, **N11** and **N20** against **1G3U** were shown in **Figure 19, 20 & 21**.



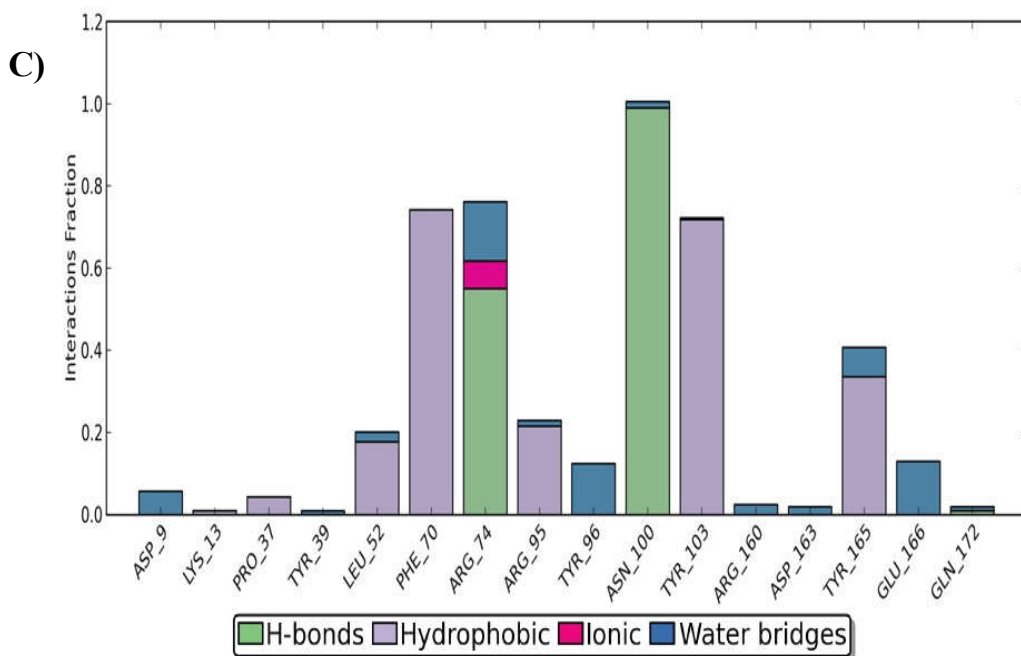
**Figure 19:** **A)** Ligand interaction pattern of the ligand **N18** against **1G3U** before MD simulation. **B)** Ligand interaction pattern with percentage of contacts of the ligand **N18** against **1G3U** after MD simulation.



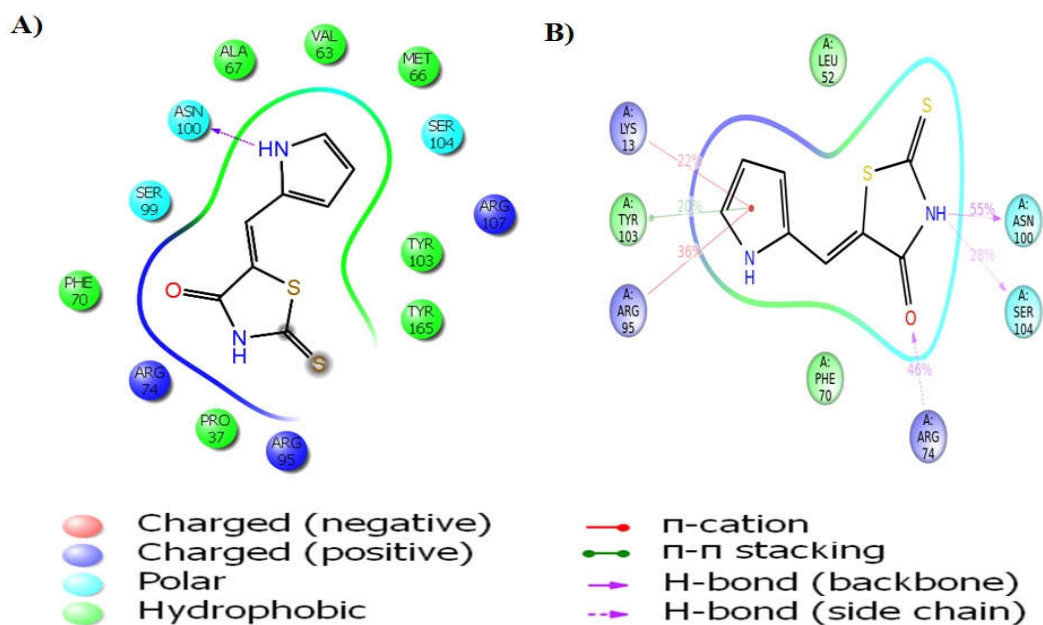
**Figure 19:** C) BAR representation of the conserved binding site residues which influenced compound N18 against 1G3U.



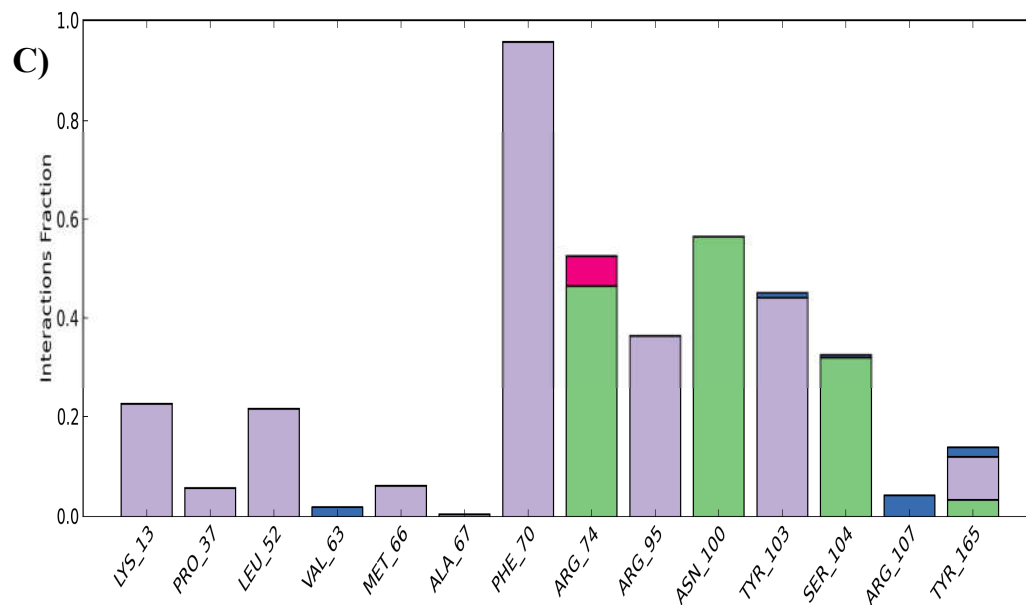
**Figure 20:** A) Ligand interaction pattern of the ligand N11 against 1G3U before MD simulation. B) Ligand interaction pattern with percentage of contacts of the ligand N11 against 1G3U after MD simulation.



**Figure 20:** C) BAR representation of the conserved binding site residues which influenced compound N11 against 1G3U.



**Figure 21:** A) Ligand interaction pattern of the ligand N20 against 1G3U before MD simulation. B) Ligand interaction pattern with percentage of contacts of the ligand N20 against 1G3U after MD simulation.



**Figure 21: C)** BAR representation of the conserved binding site residues which influenced compound **N11** against **1G3U**.



## CHAPTER 8

### *In-Vivo Efficacy*

All the animal experiments have been carried out according to the internationally valid guidelines and they are approved by the “Institutional Animal Ethical Committee [IAEC] of Committee for the Purpose of Control and Supervision on Experimentation on Animals [CPCSEA]”.

- ✓ Vide sanction letter no. 19/243/CPCSEA/IAEC/2014.
- ✓ Vide sanction letter no. 1/243/CPCSEA/IAEC/2015.
- ✓ Vide sanction letter no. CPCSEA/IAEC/2015/23.

#### **8.1. Acute Toxicity Study**

All the synthesized compounds exhibiting promising *in-vitro* antimycobacterial activity were subjected to acute toxicity studies in order to find out the toxicity induced mortality and other behavioral changes.

##### **8.1.1. Materials**

- Acute toxicity studies were carried out by acute oral toxic class method (OECD guidelines, 423).
- The animals used for acute toxicity studies were Swiss Albino mice (20-30 gm) of female sex, n=3/group, with one untreated control group.
- The compounds showing *in-vitro* inhibitory activity below 12.5 µg/ml concentrations against *Mycobacterium tuberculosis* were selected for acute oral toxicity studies. The selected compound codes were **N10, N11 to N20 and GAT**.

### ***8.1.2. Experimental***

*Preparation of the synthesized compounds and standard drug for the pharmacological study:*

The test compounds (**N10, N11 to N20 and GAT**) and the standard drug, **isoniazid** were administered orally in the form of suspension in water with 1 % w/v carboxy methyl cellulose (CMC) as the suspending agent.

#### ***Animals***

Mice were housed in individually caged system and provided with autoclaved pellet diet, bedding and water *ad libitum*. Animals were maintained in light and noise controlled environment. Animals were fasted for twelve hours before the experiment..

#### ***Acute oral toxicity studies***

The acute oral toxicity for the synthesized compounds was done by “acute oral toxic class method” (OECD guidelines, 423).<sup>152</sup> In this method, the toxicity of the selected synthesized compounds was tested by using step by step procedure, in each step three mice of a same sex was used. Before the commencement of study, the animals were kept under fasting for a period of three to four hours. The animals are deprived of food (but not water should be withheld) during the period of study. Following the period of fasting, the animals were weighed and the synthesized compounds were administered orally at a dose of 5 mg/kg/p.o. Animals were observed for any signs and symptoms of mortality and recorded for at least once during the first 30 min and from then for every 4 h for the first 24 h and the animals are kept under observation for a period of 14 days. Careful observations were made at least twice/day for the effect on “CNS, ANS, motor activity, salivation, skin coloration and other general signs of toxicity” were also observed and recorded.

As there was no mortality with 5 mg/kg for 14 days, the procedure was repeated for next higher doses till 2000 mg/kg/p.o. for all the selected synthesized compounds (**N3, N6, N10, N11 to N20 and GAT**).

### ***8.1.3. Results and discussion***

#### ***Acute oral toxicity***

The selected compounds (**N10, N11 to N20 and GAT**) had not shown any signs of toxicity up to 300 mg/kg body weight and was considered as safe (OECD-423 guidelines), but an unusual weight loss was observed with 2000 mg/kg body weight.

It was noticed that there was no toxicity at 300 mg/kg body weight, while some signs of toxicity at 2000 mg/kg body weight was recorded. This indicates that the LD<sub>50</sub> value of the tested compounds were expected to be beyond 300 mg/kg body weight and represented as class 4 (“**300 mg/kg < LD<sub>50</sub> < 2000 mg/kg**”) according to Globally Harmonized Classification System (GHS).

From the acute toxicity studies the data revealed that all the tested compounds proved to be non toxic at tested 300 mg/kg body weight dose level and well tolerated by the tested animals as their LD<sub>50</sub> values are >300 mg/kg body weight.

### ***8.2. In-vivo antimycobacterial activity***

With the acute toxicity results, the *in-vitro* anti-tubercular activity rankings and with the support of multiple molecular docking studies including molecular dynamic simulation studies, top 3 compounds were selected and subjected for the *in-vivo* antitubercular activity. The three top ranked compounds (**N11, N20 and N18**) resulting from *in-vitro* antimycobacterial activity were found to be non toxic at the tested 300 mg/kg body weight. In addition, the results of multiple molecular docking studies and

the molecular dynamic simulation studies rationalizes the selection of those three compounds for *in-vivo* efficacy study.

### **8.2.1. Materials**

- LD<sub>50</sub> determination of the test compounds was performed in Balb/c mice (20-30 gm) of either sex using standard procedures.
- *In-vivo* antimycobacterial activity was performed using Balb/c mouse model for CFU (Colony Forming Unit) and Mortality.
- Isoniazid was used as a reference standard, as it is a standard drug regimen in the management of tuberculosis.

### **8.2.2. Experimental**

#### ***Animals***

Balb/c animals were housed in individually ventilated cage system and provided with autoclaved pellet diet, bedding and water *ad libitum*. Animals were maintained in light and noise controlled environment.

#### ***Dose determination:***

LD<sub>50</sub> determination of the test sample was performed in Balb/c mice using standard procedures. >300mg per kg was observed as LD<sub>50</sub> for samples **N11**, **N18** and **N20**. Samples **N11**, **N18** and **N20** were administered at 10mg per kg orally for 10 days. At this test dose animals did not show any signs of weight loss, therefore selected for the preliminary *in-vivo* efficacy testing.

#### ***In-vivo antimycobacterial activity***

5 x 10<sup>8</sup> CFU of *Mycobacterium tuberculosis* (H37rv) was injected by lateral caudal vein of the mice. Test substance **N11**, **N18** and **N20** 10 mg/kg, **INH** 25 mg/kg

were administered orally, once daily for 4 weeks. Animals were sacrificed by cervical dislocation. CFU from lung were obtained by dissecting and weighing the lung followed by preparation of 1 mg/ml homogenate in saline. The homogenate was added to 7H11 agar medium supplemented with OADC (Oleic Albumin Dextrose Catalase) in a petridish and incubated at 37°C for 4 weeks to obtain the CFU. The CFU were counted and reported as CFU per mg of tissue.

### **8.1.3. Results and discussion**

#### ***Antitubercular activity***

The test compounds, despite of showing LD<sub>50</sub> cut of values at >300 mg/kg body weight to start with the safe low dose, 10 mg/kg body weight was selected as a dose for *in-vivo* antimycobacterial activity after testing it orally daily for 10 days.

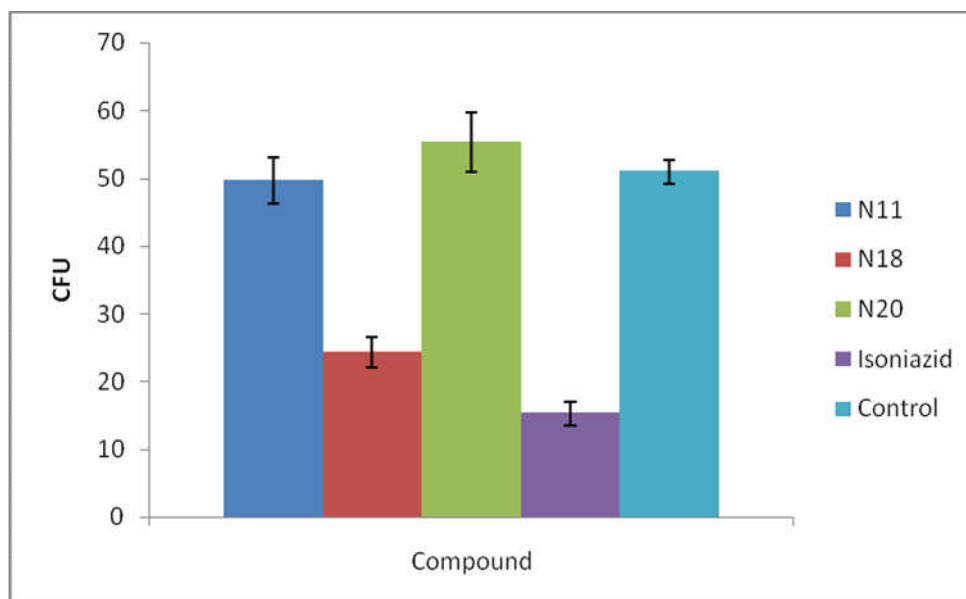
The tested compounds **N11**, **N18** and **N20** showed CFU value for antitubercular activity with  $49.67 \pm 3.480$ ,  $24.33 \pm 2.186$  and  $55.33 \pm 4.410$ , respectively, and the standard drug Isoniazid showed  $15.33 \pm 1.764$  antitubercular activity. It was found that compound **N18** was active in *in-vivo* antimycobacterial assay, when compared to the other synthesized tested compounds. The results of the *in-vivo* antitubercular activity showing CFU lung values were summarized in **Table 13** and in **Figure-22**.

It was interesting to notice that the compound **N18** decreased the bacterial load to  $24.33 \pm 2.186$  at 10 mg/kg dose, while standard drug isoniazid decreased the bacterial load to  $15.33 \pm 1.764$  at 25 mg/kg dose. Thus the study deserves for the conclusion that the CFU value obtained by compound **N18** at the dose of 10 mg/kg was found to be significant when compared to the standard drug isoniazid at 25 mg/kg dose.

**Table 13: Lung CFU lung values in animals treated with test samples and standard controls**

S.No	Compound	CFU per mg tissue			CFU lung values±SEM <sup>a</sup> Average ±SEM
		1	2	3	
1	N11	44	56	49	49.67±3.480
2	<b>N18</b>	<b>26</b>	<b>20</b>	<b>27</b>	<b>24.33±2.186</b>
3	N20	47	62	57	55.33±4.410
4	Isoniazid	12	18	16	15.33±1.764
5	Control (Untreated)	54	48	51	51.00±1.732

<sup>a</sup>CFU- Colony Forming Units , SEM- Standard Error in Mean



n=3, error bars represents SEM values (Standard Error in Mean)

**Figure 22: Lung CFU lung values in animals treated with test samples and standard controls**

# CHAPTER 9

## SUMMARY AND CONCLUSION

### 9.1. Summary

- Thirty molecules (N1 to N20, GA, GAC, GAC1, GAC5, GAC6, GAC7, GAE, GAEA, GAM and GAT) which were predicted to be effective against *Mycobacterium tuberculosis* were selected for the synthesis through computational studies. This was achieved by the molecular docking studies against the target enzyme InhA (PDB id – 2NSD) of *Mycobacterium tuberculosis*, *in-silico* ADME assessment and *in-silico* toxicity predictions.
- The thirty molecules which were selected for the synthesis belong to the following functional class,
  - ✓ 20 Thiazolidinone derivatives (N1 to N20) and
  - ✓ 10 dioxolan based analogues comprising of
    - thieno-pyrimidine core (4 compounds) (GAC, GAC1, GAC5 and GAC7),
    - thieno-pyridine core (2 compounds) (GAEA and GAM),
    - thieno-thiazine core (1 compound) (GAC6) and
    - dihydro benzo-thiophene (3 compounds) (GA, GAE and GAT).
- All the thirty molecules were synthesized. The synthesized compounds were purified and characterized. The synthesized compounds were characterized by “FT-IR, <sup>1</sup>H-NMR, <sup>13</sup>C-NMR, Mass spectra and elemental analysis”. The relative stereochemistry of one compound was confirmed by the X-Ray Crystallography.

- The physical characteristics and spectral studies like “FT-IR, <sup>1</sup>H-NMR, <sup>13</sup>C-NMR, Mass spectra and elemental analysis” confirmed the proposed structure of the synthesized compounds.
- All the synthesized compounds were investigated for their *in-vitro* anti-tubercular potential using “Microplate Alamar Blue assay” MABA Assay. All the compounds showed moderate to potent *in vitro* activity against MTB with MIC range **0.05-50 µg/ml** concentrations. Compounds **N18, N11 and N20** displayed most potent *in-vitro* activity with MICs **0.05, 0.1, 0.2 µg/ml** concentrations respectively.
- In order to correlate the *in-vitro* anti-tubercular activity results with the docking results, further docking was performed with the top 12 compounds (**N10, N11 to N20** and **GAT**) resulting from *in-vitro* anti-tubercular activity data against the multiple target enzymes of *Mycobacterium tuberculosis* {Thymidylate Kinase (PDB id – 1G3U), Diaminopimelate Decarboxylase (PDB id – 1HKV), Cyclopropane Synthase (PDB id – 1L1E), Antibiotic Resistance Protein (PDB id – 1YK3), TrpD essential for lung colonization (PDB id – 1ZVW), Thymidylate Synthase X (PDB id – 2AF6), Protein Kinase G (PDB id – 2PZI), Gyrase TypeIIA Topoisomerase (PDB id – 3UC1), L, D Transpeptidase 2 (PDB id – 3VAE)}.
- In order to rationalize the correlation between the *in-vitro* antitubercular activity and multi-target docking results a cross observational analysis was performed. The top-ranked three compounds (**N18, N11 and N20**) of *in-vitro* antitubercular activity were cross observed with their docking ranks on all the studied target enzymes for their deviations in their ranks.



- Based upon multiple target docking study results and the cross observational analysis results, the enzyme Thymidylate Kinase (PDB id – 1G3U) was found to be more appropriate target for the tested compounds that exhibited *in-vitro* antitubercular activity. Thus the scope and limitations of software and the plausible mechanism of action for the activity was proved.
- The stability of the ligand-receptor complexes were analysed by molecular dynamic simulation study. This was achieved by performing the study with the ligands **N18-1G3U**, **N11-1G3U** and **N20-1G3U** (-thymidylate kinase) complexes (top-ranked docking ligand-receptor complex). The study confirmed that the ligand-receptor complexes were stable without any notable conformational changes during the simulation run. At the end of the MD simulation, change in position and orientation of ligands in the introduced binding site were observed, which indicates the usefulness of the MD simulation for the optimization of the ligands into the target binding site.
- The compounds showing *in-vitro* inhibitory activity below 12.5 µg/ml concentrations against *Mycobacterium tuberculosis* were subjected for the acute oral toxicity studies. The selected compound codes were **N10**, **N11 to N20** and **GAT**. No signs of toxicity were noticed at the dose of 300 mg/kg b.w, while some signs of toxicity at 2000 mg/kg b.w. to the group of animals were recorded. Thus the study suggests that the LD<sub>50</sub> value of the tested compounds were expected to exceed 300 mg/kg b.w and was represented as class 4 (**300 mg/kg < LD<sub>50</sub> < 2000 mg/kg**) according to Globally Harmonized Classification System (GHS).
- Three compounds (**N11**, **N20** and **N18**) which displayed effective inhibition of *Mycobacterium tuberculosis* in *in-vitro* anti-tubercular activity were studied for

their *in-vivo* potential using Balb/c mouse model for Colony Forming Units (CFU) and Mortality. It was found that compound **N18** was active in *in-vivo* antimycobacterial assay, when compared to the other synthesized tested compounds. It was also interesting to notice that the compound **N18** decreased the bacterial load to  $24.33 \pm 2.186$  at 10 mg/kg dose, while standard drug isoniazid decreased the bacterial load to  $15.33 \pm 1.764$  at 25 mg/kg dose. Thus the study concludes that the CFU value obtained by compound **N18** at the dose of 10 mg/kg was found to be significant when compared to the standard drug isoniazid at 25 mg/kg dose.

## 9.2. Conclusion

- In the present work, simple and efficient practical methods for the synthesis of heterocyclics, which resulted from the *in-silico* approach was achieved in good yield.
- Thiazolidinone derivatives, i.e. compounds **N18**, **N11** and **N20** showed most potent inhibition in *in-vitro* antitubercular activity at MIC 0.05, 0.1 and 0.2  $\mu\text{g/ml}$  concentrations.
- *In-vivo* acute toxicity studies and *in-silico* ADME predictions reports suggest the lead compounds **N18**, **N11** and **N20** can be taken up for further studies.
- It was found that lead compound **N18** was active in *in-vivo* antimycobacterial assay, when compared to the other synthesized tested compounds.
- It was interesting to note that the compound **N18** decreased the bacterial load to  $24.33 \pm 2.186$  at 10 mg/kg dose, while standard drug isoniazid decreased the bacterial load to  $15.33 \pm 1.764$  at 25 mg/kg dose. Thus the study deserves for the conclusion that the CFU value obtained by compound **N18** at the dose of 10 mg/kg was found to be significant when compared to the standard drug

isoniazid at 25 mg/kg dose. It was also concluded that, on increasing the dose of compound **N18**, it may produce more significant results compared to the standard drug isoniazid.

- The above findings have demonstrated that the compound **N18 ((Z)-5-(3-nitrobenzylidene)-2-thioxothiazolidin-4-one)** is possibly a good anti-mycobacterial agent.

## BIBLIOGRAPHY

1. Kumar V, Abbas AK, Fausto N, Mitchell RN. Robbins Basic Pathology. Saunders Elsevier 2007; 8<sup>th</sup> ed: 516-22.
2. World Health Organization. c1948. Tuberculosis Fact Sheet. In: Geneva (Switzerland): WHO global TB programmes. November 2010.
3. Keshavjee S, Farmer P. Tuberculosis, drug, resistance, and the history of modern medicine. *New England Journal of Medicine*. 2012; 367(10): 931-6.
4. World Health Organization. c1948. Tuberculosis Fact Sheet. In: Geneva (Switzerland): WHO global TB programmes. October 2014.
5. Daniel TM. The history of tuberculosis. *Respiratory Medicine*. 2006; 100: 1862-70.
6. Hayman J. *Mycobacterium ulcerans*: an infection from Jurassic time? *Lancet*. 1984; 2: 1015-6.
7. Gutierrez MC, Brisse S, Brosch R, Fabre M, et al. Ancient origin and gene mosaicism of the progenitor of *Mycobacterium tuberculosis*. *PLOS Pathogens*. 2005; 1: e5.
8. Kapur V, Whittam TS, Musser JM. Is *Mycobacterium tuberculosis* 15,000 years old? *Journal of Infectious Diseases*. 1994; 170: 1348-9.
9. Comas I, Gagneux S. The past and future of tuberculosis research. *PLOS Pathogens*. 2009; 5(10): e1000600.
10. Goldman L, Schafer AI. Tuberculosis: disease overview. In: Goldman L, Schafer AI, editors. *Goldman's cecil medicine: expert consult premium edition*. 24th ed. St. Louis (MO): Saunders Elsevier. 2011.
11. Cruz-Knight W, Blake-Gumbs L. Tuberculosis: an overview. *Prim Care*. 2013; 40(3):743-56.

12. de Martino M, Galli L, Chiappini E. Reflections on the immunology of tuberculosis: will we ever unravel the skein? *BMC Infectious Diseases*. 2014; 14(Suppl. 1): S1.
13. Mason RJ, Broaddus VC, Martin TR, King TE, et al. Tuberculosis. In: Murray JF, Nadel JA, editors. *Murray and Nadel's textbook of respiratory medicine*. 5th ed. St. Louis (MO): Saunders Elsevier. 2010.
14. Thillai M, Pollock K, Pareek M, Lalvani A. Interferon-gamma release assays for tuberculosis: current and future applications. *Expert Review of Respiratory Medicine*. 2014; 8(1): 67-78.
15. Berry MPR, Blankley S, Graham CM, Bloom CI, O'Garra A. Systems approaches to studying the immune response in tuberculosis. *Current Opinion in Immunology*. 2013; 25(5): 579-87.
16. World Health Organization "Epidemiology". *Global tuberculosis control: epidemiology, strategy and financing*. 2009; 6-33.
17. "Improved data reveals higher global burden of tuberculosis". *WHO.int*. 22 October 2014. Retrieved on 23 October 2014.
18. GBD 2013 Mortality and Causes of Death Collaborators., "Global, regional and national age-sex specific all-cause and cause-specific mortality for 240 causes of death, 1990-2013: a systematic analysis for the Global Burden of Disease Study 2013". *Lancet*. 2014; 385 (9963): 117–171.
19. World Health Organization., "The sixteenth global report on tuberculosis-2011".
20. Fogel N. Tuberculosis: A disease. *Tuberculosis*. 2015; 95: 527-31.
21. Kumar V, Abbas AK, Aster JC, Husain AN. *Robbins basic pathology*. Saunders Elsevier. 2013; 9<sup>th</sup> ed: 493-5.
22. Mi Yan, Shutao Ma. "Recent Advances in the Research of Heterocyclic Compounds as Antitubercular Agents". *Chem Med Chem*. 2012; 7: 2063-75.

23. Gutierrez-Lugo MT, Bewley CA. Natural products, small molecules, and genetics in tuberculosis drug development. *Journal of Medicinal Chemistry*. 2008; 51(9): 2606-12.
24. Andersen P, Woodworth JS. Tuberculosis vaccine - rethinking the current paradigm. *Trends in Immunology*. 2014; 35(8): 387-95.
25. Butler R, Janice C. Centers for Disease Control and Prevention. National Institute of Allergy and Infectious Diseases (NIAID). 2007.
26. Lombardino JG, Lowe JA. The role of the medicinal chemist in drug discovery-then and now. *Nature Reviews Drug Discovery*. 2004; 3: 853-62.
27. Stratmann HG. Bad Medicine: When Medical Research Goes Wrong, Analog Science Fiction and Fact. 2010; CXXX: 20.
28. Peter Imming. Medicinal Chemistry: Definitions and objectives, drug activity phases, drug classification systems. *The Practice of Medicinal Chemistry*. 4<sup>th</sup> ed. Germany: Elsevier. 2015; 3-13.
29. Wermuth CG, Ganellin CR, Lindberg P, Mitscher LA. Glossary of terms used in medicinal chemistry. IUPAC Recommendations 1997, Part I. In: Adam J, editor. *Annual reports in medicinal chemistry*. San Diego, CA: Academic Press. 1998; 385-95.
30. Burger A. Preface. In: Hansch C, Sammes PG, Taylor JB, editors. *Comprehensive medicinal chemistry*. Oxford: Pergamon Press. 1990; 1.
31. Kore PP, Mutha MM, Antre RV, Oswal RJ, et al. Computer-aided drug design: An innovative tool for modeling. *Open Journal of Medicinal Chemistry*. 2012; 2: 139-48.
32. Lengauer T, Rarey M. Computational Methods for Biomolecular Docking. *Current Opinion in Structural Biology*. 1996; 6 (3): 402-6.
33. Jain AN. "Scoring functions for protein-ligand docking". *Current Protein and Peptide Science*. 2006; 7 (5): 407-20.

34. Lensink MF, Mendez R, Wodak SJ. "Docking and scoring protein complexes: CAPRI 3rd Edition". *Proteins: Structure, Function, and Bioinformatics*. 2007; 69 (4): 704-18.
35. Robertson TA, Varani G. "An all-atom, distance-dependent scoring function for the prediction of protein-DNA interactions from structure". *Proteins*. 2007; 66 (2): 359-74.
36. Roncaglioni A, Toropov A, Toropova AP, Benfenati E. In silico methods to predict drug toxicity. *Current Opinion in Pharmacology*. 2013; 13(5): 802-6.
37. Lipinski CA, Lombardo F, Dominy BW, Feeney PJ. Experimental and computational approaches to estimate solubility and permeability in drug discovery and development settings. *Advanced Drug Delivery Reviews*. 2001; 46: 3.
38. Pieffet G. *The Application of Molecular Dynamics Simulation Techniques and Free Energy*. Groningen: s.n 2005; 126.
39. Gokulan K, Rupp B, Pavelka MS, Jacob WR, et al. Crystal structure of *Mycobacterium tuberculosis* diaminopimelate decarboxylase, an essential enzyme in bacterial lysine biosynthesis. *Journal of Biological Chemistry*. 2003; 278(20): 18588-96.
40. Huang CC, Clare VS, Glickman MS, Jacob WR, et al. Crystal structures of mycolic acid cyclopropane synthases from *Mycobacterium tuberculosis*. *Journal of Biological Chemistry*. 2002; 277(13): 11559-69.
41. Card GL, Peterson NA, Smith CA, Rupp B, et al. The crystal structure of Rv1347c, a putative antibiotic resistance protein from *Mycobacterium tuberculosis*, reveals a GCN5-related fold and suggests an alternative function in Siderophore biosynthesis. *The Journal of Biological Chemistry*. 2005; 280(14): 13978-86.
42. Lee CE, Goodfellow C, Farah JM, Edward NB, et al. The crystal structure of TrpD, a metabolic enzyme essential for lung colonization by *Mycobacterium tuberculosis*, in complex with its substrate phosphoribosylpyrophosphate. *Journal of Molecular Biology*. 2006; 355: 784-97.

43. Sampathkumar P, Turley S, Ulmer JE, Rhie HG, et al. Structure of *Mycobacterium tuberculosis* flavin dependant thymidylate synthase (MtbThyX) at 2.0 Å resolution. *Journal of Molecular Biology*. 2003; 352(5): 1091-104.
44. Xin H, Akram A, Paul R, Montellano O. Inhibition of the *Mycobacterium tuberculosis* enoyl acyl carrier protein reductase InhA by arylamides. *Bioorganic & Medicinal Chemistry*. 2007; 15: 6649-58.
45. Li de la S, Munier LH, Gilles AM, Barzu O, et al. X-ray Structure of TMP Kinase from *Mycobacterium tuberculosis* complexed with TMP at 1.95 Å Resolution. *Journal of Molecular Biology*. 2001; 311: 87-100.
46. Scherr N, Honnappa S, Kunz G, Mueller P, et al. Structural basis for the specific inhibition of protein kinase G, a virulence factor of *Mycobacterium tuberculosis*. *PNAS*. 2007; 104(29): 12151-6.
47. Tretter EM, Berger AM. Mechanisms for Defining Supercoiling Set Point of DNA Gyrase Orthologs. *Journal of Biological Chemistry*. 2012; 287(22): 18645-54.
48. Erdemli SB, Gupta R, Bishai WR, Lamichhane G, et al. Targeting the cell wall of *Mycobacterium tuberculosis*: Structure and mechanism of L,D- transpeptidase 2. *Structure*. 2012; 20(12): 2103-15.
49. Stockwell BR. Exploring biology with small organic molecules. *Nature*. 2004; 432: 846.
50. Capan G, Ulusoy N, Ergenc N, Kiraz M. New 6-Phenylimidazo[2,1-b]thiazole Derivatives: Synthesis and Antifungal Activity. *Monatshefte für Chemie/ Chemical Monthly*. 1999; 130(11): 1399-407.
51. Kavitha CV, Basappa, Swamy SN, Mantelingu K, et al., Synthesis of new bioactive venlafaxine analogs: novel thiazolidin-4-ones as antimicrobials. *Bioorganic & Medicinal Chemistry*. 2006; 14(7): 2290-9.



52. Omar K, Geronikaki A, Zoumpoulakis P, Camoutsis C, et al. Novel 4-thiazolidinone derivatives as potential antifungal and antibacterial drugs. *Bioorganic & Medicinal Chemistry*. 2010; 18: 426-32.
53. Vigorita MG, Ottana R, Monforte F, Maccari R, et al. Synthesis and antiinflammatory, analgesic activity of 3,3'-(1,2-ethanediyl)-bis[2-aryl-4-thiazolidinone] chiral compounds. Part 10. *Bioorganic & Medicinal Chemistry Letters*. 2001; 11(21): 2791-4.
54. Ottana R, Maccari R, Barreca MT, Bruno G, et al. 5-Arylidene-2-imino-4-thiazolidinones: design and synthesis of novel anti-inflammatory agents. *Bioorganic & Medicinal Chemistry*. 2005; 13(13): 4243-52.
55. Kumar A, Rajput CS, Bhati SK. Synthesis of 3-[4'-(p-chlorophenyl)-thiazol-2'-yl]-2-[(substituted azetidinone/thiazolidinone)-aminomethyl]-6-bromoquinazolin-4-ones as anti-inflammatory agent. *Bioorganic & Medicinal Chemistry*. 2007; 15: 3089-96.
56. Karegoudar P, Prasad DJ, Ashok M, Mahalinga M, et al. Synthesis, antimicrobial and anti-inflammatory activities of some 1,2,4-triazolo[3,4-b][1,3,4]thiadiazoles and 1,2,4-triazolo[3,4-b][1,3,4]thiadiazines bearing trichlorophenyl moiety. *European Journal of Medicinal Chemistry*. 2008; 43(4): 808-15.
57. Ottana R, Carotti S, Maccari R, Landini I, et al. In vitro antiproliferative activity against human colon cancer cell lines of representative 4- thiazolidinones. Part I. *Bioorganic Medicinal Chemistry Letters*. 2005; 15: 3930-3.
58. Rao A, Carbone A, Chimirri A, De Clercq E, et al. Synthesis and anti-HIV activity of 2,3-diaryl-1,3-thiazolidin-4-ones. *Farmaco*. 2003; 58: 115-20.
59. Barreca ML, Chimirri A, De Clercq E, De Luca L, et al. Anti-HIV agents: design and discovery of new potent RT inhibitors. *Farmaco*. 2003; 58: 259-63.

60. Kucukguzel G, Kocatepe A, De clerq E, Sahin F, et al. Synthesis and biological activity of 4-thiazolidinones, thiosemicarbazides derived from diflunisal hydrazide. *European Journal of Medicinal Chemistry*. 2006; 41(3): 353-9.
61. Rawal RK, Tripathi R, Katti SB, Pannecouque C, et al. Design, synthesis, and evaluation of 2-aryl-3-heteroaryl-1,3-thiazolidin-4-ones as anti-HIV agents, *Bioorganic & Medicinal Chemistry*. 2007; 15: 1725-31.
62. Karakus S, Rollas S. Synthesis and antituberculosis activity of new N-phenyl-N'-[4-(5-alkyl/arylamino-1,3,4-thiadiazole-2-yl)phenyl]thioureas. *Farmaco*. 2002; 57(7): 577-81.
63. Babaoglu K, Page MA, Jones VC, McNeil MR, et al., Novel inhibitors of an emerging target in *Mycobacterium tuberculosis*; substituted thiazolidinones as inhibitors of dTDP-rhamnose synthesis. *Bioorganic & Medicinal Chemistry Letters*. 2003; 13: 3227-30.
64. Kachhadia VV, Patel MR, Joshi HS. Heterocyclic systems containing S/N regioselective nucleophilic competition: facile synthesis, antitubercular and antimicrobial activity of thiohydantoins and iminothiazolidinones containing the benzo[*b*]thiophene moiety. *Journal of the Serbian Chemical Society*. 2005; 70: 153-61.
65. Foroumadi A, Kargar Z, Sakhteman A, Sharifzadeh Z, et al. Synthesis and antimycobacterial activity of some alkyl [5-(nitroaryl)-1,3,4-thiadiazol-2-ylthio]propionates. *Bioorganic & Medicinal Chemistry Letters*. 2006; 16(5): 1164-7.
66. Balamurugan K, Perumal S, Sunil Kumar AR, Yogeeswari P, et al. A facile domino protocol for the regioselective synthesis and discovery of novel 2-amino-5-arylthieno[2,3-*b*]thiophenes as antimycobacterial agents. *Tetrahedron Letters*. 2009; 50: 6191-5.
67. El-Gazzar ARBA, Hussein HAR, Hafez HN. Synthesis and biological evaluation of thieno [2, 3-*d*] pyrimidine derivatives for anti-inflammatory, analgesic and ulcerogenic activity. *Acta Pharm*. 2007; 57: 395-411.

68. Abd El-Wahab A H F, Al-Fifi ZIA, Bedair AH, Ali FM, et al. Synthesis, reactions and biological evaluation of some new naphtho[2,1-*b*]furan derivatives bearing a pyrazole nucleus. *Molecules*. 2011; 16: 307-18.
69. El-mahdy KM, El-Kazak AM, Abdel-Megid M, Seada M, et al. Synthesis, characterization and biological evaluation of some new thieno[2,3-*d*]pyrimidine derivatives. *Journal of Advances in Chemistry*. 2013; 5: 581-91.
70. Karthikeyan SV, Perumal S, Arun Shetty K, Yogeewari P, et al. A microwave assisted facile regioselective Fischer indole synthesis and antitubercular evaluation of novel 2-aryl-3,4-dihydro-2H-thieno[3,2-*b*]indoles. *Bioorganic & Medicinal Chemistry Letters*. 2009; 19: 3006-9.
71. Balamurugan K, Jayachandran V, Perumal S, Manjashetty TH, et al. A microwave-assisted, facile, regioselective Friedlander synthesis and antitubercular evaluation of 2,9-diaryl-2,3-dihydrothieno-[3,2*b*]quinolones. *European Journal of Medicinal Chemistry*. 2010; 45: 682-8.
72. Kondreddi RR, Jiricek J, Srinivasa PSR, Lakshminarayana SB, et al. Design, synthesis and biological evaluation of indole-2-carboxamides, a promising class of anti-tuberculosis agents. *Journal of Medicinal Chemistry*. 2013; 01-47.
73. Soumendranath B. SAR and Pharmacophore Based Designing of Some Antimalarial and Antiretroviral Agents: An Internet Based Drug Design Approach. *Der Pharma Chemica*. 2012; 4(3): 1247-63.
74. Wermuth, C. G. Similarity in drugs: reflections on Analogue design. *Drug Discovery Today*. 2006; 11(7): 348-54.
75. Ntie Kang F. An *in silico* evaluation of the ADMET profile of the StreptomeDB database. *Springerplus*. 2013; 353(2): 01-11.

76. Ghorpade SR, Kale M, Raichurkar A, Hameed PS, et al. Thiazolopyridine ureas as novel antitubercular agents acting through inhibition of DNA Gyrase B. *Journal of Medicinal Chemistry*. 2013.
77. Martins F, Santos S, Ventura C, Elvas-Leitao R, et al. Design, synthesis and biological evaluation of novel isoniazid derivatives with potent antitubercular activity. *European Journal of Medicinal Chemistry*. 2014.
78. Nalini CN, Deepthi SR, Ramalakshmi N, Uma G. Toxicity risk assesment of Isatins. *RASAYAN J. Chem.* 2011; 4(4): 829-33.
79. Bamane RV, Chitre TS, Rakholiya VK. Molecular docking studies of quinoline-3-carbohydrazide as novel PTP1B inhibitors as potential antihyperglycemic agents. *Der Pharma Chemica*. 2011; 3(4): 227-37.
80. Raparti V, Chitre T, Bothara K, Kumar V, et al. Novel 4-(morpholin-4-yl)-N<sup>2</sup>-(arylidene)benzohydrazides: Synthesis, antimycobacterial activity and QSAR investigations. *European Journal of Medicinal Chemistry*. 2009; 44: 3954-60.
81. Renuka J, Reddy KI, Srihari K, Jeankumar VU, et al. Design, synthesis, biological evaluation of substituted benzofurans as DNA gyrase B inhibitors of *Mycobacterium tuberculosis*. *Bioorganic & Medicinal Chemistry*. 2014.
82. Haouz A, Vanheusden V, Munier-Lehmannn H, Froeyen M, et al. Enzymatic and Structural Analysis of Inhibitors Designed against *Mycobacterium tuberculosis* Thymidylate Kinase. *The Journal of Biological Chemistry*. 2003; 278(7): 4963-71.
83. Frederick WG, Jason GK, Thierry K, Matthew WD, et al. Designing novel building blocks is an overlooked strategy to improve compound quality. *Drug Discovery Today*. 2015; 20(1): 11-7.
84. Santhi N, Aishwarya S. Insights from the molecular docking of Withanolide derivatives to the target protein PknG from *Mycobacterium tuberculosis*. *Bioinformation*. 2011; 7(1): 1-4.

85. Alegaon SG, Alagawadi KR, Garg MK, Dushyant K, et al. 1,3,4-trisubstituted pyrazole analogues as promising anti-inflammatory agents. *Bioorganic Chemistry*. 2014; 54: 51-9.
86. Romano TK. Structure Based Drug Design: Docking and Scoring. *Current Protein and Peptide Science*. 2007; 8: 312-28.
87. Alegaon SG, Alagawadi KR, Vinod D, Unger B, et al. Synthesis, pharmacophore modeling, and cytotoxic activity of 2-thioxothiazolidin-4-one derivatives. *Medicinal Chemistry Research*. 2014.
88. Eleftheriou P, Geronikaki A, Hadjipavlou-Litina D, Vicini P, et al. Fragment-based design, docking, synthesis, biological evaluation and structure-activity relationships of 2-benzo/benzisothiazolimino-5-arylidene-4-thiazolidinones as cyclooxygenase/ lipoxygenase inhibitors. *European Journal of Medicinal Chemistry*. 2012; 47: 111-24.
89. Joshi SD, More UA, Koli D, Kulkarni MS, et al. Synthesis, evaluation and in silico molecular modeling of pyrrolyl-1,3,4-thiadiazole inhibitors of InhA. *Bioorganic Chemistry*. 2015; 59: 151-67.
90. Nasr T, Bondock S, Eid S. Design, synthesis, antimicrobial evaluation and molecular docking studies of some new 2,3-dihydrothiazoles and 4-thiazolidinones containing sulfisoxazole. *Journal of Enzyme Inhibition and Medicinal Chemistry*. 2015; 01-11.
91. Spadola L, Novellino E, Folkers G, Scapozza L. Homology modelling and docking studies on Varicella Zoster Virus Thymidine kinase. *European Journal of Medicinal Chemistry*. 2003; 38: 413-9.
92. Saha R, Alam MM, Akhter M. Novel hybrid-pyrrole derivatives: their synthesis, antitubercular evaluation and docking studies. *RSC Advances*. 2014.
93. Mohan SB, Ravi Kumar BVV, Dinda SC, Naik D, et al. Microwave-assisted synthesis, molecular docking and antitubercular activity of 1,2,3,4-tetrahydropyrimidine-5-carbonitrile derivatives. *Bioorganic & Medicinal Chemistry Letters*. 2012; 22: 7539-42.

94. Vilar S, Ferino G, Phatak GG, Berk B et al. Docking-based virtual screening for ligands of G protein-coupled receptors: Not only crystal structures but also in silico models. *Journal of Molecular Graphics and Modelling*. 2011; 29: 614-23.
95. Zhou Z, Felts AK, Friesner RA, Levy RM. Comparative performance of several flexible docking programs and scoring functions: enrichment studies for a diverse set of pharmaceutically relevant targets. *Journal of Chemical Information and Modeling*. 2007; 47: 1599-608.
96. Kim M, Lee KW, Cho AE. Elucidation of allosteric inhibition mechanism 2-Cys human peroxiredoxin by molecular modeling. *Journal of Chemical Information and Modeling*. 2012; 52: 3278-83.
97. Friesner RJ, Banks JL, Murphy RB, Halgren TA, et al. Glide: A new approach for rapid, accurate docking and scoring. 1. Method and assessment of docking accuracy. *Journal of Medicinal Chemistry*. 2004; 47: 1739-49.
98. Friesner RA, Murphy RB, Repasky MP, Frye LL, et al. Extra Precision Glide: Docking and Scoring Incorporating a Model of Hydrophobic Enclosure for Protein-Ligand Complexes. *Journal of Medicinal Chemistry*. 2006; 49: 6177-96.
99. Halgren TA, Murphy RB, Friesner RA, Beard HS, et al. Glide: A new approach for rapid, accurate docking and scoring. 2. Enrichment factors in database screening. *Journal of Medicinal Chemistry*. 2004; 47: 1750-9.
100. Halgren T. New method for fast and accurate binding-site identification and analysis. *Chemical Biology & Drug Design*. 2007; 69: 146-8.
101. Halgren TA. Identifying and Characterizing Binding Sites and Assessing Druggability. *Journal of Chemical Information and Modeling*. 2009; 49: 377-89.

102. Sastry GM, Adzhigirey M, Day T, Annabhimoju R, et al. Protein and ligand preparation: parameters, protocols, and influence on virtual screening enrichments. *Journal of Computer-Aided Molecular Design*. 2013.
103. Douguet D, Munier-Lehmann H, Labesse G, Pochet S. LEA3D: A computer-aided ligand design for structure-based drug design. *Journal of Medicinal Chemistry*. 2005; 48: 2457-68.
104. Unsal-Tan O, Ozadali K, Piskin K, Balkan A. Molecular modeling, synthesis and screening of some new 4-thiazolidinone derivatives with promising selective COX-2 inhibitory activity. *European Journal of Medicinal Chemistry*. 2012; 57: 59-64.
105. Raghu R, Vinod D, Leena K, Riyaz S, et al. Virtual screening and discovery of novel Aurora kinase inhibitors. *Current Topics in Medicinal Chemistry*. 2014; 14(16): 1-14.
106. Shahlaei M, Madadkar-Sobhani A, Mahnam K, Fassihi A, et al. Homology modeling of human CCR5 and analysis of its binding properties through molecular docking and molecular dynamics simulation. *Biochimica et Biophysica Acta*. 2011; 1808: 802-17.
107. Xiao J, Li Z, Sun C. Homology modeling and molecular dynamics studies of a novel C3-like ADP-ribosyltransferase. *Bioorganic & Medicinal Chemistry*. 2004; 12: 2035-41.
108. Park H, Park SY, Ryu SE. Homology modeling and virtual screening approaches to identify potent inhibitors of slingshot phosphatase 1. *Journal of Molecular Graphics and Modelling*. 2013; 39: 65-70.
109. Guo Z, Mohanty U, Noehre J, Sawyer TK, et al. Probing the  $\alpha$ -helical structural stability of stapled p53 peptides: Molecular dynamics simulations and analysis. *Chem Biol Drug Des*. 2010; 75: 348-59.
110. Shivakumar D, Williams J, Wu Y, Damm W, et al. Prediction of absolute solvation free energies using molecular dynamics free energy perturbation and the OPLS force field. *Journal of Chemical Theory Computation*. 2010; 6: 1509-19.

111. Hamama WS, Ismail MA, Shaaban S, Zoorob HH. Progress in the Chemistry of 4-Thiazolidinones. *Journal of Heterocyclic Chemistry*. 2008; 45: 939-56.
112. Havrylyuk D, Zimenkovsky B, Vasylenko O, Day CW, et al. Synthesis and Biological Activity Evaluation of 5-Pyrazoline Substituted 4-Thiazolidinones. *European Journal of Medicinal Chemistry*. 2013; 05-44.
113. Havrylyuk D, Zimenkovsky B, Karpenko O, Grellier P, et al. Synthesis of pyrazoline-thiazolidinone hybrids with trypanocidal activity. *European Journal of Medicinal Chemistry*. 2014; 85: 245-54.
114. Kuçukguzel I, Satılmış G, Gurukumar KR, Basu A, et al. 2-Heteroarylimino-5-arylidene-4-thiazolidinones as a new class of non-nucleoside inhibitors of HCV NS5B polymerase. *European Journal of Medicinal Chemistry*. 2013; 08-43.
115. Metwally MA, Abdelbasset AF, Abdel-Wahab BF. 2-Amino-4-thiazolidinones: Synthesis and reactions. *Journal of Sulfur Chemistry*. 2010; 31(4): 315-49.
116. Metwally NH. A Convenient Synthesis of Some New 5-Substituted-4-Thioxo-Thiazolidinones and Fused Thiopyrano[2,3-d]thiazole Derivatives. *Phosphorus, Sulfur, and Silicon and the Related Elements*. 2008; 183(9): 2073-85.
117. Alegaon SG, Alagawadi KR, Pawar SM, Vinod D, et al. Synthesis, Characterization and biological evaluation of thiazolidine-2, 4-dione derivatives. *Medicinal Chemistry Research*. 2013.
118. Vicini P, Geronikaki A, Incerti M, Zani F, et al. 2-Heteroarylimino-5-benzylidene-4-thiazolidinones analogues of 2-thiazolylimino-5-benzylidene-4-thiazolidinones with antimicrobial activity: Synthesis and structure–activity relationship. *Bioorganic & Medicinal Chemistry*. 2008; 16: 3714-24.



119. Aneja DK, Lohan P, Arora S, Sharma C, et al. Synthesis of new pyrazolyl-2, 4-thiazolidinediones as antibacterial and antifungal agents. *Organic and Medicinal Chemistry Letters*. 2011; 1:15.
120. Önen FE, Boum Y, Jacquement C, Spanedda MV, et al. Design, synthesis and evaluation of potent thymidylate synthase X inhibitor. *Bioorganic & Medicinal Chemistry Letters*. 2008; 18: 3628-31.
121. Onen-Bayram FE, Durmaz I, Scherman D, Herscovici J, et al. A novel thiazolidine compound induces caspase-9 dependent apoptosis in cancer cells. *Bioorganic & Medicinal Chemistry*. 2012; 20: 5094-102.
122. Ustundag GC, Satana D, Ozhan G, Capan G. Indole-based hydrazide-hydrazones and 4-thiazolidinones: synthesis and evaluation as antitubercular and anticancer agents. *Journal of Enzyme Inhibition and Medicinal Chemistry*. 2015; 1-12.
123. Crascì L, Vicini P, Incerti M, Cardile V, et al. 2-Benzisothiazolylimino-5-benzylidene-4-thiazolidinones as protective agents against cartilage destruction. *Bioorganic & Medicinal Chemistry*. 2015.
124. Wang XS, Mei-zhang M, Li Q, Sheng Yao C. Malononitrile-catalyzed and highly selective method for the synthesis of 2-((E)-1,3-diaryllallylidene)malononitriles in ionic liquid. *Synthetic Communications: An International Journal for rapid Communication and Synthetic Organic Chemistry*. 2009; 39(17): 3045-59.
125. Química C, Minho U, Gualtar C. The reaction of o-phenylenediamine with ethoxymethylene compounds and aromatic aldehydes. *Arkivoc*. 2009; xiv: 346-61.
126. Dolezel J, Hirsova P, Opletalova V, Dohnal J, et al. Rhodanineacetic acid derivatives as potential drugs: Preparation, Hydrophobic Properties and Antifungal Activity of (5-Arylalkylidene-4-oxo-2-thioxo-1,3-thiazolidin-3-yl)acetic acids. *Molecules*. 2009; 14: 4197-212;

127. Jain AK, Vaidya A, Ravichandran V, Kashaw SK, et al. Recent developments and biological activities of thiazolidinone derivatives: A review. *Bioorganic & Medicinal Chemistry*. 2012; 20: 3378-95.
128. Malipeddi H, Karigar AA, Malipeddi VR, Sikarwar MS. Synthesis and antitubercular activity of some novel thiazolidinone derivatives. *Tropical Journal of Pharmaceutical Research*. 2012; 11(4): 611-20.
129. Foreroa JSB, Carvalho EM, Juniora JJ, Silvaa FM. A new protocol for the synthesis of 2-Aminothiophenes through the Gewald reaction in solvent-free conditions. *Heterocyclic Letters*. 2011; 1(1): 61-7.
130. DurgaReddy GANK, Ravikumar R, Ravi S, Adapa SR. A CaO catalysed facile one pot synthesis of 2-Aminothiophenes using Gewald reaction. *Der Pharma Chemica*. 2013; 5(6): 294-8.
131. Kanwar S, Sharma SD. Thienopyrimidines as hetryl moiety in 2-azetidiones: Synthesis of 4-hetryl-2-azetidiones. *Indian Journal of Chemistry*. 2005; 44B: 2367-71.
132. Puterova Z, Krutosikova A, Vegh D. Gewald Reaction: Synthesis, properties and applications of substituted 2-amino thiophenes. *Arkivoc*. 2010; (i): 209-46.
133. Huang XG, Liu J, Ren J, Wang T, et al. A facile and practical one-pot synthesis of multisubstituted 2-aminothiophenes via imidazole-catalyzed Gewald reaction. *Tetrahedron*. 2011; 67: 6202-5.
134. Shearouse WC, Shumba MZ, Mack J. A Solvent-free, One-Step, One-Pot Gewald Reaction for Alkyl-aryl Ketones via mechanochemistry. *Applied Sciences*. 2014; 4: 171-9.
135. Tumer F, Ekinici D, Zilbeyaz K, Demir U. An Efficient synthesis of Substituted 4-Aryl-3-Cyano-2-Amino Thiophenes by a Stepwise Gewald Reaction. *Turk Journal of Chemistry*. 2004; 28: 395-403.

136. Al-Afaleq EI, Abubshait SA. Heterocyclic *o*-Aminonitriles: Preparation of Pyrazolo[3,4-*d*]-pyrimidines with Modification of the Substituents at the 1-Position. *Molecules*. 2001; 6: 621-38.
137. Abdelrazek FM, El-Din AMS, Mekky AE. The reaction of ethyl benzoylacetate with malononitrile: a novel synthesis of some pyridazine, pyridazino[2,3-*a*]quinazoline and pyrrole derivatives. *Tetrahedron* 2001; 57: 1813-7.
138. Buchstaller HP, Seibert CD, Lyssy RH, Frank I, et al. Synthesis of Novel 2-Aminothiophene 3-carboxylates by Variations of the Gewald Reaction. *Monatshefte für Chemie*. 2001; 132: 279-93.
139. Tormyshev VM, Trukhin DV, Rogozhnikova OY, Mikhailina TV, et al. Aryl alkyl ketones in one-pot Gewald synthesis of 2-aminothiophenes. *Synlett*. 2006; 2559-64.
140. Fleming FF, Yao L, Ravikumar PC, Funk L, et al. Nitrile-containing pharmaceuticals: efficacious roles of the nitrile pharmacophore. *Journal of Medicinal Chemistry*. 2010; 53(22): 7902-17.
141. Chavan SS, Pedgaonkar YY, Jadhav AJ, Deagani MS. Microwave accelerated synthesis of 2-aminothiophenes in ionic liquid via three component Gewald reaction. *Indian Journal of Chemistry*. 2012; 51B: 653-7.
142. Eller GA, Holzer W. First synthesis of 3-acetyl-2-aminothiophenes using the Gewald reaction. *Molecules*. 2006; 11: 371-6.
143. Awasthi D, Kumar K, Knudson SE, Slayden RA, et al. SAR studies on trisubstituted benzimidazoles as inhibitors of *Mtb* FtsZ for the development of novel antitubercular agents. *Journal of Medicinal Chemistry*. 2013; 56: 9756-70.
144. Matviiuk T, Rodriguez F, Saffon N, Mallet-Ladeira S, et al. Design, chemical synthesis of 3-(9H-fluoren-9-yl)pyrrolidine-2,5-dione derivatives and biological activity against enoyl-

- ACP reductase (InhA) and *Mycobacterium tuberculosis*. *European Journal of Medicinal Chemistry*. 2013.
145. Gasse C, Douguet D, Huteau V, Marchal G, et al. Substituted benzyl-pyrimidines targeting Thymidine monophosphate kinase of *Mycobacterium tuberculosis*: Synthesis and in vitro anti-mycobacterial activity. *Bioorganic & Medicinal Chemistry*. 2008; 16: 6075-85.
146. Kogler M, Vanderhoydonck B, De Jonghe S, Rozenski J, et al. Synthesis and evaluation of 5-substituted 20-deoxyuridine monophosphate analogues as inhibitors of flavin-dependent thymidylate synthase in *Mycobacterium tuberculosis*. *Journal of Medicinal Chemistry*. 2011; 54: 4847-62.
147. Vanheusden V, Munier-Lehmann H, Froeyen M, Busson R, et al. Discovery of bicyclic thymidine analogues as selective and high-affinity inhibitors of *Mycobacterium tuberculosis* thymidine monophosphate kinase. *Journal of Medicinal Chemistry*. 2004; 47: 6187-94.
148. Daele IV, Munier-Lehmann H, Froeyen M, Balzarini J, et al. Rational design of 5'-thiourea-substituted  $\alpha$ -thymidine analogues as Thymidine monophosphate kinase inhibitors capable of inhibiting mycobacterial growth. *Journal of Medicinal Chemistry*. 2007; 50: 5281-92.
149. Familiar O, Munier-Lehmann H, Ainsa JA, Camarasa MJ, et al. Design, synthesis and inhibitory activity against *Mycobacterium tuberculosis* thymidine monophosphate kinase of acyclic nucleoside analogues with a distal imidazoquinolinone. *European Journal of Medicinal Chemistry*. 2010; 45: 5910-18.
150. Poecke SV, Munier-Lehmann H, Helyneck O, Froeyen M, et al. Synthesis and inhibitory activity of thymidine analogues targeting *Mycobacterium tuberculosis* thymidine monophosphate kinase. *Bioorganic & Medicinal Chemistry*. 2011; 19: 7603-11.

151. Raman K, Yeturu K, Chandra N. targetTB: A target identification pipeline for *Mycobacterium tuberculosis* through an interactome, reactome and genome-scale structural analysis. *BMC Systems Biology*. 2008, 2: 109.
152. OECD guideline for testing of chemicals, Acute Oral Toxicity – Acute Toxic Class Method 423, Adopted: 17<sup>th</sup> December 2001.
153. Chepte C, Dulcescu MM, Dorohoi DO, Valeriu S, et al. Design, Synthesis and Molecular Modelling of New Thiazolidines 2,3-disubstituted with Antitumoral Activity. *Digest Journal of Nanomaterials and Biostructures*. 2012; 7(1): 287-97.
154. Pahari N, Saha D, Jain VK, Jain B, et al. Synthesis and evaluation of acute toxicity studies and analgesic characters of some novel indole derivatives. *International Journal of Pharma Sciences and Research*. 2010; 1(9): 399-408.
155. Bhaumik A, Chandra MA, Saha S, Mastanaiah J, et al. Synthesis, characterization and evaluation of anticonvulsant activity of some novel 4-thiazolidinone derivatives. *Scholars Academic Journal of Pharmacy*. 2014; 3(2): 128-32.
156. Kumar KK, Prabhu SS, Vanaja K, Mohan D. Synthesis of quinoline coupled [1, 2, 3]-triazoles as a promising class of anti-tuberculosis agents. *Carbohydrate Research*. 2011; 346: 2084-90.
157. Collins LA, Scott GF. Microplate Alamar Blue Assay versus BACTEC 460 System for High-Throughput Screening of Compounds against *Mycobacterium tuberculosis* and *Mycobacterium avium*. *Antimicrobial Agents and Chemotherapy* 1997; 41(5): 1004-9.
158. Juan-Carlos P, Anandi M, Mirtha C, Humberto G, et al. Resazurin Microtiter Assay Plate: Simple and Inexpensive Method for Detection of Drug Resistance in *Mycobacterium tuberculosis*. *Antimicrobial Agents and Chemotherapy*. 2001; 46(8): 2720-2.
159. Cappoen D, Vajs J, Uythethofken C, Virag A, et al. Anti-mycobacterial activity of 1,3-diaryltriazenes. *European Journal of Medicinal Chemistry*. 2014; 77:193-203.

160. Prithwiraj D, Yoya GK, Constant P, Bedos-Belval F, et al. Design, synthesis, and biological evaluation of new cinnamic derivatives as antituberculosis agents. *Journal of Medicinal Chemistry*. 2011; 54: 1449-61.
161. Ferreira ML, Vasconcelos TRA, Carvalho EM, Lourenço MCS, et al. Synthesis and antitubercular activity of novel Schiff bases derived from D-mannitol. *Carbohydrate Research*. 2009; 344: 2042-7.
162. Eldehna WM, Fares M, Abdel-Aziz MM, Abdel-Aziz HAA. Design, synthesis and antitubercular Activity of certain nicotinic acid hydrazides. *Molecules*. 2015; 20: 8800-15.
163. Primm TP, Franzblau SG. Recent advances in methodologies for the discovery of antimycobacterial drugs. *Current Bioactive Compounds*. 2007; 3(3): 1-8.
164. Nagesh HN, Naidu KM, Rao DH, Sridevi JP, et al. Design, synthesis and evaluation of 6-(4-((substituted-1H-1,2,3-triazol-4-yl)methyl)piperazin-1-yl)phenanthridine analogues as antimycobacterial agents. *Bioorganic & Medicinal Chemistry Letters*. 2013; 23: 6805-10.
165. Dutta NK, Asok Kumar K, Kaushiki M, Sujata GD. *In vitro* and *in vivo* antimycobacterial activity of anti-inflammatory drug, diclofenac sodium. *Indian Journal of Experimental Biology*. 2004; 42: 922-7.
166. Manna K, Yadendra KA. Potent *in vitro* and *in vivo* antitubercular activity of certain newly synthesized indophenazine 1, 3, 5-trisubstituted pyrazoline derivatives bearing benzofuran. *Medicinal Chemistry Research*. 2011; 20: 300-6.
167. Hearn MJ, Cynamon MH, Chen MF, Coppins R, et al. Preparation and antitubercular activities *in vitro* and *in vivo* of novel Schiff bases of isoniazid. *European Journal of Medicinal Chemistry*. 2009; 44: 4169-78.
168. Tyagi S, Ammerman NC, Si-Yang L, Adamson J, et al. Clofazimine shortens the duration of the first-line treatment regimen for experimental chemotherapy of tuberculosis. *PNAS*. 2015; 112(3): 869-74.

169. Sriram D, Yogeeswari P, Basha JS, Radha DR, et al. Synthesis and antimycobacterial evaluation of various 7-substituted ciprofloxacin derivatives. *Bioorganic & Medicinal Chemistry*. 2005; 13: 5774-8.
170. Sriram D, Yogeeswari P, Madhu K. Synthesis and in vitro and in vivo antimycobacterial activity of isonicotinoyl hydrazones. *Bioorganic & Medicinal Chemistry Letters*. 2005; 15: 4502-5.
171. Evaluation of antitubercular activity of nicotinic and isoniazid analogues. *ARKIVOC*. 2007; (xv): 181-91.